UNIVERSITY OF GRANADA

DEPARTMENT OF CHEMICAL ENGINEERING

NANO-MICROENCAPSULATION OF OILS RICH IN OMEGA-3 POLYUNSATURATED FATTY ACIDS BY SPRAY-DRYING AND ELECTROSPRAYING

DOCTORAL THESIS

NOR E. RAHMANI MANGLANO

2023

PROGRAMA DE DOCTORADO EN QUÍMICA

Directores
Emilia M. Guadix Escobar
Pedro J. García Moreno

Editor: Universidad de Granada. Tesis Doctorales
Autor: Nor Elena rahmani Manglano
ISBN: 978-84-1117-998-0
URI: https://hdl.handle.net/10481/84451

Acknowledgements

First of all, I would like to thank my supervisors, Emilia M. Guadix and Pedro J. García-Moreno for their invaluable help, support and guidance throughout my Ph.D. Thesis. Thank you for believing in my potential and encouraging me to be a better researcher every day. I have learnt so much from you and, for that, I am very grateful.

I would also like to thank my "supervisors abroad". Many thanks to Jose M. Lagaron and Cristina Prieto, from the Institute of Agrochemistry and Food Technology (IATA), for giving me the opportunity to work with them at the Novel Materials and Nanotechnology research group and for teaching me that electrospraying technology is not as frustrating as I thought. Many thanks also to Mogens L. Andersen, from the University of Copenhagen, for his patience teaching me how to handle and interpret the ESR results. By last, but not least, I am also very grateful to Charlotte Jacobsen and Betül Yesiltas, from the Technical University of Denmark, for providing me a great environment to do my research and for always taking the time for discussions whenever needed. Many thanks also to Aberto Rodríguez, Henriette Rifbjerg, Lis Berner and Thi Thu Trang Vu for their technical assistance and for sharing their extended expertise with me. It has been a pleasure working with you all.

Many thanks also to all the people I got to know during my research stays. Carlos, Mads, Valentina… you all made me feel like home.

Also, I would like to thank all my colleagues at the Department of Chemical Engineering, particularly Raúl and Ismael. Thank you for always helping me, for being so supportive and for always listening whenever I needed to vent, which may have been a bit too often. I am also very thankful for "los Viernes de Flota", which I hope they never end.

Moreover, I would like to thank my forever friend "Ferni". Thank you for always being there for me and for your constant support. Despite the distance, I have always felt you so close and I cannot thank you enough for that.

To Manu and Juan. To all my friends from Granada. Thank you very much.

Lastly,

To David. Thank you for being my best friend and my partner in crime. Thank you for always taking care of me. Thank you for making my life easier.

To my sister Salma, to my mom Marisa and to my dad Abderrahman. Thank you for always believing in me, for being so caring and supportive and for your unconditional love. This Ph.D. Thesis would not have been possible without you.

Table of contents

Resumen

Las numerosas evidencias científicas que hay disponibles en la actualidad relacionando el consumo de ácidos grasos poliinsaturados omega-3 (omega-3 PUFAs), especialmente el EPA y el DHA, con sus efectos beneficiosos para la salud han impulsado la investigación y el desarrollo de alimentos enriquecidos con estos compuestos bioactivos. No obstante, hasta la fecha, su inclusión en matrices alimentarias supone un reto científico-técnico para la industria alimentaria. Debido a su naturaleza poliinsaturada, los omega-3 PUFAs son altamente susceptibles de sufrir procesos de oxidación, lo que conlleva tanto la pérdida de sus propiedades nutricionales, como la alteración de las propiedades organolépticas del alimento enriquecido (p.ej., mal olor o sabor). Por esta razón, en las últimas décadas se ha impulsado el desarrollo de sistemas de vehiculización que prevengan la oxidación de una manera eficiente antes, durante y después de su inclusión en una matriz alimentaria. En este sentido, la producción de micro/nanoencapsulados de aceite de pescado, como fuente rica en omega-3 PUFAs, ha despertado un gran interés.

Las tecnologías de encapsulación se basan en la creación de una barrera física entre el aceite contenido en la matriz encapsulante y el entorno, limitando así su contacto directo con las especies prooxidantes presentes en el medio (p.ej., oxígeno). Actualmente, el secado por atomización es la tecnología más utilizada por la industria alimentaria y su aplicación para la producción de encapsulados de aceite de pescado ha sido ampliamente investigada durante las últimas décadas. Sin embargo, múltiples estudios han puesto de manifiesto que el proceso de encapsulación (i.e., emulsionado y secado a alta temperatura) y posterior almacenamiento (i.e., difusión de especies prooxidantes a través de la matriz encapsulante) resulta en la oxidación del aceite de pescado, haciendo necesario el uso de técnicas de estabilización adicionales. En este sentido, la adición de antioxidantes a la formulación se presenta como una estrategia eficaz, en especial el uso de agentes emulsionantes naturales con propiedades antioxidantes (p.ej., hidrolizados de proteína).

Recientemente, la tecnología de electroesprayado se ha propuesto como alternativa prometedora al convencional secado por atomización para la producción de encapsulados de aceite de pescado. Esta tecnología se basa en la aplicación de un campo eléctrico de alto voltaje entre el inyector, por donde circula la solución, y el colector, donde se recoge el producto seco, causando la atomización de la alimentación líquida y posterior secado a temperatura ambiente, evitando así la degradación térmica. Además, la configuración coaxial, que consiste en un inyector compuesto de dos agujas concéntricas, permite producir cápsulas cargadas de aceite de pescado sin necesidad de previamente dispersarlo o

emulsionarlo en la solución encapsulante, minimizando aún más la oxidación lipídica durante el procesado. Sin embargo, el uso a gran escala de esta tecnología se ve restringido por la baja productividad del proceso. El Electroesprayado Asistido por Gas Presurizado, EAPG según sus siglas en inglés, es una tecnología innovadora recientemente desarrollada que se basa en la atomización mecánica de la alimentación líquida dentro de la cámara de secado en la que se ha generado un campo electrostático de alto voltaje, permitiendo con ello la evaporación del disolvente a temperatura ambiente. Mediante esta tecnología, la productividad del proceso se ve aumentada considerablemente (de mg/h para el electroesprayado a escala de laboratorio a g/h para el EAPG), lo que la hace particularmente atractiva para la producción de encapsulados de pescado a gran escala.

En base a lo expuesto, el objetivo de esta Tesis Doctoral ha sido estudiar y optimizar el proceso de producción, así como investigar las propiedades físico-químicas y la bioaccesibilidad de encapsulados de aceite de pescado para su uso como sistemas de vehiculización en la producción de alimentos enriquecidos en omega-3 PUFAs. Para ello, se investigó la producción de encapsulados mediante la técnica térmica de secado por atomización y las técnicas electrohidrodinámicas de electroesprayado, tanto en la configuración monoaxial como en la coaxial.

En primer lugar, se estudió la influencia de la formulación (i.e., combinación agente encapsulante – agente emulsionante) en las propiedades físico-químicas de los encapsulados producidos mediante secado por atomización a escala de laboratorio. Se trabajó con dos carbohidratos de bajo peso molecular ampliamente utilizados como agentes encapsulantes (i.e., jarabe de glucosa, GS o maltodextrina, MD), y como agentes emulsionantes se consideró un hidrolizado de proteínas de lactosuero, con propiedades emulsionantes y antioxidantes (WPCH), y un surfactante sintético comercial (Tween 20). Los resultados mostraron que las propiedades físico-químicas (i.e., tamaño o EE) de los encapsulados no se vieron influenciadas por la formulación, al contrario que la estabilidad oxidativa. Independientemente del agente encapsulante utilizado, las cápsulas producidas con WPCH como agente emulsionante mostraron menores niveles de oxidación en comparación con las producidas con Tween 20. Por otra parte, al producir los encapsulados a escala planta piloto se observó que el agente encapsulante afectó a la estabilidad oxidativa del aceite de pescado encapsulado, siendo la combinación GS/WPCH más eficiente en prevenir la oxidación durante el almacenamiento que la combinación MD/WPCH. Sin embargo, los resultados mostraron bajos niveles de oxidación para ambas formulaciones, lo que sugirió un efecto

protector del WPCH. Por ello, se evaluó la actividad antioxidante del WPCH en comparación con otros agentes antioxidantes naturales comerciales de distinta polaridad (i.e., polares y apolares) añadidos a la formulación de los encapsulados. El uso del WPCH, con propiedades anfifílicas y con distintos mecanismos de acción en su parte polar y apolar (i.e., captador de radicales libres y quelante de metales), mejoró la estabilidad oxidativa del aceite de pescado encapsulado durante el almacenamiento en comparación con los antioxidantes comerciales naturales investigados.

Al estudiar la influencia de la formulación (i.e., agente encapsulante, GS o MD) y las condiciones de proceso (i.e., configuración del inyector monoaxial o coaxial, voltaje aplicado y caudales de alimentación) en las propiedades físico-químicas de las cápsulas producidas mediante electroesprayado a escala de laboratorio, se puso de manifiesto que las condiciones de proceso influían de una manera más sustancial que la formulación de la matriz encapsulante. La configuración monoaxial dio lugar a cápsulas con mejores propiedades de retención que las producidas en la configuración coaxial ($EE_{monoaxial}$ = 69-72% frente a $EE_{coaxial}$=53-59%) y con una alta estabilidad oxidativa. Además, también se observó que aumentar el contenido de pululano en las cápsulas producidas en la configuración coaxial redujo significativamente la oxidación del aceite encapsulado. En general, escalar el proceso de electroesprayado de escala de laboratorio a escala planta piloto (EAPG) dio lugar a cápsulas más grandes (~99% de las cápsulas < 3µm en comparación con ~99% de las cápsulas < 15µm a escala de laboratorio y EAPG, respectivamente), con mejores propiedades de retención y mejor estabilidad oxidativa. Por otro lado, se pudo observar que el contenido de compuestos volátiles de oxidación aumentó progresivamente durante el almacenamiento para las cápsulas producidas en la configuración monoaxial, en comparación con las cápsulas producidas en la configuración coaxial en las que se mantuvo prácticamente contante. Este hallazgo se atribuyó a la distinta protección ejercida por los sistemas encapsulantes frente al oxígeno ambiental, influenciada por la distribución del aceite de pescado dentro de la matriz encapsulante (i.e., distribución centralizada en coaxial frente a distribución aleatoria en monoaxial).

A través de la técnica de Resonancia Paramagnética Electrónica (RPE) se evaluó la permeabilidad al oxígeno y la estabilidad oxidativa de los encapsulados producidos a escala de laboratorio mediante las técnicas de secado por atomización y electroesprayado. Los resultados mostraron que las cápsulas menos permeables al oxígeno fueron aquellas producidas mediante secado por atomización (~95% de las cápsulas < 25µm) que, a su vez,

fueron las que mostraron la mayor estabilidad oxidativa en comparación con las producidas mediante la tecnología de electroesprayado (i.e., monoaxial o coaxial) (~95% de las cápsulas < 1.5µm) debido a su mayor tamaño. De hecho, la influencia del tamaño de partícula en la estabilidad oxidativa de los encapsulados se hizo más evidente cuando las cápsulas se produjeron a escala planta piloto mediante secado por atomización o EAPG monoaxial con distintas cargas de aceite (13, 26 o 39 wt%). Independientemente de la carga de aceite, se encontraron niveles de oxidación similares tras el almacenamiento para las cápsulas producidas mediante la misma tecnología. Sin embargo, la menor estabilidad oxidativa reportada para las cápsulas producidas mediante EAPG monoaxial se atribuyó a la mayor permeabilidad al oxígeno de la pared encapsulante a consecuencia de su menor tamaño de partícula, ya que el resto de propiedades físico-químicas de los encapsulados estudiados era similar entre las muestras (i.e., misma formulación, similar EE y similar tamaño de gota del aceite encapsulado, $p > 0.05$).

Teniendo en cuenta que la finalidad de los encapsulados producidos es el enriquecimiento en omega-3 PUFAs de una matriz alimentaria, primero se estudió la bioaccesibilidad del aceite de pescado encapsulado. Tras la digestión *in vitro* simulada de las cápsulas producidas mediante secado por atomización se observó que la extensión y el grado de digestión lipídica se vio significativamente influenciado por el agente emulsionante utilizado en la formulación (i.e., WPCH o Tween 20), y no tanto por el agente encapsulante (i.e., GS o MD). Los resultados mostraron que el WPCH usado como emulsionante fue capaz de mantener la integridad de la interfase aceite/agua durante el proceso de secado de una manera más eficiente que el Tween 20, lo que se tradujo en un menor estado de agregación de las gotas de aceite en las distintas fases del tracto gastrointestinal (GIT) simulado y, por lo tanto, en una mayor área interfacial disponible para las reacciones de digestión. Estos resultados se correlacionaron bien con los encontrados cuando se investigó la influencia de la técnica de secado en la estructura secundaria de los péptidos (WPCH) adsorbidos en la interfase aceite/agua mediante la tecnología de Dicroísmo Circular de Radiación de Sincrotrón (SRCD), que mostraron que la conformación del WPCH localizado en la interfase se mantuvo invariable antes y después del secado por atomización.

Por último, se produjeron matrices alimentarias enriquecidas en omega-3 PUFAs. Inicialmente, se investigó la influencia del sistema de vehiculización (i.e., aceite, aceite emulsionado o aceite encapsulado mediante secado por atomización) en la estabilidad física y oxidativa de una mayonesa enriquecida. La mayonesa enriquecida con el aceite

encapsulado presentó la mayor viscosidad tras la producción debido al efecto espesante de las cápsulas intactas dispersas en la matriz, lo que se tradujo en una alta estabilidad física durante el almacenamiento. Además, este sistema de vehiculización (i.e., aceite encapsulado) mejoró la estabilidad oxidativa de las mayonesas enriquecidas, lo que se atribuyó a la retención de la integridad física de la matriz encapsulante durante el procesado y posterior almacenamiento de la mayonesa, limitando así el contacto directo entre el aceite de pescado encapsulado y las especies prooxidantes presentes en el medio (i.e., oxígeno o iones metálicos). Posteriormente, se investigó la influencia de la tecnología de encapsulación en la estabilidad física y oxidativa de un aliño de ensalada enriquecido. Para ello, los encapsulados se produjeron a escala planta piloto mediante secado por atomización y EAPG monoaxial y coaxial. La estabilidad física del alimento enriquecido no se vio influenciada por el sistema de enriquecimiento, al contrario que la estabilidad oxidativa. El aliño de ensalada enriquecido con el aceite de pescado encapsulado mediante la tecnología EAPG coaxial presentó niveles bajos, y prácticamente constantes, de oxidación al contario que los aliños enriquecidos con las cápsulas producidas mediante las tecnologías de encapsulación basadas en emulsión (i.e., secado por atomización y EAPG monoaxial). Esto se atribuyó a la menor degradación inicial del aceite encapsulado mediante EAPG coaxial ya que el aceite no se emulsionó y el secado se produjo a temperatura ambiente.

En general, de los estudios llevados a cabo en la Tesis Doctoral se puede concluir que las propiedades físico-químicas de los encapsulados de aceite de pescado, influenciadas por la tecnología de encapsulación, tienen un impacto significativo en la estabilidad oxidativa del aceite. Así mismo, se ha demostrado que la encapsulación de aceite de pescado mediante la tecnología EAPG coaxial no basada en emulsión es una estrategia prometedora para la producción de alimentos ricos en omega-3 PUFAs física y oxidativamente estables.

Summary

1. INTRODUCTION

1.1 Omega-3 Polyunsaturated Fatty Acids

Omega-3 polyunsaturated fatty acids (PUFAs) are, from a structural point of view, a group of fatty acids which are characterized for having more than two double bonds, with the first doble bond located three atoms away from the terminal methyl group of the fatty acid chain (Calder, 2013). From the omega-3 PUFAs series, eicosapentaenoic acid (EPA; C20:5 n-3) and docosahexaenoic acid (DHA; C22:6 n-3) are regarded as the most important fatty acids due to the nutritional and physiological benefits related to their intake. Several epidemiological studies have stablished a relationship between a diet rich in omega-3 PUFAs with the prevention of major chronic diseases such as, cardiovascular diseases (e.g., stroke and coronary heart disease), inflammatory diseases (e.g., arthritis and asthma), neurodegenerative diseases (e.g., Alzheimer and Parkison), metabolic diseases (e.g., type 2 diabetes mellitus) or even cancer (e.g., breast cancer) (Calder, 2014; Djuricic & Calder, 2022; Punia et al., 2019). Furthermore, there is strong scientific evidence linking the consumption of omega-3 PUFAs with the preservation of normal brain or cardiac function (Calder, 2021). Based on the aforementioned research evidence, several national and global authoritative organizations have set a series of dietary intake recommendations of omega-3 PUFAs which vary depending on the age, gender and consumption purposes (Nguyen et al., 2019). For instance, in Europe, the European Food Safety Authority (EFSA) has established an adequate intake (AI) of 250 mg per day for EPA + DHA in adults and a recommended intake for pregnant or nursing women of the AI value plus 100–200 mg per day of DHA (EFSA, 2010).

From a metabolic perspective, EPA and DHA could be considered semi-essential fatty acids since, although they can be synthetized in the organism from α-linolenic acid (ALA; C18:3 n-3), the conversion extent is very low (i.e., 8% of ALA convers to EPA and 1% to DHA) (Layé et al., 2018). Therefore, to meet the intake recommendations and to have a balanced diet, a direct consumption of EPA and DHA is required. Fish and its derivatives (e.g., fish oil and fish meal) are the main source of dietary EPA and DHA (Demets & Foubert, 2021). Especially fish oil since the content of omega-3 PUFAs accounts up to 35%, depending on the parent fish (Demets & Foubert, 2021). Nonetheless, changes in the food industry and

eating habits have led to the major part of the global population (~ 80%) not reaching the recommended intake (Demets & Foubert, 2021). In this regard, enriching common food products with these bioactive lipids (e.g., fish oil) has been proposed as a promising strategy to increase the consumption of omega-3 PUFAs. Nonetheless, due to their highly unsaturated nature, these compounds are highly prone to lipid oxidation which eventually affects the product quality as it leads to the loss of nutritional properties, as well as the formation of undesirable odors and flavors. As a result, the development of fortification strategies that preserves the properties of the omega-3 PUFAs and prevent their degradation during processing and subsequent storage of the enriched foodstuff is the main technological challenge that the food industry must address when it comes to the production of fortified food products.

1.2 Lipid oxidation

Autooxidation is the most important mechanism of lipid oxidation and occurs as a free radical chain reaction in presence of oxygen (Rahmani-Manglano, García-Moreno, et al., 2020). This mechanism can be divided into three different stages: (I) initiation, (II) propagation and (III) termination, as depicted in Figure 1. In the next section, the basic principles of lipid oxidation will be briefly described. For a detailed description, please refer to Chapter I (Rahmani-Manglano, García-Moreno, et al., 2020).

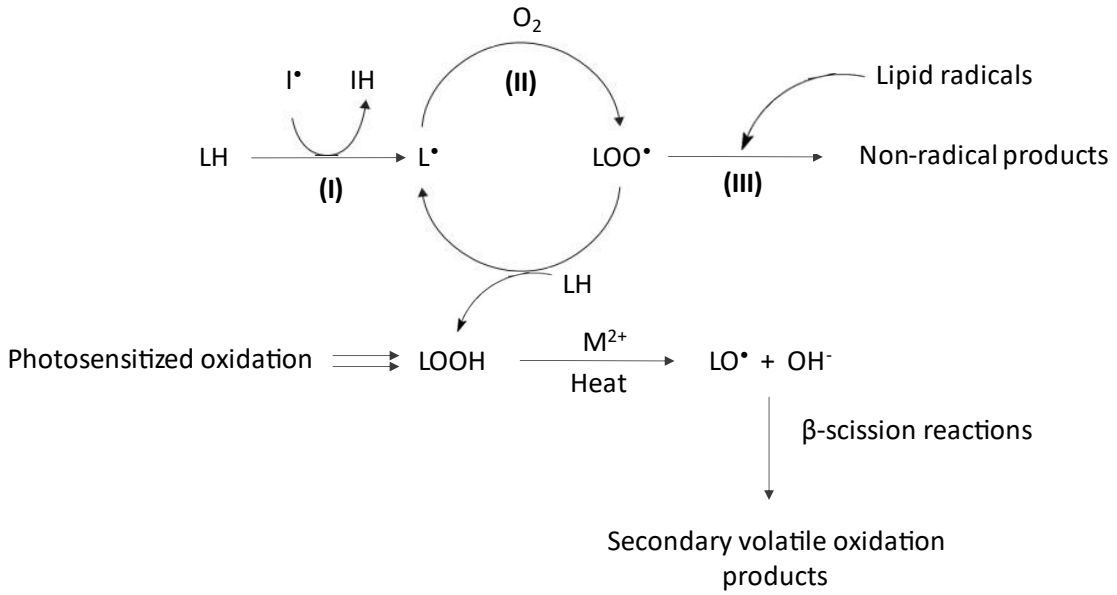

Figure 1. Autooxidation mechanism of polyunsaturated omega-3 PUFAs.

In the initiation stage (I), the unsaturated lipids lose a hydrogen atom (H^+) in the presence of initiators (e.g., heat, light or metal ions) to form very reactive free lipid radicals (alkyl radicals, $L^{\bullet}$) (Eq. 1).

$$LH + I \rightarrow IH + L^{\bullet} \quad (1)$$

Although free lipid radicals ($L^{\bullet}$) can be produced by a variety of mechanisms depending on the initiator agent, the process of transition metal-catalyzed decomposition of already existing hydroperoxides (LOOH), either as impurities or as by-products of photosensitized oxidation, is the most likely and widely accepted (Eq. 2,3). As a result, alkoxyl radicals ($LO^{\bullet}$) and peroxyl radicals ($LOO^{\bullet}$) are produced which can further initiate lipid oxidation.

$$LOOH + M^{2+} \rightarrow LO^{\bullet} + OH^{-} + M^{3+} \quad (2)$$

$$LOOH + M^{3+} \rightarrow LOO^{\bullet} + H^{+} + M^{2+} \quad (3)$$

Afterwards, in the propagation stage (II), the free lipid radicals ($L^{\bullet}$) react with oxygen to form peroxyl radicals ($LOO^{\bullet}$) (Eq. 4), which in turn react with another unsaturated lipid (LH) to form hydroperoxides (LOOH) and more free lipid radicals ($L^{\bullet}$) (Eq. 5). The hydroperoxides produced in this stage are also known as primary oxidation products and are often quantified to be used as a marker of lipid oxidation (e.g., peroxide value, PV) (Jacobsen et al., 2021).

$$L^{\bullet} + O_2 \rightarrow LOO^{\bullet} \quad (4)$$

$$LOO^{\bullet} + LH \rightarrow LOOH + L^{\bullet} \quad (5)$$

By last, in the termination stage (III), non-radical stable products are formed by the reaction of the lipid radicals formed in the initiation and propagation stages with each other. These reactions can occur through different mechanisms (e.g., condensation reaction) depending on the compounds present in the medium and the reaction conditions (e.g., temperature or pressure) and therefore, different products will be formed (Frankel, 2012). Some typical termination reactions are shown in Eq. 6-8.

$$LOO^{\bullet} + LOO^{\bullet} \rightarrow LOOL + O_2 \quad (6)$$

$$LO^{\bullet} + L^{\bullet} \rightarrow LOL \quad (7)$$

$$L^{\bullet} + L^{\bullet} \rightarrow L - L \quad (8)$$

Lipid hydroperoxides formed in the propagation stage (II) are unstable compounds that decompose through homolytic cleavage by action of heat and metal ions to alkoxyl radicals ($LO^{\bullet}$) and hydroxyl ions (OH^{-}). Generally, hydroperoxides decomposition results in the cleavage of the aliphatic chain of fatty acids, which is known as β-scission reaction, leading to the formation of low molecular weight compounds (e.g., alcohols, aldehydes and ketones). The most often identified SVOPs in oxidized fish oil are alcohols (e.g., 1-penten-3-ol), aldehydes (e.g., pentanal) and ketones (e.g., 1-penten-3-one), and to a lesser extent, hydrocarbons, furans and aromatic compounds. These compounds are referred to as secondary volatile oxidation products (SVOPs) and are responsible of the off-odor and off-flavors of oxidized omega-3 PUFAs, even at very low concentrations (e.g., flavor threshold values of vinyl ketones in the range $2 \cdot 10^{-5} – 7 \cdot 10^{-3}$ ppm). In consequence, the SVOPs are regarded as important quality markers as they can severely impact the organoleptic properties of the fortified food product.

1.3 Omega-3 delivery systems

Among the alternatives to minimize lipid oxidation during food processing and storage, the development of efficient delivery systems has been proposed as a promising approach. The basic principle of any delivery system, irrespective of its physical state (e.g., wet or dry), is to protect the oil from the environment by creating a physical barrier. Thus, the direct contact of the bioactive lipids (e.g., fish oil) with the prooxidant species present in the medium (e.g., oxygen, metal traces) is theoretically avoided, and the oxidative stability is therefore, theoretically enhanced. Whether the delivery system should be wet (e.g., fish oil-in water emulsions) or dry (e.g., fish oil loaded capsules) will be mainly determined by the nature of the food matrix.

Conventional oil-in-water (O/W) emulsions are, by nature, thermodynamically unstable systems therefore, to avoid spontaneous separation of the phases, the oil droplets need to be physically stabilized by action of emulsifiers (Berton-Carabin et al., 2014). Emulsifiers are surface-active compounds that adsorb at the O/W interface during the homogenization process and form an interfacial layer that keeps oil droplets dispersed in the aqueous phase. High molecular weight biopolymers such as proteins (e.g., casein, whey protein) and

polysaccharides (e.g., Arabic gum, modified starch) are the most common emulsifiers used in the food industry.

Apart from providing physical stability to the wet heterogeneous system (i.e., O/W emulsion), emulsifiers adsorbed at the O/W interface also play a major role on its oxidative stability as this microenvironment has been extensively proposed to be the place where lipid oxidation is initiated (i.e., contact area between prooxidant species and the oil droplets). Therefore, the interfacial properties conferred by the emulsifier will not only determine the physical stability of the emulsified systems, but they will also strongly affect its oxidative stability (Rahmani-Manglano, García-Moreno, et al., 2020). Some of the interfacial properties influencing lipid oxidation in O/W emulsions are the interfacial composition (e.g., thickness, antioxidant properties), interfacial area (e.g., droplet size) or interfacial charge (e.g., pH).

As to the interfacial layer in O/W emulsions minimize the contact between the oil and penetrating prooxidants (e.g., oxygen), emulsifiers which form thick and densely packed membranes are expected to enhance the oxidative stability of the emulsified system (Sørensen et al., 2021). Furthermore, the use of emulsifiers with antioxidant properties has been proposed to be an effective way to prevent lipid oxidation since these compounds partition at the O/W interface and thus are able to inhibit lipid oxidation at the site where it is initiated (McClements & Decker, 2018). Another factor affecting the oxidative stability of O/W emulsions is the oil droplet size since it determines the interfacial area and therefore the rate of lipid oxidation. Based on the latter, fine emulsions are expected to oxidize faster and to a higher extent than coarse emulsions however, the latter is not always true given that lipid oxidation in emulsified systems is affected by many other factors (e.g., emulsifier type and concentration, surface charge, viscosity and homogenization conditions) (Sørensen et al., 2021). Furthermore, the surface charge of the O/W interface has been proposed to greatly affect metal-catalyzed lipid oxidation in O/W emulsions (e.g., decomposition of hydroperoxides in presence of metal traces). That is because of the attraction or repulsion of positively charged metal traces by a negatively- or positively- charged O/W interface, respectively. In protein-stabilized emulsions, the interfacial charge is determined by the pH of the medium and it is generally positively-charged at acidic conditions (i.e., pH < pI). However, at low pH the solubility, and therefore the prooxidant activity, of metal traces is enhanced to react with hydroperoxides (Berton-Carabin et al., 2014).

Although conventional wet O/W emulsions have been extensively used for incorporating omega-3 PUFAs into a variety of food products (e.g., dairy products or dressings) (Ghelichi et al., 2021), dry delivery systems are more interesting from a technological point of view since they are not only more stable than wet delivery systems, but depending on the nature of the encapsulating wall (e.g., hydrophobic (bio)polymers), they can also be used in a wider range of food products (e.g., liquid to solid food products) (Sørensen et al., 2021). Therefore, in the last decades, the production of oxidatively stable micro/nanocapsules loaded with oils rich in omega-3 PUFAs (e.g., fish oil) to be used as delivery systems has become a focus for academia and industry research.

1.4 Development of dry omega-3 delivery systems: Micro/nanoencapsulation technologies

1.4.1 Spray-drying

Due to its adaptability, simplicity, low cost, ease of scaling up and high productivity, spray-drying has been historically the preferred encapsulation technology of the food industry (Rahmani-Manglano, García-Moreno, et al., 2020). Furthermore, the production of fish oil-loaded capsules by spray-drying aimed as omega-3 delivery systems has been extensively investigated over the last decades (Rahmani-Manglano, García-Moreno, et al., 2020).

In brief, spray-drying consist of a unit operation in which a liquid feed is converted into a powder product as a result of solvent evaporation by contact with air at high temperature (i.e., 150 – 220 °C) after atomization. Despite the high drying temperatures used in spray-drying, this technology has been proven to be suitable to encapsulate thermo-sensitive bioactive compounds, such as fish oil (Rahmani-Manglano, García-Moreno, et al., 2020). Due to the small droplets generated during the atomization process, at the constant-rate drying period, the internal mass transfer from the core of the droplet to the surface is high enough that allows constant moisture removal at the inlet air wet bulb temperature (T_{wb}). As evaporation occurs, the solutes accumulate at the surface of the droplet forming a semi-solid thin layer, also known as “skin” or “crust”. The development of this crust marks the beginning of falling-rate drying period in which evaporation is controlled by the water diffusion rate from the wet core of the droplet through the crust (Santos et al., 2018). During this period, the temperature of the particle increases as the water evaporation rate decreases. Nonetheless, the external mass transfer in the falling-rate drying period is also high, thus

allowing very short residence time of the particles in the drying chamber (~5 – 30s) being the temperature of the dried product exiting the equipment 15 – 20 °C lower than that of the outlet air temperature (Anandharamakrishnan et al., 2007).

The application of spray-drying to encapsulation processes, in particular omega-3 PUFAs, could be described in four basic steps: (I) preparation of the liquid feed, (II) atomization of the liquid feed, (III) solvent evaporation and (IV) collection of the dried particles (Figure 2).

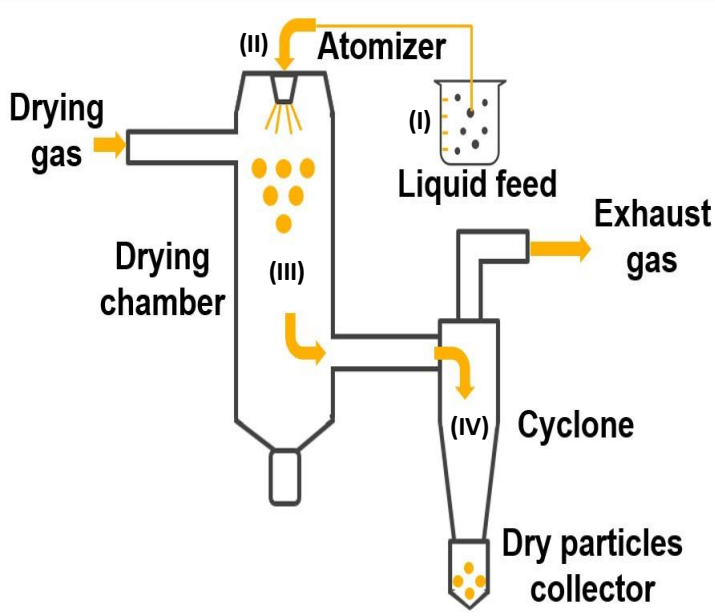

Figure 2. Schematic representation of spray-drying process.

Due to the hydrophobic nature of omega-3 PUFAs, an oil-in-water emulsion is fed to the drier. Thus, the fish oil is previously dispersed within the aqueous phase containing the encapsulating agent. The addition of an emulsifying agent will depend on whether the encapsulating material has interfacial activity or not. Afterwards, in the co-current operational mode, the emulsion is atomized into the drying chamber where it comes into contact with a current of hot drying air. As a result, water is evaporated and the liquid feed is converted into powder particles upon seconds. After water removal, the dried particles are collected as free-flowing powder, generally in a cyclone.

In order to ensure a good performance of the encapsulation process in terms of high retention of the bioactive component and high stability of the produced powder, the optimization of the feed formulation and the process variables is required. Encapsulating agents used in spray-drying processes are mainly selected based on their physicochemical properties such

as solubility, film-forming and emulsifying properties, molecular weight or glass transition temperature (T_g), among others (Gharsallaoui et al., 2007). Water is the preferred solvent for food applications, thus encapsulating agents for spray-drying applications are desired to be water-soluble (bio)polymers with low viscosity at high solids concentrations. During atomization, smaller droplets are produced from lower viscous infeed emulsions and therefore, smaller capsules are produced after drying. In addition, to enhance the retention properties of the encapsulating matrix, the encapsulating agents should exhibit: i) high emulsifying properties, in order to produce fine and stable emulsions during the processing time and ii) high film-forming and/or structural properties, in order to surround the liquid droplets upon drying. Moreover, a high T_g of the wall constituents is required to avoid sticking and agglomeration problems during drying and to maintain the integrity of the encapsulating wall during storage (e.g., avoid caking during storage) (Roos, 2010; Santos et al., 2018). Nonetheless, it has been reported that lowering the T_g of the wall constituents by adding low molecular weight carbohydrates to the formulation (e.g., maltodextrin) enhances the retention properties of the capsules by favoring the early crust formation during the drying process (Rahmani-Manglano, García-Moreno, et al., 2020).

The use of proteins (e.g., caseins, whey proteins), carbohydrates (e.g., glucose syrup, maltodextrin) and their combinations as encapsulating agents has been extensively reported in the production of fish oil-loaded capsules by spray-drying (Rahmani-Manglano, García-Moreno, et al., 2020). Generally, proteins or proteins mixtures are used alone due to their high emulsifying and film-forming properties. However, the combined use of proteins and carbohydrates is also very common because: i) carbohydrates, if not chemically modified (e.g., *n*-octenylsuccinate-derivatised starch), lack of surface-active properties and ii) carbohydrates, especially low molecular weight carbohydrates (e.g., glucose syrup), act as fillers or bulk materials, which enhances the structural properties of the encapsulating matrix (i.e., more densely packed and less porous encapsulating matrices).

The choice of the wall matrix constituents is of outmost importance as they will later determine the physicochemical properties of the system (e.g., microstructure, bulk/tapped density, moisture content or encapsulation efficiency) (Rahmani-Manglano, García-Moreno, et al., 2020). Traditionally, the encapsulation efficiency (EE) has been considered one of the most important quality markers of the outcome of the process as well as of the resulting fish oil-loaded capsules. Provided that the EE quantifies the amount of bioactive entrapped within the encapsulating matrix, the higher the EE, the better the performance of the

encapsulation process. Furthermore, in case of fish oil-loaded capsules, high EE imply a low content of unprotected non-encapsulated surface oil, therefore a high oxidative stability of encapsulated system could be expected (i.e., better protection of the encapsulated oil fraction). Nonetheless, recent studies have pointed out that, besides the content of surface oil, the oxygen diffusion within the glassy encapsulating matrix play a major role on lipid oxidation in dried heterogeneous systems (e.g., fish oil-loaded capsules) (Drusch et al., 2009; Linke, Weiss, et al., 2020).

Apart from the infeed emulsion formulation, the processing variables also influence the outcome of the encapsulation process as well as the quality of the dried product (e.g., particle size or EE). These operational variables include the inlet and outlet air temperature, the feed temperature, the drying air mass flow rate, the feed mass flow rate and the type and speed of atomization (Santos et al., 2018). Among all, the inlet drying air temperature is considered the most important when it comes to the encapsulation of thermo-labile bioactive compounds (e.g., fish oil) and it is selected based on the components to be dried. Generally, high inlet drying temperatures are preferred since it is directly related to the drying rate and the final moisture content of the product. However, there are limitations. If the drying temperature is too high, it is more likely to obtain capsules with an irregular surface morphology due to the faster particle shrinkage produced during the early stage of drying. On the other hand, too low inlet drying air temperatures may lead to a high moisture content of the dried capsules causing agglomeration of the powder (Rahmani-Manglano, García-Moreno, et al., 2020).

1.4.2 Electrospraying

In the last decades, the development of electrohydrodynamic processes as non-thermal encapsulation technologies to produce dry omega-3 delivery systems has advanced significantly (García-Moreno et al., 2021). Electrohydrodynamic technology principle is based on applying a high-voltage electrostatic field between the tip of an emitter, from which the infeed solution flows, and a grounded collector, from which the dried product is collected. Hence, when the infeed solution flows through the electrified emitter, a meniscus of conical shape, referred to as the Taylor cone, is formed at its exit as consequence of mutual charge repulsion. When the electric force overcomes the surface tension of the infeed solution, a charged jet is ejected in the direction of the collector and, depending on the properties of the infused solution (e.g., viscoelasticity), thin fibers (i.e., electrospinning) or micro/nanocapsules (i.e., electrospraying) will be produced upon drying (Rahmani-Manglano, García-Moreno, et al., 2020). Since capsules are easier to disperse than fibers,

they are preferred for food fortification purposes (Jacobsen et al., 2018). Thus, the rest of the section will cover electrospraying technology applied to the production of fish oil-loaded capsules aimed as omega-3 delivery systems.

In conventional electrospraying (i.e., monoaxial electrospraying), the fish oil-loaded emulsion/dispersion is dried by means of the high-electrostatic field applied between the emitter and the collector. Provided the low viscoelasticity of the infeed emulsion/solution, the charged jet formed destabilizes due to varicose instability producing a spray of highly charged small droplets. Due to electrostatic repulsions, these charged droplets self-disperse on their way to the collector allowing solvent evaporation at room temperature and avoiding particles agglomeration after drying (García-Moreno et al., 2021). A schematic representation of the monoaxial electrospraying process is shown in Figure 3. Generally, the basic electrospraying set up consists of a high-voltage source (up to 30 kV), a syringe pump, an emitter and a collector.

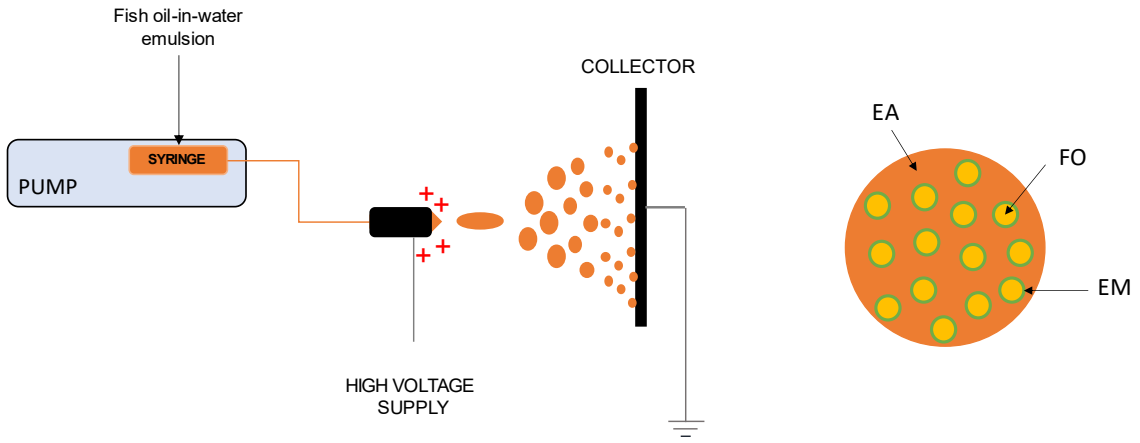

Figure 3. Schematic representation of monoaxial electrospraying process (left) and the oil distribution within the dry capsule (right). EA, encapsulating agent; FO, fish oil; EM, emulsifier.

The outcome of the electrospraying process (e.g., EE) and the physicochemical properties of the resulting capsules (e.g., particle size) are influenced by the infeed solution properties (e.g., viscosity, surface tension and conductivity) and by the operational parameters (e.g., voltage, flow rate and distance between emitter and collector) (García-Moreno et al., 2021). All these variables jointly affect the electrospraying process (i.e., the stability of the Taylor cone) thus, to ensure its reproducibility and to produce high quality encapsulates, all of them need to be optimized simultaneously. The solution properties are determined by the biopolymer type, the molecular weight, the hydrophobic/hydrophilic nature and the

concentration, as well as on the type of solvent. The processing variables include the emitter diameter, the temperature and the humidity nonetheless, the voltage applied, the infeed flow rate and the distance from the collector are regarded as the most significant. A deep discussion on the major influencing parameters, their relationship and their effect on the electrospraying process outcome can be found elsewhere (García-Moreno et al., 2021).

The main advantage of electrospraying technology over spray-drying is that heat is not required at any point of the process. Therefore, thermal degradation of thermo-sensitive bioactive compounds (e.g., fish oil) during processing is avoided. Electrospraying also allows the use of a wider variety of (bio)polymeric materials as encapsulating agents (e.g., hydrophobic proteins) compared to spray-drying using hot air as drying gas (García-Moreno et al., 2021). Furthermore, electrohydrodynamic atomization, contrary to mechanical atomization (e.g., spray-drying), produces a monodisperse distribution of smaller droplets which, after drying, results in smaller capsules with a narrower particle size distribution. This is preferred for food fortification applications since, compared to spray-dried capsules, the smaller capsules produced by electrospraying are expected to impact less the organoleptic properties of the enriched foodstuff (e.g., texture, mouth feel) and are also expected to be more bioaccessible. Nonetheless, it is important not to lose sight of the fact that smaller capsules might result in a lower oxidative stability of the encapsulated oil as a result of the increased contact area with environmental prooxidant species (e.g., oxygen), which will in turn affect the quality of the fortified food.

Coaxial electrospraying is also a promising alternative for the development of dry omega-3 delivery systems. Coaxial electrospraying modifies monoaxial electrospraying by introducing a coaxial emitter, consisting of two concentric needles, in the set up (Figure 4). Thus, two liquids can be electrosprayed simultaneously (Loscertales et al., 2002). In terms of encapsulation, the main difference between monoaxial electrospraying and coaxial electrospraying is that the former relies in the formation of an oil-in-water emulsion as feed to produce the oil-loaded capsules (i.e., emulsion-based methods), whilst by coaxial electrospraying a core/shell structure is achieved by physical separation of the core and shell solutions (Rahmani-Manglano, García-Moreno, et al., 2020). Through the inner needle of the emitter flows the core solution containing the bioactive compound (e.g., omega-3 PUFAs) and through the annular gap, between the inner and the outer needle, flows the shell solution containing the wall material. As a result, omega-3-loaded capsules can be produced by coaxial electrospraying without the need of first emulsifying or dispersing the fish oil

within the (bio)polymer-based encapsulating solution. This is particularly interesting for the development of fish oil-loaded capsules since it has been demonstrated that lipid oxidation already occurs during the homogenization step as a result of the intense mechanical stress exerted (i.e., air inclusion and distribution of prooxidant species within the liquid system) (Serfert et al., 2009). Therefore, by coaxial electrospraying, initial lipid oxidation due to processing could not be only prevented (e.g., drying occurs at ambient temperature), but could be even theoretically avoided (e.g., might not require previous homogenization) is the process is efficiently designed.

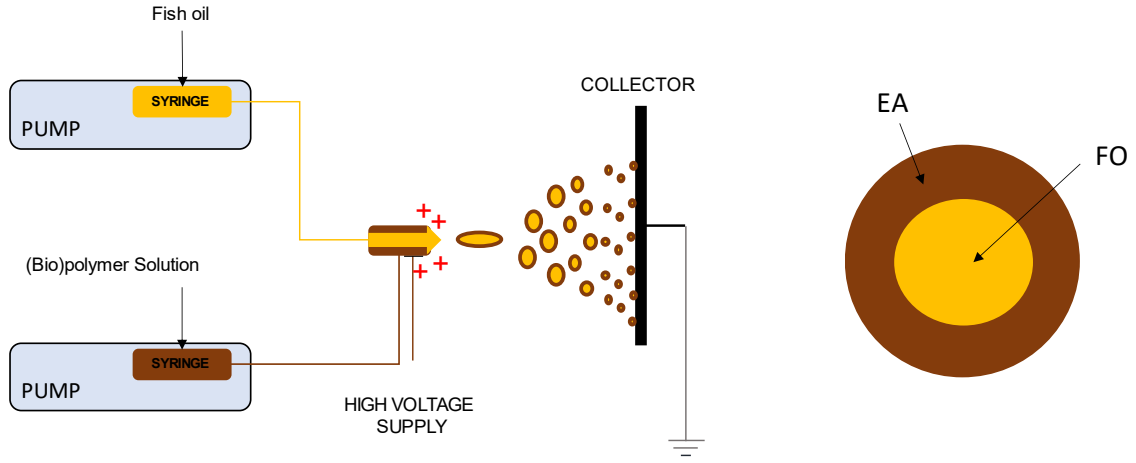

Figure 4. Schematic representation of coaxial electrospraying process (left) and the oil distribution within the dry capsule (right). EA, encapsulating agent; FO, fish oil.

Another advantage of coaxial electrospraying over emulsion-based encapsulation methods (e.g., spray-drying and monoaxial electrospraying) is that a centralized distribution of the fish oil can be achieved. The latter not only allows to produce capsules with higher load capacity, higher encapsulation efficiency or tunable wall-thickness (Jaworek, 2016), but also may result in an enhanced oxidative stability of the encapsulated fish oil. Emulsion-based encapsulation methods, such as monoaxial electrospraying, lead to a random distribution of the fish oil droplets within the encapsulating matrix which favors the presence of easily accessible surface oil (Figure 3, right). On the contrary, by optimal coaxial electrospraying, the fish oil is located as one single droplet at the core of the encapsulating matrix (Figure 4, right), thus presumably being better protected.

Over the last decade, research on the production of omega-3 delivery systems by electrospraying technology has been initiated, resulting in promising outcomes. These studies are summarized in Chapter I.

1.4.3 Electrospraying Assisted by Pressurized Gas

Overall, electrospraying technology presents multiple advantages over spray-drying when it comes to the production of fish oil-loaded capsules aimed as omega-3 delivery systems. However, its industrial use is restrained due to the low productivity of the process. To overcome this situation, Busolo et al. (2019) have recently developed a novel technology termed as "Electrospraying Assisted by Pressurized Gas".

Electrospraying Assisted by Pressurized Gas (EAPG) is an advanced high-throughput technology which is based on the combination of electrospraying and pneumatic atomization. By EAPG, the infeed emulsion/solution is mechanically atomized by a pneumatic injector within a high electric field. As a result of the high voltage applied, the liquid droplets are further disrupted allowing, again, solvent evaporation at room temperature. After drying, the capsules are collected as free-flowing powder in the collector. The basic EAPG set up consists of an injection unit, in where the atomized droplets are subjected to a high electric field, a drying camber and cyclone (Figure 5). Nowadays, this technology is available at an industrial scale (Lagaron et al., 2017).

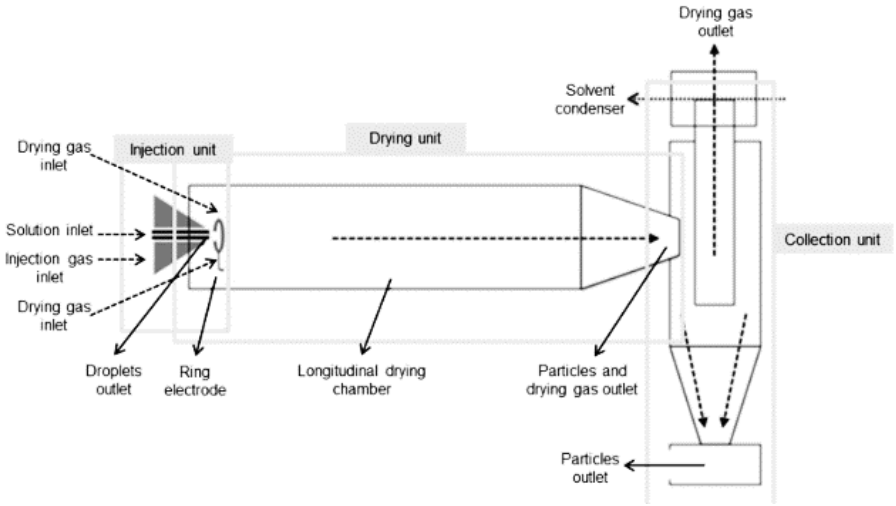

Figure 5. Schematic representation of EAPG equipment (Prieto et al., 2021).

As conventional electrospraying, EAPG technology is a versatile encapsulation technique that allows to produce encapsulated systems using matrix components of different nature (e.g., hydrophilic carbohydrates or hydrophobic proteins) (Rahmani-Manglano, García-Moreno, et al., 2020). Furthermore, capsules can be produced by coaxial EAPG by simply changing the configuration of the atomizer (i.e., coaxial nebulizer).

To date, EAPG has been demonstrated to be a promising technology to produce fish oil-loaded capsules (García-Moreno et al., 2018; Hermund et al., 2019; Miguel et al., 2019), although the physicochemical properties of the obtained capsules and the capsule-fortified fortified food matrices (e.g., mayonnaise) (Hermund et al., 2019; Miguel et al., 2019) require further improvement.

1.4.4 Additional chemical stabilization by addition of antioxidants

Although the main goal of encapsulation technologies (e.g., spray-drying or electrospraying) is to protect the encapsulated fish oil from oxidative degradation, it has been demonstrated that the onset of lipid oxidation already occurs in the early stages of processing (i.e., emulsification process). For instance, in the emulsification step, which consist in the production of a coarse emulsion followed by homogenization, the intense mechanical stress exerted results in the inclusion and distribution of prooxidants species (e.g., oxygen, metal traces) within the system. Furthermore, in most cases, the production of the infeed emulsion is accompanied by a significant temperature increase. On the other hand, in spray-drying technology, air at high temperature (e.g., ranging from ~200 °C to ~80 °C as the inlet and outlet air temperature, respectively) is used for drying which can further oxidize the fish oil, especially if the process is not efficiently design (i.e., low EE and long residence time of the capsules in the drying chamber). Additionally, lipid oxidation of the encapsulated fish oil after processing still occurs. It has been demonstrated that prooxidant species, particularly oxygen, can diffuse through the glassy encapsulating matrix triggering lipid oxidation of the embedded oil droplets (A. B. Andersen et al., 2000; Boerekamp et al., 2019; Drusch et al., 2009; Orlien et al., 2000). Indeed, it has been extensively reported in the literature that the key factor influencing the oxidative stability of oil-loaded encapsulated systems is the oxygen diffusivity through the encapsulating wall (Boerekamp et al., 2019; Drusch et al., 2009; Linke, Hinrichs, et al., 2020; Linke, Linke, et al., 2020; Linke, Weiss, et al., 2020; Rahmani-Manglano et al., 2023; Velasco et al., 2006). Therefore, to minimize lipid oxidation during processing and to enhance the oxidative stability of the encapsulated fish oil during storage, additional chemical stabilization by addition of antioxidants is required.

The addition of antioxidants of different nature (e.g., polar, non-polar) and mechanisms of action (e.g., radical scavengers, metal chelator) to fish oil-loaded capsules produced by spray-drying or electrospraying and their influence on the oxidative stability of the encapsulated system has been investigated by several authors (Rahmani-Manglano, García-Moreno, et al., 2020). Among these studies, one of the most relevant was carried out by

Serfert et al. (2009) who systematically investigated the impact of different antioxidant combinations on the oxidative stability of fish oil during the spray-drying processing stages (i.e., emulsification and drying) and later storage. The main finding of the study was that the optimal combination of antioxidants depended on the spray-drying processing step, that is the nature of the heterogeneous system (i.e., wet multiphase system consisting of emulsified fish oil or dry multiphase system consisting of encapsulated fish oil). According to these authors, an efficient stabilization of the encapsulated fish oil during storage was achieved combining rosemary extract (rich in carnosic acid) with a ternary blend of antioxidants consisting of lipophilic antioxidants (i.e., mixed tocopherols), synergistic compounds (i.e., ascorbyl palmitate) and a metal chelator (i.e., lecithin) (Serfert et al., 2009).

It is well known that the antioxidant effectiveness is determined by the chemical structure, although other factors also have an effect on the overall antioxidant activity (e.g., concentration, temperature or presence of synergistic/antagonistic species) (Shahidi & Zhong, 2011). In particular, the partition of the antioxidant in the medium based on its polarity (e.g., hydrophilic, lipophilic or amphiphilic) is regarded as one of the most significant factors influencing the antioxidant activity. In wet oil-in-water emulsions, it is generally assumed that antioxidants with a tendency to accumulate at the O/W interface are more effective preventing lipid oxidation since this microenvironment is the place where lipid oxidation is initiated (i.e., area of contact between the prooxidants and the oil) (Berton-Carabin et al., 2014). Based on the latter, the use of ingredients which exhibit both emulsifying and antioxidant activity (e.g., radical scavenging) has gained great interest as an efficient strategy to prevent lipid oxidation in wet/dry heterogeneous systems (i.e., fish oil-in-water emulsion or fish oil-loaded capsules). It is hypothesized that these ingredients would theoretically improve the oxidative stability of the emulsified, and subsequently encapsulated fish oil by inhibiting lipid oxidation at the oil/water and subsequently oil/matrix interface. Thus, stabilizing the fish oil during processing and later storage. In this regard, the use of protein hydrolysates seems to be an interesting alternative. Depending on the proteolysis conditions (e.g., type of enzyme, temperature, pH, time), protein hydrolysates show enhanced functional properties (e.g., emulsifying and antioxidant activity) with respect to the native protein (Liceaga & Hall, 2018; Peighambardoust et al., 2021). That is because the conformational changes induced during hydrolysis favors: i) the exposure of hydrophobic groups that contribute to the improved emulsifying activity and ii) the exposure of amino acid residues capable of inhibiting lipid oxidation through different mechanisms of

action (e.g., radical scavenging and/or metal chelation) (Elias et al., 2008; Liceaga & Hall, 2018; Peighambardoust et al., 2021). Furthermore, the rather small peptides produced as a result of protein hydrolysis could act as co-polymers or filler of the encapsulating wall, thus enhancing its protective effect. Hence, protein hydrolysates could improve the oxidative stability of the encapsulated fish oil, not only by chemical, but by physical means (Rahmani-Manglano, García-Moreno, et al., 2020).

1.5 Digestion and bioaccessibility of dry omega-3 delivery systems

Traditionally, the research efforts carried out in the field of omega-3 PUFAs encapsulation has been the development of oxidatively stable delivery systems during the processing chain, from the production and storage of the bioactive-loaded capsules, to the production and storage of the enriched food matrix. However, recent trends include the understanding of the stability, digestion and absorption of these bioactive lipids throughout the gastrointestinal tract (GIT).

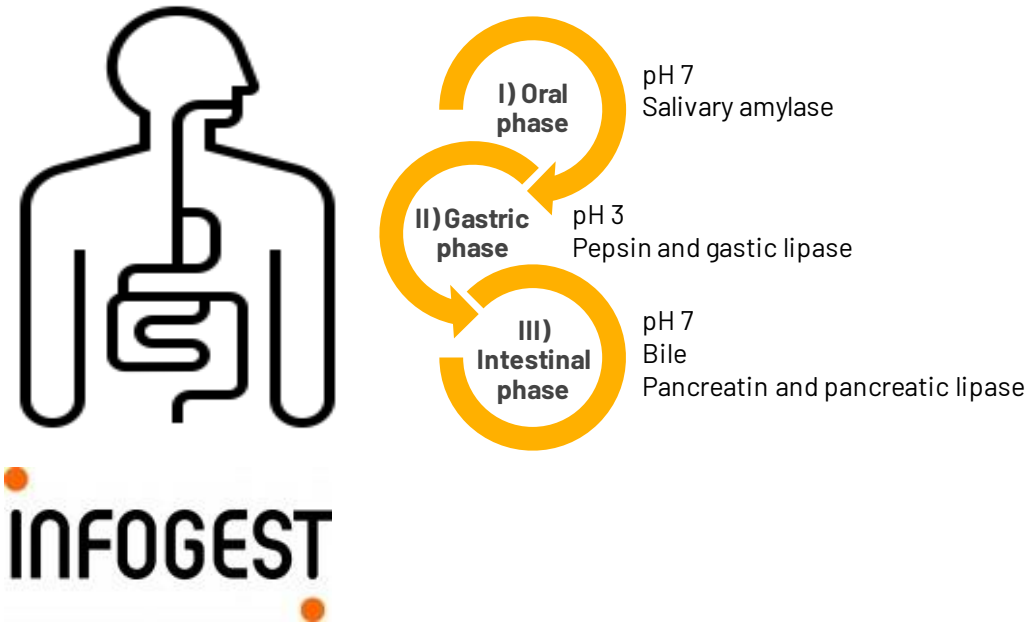

Figure 6. Schematic representation of the gastrointestinal tract (GIT) and the main phases of digestion.

Overall, food digestion is a complex process involving a number of steps in which the enzymes activity and the physicochemical properties of the food matrix play a major role (Acevedo-Fani et al., 2021). Digestion can be divided into three main phases: I) oral phase, II) gastric phase and III) intestinal phase, as shown in Figure 6 (Brodkorb et al., 2019). In the mouth, the mechanical action of chewing mixes the food with saliva to form a bolus

which is safe to swallow and suitable for further digestion. Then, the bolus moves into the stomach, where the gastric phase of digestion takes place. In this stage, proteins are fully or partially digested by action of pepsin, whilst gastric lipolysis only account to up 10 - 30% of the total lipolysis extent (Acevedo-Fani et al., 2021). Afterwards, the so-called chyme formed in the stomach enters the intestinal phase of digestion. The small intestine is the main site of digestion as it is where the conversion of nutrients into a bioaccessible form occurs. Thus, by action of the pancreatic secretions (e.g., proteases, peptidases, amylases and lipases), the protein and peptides, the carbohydrates and the lipids are converted into their respective absorbable monomeric forms. In regard to lipid digestion, it involves the interaction of the oil with bile salts and lipases.

Lipid digestion is an interfacial process since the bile salts and lipases must adsorb onto the O/W interface to catalyze lipid hydrolysis. Therefore, taking this into account, it is safe to assume that the oil droplets size, the oil droplets aggregation state and the interfacial properties will significantly influence the bioaccessibility of omega-3 PUFAs, particularly at the beginning of the intestinal phase of digestion (McClements, 2018).

Depending on the ingredients used to produce the omega-3 delivery system (i.e., the combination of emulsifier and/or encapsulating agent), the bioaccessibility of encapsulated fish oil can be lowered or enhanced (Acevedo-Fani et al., 2021). For instance, highly surface-active emulsifiers may limit the lypolisys extent by restraining the adsorption of bile salts onto the O/W interface. Besides, emulsifiers also affect the droplets aggregation state by preventing or promoting oil droplets flocculation and/or coalescence, therefore influencing the surface area available for lipid digestion (McClements, 2018). On the other hand, depending on their molecular and physicochemical properties, carbohydrates used as encapsulating agents can also impact lipid digestion through different mechanisms (Chang & McClements, 2016). Some carbohydrates: i) may adsorb onto the O/W interface, ii) may influence the droplets aggregation state or iii) may increase the viscosity of the continuous phase limiting the free flow of the digestive components (e.g., digestive enzymes and lipolysis products), among others. Likewise, the food matrix also plays a major role on the lypolisys rate and extent of encapsulated omega-3 PUFAs (Shen et al., 2011). The food structure (e.g., liquid, semi-solid or solid) is the main factor dominating lipid digestion as it can prevent the diffusion of the digestive components (i.e., bile salts and lipase) to the surface of the oil droplets (Acevedo-Fani et al., 2021). Furthermore, the type and content of the rest of the food ingredients also affects lipid hydrolysis as they can also influence the surface

area available for interfacial reactions (i.e., influencing the droplets size and aggregation state) (Shen et al., 2011).

1.6 Food enrichment with dry omega-3 delivery systems

Fish oil-loaded capsules produced either by spray-drying or EAPG have been used as omega-3 delivery systems into a wide variety of food products to investigate their influence on the physical, oxidative and/or sensory stability. These food matrices include dairy products (e.g., powdered or fermented milk) (Busolo et al., 2019; Patrick et al., 2013), baked products (e.g., bread and cookies) (Davidov-Pardo et al., 2008; Jeyakumari et al., 2016), spreads (e.g., dry-cured ham and cheese spreads) (Solomando, Antequera, González-Mohíno, et al., 2020), dressings (e.g., mayonnaise) (Hermund et al., 2019; Miguel et al., 2019; Rahmani-Manglano, González-Sánchez, et al., 2020) and meat products (e.g., sausages and burgers) (Aquilani et al., 2018; Solomando, Antequera, & Perez-Palacios, 2020).

Patrick et al. (2013) successfully enriched fermented milk with monolayered (i.e., single-shell) or multilayered (e.g., double-shell) fish oil-loaded capsules produced by spray-drying. After 28 days of storage, the fortified milk showed good sensory markers (i.e., ~6/7) irrespective of the fortification approach. Unfortunately, the oxidative stability of the enriched matrices was not evaluated. Likewise, Busolo et al. (2019) used fish oil-loaded capsules produced by EAPG within a zein-based encapsulating matrix to fortify powdered milk. After 45 days of storage, the authors found little differences between the good sensory attributes of the capsule-fortified milk compared to the control milk (i.e., without fish oil), contrary to the sample fortified with neat fish oil. This was attributed to the high EE (EE = 84%) achieved during the encapsulation process. However, the oxidative stability of the fortified food matrix was again not evaluated in this study. Regarding baked products, Davidov-Pardo et al. (2008) evaluated the physical (e.g., dough and bread texture) and organoleptic properties (e.g., fishy flavor) of fortified bread samples after enrichment with fish oil-loaded capsules produced by spray-drying within different encapsulating walls (i.e., methyl cellulose, whey protein concentrate or calcium-gelatin casein). The authors concluded that bread fortification with methyl cellulose-based capsules was an efficient strategy since this omega-3 delivery system impacted less the physical and sensory attributes of the enriched food matrix. In this line, Jeyakumari et al. (2016) investigated the influence of the encapsulating wall (i.e., fish gelatin) and the fortification approach (i.e., neat fish oil, emulsified fish oil and spray-dried encapsulated fish oil) on the oxidative stability of

enriched cookies. After 6 months of storage, the capsules-fortified cookies were the less oxidized compared to the emulsion- or neat fish oil-enriched samples, although only the maltodextrin-based capsules received a sensory evaluation score similar to that of the control cookies (i.e., without fish oil). Solomando, Antequera, González-Mohíno, et al. (2020) evaluated the physical (i.e., color), oxidative (i.e., TBAR and FFA content) and sensory stability of cheese and meat spreads fortified with spray-dried fish oil-loaded capsules after food processing and after 4 months of storage. The oxidative stability of both fortified food matrices (i.e., cheese and meat spreads) was similar after food enrichment and subsequent storage. Nonetheless, the EPA and DHA content decreased significantly after storage for the capsule-fortified cheese spread, as well as sensory attributes, contrary to the capsule-fortified meat spread which showed good oxidative and sensory stability. Moving on to the dressings, Hermund et al. (2019) enriched mayonnaise with fish oil-loaded capsules produced by EAPG in presence or absence of commercial antioxidants (i.e., δ-tocopherol and rosemary extract). Glucose syrup was used as the encapsulating agent. The authors reported a low physical and oxidative stability of the capsules-fortified mayonnaise samples (i.e., with and without antioxidants) compared to the mayonnaise fortified with neat fish oil. This was attributed to the disintegration of the water-soluble encapsulating wall during food processing and storage which caused the release of fish oil with a poorer oxidative status. Furthermore, the addition of commercial antioxidants did not exert any protective effect in the presence of iron released from egg yolk due to the lack of metal chelating activity. Conversely, Rahmani-Manglano, González-Sánchez, et al. (2020) produced a physically and oxidatively stable fortified mayonnaise using spray-dried fish oil-loaded capsules within a glucose syrup-based encapsulating wall. Whey protein concentrate hydrolysate (WPCH), exhibiting high antioxidant activity (e.g., radical scavenger and metal chelating), was used as film-forming material. The results reported by these authors suggested that the physical integrity of the encapsulating wall was retained during the optimized fortification processing, which correlated well with the physical stability markers monitored during storage (e.g., droplet size and viscosity). Likewise, the higher oxidative stability reported for the capsule-fortified mayonnaise compared to the emulsified- or neat fish oil-fortified samples was attributed to the protecting effect of the encapsulating wall. In this line, Miguel et al. (2019) produced a fortified mayonnaise with fish oil-loaded capsules produced by EAPG within a zein-based encapsulating wall with high physical and oxidative stability. This finding was attributed to the hydrophobic nature of the encapsulating wall which was able to retain its physical integrity during food processing and storage, as confirmed by the

Cryo-SEM images and the physical stability markers (e.g., droplet size and viscosity). In addition, the capsule-fortified salad dressing showed a lower PV after storage compared to the mayonnaise sample fortified with neat fish oil and, although the content of some selected SVOPs was higher for the capsule-enriched sample, this was attributed either: i) to the volatile compounds already present in the zein protein (e.g., hexanal, 3-methyl-butanal or nonanal) or ii) to fungal spoilage of the fortified food matrix (e.g., 3-methyl-1-butanol). Finally, the performance of fish oil-loaded capsules as omega-3 delivery systems in meat products has been also investigated. Aquilani et al. (2018) evaluated the effect of the fortification approach (i.e., neat fish oil or spray-dried fish oil-loaded capsules) and the storage conditions (i.e., no storage, refrigerated storage or frozen storage) on the physicochemical properties of raw and cooked burgers. After storage and cooking, the samples fortified with neat fish oil showed the lowest content of EPA and DHA and the higher TBAR value. On the contrary, the capsules-fortified burger showed similar results compared to the control sample without fish oil. Furthermore, among the refrigerated samples, the capsule-fortified burger presented better quality attributes than the control and the neat fish oil-fortified burger. In this line, Solomando, Antequera, & Pérez-Palacios (2020) also reported that the use of fish oil-loaded capsules produced by spray-drying was suitable to produce enriched dry-cured or cooked sausages without influencing their physical and oxidative stability, the organoleptic properties or the usual changes that take place during food processing (i.e., dry-curing processing or heating).

Taken altogether, the scientific evidence collected to date points out that fish oil encapsulation either by spray-drying or electrospraying is a promising approach to produce a wide range of omega-3 fortified food products. Unfortunately, none of the aforementioned studies investigated how the encapsulation technology (i.e., spray-drying or EAPG) or the fish oil load of the capsules affect the physicochemical stability of the enriched food matrix. The latter is of outmost importance in order to understand the relationship between lipid oxidation of the enriched food product and the properties of the fish oil-loaded capsules used for its enrichment.

2. OBJECTIVES

The objective of this Ph.D. Thesis was to investigate the production process and subsequently characterization and bioaccessibility of fish oil-loaded capsules aimed as omega-3 delivery systems. Both conventional thermal encapsulation techniques, such as spray-drying, and novel electrohydrodynamic techniques, such as monoaxial and coaxial electrospraying, were evaluated. To this end, the research carried out was divided into the following specific goals:

1. Study of the state of the art of omega-3 PUFAs stabilization techniques including chemical means (i.e., addition of antioxidants), physical means (i.e., conventional and novel encapsulation technologies), combined means (i.e., encapsulation in presence of antioxidants) and food enrichment (**Chapter I**).

2. Evaluation of the influence of the encapsulation technology on the physicochemical properties of fish oil-loaded capsules

   2.1 Physicochemical properties of fish oil-loaded capsules produced by spray-drying: influence of the formulation and scale-up, addition of natural antioxidants of different polarity and oil load (**Chapters II, III, VII and VIII**).

   2.2 Physicochemical properties of fish oil-loaded capsules produced by electrospraying: influence of the formulation and scale-up and oil load (**Chapters II and VIII**).

   2.3 Comparison between the physicochemical properties of spray-dried and electrosprayed capsules: evaluation of the oxygen permeability and the secondary structure of the whey protein hydrolysate used as emulsifier (**Chapters IV and V**).

3. Investigation of the influence of the formulation on the bioaccessibility of dry omega-3 delivery systems (**Chapter VI**).

4. Study of food fortification with omega-3 delivery systems: influence of the delivery system as well as of the encapsulation technology and the oil load on the physical and oxidative stability of fortified food matrices (**Chapters VII and VIII**).

3. MATERIALS AND METHODS

In this section, the main materials and the methodology used to produce and characterize the omega-3 delivery systems and the fortified food matrices are briefly described.

For further details, please refer to the respective Chapters as specified in the text and in Table 1.

3.1 Materials

Refined fish oil under the commercial name of Omega Oil 1812 TG Gold (18% EPA and 12% DHA), and provided by BASF Personal Care and Nutrition GmbH (Illertissen, Germany), was used as the omega-3 PUFAs source. Glucose syrup (GS; DE38, C*Dry GL 01934, Cargill Germany GmbH) or maltodextrin (MD; DE21, Abbott Laboratories) were used as the main encapsulating agents due their extended use in the production of fish oil-loaded capsules by spray-drying aimed for food fortification purposes. Pullulan (Hayashibara Co., Ltd., Okayama, Japan; molecular weight = 200kDa) was used as thickening agent for lab-scale electrospraying purposes to increase the viscoelasticity of the infeed emulsions and solutions, as previously reported by other authors (García-Moreno et al., 2018). Whey protein concentrate hydrolysate (WPCH), produced by enzymatic hydrolysis as described in Chapter VII, was used as the emulsifier. The performance of WPCH as emulsifying agent was compared to the commercial low molecular weight surfactant, Tween 20 (T20), purchased from by Sigma-Aldrich (T20; Darmstadt, Germany). In this Ph.D. Thesis, the use of commercial antioxidants was also evaluated. These antioxidants consisted of rosemary-based extracts and were provided by Kalsec Inc. The commercial name is as follows: Herbalox® HT-P, Herbalox® XT-O and Duralox® MAN-5.

3.2 Methodology

For the emulsion-based encapsulation methods (i.e., spray-drying and monoaxial electrospraying), fish oil-in-water emulsions were fed to the respective driers. The emulsions were produced by first dispersing the fish oil within the aqueous phase containing the encapsulating agent and the emulsifier (Ultraturrax T-25 homogenizer; IKA, Staufen, Germany). Then, the coarse emulsion was homogenized using a high-pressure homogenizer (HPH) (PandaPLUS 2000; GEA Niro Soavi, Lübeck, Germany). For coaxial

electrospraying, neat fish oil was infused as the core solution, whilst the outer solution consisted of a water-based solution containing the encapsulating agent/s dissolved. Further details on the equipment used to produce the respective fish oil-in-water emulsions and solutions and the operating conditions can be found in Chapters II-VIII.

First, the capsules were produced at lab-scale and then the process was scaled-up to pilot-pant scale. On the lab-scale, spray-drying was carried out in a Büchi B-190 spray-drier (Büchi Labortechnik, Flawill, Switzerland) at the optimized drying conditions specified in Chapters II, IV, V and VI. Electrospraying was carried out in the so-called SpinBox Electrospinning equipment developed by Bioinicia S.L. (Valencia, Spain). The operating conditions are reported in Chapters II, IV and V. On the pilot plant scale, spray-drying was conducted on a Mobile Minor spray-drier (Niro A/S, Copenhagen, Denmark) as specified in Chapters III, VII and VIII. Finally, EAPG was carried out using the pilot plant equipment Capsultek^{TM} from Bioinicia S.L. (Valencia, Spain) at the operating conditions described in Chapter VIII.

Table 1. Methodology used in the Ph.D. Thesis

Method	Description	Chapter
Enzymatic hydrolysis	Enzymatic hydrolysis of whey protein concentrate (WPC) in an automatic titrator 718 Stat Titrino using the pH-stat-method	VII
Oil droplet size	Measurement of the oil droplet size of: i) the parent emulsions, ii) the reconstituted emulsions and iii) the food matrices by laser diffraction	II, III, VI, VII, VIII
Zeta potential	Measurement of the surface charge of the fish oil droplets using a Zetasizer Ultra	VI
Microstructure	- Microstructure of the fish oil droplets determined by confocal scanning laser microscopy	VI
	- Microstructure of the fish oil-loaded capsules determined by scanning electron microscopy. The particle size was determined by the software Image J	II, III, IV, VI, VII, VIII
Load Capacity, Encapsulation Efficiency and Surface Fat (LC, EE and SF)	Extraction of the total oil and the surface oil with organic solvents. The LC, EE and/or SF were determined by: - Gravimetric method: weight difference before and after solvent evaporation	III, VI, VII
	- Spectrophotometric method: measurement of the absorbance of the oil-containing filtrate	II, VI, VIII
Synchrotron Radiation Circular Dichroism (SRCD)	Determination of the secondary structure of the native protein and the protein hydrolysate by SRCD carried out on the AU-CD beamline at the ASTRID2 synchrotron radiation source	V

Table 1. Methodology used in the Ph.D. Thesis (continued)

Method	Description	Chapter
In vitro digestion	INFOGEST pH-stat method for simulated digestion	VI
Apparent viscosity	Measurement of the apparent viscosity of the food matrices using a stress-controlled rheometer	VII, VIII
Color	Measurement of the color of the food matrices using a colorimeter	VIII
Peroxide value (PV)	Measurement of the peroxide value of the fish oil-containing lipid extracts using the colorimetric ferric-thiocyanate method	III, VII, VIII
Anisidine value (AV)	Measurement of the AV of the fish oil-containing lipid extracts according to the ISO 6885:2006 method	VII
Tocopherol content (TC)	Measurement of the tocopherol content of the fish oil-containing lipid extracts according to the American Oil Chemists' Society (AOCS) official method	VII, VIII
Secondary volatile oxidation products (SVOPs)	Measurement of the content of selected SVOPs by Gas Chromatography - Mass Spectroscopy (GC/MS). The volatile compounds were extracted from the samples by:	
	- Static headspace solid-phase microextraction into a SPME fiber	III
	- Dynamic headspace purge & trap into Tenax GR tubes	II, VII, VIII
Fourier transformed infrared spectra (FT-IR)	Recording of the FT-IR spectra of: i) the raw ingredients in the attenuated total reflection mode (ATR-FTIR) and ii) the fish oil-loaded capsules in the transmission mode (FT-IR) by infrared spectroscopy	II
Electron Spin Resonance (ESR)	Determination of the oxidative stability and oxygen permeability of oil-loaded capsules by ESR spin trapping and ESR-oximetry, respectively. The ESR spectra were recorded using a MiniScope MS5000	IV

The basic principles of the main methodologies used in the Ph.D. Thesis are described below.

3.2.1 Synchrotron Radiation Circular Dichroism

Synchrotron Radiation Circular Dichroism (SRCD) technique was used to quantitatively evaluate the secondary structure of the native protein (i.e., whey protein concentrate) and the protein hydrolysate (i.e., whey protein concentrate hydrolysate) in solution or adsorbed at O/W interface. This technique, as conventional circular dichroism (CD), measures the differential absorption of left- and right-handed circularly polarized light by a chiral sample (Wallace & Janes, 2001). Therefore, when the circularly polarized light passes through the

sample, the resulting spectrum is recorded as a function of wavelength (Figure 7). Proteins and peptides are chiral molecules due to the intrinsic chirality of its constituents, that is amino acids. Thus, although the peptide bond is not a strong chromophore itself, its abundance in proteins and peptides results in a high absorption in the far UV range (Hoffmann et al., 2016).

In SRCD, a synchrotron radiation source generates a higher flux of light compared to conventional CD which allows to reduce the signal-to-noise ratio, especially at the vacuum ultraviolet (VUV) wavelength region (<190 nm). This is particularly interesting for samples where light scattering is high (e.g., oil-in-water emulsions). Furthermore, in case of protein samples, the secondary structural changes are recorded mostly in the far-UV spectrum (91 – 200nm), thus SRCD allows a better and more accurate determination of secondary structure (Wallace & Janes, 2001). Further details on the equipment, measurement conditions and sample preparation can be found in Chapter V.

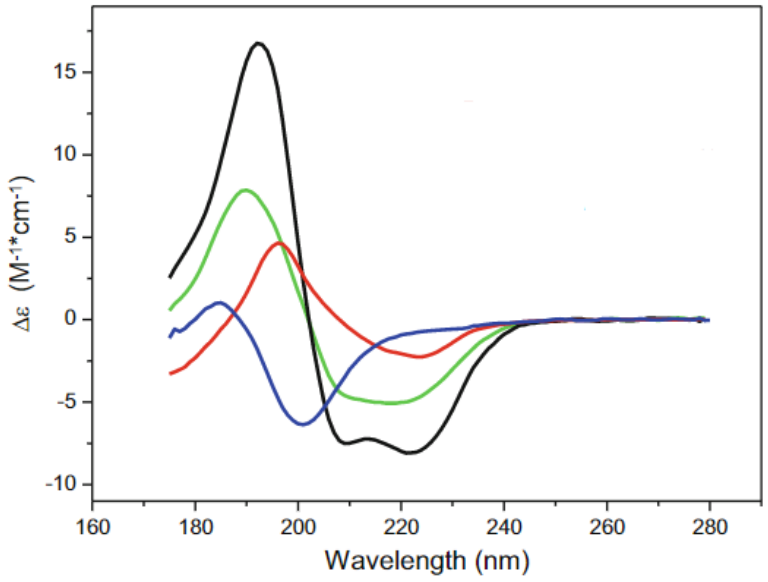

Figure 7. Examples of far UV CD spectra of proteins with high content of α-helix (black), β-strand (red), α/β protein (green) and a protein with a high content of irregular structure (blue) (Hoffmann et al., 2016).

3.2.2 Secondary volatile oxidation products (SVOPs)

The content of secondary volatile oxidation products (SVOPs) was determined by Gas Chromatography (GC) – Mass Spectrometry (MS) (GC/MS), which is based on the combination of the features of GC and MS to separate and then identify different substances within a sample. Therefore, unlike other methods used for the determination of secondary oxidation products (e.g., anisidine value), GS/MS is a specific method suitable to identify

and quantify SVOPs in complex matrices (Thomsen et al., 2016). In GC/MS, the collection of the volatile compounds released from the sample before injection in the equipment is required and, depending on the collection method, the GC/MS results can vary significantly. Static headspace solid-phase microextraction (SPME) and dynamic headspace purge & trap (DHS – P&T) are the most common collection methods (Figure 8) (Jacobsen et al., 2021).

(A) **(B)**

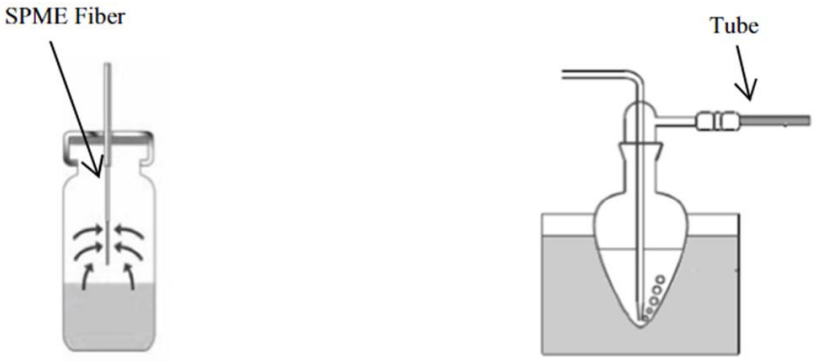

Figure 8. Schematic representation of the SPME (A) and DHS – P&T (B) collection methods (Thomsen et al., 2016).

In SPME (Figure 8A), the sample is incubated in a closed vial at a certain temperature until the equilibrium of the SVOPs between the headspace and the sample is reached. Then, the SPME fiber is introduced into the headspace to extract and adsorb the compounds, typically under stirring conditions. On the contrary, by DHS – P&T (Figure 8B), the volatile compounds are released from the incubating sample by purging through it with an inert gas (e.g., nitrogen). While purging, the released compounds are adsorbed on a thermal desorption tube containing an adsorbing material (e.g., Tenax®) (Thomsen et al., 2016). DHS – P&T is more sensitive and allows to identify more compounds than SPME because the equilibrium between the volatile compounds in the sample and in the headspace is continuously disturbed during the collection method by the purging gas. Furthermore, SPME fibers differ from batch to batch which can be problematic if the fiber breaks in the middle or at the end of the analysis (Jacobsen et al., 2021). In this Ph.D. Thesis the SVOPs were collected from the samples before analysis either by SPME or DHS – P&T. For further details on the equipment used, measurement conditions and sample preparation, please refer to Chapter III or to Chapters II, VII and VII, respectively.

3.2.3 Fourier transformed infrared spectroscopy (FT-IR)

Fourier transformed infrared spectroscopy (FT-IR) has been proven to be a suitable tool to monitor lipid oxidation in neat edible oils (Guillén & Cabo, 1999, 2000) and in encapsulated systems (Prieto & Lagaron, 2020; Unnikrishnan et al., 2019). This method relies on the distinctive vibrational mode of the different functional groups present in an organic compound, which allows its determination in the resulting spectrum (Guillén & Cabo, 1999). By this technique, quantitative analysis is also possible as the band intensity of the spectrum is proportional to the concentration of the functional group in the sample (Guillén & Cabo, 1999). In case of omega-3 PUFAs, lipid oxidation can be investigated by monitoring the absorption band corresponding to the stretching of cis-alkene groups (–HC=CH–, at 3012 cm^{-1}, Figure 9) since the decrease in the intensity of this band implies the loss of cis double bonds (García-Moreno et al., 2018). In the current Ph.D. Thesis, the FT-IR spectra of the fish oil-loaded capsules over storage was recorded in the transmission mode (IR) which allowed to significantly decrease the amount of sample required for the analysis (i.e., 1.5 mg of powder per replicate). Further details on the equipment, measurement conditions and sample preparation can be found in Chapter II.

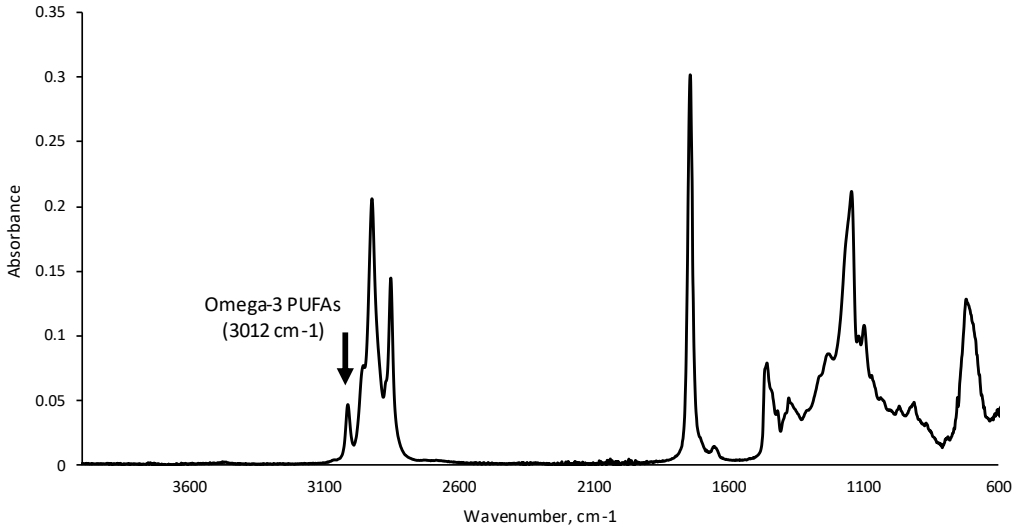

Figure 9. ATR-FTIR spectra of the fish oil used in the Ph.D. Thesis.

3.2.4 Electron Spin Resonance (ESR)

Electron Spin Resonance (ESR), also referred as Electron Paramagnetic Resonance (EPR), is the main spectroscopic method for detection of radicals (M. L. Andersen, 2021). This technique is based on the detection of the absorption of electromagnetic radiation when the unpaired electrons of a paramagnetic material transitions between specific energy levels in

the presence of a strong magnetic field (M. L. Andersen, 2021). These energy levels are quantized, meaning that are specific and that can only take on certain discrete values which are in turn determined by the angular momentum (i.e., spin) of the unpaired electrons. Generally, the ESR spectra are recorded by keeping constant the electromagnetic radiation frequency and scanning the magnetic field. A peak in the absorption will occur when the magnetic field tunes the two spin states so that their energy difference matches the energy of the radiation. In turn, paramagnetic nuclei can interact with the unpaired electrons causing the splitting of the observed ESR lines in what is known as "hyperfine coupling" or "hyperfine interactions". Based on the ESR-spectra splitting patterns and the hyperfine coupling constant, important information about the sample can be obtained (e.g., the structure of the radicals) (M. L. Andersen & Skibsted, 2018). ESR technique has been extensively used to monitor lipid oxidation of omega-3 PUFAs (i.e., ESR-spin trapping) as well as the oxygen permeability (i.e., ESR-oximetry) of foods and oil-loaded systems (M. L. Andersen, 2021; M. L. Andersen & Skibsted, 2018; Zhou et al., 2011). In brief, ESR-spin trapping consists in the indirect measurement of the highly reactive lipid-derived radicals (e.g., alkyl radicals) through the formation of stable and detectable radicals (spin adducts) (Figure 10). Thus, it is generally assumed that the higher level of radicals detected by ESR (related to the peak-to-peak high of the central line of the spectrum), the higher the oxidation extent. On the other hand, ESR-oximetry is based on the broadening of the ESR spectra of stable radicals (i.e., paramagnetic spin probes) in the presence of oxygen, which is a paramagnetic substance itself. The line broadening of the spin probe-ESR spectra is proportional to the concentration of oxygen which allows to evaluate the oxygen permeability of a given system and quantification of the oxygen concentration through calibration curves (Figure 11). For further details on the ESR technique, the equipment used, the measurement conditions and the sample preparation, please refer to Chapter IV.

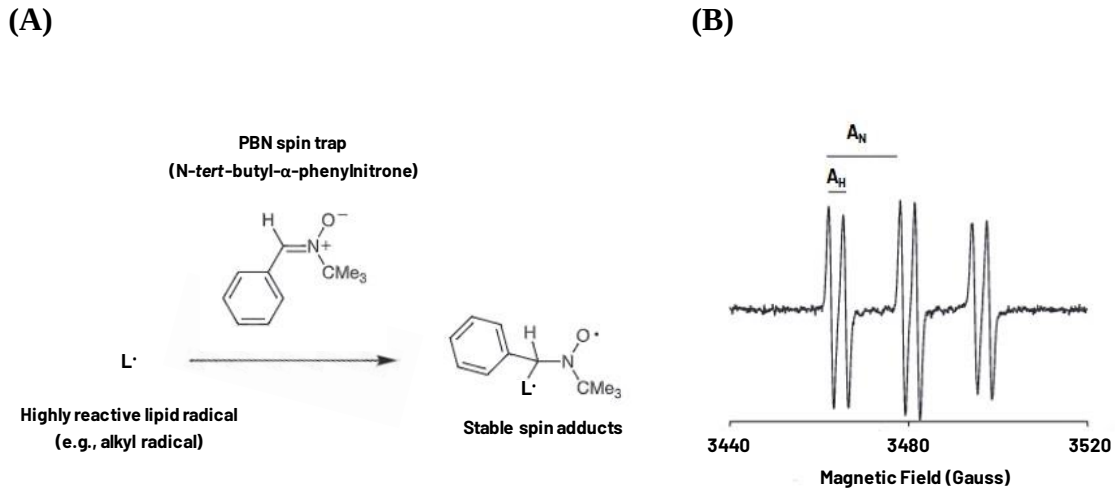

Figure 10. Schematic representation of the generation of spin adducts by addition of a lipid radical (L˙) to the PBN-spin trap (A) and typical PBN-ESR spectrum with the hyperfine coupling constants A_H and A_N (M. L. Andersen, 2021).

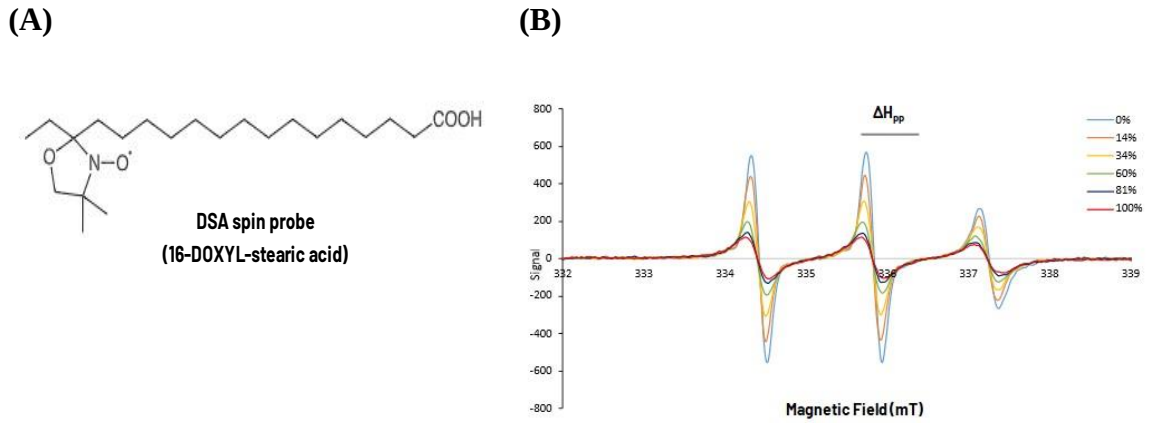

Figure 11. Molecular structure of 16-DSA spin probe (A) and typical broadening of the DSA-ESR spectrum exposed to atmospheres with different oxygen concentrations.

4. RESULTS AND DISCUSSIONS

4.1 State of the art of the omega-3 PUFAs stabilization techniques

The health benefits attributed to the intake of omega-3 PUFAs (i.e., EPA and DHA) have driven the research and development of fortified food products rich in these bioactive compounds. However, their inclusion into complex food matrices is still challenging for the food industry due to their inherent drawbacks, especially their utterly low oxidative stability, which makes necessary the design of efficient omega-3 PUFAs delivery systems. In this regard, the production of stable micro/nanocapsules loaded with oils rich in omega-3 PUFAs (e.g., fish oil) has been proposed as a promising approach.

Chapter I aimed to review the most important advances of the last decades regarding omega-3 PUFAs stabilization techniques, including chemical (i.e., addition of antioxidants), physical (i.e., encapsulation by spray-drying or electrospraying) or combined means (i.e., encapsulation in presence of antioxidants). Food fortification with dry omega-3 delivery systems is also covered in Chapter I.

Table 2 summarizes the state of the art of the current knowledge on the stabilization of omega-3 PUFAs by spray-drying and electrospraying technologies and also collect the extended knowledge that this Ph.D. Thesis provides. The results obtained from each of the studies carried out in the Ph.D. Thesis will be thoroughly discussed in the next Sections.

Table 2. State of the art of the omega-3 PUFAs stabilization techniques and the extended knowledge provided by this Ph.D. Thesis

Current knowledge	Extended knowledge
Spray-drying	
1) Combination of LMW carbohydrates used as the encapsulating agent (e.g., GS) with protein hydrolysates exhibiting emulsifying and antioxidant properties *LMW, low molecular carbohydrates	Influence of the infeed emulsion formulation on the physicochemical properties of fish oil-loaded capsules: comparison of the performance of whey protein hydrolysate (WPCH), exhibiting emulsifying and antioxidant properties, with a synthetic surfactant widely used in the food industry (Tween 20) in presence of two commonly used LMW carbohydrates as the encapsulating agents (i.e., GS or MD).
2) Chemical stabilization of the encapsulated fish oil with antioxidants of different polarity	Influence of the antioxidant location within dry emulsions: comparison of the performance of whey protein hydrolysate (WPCH), used as an antioxidant with amphiphilic properties, with different commercial natural antioxidants of different polarity (i.e., polar or non-polar rosemary-based extracts).
3) Bioaccessibility of encapsulated marine oils	Influence of the infeed emulsion formulation on: i) the physicochemical changes of the capsules within the simulated gastrointestinal tract (i.e., oil droplet size, microstructure and ζ-potential) and ii) on the bioaccessibility of encapsulated fish oil (i.e., release of free fatty acids).
4) Fortification of a wide range of food matrices with fish oil-loaded capsules produced by spray-drying	Influence of the nature of the fish oil-loaded delivery system (i.e., neat fish oil, emulsified fish oil or encapsulated fish oil) on the physical and oxidative stability of a fortified food matrix.
	Influence of the fish oil load of the capsules on the physical and oxidative stability of a fortified food matrix.

Table 2. State of the art of the omega-3 PUFAs stabilization techniques and the extended knowledge provided by this Ph.D. Thesis (continued)

Current knowledge	Extended knowledge
Electrospraying	
1) Production of fish oil-loaded capsules by conventional electrospraying in the monoaxial and in the coaxial configuration using LMW carbohydrates (e.g., GS) and/or proteins (e.g., zein) as the encapsulating agents	Influence of the formulation: Production of fish oil-loaded capsules by conventional monoaxial electrospraying using WPCH as the emulsifier in combination of LMW carbohydrates as the encapsulating agents (i.e., GS or MD).
	Production of neat fish oil-loaded capsules by conventional coaxial electrospraying in combination of LMW carbohydrates as the encapsulating agents (i.e., GS or MD).
2) Production of fish oil-loaded capsules by Electrospraying Assisted by Pressurized Gas (EAPG) in the monoaxial configuration using LMW carbohydrates (e.g., GS) and/or proteins (e.g., zein) as the encapsulating agents	Production of fish oil-loaded capsules by EAPG in the monoaxial configuration using WPCH as the emulsifier in combination of GS as the encapsulating agent.
	Production of neat fish oil-loaded capsules by EAPG in the coaxial configuration using WPCH in combination of GS as the encapsulating agents.
3) Fortification of food matrices with fish oil-loaded capsules produced by EAPG in the monoaxial configuration	Influence of the EAPG technique (i.e., monoaxial or coaxial) on the physical and oxidative stability of a fortified food matrix.
	Influence of the fish oil load of the capsules produced by monoaxial EAPG on the physical and oxidative stability of a fortified food matrix.

Table 2. State of the art of the omega-3 PUFAs stabilization techniques and the extended knowledge provided by this Ph.D. Thesis (continued)

Current knowledge	Extended knowledge
Spray-drying vs. Electrospraying	
It has not been studied before	Comparative studies on the influence of the encapsulation technology on:
	- the oxidative stability of fish oil-loaded capsules produced: i) by spray-drying and conventional monoaxial or coaxial electrospraying at lab-scale and ii) by spray-drying and EAPG in the monoaxial or coaxial configuration at pilot plant scale.
	- the oxygen permeability of the encapsulating wall of the capsules produced by spray-drying and conventional monoaxial or coaxial electrospraying at lab-scale.
	- the secondary structure of WPCH, used as the emulsifier, adsorbed at the O/W interface before and after spray-drying or conventional monoaxial electrospraying processing at lab-scale.

4.2 Influence of the encapsulation technology on the physicochemical properties of fish oil-loaded capsules

4.2.1 Physicochemical properties of fish oil-loaded capsules produced by spray-drying

The influence of the formulation (i.e., combination of encapsulating agents and emulsifiers) on the oxidative stability of fish oil-loaded capsules produced by spray-drying was investigated. To this end, GS and MD were selected as the encapsulating agents due to their extended use in the field of spray-drying. Due to their lack of surface-active properties, these ingredients were combined either with WPCH or T20 as emulsifiers. The fish oil-in-water emulsions were produced with a fixed protein/oil ratio of 0.4 and the concentration of T20 was optimized to achieve a similar oil droplet size distribution of that of the WPCH-stabilized emulsions.

When producing the fish oil-loaded capsules at lab-scale (**Chapter II**), our results showed that irrespective of the ingredients combination (i.e., WPCH+GS, WPCH+MD, T20+GS or T20+MD), fine and monodispersed emulsions with similar oil droplets size and oil droplets size distributions were produced. Furthermore, a minor impact of the formulation was also observed after drying in regards to the morphology and size of the capsules since spherical

capsules of smooth surfaces were produced for every emulsifier/encapsulating agent combination, with mean diameters varying from 8.57 ± 5.30 – 9.77 ± 5.36 μm ($p > 0.05$) (more than 90% of the capsules < 20μm). Although the emulsifier used was shown to influence the stability of the O/W interface upon spray-drying (as will be further discussed in Section 4.4), capsules with high and similar EE values were produced irrespective of the formulation (Figure 19, EE > 84%, $p > 0.05$). Therefore, the different oxidative stability reported for the encapsulated systems could not be attributed to the amount of non-encapsulated surface oil, but to the formulation of the encapsulating matrix. Highly oxidatively stable capsules were produced from the WPCH-stabilized emulsions regardless of the encapsulating agent used (i.e., GS or MD), as confirmed by the low content of SVOPs developed upon 6 weeks of storage at ambient temperature (Figure S 3). Nonetheless, substituting WPCH for T20 affected the overall oxidative stability of the fish oil-loaded capsules, especially in presence of MD (Figure S 3). This finding was attributed to the higher molecular weight of MD compared to GS, which resulted in less dense and more porous encapsulating walls as previously reported by other authors (Drusch et al., 2009). Furthermore, it was also pointed out that T20 lacks of antioxidant activity contrary to WPCH (Padial-Domínguez et al., 2020) which could have exerted a protective effect when located at the oil/matrix interface, as will be discussed below. The influence of the formulation on the oxidative stability of the fish oil-loaded capsules was further investigated at pilot plant scale (**Chapter VII**). In the study, the capsules were produced by spray-drying WPCH-stabilized emulsions in presence of GS or MD as the encapsulating agent. Furthermore, the effect of the storage temperature on lipid oxidation was also evaluated (i.e., 4 or 25 °C). Scaling up the spray-drying process resulted in larger capsules as a result of the higher infusing flow rate of the infeed emulsions and the type of atomizer compared to spray-drying carried out at lab-scale (rotary atomizer vs. 2-fluids nozzle) (mean particle size in the range 12.5 ± 5.5 – 16.8 ± 10.2 μm, $p \leq 0.05$). Furthermore, the capsules produced using MD as the encapsulating agent were significantly larger compared to those produced with GS (i.e., 93% and 71% of the capsules < 20μm for the GS- and MD-based capsules, respectively), most likely as a result of the increased viscosity of the MD-based infeed emulsion due to its higher molecular weight. In turn, the larger particle size obtained at pilot plant scale might be also related to the higher EE reported for these capsules (EE ~98%) since larger capsules result in thicker encapsulating walls (for a fixed oil load) resulting in a better entrapment of the fish oil droplets within the encapsulating matrix (Ramakrishnan et al., 2014). As expected, our results showed that increasing the storage temperature resulted in a higher lipid oxidation

rate and extent irrespective of the formulation. Moreover, our results indicated that the wall matrix composition played a major role on the oxidative stability of the encapsulated fish oil. Although highly oxidatively stable capsules were produced regardless of the wall composition, as confirmed by the low PV and the content of SVOPs developed after 6 weeks of storage (Figure 46 and Figure 47, respectively), the capsules produced with GS as the encapsulating agent were significantly less oxidized at the two values of temperature assayed (4 and 25 °C). The latter was once again ascribed to the different molecular weight of the encapsulating agents (i.e., GS or MD), influencing the permeability of the wall matrix (e.g., permeability to prooxidant species such as oxygen) (Drusch et al., 2009). Nonetheless, the significantly higher oxidative stability reported for the aforementioned system (i.e., WPCH+GS) could not only be attributed to the protective effect of GS used as wall constituent. In a previous study, Tamm et al. (2015) reported that spray-drying GS-based fish oil-in-water emulsions stabilized with hydrolyzed β-Lactoglobulin resulted in a higher oxidative stability of the capsules compared to the capsules produced using the unmodified protein as the emulsifier. This was attributed to the enhanced emulsifying and antioxidant activity (e.g., radical scavenger) of the protein hydrolysates that efficiently stabilized the encapsulated fish oil by exerting a protective effect when located at the oil/matrix interface after drying.

To further investigate the protective effect of the WPCH produced in this Ph.D. Thesis and the influence of the location of the antioxidants within the dried matrix on the oxidative stability of the encapsulated fish oil, its performance as antioxidant was compared to three commercial natural antioxidants of different polarity (i.e., polar or non-polar) (**Chapter III**). These antioxidants consisted in rosemary-based extracts as follows: i) a water-soluble rosemary extract (K1), ii) an oil-soluble rosemary extract (K2), iii) an oil-soluble mixture of antioxidants including rosemary extract, tocopherols, ascorbic acid, citric acid and lecithin (K3). The fish oil-loaded capsules were produced at pilot plant scale using T20 as the emulsifier and GS as the encapsulating agent. Our results showed that the physicochemical properties of the encapsulated systems (i.e., morphology, size and EE) were similar irrespective of the antioxidant used in the formulation (Figure 23and Figure 24, respectively). However, significant differences were observed with respect to the oxidative stability of the capsules. The water-soluble rosemary extract was the less efficient antioxidant preventing lipid oxidation during processing and subsequent storage since this system presented the highest PV after drying and the highest content of SVOPs at the

beginning and at the end of the storage time (6 weeks at ambient temperature) (Figure 25 and Figure 26, respectively). The lower antioxidant efficacy of K1 antioxidant was attributed to its preferential partition at the water phase of the wet spray-dried emulsion, far from the O/W interface where lipid oxidation is initiated in liquid heterogeneous systems (Berton-Carabin et al., 2014), resulting in its preferential location in the glassy matrix after drying, where the mobility towards oxidizing lipids is significantly reduced (Barden & Decker, 2013). On the contrary, the capsules containing the lipid-soluble antioxidants (i.e., K2 and K3) showed the lowest PV after drying, closely followed by the WPCH-containing sample (Figure 25). Nonetheless, WPCH was demonstrated to significantly reduce lipid oxidation of the encapsulated fish oil during storage, as confirmed by the lower amount and content of the SVOPs developed (Figure 26). The latter was discussed on the basis of the proved high interfacial adsorption of WPCH at the O/W interface in emulsions (Ruiz-Álvarez et al., 2022), leading to its preferential location at the oil/matrix interface after drying. Furthermore, WPCH exhibits high antioxidant activity through different mechanisms of action (e.g., metal chelating and radical scavenger) both at its polar part and its non-polar part (Padial-Domínguez et al., 2020), which combined with the antioxidant activity of the non-polar tocopherols (e.g., gamma-tocopherol) already present in the commercial fish oil, resulted in an enhanced oxidative stability of the encapsulated system.

Finally, the influence of the fish oil load (i.e., 13, 26 or 39 wt% fish oil load) on the oxidative stability of the encapsulated systems was investigated (**Chapter VIII**). The capsules were produced at pilot plant scale from WPCH-stabilized emulsions using GS as the encapsulating agent. Irrespective of the oil load, the protein/oil ratio was fixed to 0.4. Interestingly, increasing the oil load did not affect the oil droplet size of the wet spray-dried emulsions nor the outcome of the spray-drying process since capsules with the desired load capacity and high EE were produced (Figure 53, EE > 95%, $p > 0.05$). However, smoother capsules were produced as the oil load increased (Figure 51), which was attributed to the higher protein content of the infeed emulsions at the same drying conditions (higher WPCH content for higher oil loads because the protein/oil ratio was fixed to 0.4) (Both et al., 2018). Nonetheless, the particle size distribution was not influenced by the formulation (mean particle size in the range 17.0 ± 8.1 – 17.3 ± 7.6μm, $p > 0.05$, Figure 52). In regard to lipid oxidation, our results showed that the fish oil load of the encapsulated systems did not influence the oxidation rate and extent, as confirmed by the similar content of SVOPs developed after 6 weeks of storage at ambient temperature among the samples (Figure 54, p

> 0.05). These findings are in line with those reported by Linke et al. (2021) who stated that lipid oxidation of encapsulated systems is affected by the oxygen supply rather than by the oil load, which will be further discussed in depth in Section 4.2.3.

4.2.2 Physicochemical properties of fish oil-loaded capsules produced by electrospraying

Following the same reasoning as for the spray-dried capsules, the influence of the formulation (i.e., encapsulating agent), the emitter configuration (i.e., monoaxial and coaxial) and the processing conditions (i.e., infusing flow rate and voltage applied) was first investigated for the fish oil-loaded capsules produced by conventional electrospraying (**Chapter II**). For comparative purposes, GS or MD were used as the encapsulating agents and pullulan was added to the formulation as thickening agent. For monoaxial electrospraying, the infeed emulsions were produced using WPCH as the emulsifier to a fixed protein/oil ratio of 0.4. For coaxial electrospraying, neat fish oil was infused as the core solution, whilst the biopolymer-based shell solutions were produced following two different approaches. In the first approach, the encapsulating agent and pullulan (i.e., 1 or 2 wt%) were dissolved in distilled water and stirred overnight before processing and in the second approach, the shell solution with a higher load of pullulan (i.e., 3 wt%) was passed through a high-pressure homogenizer (HPH) prior electrospraying. For further details on the formulation, the production of the infeed emulsions/solutions and the production of the fish oil-loaded capsules, please refer to Chapter II.

The main parameters influencing the physicochemical properties of the capsules (i.e., morphology, size and EE) were the emitter configuration and the processing conditions, while the formulation (based on the encapsulating agent used) had a minor effect. In brief, monoaxial electrospraying led to smoother capsules contrary to coaxial electrospraying, which resulted in dented particles irrespective of the shell solution formulation and production approach (i.e., with or without HPH) (Figure 17). Furthermore, small fibrils interconnecting the capsules were observed regardless of the emitter configuration (i.e., monoaxial or coaxial) (Figure 17), which is ascribed to the presence of pullulan in the formulation of the electrosprayed emulsions/solutions. Increasing the infusing flow rate led to larger capsules (coaxially electrosprayed capsules were larger than monoaxially electrosprayed capsules), although a narrow particle size distributions of small particles (0.5 – 3 µm) were obtained regardless of the emitter configuration (Figure 18). As for the EE, monoaxial electrospraying resulted in a better entrapment of the fish oil within the

encapsulating matrix during processing (EE = 69 – 72%, $p > 0.05$) compared to coaxial electrospraying (EE = 53 – 59%, $p > 0.05$) (Figure 19) due to the lack of surface-active properties of the encapsulating agents used the in absence of an emulsifier. Furthermore, increasing the content of pullulan in the shell solution did not improve the retention properties of the encapsulating wall (Figure 19).

Regarding lipid oxidation, the monoaxially electrosprayed capsules were more oxidized after processing than the coaxially electrosprayed capsules, as confirmed by the higher initial content of the selected SVOPs (e.g., 2-ethyl-furan) (Figure 21 and Figure S 3). This finding was attributed to the production and subsequent storage of the emulsions throughout the processing time (36 h), leading to physical destabilization (Figure S 1) and presumably, initial lipid oxidation. Moreover, the monoaxially electrosprayed capsules presented a relatively high content of non-encapsulated surface oil (Figure 19) which could have been oxidized during the processing time between batches (30 min). Nonetheless, the initial content of SVOPs did not significantly increase over storage (Figure S 3). This is in line with our previous observations for the spray-dried capsules (Section 4.2.1) in which WPCH, used as the emulsifier exhibiting film-forming and antioxidant properties, and combined with low molecular weight carbohydrates as bulk materials (i.e., GS or MD) resulted in highly oxidatively stable capsules during storage.

Conversely, the coaxially electrosprayed capsules showed low and comparable amounts of the selected SVOPs after drying irrespective of the shell solution production approach (Figure S 3, $p > 0.05$). However, based on the FT-IR results and the content of selected SVOPs derived from the oxidation of omega-3 PUFAs (i.e., 2-ethyl-furan, 1-penten-3-ol and (*E*,*E*)-2,4-heptadienal) developed throughout storage, the capsules produced by coaxial electrospraying without previous HPH of the shell solution (i.e., with lower pullulan concentration) were significantly oxidized (Figure 20 and Figure 21, respectively). In contrast, the capsules produced by coaxial electrospraying with previous HPH of the sell solution enhanced the oxidative stability of the encapsulated neat fish oil to levels comparable to the emulsion-based encapsulation method (i.e., monoaxial electrospraying) (Figure 21 and Figure S 3). Generally, a low oxidative stability of encapsulated systems is related to a high amount of unprotected non-encapsulated surface oil since this fraction is in direct contact with prooxidant species (e.g., oxygen) and therefore is more susceptible to undergo lipid oxidation (Drusch & Berg, 2008; Linke, Weiss, et al., 2020). Nonetheless, the differences observed between the coaxially electrosprayed systems could not be attributed

to the amount of easily-oxidized surface oil as it was similar among the samples (Figure 19), $p > 0.05$). Increasing the content of pullulan in the shell solution resulted in larger capsules (Figure 18) and therefore in a lower surface-to-volume ratio and in thicker encapsulating walls for a fixed oil load (~ 13 wt%), both influencing oxygen diffusivity through the encapsulating wall (Linke, Hinrichs, et al., 2020). Thus, our result pointed out that the physicochemical properties of the capsules influencing the oxygen uptake during storage (e.g., particle size) played a major role on lipid oxidation rather than the content of non-encapsulated surface oil, as will be further discussed in Section 4.2.3.

Overall, the results reported for the fish oil-loaded capsules produced by conventional electrospraying (Chapter II) are in line with our findings when the capsules were produced by EAPG in the monoaxial or in the coaxial configuration at a fixed oil load of ~ 13 wt% using GS as the encapsulating agent (**Chapter VIII**). In this study, the coaxially EAPG capsules showed low concentrations of the selected SVOPs after storage, and in most cases not significantly different from that of the beginning of the storage time (e.g., (*E,E*)-2,4-heptadienal or pentanal) (Figure 54). These results suggested that the coaxially-EAPG neat fish oil was more efficiently protected from lipid oxidation than the monoaxially-EAPG fish oil. By optimal coaxial electrospraying, the oil is theoretically located at the core of the encapsulating matrix as a single droplet, whilst by emulsion-based encapsulation methods (i.e., monoaxial electrospraying), a random distribution of oil droplets within the system is achieved. Therefore, whilst prooxidant species (e.g., oxygen) ought to penetrate throughout the encapsulating wall to reach the oily core in coaxially electrosprayed capsules to trigger lipid oxidation, it could be more easily initiated for the monoaxially electrosprayed systems where the oil droplets are dispersed in the encapsulating matrix near to the capsules surface, especially when the particle size is notably small (the mean particle size was in the range 3.2 ± 2.1 – 4.9 ± 2.4 μm irrespective of the emitter configuration, Figure 52). In addition, it should be noted that the capsules produced by coaxial EAPG contained WPCH in the formulation of the shell solution, contrary to when the fish oil-loaded capsules were produced by conventional electrospraying (Chapter II). Thus, although the EE results showed that coaxial EAPG did not improve the retention properties of the encapsulating wall during processing compared to conventional coaxial electrospraying in the presence of GS as the encapsulating agent ($EE_{EAPG\text{-}co\text{-}13}$ = ~50%, Figure 53B; EE_{co} = 53-59%, Figure 19), the oxidative stability results suggested otherwise. It has been reported that the contribution of the non-encapsulated oil fraction to the overall lipid oxidation is minor when its

concentration is rather low compared to the fraction of the encapsulated oil (Linke, Weiss, et al., 2020). Therefore, our results pointed out that the fraction of non-encapsulated surface oil was overestimated for the coaxially-EAPG capsules as a result of the EE measurements (i.e., immersion of the capsules in the extracting solvent and shaking of the mixture for a certain time) which presumably extracted a portion of the theoretically centralized encapsulated oil through cracks or capillary present on the capsules surface (Drusch & Berg, 2008). In this line, the influence of WPCH on the outcome of coaxial-EAPG process was further confirmed when the capsules were produced at different GS:WPCH ratios in the shell solution formulation (GS:WPCH = 100:0, ~82:18, 60:40, ~28:72 or 0:100) when neat fish oil was infused as the core solution (**Appendix I).** The results showed that, by coaxial EAPG, the fish oil was not effectively retained within the matrix when GS alone was used as the encapsulating agent (EE = 0%), in contrast to when the concentration of WPCH in the shell solution was increased (EE = ~50 - 70%, Figure I 2B). It should be noted, however, that the highest EE (EE = ~84%) was achieved when the encapsulating wall consisted of GS alone and the core solution consisted in emulsified fish oil (i.e., WPCH-stabilized fish oil-in-water emulsion, 15 wt% fish oil load) (Figure I 2B). These results further highlighted that the outcome of the coaxial electrospraying process is influenced by the properties of the encapsulating agent/s used and that ingredients with amphiphilic properties are required to improve the retention properties of the encapsulating wall, especially when neat fish oil is infused as the core solution.

On the other hand, EAPG processing (Chapter VIII) also resulted in a better performance of the encapsulation process in the monoaxial configuration compared to conventional monoaxial electrospraying (Chapter II) when GS was used as the encapsulating agent ($EE_{EAPG\text{-}mo\text{-}13}$ = 94%, Figure 53B; EE_{mo} = 72%, Figure 19). In addition, although our results showed that the monoaxially-EAPG system oxidized throughout storage, the final content of the selected SVOPs developed was lower compared to that found in the capsules produced by conventional electrospraying (e.g., 1-penten-3-ol or (*E*,*E*)-2,4-heptadienal) (Figure 54 and Figure 21, respectively). It should be noted that in Figure 21 the results are expressed as ng/g powder whilst in Figure 54 the results are expressed as ng/g oil.

Altogether, in line with our previous observations for the spray-dried capsules, scaling-up the electrospraying process from lab-scale (i.e., conventional electrospraying) to pilot plant scale (i.e., EAPG) resulted in larger capsules (Figure 52) with enhanced retention properties (Figure 53B). Furthermore, it should be also noted that the small fibrils interconnecting the

capsules produced at lab-scale (Figure 17) were not observed when the capsules were produced by EAPG (Figure 51). By EAPG, the infeed solution/emulsion is first mechanically atomized and then subjected to a high electric field (i.e., electrohydrodynamic atomization), thus the "Taylor cone" is not formed at the tip of the emitter as occur when the solution/emulsions are subjected to electrohydrodynamic atomization at lab-scale. Therefore, by EAPG, not only the throughput of the process is significantly enhanced by allowing to increase the infusing flow rate/s (i.e., from 0.2 – 0.6 mL/h to 60 – 600 mL/h for Chapter II and Chapter VIII, respectively) as a result of the combined atomization techniques (i.e., mechanical atomization followed by electrohydrodynamic atomization) without significantly affecting the particle size distribution (i.e., narrow particle size distribution of small capsules), but also allows to electrospray solutions/emulsion with low viscoelasticity without the need of adding a "spin aid (bio)polymer" (i.e., pullulan). In addition, WPCH, with film-forming and antioxidant properties, combined with the low-molecular-weight GS as bulk material, resulted in fish oil-loaded capsules with a high oxidative stability, especially those produced in the coaxial configuration due to the centralized distribution of the encapsulated fish oil within the matrix.

Finally, it is also particularly interesting to note that increasing the fish oil load of the monoaxially-EAPG capsules (i.e., 13, 26 or 39 wt% fish oil load) did not affect the outcome of the encapsulation process (EE = 83 – 97%, $p > 0.05$, Figure 53B) despite the small particle size of the capsules produced (the mean particle size was in the range 4.2 ± 2.6 – 4.9 ± 2.4 µm for the monoaxially-EAPG capsules, Figure 52). Furthermore, the oil droplet size of the reconstituted emulsions was fairly similar to that of the parent emulsions fed to the EAPG drier (Figure S 29), which implies that the integrity of the WPCH-based interfacial layer was efficiently retained during processing despite the combined atomization mechanisms (i.e., mechanical atomization followed by electrohydrodynamic atomization). Moreover, and also in line with the results found for the spray-dried capsules produced at pilot plant scale (Section 4.2.1), the oil load did not influence the oxidative stability of the monoaxially-EAPG capsules, as will be further discussed below (Section 4.2.3).

4.2.3 Comparison between the physicochemical properties of spray-dried and electrosprayed capsules

As extensively reported throughout the document, the physicochemical properties of the fish oil-loaded capsules (e.g., wall matrix composition or particle size, among others) influencing the oxygen diffusivity through the encapsulating wall were suggested to play major role on

their oxidative stability. Therefore, Electron Spin Resonance (ESR) technique was used to evaluate the oxidative stability (ESR-spin trapping) and, in turn, the oxygen permeability (ESR-oximetry) of the fish oil-loaded capsules produced by the different technologies investigated in this Ph.D. Thesis (**Chapter IV**). In the study, the capsules were produced by spray-drying and conventional electrospraying, both at lab-scale, using GS as the encapsulating agent. For the emulsion-based encapsulation methods (i.e., spray-drying and monoaxial electrospraying), WPCH was used as the emulsifier. For coaxial electrospraying, neat fish oil was infused as the core solution. ESR-spin trapping was used to monitor the course of lipid oxidation throughout storage by measuring the peak-to-peak amplitude of the central line of the PBN-ESR spectra of the samples. On the other hand, ESR-oximetry was used to evaluate the gas permeability of the encapsulating systems by measuring the broadening or the narrowing of the central line width (ΔH_{pp}) of the DSA-ESR spectra of the samples upon oxygen or nitrogen exposure, respectively.

ESR-spin trapping results showed a low and rather constant peak-to-peak amplitude for the capsules produced by electrospraying during 25 days of storage, regardless of the emitter configuration (i.e., monoaxial or coaxial) (Figure 30). Conversely, the peak-to-peak amplitude of the PBN-ESR spectrum of the capsules produced by spray-drying showed a lag phase of 4 days, followed by a sharp increase up to day 21 and then a slight decrease (Figure 30). The peak-to-peak amplitude, meaning the signal intensity of the ESR spectrum, is proportional to the concentration of lipid-derived-radicals. Thus, it is generally assumed that the higher levels of radicals detected, the higher the oxidation extent (Boerekamp et al., 2019). However, our results suggested otherwise. In conditions of advanced lipid oxidation, where the concentration of lipid-derived-radicals is high, they can react with each other and with PBN-spin adducts giving rise to ESR-silent compounds (i.e., non-detectable diamagnetic species) leading to a situation where low levels of radicals can be detected in markedly oxidized samples. Therefore, the low and constant levels of lipid-derived-radical detected by ESR-spin trapping for the capsules produced by electrospraying (i.e., monoaxial and coaxial) suggested a faster lipid oxidation during the early stages of storage rather than a high oxidative stability. In this line, the ESR-oximetry results showed that the oxygen inside the spray-dried capsules reached the equilibrium with the surrounding pure oxygen atmosphere significantly slower than the monoaxially electrosprayed capsules (i.e., ~2 h and ~10 min, respectively) (Figure 32). This finding clearly indicates a higher oxygen permeability of the monoaxially electrosprayed capsules. This was attributed to the

significantly smaller capsule size of the monoaxially electrosprayed capsules (~95% of the capsules < 1.5µm) compared to the spray-dried capsules (~95% of the capsules < 25µm) (Figure 28) which, for a fixed oil load, results in: i) an increased specific surface area available for the oxygen diffusion process and ii) thinner encapsulating walls, which implies a shorter diffusion path to the core of the capsules. Unfortunately, the oxygen permeability of the coaxially electrosprayed capsules could not be evaluated by ESR technology since the MCT oil used in the study containing the DSA probe was extracted during sample preparation (Figure S 6) (please, refer to Chapter IV for further details).

Overall, the oxygen permeability results correlated well with the oxidative stability measured for the fish oil-loaded capsules by ESR technology, with the spray-dried capsules showing the lower oxygen permeability and the higher oxidative stability. Furthermore, these findings were in turn in agreement with our previous study investigating the influence of the encapsulation technology (i.e., spray-drying or monoaxial/coaxial electrospraying) on the oxidative stability of fish oil-loaded capsules produced at lab-scale (**Chapter II**). Our results showed that the spray-dried capsules were the most oxidatively stable compared to those produced by monoaxial or coaxial electrospraying, as confirmed by the low content of SVOPs (e.g., 2-ethylfuran, hexanal) (Figure 21 and Figure S 3) found before and after storage. Therefore, it is confirmed that the physicochemical properties of the capsules influence the oxygen permeability of the encapsulating wall (i.e., larger particle size of the spray-dried capsules), affecting oxidative stability.

The influence of the encapsulation technology on the oxidative stability of the fish oil-loaded capsules was even more evident when the capsules were produced at pilot plant scale with different oil loads (i.e., 13, 26 and 39 wt%) (**Chapter VIII**). Interestingly, our results showed that the encapsulation technology (i.e., spray-drying or monoaxial/coaxial EAPG) used to produce the capsules significantly influenced their oxidative stability, but not the oil load. The capsules produced by spray-drying and coaxial EAPG were significantly less oxidized after storage compared to the monoaxially-EAPG capsules irrespective of the oil load, as confirmed by the low, and in most cases similar, content of SVOPs developed throughout storage (e.g., (*Z*)-4-heptenal, (*E*,*E*)-2,4-heptadienal or pentanal) (Figure 54). Thus, the differences observed for the oxidative stability of the capsules produced by the emulsion-based encapsulation methods (i.e., spray-drying or monoaxial EAPG) could be only attributed to the significantly different capsules size influencing the oxygen uptake (Figure 52) since the formulation, the EE (Figure 53B) and the droplet size of the encapsulated fish

oil (Figure S 29) was not significantly different among the samples. In turn, the improved oxidative stability reported for the coaxially-EAPG capsules over the monoaxially-EAPG capsules was attributed to the fish oil distribution within the encapsulating matrix as a result of the different processing conditions (i.e., different emitter configuration). As previously discussed, our results suggested that lipid oxidation could be more easily initiated by the diffusing oxygen when the fish oil is randomly distributed within the encapsulating matrix, as is the case of the monoaxially-EAPG capsules, contrary to when the oil is embedded in the core of the matrix, as is the case of the coaxially-EAPG capsules. Therefore, taking into account that the oxidative stability of the coaxially-EAPG capsules was comparable to the oxidative stability of the spray-dried capsules (Figure 54), the oil distribution within the encapsulating matrix seems to strongly influence the oxidative stability of the encapsulated fish oil, especially when the particle size is significantly reduced.

Altogether, our results confirm the key role of oxygen permeability on the oxidative stability of the encapsulated fish oil and how it is strongly influenced by the physicochemical properties of the capsules (e.g., particle size), which are in turn influenced by the encapsulation technology (i.e., spray-drying, monoaxial electrospraying/EAPG or coaxial electrospraying/EAPG).

ESR technology was also aimed to investigate the oxidative stability of fish oil-loaded capsules produced by conventional electrospraying (i.e., monoaxial electrospraying) using hydrophobic proteins as the encapsulating agent (i.e., kafirin or zein) (**Appendix II**). Unfortunately, after drying, the characteristic spectra of the PBN-adducts formed in oil-containing samples (i.e., bulk oil, emulsified oil or encapsulated oil) consisting of three broad lines (Boerekamp et al., 2019; Velasco et al., 2005, 2021) was not observed (Figure II 3E,F). On the contrary, the spectra of the kafirin- and zein-based capsules corresponded to PBN-adducts formed with protein radicals of low mobility, thus lipid oxidation could not be monitored throughout storage. Interestingly, our results also showed that native kafirin does not have free radicals (Figure II 3A), but develops them upon electrospraying (Figure II 3C), conversely to native zein which has free radicals (Figure II 3B).

Finally, the influence of the encapsulation technology (i.e., spray-drying or monoaxial electrospraying) on the secondary structure of WPCH used as emulsifier with film-forming and antioxidant activity in the production of dry fish oil-loaded delivery systems was investigated (**Chapter V**). Previous studies have evaluated the interfacial properties (i.e., interfacial tension and viscoelasticity of the interfacial peptide layer) of WPCH at different

pH (i.e., pH 2 and pH 8) and their effect on the physical stability of fish oil-in-water emulsions (Ruiz-Álvarez et al., 2022). Nonetheless, the structural organization of WPCH adsorbed at the O/W interface was not reported. The latter is of outmost importance since the conformational structure of emulsifier peptides adsorbed at the interface will affect the mechanical properties of the interfacial peptide-based layer (i.e., viscoelasticity) which will further determine the outcome of the emulsion-based encapsulation process (i.e., EE) as well as the oxidative stability of the emulsion-based dry delivery systems. Moreover, other factors such as the encapsulating agent and the drying technique might affect the structural conformation of peptides at the O/W interface both before and after processing. Therefore, to gain insight into the structural organization of WPCH used as emulsifier in the production of dry delivery systems, its secondary structure upon adsorption at the oil/water interface before and after drying (i.e., spray-drying or conventional monoaxial electrospraying) was investigated by means of Synchrotron Radiation Circular Dichroism (SRCD) (Chapter V). The influence of the pH (i.e., pH 2 or pH 8) on the secondary structure of WPCH and its thermal stability was also studied.

Our results showed that enzymatic hydrolysis of whey protein concentrate (WPC, Alcalase® 2.4L, pH 8, 50 °C, DH = 10%) resulted in peptides (i.e., WPCH) with a lower α-helix structure (< 10%) and higher unordered regions (~60% of turns and unordered region) in solution irrespective of the pH when compared to the whey protein concentrate (Figure 34A). However, upon adsorption at the O/W interface, the content of α-helical structure significantly increased at expenses of the β-sheet conformation (Figure 34B) as a result of the reorientation of hydrophobic residues towards the oil phase (Zhai et al., 2011). Although a slightly higher α-helical content was found for WPCH adsorbed at the O/W interface at pH 8 (Figure 34B), the pH had a minor influence the secondary structure of WPCH in emulsions which is an indicative that the hydrophobic interactions played a major role over electrostatic interaction (driven by the pH) on the conformational changes of WPCH in liquid heterogeneous systems (i.e., oil-in-water emulsions). Furthermore, our results showed that these hydrophobic interactions were enhanced for the WPCH compared to the native protein (WPC) (i.e., the content of non-native α-helical structure significantly increased in emulsion for WPCH contrary to WPC, Figure 34B) as a result of the smaller and more flexible peptides produced by enzymatic hydrolysis (O'Regan & Mulvihill, 2010; Rahali et al., 2000; Ruiz-Álvarez et al., 2022) . In addition, the adsorption of WPCH at the O/W interface slightly enhanced its thermal stability regardless of the pH (i.e., pH 2 or pH 8) (Figure 36). However,

our result showed that the thermal stress exerted during spray-drying did not cause the denaturation of the peptides adsorbed at the O/W interface since the more α-helix-rich secondary structure of WPCH in emulsion before and after drying was practically unaltered irrespective of the encapsulating agent used (i.e., GS or MD) (Figure 38A,B). Conversely, although conventional monoaxial electrospraying was carried out at ambient temperature, the high voltage applied caused structural changes in the WPCH-based interfacial layer after drying with respect to the parent electrosprayed emulsions (i.e., high content of irregular structure after drying) (Figure 38C,D) suggesting denaturation of the adsorbed peptides upon conventional monoaxial electrospraying (Perez & Pilosof, 2004; Xiang et al., 2008).

4.3 Digestion and bioaccessibility of dry omega-3 delivery systems

The influence of the infeed emulsion formulation on the bioaccessibility of the encapsulated fish oil was investigated (**Chapter VI**). For this purpose, the fish oil-loaded capsules were produced by spray-drying WPCH-stabilized emulsions at lab-scale using GS or MD as the encapsulating agents. Furthermore, the influence of WPCH used as emulsifier on lipid digestion was compared to T20, being the latter a commercial surfactant used in the food industry. After production, the capsules were subjected to a three-phase *in vitro* digestion (i.e., oral phase, gastric phase and intestinal phase) and the changes in the physicochemical properties of the re-dispersed capsules were monitored throughout the different phases of the gastrointestinal tract (GIT) (i.e., droplet size, microstructure and ζ-potential).

The infeed emulsions formulation did not influence the microstructure of the infeed emulsions before processing (i.e., droplet size) (Figure 41) nor the microstructure of the dried capsules (i.e., morphology and size) (Figure 39 and Figure 40A). However, the emulsifier used (i.e., WPCH or T20) affected the outcome of the spray-drying process, and more significantly, the outcome of lipid digestion. WPCH retained the integrity of the O/W interface more efficiently than T20 during processing as confirmed by the higher EE reported for the WPCH-based capsules irrespective of the encapsulating agent used (i.e., GS or MD) (Figure 40B). The latter was attributed to the high viscoelastic behavior of the WPCH-based interfacial layer (Ruiz-Álvarez et al., 2022) which was able to withstand the mechanical stresses exerted during spray-drying (e.g., atomization). This was further confirmed by the similar oil droplet size distribution of the reconstituted emulsions after re-dispersion of the capsules in the simulated GIT fluid (i.e., salivary fluid) (Figure 41A,B) as well as by the smaller oil droplets observed by confocal microscopy (Figure 42A), contrary to the T20-

based re-dispersed capsules (Figure 41C,D and Figure 42A). It is also worth mentioning that after processing the interfacial charge of the WPCH-based interfacial film did not vary with respect to the parent emulsion before drying (Figure 43). Altogether, these finding are in line with Chapter V reporting that spray-drying does not affect the secondary structure of WPCH adsorbed at the O/W interface irrespective of the encapsulating agent used (i.e., GS or MD). After the gastric phase of lipid digestion, a population of large oil droplets could be observed for the WPCH-based capsules (Figure 41A,B). Moreover, the surface charge of the peptides' interfacial layer, now positive due to the pH of the medium (i.e., the pH of the gastric phase was fixed to pH 3 and the pI of WPCH is 4.06 (Ruiz-Álvarez et al., 2022)), slightly decreased (Figure 43). This was attributed to the partial digestion of the WPCH-based interfacial layer by action of pepsin present in the simulated gastric fluid which: i) led to the reduction of the surface charge and ii) resulted in smaller peptides unable to prevent oil droplets coalescence, both resulting in larger oil droplets. Likewise, the results obtained for the T20-based capsules suggested further coalescence of the already coalesced oil droplets, as shown by the significantly different oil droplet size distribution before and after gastric digestion (Figure 41C,D), which may also be an indicative that the integrity of the T20-based interfacial layer was not retained after processing. At the beginning of the intestinal phase of lipid digestion, the oil droplet size distribution was displaced to lower diameter values for both systems (i.e., WPCH- and T20-bases systems) (Figure 41) by action of the bile salts present in the simulated intestinal fluid, although it was more pronounced in case of the WPCH-based capsules (i.e., the main peak of the WPCH-based capsules was centered at ~0.7 – 0.9 μm) (Figure 41A,B). The latter led to an increased specific surface area for lipases to adsorb, and in consequence, a higher lipolysis rate and extent (Figure 44). On the contrary, bile salts adsorption at the O/W interface of the T20-bases capsules was hindered due to the high surface-activity of T20 (Salvia-Trujillo et al., 2021) which significantly reduced lipid digestion.

Interestingly, the encapsulating agent used in the formulation of the infeed emulsions (i.e., GS or MD) did not significantly affect the bioaccessibility of the encapsulated fish oil. Nonetheless, the percentage of free fatty acids (FFA) released was slightly lower for the MD-containing capsules (Figure 44B). This finding was attributed to the higher viscosity of the continuous phase in presence of MD due to it higher molecular weight, which might have difficulted the diffusion of the GIT components (i.e., digestive enzymes) through the digestive medium.

4.4 Food enrichment with dry omega-3 delivery systems

The influence of the delivery system on the physical and oxidative stability of a fortified food matrix was first investigated (**Chapter VII**). In the study, low-fat mayonnaise was enriched with: i) neat fish oil, ii) a WPCH-stabilized fish oil-in-water emulsion and iii) spray-dried fish oil-loaded capsules produced at pilot plant scale with WCPH and GS as the emulsifier and the encapsulating agent, respectively. The enriched mayonnaise samples were then stored at ambient temperature during 28 days.

After production, the mayonnaise sample enriched with neat fish oil showed the highest proportion of large oil droplets (Figure 48A), in line with the significantly higher D[3,2] and D[4,3] values reported for the aforementioned sample (i.e., D[3,2] = 1.55 ± 0.02 μm and D[4,3] = 2.72 ± 0.04 μm, $p \leq 0.05$, Table 8). On the contrary, the mayonnaise samples fortified with the emulsified or the encapsulated fish oil showed the highest proportion of small oil droplets, with the first peak of the respective distributions overlapping at ~0.13μm (Figure 48A). This peak in turn overlapped with the oil droplet size distribution of the emulsion fed to the spray-drier, which suggested that the integrity of the fish oil-loaded delivery systems (i.e., fish oil-in-water emulsion or fish oil-loaded capsules) was retained during food processing. These results further correlated with the small, and not significantly different, D[3,2] values of the mayonnaise samples fortified with the emulsified or the encapsulated fish oil (Table 8). Nonetheless, the D[4,3] values were significantly smaller for the mayonnaise sample fortified with the encapsulated fish oil since the capsules were mechanically dispersed into an already produced mayonnaise, which further reduced the size of the bulk oil droplets (i.e., sunflower oil droplets). After storage, the droplet size of the mayonnaise sample enriched with neat fish oil decreased, contrary to the oil droplet size of the mayonnaise samples fortified with the emulsified or the encapsulated fish oil which slightly increased (Table 8). The latter was attributed: i) to the disintegration of oil floccules present after production of the neat fish oil-enriched sample and to ii) the partial physical destabilization or partial physical disintegration of the fish oil-loaded delivery systems (i.e., fish oil-in-water emulsion or fish oil-loaded capsules) leading to flocculation and/or coalescence of the oil droplets released from the delivery system. Overall, these findings correlated well with the apparent viscosity reported for the mayonnaise samples after production and after storage, with the sample fortified with neat fish oil showing the larger oil droplets, and therefore, the lower apparent viscosity at both sampling points. Furthermore, the apparent viscosity of the mayonnaise samples fortified with the emulsified

or the encapsulated fish oil did not significantly change after storage due to the enhanced physical stability of these samples as a result of their high viscosity after production. Nonetheless, the higher apparent viscosity was found for the mayonnaise sample fortified with the encapsulated fish oil, being this fact attributed to the thickening effect of the intact capsules dispersed in the continuous phase of the food matrix.

As for the oxidative stability, the PV of the enriched mayonnaise samples was low and comparable after production (PV ~4 – 5 meqO_2/kg oil, $p > 0.05$, Figure 49) and the course of lipid oxidation showed a lag phase up to the second week of storage, irrespective of the fortification approach (i.e., neat fish oil, emulsified fish oil or encapsulated fish oil). However, from week 2 onwards, the PV of the three mayonnaise samples increased progressively to values significantly different among the systems (Figure 49, $p \leq 0.05$). After storage, the highest PV was found for the sample fortified with neat fish oil, followed by the sample fortified with encapsulated fish oil and by last, by the sample fortified with emulsified fish oil (Figure 49). However, low PVs might be indicative of an advanced oxidation state due to hydroperoxides decomposition to secondary volatile oxidation products (e.g., 2-alkenals or 2,4-alkadienals) rather than being indicative of high oxidative stability. This was further confirmed by the anisidine value (AV) of the fortified samples, with that enriched with the emulsified fish oil showing a sharp increase from day 21 onwards, contrary to the samples fortified with either the neat fish oil or the encapsulated fish oil which AV was rather constant throughout storage (Figure 50). The lower oxidative stability found the mayonnaise sample fortified with the emulsified fish oil was discussed on the basis of the poorer oxidative status of the fish oil as a result of the production of the delivery system itself (i.e., oxygen inclusion and distribution during the emulsification step). Therefore, the significantly higher oxidative stability reported for the capsule-fortified mayonnaise sample might indicate that the integrity of the encapsulating wall was efficiently retained during processing and subsequent storage of the food matrix, thus limiting the contact of the fish oil with prooxidant species (e.g., oxygen or metal ions).

Afterwards, the influence of the physicochemical properties of fish oil-loaded produced by spray-drying or EAPG on the physical and oxidative stability of a fortified food matrix was investigated (**Chapter VIII**). For comparative purposes, a salad dressing was selected as the food model system. The fish oil-loaded capsules were produced at pilot plant scale either by spray-drying or by EAPG in the monoaxial or in the coaxial configuration using GS as the encapsulating agent and WPCH as the emulsifier at three fixed fish oil loads (i.e., 13, 26 or

39 wt%) keeping constant the ratio protein/oil at 0.4. Based on the results for the physicochemical properties of the capsules (e.g., size, EE or oxidative stability), the salad dressing samples were fortified with the selected capsules as follows: i) spray-dried and monoaxially-EAPG capsules with 13 or 39 wt% fish oil load, and ii) coaxially-EAPG capsules with 13 wt% fish oil load. A salad dressing sample fortified with neat fish oil was also produced as a control. The enriched salad dressing samples were then stored at ambient temperature during 28 days.

In line with our previous observations (Chapter VII), the salad dressing samples fortified with the capsules produced by the emulsion-based encapsulation methods (i.e., spray-drying or monoaxial EAPG) presented the highest proportion of small oil droplets after production irrespective of the oil load (i.e., 13 or 39 wt%) (Figure S 30A). Furthermore, the peak of the aforementioned salad dressing samples was centered at the same diameter values as the peak of the emulsion-based capsules after redispersion in water (~0.3 – 0.4μm, Figure S 30A and Figure S 29B, respectively) which indicates that the integrity of the encapsulating wall was retained after food processing. On the contrary, but also in line with our previous observations, the salad dressing samples fortified with the coaxially-EAPG capsules or the neat fish oil showed a low proportion of small oil droplets after food processing since in both cases the oil was not emulsified before food fortification. These observations in turn correlated with the D[3,2] and D[4,3] values of the salad dressing samples after production, with the samples fortified with the emulsion-based capsules showing significantly lower D[3,2] irrespective of the oil load (D[3,2] ~0.9 μm, $p \leq 0.05$, Table 9). It was explained due to the small fish oil droplets dispersed in the matrix. The sample fortified with neat fish oil showed the highest D[4,3], meaning larger bulk rapeseed oil droplets, because the sample was not subjected to further mixing after production (i.e., mechanical dispersion of the capsules) (D[4,3] ~25 μm, $p \leq 0.05$, Table 9). After storage, no creaming or phase separation was observed for any of the fortified salad dressings and minor changes on the oil droplets size was observed (Table 9). As previously discussed, the increase in the D[3,2] and D[4,3] values of the samples fortified with the coaxially electrosprayed capsules or neat fish oil suggested the disruption of oil floccules present after food processing. On the other hand, the increase in the D[3,2] and D[4,3] values of the salad dressing samples fortified with the emulsion-based capsules suggested oil flocculation/coalescence due to a partial, although limited, disintegration of the encapsulating matrix. As expected, all the fortified salad dressing samples showed pseudoplastic behavior due to the nature of the food model system

(Ma et al., 2013) (Figure S 31) and the apparent viscosity was influenced by the oil load of the capsules rather than by the encapsulation technology used for their production (Table 9). Higher viscosity values were found for the capsule-fortified salad dressing samples, contrary to sample fortified to neat fish oil due to the thickening effect of the intact capsules within the matrix, and the viscosity increased as the oil load of the capsules decreased (Table 9). Furthermore, minor, and in most cases not significant, changes were observed for the apparent viscosity values after storage irrespective of the fortification approach (Table 9), further confirming the high physical stability of the fortified salad dressings. In addition, minor changes were also observed for the yellowness index (YI) of the fortified salad dressings before and after storage, which also implies a high chemical stability of the samples (i.e., non-enzymatic browning reactions did not occur during the storage time).

Overall, the oxidative stability of the capsule-fortified salad dressing correlated well with the oxidative stability of the delivery systems. A sharp increase in the PV was observed for the dressing samples fortified with the monoaxially-EAPG capsules irrespective of the oil load (i.e., 13 or 39 wt%), whilst a sustained increased was observed for the dressing samples fortified with the capsules produced by spray-drying (Figure 55A). On the contrary, and although the PV increased throughout storage, the salad dressing samples fortified with either the coaxially-EAPG capsules or the neat fish oil were significantly less oxidized (PV < 1.5 meqO_2/kg oil, $p > 0.05$, Figure 55A). These findings were in turn in line with the content of the selected SVOPs developed during storage, being the most oxidized samples those enriched with the monoaxially-EAPG capsules, followed by those enriched with the spray-dried capsules and then by the samples fortified with either the coaxially-EAPG capsules and the neat fish oil, with no significant differences among the latter (e.g., 2-ethylfuran, 1-penten-3-ol or (*E*,*E*)-2,4-heptadienal) (Figure 55B-F). Therefore, taking into account that the tocopherol content of the fortified dressings was similar among the samples and that it did not vary throughout storage (Figure S 32), the higher oxidative stability observed for the salad dressings enriched with the non-emulsion-based delivery systems (i.e., coaxially-EAPG capsules or the neat fish oil) was attributed to the better oxidative status of the fish oil prior to food fortification. By coaxial EAPG, neat fish oil was infused as the core solution therefore initial lipid oxidation caused by the emulsification step (i.e., air inclusion and temperature increase) was avoided. Furthermore, drying was carried out at ambient temperature, thus thermal degradation of the fish oil did not occur. The latter was further confirmed by the lower content of all the selected SVOPs found in the coaxially-

EAPG capsules right after production (Figure 54), which in turn confirms that the onset of lipid oxidation occurred during processing for the capsules produced by the emulsion-based encapsulation methods (i.e., spray-drying and monoaxial EAPG by air inclusion and temperature increase during fish oil emulsification, and presumably thermal degradation during spray-drying). Thus, the different oxidation rate and extent observed for the dressing samples fortified with the emulsion-based capsules (i.e., spray-dried or monoaxially-EAPG capsules) (Figure 55) was attributed to their different physicochemical properties influencing the diffusivity of prooxidant species through the encapsulating wall (i.e., particle size) (as previously discussed in Section 4.2.3). Therefore, our results show that a poorer initial oxidative status of the fish oil-loaded delivery system used for food fortification purposes significantly affect the oxidative stability of the enriched food matrix, especially when the particle size is significantly reduced.

5. REFERENCES

Acevedo-Fani, A., Guo, Q., Nasef, N., & Singh, H. (2021). Aspects of food structure in digestion and bioavailability of LCn-3PUFA-rich lipids. In P. J. García-Moreno, C. Jacobsen, A.-D. M. Sørensen, & B. Yesiltas (Eds.), *Omega-3 Delivery Systems* (pp. 427–448). Academic Press. https://doi.org/10.1016/b978-0-12-821391-9.00003-x

Anandharamakrishnan, C., Rielly, C. D., & Stapley, A. G. F. (2007). Effects of process variables on the denaturation of whey proteins during spray drying. *Drying Technology*, *25*(5), 799–807. https://doi.org/10.1080/07373930701370175

Andersen, A. B., Risbo, J., Andersen, M. L., & Skibsted, L. H. (2000). Oxygen permeation through an oil-encapsulating glassy food matrix studied by ESR line broadening using a nitroxyl spin probe. *Food Chemistry*, *70*(4), 499–508. www.elsevier.com/locate/foodchem

Andersen, M. L. (2021). Lipid oxidation studied by electron paramagnetic resonance (EPR). In *Omega-3 Delivery Systems*. Elsevier Inc. https://doi.org/10.1016/b978-0-12-821391-9.00004-1

Andersen, M. L., & Skibsted, L. H. (2018). ESR Spectroscopy for the Study of Oxidative Processes in Food and Beverages. In *Modern Magnetic Resonance* (pp. 1–14). Springer International Publishing. https://doi.org/10.1007/978-3-319-28275-6_25-1

Aquilani, C., Pérez-Palacios, T., Sirtori, F., Jiménez-Martín, E., Antequera, T., Franci, O., Acciaioli, A., Bozzi, R., & Pugliese, C. (2018). Enrichment of Cinta Senese burgers with omega-3 fatty

acids. Effect of type of addition and storage conditions on quality characteristics. *Grasas y Aceites*, *69*(1). https://doi.org/10.3989/gya.0671171

Barden, L., & Decker, E. A. (2013). Lipid oxidation in low-moisture food: A review. In *Critical Reviews in Food Science and Nutrition* (Vol. 56, Issue 15, pp. 2467–2482). Taylor and Francis Inc. https://doi.org/10.1080/10408398.2013.848833

Berton-Carabin, C. C., Ropers, M. H., & Genot, C. (2014). Lipid Oxidation in Oil-in-Water Emulsions: Involvement of the Interfacial Layer. *Comprehensive Reviews in Food Science and Food Safety*, *13*(5), 945–977. https://doi.org/10.1111/1541-4337.12097

Boerekamp, D. M. W., Andersen, M. L., Jacobsen, C., Chronakis, I. S., & García-Moreno, P. J. (2019). Oxygen permeability and oxidative stability of fish oil-loaded electrosprayed capsules measured by Electron Spin Resonance: Effect of dextran and glucose syrup as main encapsulating materials. *Food Chemistry*, *287*, 287–294. https://doi.org/10.1016/j.foodchem.2019.02.096

Both, E. M., Karlina, A. M., Boom, R. M., & Schutyser, M. A. I. (2018). Morphology development during sessile single droplet drying of mixed maltodextrin and whey protein solutions. *Food Hydrocolloids*, *75*, 202–210. https://doi.org/10.1016/j.foodhyd.2017.08.022

Brodkorb, A., Egger, L., Alminger, M., Alvito, P., Assunção, R., Ballance, S., Bohn, T., Bourlieu-Lacanal, C., Boutrou, R., Carrière, F., Clemente, A., Corredig, M., Dupont, D., Dufour, C., Edwards, C., Golding, M., Karakaya, S., Kirkhus, B., Le Feunteun, S., … Recio, I. (2019). INFOGEST static in vitro simulation of gastrointestinal food digestion. *Nature Protocols*, *14*(4), 991–1014. https://doi.org/10.1038/s41596-018-0119-1

Busolo, M. A., Torres-Giner, S., Prieto, C., & Lagaron, J. M. (2019). Electrospraying assisted by pressurized gas as an innovative high-throughput process for the microencapsulation and stabilization of docosahexaenoic acid-enriched fish oil in zein prolamine. *Innovative Food Science and Emerging Technologies*, *51*, 12–19. https://doi.org/10.1016/j.ifset.2018.04.007

Calder, P. C. (2013). Nutritional benefits of omega-3 fatty. In *Food Enrichment with Omega-3 Fatty Acids* (pp. 3–26). Woodhead Publishing Limited. https://doi.org/10.1533/978-0-85709-886-3.1.3

Calder, P. C. (2014). Very long chain omega-3 (n-3) fatty acids and human health. *European Journal of Lipid Science and Technology*, *116*(10), 1280–1300. https://doi.org/10.1002/ejlt.201400025

Calder, P. C. (2021). Health benefits of omega-3 fatty acids. In P. J. García-Moreno, C. Jacobsen, A.-D. Moltke-Sørensen, & B. Yesiltas (Eds.), *Omega-3 Delivery Systems* (pp. 25–53). Academic Press. https://doi.org/10.1016/b978-0-12-821391-9.00006-5

Chang, Y., & McClements, D. J. (2016). Influence of emulsifier type on the in vitro digestion of fish oil-in-water emulsions in the presence of an anionic marine polysaccharide (fucoidan): Caseinate, whey protein, lecithin, or Tween 80. *Food Hydrocolloids*, *61*, 92–101. https://doi.org/10.1016/j.foodhyd.2016.04.047

Davidov-Pardo, G., Roccia, P., Salgado, D., León, A. E., & Pedroza-Islas, R. (2008). Utilization of Different Wall Materials to Microencapsulate Fish Oil Evaluation of its Behavior in Bread Products. *American Journal of Food Technology*, *3*(6), 384–393. https://doi.org/10.3923/ajft.2008.384.393

Demets, R., & Foubert, I. (2021). Traditional and novel sources of long-chain omega-3 fatty acids. In *Omega-3 Delivery Systems: Production, Physical Characterization and Oxidative Stability* (pp. 3–23). Elsevier. https://doi.org/10.1016/B978-0-12-821391-9.00013-2

Djuricic, I., & Calder, P. C. (2022). Polyunsaturated fatty acids and metabolic health: novel insights. In *Current Opinion in Clinical Nutrition and Metabolic Care* (Vol. 25, Issue 6, pp. 436–442). Lippincott Williams and Wilkins. https://doi.org/10.1097/MCO.0000000000000865

Drusch, S., & Berg, S. (2008). Extractable oil in microcapsules prepared by spray-drying: Localisation, determination and impact on oxidative stability. *Food Chemistry*, *109*(1), 17–24. https://doi.org/10.1016/j.foodchem.2007.12.016

Drusch, S., Rätzke, K., Shaikh, M. Q., Serfert, Y., Steckel, H., Scampicchio, M., Voigt, I., Schwarz, K., & Mannino, S. (2009). Differences in free volume elements of the carrier matrix affect the stability of microencapsulated lipophilic food ingredients. *Food Biophysics*, *4*(1), 42–48. https://doi.org/10.1007/s11483-008-9100-9

EFSA. (2010). Scientific Opinion on Dietary Reference Values for fats, including saturated fatty acids, polyunsaturated fatty acids, monounsaturated fatty acids, trans fatty acids, and cholesterol. *EFSA Journal*, *8*(3), 1–107. https://doi.org/10.2903/j.efsa.2010.1461

Elias, R. J., Kellerby, S. S., & Decker, E. A. (2008). Antioxidant activity of proteins and peptides. *Critical Reviews in Food Science and Nutrition*, *48*(5), 430–441. https://doi.org/10.1080/10408390701425615

Frankel, E. N. (2012). Free radical oxidation. In *Lipid Oxidation* (2nd Ed., pp. 15–24). Woodhead Publishing Limited. https://doi.org/10.1533/9780857097927.15

García-Moreno, P. J., Pelayo, A., Yu, S., Busolo, M., Lagaron, J. M., Chronakis, I. S., & Jacobsen, C. (2018). Physicochemical characterization and oxidative stability of fish oil-loaded electrosprayed capsules: Combined use of whey protein and carbohydrates as wall materials. *Journal of Food Engineering*, *231*, 42–53. https://doi.org/10.1016/j.jfoodeng.2018.03.005

García-Moreno, P. J., Rahmani-Manglano, N. E., Chronakis, I. S., Guadix, E. M., Yesiltas, B., Sørensen, A.-D. M., & Jacobsen, C. (2021). Omega-3 nano-microencapsulates produced by electrohydrodynamic processing. In P. J. García-Moreno, C. Jacobsen, A.-D. M. Sørensen, & B. Yesiltas (Eds.), *Omega-3 Delivery Systems. Production, Physical Characterization and Oxidative Stability* (pp. 345–370). Academic Press. https://doi.org/10.1016/b978-0-12-821391-9.00017-x

Gharsallaoui, A., Roudaut, G., Chambin, O., Voilley, A., & Saurel, R. (2007). Applications of spray-drying in microencapsulation of food ingredients: An overview. In *Food Research International* (Vol. 40, Issue 9, pp. 1107–1121). https://doi.org/10.1016/j.foodres.2007.07.004

Ghelichi, S., Hajfathalian, M., García-Moreno, P. J., Yesiltas, B., Moltke-Sørensen, A.-D., & Jacobsen, C. (2021). Food enrichment with omega-3 polyunsaturated fatty acids. In P. J. García-Moreno, C. Jacobsen, A.-D. M. Sørensen, & B. Yesiltas (Eds.), *Omega-3 Delivery Systems* (pp. 395–425). Academic Press. https://doi.org/10.1016/b978-0-12-821391-9.00020-x

Guillén, M. D., & Cabo, N. (1999). Usefulness of the frequency data of the Fourier transform infrared spectra to evaluate the degree of oxidation of edible oils. *Journal of Agricultural and Food Chemistry*, *47*(2), 709–719. https://doi.org/10.1021/jf9808123

Guillén, M. D., & Cabo, N. (2000). Some of the most significant changes in the Fourier transform infrared spectra of edible oils under oxidative conditions. *Journal of the Science of Food and Agriculture*, *80*(14), 2028–2036. https://doi.org/10.1002/1097-0010(200011)80:14<2028::AID-JSFA713>3.3.CO;2-W

Hermund, D., Jacobsen, C., Chronakis, I. S., Pelayo, A., Yu, S., Busolo, M., Lagaron, J. M., Jónsdóttir, R., Kristinsson, H. G., Akoh, C. C., & García-Moreno, P. J. (2019). Stabilization of Fish Oil-Loaded Electrosprayed Capsules with Seaweed and Commercial Natural Antioxidants: Effect on the Oxidative Stability of Capsule-Enriched Mayonnaise. *European Journal of Lipid Science and Technology*, *121*(4). https://doi.org/10.1002/ejlt.201800396

Hoffmann, S. V., Fano, M., & van de Weert, M. (2016). Circular Dichroism Spectroscopy for Structural Characterization of Proteins. In *Analytical Techniques in the Pharmaceutical Sciences* (pp. 223–251). https://doi.org/10.1007/978-1-4939-4029-5_6

Jacobsen, C., García-Moreno, P. J., Mendes, A. C., Mateiu, R. V., & Chronakis, I. S. (2018). Use of Electrohydrodynamic Processing for Encapsulation of Sensitive Bioactive Compounds and Applications in Food. *Annual Review of Food Science and Technology*, *9*(1), 525–549. https://doi.org/10.1146/annurev-food-030117-012348

Jacobsen, C., García-Moreno, P. J., Yesiltas, B., & Sørensen, A. D. M. (2021). Lipid oxidation and traditional methods for evaluation. In *Omega-3 Delivery Systems: Production, Physical*

Characterization and Oxidative Stability (pp. 183–200). Elsevier. https://doi.org/10.1016/B978-0-12-821391-9.00009-0

Jaworek, A. (2016). Electrohydrodynamic microencapsulation technology. In *Encapsulations. Nanotechnology in the Agri-Food Industry, Volume 2* (pp. 1–45). Elsevier. https://doi.org/10.1016/b978-0-12-804307-3.00001-6

Jeyakumari, A., Janarthanan, G., Chouksey, M. K., & Venkateshwarlu, G. (2016). Effect of fish oil encapsulates incorporation on the physico-chemical and sensory properties of cookies. *Journal of Food Science and Technology*, *53*(1), 856–863. https://doi.org/10.1007/s13197-015-1981-2

Lagaron, J. M., Castro, S., Galan, D., & Valle, J. M. (2017). *Installation and procedure of industrial encapsulation of thermolabile substances. P201631725.*

Layé, S., Nadjar, A., Joffre, C., & Bazinet, R. P. (2018). Anti-inflammatory effects of omega-3 fatty acids in the brain: Physiological mechanisms and relevance to pharmacology. *Pharmacological Reviews*, *70*(1), 12–38. https://doi.org/10.1124/pr.117.014092

Liceaga, A. M., & Hall, F. (2018). Nutritional, functional and bioactive protein hydrolysates. In *Encyclopedia of Food Chemistry*. Elsevier. https://doi.org/10.1016/B978-0-08-100596-5.21776-9

Linke, A., Hinrichs, J., & Kohlus, R. (2020). Impact of the powder particle size on the oxidative stability of microencapsulated oil. *Powder Technology*, *364*, 115–122. https://doi.org/10.1016/j.powtec.2020.01.077

Linke, A., Linke, T., & Kohlus, R. (2020). Contribution of the Internal and External Oxygen to the Oxidation of Microencapsulated Fish Oil. *European Journal of Lipid Science and Technology*, *1900381*, 1900381. https://doi.org/10.1002/ejlt.201900381

Linke, A., Weiss, J., & Kohlus, R. (2020). Oxidation rate of the non-encapsulated- and encapsulated oil and their contribution to the overall oxidation of microencapsulated fish oil particles. *Food Research International*, *127*(September 2019), 108705. https://doi.org/10.1016/j.foodres.2019.108705

Linke, A., Weiss, J., & Kohlus, R. (2021). Impact of the oil load on the oxidation of microencapsulated oil powders. *Food Chemistry*, *341*(September 2020), 128153. https://doi.org/10.1016/j.foodchem.2020.128153

Loscertales, I. G., Barrero, A., Guerrero, I., Cortijo, R., Marquez, M., & Gañán-Calvo, A. M. (2002). Micro/nano encapsulation via electrified coaxial liquid jets. *Science*, *295*(5560), 1695–1698. https://doi.org/10.1126/science.1067595

Ma, Z., Boye, J. I., Fortin, J., Simpson, B. K., & Prasher, S. O. (2013). Rheological, physical stability, microstructural and sensory properties of salad dressings supplemented with raw and thermally treated lentil flours. *Journal of Food Engineering*, *116*(4), 862–872. https://doi.org/10.1016/j.jfoodeng.2013.01.024

McClements, D. J. (2018). Enhanced delivery of lipophilic bioactives using emulsions: A review of major factors affecting vitamin, nutraceutical, and lipid bioaccessibility. *Food and Function*, *9*(1), 22–41. https://doi.org/10.1039/c7fo01515a

McClements, D. J., & Decker, E. (2018). Interfacial Antioxidants: A Review of Natural and Synthetic Emulsifiers and Coemulsifiers That Can Inhibit Lipid Oxidation. *Journal of Agricultural and Food Chemistry*, *66*(1), 20–25. https://doi.org/10.1021/acs.jafc.7b05066

Miguel, G. A., Jacobsen, C., Prieto, C., Kempen, P. J., Lagaron, J. M., Chronakis, I. S., & García-Moreno, P. J. (2019). Oxidative stability and physical properties of mayonnaise fortified with zein electrosprayed capsules loaded with fish oil. *Journal of Food Engineering*, *263*, 348–358. https://doi.org/10.1016/j.jfoodeng.2019.07.019

Nguyen, Q. V., Malau-Aduli, B. S., Cavalieri, J., Malau-Aduli, A. E. O., & Nichols, P. D. (2019). Enhancing omega-3 long-chain polyunsaturated fatty acid content of dairy-derived foods for human consumption. *Nutrients*, *11*(4), 1–23. https://doi.org/10.3390/nu11040743

O'Regan, J., & Mulvihill, D. M. (2010). Sodium caseinate-maltodextrin conjugate hydrolysates: Preparation, characterisation and some functional properties. *Food Chemistry*, *123*(1), 21–31. https://doi.org/10.1016/j.foodchem.2010.03.115

Orlien, V., Andersen, A. B., Sinkko, T., & Skibsted, L. H. (2000). Hydroperoxide formation in rapeseed oil encapsulated in a glassy food model as influenced by hydrophilic and lipophilic radicals. *Food Chemistry*, *68*, 191–199. https://doi.org/https://doi.org/10.1016/S0308-8146(99)00177-6

Padial-Domínguez, M., Espejo-Carpio, F. J., García-Moreno, P. J., Jacobsen, C., & Guadix, E. M. (2020). Protein derived emulsifiers with antioxidant activity for stabilization of omega-3 emulsions. *Food Chemistry*, *329*(127148). https://doi.org/10.1016/j.foodchem.2020.127148

Patrick, K. E., Lv, Y., Muhamyankaka, V., Ocen, D., Ntsama, I. S. B., & Zhang, X. (2013). Development of EPA-DHA Microcapsules Supplemented Probiotic Fermented Milk. *Akademik Gıda*, *11*(3–4), 6–15. http://www.academicfoodjournal.com

Peighambardoust, S. H., Karami, Z., Pateiro, M., & Lorenzo, J. M. (2021). A review on health-promoting, biological, and functional aspects of bioactive peptides in food applications. *Biomolecules*, *11*(5), 1–21. https://doi.org/10.3390/biom11050631

Perez, O. E., & Pilosof, A. M. R. (2004). Pulsed electric fields effects on the molecular structure and gelation of β-lactoglobulin concentrate and egg white. *Food Research International*, *37*(1), 102–110. https://doi.org/10.1016/j.foodres.2003.09.008

Prieto, C., Evtoski, Z., Pardo-Figuerez, M., Hrakovsky, J., & Lagaron, J. M. (2021). Nanostructured Valsartan Microparticles with Enhanced Bioavailability Produced by High-Throughput Electrohydrodynamic Room-Temperature Atomization. *Molecular Pharmaceutics*, *18*(8), 2947–2958. https://doi.org/10.1021/acs.molpharmaceut.1c00098

Prieto, C., & Lagaron, J. M. (2020). Nanodroplets of docosahexaenoic acid-enriched algae oil encapsulated within microparticles of hydrocolloids by emulsion electrospraying assisted by pressurized gas. *Nanomaterials*, *10*(2). https://doi.org/10.3390/nano10020270

Punia, S., Sandhu, K. S., Siroha, A. K., & Dhull, S. B. (2019). Omega 3-metabolism, absorption, bioavailability and health benefits–A review. *PharmaNutrition*, *10*, 100162. https://doi.org/10.1016/j.phanu.2019.100162

Rahali, V., Chobert, J. M., Haertlé, T., & Guéguen, J. (2000). Emulsification of chemical and enzymatic hydrolysates of β-lactoglobulin: Characterization of the peptides adsorbed at the interface. *Nahrung - Food*, *44*(2), 89–95. https://doi.org/10.1002/(sici)1521-3803(20000301)44:2<89::aid-food89>3.0.co;2-u

Rahmani-Manglano, N. E., García-Moreno, P. J., Espejo-Carpio, F. J., Pérez-Gálvez, A. R., & Guadix-Escobar, E. M. (2020). The Role of Antioxidants and Encapsulation Processes in Omega-3 Stabilization. In M. A. Aboudzadeh (Ed.), *Emulsion-based Encapsulation of Antioxidants. Food Bioactive Ingredients.* (pp. 339–386). Springer, Cham. https://doi.org/10.1007/978-3-030-62052-3_10

Rahmani-Manglano, N. E., González-Sánchez, I., García-Moreno, P. J., Espejo-Carpio, F. J., Jacobsen, C., & Guadix, E. M. (2020). Development of fish oil-loaded microcapsules containing whey protein hydrolysate as film-forming material for fortification of low-fat mayonnaise. *Foods*, *9*(5). https://doi.org/10.3390/foods9050545

Rahmani-Manglano, N. E., Guadix, E. M., Jacobsen, C., & García-Moreno, P. J. (2023). Comparative Study on the Oxidative Stability of Encapsulated Fish Oil by Monoaxial or Coaxial Electrospraying and Spray-Drying. *Antioxidants*, *12*(2). https://doi.org/https://doi.org/10.3390/antiox12020266

Ramakrishnan, S., Ferrando, M., Aceña-Muñoz, L., Mestres, M., De Lamo-Castellví, S., & Güell, C. (2014). Influence of Emulsification Technique and Wall Composition on Physicochemical Properties and Oxidative Stability of Fish Oil Microcapsules Produced by Spray Drying. *Food and Bioprocess Technology*, *7*(7), 1959–1972. https://doi.org/10.1007/s11947-013-1187-4

Roos, Y. H. (2010). Glass transition temperature and its relevance in food processing. *Annual Review of Food Science and Technology*, *1*(1), 469–496. https://doi.org/10.1146/annurev.food.102308.124139

Ruiz-Álvarez, J. M., del Castillo-Santaella, T., Maldonado-Valderrama, J., Guadix, A., Guadix, E. M., & García-Moreno, P. J. (2022). pH influences the interfacial properties of blue whiting (M. poutassou) and whey protein hydrolysates determining the physical stability of fish oil-in-water emulsions. *Food Hydrocolloids*, *122*(107075). https://doi.org/10.1016/j.foodhyd.2021.107075

Salvia-Trujillo, L., McClements, D. J., & Martín-Belloso, O. (2021). Nanoemulsion design for the delivery of omega-3 fatty acids: formation, oxidative stability, and digestibility. In P. J. García-Moreno, C. Jacobsen, A.-D. M. Sørensen, & B. Yesiltas (Eds.), *Omega-3 Delivery Systems* (pp. 295–319). Academic Press. https://doi.org/10.1016/b978-0-12-821391-9.00016-8

Santos, D., Maurício, A. C., Sencadas, V., Santos, J. D., Fernandes, M. H., & Gomes, P. S. (2018). Spray Drying: An Overview. *Biomaterials - Physics and Chemistry - New Edition*. https://doi.org/10.5772/intechopen.72247

Serfert, Y., Drusch, S., & Schwarz, K. (2009). Chemical stabilisation of oils rich in long-chain polyunsaturated fatty acids during homogenisation, microencapsulation and storage. *Food Chemistry*, *113*(4), 1106–1112. https://doi.org/10.1016/j.foodchem.2008.08.079

Shahidi, F., & Zhong, Y. (2011). Revisiting the polar paradox theory: A critical overview. *Journal of Agricultural and Food Chemistry*, *59*(8), 3499–3504. https://doi.org/10.1021/jf104750m

Shen, Z., Apriani, C., Weerakkody, R., Sanguansri, L., & Augustin, M. A. (2011). Food matrix effects on in vitro digestion of microencapsulated tuna oil powder. *Journal of Agricultural and Food Chemistry*, *59*(15), 8442–8449. https://doi.org/10.1021/jf201494b

Solomando, J. C., Antequera, T., González-Mohíno, A., & Perez-Palacios, T. (2020). Fish oil/lycopene microcapsules as a source of eicosapentaenoic and docosahexaenoic acids: a case study on spreads. *Journal of the Science of Food and Agriculture*, *100*(5), 1875–1886. https://doi.org/10.1002/jsfa.10188

Solomando, J. C., Antequera, T., & Perez-Palacios, T. (2020). Evaluating the use of fish oil microcapsules as omega-3 vehicle in cooked and dry-cured sausages as affected by their processing, storage and cooking. *Meat Science*, *162*. https://doi.org/10.1016/j.meatsci.2019.108031

Sørensen, A.-D. M., García-Moreno, P. J., Yesiltas, B., & Jacobsen, C. (2021). Introduction to delivery systems and stability issues. In *Omega-3 Delivery Systems* (pp. 107–117). Elsevier. https://doi.org/10.1016/b978-0-12-821391-9.00015-6

Tamm, F., Gies, K., Diekmann, S., Serfert, Y., Strunskus, T., Brodkorb, A., & Drusch, S. (2015). Whey protein hydrolysates reduce autoxidation in microencapsulated long chain polyunsaturated fatty acids. *European Journal of Lipid Science and Technology*, *117*(12), 1960–1970. https://doi.org/10.1002/ejlt.201400574

Thomsen, B. R., Yesiltas, B., Sørensen, A. D. M., Hermund, D. B., Glastrup, J., & Jacobsen, C. (2016). Comparison of Three Methods for Extraction of Volatile Lipid Oxidation Products from Food Matrices for GC–MS Analysis. *JAOCS, Journal of the American Oil Chemists' Society*, *93*(7), 929–942. https://doi.org/10.1007/s11746-016-2837-2

Unnikrishnan, P., Puthenveetil Kizhakkethil, B., Annamalai, J., Ninan, G., Aliyamveetil Abubacker, Z., & Chandragiri Nagarajarao, R. (2019). Tuna red meat hydrolysate as core and wall polymer for fish oil encapsulation: a comparative analysis. *Journal of Food Science and Technology*, *56*(4), 2134–2146. https://doi.org/10.1007/s13197-019-03694-w

Velasco, J., Andersen, M. L., & Skibsted, L. H. (2005). Electron spin resonance spin trapping for analysis of lipid oxidation in oils: Inhibiting effect of the spin trap α-phenyl-N-tert-butylnitrone on lipid oxidation. *Journal of Agricultural and Food Chemistry*, *53*(5), 1328–1336. https://doi.org/10.1021/jf049051w

Velasco, J., Andersen, M. L., & Skibsted, L. H. (2021). ESR spin trapping for in situ detection of radicals involved in the early stages of lipid oxidation of dried microencapsulated oils. *Food Chemistry*, *341*(June 2020), 128227. https://doi.org/10.1016/j.foodchem.2020.128227

Velasco, J., Marmesat, S., Dobarganes, C., & Márquez-Ruiz, G. (2006). Heterogeneous aspects of lipid oxidation in dried microencapsulated oils. *Journal of Agricultural and Food Chemistry*, *54*(5), 1722–1729. https://doi.org/10.1021/jf052313p

Wallace, B. A., & Janes, R. W. (2001). Synchrotron radiation circular dichroism spectroscopy of proteins: Secondary structure, fold recognition and structural genomics. *Current Opinion in Chemical Biology*, *5*(5), 567–571. https://doi.org/10.1016/S1367-5931(00)00243-X

Xiang, B. Y., Ngadi, M. O., Simpson, M. V, & Ochoa-Martínez, L. A. (2008). Effect of pulsed electric field on structural modification and thermal properties of whey protein isolate. *CSBE/SCGAB 2008 Annual Conference*, *July*, 15. https://bit.ly/2PlvkJ7

Zhai, J., Wooster, T. J., Hoffmann, S. V., Lee, T. H., Augustin, M. A., & Aguilar, M. I. (2011). Structural rearrangement of β-lactoglobulin at different oil-water interfaces and its effect on emulsion stability. *Langmuir*, *27*(15), 9227–9236. https://doi.org/10.1021/la201483y

Zhou, Y. T., Yin, J. J., & Lo, Y. M. (2011). Application of ESR spin label oximetry in food science. In *Magnetic Resonance in Chemistry* (Vol. 49, Issue SUPPL. 1). https://doi.org/10.1002/mrc.2822

CHAPTERS

I. The Role of Antioxidants and Encapsulation Processes in Omega-3 Stabilization *

In the last years the production of functional food systems enriched with omega-3 polyunsaturated fatty acids (ω-3 PUFAs) has gained great interest, not only because of the health benefits attributed especially to eicosapentaenoic acid (EPA; C20: 5 n-3) and docosahexaenoic acid (DHA; C22:6 n-3), but also because the imbalanced intake ratio of omega-6/omega-3 in Western diets. However, ω-3 PUFAs are highly prone to lipid oxidation. This is a big drawback since it leads to the loss of their nutritional properties together with the appearance of odor/flavor active compounds and other toxic lipid oxidation products. In this regard, the development of efficient delivery systems (e.g., emulsions or encapsulates) which prevent ω-3 PUFAs oxidation when incorporated to complex food matrices is of great importance. This chapter aims to review the most important advances of the last decade regarding ω-3 PUFAs stabilization techniques, either by chemical means (e.g., addition of antioxidants), physical means (e.g., encapsulation) or both (e.g., ω-3 PUFAs encapsulation in presence of antioxidants) and subsequent addition to food matrices. In addition, the new trends in electrohydrodynamic processing (electrospraying and coaxial electrospraying) in order to produce ω-3 PUFAs-loaded encapsulates are also discussed.

* BOOK CHAPTER: N.E. Rahmani-Manglano, P.J. García-Moreno, F.J. Espejo-Carpio, A.R. Pérez-Gálvez & E.M. Guadix-Escobar. (2020). The Role of Antioxidants and Encapsulation Processes in Omega-3 Stabilization. In*:* *Emulsion-based Encapsulation of Antioxidants*, 339-386

1. OMEGA-3 POLYUNSATURATED FATTY ACIDS

Over the last decades the importance of ω-3 PUFAs, especially EPA and DHA, in human nutrition has been the focus of scientific research since these long chain fatty acids have been considered to improve human health as a result of their influence in cell and tissue function (Calder, 2014). High ω-3 PUFAs intake has been associated with a reduced risk of suffering from major chronic diseases such as cardiovascular diseases (CVD) (e.g., coronary heart disease (CHD) and stroke), some cancers (e.g., colorectal, prostate and lung cancer), hypertension, inflammatory diseases (e.g., arthritis, psoriasis and asthma), neurodegenerative diseases (e.g., Alzheimer and Parkinson), type-2 diabetes and obesity (Calder, 2014; Nguyen et al., 2019; Punia et al., 2019). In addition, it is well known that DHA plays an important structural role in the brain and eye since it is the main ω-3 PUFA in the brain (Layé et al., 2018) and it constitutes more than 50% of the fatty acids present in the outer segments of the retina (Calder, 2014). Thus, DHA supply is essential, especially when these tissues are developing (from gestation to 18 months after birth) for optimal neurodevelopment (memory and learning ability) and visual development for fetus and infants (Calder, 2014; Jacobsen, 2016). Despite all the research carried out in this field, there are still some controversies regarding the role of ω-3 PUFAs and their beneficial effects in the prevention of some health conditions (e.g., mental disorders, diabetes or obesity) (Nguyen et al., 2019). However, there is strong scientific evidence establishing a cause-and-effect relationship between ω-3 PUFAs consumption and some beneficial physiological effects (e.g., maintenance of normal brain function or cardiac function). Based on the later, the European Food Safety Authority (EFSA) has allowed the use of different health claims for EPA and/or DHA pursuant to Article 13(1) and Article 14 of Regulation (EC) No 1924/2006 (Table 3). In the USA, the Food and Drug Administration (FDA) has recently summited a letter of enforcement discretion, which allows the use of different qualified health claims regarding the relationship between ω-3 PUFAs intake and reduction of blood pressure in general population, provided that the dietary supplement and/or conventional food contains at least 0.8 g EPA and DHA combined per serving (FDA, 2019). However, as the scientific evidence is considered insufficient and inconsistent by the agency, the qualified health claim must be accompanied by a disclaimer (FDA, 2019).

Table 3. Summary of EFSA's allowed health claims for ω-3 PUFAs.

ω-3 PUFAs	Health Claim	Target Population	Dose	Reference
EPA + DHA	Maintenance of normal blood pressure	Adult men and women	3 g EPA and DHA per day	(EFSA, 2009)
	Maintenance of normal cardiac function	General population	250 mg EPA and DHA per day	(EFSA, 2010c)
	Maintenance of normal (fasting) blood concentration of triglycerides	Adult men and women	2 g EPA and DHA per day	(EFSA, 2010c)
DHA	Maintenance of normal (fasting) blood concentration of triglycerides	Adult men and women	2 g DHA per day in one or more servings	(EFSA, 2010b)
	Maintenance of normal brain function	General population	250 mg DHA in one or more servings	(EFSA, 2010b)
	Maintenance of normal vision	General population	250 mg DHA in one or more servings	(EFSA, 2010b)
	DHA contributes to normal brain development	Older infants and young children (> 6 - 24 m.o.)	100 mg DHA in one or more servings	(EFSA, 2014)
		Children (2 - 18 y.o.)	250 mg DHA in one or more servings	

Abbreviations: m.o.: months old; y.o.: years old.

Because of the recognized health benefits derived from ω-3 PUFAs consumption, several authoritative bodies and expert scientific organizations have set a series of recommendations to increase their intake. Internationally, the Food and Agriculture Organization of the United Nations (FAO) recommends a daily intake of 250 mg of EPA+DHA for adult men and non-pregnant and non-lactating adult women. The minimum intake recommended in case of adult pregnant or lactating women, in order to assure adult health and fetal and infant development, for EPA+DHA is 300 mg per day of which at least 200 mg per day should be DHA. The EPA+DHA intake recommendation for children is: (i) 100 – 150 mg/day for children from 2 to 4 years old, (ii) 150 – 200 mg/day for children from 4 to 6 years old and (iii) 200 – 300 mg/day for children from 6 to 10 years old (FAO, 2010). In Europe, the EFSA set an adequate intake (AI) of 250 mg per day for EPA+DHA in adults, while for pregnant or lactating women the recommended intake is that of the AI value plus 100 – 200 mg per day of DHA. In case of infants (from 6 months to 2 years), the AI is set to 100 mg per day

of DHA. From 2 years onwards the AI is that for adults (250 mg per day of EPA+DHA) (EFSA, 2010a). Moreover, the EFSA has set a recommended intake for EPA+DHA of 250 – 500 mg per day for European adults based on cardiovascular risk considerations (EFSA, 2012).

EPA and DHA can be synthetized in the organism from α-linolenic acid (ALA; C18:3 n-3), which is the precursor of the ω-3 PUFAs family. This fatty acid is in turn synthesized from linoleic acid (LA; C18:2 n-6) in a desaturation reaction catalysed by Δ15-desaturase enzyme, which is only found in plants. Thus, ALA is considered as an essential fatty acid since it cannot be synthesized de novo by humans and it needs to be provided in the diet. ALA is naturally found in seeds, nuts and seed oils (e.g., flaxseeds, walnuts or soybean oil) (Calder, 2013). When ALA enters the human body, it converts to EPA and DHA by the metabolic path shown in Figure 12. This synthesis occurs mainly in the liver but in a very little extent since only about 8% of ALA convers to EPA and 1% to DHA (Layé et al., 2018). The synthesis reaction is also very slow. Moreover, the metabolic path of conversion from ALA to EPA is in direct competition with the metabolic path of conversion of LA (ω-6 PUFAs family precursor) to arachidonic acid (ARA; C20:4 n-6), since both reactions are catalysed by the same enzymes (Δ6-desaturase, Elongase and Δ5-desaturase) (Calder, 2013).

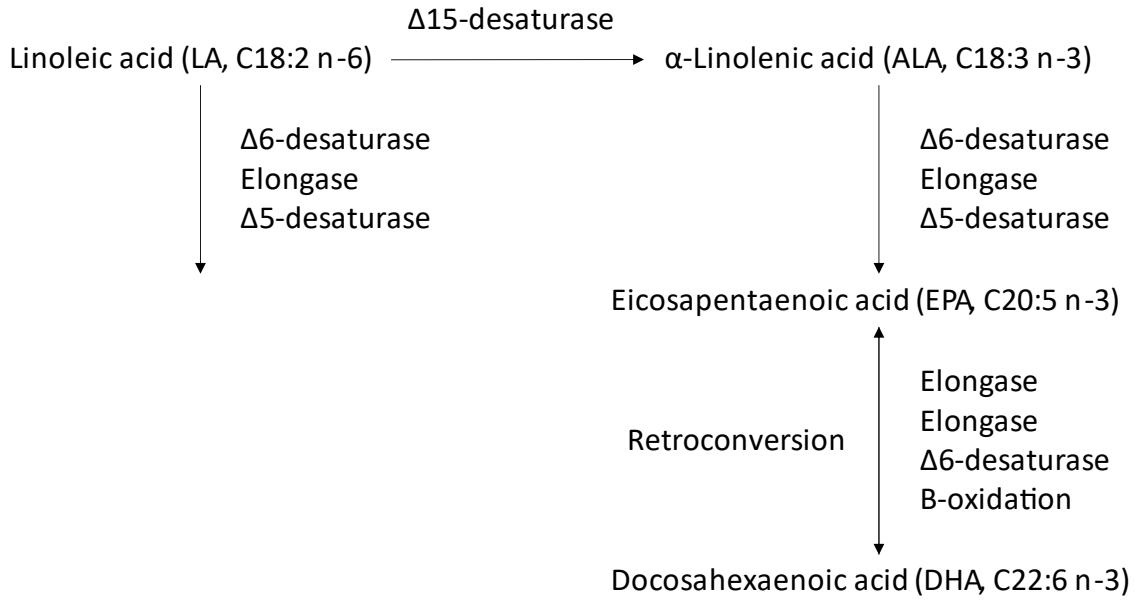

Figure 12. Metabolic pathway of biosynthesis of α-linolenic acid (ALA), eicosapentaenoic acid (EPA) and docosahexaenoic acid (DHA).

Changes in food technology and eating habits in industrial societies have led to an unbalanced intake ratio omega-6/omega-3 of ~20/1 due to a high consumption of vegetables oils (e.g., corn oil) (Simopoulos, 2011). This situation interferes with ω-3 PUFAs metabolism and, since ω-6 PUFAs are more present in current human diets, the synthesis of ω-6 PUFAs in the organism is quantitatively more important. The increase of ω-6 PUFAs in diet exert a proinflammatory and prothrombotic effect, which is a risk factor for major chronic diseases such as CHD, obesity or diabetes, among others (Simopoulos, 2016). Thus, direct ω-3 PUFAs (e.g., EPA and DHA) intake is required for a balanced diet.

The main sources of dietary EPA and DHA are fish, krill, algae and other seafood (e.g., crab, prawns, lobsters or mussels) together with marine oils. However, these long chain polyunsaturated fatty acids (LC ω-3 PUFAs) are also modestly present in some other animal-derived foodstuff (e.g., meat, milk or eggs) (Calder, 2014; Nguyen et al., 2019). Among fishes, two categories are distinguished: (i) lean fish, which stores lipid in the liver (e.g., cod, haddock and plaice) and (ii) fatty fish, which stores lipid in the flesh (e.g., salmon, mackerel, herring, sardines, trout and tuna) (Calder, 2013). Due to differences in the diet and metabolism, the amount and ratio of EPA and DHA vary depending on fish type and species. Fatty fishes' content per serving of dietary ω-3 PUFAs is up to 10-folds those of lean fishes (Calder, 2013, 2014). On the other hand, marine oils are those obtained from the flesh or liver of the fish, crustaceans, cephalopods (e.g., squid) or marine mammals (Jacobsen, 2016). Flesh fish oils are produced from the flesh of fatty fishes (e.g., sardine, anchovy, tuna, pollack, salmon and catfish) and are the most manufactured among the marine oils, while liver fish oils are obtained from the liver of lean fishes (e.g., cod, hake, halibut and shark) and constitutes less than 3% of the total marine oils production (Jacobsen, 2016). In most fish oils (flesh fish oils and liver fish oils), EPA and DHA are present as triacylglycerides (TAG). However, the amount and ratio of these LC ω-3 PUFAs, once again, differs among oils. Other sources of marine oil are algae and krill. Krill oil contains ω-3 PUFAs in the form of phospholipids whilst algae oil contains such fatty acids in the form of TAG. Algae oils are of great interest, especially in infant formulas production, since their DHA content is up to 52% (Jacobsen, 2016).

Nowadays, fish, krill, algae and marine oils consumption is insufficient to meet the requirements of a healthy diet. In this sense, food industry aims to produce added-value food products enriched mainly with fish oil containing high levels of EPA and DHA. However, due to the characteristic fishy flavor of marine oils and their prone to oxidation, efficient

delivery systems capable of masking the taste and preventing lipid oxidation needs to be designed.

2. LIPID OXIDATION

Due to the high degree of unsaturation, LC ω-3 PUFAs (e.g., EPA and DHA) are very prone to oxidation leading to the loss of their nutritional properties and to the formation of several off-odor and off-taste compounds (e.g., propanal) and other toxic compounds (e.g., malonaldehyde).

Lipid oxidation occurs through different mechanisms such as enzymatic oxidation, photo-oxidation and autoxidation, being the latter the most important one. While enzymatic oxidation takes place in presence of lipoxygenase enzymes and mainly affects vegetal oils, photo-oxidation occurs in presence of light and/or photosensitizers (e.g., pigments). Although photo-oxidation is not the main oxidation mechanism, it is of great importance since it influences autoxidation mechanism and the distribution of primary oxidation compounds (Frankel, 2012c).

Autoxidation occurs as a free radical chain reaction when oxygen in its ground state reacts with unsaturated lipids under mild conditions (Frankel, 2012a). The sequence of reactions taking place can be classified into three stages, namely: (I) initiation, (II) propagation and (III) termination (Figure 13).

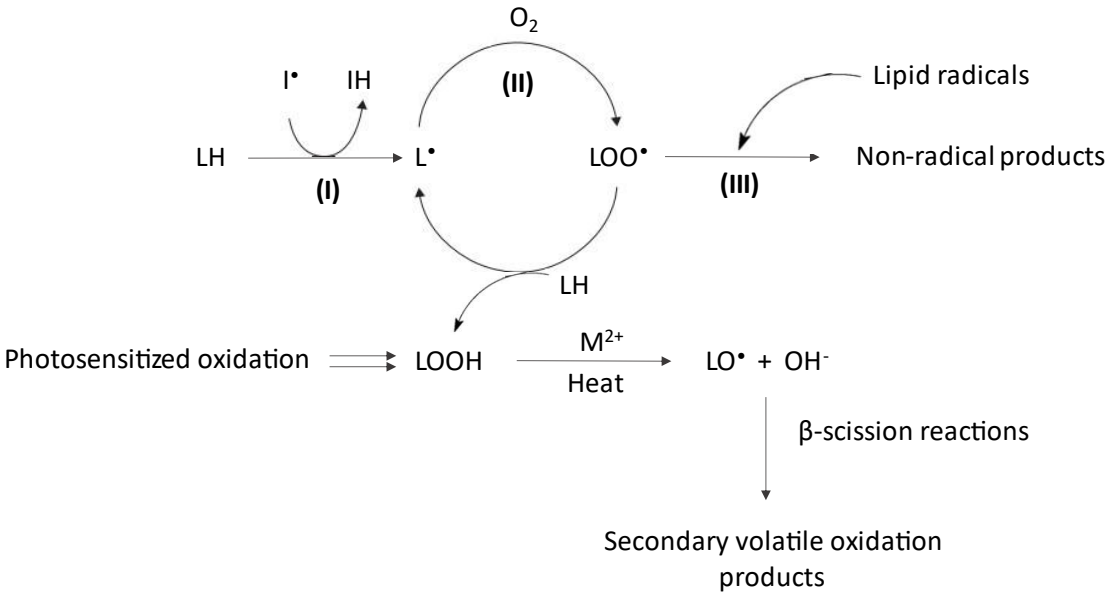

Figure 13. Schematic representation of main lipid oxidation mechanisms.

The initiation stage is characterized by the formation of very reactive lipid free radicals (or alkyl radicals) (L•) due to the loss of a hydrogen atom (H+) by an unsaturated lipid (LH) in the presence of initiators (e.g., heat, light or redox metals) (reaction 1).

$$LH + I \rightarrow IH + L^{\bullet} \quad (9)$$

Depending on the initiator agent, lipid free radicals (L•) are produced by different mechanisms. The most likely and widely accepted initiation process is the transition metal-catalyzed decomposition of already present hydroperoxides (LOOH), either as impurities or as products of photosensitized oxidation. As a result of reactions 2 and 3, alkoxyl radicals (LO•) and peroxyl radicals (LOO•) are produced which, in turn, can further initiate lipid oxidation.

$$LOOH + M^{2+} \rightarrow LO^{\bullet} + OH^{-} + M^{3+} \quad (10)$$

$$LOOH + M^{3+} \rightarrow LOO^{\bullet} + H^{+} + M^{2+} \quad (11)$$

Subsequently, in the propagation stage, the alkyl radicals (L•) react with molecular oxygen to form peroxyl radicals (LOO•) (reaction 4). These products are also very unstable and reactive and can react with another unsaturated lipid (LH) in a hydrogen transfer reaction to form hydroperoxides (LOOH) and more alkyl radicals (L•) (reaction 5). The hydroperoxides (or peroxides) produced in this stage are known as primary oxidation products.

$$L^{\bullet} + O_2 \rightarrow LOO^{\bullet} \quad (12)$$

$$LOO^{\bullet} + LH \rightarrow LOOH + L^{\bullet} \quad (13)$$

Reaction 5 is rate-determining since it is slower than reaction 4 and will occur selectively for the weakest bounded hydrogen (allylic hydrogen) until the reaction is interrupted either by action of an external agent (e.g., antioxidant) or by unavailability of a hydrogen source. Thus, the probability of undergoing autoxidation in lipids will depend on the number of allylic methylene groups, i.e., the degree of unsaturations. In case of LC ω-3 PUFAs, the probability to undergo autoxidation is linearly related to the number of methylene-interrupted carbons (bis-allylic positions) present in the fatty esters and depending on their position, different hydroperoxides are obtained. EPA produces the eight 5-, 8-, 9-, 11-, 12-, 14-, 15-, and 18-hydroperoxides, while DHA produces the ten 4-, 7-, 8-, 10-, 11-, 13-, 14-, 16-, 17-, and 20-hydroperoxides (Frankel, 2012a).

Finally, in the termination stage, the lipid radicals formed in the initiation and propagation stages accumulate and react with each other to produce non-radical stable compounds. Depending on the compounds present and the reaction conditions (e.g., pressure and temperature), different reactions will occur such as formation of alcohols or condensation reactions, thus, different compounds will be produced (e.g., alcohols or dimers) (Frankel, 2012a). The main condensation reactions are showed below (reactions 6 to 8).

$$LOO^{\bullet} + LOO^{\bullet} \rightarrow LOOL + O_2 \quad (14)$$

$$LO^{\bullet} + L^{\bullet} \rightarrow LOL \quad (15)$$

$$L^{\bullet} + L^{\bullet} \rightarrow L - L \quad (16)$$

During the initiation and propagation stages of autoxidation, lipid hydroperoxides accumulate; however, due to their high instability, they start to decompose leading to the formation of a large variety of organic compounds such as polymers, monomers and volatiles compounds. Among these, the focus has been traditionally placed on small molecular weight volatile compounds since these are responsible of the loss of the organoleptic properties of food lipids by the production of unpleasant odors and flavors. Hydroperoxides decompose through homolytic cleavage by action of heat or metal ions (e.g., haeme iron) producing alkoxyl radicals (LO•) and hydroxyl ions (OH-). These radicals are very reactive and generally cause the cleavage of the aliphatic chain of fatty acids in what is known as β-scission reaction. As a result, low molecular weight compounds are produced such as alcohols, aldehydes, ketones, furans, alkanes and alkenes. The β-scission reactions products will vary depending on the original hydroperoxide structure. In case of fish oil, the most often identified volatile compounds are alcohols, aldehydes and ketones, and to a lesser extent, hydrocarbons, furans and aromatic compounds (Frankel, 2012b; Horiuchi et al., 1998). Since these compounds are odor active, they are susceptible to be quality indicators of fish oil as well (Table 4).

Table 4. Fish oil volatile compounds as quality indicators (Frankel, 2012b; Yeşiltaş, 2019).

Compound	Fish Oil Quality Indicator	Odour description	Thresholds, ppm
Substituted furans	2-Ethylfuran	flower	2-27
Vinyl alcohols	1-Penten-3-ol	sweet	0.5-3
Alkanals	Propanal	sharp-irritating	0.04-1
2-Alkenals	2-Pentenal/2-Hexenal	pungent, glue, green/sour, green	0.04-2.5
(*E*,*E*)-2,4-Alkadienals	(*E*,*E*)-2,4-Heptadienal	green, rancid hazel nuts	0.04-0.3
Vinyl ketones	1-Penten-3-one	pungent, rancid green, sharp fishy	$2 \cdot 10^{-5}$-$7 \cdot 10^{-3}$

Other LC ω-3 PUFAs secondary oxidation products that need attention are malonaldehyde (MDA) and 4-hydroxy-2-hexenal (HHE) due to their toxicity. Both aldehydes, bis-aldehyde and α,β-unsaturated aldehyde, respectively are very reactive and can interact with biomolecules such as DNA and proteins (structural and metabolic) leading to the formation of lipooxidation end products. Aldehyde modified molecules and their biological implications have been related to major chronic diseases such as cancer, neurodegenerative diseases, kidney disease or diabetes, among others (Guéraud et al., 2010; Vieira et al., 2017). MDA reacts with proteins and DNA by acting as a crosslinker and it is considered to be more mutagenic, whilst HHE can modify nucleophile species such as proteins, membranes or nucleic acids due to its electrophilic properties, thus exerting cytotoxic activity (Guéraud et al., 2010).

Alternatives to minimize lipid oxidation of LC ω-3 PUFAs during incorporation into food matrices include the addition of antioxidants and the development of delivery systems such as fish oil-in-water emulsions or fish oil nano-microencapsulates, which will be discussed in thoroughly in the next sections.

3. ANTIOXIDANTS

Antioxidants have a key role in preventing lipid oxidation, since they can delay, control or inhibit oxidation reactions. Antioxidants can be classified by their mechanism of action as primary or secondary antioxidants. Primary antioxidants, known as chain-breaking antioxidants, are able to neutralize free radicals by either donating a hydrogen atom or by a single electron transfer mechanism. Therefore, these antioxidants play a crucial role in lipid

oxidation since they can react with the formed lipid radicals (L•) and convert them into more stable non-radical products avoiding further decomposition of the lipids. Meanwhile, secondary antioxidants prevent lipid oxidation by several mechanisms such as chelation of pro-oxidant metals ions, regeneration of primary antioxidants, decomposition of hydroperoxides (LOOH) and scavenging of oxygen, among others (Decker, 2002).

According to food regulation, antioxidants must have a required daily intake value. This has limited their use in foods to a few compounds such as synthetic phenols and vitamins. The increasing interest towards natural ingredients, which has not the potential health hazards of synthetic compounds, has boosted the research on natural antioxidants. However, only few antioxidants from natural sources have been accepted by food regulation and some of them are not commercialized as antioxidants but as flavorings, binders, etc. Below we provide information about the most common used antioxidants in foods, which include those used in the stabilization of LC ω-3 PUFAS.

3.1 Carotenoids and Xanthophylls

Carotenoids are lipophilic pigments that contain and confer the yellow, orange or red color to a wide variety of foods. Furthermore, they comprise a group of important antioxidants in plant-derived food. Its antioxidant activity is based on their capacity to quench singlet oxygen and scavenge free radicals. However, some factors such as structure or the potential for interaction with other antioxidants could reduce their antioxidant effect or even induce a pro-oxidant effect in vitro and in vivo (Young & Lowe, 2001). The main molecules used in foods are β-carotene (E160a), lycopene (E160d), astaxanthin (E160a), β-cryptoxanthin (E160a), capsanthin (E160c), lutein (E161) and zeaxanthin (E160a).

3.2 Synthetic Phenolic Antioxidants

Many phenolic compounds synthetically produced exhibit better antioxidant activity than natural antioxidants and are available at relatively cheaper prices. The inhibition of the lipid oxidation process is produced by trapping the peroxyl (LOO•) or alkoxyl radicals (LO•). Nevertheless, its toxicological effects have been the subject of controversy since some animal studies have linked synthetic phenolic antioxidants with an increased risk of cancer (Hocman, 1988; Oikawa et al., 1998), being the cause for their replacement in food applications. The most common molecules are propyl gallate (PG; E310), octyl gallate (OG; E311), dodecyl gallate (DG; E312), butylated hydroxyltoluene (BHT; E321), butylated

hydroxylanisole (BHA; E320) and tertiary-butylhydroquinone (TBHQ; E319). The use of these compounds in foods is strictly regulated and varies in different countries. In Europe, the directive 2006/52/EC allows their use in a limited number of food products. Particularly, BHT is only permitted in fats and oils.

3.3 Metal Chelators

Metal chelators are added into food owing to its ability to minimize the participation of metal ions in redox reactions. Food chelators usually have O-containing ligands, which would stabilize iron and copper in their oxidized form. In this way, chelators work as preventive antioxidants by: (i) obstructing the activity of catalytic metals and thus eliminating the initial oxidation step, and (ii) by avoiding the metal-catalyzed decomposition of peroxides (LOOH) to secondary oxidation products. Some of the most studied metal chelators are ethylenediaminetetraacetic acid (EDTA; E385), sodium tripolyphosphate (STPP; E451i), citric acid (E330) and its salts such as sodium citrate (E331), potassium citrate (E332) and calcium citrate (E333). These compounds are allowed as food additives in the European Union and United States. Particularly, sodium salts of EDTA are not allowed in Europe.

Furthermore, others compounds have been shown metal chelating capacity. Flavonoids are plant derived compounds with variable polyphenolic structure. Flavonoids such as kaempferol, quercetin, myricetin, luteolin, naringenin, and catechin are able of complexing Cu^{2+} and Fe^{3+} (Fernandez et al., 2002). Carnosine and other chelating peptides are able of chelating cupper ions and iron respectively (Guo et al., 2014; Velez et al., 2008). However, none of these compounds has been authorized as food additive by European regulations.

3.4 Protein Hydrolysates

Peptides are biopolymers formed by amino acids linked by peptide bonds. Hydrolysates are a complex mixture of peptides with different chain length and amino acids composition, which are preferably obtained by enzymatic hydrolysis. Numerous food proteins, such as milk, meat, fish, egg, seeds etc., have been described as source of antioxidant hydrolysates/peptides (Samaranayaka & Li-Chan, 2011). Antioxidant hydrolysates/peptides have been reported to be able to inhibit lipid peroxidation in model food systems such as fish oil-in-water emulsions (García-Moreno et al., 2016) by exhibiting both radical scavenging and metal chelating activities. The structure and sequence of amino acids influence the antioxidant properties of peptides. Generally, short-chain peptides and the presence of amino

acids such as tyrosine (Tyr), tryptophan (Trp), phenylalanine (Phe), lysine (Lys), methionine (Met) and histidine (His) are present in antioxidant peptides (Power et al., 2013). Food regulation do not consider protein hydrolysates as antioxidant additives; however, it could be used as a source of protein.

3.5 Tocopherols and Tocotrienols

Tocopherols and tocotrienols are one of the most well-known natural antioxidants. They are referred by the common term Vitamin E when they are coexisting with lipids in a biological setting. This group includes eleven different compounds, which differ in the number and position of methyl groups in the chromane ring. Moreover, for tocopherols the side chain in C-2 is saturated, while tocotrienols have an unsaturated side chain. All of them act as peroxyl (LOO•) or alkoxyl radical (LO•) scavengers. Normally, they are commercially extracted from vegetable oil sludge, especially soybean oil. The main food additives are α-tocopherol (E307), γ-tocopherol (E308), δ-tocopherol (E309), the rest of tocopherols and tocotrienols (Trolox, 2,2,5,7,8-Pentamethyl-6-chromanol, β-tocopherol, α-tocotrienol, β-tocotrienol, γ-tocotrienol, δ-tocotrienol and Plastochromanol are regulated as tocopherol-rich extract (E-306). They can be employed in dietary foods and infant formula.

3.6 Ascorbic Acid and Its Derivatives

Ascorbic acid (vitamin C) and its derivatives are a group of antioxidant compounds widely used as a food additive. They have a resonance structure that provides a high reducing activity. Ascorbic acid (E300) and its sodium (E301) and calcium (E302) salts as well as Ascorbyl palmitate (E304) are considered as safe food additives. In contrast, in Europe, Erythorbic acid (E315) and Sodium erythorbate (E316) are only permitted in cured products and preserved products.

3.7 Spice and Plant Extracts

Recently, natural alternatives to synthetic antioxidants have been widely studied to protect the flavor/odor and nutritional value of foods. These extracts present radical scavenging activity, reducing power and metal chelating capacity (Embuscado, 2015). Rosemary and sage extracts are interesting antioxidants because of its high content in antioxidant phenolic compounds such as carnosol, carnosic acid, rosmanol, episormanol, isorosmanol,

rosmaridiphenol, rosmariquinone, rosmarinic acid or rosmadial (Berdahl & McKeague, 2015). Tea extract is also an important source of polyphenols. The main compounds present in tea extract are epicatechin, epigallocatechin, epicatechin gallate, epigallocatechin gallate or theaflavin (Karaosmanoglu & Kilmartin, 2015). Similarly, numerous antioxidants have been identified in herb and spice extracts, namely caffeic acid, capsaicin, carotol, curcumin, eriodictyol, eugenol, etc. However, some of these extracts such as rosemary and sage extracts have the drawback of having a detectable flavor. The Food and Drug Administration refers to natural ingredients as "ingredients extracted directly from plants or animal products as opposed to being produced synthetically." In Europe, the use of rosemary extract (E392) is regulated by directives 2010/67/EU and 2010/69/EU.

4. DELIVERY SYSTEMS

Besides the addition of antioxidants, several strategies have been investigated for the successful incorporation of LC ω-3 PUFAs into food matrices. Particularly, significant research has been carried out on the development of specific delivery LC ω-3 PUFAs systems such as fish oil-in-water emulsions and dried microencapsulates loaded with fish oil. The efforts have been focused on the enhancement of the oxidative stability of the delivery systems as well as on the chemical (e.g., oxidative stability) and physical stability (e.g., texture) of the enriched foods.

4.1 Oil-in-Water Emulsions

The formation and physical stabilization of oil-in-water emulsions requires the use of emulsifiers, which reduces interfacial intension favoring droplet disruption and provides steric and/or electrostatic repulsive forces (McClements & Jafari, 2018). Physical and oxidative stability of oil-in-water emulsions are tightly related, and both are mainly affected by interfacial properties (e.g., thickness, porosity, charge, antioxidant activity) conferred by the emulsifier used (Berton-Carabin et al., 2018). Common emulsifiers for the stabilization of fish oil-in-water emulsions are biopolymers such as milk proteins (e.g., caseins and whey protein) (Horn, Nielsen, et al., 2012), and combinations of milk proteins and natural surfactants such as phospholipids (García-Moreno et al., 2014; Yesiltas, García-Moreno, et al., 2019). Both milk proteins and phospholipids exhibit antioxidant activities such as radical scavenging and chelating activities (Díaz et al., 2003; García-Moreno et al., 2014), which

are properties desired at the interface where lipid oxidation is initiated in oil-in-water emulsions. Lately, alternative protein emulsifiers showing antioxidant activities have been reported. For instance, García-Moreno et al. (2016) indicated the feasibility to use sardine protein hydrolysates with low degree of hydrolysis obtained by subtilisin for the physical and oxidative stabilization of fish oil-in-water emulsions. Recently, Yesiltas et al. (2018; 2019) reported the advantages of using emulsifiers with covalently attached caffeic acid for the stabilization of fish oil-in-water emulsions. These studies confirmed the importance of having antioxidants at the interface for improving the oxidative stability of the emulsions.

Other factors affecting lipid oxidation in oil-in-water emulsions are droplet size, viscosity, pH and surface charge.

Droplet size determines the interfacial area in the emulsion, which is in fact the contact area between pro-oxidants and lipids. Theoretically, low droplet size is desired for a high physical stability of the emulsion and should imply low oxidative stability of the emulsion due to an increased in interfacial area. Nonetheless, contradictory results have been reported on the effect of droplet size on oxidative stability in emulsions (Jacobsen et al., 2000; Let, Jacobsen, Sørensen, et al., 2007), which denoted that other factors, for instance interfacial properties have a greater influence on lipid oxidation in emulsion systems.

Viscosity of the emulsions is an important variable affecting both physical and oxidative stability of these heterogeneous systems. This is because viscosity controls both the mobility of oil droplets (e.g., by minimizing physical destabilization phenomena) (McClements, 2005) and the mobility of pro-oxidants such as metal ions and lipid radicals decreasing rate of lipid oxidation (Shimada et al., 1996). Viscosity of oil-in-water emulsions is controlled by addition of stabilizers, commonly high molecular weight carbohydrates such as pectin, guar and xanthan gums.

Surface charge of oil droplets greatly affects lipid oxidation in oil-in-water emulsions. In the case of proteins used as emulsifiers, the pH of the emulsion will determine the charge of the interfacial protein layer. This might be of special importance in the case of metal-catalyzed lipid oxidation, since theoretically metal ions will be attracted to the interface when having negative surface charge, thus favoring lipid oxidation. On the contrary, trace of metals will be repelled from the interface in emulsions with positive surface charge, reducing lipid oxidation (Mei et al., 1998). However, at low pH, which is generally required to charge positively most of protein-based emulsifiers, the solubility of trace of metals increases. Thus,

as consequence of an increased solubility, iron also becomes more active in acidic conditions to catalyze lipid oxidation via decomposition of hydroperoxides (Berton-Carabin et al., 2014).

In addition, oxidative stability of emulsions can be further improved by addition of antioxidants. For this purpose, phenolic compounds such as ferulic acid, caffeic acid have been widely used in oil-in-water emulsions to reduce lipid oxidation (Sørensen et al., 2008). These are hydrophilic compounds that will be located in the aqueous phase, thus mainly scavenging radicals in the continuous aqueous phase. In the last years, extensive research has been carried out on the lypophilization of phenolic compounds in order to modify their hydrophilic/hydrophobic ratio, which allows the location of these antioxidant compounds at the interface of oil-in-water emulsions. Interestingly, it has been reported that the optimum alkyl chain length for the phenolipids is determined by several factors such as the type of antioxidants to be lypophilized, type of emulsifiers used to stabilize the emulsion as well as the food system where the emulsion will be incorporated (Alemán et al., 2015; Laguerre et al., 2010).

A common strategy to protect the lipid ingredients of ω-3 PUFA fortified foods against oxidation is their incorporation into food matrices as delivery systems, such as microcapsules or oil-in-water emulsions. Fish oil emulsions are often used as oil carrier in liquid or semisolid products such as milk, cheese cream, mayonnaise, salad dressing or yoghurt. The market of ω-3 PUFAs enriched dairy products has undergone a sharp increase since the 2000s, followed by bakery goods. Oil addition to dairy products and beverages is favored by their low storage temperature, commonly under refrigerated or frozen conditions, which restrain lipid oxidation.

Driven by the improvements in mixing and homogenization equipment, fish oil has been successfully incorporated into liquid and semiliquid products, ensuring acceptable levels of oxidative stability. The susceptibility of the fortified food to lipid oxidation depends to large extent on the nature of both the emulsifier protein and the food matrix. To this regard, Horn et al. (2012) studied the effect of three emulsifiers including caseinates, whey proteins and a mixture of milk proteins and phospholipids on the oxidative stability of cream cheese fortified with 70% fish oil-in-water emulsion. The authors reported that both whey- and casein-based delivery emulsions provided poorer oxidative stability to the cheese cream, compared to direct addition of bulk oil. This fact was attributed to the lipid oxidation induced during emulsion preparation where temperature rose up to 65 °C. Under the same processing

conditions, the emulsion employing a mixture of milk proteins and phospholipids as emulsifier presented better oxidative stability than direct addition of bulk oil. This result confirmed the role of milk phospholipids in reducing the exposure of oil droplets to oxidation agents.

Concerning the nature of the food matrix, Let et al. (2007) studied the oxidative stability of milk, yoghurt and dressing fortified by 50% oil-in-water emulsions employing whey proteins as emulsifiers. Fortification of milk beverages with fish oil-in-water emulsions provided larger oxidative stability that direct incorporation of bulk oil. In contrast, the content of secondary volatile oxidation products (SVOP) and sensory data showed the opposite behavior for yoghurt and dressing, despite the fact that processing conditions and protein emulsifier were the same.

Early approaches to produce ω-3 PUFAs fortified mayonnaise, where vegetable oil was partially replaced by fish oil (Jacobsen et al., 2001), were hindered by the high content of protein-bound iron present in the egg yolk. Low pH levels activate iron as catalyzer of lipid oxidation reactions, limiting the stability of such emulsions. Further research on low pH systems proved that oxidative stability of ω-3 PUFAs fortified mayonnaises can be improved by adding antioxidants, either commercial synthetic chelators (Alemán et al., 2015; Haahr & Jacobsen, 2008) or natural-based extracts (D. B. Hermund et al., 2015).

Margarines and spreadable fats are another range of foodstuffs where ω-3 PUFAs fortification leads to limited oxidative and sensory quality. To this regard, Kolanowski et al. (2004) incorporated up to 30 g·kg-1 of fish oil into a reduced-fat spread containing 450 g·kg-1 of rapeseed oil. The fortified product was stabilized by a combination of antioxidants (α-tocopherol, ascorbyl palmitate and rosemary extract) added at ratio 1:10 w/w with respect to the amount of fish oil. The enriched product could be stored for up to 3 months without significant decrease in both oxidative (e.g., peroxide and acid values) and sensory parameters (e.g., hardness, consistency, spreadability, fishy odor development).

Few studies deal with the ω-3 PUFAs enriched emulsions other than dairy products. For instance, Song et al. (2011) evaluated the oxidative stability of chocolate ice cream, which was fortified with omega-3 oil emulsion containing *Bificobacterium longum* as probiotics. Despite the good results on oxidative stability and probiotic bioavailability of the fortified product, the sensory analysis showed low acceptability scores due to the detection of fishy odors.

4.2 Microencapsulates

Encapsulation technology consist of coating substances (core material) within a homogeneous/heterogeneous matrix (encapsulating agent/s) at the micro- or nano-scale. Using this technology, a physical barrier is developed between the inner substance and the environment which prevents its degradation and facilitates its handling and transportation. It also can be used as a control time-release mechanism. Food industry has been using this technology over the last decades in the production of added-value food products fortified with different sensitive bioactive compounds such as vitamins, polyphenolic antioxidants, probiotics and ω-3 PUFAs. Encapsulation can be achieved by physical (e.g., spray-drying), physico-chemical (e.g., coacervation) or chemical (e.g., polymerization) means and several encapsulating agents are used for encapsulation of food bioactives, provided that they are biocompatible and food-grade. The most common wall materials in food applications are carbohydrates (e.g., maltodextrins, glucose syrup) and proteins (e.g., casein, whey protein), although gums (e.g., sodium alginate, guar gum), lipids (e.g., wax) and cellulose and its derivatives (e.g., carboxymethylcelullose) are also used (Desai & Park, 2005). The choice of the encapsulation technique together with the encapsulating agent depends on different aspects such as the desired size of the particles, the food matrix in which the capsules will be incorporated and the controlled release of the substance, if required (Encina et al., 2016).

ω-3 PUFAs encapsulation and subsequent addition to complex food matrices still represents an important challenge to food industry due to their hydrophobic nature, which results in low solubility in most food systems, and utterly low oxidative stability. In this regard, fish oil encapsulation has gained great attention, not only to prevent its oxidation during processing, but to maintain the organoleptic properties of the fortified food by masking its flavor and oily texture. In the next sections, we provide the state-of-the art on the encapsulation of fish oil by spray-drying, as the most used encapsulation technique, and by electrospraying as an emerging encapsulation technology.

4.2.1 Spray-Dried Microencapsulates

Spray-drying is the preferred encapsulation technology in food industry due to its versatility, simplicity, low cost, ease to scale-up and good quality encapsulates. This technique consists of the atomization of a liquid feed (solution, dispersion or emulsion) into a hot gas stream (air or nitrogen), to obtain powder almost instantly in 5 – 30s (Desai & Park, 2005). The size of the resulting capsules range in the micro-scale, ~ 10μm – 3mm, and depends on the liquid

feed properties (e.g., viscosity) and the drying process conditions (e.g., atomization speed) (Gharsallaoui et al., 2007). Despite the use of high drying temperatures, this method is suitable to encapsulate heat-sensitive bioactive compounds with minimal thermal degradation due to the small droplet sizes generated during the atomization process (Espejo-Carpio et al., 2013). As a consequence: (i) the internal mass transfer rate, from the core of the droplet to the surface, is high enough to evaporate most of the solvent at the wet bulb temperature (T_{wb}) of the inlet air and, (ii) the external mass transfer, from the surface of the droplet to the air, is high enough to assure short contact time for drying, hence very short residence time of the capsules in the drying chamber. The resulting powder is collected in a cyclone where it is separated from the outer drying gas. Moreover, as it is a moisture removal technique, powders with low moisture content (MC, MC < 5%) and low water activity (aw) are produced, assuring their microbiological stability against chemical or biological degradations (Gharsallaoui et al., 2007).

4.2.1.1 Type of Encapsulating and Emulsifying Agents

Optimization of the feed formulation and the process variables is required to achieve an efficient encapsulation process to obtain good quality microcapsules in terms of high stability and high load capacity. The preparation of the liquid feed, regardless of the hydrophilic/hydrophobic nature of the core and wall materials, requires the dispersion of the bioactive compound in the encapsulating solution. Water is the preferred solvent in food applications, thus for encapsulating ω-3 PUFAs (e.g., fish oil), an emulsification process is commonly carried out to disperse the oil in the water-based biopolymer solutions. Encapsulating agents for fish oil microencapsulation purposes are desired to be water soluble biopolymers at high solids concentration leading to low viscosity solutions. Low viscosity is preferred since it allows to obtain smaller atomized droplets, hence smaller microcapsules. In addition, high coating and emulsifying properties are required to achieve high encapsulation efficiencies (EE) (Encina et al., 2016).

Proteins, carbohydrates and their combinations have been the most extensively used wall materials for fish oil microencapsulation, although the use of gums (e.g., gum Arabic) and cellulose derivatives (e.g., sodium carboxymethyl cellulose) have also been reported (Table 5).

Proteins alone or mixtures have been used for the production of fish oil microcapsules due to their high emulsifying and film-forming properties. Among proteins, those of animal

sources such as milk proteins (e.g., sodium caseinate or whey protein) or gelatin (e.g., fish gelatin) are the most commonly reported. Aghbashlo et al. (2013) investigated the influence of the wall material composition and the inlet drying temperature (140 – 180 °C) in microcapsules properties using milk proteins as the bulk materials namely, skim milk powder (SMP), whey protein concentrate (WPC), whey protein isolate (WPI) and WPI (80 %) combined with milk protein concentrate (MPC) or sodium caseinate (CAS) (20%). The core to wall ratio was set to 1:2 leading to a theoretically oil load of 33.33 %. The EE varied from 40.59 ± 1.28 % to 81.94 ± 0.24 % and the particle size was in the range of 1.37 – 4.59 µm, being both significantly influenced by the drying temperature (the higher the drying temperature, the higher the EE and the larger the particle size). The highest EE (~ 82 %) and lowest hydroperoxides content (PV) after drying at 180 °C corresponded to the SMP-based microcapsules, which led to increase their PV from 6.15 to 8.35 meq peroxide/kg oil over the storage time (25 °C during 4 weeks). The authors attributed this observation to the physical and chemical changes of the wall during storage time, which allowed oil diffusivity from the core to the surface (decreasing the EE to 59.35 %) and oxygen diffusivity from the surface to the core thus favoring lipid oxidation. In a recent study, Lehn et al. (2018) investigated the suitability of pure whey (W) alone or the blend W-Permeate (WP) as encapsulating agent(s) for ω-3 PUFAs microencapsulation (carp oil and chia oil) in presence of gum acacia and soybean lecithin as emulsion adjuvants. The oil load of the microcapsules was set to 26 % and the drying conditions were fixed to 125/105 °C as the inlet and outlet temperature, respectively. The type of oil and the wall composition highly influenced the EE. In the case of fish oil, the EE varied from 45.72 ± 3.04 % to 90.65 ± 0.96 % when W and WP were used as the bulk materials, respectively, and the particle size ranged from 10 to 150 µm. WP-based fish oil microcapsules were oxidatively stable during the storage time (30 days at 25 °C) being this fact attributed to its high encapsulation efficiency. Moreover, the use of fish gelatin alone as encapsulating agent for the production of fish oil microcapsules has also been reported (Jeyakumari et al., 2016). In this case the emulsion was produced using milk as the solvent and the core:wall ratio was set to 1:2, leading to theoretical oil load of 33.33 % in the microcapsules. The EE after drying at 160/80 °C temperatures pair was of 46.83 %. In this study, the oxidative stability of the encapsulates was not measured.

In the last years, plant proteins have gained great interest in order to substitute animal-derived proteins since they are sustainable, no subjected to any religious or diet restrictions

(e.g., vegetarian or vegan diets), low cost and reduce the risk of spreading diseases such as mad cow disease (bovine spongiform encephalitis). Oilseed and cereals (e.g., barley) were used as proteins sources, although pulses-derived proteins (e.g., soy, peas, chickpeas and lentils) are the most commonly employed (C. Chang & Nickerson, 2018). Wang et al. (2011) produced fish oil microcapsules (50 % oil load) using barley proteins (glutelin (G), hordein (H) and mixtures 1:2, 1:1, 2:1) from a water-based emulsion without the need of additional crosslinkers nor the use of organic solvents. The drying process was carried out at 150 °C (inlet temperature) and the EE ranged from 92.9 – 100 %. During storage time (40 °C during 8 weeks), the PV of all encapsulates gradually increased reaching the maximum content after 3 – 4 weeks (45 – 76 meq peroxide/kg oil). The sample with the highest content of H (G:H ratio of 1:2) showed the better protective effect against lipid oxidation. More recently, Di Giorgio et al. (2019) microencapsulated fish oil using soybean protein isolate (SPI) as the only wall constituent at different core:wall ratios (1:1 – 1:4). In this case, the concentration of the encapsulating agent in the emulsion and its production process played a major role on the microcapsules properties after drying (180/96 °C inlet/outlet temperature, respectively). The highest EE (88.74 ± 3.15 %) was achieved at the 1:4 ratio when the emulsion was prepared by mechanical stirring (Ultraturrax, U) followed by ultrasonic homogenization (Ultrasound, US). However, despite the higher EE, this sample had the highest PV and TBARS (thiobarbituric acid reactive substance) value after drying among those produced under the same conditions (U and US treatment of the emulsion prior drying) at lower core:wall ratios. This was attributed to: (i) the faster crust formation as consequence of an increase in the protein content, leading to an increased resistance to evaporation, thus an increase of particle temperature, and (ii) trace metals (iron and copper) present in the SPI. Nevertheless, these encapsulates were reported to maintain the oil oxidative stability over time, studied by RANCIMAT accelerated oxidation test method (90 °C and 20 L/h of air stream), since the induction period (IP, over 3 h) was similar to the non-encapsulated oil (IP = 3.9 h) and higher of those of lower core:wall ratios (except for the 1:1 sample).

Despite their high film-forming properties, proteins are frequently combined with low molecular weight carbohydrates since these acts as a wall filling material, which lead to less porous and more uniform matrices. Moreover, the presence of low molecular weight carbohydrates influences the drying behavior of the droplets by modifying the wall material glass transition temperature (Tg), and thus influencing the crust formation. Moreover, the compounds derived from Maillard reaction occurring between proteins and reducing sugars

at high temperatures (e.g., melanoidins) have been reported to change the physical and antioxidant properties of the wall leading to additional core stabilization. Aghbashlo et al. (2012) encapsulated fish oil using SPM alone or in combination with maltodextrin (MD), lactose (L) or sucrose (S) (70% SMP + 30% carbohydrate) with the inlet drying temperature and the core:wall ratio set to 175 °C and 1:2, respectively. The blends SMP-L and SMP-S enhanced the EE of the microcapsules by decreasing the wall composites Tg, thus favoring a fast crust formation and preventing the oil diffusivity across the encapsulating wall (84.96 ± 0.03 % and 84.92 ± 0.19 %, respectively). The faster crust formation also led to larger microcapsules (5.21 and 5.37 μm, respectively) and lower PV after drying (5.95 ± 0.05 and 5.95 ± 0.15 meq peroxide/kg oil, respectively) since less oil was exposed to the drying air at high temperature. However, the similarities in EE for both powders, despite the different nature of the sugar composites, led to conclude that Maillard reaction between the protein and carbohydrate constituents of the wall matrix did not occur. These results are in line with those reported from Aghbashlo et al. (2013), who attributed the better retention properties of the SMP-based powders to the presence of lactose in the intrinsic chemical composition of the matrix, thus enhancing the drying behavior by favoring the crust formation. However, in this case the authors discussed that the better wall properties could be also attributed to Maillard reaction products (e.g., protein-carbohydrate conjugates). Pourashouri et al. (2014) reported that fish oil encapsulates with fish gelatin (Ge) and MD as wall material composites, over those formulated with chitosan (Cs) and MD, had better retention properties (higher EE). These results were explained on the basis of lower Tg of the encapsulating material in presence of Ge which favored the crust formation leading to: (i) higher EE (85.36 ± 1.91 % over 71.84 ± 1.51 % for Ge-MD and Cs-MD microcapsules, respectively), and (ii) larger particle size (D[3,2] = 6.54 μm and D[3,2] = 5.92 for Ge-MD and Cs-MD microcapsules, respectively). The authors also stated that Maillard reaction products might also have favored the formation of a tough skin. However, the previous results differ from those reported by Huang et al. (2014) who did find that the addition of trehalose to the emulsion formulation (7.0 wt% tilapia oil, 4.5 wt% gelatin, 0.5 wt% xantham gum and 13.2 wt% S or S:trehalose (7:3)) increased the EE by increasing the wall composites Tg. The Tg were of 83.8 °C for the sample containing only S (EE = 80.4 ± 1.13 %) and 96.0 °C when trehalose was added to the formulation (EE = 87.0 ± 0.74 %).

Furthermore, due to the lack of interfacial activity of low molecular weight carbohydrates, they have been used lonely as wall material constituents in presence of surface-active

compounds. For instance, Drusch et al. (2009) used glucose syrup (GS, dextrose equivalent, DE38), MD (DE18), maltose (M, DE50) and the mixtures MD-GS or MD-M (DE38) as bulk agents in presence of n-octenylsuccinate-derivatised starch (n-OSA-starch) to produce fish oil microcapsules with an oil load of 40 %. The drying conditions were set to 180/70 °C as the inlet and outlet temperature, respectively. The particle size (d90) ranged from 49.9 – 63.1 µm and the amount of extractable oil (non-encapsulated oil) varied between 3.14 – 7.00 %, meaning high EE. Other GS-based microcapsules have been produced in presence of n-OSA-starch (Serfert, Drusch, & Schwarz, 2009; Serfert, Drusch, Schmidt-Hansberg, et al., 2009), whey protein or whey protein hydrolysate (β-lactoglobulin) (Tamm et al., 2015), fish protein hydrolysates (Morales-Medina et al., 2016) and sugar beet pectin (Polavarapu et al., 2011) as emulsifiers with different oil loads (14.33 – 40 %) but similar encapsulation efficiencies (over 90 %) (Table 5). Furthermore, the production of MD-based microencapsulates has also been reported. Jeyakumari et al. (2016) produced fish oil microcapsules using MD (DE16) as the bulk material from a milk-based emulsion, achieving an encapsulation efficiency of 49.34 %. Moreover, Linke et al. (2020) successfully encapsulated fish oil (40 % oil load) using MD (DE21) and soy protein isolate (SPI) at different protein:core ratios (0.02:1 – 0.22:1). The amount of emulsifier strongly influenced the EE (at the same emulsion homogenization pressure) and varied from 53.82 ± 1.07 % (0.02:1 ratio) to 93.44 ± 0.05 % (0.13:1 ratio). The particle size (d50,3) in this case ranged from 86.2 – 115.6 µm.

By last, Binsi et al. (2017) encapsulated sardine oil (20 % oil load) using CAS as wall polymer and gum Arabic (GA) as wall co-polymer by spray-drying at 160 °C (inlet temperature). The EE after drying the fish oil emulsion ascended to 69%. Karim et al. (2016) used two different hydroxypropyl methylcellulose (HPMC) (15 or 5 cps) and their mixtures to produce menhaden fish oil microcapsules. The drying conditions were fixed to 180/80 °C temperatures pair, but the core:wall ratio varied from 1:1 to 1:0.25, thus varying the oil load. The EE ranged from 67.33 ± 0.15 % to 74.75 ± 0.39 %, whilst the particle size (D[4,3]) varied from 18.32 ± 0.04 to 54.67 ± 0.09 µm. The core:wall ratio of 1:1 resulted in the largest particles size and the highest EE. Patrick et al. (2013) produced single-shell and double-shell fish oil microcapsules by using GA, sodium carboxymethyl cellulose (NaCMC) and sodium polyphosphate at an inlet air temperature of 180 °C. The microcapsules total oil content was of 10.86 ± 0.33 % (EE = 75.20 ± 0.73 %) and 11.92 ± 0.25 % (EE = 82.81 ± 0.61 %) for the single-shell and double shell, respectively.

The choice of the proper encapsulating agent is of vital importance since it will further determine the microcapsules properties (e.g., particle size, bulk density, MC or PV) being EE the most important. This parameter not only quantifies the yield of the drying process regarding the oil load of the particles (core retention), but also allows to predict oxidative stability of the powder. By determining the EE, the amount of non-encapsulated oil is indirectly quantified, being the latter the amount of unprotected oil susceptible to degradation by action of pro-oxidant agents (e.g., oxygen or light). It has been assumed, in consequence, that the higher the EE, the highest the degree of protection of the wall material and the higher the oxidative stability of the encapsulated oil (lower PV and SVOP content). However, not always is possible to predict the oxidative stability of the core based on this parameter since: (i) pro-oxidant species are present in the parent emulsion (e.g., transition metals or oxygen) as a consequence of the emulsification process, and (ii) pro-oxidant species which diffuses through the wall matrix (e.g., oxygen) also affects the extent of encapsulated oil oxidation. In this regard, Linke et al. (2020) investigated the oxidation rate of the non-encapsulated and encapsulated oil fractions and their contribution to overall oxidation in fish oil microcapsules and concluded that, although non-encapsulated fraction oxidized ~7 times faster than its encapsulated counterpart, its contribution to overall lipid oxidation was negligible due to its low amount on particles surface (~ 2 – 18%). Moreover, oxidation of the encapsulated oil during storage time, despite being totally embedded within the wall matrix, suggested oxygen diffusion through the capsules wall. Hence, structural particle properties such as load capacity, specific surface area of oil droplets and microparticles size play a major role on encapsulated oil oxidation by affecting the oxygen supply. These results are in line with those reported by Drusch et al. (2009) and Serfert et al. (2009) who attributed the differences in lipid oxidation course among samples to the oxygen diffusivity through the wall matrix (influenced by the differences in the molecular weight profile of the constituents) since the EE was not significantly different. Moreover, the latter authors investigated the influence of oxygen present in the drying medium (air or nitrogen) or dissolved in the parent emulsion (consequence of the shearing forces) in the microcapsules oxidative stability during storage and concluded that the course of lipid oxidation was rather determined by the oxygen present in the emulsion than in the drying gas. Hence, lipid oxidation already occurs in the microcapsules production in both the emulsion preparation (air inclusion by action of mechanical and shearing forces) and subsequent drying at high temperature.

Table 5. Recent studies on ω-3 PUFAs encapsulation by spray-drying.

Encapsulating Agent/s (EA)	Emulsifier	FO:EA	Antioxidants	Gas: Inlet/Outlet (T°)	LC/EE (EO*)	Capsules size	Oxidative Stability	References
Skim milk powder (SMP)				Air: 140/NR °C			SMP capsules (Inlet T: 180 °C)	
Whey Protein Concentrate (WPC)				Air: 160/NR °C			25 °C/4 weeks	
Whey Protein Isolate (WPI)	-	1:02	-	Air: 180/NR °C	Theoretical LC: 33.33 %; EE: 40.59 - 81.94 %	1.37 - 4.59 µm	PV	(Aghbashlo et al., 2013)
WPI:Milk Protein Concentrate								
WPI:Sodium Caseinate								
Pure whey (W)	Gum Acacia:Soybean	1:2.85	-	Air: 125/105 °C	LC: 13.7 - 18.4 %; EE: 45.72 - 90.65 %	10 - 150 µm	25 °C/30 days/darkness	(Lehn et al., 2018)
W:Whey Permeate (WP)	Lecithin						PV	
Fish gelatin	-	1:02	-	Air: 160/80 °C	Theoretical LC: 33.33 %; EE: 46.83 - 49.34 %	-	Room temperature/6 months	(Jeyakumari et al., 2016)
Maltodextrin							TBARS	
Hordein (H)				Air: 120/60 ± 5 °C			40 °C/8 weeks	
Glutelin (G)	-	1:01	-	Air: 150/60 ± 5 °C	LC: 46.5 - 50.1 %; EE: 92.9 - 100.2 %	1 - 5 µm	PV	(Wang et al., 2011)
G:H = 1:2, 1:1, 2:1				Air: 180/60 ± 5 °C				
		1:01					No storage analysis	
		1:02			LC: 12.14 - 48.77 %; EE: 57.73 - 88.74 %		PV	
Soybean Protein Isolate (SPI)	-	1:03	-	Air: 180 ± 2/96 ± 8 °C		15 - 20 µm	TBARS	(Di Giorgio et al., 2019)
		1:04					RANCIMAT test	
Skim milk powder (SMP)							No storage analysis	
SMP:Maltodextrin							PV	
SMP:Lactose	Tween 20 (T20)	1:02	-	Air: 175/95 - 98 °C	Theoretical LC: 33.33 %; EE: 76.22 - 85.12 %	3.07 - 5.37 µm		(Aghbashlo et al., 2012)
SMP:Sucrose								

Fish gelatin (Ge):Maltodextrin (MD) Chitosan (Cs):MD Ge:Cs:MD Ge:Microbial transgluminase:MD	-	1:04	-	Air: 180 ± 0.5/90 ± 5 °C	LC: 16.04 - 21.98 %; EE: 67.35 - 88.01 %	D[3,2]: 5.42 - 8.76 µm	-	(Pourashouri et al., 2014)
Gelatin (Ge):Xanthan gum (XG):Sucrose (S) Ge:XG:S:Trehalose Sucrose:Trehalose = 10:0 - 6:4	-	~ 1:2.6	-	Air: 110 - 120/NR °C	Theoretical LC: 28 %; EE: 59.4 - 91.4 %	-	No storage analysis PV	(Huang et al., 2014)
Glucose syrup Maltodextrin Maltose	n-OSA starch	1:1.5	-	Air: 180/70 °C	Theoretical LC: 40 %; EO: 3.42 - 7.00 %	d90: 49.9 - 63.1 µm	20 °C/33 %(RH)/8 weeks PV SVOP	(Drusch et al., 2009)
Glucose syrup	n-OSA starch	1:1.5	-	Air: 160/70 °C Air: 210/90°C N2: 180/70 °C	Theoretical LC: 40 %; EO: 3.60 - 7.50 %	d90: 34.6 - 44.2 µ	20 °C/33 %(RH)/56 days PV SVOP	(Serfert, Drusch, Schmidt-Hansberg, et al., 2009)
Glucose syrup	n-OSA starch	1:1.5	α-Tocopherol δ-Tocopherol corbyl palmita Citrem Lecithin osemary extra	Air: 180/70 °C	Theoretical LC: 40 %; EO: 2.63 - 3.83 %	-	20 °C/33 %(RH)/8 weeks PV SVOP	(Serfert, Drusch, & Schwarz, 2009)
Glucose syrup	β-lactoglobulin (β-LG) globulin hydrolysate (β	~ 1:2.2	-	Air: 180/70 °C	Theoretical LC: ~ 31 %; EE: 98.7 - 99.5 %	-	20 °C/33 %(RH)/11 weeks PV	(Tamm et al., 2015)
Glucose syrup	Fish Protein Hydrolysates (FPH)	1:06	-	Air: 180/70 °C	Theoretical LC: 14.33 %; EE: 98.0 %	-	20 °C/33 %(RH)/12 weeks PV	(Morales-Medina et al., 2016)

Glucose syrup	Sugar beet pectin (SBP)	1:02 1:03	Extra virgin olive oil (EVOO)	Air: 180/80 °C	LC: 24.38 - 49.22 %; EE: 90.42 - 97.87 %	-	25 °C/3 months SVOP Induction Period	(Polavarapu et al., 2011)
Maltodextrin	Soy Protein Isolate (SPI Protein:Oil: 0.02:1 - 0.22:	1:1.5	-	Air: 160/85 °C	LC: 37.34 - 40.71 %; EE: 53.82 - 94.10 %	d50,3 : 74.1 - 168.9 µm	27 ± 2 °C/6 weeks PV	(Linke et al., 2020)
Sodium Caseinate:Gum Arabic	-	1:04	Sage polyphenols	Air: 160/80 °C	LC: 12.50 - 12.72 %; EE: 68.99 - 73.21 %	107 - 115 nm	60 °C/7 days PV TBARS	(Binsi et al., 2017)
Hydroxypropyl methylcellulose (15cps + 5 cps)	-	1:01 1:0.75 1:0.5 1:0.25	-	Air: 180 ± 1/80 ± 1 °C	Theoretical LC: 50 - 80 %; EE: 67.33 - 74.75 %	D[4,3]: 18.32 - 54.67 µm	4 °C/28 days PV	(Karim et al., 2016)
Gum Arabic (GA):Sodium Carboxymethyl cellulose (NaCMC) GA:NaCMC:Sodium polyphosphate	-	NR	-	Air: 180/90 °C	LC: 10.86 - 11.92 %; EE: 75.20 - 82.81 %	-	No storage analysis PV AV TOTOX TBARS after 28 days of storage	(Patrick et al., 2013)
Maltodextrin (MD):Bovine Gelatin (BG) Chitosan (Cs):BG:MD	-	1:04	Oregano extract	Air: 180/90 °C	LC: 12.45 - 13.25 %; EE: 68.94 - 81.88 %	1.82 - 15 µm	days; 28 ± 2 °C/4 weeks; 4 °C/4 PV TBARS	(Jeyakumari et al., 2018)
Maltodextrin (MD):Gum Arabic (GA):Sodium Caseinate (CAS) MD:GA:CAS:Tuna Protein Hydrolysate (TPH) MD:GA:TPH	-	1:05	Tuna Protein Hydrolysate	Air: 160/80 °C	Theoretical LC: ~ 17 %; EE: 73.89 - 78.73 %	1.03 - 15.3 µm	/1 week; 28 °C/4 weeks; 4 °C/4 v PV TBARS	(Unnikrishnan et al., 2019)

Skipjack roe protein hydrolysate (SRPH)	-	1:04	annic acid (TA ed tannic acid	Air: 200 ± 2/108 ± 2 °C	Theoretical LC: 20 %; EE: 13 - 55 %	6.16 - 17.07 µm	30 ± 1 °C/4 weeks PV TBARS SVOP	(Intarasirisawat et al., 2015)
Vanilic acid grafted chitosan (Va-g-Ch)	Tween 20 (T20)	1:2.3	-	Air: 140/77 °C	Theoretical LC: 30 %; EE: 84 %	2.3 µm PDI: 0.345	Ambient temperature/4 weeks PV TBARS RANCIMAT test	(Vishnu et al., 2017)
Maltodextrin:Chitosan	β-lactoglobulin ol-modified β-lactoglob	1:1.65	-	Air: 160/NR °C Air: 170/NR °C Air: 180/NR °C	Theoretical LC: ~ 38 %; EE: 71.63 - 94.90 %	-	-	(H. W. Chang et al., 2020)
Barley β-D-glucan:Waxy Maize Modified Starch	Tween 80 (T80)	1:03	-	Air: 154/70 °C	Theoretical LC: 25 %; EE: 79.9 %	PDI: 1.07	Storage temperature NR/5 days TBARS	(Kurek et al., 2018)

*Abbreviations: EA, encapsulating agent; FO, fish oil; LC, load capacity; EE, encapsulation efficiency; EO, extractable oil; PV, hydroperoxides content; TBARS, thiobarbituric acid reactive substances; SVOP, secondary volatile oxidation products; AV, anisidine value; TOTOX, total oxidation; NR, not reported.

4.2.1.2 Spray-Drying Processing Variables

Regarding the spray-drying process, there are several operational variables to be optimized such as the inlet and outlet air temperatures, feed temperature, drying air mass flow rate, feed mass flow rate and type and speed of atomization. All these variables affect the final quality of the capsules (e.g., MC, particle size, EE or PV after drying). Nonetheless, inlet drying air temperature is regarded as the most important factor for encapsulation of heat-sensitive bioactives compounds (e.g., fish oil). This parameter is mostly selected according to the type of product to be dried. Although high drying temperatures are preferred, since temperature is directly related to drying rate and final water content, there are limitations. Wang et al. (2011) encapsulated fish oil using barley protein as the encapsulating agent and reported that the highest inlet temperature studied (180 °C) led to a less uniform particle size distribution composed of particles of irregular shape. This finding was attributed to the faster particle shrinkage, produced during the early stage of drying, caused by a too high drying temperature. On the other hand, at the lowest inlet temperature studied (120 °C) the high MC of the dried capsules caused agglomeration. Different studies have been carried out to determine the influence of the drying air temperature in fish oil microcapsules properties. For instance, as previously mentioned, Aghbashlo et al. (2013) produced milk protein-based microcapsules at three different inlet temperatures (140 °C, 160 °C and 180 °C) and reported that the EE, particle size and initial PV were positively correlated with the inlet drying temperature. On the other hand, as the drying temperature increased, MC and bulk density decreased. Serfert et al. (2009) found the same trend regarding initial PV, particle size and bulk density when fish oil microcapsules were produced using GS in presence of n-OSA-starch. However, in this study the EE decreased as the inlet drying temperature increased, being this finding attributed to the formation of vacuoles and to a higher porosity as consequence of a high inlet temperature.

4.2.1.3 Stabilization by Addition of Antioxidants

Although microencapsulation itself prevents lipid oxidation, additional stabilization techniques are required since it has been demonstrated that oxidation already occurs in the early stages of microcapsules production process and during storage time. In this regard, scientists have studied the addition of antioxidants to the formulation. Serfert et al. (2009) investigated the effect of a combination of various antioxidants of different natures (α-tocopherol, δ-tocopherol, ascorbyl palmitate, citrem, lecithin and rosemary extract) in the different process stages of microencapsulation and during storage. The capsules were

produced using GS in presence of n-OSA-starch as the encapsulating agent, with 40 % oil load, and the drying process was carried out at 180/70 °C temperatures setting. The main finding of this study was that the optimal combination of antioxidants depended on the microencapsulation process step, thus on the characteristics of the heterogenous system. An efficient stabilization during storage of both the emulsion and the microcapsules was achieved by using a ternary combination of antioxidants (tocopherols, ascorbyl palmitate and lecithin) in presence of rosemary extract. Jeyakumari et al. (2018) investigated the effect of the adding oregano extract on the oxidative stability of microencapsulated fish during storage at three different temperatures (4 °C, 28 °C and 60 °C). The wall material consisted of MD and bovine gelatin (BG) with or without Cs and the drying conditions were set to 180/90 °C as the inlet and outlet temperatures, respectively. The microcapsules oil load was of 20 % and the oregano extract was dissolved in the fish oil prior to emulsification. Regardless of the storage temperature, the microcapsules containing the fish oil-oregano blend had the lowest PV and TBARS value over storage time, being this attributed to the phenolic compounds present in oregano extract, which effectively protected fish oil against oxidation. Furthermore, the results suggested that the storage temperature strongly influenced the course of lipid oxidation. The smaller values reported of PV and TBARS value were those of the sample containing oregano extract at 4 °C of storage temperature. Binsi et al. (2017) produced sardine oil microcapsules in presence of sage polyphenols (SP). The course of lipid oxidation under accelerated conditions (60 °C during 7 days) showed that, although the addition of SP enhanced oxidative stability of the microcapsules (lower PV and TBARS value over storage time). This occurred rather by a physical mechanism of protection than an antioxidative effect (e.g., radical scavenging). The authors reported that SP acted as protein crosslinkers, which stabilized the wall matrix and favoured the crust formation during the early stages of drying. This led to higher EE compared to the sample without SP (73.21 % over 68.99 %). Polavarapu et al. (2011) investigated the addition of extra virgin olive oil (EVOO) as antioxidant to produce fish oil microcapsules with GS and sugar beet pectin (SBP) as wall materials. Two different encapsulates with different oil loads were produced (25 % and 50 % oil) at 180/80 °C temperatures pair. The course of lipid oxidation was assessed by quantifying the propanal and hexanal content over 3 months at 25 °C and under accelerated storage conditions (80 °C and oxygen pressure of 0.5 bar). The SVOP content showed that the addition of EVOO to the formulation did not enhance fish oil oxidative stability neither in the microcapsules production nor in storage time. This finding did not correlate with the results reported under accelerated storage conditions, which

indicated that the addition of EVOO to the formulation extended the IP in the microcapsules (~7.90 – 11.95 h). In general, the authors attributed the low oxidative stability of the microcapsules to the presence of trace metals in SBP, which could not be averted by the addition of EVOO.

Lately, the use of protein hydrolysates/peptides, having both emulsifying and antioxidant properties is gaining an increasing interest. This is because the location of the antioxidants in the oil-in-water emulsions, and thus in the dried encapsulate, determines their antioxidant activity, which is increased when the antioxidants are located at the oil-water interface. It is thought that at the oil-water or oil-encapsulating agent interfaces autoxidation process begins since pro-oxidants species (e.g., metals) contact the oil and where emulsifiers/surfactants are absorbed. Therefore, the use of emulsifying compounds with antioxidant properties (e.g., radical scavenging) would theoretically improve the oxidative stability of microencapsulated fish oil by inhibiting lipid oxidation at contact area between pro-oxidants and lipids. Moreover, protein hydrolysis enhances both hydrolysates emulsifying properties and the wall matrix protective effect since the smaller peptides size generated act rather as copolymers or fillers of the wall. Hence, protein hydrolysates are thought to improve microencapsulated fish oil oxidative stability by physical and chemical means. In this regard, different studies have been carried out. For instance, Tamm et al. (2015) encapsulated fish oil using GS in presence of β-lactoglobulin (β-LG) or β-lactoglobulin hydrolysates (β-LGH) by spray-drying at 180/70 °C temperature pair (theoretical oil load of ~ 31 %). The hydrolysates were produced to two different degrees of hydrolysis (DH = 3 % and DH = 6 %) by two different enzymes; trypsin (T) and alcalase (A). The EE achieved after drying was high and similar among samples (98.7 % - 99.5 %). Therefore, the different trend of PV curves during storage suggested an enhanced oxidative stability of the encapsulates by the addition of β-LGH (except for β-LGH, DH = 3 %, A). However, in this study the antioxidant activity of the hydrolysates was not assessed (e.g., DPPH scavenging activity) and the differences in the hydrolysates protective effect were attributed to the different peptide profiles as a consequence of the hydrolysates production. The lower PV after the storage time was reported for the sample containing β-LGH, DH = 6 %, produced with T (PV = 39.6 ± 5.9 mmol/kg oil). On the other hand, Morales-Medina et al. (2016) produced fish oil microcapsules with GS and fish protein hydrolysates (FPH, sardine and horse mackerel) to a DH = 5 % by using A or T. The drying process was carried out at 180/70 °C inlet/outlet temperatures and the oil load of the encapsulates was of 14.33 %. The addition of the FPH

to the formulation efficiently stabilized the emulsions prior and during drying (EE = 98.0 ± 0.1 %), however, it could not be established a relationship between the antioxidant activity of the hydrolysates and the course of lipid oxidation. Neither differences in the oxidative stability among samples were observed during the storage time (20 °C, 33 % of relative humidity (RH), 12 weeks) nor by using different substrates (fish species) or enzymes. In this line, Unnikrishnan et al. (2019) studied the suitability of tuna red meat hydrolysate (TPH, DH ~ 30 %) to enhance the oxidative stability of encapsulated sardine oil. For this purpose, TPH was rather used as encapsulating agent or as core polymer. The microcapsules were produced at a core:wall ratio of 1:5 and the spray-drying process was carried out at 180/70 °C inlet/outlet temperatures (EE = 73.89 ± 1.53 % - 78.73 ± 1.94 %). The oxidative stability during storage (1 or 4 weeks) at three different temperatures (4 °C, 28 °C and 60 °C) was assessed by measuring the PV and TBARS value. The results showed that the presence of TPH as a wall co-polymer (in presence of CAS, MD and GA) or in the core, led to an increase in EE. However, the highest oxidative stability of sardine oil during storage (regardless of the temperature) was achieved when TPH was used as core material. Besides, the total replacement of CAS with TPH led to the less oxidatively stable encapsulates although the EE after drying was relatively high (76.64 ± 1.17 %). Moreover, Intarasirisawat et al. (2015) investigated the effect of adding natural antioxidants (tannic acid, TA or oxidized tannic acid, OTA) to the microencapsulates formulation produced with skipjack roe protein hydrolysate (SRPH, DH = 5 %) as the sole wall material, which also exhibit antioxidant activity. The spray-drying process was carried out at 200/108 °C temperature pair. The results showed that SRPH was not suitable as sole wall material due to the low EE achieved after drying (13 %), however it was slightly improved in presence of TA and OTA (28 % and 55 %, respectively). The higher EE value found in presence of OTA was attributed to its crosslinking properties. Regarding the oxidative stability, it was assessed by quantifying the PV, TBARS value and SVOP content after 4 weeks of storage at 30 °C. The results suggested that the presence of OTA and TA improved the oxidative stability of the encapsulates compared to the microcapsules with SRPH alone, however, the reduced form of TA was more efficient than the oxidized form (OTA).

In the last years, the production of fish oil microcapsules using biofunctional compounds as wall materials has gained increasing interest, not only to enhance the oxidative stability of the capsules, but also to provide additional health benefits derived from the wall matrix constituents. Chitosan (Cs) is one of the most abundant natural polysaccharides and its

incorporation into the diet has been related to promote cardio-protective and hypolipidemic effects (Vishnu et al., 2017). In this regard, Vishnu et al. (2017) successfully produced functional sardine oil microcapsules with high oxidative stability by using vanillic acid grafted Cs (Va-g-Ch), an antioxidant-Cs conjugate, as encapsulating agent. The oil load of the capsules was of 30 % and the drying process was carried out at 140/70 °C inlet/outlet temperatures (EE = 84 ± 0.84 %). The PV after the storage time (4 weeks at ambient temperature) became 5.5 ± 0.51 meq peroxide/kg oil and the TBARS value trend indicated that low content of secondary oxidation products was produced. Moreover, the accelerated RANCIMAT test (100 °C and 20 mL/h air flow) showed that the IP of the microcapsules was ~ 11 times higher than that of the sardine oil (7.67 ± 0.05 h over 0.67 ± 0.01 h) indicating a protective effect of the wall matrix. More recently, Chang et al. (2020) used thiol-modified β-lactoglobulin fibril/Cs complex in presence of MD to produce fish oil microcapsules (theoretical oil load of ~ 37 %) at different inlet air temperatures (160 – 180 °C). In all cases the EE achieved was high (89.40 ± 1.80 % - 93.53 ± 1.57 %), not being much affected by the inlet temperature. Unfortunately, the oxidative stability of the encapsulates was not investigated in this study. On the other hand, Kurek et al. (2018) encapsulated cod liver oil in a barley β-D-glucan – waxy maize modified starch blend. β-D-glucan has been related to lower glycemic and insulin responses, lipid metabolism and blood cholesterol levels (Kurek et al., 2018). The ratio of encapsulating agents varied to optimize the wall formulation, and so did the inlet drying temperatures (154 °C – 180 °C) in the experimental design leading to a total of 13 experimental runs. The results from the optimization study showed that the optimum wall matrix consisted of 85 % β-D-glucan (15 % waxy maize modified starch) and that the optimum inlet drying temperature was 154 °C. Under these conditions the encapsulates had an EE of 79.9 % and TBARS value of 1.16 mg MDA/kg powder after drying.

4.2.1.4 Bioaccessibility and Food Enrichment

Although the purpose of producing fish oil microcapsules is to manufacture foods enriched with ω-3 PUFAs to improve peoples' health, only few studies have been carried out regarding the fate of the encapsulated oil in the food matrix (Binsi et al., 2017) and on its gastrointestinal tract (GIT) release (Binsi et al., 2017; Unnikrishnan et al., 2019; Vishnu et al., 2017) (Table 5). The latter is of great importance since the oral bioavailability of TAG (e.g., EPA and DHA) is determined by GIT absorption of TAG residues (e.g., monoglycerides) from gastric and pancreatic lipases hydrolysis. Furthermore, as most of the

encapsulating agents used are water soluble-biopolymers (carbohydrates and proteins), little research has been conducted in order to incorporate fish oil microcapsules into water-based foodstuff (Jeyakumari et al., 2016; Patrick et al., 2013). Binsi et al. (2017) investigated the release of encapsulated oil in both the food system (using buffered saline solution) and GIT (using simulated gastric and intestinal fluids) from microcapsules produced in presence (SOE) or absence (FOE) of sage extract. The authors reported that sage extract enhanced the matrix resistance to water, thus preventing its disintegration and subsequent oil leakage when added to a food matrix (19.74 % of oil release after 4 hours of incubation in the buffered saline solution over 55.22 % of oil release in the FOE sample). Regarding the simulated GIT, the total oil release was higher for the FOE sample due to its poorer structural integrity (87.12 ± 0.93 % over 79.27 ± 0.75 % of total oil release), whereas the retention properties (EE), the oxidative stability and the water resistance were enhanced by adding SP to the formulation. In this line, Unnikrishnan et al. (2019) reported that the incorporation of TPH to the MD/GA-based wall formulation of the encapsulates, resulted in an increased structural stabilization, thus retarding the oil release in the gastric phase of digestion. On the other hand, the encapsulates produced with MD and GA in presence of CAS led to a higher oil release in both the gastric and intestinal phase of digestion, amounting to 88.7 – 93.6 % of total oil release after 5 h of incubation. Moreover, Vishnu et al. (2017) reported that Va-g-Cs as the sole encapsulating agent allowed to achieve a sustained oil release in GIT, since after gastric and intestinal digestion phases, the total oil release was of 66 ± 0.21 %. Karim et al. (2016) studied the GIT oil release of microencapsulates produced using blends of HPMC of different viscosities (5 or 15 cps) at different concentrations in the infeed emulsion (1.25 – 5 %). The oil content was fixed to 5 % in the emulsions. The results showed that the gastric and subsequent intestinal digestions were highly influenced by the concentration of polymer in the formulation, being both negatively correlated, since the highest percentage of oil released (81.27 ± 1.04 %) corresponded to the sample with the lowest HPMC blend content in the emulsion (1.25 %). On the other hand, at the same polymer concentration of the infeed emulsion (5 %) the highest oil release percentage was reported for the sample containing 100 % HPMC 15 cps in both gastric digestion (22.00 ± 1.45 %) and gastric digestion followed by intestinal digestion (51.83 ± 2.18 %), respectively.

Regarding food fortification with ω-3 PUFAs by addition of fish oil microcapsules, Patrick et al. (2013) successfully produced a probiotic fermented milk by adding single-shell (MFO1) or double-shell (MFO2) fish oil encapsulates using GA, NaCMC and sodium

polyphosphate as wall materials. The PV after drying was of 2.98 ± 0.12 meq peroxides/kg oil in MFO1 sample and 2.09 ± 0.05 meq peroxides/kg oil in MFO2 sample. A sensory analysis was conducted on day 2 and day 28 of storage at 4 °C, and all types of fermented milk (including a control fermented milk without encapsulates) received an average score of 5.65/7. Unfortunately, the oxidative stability of the fortified milk over storage time was not investigated. Jeyakumari et al. (2016) produced fortified cookies by adding fish oil encapsulates to the recipe. The oxidative stability of the cookies was assessed by TBARS value over 6 months of storage at room temperature and a sensory evaluation was conducted over the fresh cookies (after baking) by a panel of 10 experts. The results showed that the cookies containing the fish oil encapsulates, regardless of the encapsulating agent (Ge or MD), had the lowest TBARS value over all the storage time compared to other cookies samples containing fish oil (e.g., cookies with emulsified or neat fish oil), being this value comparable with the control cookies (without fish oil). However, only the MD-based encapsulates received a sensory evaluation score similar to that of the control cookies (3.5 ± 0.15 and 3.5 ± 0.08 for the MD-cookies and the control cookies, respectively).

4.2.2 Mono-Axially Electrosprayed Microencapsulates

Electrospraying is an affordable and scalable emerging technology for the production of bioactive encapsulates, which has emerged as an alternative to conventional spray-drying (Jacobsen et al., 2018). This technique, which is included within the so called electrohydrodynamic processes, allows to produce nano-microcapsules by means of high voltage. A schematic representation of the process is shown in Figure 14.

Electrohydrodynamic technology principle is based on applying a high-voltage electrostatic field to charge the surface of encapsulating agents (e.g., biopolymers) solution droplets (Jacobsen et al., 2018). Hence, when the liquid feed is injected through an electrified capillary tube, as consequence of mutual charge repulsion, a meniscus of conical shape (Taylor cone) is formed at the exit. When the electric force overcomes the solution surface tension, a charged jet is ejected from the tip of the Taylor cone and, depending on the jet stability, fibers (electrospinning) or capsules (electrospraying) are produced. At low biopolymer concentrations (low viscoelasticity of the solution) the jet destabilizes and forms a spray of charged droplets, which solidifies through solvent evaporation, and are gathered on a grounded or oppositely charged collector (García-Moreno et al., 2017). The main advantage of electrospraying technology over spray-drying, regarding heat-sensitive bioactive compounds such as ω-3 PUFAs, is that heat is not required at any point of the

process. The evaporation of the solvent in which the encapsulating agent/bioactive are dispersed occurs at ambient temperature, thus thermal degradation is avoided. Furthermore, the resulting encapsulates are smaller (submicron diameter) than those produced by spray-drying (micron diameter) and present larger surface-to-volume ratio, leading to highly bioaccessible encapsulates with little detrimental organoleptic changes when incorporated into food matrices (e.g., unwanted mouthfeel).

Similar to spray-drying technology, the nano-microcapsules properties (e.g., morphology, particle size, or EE) obtained by electrospraying depend on both: (i) the electrospraying process variables (e.g., voltage, flow rate and distance from the collector) and (ii) the biopolymer solution properties (e.g., viscosity, surface tension and conductivity). The latter are of special interest since these will determine the morphology of the encapsulates (e.g., fibers, beaded fibers, capsules or fiber-interconnected capsules) and depend mainly on the biopolymer type, molecular weight, hydrophobic/hydrophilic nature and concentration, as well as on the type of solvent. Table 6 shows the advances made in the last decade in the encapsulation ω-3 PUFAs by electrospraying. In these studies, proteins (e.g., zein, WPC or gelatin), carbohydrates (e.g., dextran or GS) and protein-carbohydrates blends (e.g., WPI-GS or dextran blends) have been reported as suitable encapsulating biopolymers.

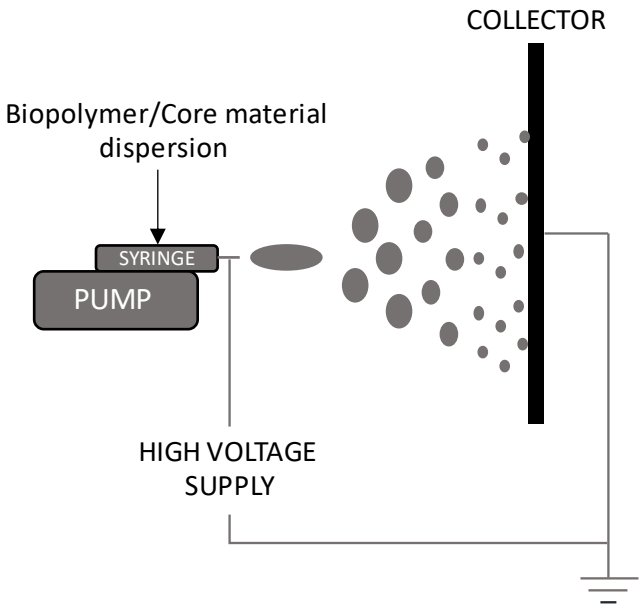

Figure 14. Scheme of electrospraying process.

4.2.2.1 Type and Concentration of Wall Materials

Torres-Giner et al. (2010) produced DHA encapsulates using zein prolamine (a hydrophobic corn protein) as wall material by electrospraying means at lab-scale. In this study, a

biopolymer/DHA solution was prepared in aqueous ethanol (85 wt% ethanol) at a core:wall ratio of 1:2 (theoretical oil load of 33.33 %). Subsequently, the solution was electrosprayed under a steady flow rate of 0.20 mL/h, 12 kV and under air atmosphere at 18 °C (RH = 40 %). The collector was placed 15 cm apart from the ejecting needle. The resulting DHA-capsules presented a smoother surface than zein encapsulates without DHA, and had an average diameter of 490 ± 200 nm. However, nano-sized fibers interconnecting the capsules could be observed. Regarding the oxidative stability of the encapsulates, based on SVOP, zein efficiently protected DHA from oxidation. The content of propanal, 2,4 – heptadienal and 2,4,7 – decatrienal, which are common compounds derived from oxidation of fish oil ω-3 PUFAs, were significantly lower in the encapsulates compared to those reported for neat DHA. For instance, after 1 week of storage at 18 °C, the relative peak area of propanal in neat DHA amounted to 5.62 %, whilst for DHA-capsules was of 0.78 %. Moomand & Lim (2015) also encapsulated fish oil within a zein matrix (30 % of oil load) at different protein concentrations (10 or 20 wt %) using aqueous solutions of ethanol or isopropanol (70 wt %). The electrospraying process was carried out at lab-scale at a pump flow rate of 1 mL/h and 20 kV. The ambient conditions were controlled at 20 ± 2 °C and 40 % RH, and the collector was placed at 20 cm from the ejecting needle. The authors reported that decreasing the zein concentration from 20 to 10 wt % led to the formation of capsules instead of fibres due to a lower viscosity of the infeed solution. In addition, the solvent used to disperse the biopolymer together with the oil phase influenced the particle size. The ethanol-based solution led to particles of diameters ranging from 400 – 500 nm, whilst the isopropanol-based particles varied from 600 to 800 nm.

Gómez-Mascaraque & López-Rubio (2016) carried out a comparative study between spray-drying and electrospraying using WPC, SPI and gelatin (G) as wall materials. ALA was used as the core bioactive and the encapsulates were produced to a fixed ALA load of 10 %, regardless of the drying procedure. The scanning electron microscopy (SEM) images showed that spray-dried capsules were larger and had a wider particle size distribution than those produced by electrospraying. Moreover, the fourier transform infrared (FT-IR) spectra analysis suggested that the bioactive encapsulated in spray-dried capsules was degraded during processing since the characteristic ω-3 PUFA absorption band was not detected. The authors attributed this finding to the high inlet drying temperature used in the spray-drying process (90 °C). Conversely, electrosprayed capsules produced with WPC and SPI, which were produced at a steady flow rate of 0.15 mL/h and by applying 15 – 17 kV (Table 6),

evidenced ALA presence during storage as measured by FT-IR. Thus, these results suggested an enhanced oxidative stability of ALA-loaded electrosprayed capsules produced with WPC and SPI, compared to ALA-loaded spray-dried capsules.

García-Moreno et al. (2017) optimized the biopolymer solution formulation to produce fish oil electrosprayed capsules in lab-scale using dextran (D, molecular weight = 70 kDa, dextran70) as wall material. The polymer was dissolved in water at different concentrations (20 – 40 wt %), whilst the oil load of the encapsulates was fixed to 10 %. It should be mentioned that the oil was introduced to the infeed solution as a fish oil-in-water emulsion stabilized with WPI. The electrospraying process was conducted at a flow rate of 0.01 mL/min, 20 kV, under inert atmosphere (nitrogen) and the collector was placed at 15 cm from the needle. In the study, the authors reported that increasing the polymer concentration resulted in the formation of fibers instead of capsules, being this fact attributed to an increase of the solution viscosity. The oxidative stability of these encapsulates is discussed below in section 4.2.2.2. More recently, the same authors (García-Moreno et al., 2018) produced fish oil encapsulates by electrospraying using D (molecular weight = 70 kDa, dextran70) or GS (DE38, molecular weight = 12.5 kDa) as wall materials in presence of WPC. In both cases, pullulan (P, molecular weight = 200 kDa) was added to the formulation as thickening agent to increase the stability of the Taylor cone at high flow rates (up to 0.012 mL/min). The oil was added to the infeed solution as neat oil to a final oil load of the encapsulates of 20 %, followed by subsequent emulsification process. The electrospraying process was carried out at lab-scale at a flow rate ranging from 0.003 – 0.012 mL/min and 17 – 20 kV, depending on the biopolymer solution, being the collector placed at 15 cm from the needle. In case of dextran70 solution, the authors reported that decreasing the polymers concentration (2 wt% to 1 wt% for P and 20 wt% to 15 wt% D) avoided capsules' fibril defects but also led to a reduction in the process flow rate. Both facts were attributed to a reduction in polymer chain entanglements and viscosity of the infeed emulsion. On the other hand, increasing the P concentration from 2 wt% to 4 wt% in the GS emulsion (15 wt%) had no effect on the microstructures morphology since capsules were obtained in this range of P content. However, at 4 wt% P, although the droplets size of the emulsion increased, the electrospraying process flow rate was higher (0.010 mL/h at 4wt% P over 0.007 mL/h at 2 wt% P), thus favoring microcapsules productivity. The oxidative stability of the resulting encapsulates is discussed in the next section (section 4.2.2.2).

Oxygen permeability trough the wall matrix has been reported to have a major impact on encapsulates oxidative stability. Indeed, this fact is even more relevant in electrosprayed capsules since the smaller particle size leads to an increase in the surface-to-volume ratio and a reduction in the thickness of the wall matrix. In this regard, Boerekamp et al. (2019) studied the influence of the wall material in oxygen permeability and its impact on encapsulated fish oil oxidative stability by electron spin resonance (ESR). D or GS were used as the wall materials in presence of P and WPI and MCT oil or fish oil were encapsulated to investigate both the oxygen permeability and oxidative stability, respectively. The electrospraying process was carried out at lab-scale under controlled ambient conditions (20 ± 4 °C and 17 – 46 % RH), at a flow rate ranging from 0.003 – 0.010 mL/min and an applied voltage of 15 – 20 kV (Table 6). The oxygen permeability results showed that, although both encapsulates were in a glassy state at ambient conditions, D-based capsules were more permeable to oxygen than GS-based encapsulates. This was attributed by the authors to a more effective packaging of GS in the wall matrix due to its lower molecular weight (12.5 kDa over 70 kDa of D), which resulted in less free volume, thus less oxygen permeability. Moreover, the encapsulates oxidative stability based on ESR results, showed that GS-based capsules were less oxidized over the storage time (50 °C during 16 days) that D-based capsules, meaning that oxygen diffusivity trough the wall matrix played a major role on oxidative stability of fish oil-loaded electrosprayed capsules.

4.2.2.2 Oil Emulsification Approach

In emulsion-based electrospraying processes (e.g., when using water-based polymers solution) both the emulsification approach and the oil introduction method in the infeed emulsion (emulsified oil or neat oil) play a major role on microcapsules properties such as particle size, EE and oxidative stability. Paximada et al. (2018) studied the influence of the emulsification process regarding the homogenization pressure (1000 or 2000 bar) and number of passes (1, 2, 4 and 8) in the fish oil-loaded electrosprayed encapsulates properties (particle size, EE). The capsules were produced using WPI as wall material in presence of MD and tween 20 (T20) at a core:wall ratio of 1:1.4 (theoretical oil load of ~ 42 %). The electrospraying process was carried out at a constant flow rate of 0.02 mL/min, applying a voltage of 18 kV and with the collector placed at 18 cm from the needle. The authors reported that the smaller the emulsion oil droplet size (achieved by increasing the homogenization pressure and number of passes), the smaller as the electrosprayed particles size. Moreover, the EE was also affected by the emulsification conditions since the particles produced from

emulsions homogenized at 1000 bar led to lower EE values (60 – 80 %) than those homogenized at 2000 bar (EE = 70 – 98 %). In the study, the most stable emulsion system attending to the smallest oil droplet size was the one that produced at 2000 bar after 8 passes (d50 = 95 nm). However, this emulsion did not produce any powder due to its high viscosity, which affected the electrospraying process. Gómez-Mascaraque & López-Rubio (2016) produced ALA-encapsulates using WPC, SPI and gelatin (Gel) as wall materials. The authors reported that the emulsification approach affected both the oil droplets size distribution in the water-based (WPC and SPI) or acetic acid-based (Gel) infeed emulsions and the EE of the resulting encapsulates (EE = 23 ± 12 – 67 ± 5 %). Although mechanical stirring (U) followed by US led to smaller droplets sizes in the emulsions, the EE of the encapsulates was also lower. This fact was attributed to thermal degradation of ALA in the US treatment, which raised the emulsion temperature up to 45 °C. The oxidative stability of the electrosprayed encapsulates was assessed by studying the degradation profile (by FT-IR) under accelerated oxidation conditions (80 °C during 2 days) and the results indicated that, although the WPC and SPI-based encapsulates presented higher stability than neat ALA, both the emulsification approach and the encapsulating agent had little impact on lipid oxidation course. On the other hand, G-based encapsulates did not exert any protective effect against ALA oxidation (on the contrary accelerated its degradation), probably due to the presence of residual solvent in these capsules.

García-Moreno et al. (2018) produced carbohydrate-based (P or D) electrosprayed capsules in pilot plant scale by using two different emulsification approaches namely, high pressure homogenization and rotor-stator homogenization. In this study the authors found that the EE of the encapsulates did not correlate with the oil droplets size in the emulsions since rotor-stator homogenization, which led to the larger oil droplets size, also led to the highest EE values of the encapsulates in both emulsions (97.1 ± 0.9 % for D-based encapsulates and 85.7 ± 0.3 % for GS-based encapsulates, respectively). However, D-based capsules presented smaller oil droplets size and higher EE compared to GS-based capsules regardless of the emulsification approach. In all cases, the initial PV of the encapsulated oil was higher than that of neat oil, and both the emulsification approach and the encapsulating agent had little effect. However, during storage time (20 °C during 21 days) the encapsulates produced from high-pressure homogenized emulsions presented lower oxidative stability than those produced from rotor-stator homogenized emulsions, based on PV and SVOP content trends. Moreover, although the PV trend during storage did not show significant differences

regarding the encapsulating agents, differences were observed in the SVOP trends. The results showed that GS-based encapsulates were the most oxidatively stable over storage time, despite their higher extractable oil content. This finding was attributed by the authors to less free volume of the GS wall matrix due to its lower molecular weight (12.5 kDa over 70 kDa of P), which reduced oxygen diffusivity. Regarding oil addition method to the infeed emulsion, García-Moreno et al. (2017) produced D-based electrosprayed capsules (both in lab-scale and pilot plant scale) by using two different oil-incorporation approaches: (i) fish oil-in-water emulsion (EFO) stabilized with WPI, and (ii) neat fish oil (NFO) using T20 as emulsifier. The optimized biopolymer solution consisted of D (molecular weight = 70 kDa) at 25 wt% in water and the oil load of the particles was fixed to 10 %, regardless of the oil-addition method. Although oil incorporated as NFO led to larger capsules due to the larger oil droplets size in the emulsion, the EE in these capsules was higher when compared to the encapsulates where the oil was added as EFO, even having smaller droplet sizes in the latter (75.5 ± 0.9 % for NFO over 68.3 ± 0.3 % for EFO). Furthermore, regarding PV after lab-scale production (2 h batches), the results showed that the oil-addition approach had little impact on fish oil oxidative stability, being both encapsulates relatively oxidized after production (43.9 ± 19.8 meq O2/kg oil for NFO and 48.1 ± 4.0 meq O2/kg oil for EFO). However, at pilot plant scale production, NFO-addition led to less oxidized encapsulates with PV of 21.2 ± 9.5 meq O2/kg oil after production, when compared to EFO-based encapsulates (PV=62.3 ± 4.5 meq O2/kg oil).

4.2.2.3 High-Throughput Electrospraying, Addition of Antioxidants and Food Enrichment

Typically, one of the main drawbacks of electrospraying technology has been its low productivity as consequence of the low flow rates achieved during processing. To overcome this situation, Busolo et al. (Busolo et al., 2019) have recently developed a novel electrospraying technology, namely Electrospraying Assisted by Pressurized Gas (EAPG), which allows to increase the capsules production by atomizing the infeed solution into a high electrostatic field by means of compressed air. The equipment consists of an injection unit, a drying camber and a cyclone to collect the dry encapsulates as free-flowing powder. The authors had first used this technology to produce DHA-enriched fish oil encapsulates within a zein matrix (core:wall ratio of 1:2) to produce fortified milk. The electrospraying process was conducted by EAPG under controlled ambient conditions (25 °C and 40 % RH) at a feed flow rate of 10 mL/min, 20 kV and an air atomizing pressure of 10 L/min, whilst the infeed

solution was constantly bubbled with nitrogen. The resulting powder had a mean size of 1.4 ± 0.8 μm, an EE of 84 ± 1 % and an initial PV of ~ 1.5 meq peroxide/kg oil. The oxidative stability of the encapsulates was studied under different storage conditions by varying the temperature (5 °C to 23 °C), RH (0 % to 65 %) and environment (dark/light, or air/vacuum) up to 45 days. In all cases, the oxidation rate of DHA neat oil was higher than that of the encapsulates, thus indicating effective protection of the zein matrix against lipid oxidation. However, the highest oxidative stability was achieved at ambient conditions (23 °C and 65 % RH) at dark and under vacuum in both neat oil (18 meq peroxide/kg oil) and encapsulates (< 2 meq peroxide/kg oil), which meant that oxygen had a greater influence on lipid oxidation than temperature and humidity. In addition, regarding production of fortified milk, the encapsulates were easier to disperse in the milk preparation than neat oil and did not present any lumps or oil droplets. Moreover, the panelists who evaluated the fortified milk organoleptic properties, found little differences compared to the blank (unfortified milk) even when the milk was prepared with encapsulates stored for 45 days (at -1 °C in the dark and under vacuum).

EAPG technology has been also used to produce carbohydrate-based (D. Hermund et al., 2019a) and protein-based (Miguel et al., 2019) encapsulates in order to produce fortified foodstuff (Table 6). Hermund et al. (D. Hermund et al., 2019b) produced fish oil encapsulates within a GS or D matrix in presence and absence of antioxidants (seaweed extract or δ-tocopherol and rosemary extract) to produce fortified mayonnaise. The biopolymer solution formulation consisted of WPC, P and GS or D. The seaweed extract was added to both solutions, while commercial natural antioxidants were only added to the GS-based formulation. The oil was introduced to the infeed emulsion as an oil-in-water emulsion stabilized with citrem to a final oil load of the encapsulates of 20 %. The electrospraying process was carried out at a flow rate of 1.8 mL/min and 15 kV under controlled ambient conditions (24 °C and 40 % RH) leading to small capsules (< 3 μm) with high EE (83.2 ± 0.5 % - 90.4 ± 0.1 %). The authors reported that the addition of antioxidants, compared to other previous results, did not enhanced encapsulates oxidative stability during storage (20 °C during 21 days in the dark) based on PV. However, the addition of commercial antioxidants lowered the content of some SVOP ((E)-2-pentenal and nonanal) in GS-based capsules. Conversely, the addition of seaweed extract exerted a pro-oxidative effect on the latter encapsulates leading to a final PV of 34.6 ± 0.5 meq peroxide/kg oil after 21 days of storage. The content of some SVOP such as 1-penten-3-ol and nonanal increased

as well. Nonetheless, the addition of seaweed extract to D-based encapsulates exhibited an antioxidative effect based on SVOP trends, except for 1-penten-ol. This fact was attributed to the pro-oxidant species present in the seaweed extract (e.g., pigments or metals), which catalyzed non-encapsulated oil oxidation more efficiently in GS encapsulates as this samples presented the lowest EE (85.7 ± 0.4 % over 90.4 ± 0.1 % for the D-based encapsulates). These authors also evaluated the oxidative stability of GS capsules-enriched mayonnaise (in presence or absence of commercial antioxidants) compared to mayonnaise fortified by adding NFO. The addition of encapsulates to an already formed mayonnaise led to an increase in the oil droplets size compared to mayonnaise fortified with NFO, indicating that the capsules could have disintegrated leading to unencapsulated oil which could flocculate/coalesce. The results also showed that GS-based encapsulates acted as a thickening agent since the apparent viscosity of capsules-enriched mayonnaise also increased. Regarding oxidative stability, all the mayonnaise samples presented a low initial PV (< 0.5 meq peroxides/kg oil), but the trends in lipid oxidation over the storage time (20 °C in the dark during 21 days) significantly differed. The results showed that the addition of encapsulates, either in presence or absence of antioxidants, did not improve the oxidative stability of the mayonnaise since both the PV and SVOP content were higher during the storage time compared to mayonnaise fortified with NFO. The authors attributed this finding to a release of oil with poorer oxidative status as consequence of the encapsulation process, caused by the encapsulates disintegration in the food matrix. Moreover, the most oxidized mayonnaise after the storage time was that fortified with encapsulates containing natural antioxidants (~ 12 meq peroxide/kg oil), which did not exert any protective effect in presence of iron released from egg yolk due to the lack of metal chelating activity. Miguel et al. (2019) encapsulated fish oil by EAPG using zein as encapsulating agent (20 % oil load) with food fortification purposes (low fat mayonnaise). The EAPG process was carried out under ambient controlled conditions (24 °C and 40 % RH) at an infeed solution flow rate of 1.4 mL/min, 10 kV and with an air pressure of 10 L/h (Table 6), resulting in encapsulates with a mean diameter of 2.4 ± 0.7 μm and an EE of 83 ± 1 %. Cryo-SEM images of fortified mayonnaise showed that zein encapsulates remained intact after foodstuff production, which correlated well with its higher apparent viscosity (compared to mayonnaise fortified with NFO) due to encapsulates thickening activity. Besides, mayonnaise fortified with encapsulated fish oil presented a larger oil droplets size of approximately 2.5-fold that of NFO fortified mayonnaise (D[4,3] = 39.7 ± 0.2 μm, over D[4,3] = 16.2 ± 2.7 μm). The oxidative stability of the enriched mayonnaise was assessed by measuring the PV and SVOP

content during 21 days of storage at 25 °C in the dark. The results showed that initial PV of the encapsulates-fortified mayonnaise were 4-fold that of NFO-fortified mayonnaise (2.1 ± 0.1 meq peroxide/kg oil), however this value did not change significantly over the storage time. Conversely, PV of NFO-fortified mayonnaise increased drastically after 14 days of storage. Regarding SVOP, the results suggested that the higher values found in encapsulates-fortified mayonnaise was due to: (i) volatile compounds already present in the zein protein (e.g., hexanal, 3-methyl-butanal or nonanal), and (ii) fungal spoilage of the mayonnaise (e.g., 3-methyl-1-butanol).

4.2.2.4 Bioaccessibility

Since the main purpose of designing efficient ω-3 PUFAs (e.g., fish oil) delivery systems is to increase oral EPA and DHA bioavailability, the core bioactive release in the GIT should be also studied. Moomand & Lim (2015) investigated the release profile of zein-based fish oil encapsulates (fibers or capsules) in the GIT under simulated gastric fluid (SGF) conditions (with and without pepsin) and under simulated intestinal fluid (SIF) conditions (with and without pancreatin), separately. The oil release profile under sequential exposure to SGF and SIF, in presence or absence of digestive enzymes, was also evaluated. The results showed that the release profile of encapsulated fish oil was influenced by GIT erosion behavior of the wall material, being the release rate higher under SGF conditions (pH = 2) than under SIF conditions (pH = 6.8), in absence of digestive enzymes. Furthermore, the presence of digestive enzymes favored oil release under both GIT conditions. These findings correlated well when sequential exposure to SGF and SIF was investigated since the release values obtained where comparable to those reported for SGF conditions alone. After sequential GIT study, the oil released in absence of enzymes ranged between 77 – 87 %, whilst in presence of enzymes amounted to 86 – 95 %.

Table 6. Recent studies on ω-3 PUFAs encapsulation by electrospraying.

ω-3 source	Encapsulating Agent(s)	Solvent(s)	Emulsifier(s)	Processing conditions	LC/EE	Capsules size	Oxidative Stability	Food application	References
Cod liver oil	Dextran	Water	WPI Tween 20 (T20)	Lab scale: 20 kV, 0.01 mL/min, 15 cm No T or RH control P-P scale: 24 needles, 42 kV, 5 mL/h, 10 cm No T or RH control	Theoretical LC: 10 %; EE: 68.3 - 75.5 %	0.1 - 3.3 µm	No storage analysis PV SVOP	NR	(García-Moreno et al., 2017)
DHA	Zein	Ethanol/Water 85/15, (v/v) %	-	12 kV, 0.20 mL/h, 15 cm 18 °C, 40 %(RH)	Theoretical LC: 33.33 %; EE: NR	490 ± 200 nm	18 °C/40 %(RH)/7 days SVOP	NR	(Torres-Giner et al., 2010)
Fish oil	Zein	Ethanol/Water Isopropanol/Water 70/30, (w/w) %	-	20 kV, 1 mL/h, 20 cm 21 ± 2 °C, 40 %(RH)	Theoretical LC: 30 %; EE: NR	400 - 500 nm 600 - 800 nm	-	NR	(Moomand & Lim, 2015)
ALA	Whey protein concentrate (WPC) Soy Protein Isolate (SPI) Gelatin (Gel)	Water Acetic acid, 20 % (v/v)	Tween 20 (T20)	15 - 17 kV, 0.15 mL/h, 10 cm No T or RH control	Theoretical LC: 10 %; EE (based on FT-IR absorbance measurements): 23 - 67 %	0.25 - 3.25 µm	80 °C/120 h FT-IR absorbance measurements	NR	(Gómez-Mascaraque & López-Rubio, 2016)
Cod liver oil	Dextran:Pullulan Glucose Syrup:Pullulan	Water	WPC Citrem	Lab scale: 17 - 20 kV, 0.18 - 0.72 mL/h, 15 cm No T or RH control EAPG: 10 - 15 kV, 90 - 108 mL/h 24 °C, 40 %(RH)	Theoretical LC: 20 %; EE (EAPG): 78.1 - 91.7 %	Lab scale: 60 - 70 % of capsules < 1 µm EAPG: 70 % of capsules < 3 µm	20 °C/21 days PV SVOP	NR	(García-Moreno et al., 2018)
MCT oil Fish oil	Dextran:Pullulan Glucose Syrup:Pullulan	Water	WPC Citrem	15 - 20 kV, 0.18 - 0.60 mL/h, 15 cm 24 ± 4 °C, 17 - 46 %(RH)	Theoretical LC: 20 %; EE: NR	Dextran: 1.26 ± 0.57 µm Glucose: 1.39 ± 0.52 µm	50 °C/16 days Electron Spin Resonance (ESR)	NR	(Boerekamp et al., 2019)

Fish oil	Whey protein Isolate:Maltodextrin	Water	Tween 20 (T20	18 kV, 1.2 mL/h, 13 cm No T or RH control	Theoretical LC: ~ 42 %; EE: 60 - 98 %	d50 = 198 - 974 nm	-	NR	(Paximada et al., 2018)
Fish oil (DHA)	Zein	Ethanol/Water 85/15, (v/v) %	-	EAPG: 20 kV, 10 mL/min, air pressure of 10 L/mi 25 °C, 40 %(RH)	Theoretical LC: 33.33 %; EE: 84 %	1.4 ± 0.8 µm	°C/0 %(RH)/45 days/air and darknes 23 °C/0 %(RH)/45 days/air and light /65 %(RH)/45 days/vacuum and darl PV	Powdered milk	(Busolo et al., 2019)
Cod liver oil	Dextran:Pullulan Glucose Syrup:Pullulan	Water	WPC Citrem	EAPG: 15 kV, 1.8 mL/min, air pressure NR 24 °C, 40 %(RH)	Theoretical LC: 20 %; EE: 83.2 - 90.4 %	Dextran: ~ 80 % of capsules < 2 µm Glucose: ~ 80 % of capsules < 3 µm	20 °C/21 days/darkness PV SVOP	..ight mayonnaise	(D. Hermund et al., 2019b)
Cod liver oil	Zein	Ethanol/Water 85/15, (v/v) %	-	EAPG: 10 kV, 1.4 mL/min, air pressure 10 L/min 24 °C, 40 %(RH)	Theoretical LC: 20 %; EE: 83 %	2.4 ± 0.7 µm	20 °C/35 days/darkness PV SVOP	ow-fat mayonnais	(Miguel et al., 2019)

*Abbreviations: LC, load capacity; EE, encapsulation efficiency; ALA, α-linolenic acid; DHA, docosahexaenoic; WPC, whey protein concentrate; WPI, whey protein isolate; EAPG, electrospraying assisted by pressurized gas; PV, hydroperoxides content; SVOP, secondary volatile oxidation products; FT-IR: Fourier transform infrared; NR: not reported.

4.2.3 Coaxially-Electrosprayed Microcapsules

Coaxial electrospraying is an emerging technology, which modifies monoaxial processing by introducing a coaxial capillary nozzle allowing to electrospray two liquids simultaneously (Jaworek, 2016). There are some differences between these two technologies. Monoaxial electrospraying rely on chemical means to form a core/shell structure by dispersing the core material in the encapsulating agent solution by using emulsifiers or surface-active biopolymers, while coaxial electrospraying achieves the core/shell structure by physical separation of the solutions (Figure 15). The latter leads to: (i) a centralized distribution of the encapsulated compounds (Loscertales et al., 2002), (ii) higher LC, and (iii) higher EE (Jaworek, 2016). In addition, co-axial electrospraying allows producing microcapsules from two immiscible liquids without the need of preparing an emulsion. This is of great interest in terms of ω-PUFAs (e.g., fish oil) encapsulation since it has been demonstrated that the emulsification step initiate lipid oxidation by means of mechanical stress and shear forces, which favors pro-oxidant species inclusion and/or distribution (e.g., oxygen or metal ions).

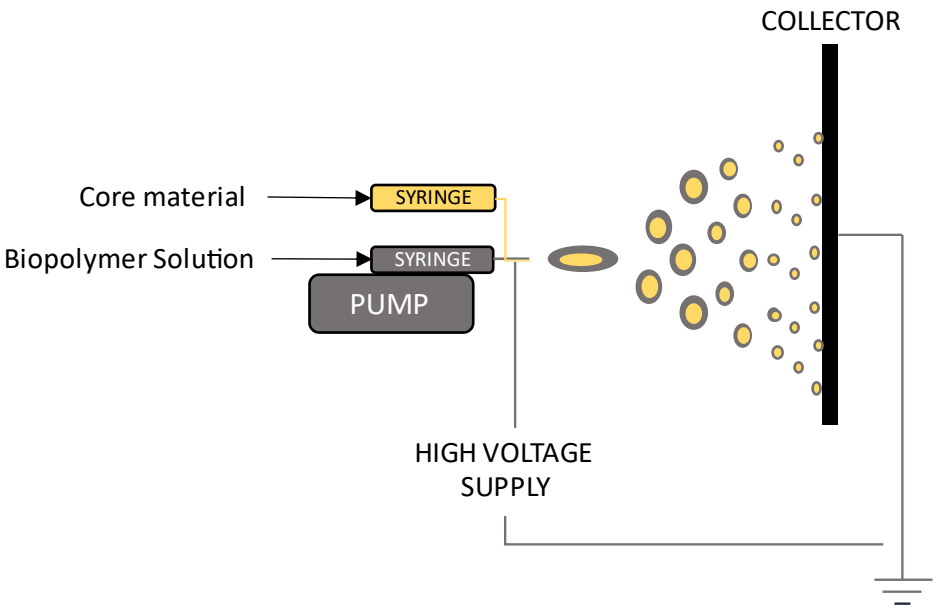

Figure 15. Scheme of coaxial electrospraying process.

As electrohydrodynamic methods, coaxial electrospraying consist of applying high-voltage electrostatic field between the coaxial nozzle and the collector to produce core/shell-structured powder. Through the inner needle, the core material flows and through the annular gap, between the inner and the outer needle, the polymer solution flows. Both liquids are at the same potential. In this technology, the driving liquid is referred to the one with the highest

conductivity, which is usually the outer liquid, although it could also be the inner solution (Loscertales et al., 2002). Process parameters (e.g., applied voltage or inner/outer flow rate ratio) and the driving liquid properties (e.g., viscosity or conductivity) will determine the process throughput (stable Taylor cone) and the nano-microcapsules properties such as particle size and wall thickness. Thus, encapsulates of poorly conductive core materials (e.g., fish oil) can be produced if the encapsulating agent solution (driving liquid) is conductive enough.

Coaxial electrospraying technology has been successfully used to encapsulate bioactive compounds for pharmaceutical purposes (e.g., drug delivery systems) (Chen et al., 2019). Nonetheless little research work is available on coaxial encapsulation of bioactives for food fortification purposes. In one important study, Yang et al. (2017) first produced fish oil-loaded fibers in presence of zein (core solution) using poly- vinylpyrrolidone (PVP) as wall material (outer solution) which led to high quality encapsulates (oil load of 14.5 %, EE of 96.9 % and average diameter of the fibers of 560 nm) with enhanced oxidative stability and favorable oil release behavior. However, to the best of the authors' knowledge, Gómez-Mascaraque et al. (2019) reported for the first time the production of ω-3 PUFAs encapsulates by coaxial electrospraying within food-grade wall matrices and using food grade solvents. In this study, the authors successfully encapsulated ALA-zein solutions (core material) within a zein or G matrix (wall material) at a final oil load of 10 %. The coaxial electrospraying process was carried out at flow rates of 0.05 mL/h and 0.15 mL/h for the inner and outer solution respectively, and the voltage applied ranged from 13 kV to 18 kV. The collector was placed at 10 cm from the coaxial nozzle. Regarding morphology and size of the encapsulates, the authors reported that neither the incorporation of ALA to the zein solution nor the incorporation of an additional zein layer, affected the morphology or the size of the encapsulates. However, the addition of G led to larger capsules and broader particles size distribution together with the appearance of fibril defects. Furthermore, the results showed that the EE was higher for both coaxial encapsulates than monoaxial zein-based capsules, being the highest EE greater than 80 % in the zein-zein system. Nonetheless, the latter exerted a less efficient protective effect against ALA degradation under accelerated oxidation conditions (80 °C) than the G-zein system despite its lower EE. This fact was attributed by the authors to the lower affinity of ALA with G (outer wall layer), which could have result on less content of ALA in the capsules surface.

5. CONCLUSIONS AND FUTURE PERSPECTIVES

The production of fortified food-stuff containing ω-3 PUFAs in the form of fish oil is indeed possible by designing efficient delivery systems, which prevent both lipid oxidation and subsequent odor/texture deterioration of the food matrix. In this regard, the production of fish oil-in-water emulsions and fish oil microcapsules, in presence or not of antioxidants, has been widely investigated with promising outcomes. Spray-drying is currently the most used encapsulation technique in food industry, however the use of high drying temperatures together with the fact that most of the encapsulating agents are water soluble restrict its use for ω-3 PUFAs food fortification purposes. As an alternative, new technologies such as electrospraying and coaxial electrospraying, based on applying high-voltage electrostatic field to produce the encapsulates, are arising as promising encapsulation methods. Nonetheless, the main drawback of the latter technologies is the low throughput of the process, especially when food-grade biopolymers are used as encapsulating agents. Thus, further research is needed to increase the process production yield of mono- and co-axial electrospraying and to investigate the addition of the resulting electrosprayed encapsulates to complex food matrices.

6. REFERENCES

Aghbashlo, M., Mobli, H., Madadlou, A., & Rafiee, S. (2012). The correlation of wall material composition with flow characteristics and encapsulation behavior of fish oil emulsion. *Food Research International*, *49*(1), 379–388. https://doi.org/10.1016/j.foodres.2012.07.031

Aghbashlo, M., Mobli, H., Madadlou, A., & Rafiee, S. (2013). Influence of Wall Material and Inlet Drying Air Temperature on the Microencapsulation of Fish Oil by Spray Drying. *Food and Bioprocess Technology*, *6*(6), 1561–1569. https://doi.org/10.1007/s11947-012-0796-7

Alemán, M., Bou, R., Guardiola, F., Durand, E., Villeneuve, P., Jacobsen, C., & Sørensen, A. D. M. (2015). Antioxidative effect of lipophilized caffeic acid in fish oil enriched mayonnaise and milk. *Food Chemistry*, *167*, 236–244. https://doi.org/10.1016/j.foodchem.2014.06.083

Berdahl, D. R., & McKeague, J. (2015). Rosemary and sage extracts as antioxidants for food preservation. In *Handbook of Antioxidants for Food Preservation* (pp. 177–217). Woodhead Publishing. https://doi.org/10.1016/B978-1-78242-089-7.00008-7

Berton-Carabin, C. C., Ropers, M. H., & Genot, C. (2014). Lipid Oxidation in Oil-in-Water Emulsions: Involvement of the Interfacial Layer. *Comprehensive Reviews in Food Science and Food Safety*, *13*(5), 945–977. https://doi.org/10.1111/1541-4337.12097

Berton-Carabin, C. C., Sagis, L., & Schroën, K. (2018). Formation, Structure, and Functionality of Interfacial Layers in Food Emulsions. *Annual Review of Food Science and Technology*, *9*(1), 551–587. https://doi.org/10.1146/annurev-food-030117-012405

Binsi, P. K., Nayak, N., Sarkar, P. C., Jeyakumari, A., Muhamed Ashraf, P., Ninan, G., & Ravishankar, C. N. (2017). Structural and oxidative stabilization of spray dried fish oil microencapsulates with gum arabic and sage polyphenols: Characterization and release kinetics. *Food Chemistry*, *219*, 158–168. https://doi.org/10.1016/j.foodchem.2016.09.126

Boerekamp, D. M. W., Andersen, M. L., Jacobsen, C., Chronakis, I. S., & García-Moreno, P. J. (2019). Oxygen permeability and oxidative stability of fish oil-loaded electrosprayed capsules measured by Electron Spin Resonance: Effect of dextran and glucose syrup as main encapsulating materials. *Food Chemistry*, *287*, 287–294. https://doi.org/10.1016/j.foodchem.2019.02.096

Busolo, M. A., Torres-Giner, S., Prieto, C., & Lagaron, J. M. (2019). Electrospraying assisted by pressurized gas as an innovative high-throughput process for the microencapsulation and stabilization of docosahexaenoic acid-enriched fish oil in zein prolamine. *Innovative Food Science and Emerging Technologies*, *51*, 12–19. https://doi.org/10.1016/j.ifset.2018.04.007

Calder, P. C. (2013). Nutritional benefits of omega-3 fatty. In *Food Enrichment with Omega-3 Fatty Acids* (pp. 3–26). Woodhead Publishing Limited. https://doi.org/10.1533/978-0-85709-886-3.1.3

Calder, P. C. (2014). Very long chain omega-3 (n-3) fatty acids and human health. *European Journal of Lipid Science and Technology*, *116*(10), 1280–1300. https://doi.org/10.1002/ejlt.201400025

Chang, C., & Nickerson, M. T. (2018). Encapsulation of omega 3-6-9 fatty acids-rich oils using protein-based emulsions with spray drying. *Journal of Food Science and Technology*, *55*(8), 2850–2861. https://doi.org/10.1007/s13197-018-3257-0

Chang, H. W., Tan, T. B., Tan, P. Y., Nehdi, I. A., Sbihi, H. M., & Tan, C. P. (2020). Microencapsulation of fish oil-in-water emulsion using thiol-modified β-lactoglobulin fibrils-chitosan complex. *Journal of Food Engineering*, *264*(July 2019), 109680. https://doi.org/10.1016/j.jfoodeng.2019.07.027

Chen, C., Liu, W., Jiang, P., & Hong, T. (2019). Coaxial electrohydrodynamic atomization for the production of drug-loaded micro/nanoparticles. *Micromachines*, *10*(2). https://doi.org/10.3390/mi10020125

Decker, E. A. (2002). Antioxidant Mechanisms. In *Food Lipids: Chemistry, Nutrition, and Biotechnology* (pp. 397–422). CRC Press. https://doi.org/10.1201/9781420046649.ch18

Desai, K. G. H., & Park, H. J. (2005). Recent developments in microencapsulation of food ingredients. *Drying Technology:An International Journal*, *23*(7), 1361–1394. https://doi.org/10.1081/DRT-200063478

Di Giorgio, L., Salgado, P. R., & Mauri, A. N. (2019). Encapsulation of fish oil in soybean protein particles by emulsification and spray drying. *Food Hydrocolloids*, *87*(September 2018), 891–901. https://doi.org/10.1016/j.foodhyd.2018.09.024

Díaz, M., Dunn, C. M., McClements, D. J., & Decker, E. A. (2003). Use of caseinophosphopeptides as natural antioxidants in oil-in-water emulsions. *Journal of Agricultural and Food Chemistry*, *51*(8), 2365–2370. https://doi.org/10.1021/jf025984l

Drusch, S., Rätzke, K., Shaikh, M. Q., Serfert, Y., Steckel, H., Scampicchio, M., Voigt, I., Schwarz, K., & Mannino, S. (2009). Differences in free volume elements of the carrier matrix affect the stability of microencapsulated lipophilic food ingredients. *Food Biophysics*, *4*(1), 42–48. https://doi.org/10.1007/s11483-008-9100-9

EFSA. (2009). Scientific Opinion on the substantiation of health claims related to EPA, DHA, DPA and maintenance of normal blood pressure (ID 502), maintenance of normal HDL-cholesterol concentrations (ID 515), maintenance of normal (fasting) blood concentrations of tr. *EFSA Journal*, *7*(9), 1–26. https://doi.org/10.2903/j.efsa.2009.1263

EFSA. (2010a). Scientific Opinion on Dietary Reference Values for fats, including saturated fatty acids, polyunsaturated fatty acids, monounsaturated fatty acids, trans fatty acids, and cholesterol. *EFSA Journal*, *8*(3), 1–107. https://doi.org/10.2903/j.efsa.2010.1461

EFSA. (2010b). Scientific Opinion on the substantiation of health claims related to docosahexaenoic acid (DHA) and maintenance of normal (fasting) blood concentrations of triglycerides (ID 533, 691, 3150), protection of blood lipids from oxidative damage (ID 630), contr. *EFSA Journal*, *8*(10), 1–27. https://doi.org/10.2903/j.efsa.2010.1734

EFSA. (2010c). Scientific Opinion on the substantiation of health claims related to eicosapentaenoic acid (EPA), docosahexaenoic acid (DHA), docosapentaenoic acid (DPA) and maintenance of normal cardiac function (ID 504, 506, 516, 527, 538, 703, 1128, 1317, 1324, 1325). *EFSA Journal*, *8*(10), 1–32. https://doi.org/10.2903/j.efsa.2010.1796

EFSA. (2012). *Scientific Opinion on the Tolerable Upper Intake Level of eicosapentaenoic acid (EPA), docosahexaenoic acid (DHA) and docosapentaenoic acid*. *10*(7), 1–48. https://doi.org/10.2903/j.efsa.2012.2815.Available

EFSA. (2014). Scientific Opinion on the substantiation of a health claim related to DHA and contribution to normal brain development pursuant to Article 14 of Regulation (EC) No 1924/2006. *EFSA Journal*, *12*(10), 1–8. https://doi.org/10.2903/j.efsa.2014.3840

Embuscado, M. E. (2015). Spices and herbs: Natural sources of antioxidants - A mini review. *Journal of Functional Foods*, *18*, 811–819. https://doi.org/10.1016/j.jff.2015.03.005

Encina, C., Vergara, C., Giménez, B., Oyarzún-Ampuero, F., & Robert, P. (2016). Conventional spray-drying and future trends for the microencapsulation of fish oil. *Trends in Food Science and Technology*, *56*, 46–60. https://doi.org/10.1016/j.tifs.2016.07.014

Espejo-Carpio, F. J., Guadix, A., & Guadix, E. M. (2013). Spray Drying of Goat Milk Protein Hydrolysates with Angiotensin Converting Enzyme Inhibitory Activity. *Food and Bioprocess Technology*, *7*(8), 2388–2396. https://doi.org/10.1007/s11947-013-1230-5

FAO. (2010). Fats and fatty acids in human nutrition. Proceedings of the Joint FAO/WHO Expert Consultation. In *Annals of nutrition & metabolism* (Vol. 55, Issues 1–3). https://doi.org/10.1159/000228993

FDA. (2019). *Letter of Enforcement Discretion. Petition for a Health Claim for Eicosapentaenoic Acid and Docosahexaenoic Acid and Reduction of Blood Pressure in the General Population (Docket No. FDA-2014-Q-1146)* (pp. 1–79).

Fernandez, M. T., Mira, M. L., Florêncio, M. H., & Jennings, K. R. (2002). Iron and copper chelation by flavonoids: an electrospray mass spectrometry study. *Journal of Inorganic Biochemistry*, *92*(2), 105–111. https://doi.org/10.1016/S0162-0134(02)00511-1

Frankel, E. N. (2012a). Free radical oxidation. In *Lipid Oxidation* (2nd Ed., pp. 15–24). Woodhead Publishing Limited. https://doi.org/10.1533/9780857097927.15

Frankel, E. N. (2012b). Methods to determine extent of oxidation. In *Lipid Oxidation* (2nd Ed., pp. 99–127). Woodhead Publishing Limited. https://doi.org/10.1533/9780857097927.99

Frankel, E. N. (2012c). Photooxidation of unsaturated fats. In *Lipid Oxidation* (2nd Ed., pp. 51–66). Woodhead Publishing Limited. https://doi.org/10.1533/9780857097927.51

García-Moreno, P. J., Guadix, A., Guadix, E. M., & Jacobsen, C. (2016). Physical and oxidative stability of fish oil-in-water emulsions stabilized with fish protein hydrolysates. *Food Chemistry*, *203*, 124–135. https://doi.org/10.1016/j.foodchem.2016.02.073

García-Moreno, P. J., Horn, A. F., & Jacobsen, C. (2014). Influence of casein-phospholipid combinations as emulsifier on the physical and oxidative stability of fish oil-in-water emulsions. *Journal of Agricultural and Food Chemistry*, *62*(5), 1142–1152. https://doi.org/10.1021/jf405073x

García-Moreno, P. J., Özdemir, N., Stephansen, K., Mateiu, R. V., Echegoyen, Y., Lagaron, J. M., Chronakis, I. S., & Jacobsen, C. (2017). Development of carbohydrate-based nano-microstructures loaded with fish oil by using electrohydrodynamic processing. *Food Hydrocolloids*, *69*, 273–285. https://doi.org/10.1016/j.foodhyd.2017.02.013

García-Moreno, P. J., Pelayo, A., Yu, S., Busolo, M., Lagaron, J. M., Chronakis, I. S., & Jacobsen, C. (2018). Physicochemical characterization and oxidative stability of fish oil-loaded electrosprayed capsules: Combined use of whey protein and carbohydrates as wall materials. *Journal of Food Engineering*, *231*, 42–53. https://doi.org/10.1016/j.jfoodeng.2018.03.005

Gharsallaoui, A., Roudaut, G., Chambin, O., Voilley, A., & Saurel, R. (2007). Applications of spray-drying in microencapsulation of food ingredients: An overview. In *Food Research International* (Vol. 40, Issue 9, pp. 1107–1121). https://doi.org/10.1016/j.foodres.2007.07.004

Gómez-Mascaraque, L. G., & López-Rubio, A. (2016). Protein-based emulsion electrosprayed micro- and submicroparticles for the encapsulation and stabilization of thermosensitive hydrophobic bioactives. *Journal of Colloid and Interface Science*, *465*, 259–270. https://doi.org/10.1016/j.jcis.2015.11.061

Gómez-Mascaraque, L. G., Tordera, F., Fabra, M. J., Martínez-Sanz, M., & Lopez-Rubio, A. (2019). Coaxial electrospraying of biopolymers as a strategy to improve protection of bioactive food ingredients. *Innovative Food Science and Emerging Technologies*, *51*, 2–11. https://doi.org/10.1016/j.ifset.2018.03.023

Guéraud, F., Atalay, M., Bresgen, N., Cipak, A., Eckl, P. M., Huc, L., Jouanin, I., Siems, W., & Uchida, K. (2010). Chemistry and biochemistry of lipid peroxidation products. *Free Radical Research*, *44*(10), 1098–1124. https://doi.org/10.3109/10715762.2010.498477

Guo, L., Harnedy, P. A., Li, B., Hou, H., Zhang, Z., Zhao, X., & FitzGerald, R. J. (2014). Food protein-derived chelating peptides: Biofunctional ingredients for dietary mineral bioavailability enhancement. *Trends in Food Science and Technology*, *37*(2), 92–105. https://doi.org/10.1016/j.tifs.2014.02.007

Haahr, A. M., & Jacobsen, C. (2008). Emulsifier type, metal chelation and pH affect oxidative stability of n-3-enriched emulsions. *European Journal of Lipid Science and Technology*, *110*(10), 949–961. https://doi.org/10.1002/ejlt.200800035

Hermund, D. B., Yeşiltaş, B., Honold, P., Jónsdóttir, R., Kristinsson, H. G., & Jacobsen, C. (2015). Characterisation and antioxidant evaluation of Icelandic F. vesiculosus extracts in vitro and in fish-oil-enriched milk and mayonnaise. *Journal of Functional Foods*, *19*, 828–841. https://doi.org/10.1016/j.jff.2015.02.020

Hermund, D., Jacobsen, C., Chronakis, I. S., Pelayo, A., Yu, S., Busolo, M., Lagaron, J. M., Jónsdóttir, R., Kristinsson, H. G., Akoh, C. C., & García-Moreno, P. J. (2019a). Stabilization of Fish Oil-Loaded Electrosprayed Capsules with Seaweed and Commercial Natural Antioxidants: Effect on the Oxidative Stability of Capsule-Enriched Mayonnaise. *European Journal of Lipid Science and Technology*, *121*(4). https://doi.org/10.1002/ejlt.201800396

Hermund, D., Jacobsen, C., Chronakis, I. S., Pelayo, A., Yu, S., Busolo, M., Lagaron, J. M., Jónsdóttir, R., Kristinsson, H. G., Akoh, C. C., & García-Moreno, P. J. (2019b). Stabilization of Fish Oil-Loaded Electrosprayed Capsules with Seaweed and Commercial Natural Antioxidants: Effect on the Oxidative Stability of Capsule-Enriched Mayonnaise. *European Journal of Lipid Science and Technology*, *121*(4). https://doi.org/10.1002/ejlt.201800396

Hocman, G. (1988). Chemoprevention of cancer: Phenolic antioxidants (BHT, BHA). *International Journal of Biochemistry*, *20*(7), 639–651. https://doi.org/10.1016/0020-711X(88)90158-9

Horiuchi, M., Umano, K., & Shibamoto, T. (1998). Analysis of Volatile Compounds Formed from Fish Oil Heated with Cysteine and Trimethylamine Oxide. *Journal of Agricultural and Food Chemistry*, *46*(12), 5232–5237. https://doi.org/10.1021/jf980482m

Horn, A. F., Green-Petersen, D., Nielsen, N. S., Andersen, U., Hyldig, G., Søgaard Jensen, L. H., Horsewell, A., & Jacobsen, C. (2012). Addition of fish oil to cream cheese affects lipid oxidation, sensory stability and microstructure. *Agriculture (Switzerland)*, *2*(4), 359–375. https://doi.org/10.3390/agriculture2040359

Horn, A. F., Nielsen, N. S., Jensen, L. S., Horsewell, A., & Jacobsen, C. (2012). The choice of homogenisation equipment affects lipid oxidation in emulsions. *Food Chemistry*, *134*(2), 803–810. https://doi.org/10.1016/j.foodchem.2012.02.184

Huang, H., Hao, S., Li, L., Yang, X., Cen, J., Lin, W., & Wei, Y. (2014). Influence of emulsion composition and spray-drying conditions on microencapsulation of tilapia oil. *Journal of Food Science and Technology*, *51*(9), 2148–2154. https://doi.org/10.1007/s13197-012-0711-2

Intarasirisawat, R., Benjakul, S., Vissessanguan, W., Maqsood, S., & Osako, K. (2015). Skipjack roe protein hydrolysate combined with tannic acid increases the stability of fish oil upon microencapsulation. *European Journal of Lipid Science and Technology*, *117*(5), 646–656. https://doi.org/10.1002/ejlt.201400247

Jacobsen, C. (2016). Fish Oils: Composition and Health Effects. *Encyclopedia of Food and Health*, 686–692. https://doi.org/10.1016/B978-0-12-384947-2.00295-6

Jacobsen, C., García-Moreno, P. J., Mendes, A. C., Mateiu, R. V., & Chronakis, I. S. (2018). Use of Electrohydrodynamic Processing for Encapsulation of Sensitive Bioactive Compounds and

Applications in Food. *Annual Review of Food Science and Technology*, *9*(1), 525–549. https://doi.org/10.1146/annurev-food-030117-012348

Jacobsen, C., Hartvigsen, K., Lund, P., Thomsen, M. K., Skibsted, L. H., Adler-Nissen, J., Hølmer, G., & Meyer, A. S. (2000). Oxidation in fish oil-enriched mayonnaise. 3. Assessment of the influence of the emulsion structure on oxidation by discriminant partial least squares regression analysis. *European Food Research and Technology*, *211*, 86–98. https://doi.org/10.1007/s002179900132

Jacobsen, C., Timm, M., & Meyer, A. (2001). Oxidation in fish oil enriched mayonnaise: Ascorbic acid and low pH increase oxidative deterioration. *Journal of Agricultural and Food Chemistry*, *49*(8), 3947–3956. https://doi.org/10.1021/jf001253e

Jaworek, A. (2016). Electrohydrodynamic microencapsulation technology. In *Encapsulations. Nanotechnology in the Agri-Food Industry, Volume 2* (pp. 1–45). Elsevier. https://doi.org/10.1016/b978-0-12-804307-3.00001-6

Jeyakumari, A., Janarthanan, G., Chouksey, M. K., & Venkateshwarlu, G. (2016). Effect of fish oil encapsulates incorporation on the physico-chemical and sensory properties of cookies. *Journal of Food Science and Technology*, *53*(1), 856–863. https://doi.org/10.1007/s13197-015-1981-2

Jeyakumari, A., Zynudheen, A. A., Parvathy, U., & Binsi, P. K. (2018). Impact of chitosan and oregano extract on the physicochemical properties of microencapsulated fish oil stored at different temperature. *International Journal of Food Properties*, *21*(1), 942–955. https://doi.org/10.1080/10942912.2018.1466319

Karaosmanoglu, H., & Kilmartin, P. A. (2015). Tea extracts as antioxidants for food preservation. In *Handbook of Antioxidants for Food Preservation* (pp. 219–233). Woodhead Publishing. https://doi.org/10.1016/B978-1-78242-089-7.00009-9

Karim, F. T., Zaidul, I. S. M., Ghafoor, K., Al-Juhaimi, F. Y., Jalil, R. ul, Awang, M. B., Amid, M., Hossain, M. S., & Khalil, H. P. S. A. (2016). Microencapsulation of Fish Oil Using Hydroxypropyl Methylcellulose As a Carrier Material by Spray Drying. *Journal of Food Processing and Preservation*, *40*(2), 140–153. https://doi.org/10.1111/jfpp.12591

Kolanowski, W., Swiderski, F., Jaworska, D., & Berger, S. (2004). Stability, sensory quality, texture properties and nutritional value of fish oil-enriched spreadable fat. *Journal of the Science of Food and Agriculture*, *84*(15), 2135–2141. https://doi.org/10.1002/jsfa.1770

Kurek, M. A., Moczkowska, M., Pieczykolan, E., & Sobieralska, M. (2018). Barley β-D-glucan – modified starch complex as potential encapsulation agent for fish oil. *International Journal of Biological Macromolecules*, *120*, 596–602. https://doi.org/10.1016/j.ijbiomac.2018.08.131

Laguerre, M., López Giraldo, L. J., Lecomte, J., Figueroa-Espinoza, M. C., Baréa, B., Weiss, J., Decker, E. A., & Villeneuve, P. (2010). Relationship between hydrophobicity and antioxidant ability of "phenolipids" in emulsion: A parabolic effect of the chain length of rosmarinate esters. *Journal of Agricultural and Food Chemistry*, *58*(5), 2869–2876. https://doi.org/10.1021/jf904119v

Layé, S., Nadjar, A., Joffre, C., & Bazinet, R. P. (2018). Anti-inflammatory effects of omega-3 fatty acids in the brain: Physiological mechanisms and relevance to pharmacology. *Pharmacological Reviews*, *70*(1), 12–38. https://doi.org/10.1124/pr.117.014092

Lehn, D. N., Esquerdo, V. M., Dahlem Júnior, M. A., Dall'Agnol, W., dos Santos, A. C. F., de Souza, C. F. V., & de Almeida Pinto, L. A. (2018). Microencapsulation of different oils rich in unsaturated fatty acids using dairy industry waste. *Journal of Cleaner Production*, *196*, 665–673. https://doi.org/10.1016/j.jclepro.2018.06.127

Let, M. B., Jacobsen, C., & Meyer, A. S. (2007). Lipid oxidation in milk, yoghurt, and salad dressing enriched with neat fish oil or pre-emulsified fish oil. *Journal of Agricultural and Food Chemistry*, *55*(19), 7802–7809. https://doi.org/10.1021/jf070830x

Let, M. B., Jacobsen, C., Sørensen, A. D. M., & Meyer, A. S. (2007). Homogenization conditions affect the oxidative stability of fish oil enriched milk emulsions: Lipid oxidation. *Journal of Agricultural and Food Chemistry*, *55*(5), 1773–1780. https://doi.org/10.1021/jf062391s

Linke, A., Weiss, J., & Kohlus, R. (2020). Oxidation rate of the non-encapsulated- and encapsulated oil and their contribution to the overall oxidation of microencapsulated fish oil particles. *Food Research International*, *127*(September 2019), 108705. https://doi.org/10.1016/j.foodres.2019.108705

Loscertales, I. G., Barrero, A., Guerrero, I., Cortijo, R., Marquez, M., & Gañán-Calvo, A. M. (2002). Micro/nano encapsulation via electrified coaxial liquid jets. *Science*, *295*(5560), 1695–1698. https://doi.org/10.1126/science.1067595

McClements, D. J. (2005). *Food Emulsions: Principles, Practices, and Technologies*. CRC Press.

McClements, D. J., & Jafari, S. M. (2018). Improving emulsion formation, stability and performance using mixed emulsifiers: A review. *Advances in Colloid and Interface Science*, *251*, 55–79. https://doi.org/10.1016/j.cis.2017.12.001

Mei, L., McClements, D. J., Wu, J., & Decker, E. A. (1998). Iron-catalyzed lipid oxidation in emulsion as affected by surfactant, pH and NaCl. *Food Chemistry*, *61*(3), 307–312. https://doi.org/10.1016/S0308-8146(97)00058-7

Miguel, G. A., Jacobsen, C., Prieto, C., Kempen, P. J., Lagaron, J. M., Chronakis, I. S., & García-Moreno, P. J. (2019). Oxidative stability and physical properties of mayonnaise fortified with

zein electrosprayed capsules loaded with fish oil. *Journal of Food Engineering*, *263*, 348–358. https://doi.org/10.1016/j.jfoodeng.2019.07.019

Moomand, K., & Lim, L. T. (2015). Properties of Encapsulated Fish Oil in Electrospun Zein Fibres Under Simulated In Vitro Conditions. *Food and Bioprocess Technology*, *8*(2), 431–444. https://doi.org/10.1007/s11947-014-1414-7

Morales-Medina, R., Tamm, F., Guadix, A. M., Guadix, E. M., & Drusch, S. (2016). Functional and antioxidant properties of hydrolysates of sardine (S. pilchardus) and horse mackerel (T. mediterraneus) for the microencapsulation of fish oil by spray-drying. *Food Chemistry*, *194*, 1208–1216. https://doi.org/10.1016/j.foodchem.2015.08.122

Nguyen, Q. V., Malau-Aduli, B. S., Cavalieri, J., Malau-Aduli, A. E. O., & Nichols, P. D. (2019). Enhancing omega-3 long-chain polyunsaturated fatty acid content of dairy-derived foods for human consumption. *Nutrients*, *11*(4), 1–23. https://doi.org/10.3390/nu11040743

Oikawa, S., Nishino, K., Oikawa, S., Inoue, S., Mizutani, T., & Kawanishi, S. (1998). Oxidative DNA damage and apoptosis induced by metabolites of butylated hydroxytoluene. *Biochemical Pharmacology*, *56*(3), 361–370. https://doi.org/10.1016/S0006-2952(98)00037-9

Patrick, K. E., Lv, Y., Muhamyankaka, V., Ocen, D., Ntsama, I. S. B., & Zhang, X. (2013). Development of EPA-DHA Microcapsules Supplemented Probiotic Fermented Milk. *Akademik Gıda*, *11*(3–4), 6–15. http://www.academicfoodjournal.com

Paximada, P., Howarth, M., & Dubey, B. (2018). Electrosprayed particles derived from nano-emulsions as carriers of fish oil. *TechConnect Briefs 2018 - Advanced Materials*, *3*, 1–4.

Polavarapu, S., Oliver, C. M., Ajlouni, S., & Augustin, M. A. (2011). Physicochemical characterisation and oxidative stability of fish oil and fish oil-extra virgin olive oil microencapsulated by sugar beet pectin. *Food Chemistry*, *127*(4), 1694–1705. https://doi.org/10.1016/j.foodchem.2011.02.044

Pourashouri, P., Shabanpour, B., Razavi, S. H., Jafari, S. M., Shabani, A., & Aubourg, S. P. (2014). Impact of Wall Materials on Physicochemical Properties of Microencapsulated Fish Oil by Spray Drying. *Food and Bioprocess Technology*, *7*(8), 2354–2365. https://doi.org/10.1007/s11947-013-1241-2

Power, O., Jakeman, P., & Fitzgerald, R. J. (2013). Antioxidative peptides: Enzymatic production, in vitro and in vivo antioxidant activity and potential applications of milk-derived antioxidative peptides. *Amino Acids*, *44*(3), 797–820. https://doi.org/10.1007/s00726-012-1393-9

Punia, S., Sandhu, K. S., Siroha, A. K., & Dhull, S. B. (2019). Omega 3-metabolism, absorption, bioavailability and health benefits–A review. *PharmaNutrition*, *10*, 100162. https://doi.org/10.1016/j.phanu.2019.100162

Samaranayaka, A. G. P., & Li-Chan, E. C. Y. (2011). Food-derived peptidic antioxidants: A review of their production, assessment, and potential applications. *Journal of Functional Foods*, *3*(4), 229–254. https://doi.org/10.1016/j.jff.2011.05.006

Serfert, Y., Drusch, S., Schmidt-Hansberg, B., Kind, M., & Schwarz, K. (2009). Process engineering parameters and type of n-octenylsuccinate-derivatised starch affect oxidative stability of microencapsulated long chain polyunsaturated fatty acids. *Journal of Food Engineering*, *95*(3), 386–392. https://doi.org/10.1016/j.jfoodeng.2009.05.021

Serfert, Y., Drusch, S., & Schwarz, K. (2009). Chemical stabilisation of oils rich in long-chain polyunsaturated fatty acids during homogenisation, microencapsulation and storage. *Food Chemistry*, *113*(4), 1106–1112. https://doi.org/10.1016/j.foodchem.2008.08.079

Shimada, K., Okada, H., Matsuo, K., & Yoshioka, S. (1996). Involvement of chelating action and viscosity in the antioxidative effect of xanthan in an oil/water emulsion. *Bioscience, Biotechnology and Biochemistry*, *60*(1), 125–127. https://doi.org/10.1271/bbb.60.125

Simopoulos, A. P. (2011). Evolutionary aspects of diet: The omega-6/omega-3 ratio and the brain. *Molecular Neurobiology*, *44*, 203–215. https://doi.org/10.1007/s12035-010-8162-0

Simopoulos, A. P. (2016). An increase in the Omega-6/Omega-3 fatty acid ratio increases the risk for obesity. *Nutrients*, *8*(3), 1–17. https://doi.org/10.3390/nu8030128

Song, D., Khouryieh, H., Abughazaleh, A. A., Salem, M. M. E., Hassan, O., & Ibrahim, S. A. (2011). Sensory properties and viability of probiotic microorganisms in chocolate ice cream supplemented with omega-3 fatty acids. *Milchwissenschaft*, *66*(2), 172–175.

Sørensen, A. D. M., Haahr, A. M., Becker, E. M., Skibsted, L. H., Bergenståhl, B., Nilsson, L., & Jacobsen, C. (2008). Interactions between iron, phenolic compounds, emulsifiers, and pH in omega-3-enriched oil-in-water emulsions. *Journal of Agricultural and Food Chemistry*, *56*(5), 1740–1750. https://doi.org/10.1021/jf072946z

Tamm, F., Gies, K., Diekmann, S., Serfert, Y., Strunskus, T., Brodkorb, A., & Drusch, S. (2015). Whey protein hydrolysates reduce autoxidation in microencapsulated long chain polyunsaturated fatty acids. *European Journal of Lipid Science and Technology*, *117*(12), 1960–1970. https://doi.org/10.1002/ejlt.201400574

Torres-Giner, S., Martinez-Abad, A., Ocio, M. J., & Lagaron, J. M. (2010). Stabilization of a nutraceutical omega-3 fatty acid by encapsulation in ultrathin electrosprayed zein prolamine. *Journal of Food Science*, *75*(6). https://doi.org/10.1111/j.1750-3841.2010.01678.x

Unnikrishnan, P., Puthenveetil Kizhakkethil, B., Annamalai, J., Ninan, G., Aliyamveetil Abubacker, Z., & Chandragiri Nagarajarao, R. (2019). Tuna red meat hydrolysate as core and wall polymer

for fish oil encapsulation: a comparative analysis. *Journal of Food Science and Technology*, *56*(4), 2134–2146. https://doi.org/10.1007/s13197-019-03694-w

Velez, S., Nair, N. G., & Reddy, V. P. (2008). Transition metal ion binding studies of carnosine and histidine: Biologically relevant antioxidants. *Colloids and Surfaces B: Biointerfaces*, *66*(2), 291–294. https://doi.org/10.1016/j.colsurfb.2008.06.012

Vieira, S. A., Zhang, G., & Decker, E. A. (2017). Biological Implications of Lipid Oxidation Products. *JAOCS, Journal of the American Oil Chemists' Society*, *94*(3), 339–351. https://doi.org/10.1007/s11746-017-2958-2

Vishnu, K. V., Chatterjee, N. S., Ajeeshkumar, K. K., Lekshmi, R. G. K., Tejpal, C. S., Mathew, S., & Ravishankar, C. N. (2017). Microencapsulation of sardine oil: Application of vanillic acid grafted chitosan as a bio-functional wall material. *Carbohydrate Polymers*, *174*, 540–548. https://doi.org/10.1016/j.carbpol.2017.06.076

Wang, R., Tian, Z., & Chen, L. (2011). A novel process for microencapsulation of fish oil with barley protein. *Food Research International*, *44*(9), 2735–2741. https://doi.org/10.1016/j.foodres.2011.06.013

Yang, H., Wen, P., Feng, K., Zong, M. H., Lou, W. Y., & Wu, H. (2017). Encapsulation of fish oil in a coaxial electrospun nanofibrous mat and its properties. *RSC Advances*, *7*, 14939–14946. https://doi.org/10.1039/c7ra00051k

Yeşiltaş, B. (2019). *Lipid oxidation in high fat omega-3 delivery emulsions* (pp. 1–276).

Yesiltas, B., García-Moreno, P. J., Sørensen, A. D. M., Akoh, C. C., & Jacobsen, C. (2019). Physical and oxidative stability of high fat fish oil-in-water emulsions stabilized with sodium caseinate and phosphatidylcholine as emulsifiers. *Food Chemistry*, *276*, 110–118. https://doi.org/10.1016/j.foodchem.2018.09.172

Yesiltas, B., García-Moreno, P. J., Sørensen, A. D. M., Anankanbil, S., Guo, Z., & Jacobsen, C. (2018). Effects of Modified DATEMs with Different Alkyl Chain Lengths on Improving Oxidative and Physical Stability of 70% Fish Oil-in-Water Emulsions. *Journal of Agricultural and Food Chemistry*, *66*, 12512–12520. https://doi.org/10.1021/acs.jafc.8b04091

Yesiltas, B., Sørensen, A. D. M., García-Moreno, P. J., Anankanbil, S., Guo, Z., & Jacobsen, C. (2019). Modified phosphatidylcholine with different alkyl chain length and covalently attached caffeic acid affects the physical and oxidative stability of omega-3 delivery 70% oil-in-water emulsions. *Food Chemistry*, *289*, 490–499. https://doi.org/10.1016/j.foodchem.2019.03.087

Young, A. J., & Lowe, G. M. (2001). Antioxidant and prooxidant properties of carotenoids. *Archives of Biochemistry and Biophysics*, *385*(1), 20–27. https://doi.org/10.1006/abbi.2000.2149

II. Comparative Study on the Oxidative Stability of Encapsulated Fish Oil by Monoaxial or Coaxial Electrospraying and Spray-Drying *

The impact of the encapsulation technology on the oxidative stability of fish-oil-loaded capsules was investigated. The capsules (ca. 13 wt% oil load) were produced via monoaxial or coaxial electrospraying and spray-drying using low molecular weight carbohydrates as encapsulating agents (e.g., glucose syrup or maltodextrin). The use of spray-drying technology resulted in larger capsules with higher encapsulation efficiency (EE > 84%), whilst the use of electrospraying produced encapsulates in the sub-micron scale with poorer retention properties (EE < 72%). The coaxially electrosprayed capsules had the lowest EE values (EE = 53–59%), resulting in the lowest oxidative stability, although the lipid oxidation was significantly reduced by increasing the content of pullulan in the shell solution. The Emulsion-based encapsulates (spray-dried and monoaxially electrosprayed capsules) presented high oxidative stability during storage, as confirmed by the low concentration of selected volatiles (e.g., (*E,E*)-2,4-heptadienal). Nonetheless, the monoaxially electrosprayed capsules were the most oxidized after production due to the emulsification process and the longer processing time.

* JOURNAL PAPER: N.E. Rahmani-Manglano, E.M. Guadix, C. Jacobsen, P.J. García-Moreno. (2023). Comparative Study on the Oxidative Stability of Encapsulated Fish Oil by Monoaxial or Coaxial Electrospraying and Spray-Drying. *Antioxidants*, 12(2), 266 (IF: 7.675; category: FOOD SCIENCE & TECHNOLOGY - SCIE; position: 12/144; Q1/D1)

1. INTRODUCTION

Food fortification with omega-3 polyunsaturated fatty acids (PUFAs), especially EPA (C20:5 n-3) and DHA (C22:6 n-3), has become a focus of scientific research as a result of the recognized health benefits derived from their consumption (Djuricic & Calder, 2021). However, their inclusion into complex food matrices still poses a challenge for the food industry due to their low oxidative stability, which eventually affects the organoleptic and the nutritional properties of the final food product (Ghelichi et al., 2021). In this regard, micro/nanoencapsulation of oils rich in EPA and DHA (e.g., fish oil) to be used as ome-ga-3 delivery systems stands out as the approach with the highest potential (Rahmani-Manglano, García-Moreno, et al., 2020).

Spray-drying is the preferred encapsulation technique in the food industry due toits multiple advantages, such as the high throughput and low cost (Drosou et al., 2017). Furthermore, the encapsulation of fish oil by spray-drying, as a source of omega-3 PUFAs, has been widely studied over the last decades (Rahmani-Manglano, García-Moreno, et al., 2020). However, this technology also presents some disadvantages. It has been demonstrated that fish oil emulsification and drying at high temperatures(160–200◦C) results in initial lipid oxidation (Serfert et al., 2009). Moreover, the large size range (~5–100μm) and the broad particle size distribution of the resulting microcapsules may limit their use for certain food applications. Therefore, novel encapsulation technologies such as electrospraying have emerged as alternatives to conventional spray-drying.

Electrospraying technology is based on applying a high-voltage electrostatic field between the end of an emitter and a grounded collector to cause the ejection of a solution (García-Moreno et al., 2021). When the electric force overcomes the surface tension of the solution droplet formed at the tip of the emitter, a charged jet is ejected in the direction of the collector. At sufficiently low viscoelasticity of the solution, the jet destabilizes, forming a spray of highly charged small droplets. These droplets self-disperse on their way to the collector due to electrostatic repulsion, avoiding particle agglomeration or coagulation (García-Moreno et al., 2021). One of the advantages of electrospraying over spray-drying is that heat is not required at any point in the process, since solvent evaporation occurs at ambient temperature when the droplets travel on their way to the collector. Moreover, contrary to the mechanically atomized droplets produced by spray-drying, the electrosprayed

liquid droplets are smaller and show a monodisperse particle size distribution (Jaworek & Sobczyk, 2008), which results in highly bioaccessible capsules with little organoleptic changes when incorporated into a food matrix. Nonetheless, it should be born in mind that smaller capsules may be more prone to oxidation due to an increased contact area between the lipids and prooxidants (García-Moreno, Özdemir, et al., 2017). Fish-oil-loaded capsules have been produced by electrospraying in the monoaxial configuration with promising outcomes (García-Moreno et al., 2021). However, some authors reported initial lipid oxidation when water-soluble(bio)polymers were used as the encapsulating agent as a consequence of the emulsification process before drying (García-Moreno et al., 2018; Prieto & Lagaron, 2020).

Coaxial electrospraying modifies the monoaxial electrospraying process by introducing a coaxial emitter, which allows to electrospray two liquids simultaneously (Loscertales et al., 2002). In brief, through the inner needle of the emitter flows the bioactive ingredient, and through the annular gap, between the inner and the outer needle, flows the (bio)polymer-based solution used as the encapsulating agent (Rahmani-Manglano, García-Moreno, et al., 2020). This technology is particularly interesting since it allows to produce capsules from two immiscible liquids without the need of producing first a dispersion or an emulsion of the bioactive compound. Thus, the initial fish oil oxidation caused by emulsification could be theoretically avoided by producing the capsules in the coaxial configuration. Furthermore, emulsion-based encapsulation methods (e.g., spray-drying) lead to a random distribution of oil droplets within the encapsulating matrix, favoring the presence of easily accessible surface oil. On the contrary, the use of optimum coaxial electrospraying could lead to a centralized distribution of the oil within the (bio)polymer-based wall, whose thickness can be easily controlled (Loscertales et al., 2002). Therefore, capsules with a higher load capacity and encapsulation efficiency (EE) might be produced (Rahmani-Manglano, García-Moreno, et al., 2020). Despite the potential advantages of coaxial electrospraying over its monoaxial counterpart, only one study has been reported in the literature on the encapsulation of the short-chainomega-3 fatty acidα-linolenic acid (ALA) using proteins as encapsulating agents (e.g., zein or gelatin) (Gómez-Mascaraque et al., 2019). These authors observed that coaxial electrospraying resulted in better entrapment of the core material within the encapsulating matrix compared to monoaxial electrospraying. However, the oxidative stability of the resulting coaxial encapsulates was only improved when gelatin was used as the outer encapsulating agent, and not zein, which does not correlate with the EE values reported.

Low molecular weight (LMW) carbohydrates such as glucose syrup (GS) and maltodextrin (MD) have been extensively used for the encapsulation of fish oil by spray-drying (Rahmani-Manglano, García-Moreno, et al., 2020), and their use has also been reported in the encapsulation of omega-3 PUFAs using monoaxial electrospraying technology (García-Moreno et al., 2018; Prieto & Lagaron, 2020). Nonetheless, to the best of the authors' knowledge, fish-oil-loaded capsules have not yet been produced by coaxial electrospraying using GS or MD as the main encapsulating agent. In addition, a systematic study about the impact of the encapsulation technology on the oxidative stability of fish-oil-loaded capsules has not yet been reported.

Taken altogether, the objective of this work was to investigate the production of fish-oil-loaded capsules using different encapsulation technologies such as spray-drying and monoaxial or coaxial electrospraying using GS or MD as the main encapsulating agent. Whey protein concentrate hydrolysate (WPCH), with high emulsifying and antioxidant activity (Padial-Domínguez et al., 2020; Rahmani-Manglano, González-Sánchez, et al., 2020), was used for the first time as the emulsifier in the production of fish-oil-loaded capsules via monoaxial electrospraying. For coaxial electrospraying, neat fish oil was infused as the core solution. The resulting encapsulates were characterized in terms of their morphology, particle size distribution, and encapsulation efficiency, and their oxidative stability was monitored over six weeks of storage at ambient temperature by recording their Fourier transformed infrared spectra (FT-IR) and quantifying their contents of selected secondary volatile oxidation products (SVOPs). Thus, this research advances our understanding on the relation between the lipid oxidation of encapsulated fish oil and the encapsulation technology used to produce such encapsulates. The latter will allow the better design of dried omega-3 delivery systems with enhanced oxidative stability.

2. MATERIALS AND METHODS

2.1 Materials

The refined fish oil (Omega Oil 1812 TG Gold) was purchased from BASF Personal Careand Nutrition GmbH (Illertissen, Germany) and stored at−80◦C until use. The Tween-20(T20) was obtained from Sigma-Aldrich (Darmstadt, Germany) and CITREM (GRINDSTED®CITREM LR 10 EXTRA MT) were provided by Danisco (Copenhagen,

Denmark). The pullulan (P) was kindly donated by Hayashibara Co., Ltd. (Okayama, Japan). The glucose syrup (GS; DE38, C*Dry 1934) was supplied by Cargill Germany GmbH (Krefeld, Germany). The maltodextrin (MD; DE21) and whey protein concentrate (ca. 35 wt% protein content) were generously donated by Abbott Laboratories S.A. (Granada, Spain). The whey protein concentrate hydrolysate (WPCH) used as an emulsifier was produced in an automatic titrator (718 StatTitrino; Metrohm AG, Herisau, Switzerland) using Alcalase 2.4 L to a degree of hydrolysis of10% (DH10), as described by Rahmani-Manglano et al. (2020). Then, the hydrolysate (WPCH)was freeze dried and stored at 4◦C until further use. The rest of the reagents used for the analysis were of analytical grade.

2.2 Production of the Spray-Dried Capsules

Fish-oil-in-water emulsions were produced by dispersing the fish oil (5 wt%) in the aqueous phase containing the encapsulating agent (GS or MD) and the emulsifier (WPCH or T20). The total solid content of the emulsions was fixed to 34 wt%, leading to a final oil load of the microcapsules of ca. 13 wt%. Therefore, depending on the emulsifier used (WPCH = 6 wt% or T20 = 0.35 wt%), the concentrations of the encapsulating agent varied (28 wt% or 34 wt%, respectively). The concentration of T20 was optimized to achieve a similar oil droplet size distribution to that of the WPCH-based emulsions (data not shown). The emulsions prepared with WPCH as the emulsifier had a final protein content of 2 wt%, resulting in a protein/oil ratio (P/O ratio) of 0.4. The spray-dried emulsions were produced as follows. First, a coarse emulsion was prepared by adding the oil to the aqueous phase during the first minute of mixing at 15,000 rpm using an UltraturraxT-25 homogenizer (IKA, Staufen, Germany). The total mixing time was 2 min. Then, the pre-emulsion was homogenized in a high-pressure homogenizer (PandaPLUS 2000; GEANiro Soavi, Lübeck, Germany) at a pressure range of 450/75 bar and by applying 3 passes. Right after production, the emulsions were subjected to spray-drying in a laboratory-scale spray-drier (Büchi B-190; Büchi Labortechnik, Flawill, Switzerland) at 180 and 90◦C for the inlet and outlet temperatures, respectively. The drying air flow was fixed to 25 Nm3/h.

2.3 Production of the Electrosprayed Capsules

2.3.1 Monoaxially Electrosprayed Capsules

First, fish-oil-in-water emulsions were produced. The aqueous phase consisted of WPCH (4.3 wt%), P (3.0 wt%), and the main encapsulating agent (GS or MD, 15 wt%), which were dissolved in distilled water and stirred overnight (500 rpm) at ambient temperature. Then, the CITREM (1 wt%)/fish oil (3.7 wt%) mixture was dispersed in the aqueous phase using a rotor-stator homogenizer prior to high-pressure homogenization, as described in Section 2.2. The resulting fish-oil-in-water emulsions also had a P/O ratio of 0.4, and the final oil load of the microcapsules was ca. 13 wt%. Immediately after production, the emulsions were subjected to electrospraying. The electrospraying process was carried out using a system consisting of a drying chamber equipped with a variable high-voltage power supply (up to 30 kV), a syringe pump, and a 15×15 cm collector plate made of stainless steel (SpinBox Electrospinning; Bioinicia, Valencia, Spain). The emulsions were loaded into a 5 mL syringe, which was placed in the syringe pump and connected to the monoaxial emitter via a PTFE tube. A 16G needle (Proto Advantage, Hamilton, ON, Canada) was coupled to the monoaxial emitter and the needle tip was placed 15 cm apart from the collector plate (horizontal conformation). The flow rate (0.2 or 0.3 mL/h) and the voltage (17–20 kV) were optimized for each emulsion in order to avoid dripping and droplets in the collector. The electrospraying process was carried out at ambient temperature and ambient relative humidity (21–29◦C, 22–48% RH) in batches of 30 min. Between batches, the remaining emulsion was gently stirred (100 rpm) to minimize the physical destabilization of the emulsion and the oil droplet size was monitored during the processing time (0 h, 24 h, and 36 h) via laser diffraction in a Mastersizer 2000 system,(Malvern Instruments, Ltd., Worcestershire, UK) as described elsewhere (Rahmani-Manglano, González-Sánchez, et al., 2020). The powder collected from the different batches was gently mixed before sampling to ensure that the analyzed samples were homogeneous and representative of the obtained material.

2.3.2 Coaxially Electrosprayed Capsules

For the coaxial electrospraying, the biopolymer solution flowing through the annular gap between the inner and outer needles was produced following two different approaches. In the first approach, the encapsulating agent (GS or MD, 15 wt%), P (1 or 2 wt% for MD and GS, respectively), and T20 (1 wt%) were dissolved in distilled water and stirred overnight

(500 rpm) at ambient temperature before electrospraying. In the second approach, the encapsulating agent (GS or MD, 15 wt%), P (3 wt%), and T20 (1 wt%) were dissolved in distilled water and stirred overnight (500 rpm). Afterwards, the biopolymer solution was passed through a high-pressure homogenizer (450/75 bar, 3 passes) prior to electrospraying. The electrospraying process was carried out in the setup described in Section 2.3.1,but this time a coaxial emitter consisting of two concentric needles was used. Thus, two syringe pumps working simultaneously were used. The neat fish oil was infused through the inner needle (ID/OD = 0.6/0.9 mm), and through the annular gap between needles flowed the biopolymer solution (outer needle 16G). The outer flow rate (F1) was fixed to0.36 or 0.60 mL/h and the inner flow rate (F2) was adjusted to achieve a final oil load in the microcapsules of ca. 13 wt% (F2 = 0.012 or 0.021 mL/h, respectively). The voltages varied from 10 to 13.5 kV and from 16 to 18 kV depending on the flow rates used for the GS- or MD-based shell solutions. The flow rates and voltage combinations were optimized in order to avoid dripping and droplets in the collector. The process was conducted at ambient temperature and ambient relative humidity (21–30◦C, 23–51% RH) in batches of 60 min. The powders collected from the different batches were gently mixed before sampling to ensure that the analyzed samples were homogeneous and representative of the obtained material.

2.4 Characterization of the Capsules

2.4.1 Morphology and Particle Size Distribution

The morphology of the capsules was investigated via scanning electron microscopy (SEM) using an FESEM microscope (LEO 1500 GEMINI, Zeiss, Germany). Depending on the microencapsulation technology used, a thin layer of microcapsules (i.e., spray-drying) or a piece of approximately 0.5×0.5 cm aluminum foil containing the sample (i.e., electrospraying) was placed on the carbon tape and carbon-coated using an EMITECHK975X Turbo-Pumped Thermal Evaporator (Quorum Technologies, UK). The SEM images were acquired in the range of 500×–15K×magnification with a 5 kV accelerating voltage. The particle size distributions and mean diameters were determined by measuring 180 randomly selected capsules using ImageJ software (National Institute of Health).

2.4.2 Encapsulation Efficiency

The encapsulation efficiency (EE) of the capsules was measured as described by Prieto and Lagaron (2020) with some modifications. Approximately 25 mg of microcapsules was immersed in 10 mL of hexane and gently shaken for 30 s. Then, the mixture was filtered into a pyrex tube and the absorbance of the filtrate was measured at 250 nm in a UV-Vis double beam spectrophotometer (Thermo Spectronic Helios Alpha 9423 UVA 1002E, Thermo Fisher Scientific, Waltham, MA, USA). The amount of oil contained in the filtrate was determined from a calibration curve (R2= 0.99) prepared by dissolving various quantities of fish oil in hexane (0.1–2.0 mg/mL). The EE and was calculated as follows:

$$EE, \% = \frac{A - B}{A} \cdot 100 \quad (17)$$

where A refers to the total oil load of the microcapsules (g) and B to the easily extractable oil (g). The measurements were carried out in triplicate. The total oil load of the microcapsules was determined by extracting the fish oil using a hexane/2-propanol (1:1, v/v) solvent. For the extraction, ca. 50 mg of powder was dissolved by adding 10 mL of distilled water, and the total oil load was determined by measuring the absorbance of the lipid extract, as previously described by Rahmani-Manglano et al. (2022). The measurements were carried out in triplicate.

2.5 Oxidative Stability

To monitor the oxidative stability, 10 mg of capsules was stored in a 2 mL plastic Eppendorf tube at 25◦C in the dark for 6 weeks for the FT-IR analysis. For the measurement of secondary volatile oxidation products, 150 mg of capsules was stored in a 2 mL plastic Eppendorf tube at 25◦C in the dark for 6 weeks. Samples were taken at week 0, 2, 4, and 6for the analysis.

2.5.1 Fourier Transform Infrared Spectra (FT-IR) Analysis

FT-IR spectra of the capsules were recorded on a JASCO FT/IR 6200 (Madrid, Spain) spectrometer operating in transmission mode. Approximately 1.5 mg of capsules was dispersed in ca. 150 mg of spectroscopic-grade potassium bromide (KBr) and subsequently ground. Then, a pellet was formed by compressing the mixture at ca. 150 MPa. All spectra were recorded within the wavenumber range of 4000–400 cm^{-1} by averaging 100 scans at 2

cm^{-1} resolution. The pellets were produced in triplicate for each sampling point and the measurements were carried out immediately after pellet production. For the raw ingredients used to produce the capsules (i.e., fish oil, GS, and T20), the attenuated total reflection (ATR)–FTIR spectra were recorded with the same equipment and conditions.

2.5.2 Secondary Volatile Oxidation Products – Dynamic Headspace GC-MS

Approximately 50 mg of microcapsules and 5 mg of internal standard (4-methyl-1-pentanol, 30μg/g water) were weighed out in a 100 mL pear-shaped bottle, to which 5 mL of distilled water and 1 mL of antifoam (Synperonic 800μL/L water) were added. The bottle was heated to 45◦C in a water bath while being purged with nitrogen (flow 250 mL/min,30 min). Volatile secondary oxidation products were trapped on Tenax GR tubes. The volatiles were desorbed again via heating (200◦C) in an Automatic Thermal Desorber (ATD-400, Perkin Elmer, Norwalk, CN, USA), cryofocused on a cold trap (−30◦C), and released again (220◦C), which led to a gas chromatograph (HP 5890IIA, Hewlett Packard, Palo Alto, CA, USA; Column: DB-1701, 30 m×0.25 mm×1.0μm; J&W Scientific, Santa Clara, CA, USA). The oven program had an initial temperature of 45◦C for 5 min, increasing by 1.5◦C/min until 55◦C, 2.5◦C/min until 90◦C, and 12.0◦C/min until 220◦C, where the temperature was kept for 4 min. The individual compounds were analyzed using mass-spectrometry (HP 5972 mass-selective detector, Agilent Technologies, USA; electron ionization mode, 70 eV; mass-to-charge scan ratios between 30 and 250). The individual compounds were identified via both 186 MS library searches (Wiley 138 K, John Wileyand Sons, Hewlett-Packard) and using authentic external standards, which was quantified through calibration curves. The external standards employed were 2-ethylfuran, 1-penten-3-ol, hexanal, heptanal, and (*E*,*E*)-2,4-heptadienal (Sigma-Aldrich, Brøndby, Denmark),and the standard solutions were directly injected into the Tenax tubes. The samples were analyzed in triplicate.

2.6 Statistical analysis

The data were subjected to a one-way analysis of variance (ANOVA) using Statgraphics version 5.1 (Statistical Graphics Corp., Rockville, MD, USA). Tukey's HSD multiple range test was used at the 95% confidence level ($p < 0.05$) to determine significant differences between mean values.

3. RESULTS AND DISCUSSION

3.1 Characterization of the Capsules

3.1.1 Morphology and Particle Size Distribution

Figure 16 shows that spherical, non-agglomerated capsules were produced by spray-drying. Contrary to the discrete particles obtained for the spray-dried systems (Figure 16), thin fibers interconnecting the capsules could be observed in all the electrosprayed samples, irrespective of the emitter configuration (monoaxial or coaxial) (Figure 17). This has been attributed to the presence of pullulan in the different formulations, which is used as a "spin aid (bio)polymer" to increase the stability of the electrospraying process, al-lowing work at high flow rates (e.g., leading to increased throughput) (García-Moreno et al., 2021). Pullulan is an edible, water-soluble, non-ionic polysaccharide with great spinnability in water-based solutions (Stijnman et al., 2011), which has been previously used in the production of fish-oil-loaded nanofibers as the main biopolymer (García-Moreno, Damberg, et al., 2017; García-Moreno, Özdemir, et al., 2017) or in the production of fish-oil-loaded nanocapsules within carbohydrate-based matrices as a thickening agent (García-Moreno et al., 2018). In the current study, the pullulan concentration was optimized in order to increase the viscoelasticity of the emulsions or solutions, allowing stable processing conditions at high flow rates (e.g., no dripping and droplets in the collector), but avoiding the formation of thick or strong fibers. Thus, the samples gathered from the collector plate had the appearance of a flowing powder, which led us to conclude that the fibrils observed were easily disrupted when subjected to mechanical forces (e.g., detachment of samples from the collector with a spatula). It should be noted that powder and capsules are preferred to fibers for the enrichment of food matrices due to their better dispersibility (Jacobsen et al., 2018).

Figure 18 shows the particle size distribution of the different capsules obtained in this study. No significant differences were observed in the mean diameter of the spray-dried capsules or in their particle size distribution regardless of the encapsulating agent (e.g., GS or MD) or the emulsifier (e.g., WPCH or T20) used in the formulation. The mean diameters of the spray-dried capsules obtained with GS or MD as encapsulating agents ranged from 8.57 ± 5.30μm to 9.77 ± 5.36μm ($p > 0.05$), and more than 90% of the particles had a size below 20μm (Figure 18A). Moreover, it is noteworthy that the particle size distribution of the capsules produced by spray-drying was significantly wider (ranging from below 5 to over

35μm) (Figure 18A) compared to that of the electrosprayed capsules (ranging from below 0.5 to over 3μm) (Figure 18B).

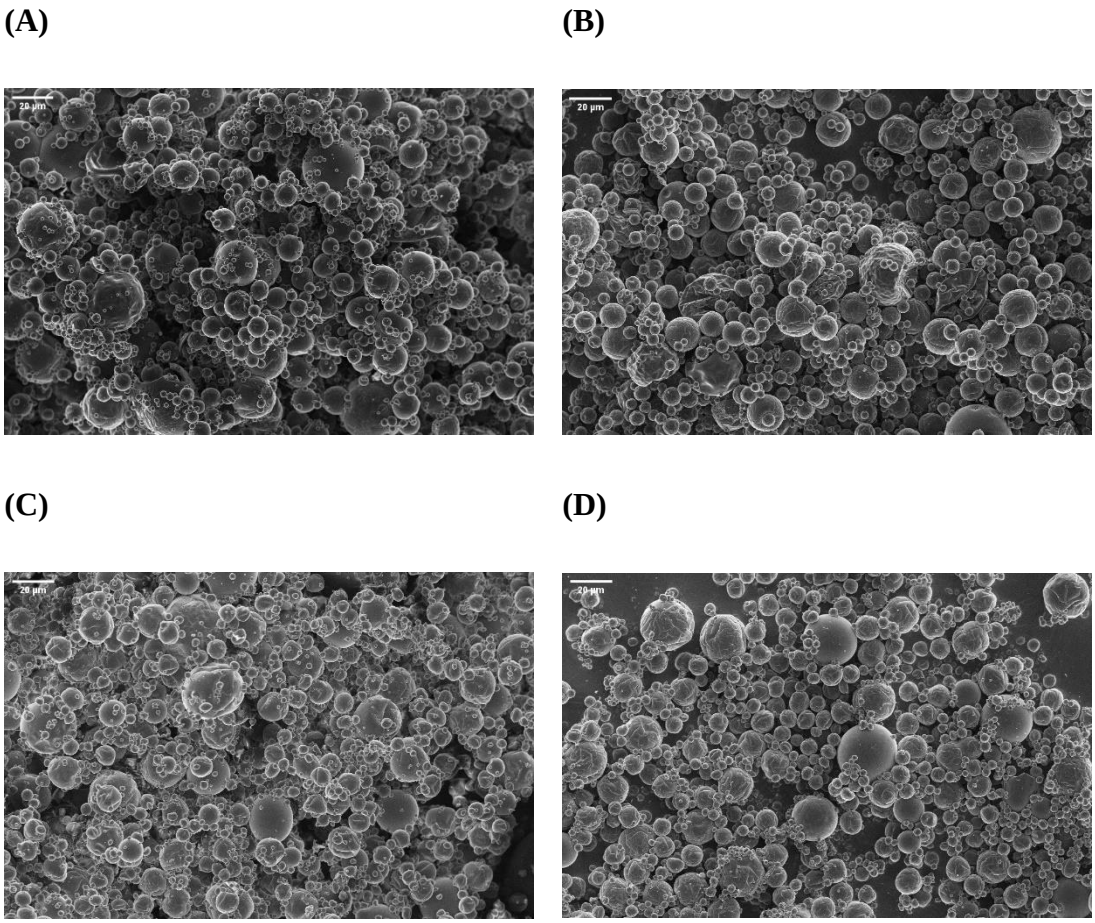

Figure 16. SEM images (A-D) of the spray-dried capsules loaded with fish oil: W-GS (A); T-GS (B); W-MD (C); T-MD (D). Scale bar: 20 μm.

As in the case of spray-drying, the monoaxially electrosprayed capsules (GS-mo and MD-mo samples) (Figure 17A,B) did not show significant differences regarding their morphology and size, irrespective of the encapsulating agent employed (mean diameters of 0.6 ± 0.3μm and 0.7 ±0 .3μm for GS-mo and MD-mo, respectively). Furthermore, in line with the spray-dried capsules, the monoaxially electrosprayed capsules mostly showed spherical shapes with smooth surfaces, although some dented particles could be also spotted (Figure 17A,B). It is worth noting that more than 80% of the monoaxially electrosprayed capsules were below 1μm (Figure 17B). These results are in line with those previously reported by García-Moreno et al. (2018), who also produced spherical capsules with smooth surfaces when electrospraying fish-oil-in-water emulsions containing GS or dextran as encapsulating agents (70% of the capsules below 1μm).

Interestingly, despite the differences in the formulation of the biopolymer-based shell solutions (pullulan content) and the production process (with or without high-pressure homogenization, HPH), the morphologies of the coaxially electrosprayed capsules were fairly similar among the samples (Figure 17C–F). For the GS-co and MD-co samples (without HPH), the differences in the formulation of the shell solutions depended on the different molecular weights of the carbohydrates as a consequence of their dextrose equivalence (DE) values (DE38 for GS and DE21 for MD). Increasing the DE of a carbohydrate leads to smaller oligosaccharides with a lower molecular weight, which results in solutions with lower viscoelasticity at the same (bio)polymer concentration (Siemons et al., 2020). Hence, it was necessary to increase the pullulan concentration for the GS-based shell solution when compared to the MD-based solution in order to achieve a stable electrospraying process (2 wt% P for the GS-based shell solution over 1 wt% P for the MD-based shell solution). On the other hand, when the shell solution was subjected to HPH prior to electrospraying, the same content of pullulan in the GS- or MD-based formulations (3 wt% P) allowed the stabilization of the electrospraying process. It is noteworthy that despite the higher content of pullulan in the -HPH-co shell solutions, no differences were observed in the amount or thickness of the fibril defects between the coaxially electrosprayed capsules (Figure 17C–F), which is explained by the break of the pullulan polymer chains during homogenization at high pressures.

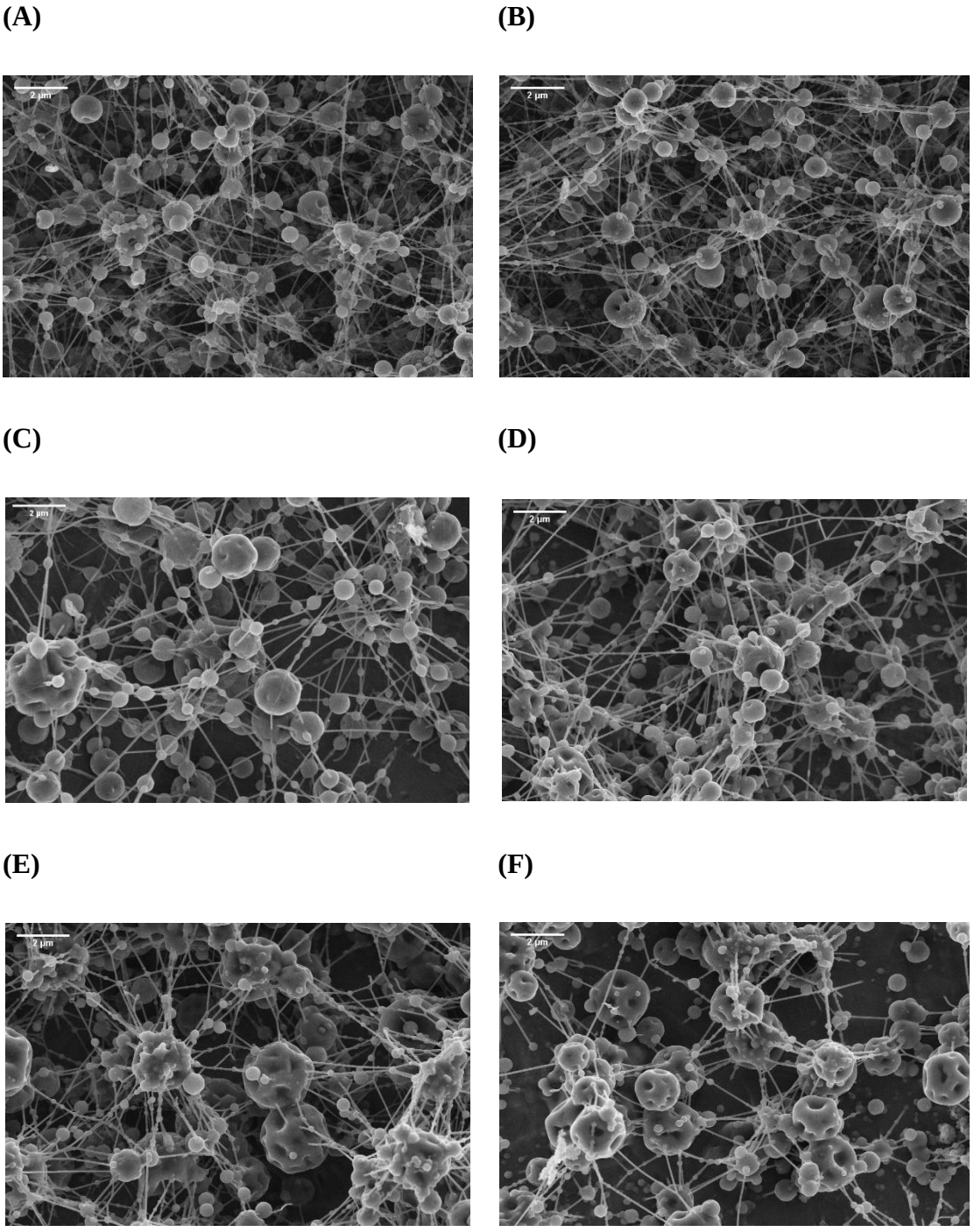

Figure 17. SEM images (A-F) of the electrosprayed capsules (monoaxial and coaxial) loaded with fish oil: GS-mo (monoaxial) (A); MD-mo (monoaxial) (B); GS-co (coaxial) (C); MD-co (coaxial) (D); GS-HPH-co (coaxial) (E); MD-HPH-co (coaxial) (F). Scale bar: 2 µm.

Overall, regarding the electrosprayed systems (monoaxial and coaxial), it should be noted that coaxially electrosprayed capsules showed more and larger dents on the capsules' surface compared to monoaxially electrosprayed systems (Figure 17). The morphology development of dried particles is highly influenced by the rheological properties of the skin, as well as the subsequent crust, formed during the drying process. Elastic skins are able to withstand

internal and surface stresses that occur during drying, leading to smooth particles, whilst viscous skins deform, leading to wrinkled, folded, or dented particles (Siemons et al., 2020). LMW carbohydrates-based solutions have been reported to exhibit a viscous behavior upon drying, causing the deformation of the particle surfaces (Siemons et al., 2020), thereby explaining the large dents observed in the coaxially electrosprayed systems compared to the monoaxially electrosprayed capsules. This is explained on the basis that for the monoaxial electrospraying, a fish-oil-in-water emulsion was infused to produce the capsules, whilst for the coaxial electrospraying, the shell processing solution consisted of a GS- or MD-based solution. Moreover, significantly larger capsules were produced via coaxial electrospraying over monoaxial electrospraying (Figure 18B). This was related to the electrospraying processing conditions, especially the operating flow rates. At high infusing flow rates, larger droplets are formed at the tip of the emitter, meaning larger capsules are obtained after drying. Hence, the -mo capsules (ca. 85% of the capsules < 1μm) were smaller than the -co capsules (ca. 45% of the capsules < 1μm), which at the same time were smaller than the -HPH-co capsules (ca. 25% of the capsules < 1μm). Stable processing conditions could be achieved at higher flow rates for the -HPH-co systems (over the -co systems) due to their higher pullulan content in the shell solution formulation (0.36 mL/h for -co systems and 0.60 mL/h for -HPH-co systems). The latter, together with the differences in the solid contents of the shell solutions (i.e., 16 wt% solids for MD-co over 18 wt% solids for MD-HPH-co), explains the differences observed in the particle size ($p < 0.05$) and throughput of the process (from ca. 80 mg/h for -co capsules to ca. 143 mg/h for -HPH-co capsules). Nonetheless, although the infusion flow rate increased by up to two times for the production of -HPH-co systems compared to -co systems, the size of the capsules did not increase in the same proportion as a consequence of the higher voltage applied during the -HPH-co capsule production process (ca. 18 kV for -HPH-co over ca. 13.5 kV for -co electrospraying). Higher processing voltages favor jet breakage into smaller droplets due to increased electrostatic charge repulsion, leading to smaller capsules after solvent evaporation (García-Moreno et al., 2021).

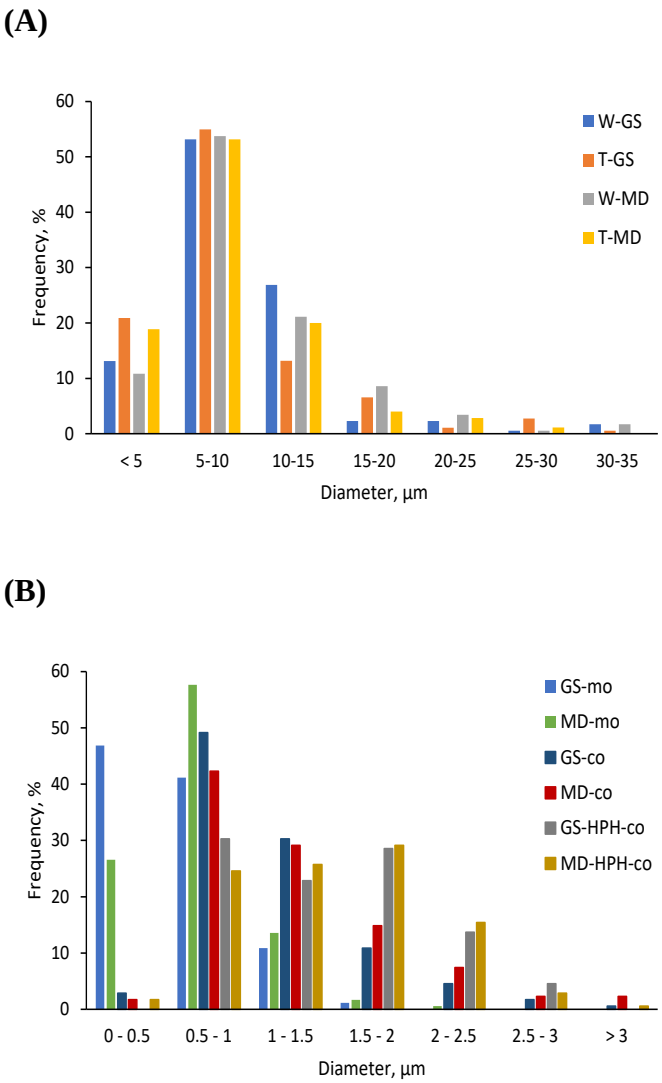

Figure 18. Particle size distribution of the capsules produced by: spray-drying (A) and electrospraying (monoaxial and coaxial) (B).

3.1.2 Encapsulation Efficiency (EE)

Significant differences ($p < 0.05$) were observed in the EE values depending on the encapsulation technique used to produce the fish-oil-loaded capsules (i.e., spray-drying, monoaxial electrospraying, or coaxial electrospraying) (Figure 19). The highest EE was obtained for the spray-dried systems (EE = 84–90%), followed by the monoaxially electro-sprayed (EE = 69–72%) and coaxially electrosprayed systems (EE = 53–59%), respectively. For emulsion-based encapsulation techniques, such as spray-drying and monoaxial electrospraying, the EE is closely related to the infeed emulsion formulation and its physical stability. The drying of physically stable monodisperse emulsions of small oil droplets results in the better entrapment of the oil within the encapsulating matrix (Paximada et al., 2018; Ramakrishnan et al., 2014). Furthermore, it has been reported that for a fixed oil load,

increasing the wall material concentration improves the EE (Drosou et al., 2017). Therefore, the differences in the EE values reported for the spray-drying and monoaxial electrospraying encapsulation techniques could be related to the different emulsion formulations and their characteristics before and during (e.g., oil droplet size). From our previous work, it could be observed that all the emulsions fed to the spray-drier presented a monomodal oil droplet size distribution with D[4,3] values ranging from 0.45 ± 0.01 µm to 0.56 ± 0.01 µm (Rahmani-Manglano et al., 2022). Conversely, the emulsions subjected to monoaxial electrospraying in this study showed both wider (GS-mo) and bimodal (MD-mo) droplet size distributions before processing (see Figure S 1 in the Supplementary Material) as wells as higher D[4,3] values, thus larger oil droplets (D[4,3] = 1.01 ± 0.34 µm and 1.60 ± 0.54 µm, respectively).

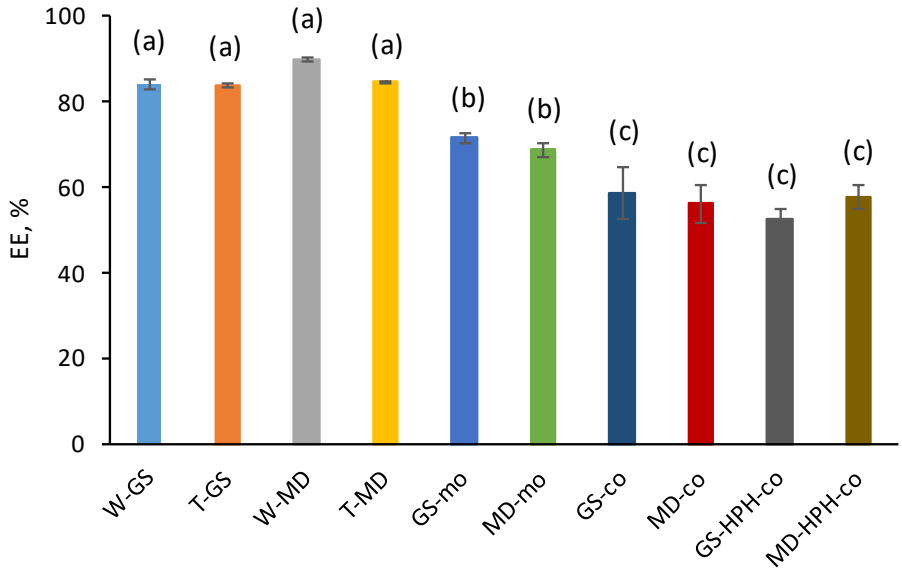

Figure 19. Encapsulation efficiency (EE) of the fish-oil loaded capsules produced by spray-drying or electrospraying (monoaxial and coaxial). Samples followed by a letter, a-c, indicates statistical differences ($p \leq 0.05$) between microcapsules.

For monoaxial electrospraying, the emulsions were produced by dispersing the oil phase, consisting of a CITREM (1 wt%)/fish oil (3.7 wt%) mixture, within the aqueous sphase, containing the encapsulating agent (GS or MD, 15 wt%), the emulsifier (WPCH,4.3 wt%), and pullulan (3 wt%). Both the presence of pullulan in the aqueous phase and CITREM in the oil phase may have increased their respective viscosities to an extent, resulting in poorer emulsification, leading to emulsions of larger oil droplets. Moreover, although the electrosprayed emulsions were gently stirred during the total processing time to minimize their physical destabilization, this was not totally achieved (see Figure S 1 in the Supplementary Materials). After 36 h, the GS-mo emulsion showed a relatively wider

monomodal oil droplet size distribution and the main peak was displaced to larger diameter values when compared to at 0 h (main peak centered at ca. 3μm after 36 h) (see Figure S 1A of the Supplementary Materials). Likewise, for the MD-mo emulsion, the proportion of the first peak of the bimodal droplet size distribution decreased as the proportion of the second peak increased and was progressively displaced to larger diameter values (second peak centered at ca. 5μm after 36 h; see Figure S 1B of the Supplementary Materials). These results suggest that the electrosprayed emulsions suffered physical destabilization during processing, favoring the presence of easily extractable surface oil in the electrosprayed capsules. In addition, for a fixed oil load, an increased particle size implies thicker encapsulating walls, resulting in better entrapment of the oil droplets within the encapsulating matrix (Ramakrishnan et al., 2014). Therefore, the significantly different capsules sizes ($p < 0.05$)as a result of the different atomization processes of both techniques could further explain the lower EE values reported for the -mo systems over the spray-dried capsules ($p < 0.05$).Nonetheless, the EE values reported for the capsules produced by monoaxial electrospraying in the current work contrast with previous studies on the encapsulation of fish oil by monoaxial electrospraying within carbohydrate-based matrices. García-Moreno et al. (2018, 2017) produced fish-oil-loaded microcapsules using dextran or GS as the encapsulating agents, with EE values ranging from 76 to 92%, depending on the production process (conventional electrospraying or electrospraying assisted by pressurized gas, EAPG). Likewise, Prieto and Lagaron (2020) reported similar EE values when encapsulating algae oil within a maltodextrin-based matrix using EAPG (EE = 77% for an oil load of 10 wt%). It should be noted, however, that finer emulsions were produced in the aforementioned studies (García-Moreno et al., 2018; García-Moreno, Özdemir, et al., 2017; Prieto & Lagaron, 2020).

The coaxially electrosprayed capsules presented the lowest EE values (EE = 53–59%), regardless of the shell solution formulation or production process (-co or -HPH-co capsules) ($p > 0.05$) (Figure 19). These low EE values could be attributed to the lack of surface-active properties of the LMW carbohydrates used as encapsulating agents (i.e., GS or MD) (Hogan et al., 2001), which could have resulted in reduced entrapment of the fish oil within the encapsulating matrix during processing. Moreover, the lower EE values are in agreement with the large dents observed on the surfaces of the coaxially electrosprayed capsules (Figure 17C–F), which were related to the presence of non-encapsulated oil droplets and to higher access of the extracting solvent to the encapsulated oil once the non-encapsulated oil fraction

is removed (Drusch & Berg, 2008). These results highlight that the outcome of the coaxial electrospraying process is influenced by the properties of the encapsulating agent/s used and that ingredients with amphiphilic properties are required to improve the retention properties of the encapsulating wall, especially when neat fish oil is infused as the core solution.

Overall, our EE results for the electrospraying processes (monoaxial vs. coaxial) contrast with those reported by other authors (Gómez-Mascaraque et al., 2019; Pérez-Masiá et al., 2015). Pérez-Masiá et al. (2015) found that the coaxially electrosprayed capsules resulted in higher EE (based on intact lycopene) compared to those produced by monoaxial electrospraying when dextran was used as the encapsulating agent (EEcoaxial = 58% over EEmonoaxial = 26%). The authors attributed this to the low physical stability of the emulsion during monoaxial processing. Nonetheless, it should be noted that the EE value reported by the aforementioned authors for the coaxially electrosprayed system using carbohydrates as wall materials to encapsulate a hydrophobic bioactive is in line with the EE values obtained in the current work (EEcoaxial = 53–59%). Similarly, Gómez-Mascaraque et al. (2019) produced α-linolenic acid (ALA)-loaded microcapsules within protein-based matrices (i.e., zein) via monoaxial and coaxial electrospraying. These authors found higher EE values for the coaxial encapsulates (EEcoaxial = ca. 90% over EEmonoaxial = ca. 70%) when using an extra shell layer based on zein, but no significant differences were observed when gelatin was employed as the extra shell layer. Furthermore, contrary to our study, the core material that these authors used was a zein/ALA solution and not only ALA. This could explain the higher EE values reported for the zein-based coaxially electrosprayed systems, since the resulting capsules consisted of an outer zein-based layer coating the inner zein-containing matrix, leading to better bioactive entrapment due to the surface-active and encapsulating properties of zein (Gómez-Mascaraque & López-Rubio, 2016). Interestingly, the EE value reported for the monoaxial zein/ALA system by Gómez-Mascaraque et al. (2019) is in line with the EE values reported in this study when fish-oil-in-water emulsions stabilized with WPCH were electrosprayed in the monoaxial configuration (EEmonoaxial = 69–72%). WPCH has been proven to possess great emulsifying and film-forming properties (Padial-Domínguez et al., 2020; Rahmani-Manglano, González-Sánchez, et al., 2020), which may have favored the monoaxial electrospraying outcome by (i) stabilizing the fish oil droplets in the emulsion during processing and (ii) increasing the biopolymer-based wall matrix retention properties during and after drying.

3.2 Oxidative Stability of the Capsules

3.2.1 FT-IR

First, the oxidative stability of the different types of capsules was evaluated via FT-IR by monitoring the changes in the characteristic absorption bands of omega-3 PUFAs during the storage time. Although information on the initial oxidation status of the encapsulated oil is not provided by FT-IR analysis, this technique has been proven to be a useful tool to evaluate the oxidation stage of neat edible oils (Guillén & Cabo, 1999, 2000) and has been extensively used to monitor the oxidative stability of capsules loaded with omega-3 PUFA-rich oils produced either by spray-drying (Binsi et al., 2017; Unnikrishnan et al., 2019) or electrospraying (monoaxial and coaxial) (García-Moreno et al., 2018; Gómez-Mascaraque et al., 2019; Prieto & Lagaron, 2020).

For omega-3 PUFA-rich oils, the characteristic absorption band corresponds to the stretching of cis-alkene groups (–HC=CH–) at 3012 cm^{-1}, and a decrease in the intensity of this band (due to the loss of cis double bonds) has been proposed as a marker of lipid oxidation (Guillén & Cabo, 1999). Thus, the intensity of this band was monitored during the storage time. The band at 1456 cm^{-1}, assigned to rocking vibrations of C–H bonds of cis-disubstituted alkenes, was used as the internal standard for normalization purposes, since this band remains unchanged during the lipid oxidation of omega-3 PUFA-rich oils (e.g., algae oil rich in DHA), as reported by other authors (Prieto & Lagaron, 2020). Therefore, for each sampling point, the relative absorbance was calculated (A_{3012}/A_{1456}) and the results were normalized to the initial relative absorbance value (week 0) for a better comparison among the samples. The ATR-FTIR spectra of the fish oil, the GS, and the T20 used in the study are shown in Figure S 2 in the Supplementary Materials, where it can be seen that the band at 3012 cm⁻1 does not overlap with the infrared bands of the other ingredients. The spectra of the rest of the ingredients used in the production of the capsules also did not overlap with the fish oil band at 3012 cm^{-1}, as can be seen elsewhere (García-Moreno, Özdemir, et al., 2017; Prieto & Lagaron, 2020).

Overall, a slight decrease in the normalized absorbance values was observed during storage for all samples (Figure 20), which indicates that the capsules produced by the different encapsulation techniques were not extensively oxidized based on the reduction in the characteristic omega-3 absorption band (at 3012 cm^{-1}). Likewise, García-Moreno et al. (2018) did not observe a significant decrease in the normalized absorbance of the band at

3012 cm^{-1} in fish-oil-loaded capsules produced via monoaxial electrospraying using dextran or GS as the encapsulating biopolymer after 21 days of storage at 20 °C. Nonetheless, Figure 20 shows a more pronounced decrease in the normalized absorbance for GS-co and MD-co samples, indicating that these capsules were the less oxidatively stable during storage, while no clear differences could be observed for the rest of the systems, regardless of the encapsulating agent used or the encapsulation technique (i.e., spray-dried, -mo, and -HPH-co systems). Low oxidative stability in encapsulated oils is often related to low EE values, since unprotected surface oil is extremely prone to oxidation due to direct contact with prooxidant species (e.g., oxygen) (Drusch & Berg, 2008). However, the lower oxidative stability observed in the -co systems cannot be only attributed to a higher content of easily oxidized surface oil, since the EE values reported for the -HPH-co capsules were not significantly different ($p > 0.05$) (Figure 19). Therefore, our results show that although the HPH treatment of the shell solution prior to coaxial electrospraying did not improve the oil retention properties of the encapsulating wall during processing, it did improve the oxidative stability of the -HPH-co systems over the -co systems. The latter suggests that the physicochemical properties of the coaxial capsules (e.g., particle size, thickness of the encapsulating wall, permeability to oxygen) significantly influenced the lipid oxidation rather than the non-encapsulated oil, which will be further discussed below.

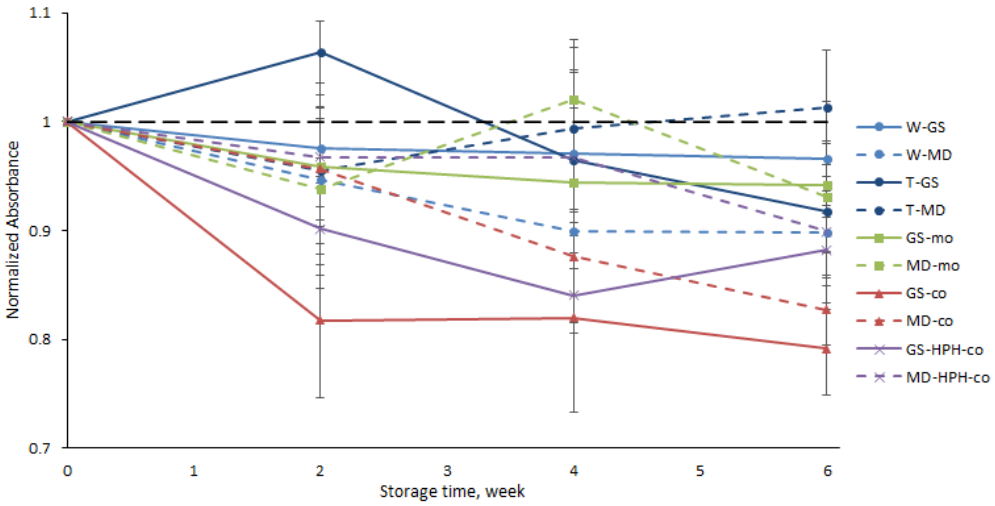

Figure 20. Oxidative stability levels measured using FT-IR of the of the fish-oil-loaded capsules produced by spray-drying or electrospraying (monoaxial and coaxial) during storage.

3.2.2 Secondary Volatile Oxidation Products (SVOPs)

To further investigate the oxidative stability of the fish-oil-loaded capsules, the contents of selected secondary volatile oxidation products (SVOPs) were measured during 6 weeks of storage at 25 °C. (Figure 21). Volatiles such as 2-ethylfuran, 1-penten-3-ol, and (*E*,*E*)-2,4-heptadienal are typical compounds derived from the oxidation of omega-3 PUFAs related to unpleasant odors (e.g., flower, sweet or green) at low threshold values (e.g., 1-penten-3-ol = 0.5–3 ppm) (Rahmani-Manglano, García-Moreno, et al., 2020). Hexanal and heptanal, despite being compounds derived from the oxidation of omega-6 and omega-9 fatty acids, respectively, have also been identified in oxidized fish oils (García-Moreno et al., 2018; Shahidi, 2001). The odors of these SVOPs are described as grassy, fruity, green, or sharp, and their threshold values are also considerably low (0.014–1 ppm) (Shahidi, 2001).

Considering the results obtained for the SVOPs derived from the oxidation of omega-3 PUFAs (Figure 21A–C), the same trend as for the FT-IR analysis can be observed: the most oxidized samples after storage were the -co systems, whilst for the rest of the capsules (i.e., -HPH-co, -mo, and spray-dried capsules) no significant differences could be observed at the end of the storage time (Figure 21A–C; $p > 0.05$). Furthermore, irrespective of the SVOP considered (i.e., 2-ethylfuran, 1-penten-3-ol, and (*E*,*E*)-2,4-heptadienal), the same oxidation trend could be observed for the -co capsules. First, a slight increase in the concentration occurred during the first two weeks of storage, followed by a sharp increase from week 2 onwards (Figure 21A–C). Nonetheless, as previously discussed, the lower oxidative stability found for the -co capsules cannot only be attributed to their high content of surface oil, since the EE values reported for the coaxially electrosprayed systems (i.e., -co and -HPH-co systems) were not significantly different among the samples (Figure 19; $p > 0.05$).

Oxygen's solubility and diffusion through the encapsulating wall have been proven to play a key role in the lipid oxidation of encapsulated fish oil (Boerekamp et al., 2019). Both are influenced by several factors, such as the type of encapsulating (bio)polymer and its properties (e.g., molecular weight and permeability to oxygen), the thickness of the encapsulating wall (e.g., solids content, oil load), and the capsule size (e.g., surface-to-volume ratio) (Boerekamp et al., 2019). Therefore, the different oxidation rates and extents observed in the coaxially electrosprayed systems (i.e., -co and -HPH-co systems) could be attributed to the different physicochemical properties of the capsules influencing the oxygen diffusivity.

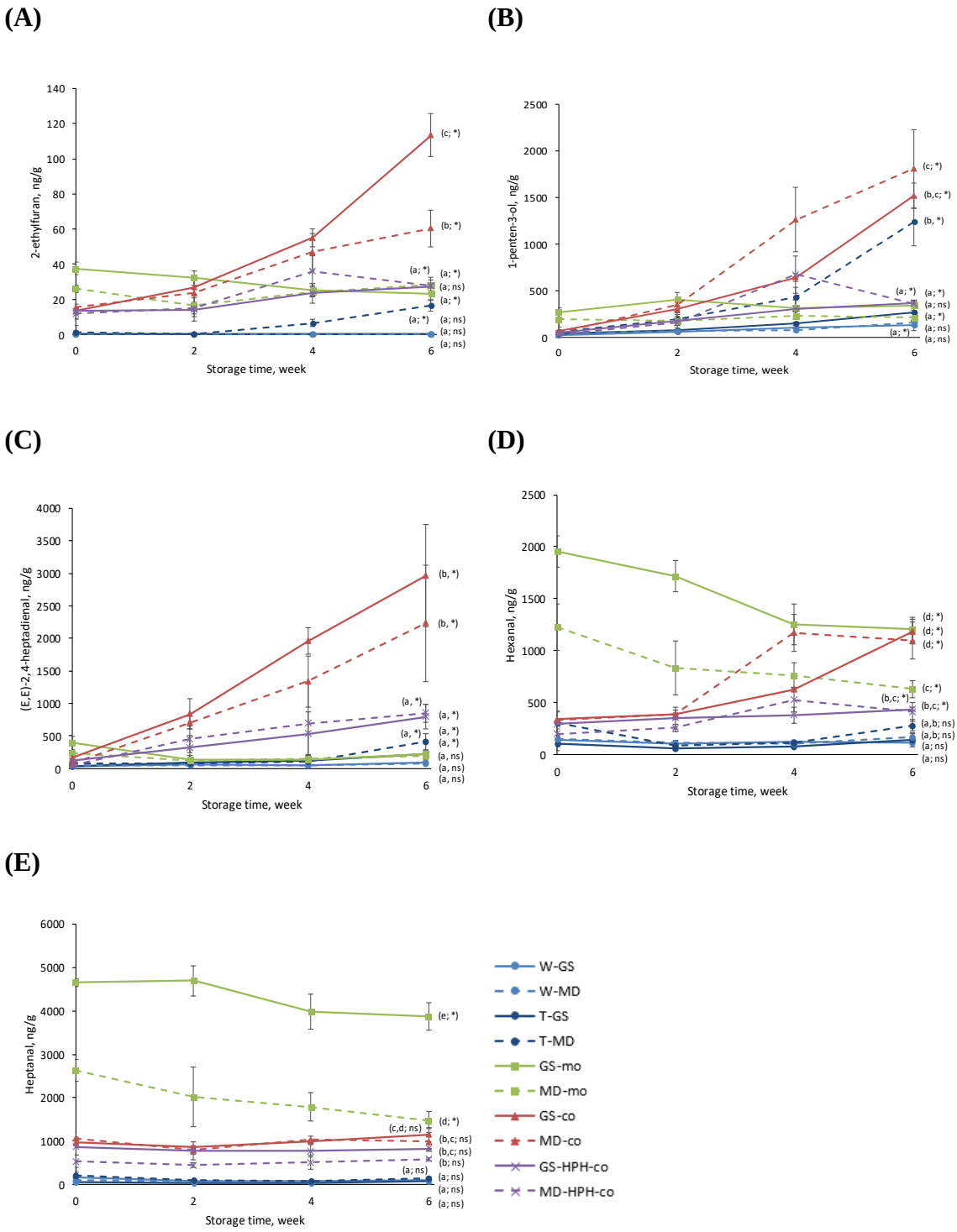

Figure 21. Secondary volatile oxidation products (SVOPs) of the fish-oil-loaded capsules produced by spray-drying or electrospraying (monoaxial and coaxial) during storage: 2-ethylfuran (A); 1-penten-3-ol (B); (E,E)-2,4-heptadienal (C); hexanal (D); heptanal (E).

Smaller capsules, as is the case for -co systems compared to -HPH-co capsules (Figure 18B; $p < 0.05$), result in an increased contact area with environmental prooxidants (e.g., oxygen), which facilitates their diffusion through the encapsulating matrix, thereby promoting lipid

oxidation (Boerekamp et al., 2019). Additionally, for a fixed oil load, smaller capsules result in thinner and, therefore, more permeable encapsulating walls. This, together with the higher content of pullulan in the -HPH-co capsules, may explain their higher oxidative stability, since pullulan acts as an efficient oxygen barrier due to its intrinsic impermeability to oxygen (Bakry et al., 2016). Moreover, the breakage of the pullulan chains during HPH for -HPH-co samples may have contributed to the formation of a more densely packed dry matrix, which may have limited the oxygen diffusion to a higher extent, although the latter requires further research. Nonetheless, the significantly higher oxidation rate and extent observed in -co systems cannot only be attributed to the physicochemical properties of the capsules in regard to their size and the thickness of the encapsulating wall. Contrary to emulsion-based methods, which lead to capsules consisting of small discrete oil droplets distributed within the dried encapsulating matrix, coaxially electrosprayed capsules consist, theoretically, of an oil droplet located in the core coated with the dried encapsulating wall. It is well known that lipid oxidation occurs as a chain reaction between lipid radicals and oxygen until it is interrupted either by the action of an external agent (e.g., antioxidant) or by the unavailability of an oxygen or hydrogen source (Rahmani-Manglano, García-Moreno, et al., 2020). Therefore, whilst emulsion-based encapsulates will oxidize progressively as the oxygen diffuses from the surface to the core, reaching the different oil droplets, lipid oxidation will propagate faster and more easily in coaxially electrosprayed systems once the oxygen reaches the oily core. This could be a further indication that for -HPH-co capsules, the oxygen diffusivity through the encapsulating matrix was prevented more efficiently than for -co capsules, since although lipid oxidation occurred, these samples were significantly less degraded at the end of the storage time, showing a lipid oxidation extent comparable to that of the emulsion-based encapsulates (Figure 21A–C).

Interestingly, the monoaxially electrosprayed capsules were the most oxidized after processing, as shown by their significantly higher content in the selected volatiles studied at the beginning of the storage time (Figure 21 and see also Figure S 3A in the Supplementary Materials; $p < 0.05$). As previously mentioned, the monoaxially electrosprayed emulsions contained CITREM, which according to the supplier, was made from refined sunflower oil. Sunflower oil is rich in omega-6 PUFAs, and both hexanal and heptanal have been identified in neat sunflower oil (Xu et al., 2018). In addition, the sunflower oil emulsification process favors both the generation and release of SVOPs (van Ruth & Roozen, 2000), which could explain the significantly higher initial concentrations of hexanal and heptanal found in the -

mo capsules after production (Figure 21D,E, $p < 0.05$). In addition, the monoaxially electrosprayed emulsions were stored between batches for a total processing time of 36 h, which resulted in physical destabilization, and consequently in a relatively high content of non-encapsulated surface oil (Figure 19). Indeed, it has been reported that the oxidative stability of emulsions is directly related to their physical stability, with fine and physically stable emulsions being less prone to lipid oxidation (Padial-Domínguez et al., 2020). Therefore, the higher content of SVOPs found in the -mo capsules at the beginning of the storage time (Figure 21) could be attributed to the production and subsequent storage of the emulsions during processing and to the lipid oxidation of the non-encapsulated oil fraction during the processing time between batches. Conversely, spray-dried emulsions were dried right after production, and the spray-drying process led to capsules with better retention properties, as confirmed by their higher EE values (Figure 19). This, together with the short residence time of the spray-dried capsules in the drying chamber, could explain their low contents in the selected volatiles at the beginning of the storage time (see Figure S 3 in the Supplementary Materials). Likewise, low initial lipid oxidation was observed for -HPH-co systems (see Figure S 3 in the Supplementary Materials), which has been attributed to the absence of the emulsification step in the production of these systems. Nonetheless, despite the higher content of the selected volatiles found at the beginning of the storage time for -mo systems, their concentration did not significantly increase during storage (see Figure S 3 in the Supplementary Materials). The monoaxially electrosprayed capsules (i.e., GS-mo and MD-mo) contained WPCH and pullulan in the formulation. WPCH possesses both film-forming and antioxidant properties (e.g., radical scavenging and metal chelating), and combined with LMW carbohydrates as bulk materials, this leads to highly stable capsules in terms of lipid oxidation, as confirmed in our previous work (Rahmani-Manglano, González-Sánchez, et al., 2020). This, together with the intrinsic oxygen-impermeability of pullulan and the breakage of the pullulan chains during the emulsification process, may have contributed to the formation of a highly dense encapsulating matrix with enhanced impermeable properties, which could explain why the initial contents of the volatiles did not increase during storage. It is noteworthy, however, that the concentrations of both hexanal and heptanal significantly decreased for the -mo systems during the course of the lipid oxidation (Figure 21D,E; $p < 0.05$). This could be explained on the basis of aldehyde decomposition as a result of the so called non-enzymatic browning reactions taking place in the presence of the WPCH amino groups (Xiang et al., 2021), as previously observed by other authors (Carneiro et al., 2013; Henna Lu et al., 2013).

Finally, high oxidative stability was observed for the spray-dried capsules, which showed both low initial and low final contents for all selected volatiles (Figure 21). As previously mentioned, the use of spray-drying technology resulted in large capsules (Figure 18A), leading to (i) thicker encapsulating walls for the same oil load and (ii) a significantly reduced surface-to-volume ratio, both affecting the oxygen diffusivity through the encapsulating wall. In addition, the high EE values reported for these samples confirmed the low content of easily oxidized non-encapsulated surface oil. Furthermore, substituting WPCH for T20 as the emulsifier did not significantly affect the overall oxidative stability of the spray-dried systems, except for the T-MD sample (see Figure S 3 in the Supplementary Materials). The latter has been attributed to the higher molecular weight of the MD due to its lower DE, which may have resulted in a more porous encapsulating wall. Additionally, contrary to the WPCH, T20 lacks antioxidant properties, meaning lipid oxidation occurring at the oil–encapsulating agent interface could not be prevented.

4. CONCLUSIONS

To the best of the authors' knowledge, neat fish-oil-loaded capsules were for the first time produced via coaxial electrospraying using LMW carbohydrates (i.e., glucose syrup (GS) or maltodextrin (MD)) as the encapsulating agents. Furthermore, in the study, fish-oil-loaded capsules were also produced by spray-drying and monoaxial electrospraying in the presence of GS or MD, using whey protein concentrate hydrolysate (WPCH) as the emulsifier. Our results show that the physicochemical properties of the capsules (e.g., the particle size or EE) were significantly influenced by the encapsulation technology. As expected, larger capsules were produced using spray-drying over electrospraying technology, and the particle size distribution was also broader. Moreover, the use of emulsion-based encapsulation methods (i.e., spray-drying and monoaxial electrospraying) resulted in better entrapment of the fish oil within the encapsulating matrix (EE > 69%) compared to coaxial electrospraying (EE = 53–59%), due to the lack of surface-active properties of the main encapsulating agents used (i.e., GS or MD). This explained the lowest oxidative stability observed for the coaxially electrosprayed capsules. However, despite the higher content of non-encapsulated oil in the aforementioned systems, their oxidative stability could be significantly enhanced by increasing the content of pullulan in the shell solution. This was attributed to the larger size of the resulting capsules and to the higher content of pullulan in the encapsulating matrix, both influencing the oxygen diffusivity through the encapsulating wall. The use of

emulsion-based encapsulation methods led to capsules with high oxidative stability, as confirmed by the low contents of SVOPs (i.e., 2-ethylfuran, (*E*,*E*)-2,4-heptadienal) found at the end of the storage time. Nonetheless, the monoaxially electrosprayed capsules were the most oxidized right after production due to the emulsification process, together with a larger time span between the emulsion production and drying.

5. REFERENCES

Acevedo-Fani, A., Guo, Q., Nasef, N., & Singh, H. (2021). Aspects of food structure in digestion and bioavailability of LCn-3PUFA-rich lipids. In P. J. García-Moreno, C. Jacobsen, A.-D. M. Sørensen, & B. Yesiltas (Eds.), Omega-3 Delivery Systems (pp. 427–448). Academic Press. https://doi.org/10.1016/b978-0-12-821391-9.00003-x

Bakry, A. M., Fang, Z., Ni, Y., Cheng, H., Chen, Y. Q., & Liang, L. (2016). Stability of tuna oil and tuna oil/peppermint oil blend microencapsulated using whey protein isolate in combination with carboxymethyl cellulose or pullulan. *Food Hydrocolloids*, *60*, 559–571. https://doi.org/10.1016/j.foodhyd.2016.04.026

Binsi, P. K., Nayak, N., Sarkar, P. C., Jeyakumari, A., Muhamed Ashraf, P., Ninan, G., & Ravishankar, C. N. (2017). Structural and oxidative stabilization of spray dried fish oil microencapsulates with gum arabic and sage polyphenols: Characterization and release kinetics. *Food Chemistry*, *219*, 158–168. https://doi.org/10.1016/j.foodchem.2016.09.126

Boerekamp, D. M. W., Andersen, M. L., Jacobsen, C., Chronakis, I. S., & García-Moreno, P. J. (2019). Oxygen permeability and oxidative stability of fish oil-loaded electrosprayed capsules measured by Electron Spin Resonance: Effect of dextran and glucose syrup as main encapsulating materials. *Food Chemistry*, *287*, 287–294. https://doi.org/10.1016/j.foodchem.2019.02.096

Carneiro, H. C. F., Tonon, R. v., Grosso, C. R. F., & Hubinger, M. D. (2013). Encapsulation efficiency and oxidative stability of flaxseed oil microencapsulated by spray drying using different combinations of wall materials. *Journal of Food Engineering*, *115*(4), 443–451. https://doi.org/10.1016/j.jfoodeng.2012.03.033

Djuricic, I., & Calder, P. C. (2021). Beneficial outcomes of omega-6 and omega-3 polyunsaturated fatty acids on human health: An update for 2021. *Nutrients*, *13*(7). https://doi.org/10.3390/nu13072421

Drosou, C. G., Krokida, M. K., & Biliaderis, C. G. (2017). Encapsulation of bioactive compounds through electrospinning/electrospraying and spray drying: A comparative assessment of food-

related applications. *Drying Technology*, *35*(2), 139–162. https://doi.org/10.1080/07373937.2016.1162797

Drusch, S., & Berg, S. (2008). Extractable oil in microcapsules prepared by spray-drying: Localisation, determination and impact on oxidative stability. *Food Chemistry*, *109*(1), 17–24. https://doi.org/10.1016/j.foodchem.2007.12.016

García-Moreno, P. J., Damberg, C., Chronakis, I. S., & Jacobsen, C. (2017). Oxidative stability of pullulan electrospun fibers containing fish oil: Effect of oil content and natural antioxidants addition. *European Journal of Lipid Science and Technology*, *119*(12). https://doi.org/10.1002/ejlt.201600305

García-Moreno, P. J., Özdemir, N., Stephansen, K., Mateiu, R. v., Echegoyen, Y., Lagaron, J. M., Chronakis, I. S., & Jacobsen, C. (2017). Development of carbohydrate-based nano-microstructures loaded with fish oil by using electrohydrodynamic processing. *Food Hydrocolloids*, *69*, 273–285. https://doi.org/10.1016/j.foodhyd.2017.02.013

García-Moreno, P. J., Pelayo, A., Yu, S., Busolo, M., Lagaron, J. M., Chronakis, I. S., & Jacobsen, C. (2018). Physicochemical characterization and oxidative stability of fish oil-loaded electrosprayed capsules: Combined use of whey protein and carbohydrates as wall materials. *Journal of Food Engineering*, *231*, 42–53. https://doi.org/10.1016/j.jfoodeng.2018.03.005

García-Moreno, P. J., Rahmani-Manglano, N. E., Chronakis, I. S., Guadix, E. M., Yesiltas, B., Sørensen, A.-D. M., & Jacobsen, C. (2021). Omega-3 nano-microencapsulates produced by electrohydrodynamic processing. In P. J. García-Moreno, C. Jacobsen, A.-D. M. Sørensen, & B. Yesiltas (Eds.), *Omega-3 Delivery Systems. Production, Physical Characterization and Oxidative Stability* (pp. 345–370). Academic Press. https://doi.org/10.1016/b978-0-12-821391-9.00017-x

Ghelichi, S., Hajfathalian, M., García-Moreno, P. J., Yesiltas, B., Moltke-Sørensen, A.-D., & Jacobsen, C. (2021). Food enrichment with omega-3 polyunsaturated fatty acids. In P. J. García-Moreno, C. Jacobsen, A.-D. M. Sørensen, & B. Yesiltas (Eds.), *Omega-3 Delivery Systems* (pp. 395–425). Academic Press. https://doi.org/10.1016/b978-0-12-821391-9.00020-x

Gómez-Mascaraque, L. G., & López-Rubio, A. (2016). Protein-based emulsion electrosprayed micro- and submicroparticles for the encapsulation and stabilization of thermosensitive hydrophobic bioactives. *Journal of Colloid and Interface Science*, *465*, 259–270. https://doi.org/10.1016/j.jcis.2015.11.061

Gómez-Mascaraque, L. G., Tordera, F., Fabra, M. J., Martínez-Sanz, M., & Lopez-Rubio, A. (2019). Coaxial electrospraying of biopolymers as a strategy to improve protection of bioactive food

ingredients. *Innovative Food Science and Emerging Technologies*, *51*, 2–11. https://doi.org/10.1016/j.ifset.2018.03.023

Guillén, M. D., & Cabo, N. (1999). Usefulness of the frequency data of the Fourier transform infrared spectra to evaluate the degree of oxidation of edible oils. *Journal of Agricultural and Food Chemistry*, *47*(2), 709–719. https://doi.org/10.1021/jf9808123

Guillén, M. D., & Cabo, N. (2000). Some of the most significant changes in the Fourier transform infrared spectra of edible oils under oxidative conditions. *Journal of the Science of Food and Agriculture*, *80*(14), 2028–2036. https://doi.org/10.1002/1097-0010(200011)80:14<2028::AID-JSFA713>3.3.CO;2-W

Henna Lu, F. S., Nielsen, N. S., & Jacobsen, C. (2013). Comparison of two methods for extraction of volatiles from marine PL emulsions. *European Journal of Lipid Science and Technology*, *115*(2), 246–251. https://doi.org/10.1002/ejlt.201200128

Hogan, S. A., McNamee, B. F., O'Riordan, E. D., & O'Sullivan, M. (2001). Emulsification and microencapsulation properties of sodium caseinate/carbohydrate blends. *International Dairy Journal*, *11*(3), 137–144. https://doi.org/10.1016/S0958-6946(01)00091-7

Jacobsen, C., García-Moreno, P. J., Mendes, A. C., Mateiu, R. V., & Chronakis, I. S. (2018). Use of Electrohydrodynamic Processing for Encapsulation of Sensitive Bioactive Compounds and Applications in Food. *Annual Review of Food Science and Technology*, *9*(1), 525–549. https://doi.org/10.1146/annurev-food-030117-012348

Jaworek, A., & Sobczyk, A. T. (2008). Electrospraying route to nanotechnology: An overview. *Journal of Electrostatics*, *66*(3–4), 197–219. https://doi.org/10.1016/j.elstat.2007.10.001

Loscertales, I. G., Barrero, A., Guerrero, I., Cortijo, R., Marquez, M., & Gañán-Calvo, A. M. (2002). Micro/nano encapsulation via electrified coaxial liquid jets. *Science*, *295*(5560), 1695–1698. https://doi.org/10.1126/science.1067595

Padial-Domínguez, M., Espejo-Carpio, F. J., García-Moreno, P. J., Jacobsen, C., & Guadix, E. M. (2020). Protein derived emulsifiers with antioxidant activity for stabilization of omega-3 emulsions. *Food Chemistry*, *329*(127148). https://doi.org/10.1016/j.foodchem.2020.127148

Paximada, P., Howarth, M., & Dubey, B. (2018). Electrosprayed particles derived from nano-emulsions as carriers of fish oil. *TechConnect Briefs 2018 - Advanced Materials*, *3*, 1–4.

Pérez-Masiá, R., Lagaron, J. M., & Lopez-Rubio, A. (2015). Morphology and Stability of Edible Lycopene-Containing Micro- and Nanocapsules Produced Through Electrospraying and Spray Drying. *Food and Bioprocess Technology*, *8*(2), 459–470. https://doi.org/10.1007/s11947-014-1422-7

Prieto, C., & Lagaron, J. M. (2020). Nanodroplets of docosahexaenoic acid-enriched algae oil encapsulated within microparticles of hydrocolloids by emulsion electrospraying assisted by pressurized gas. *Nanomaterials*, *10*(2). https://doi.org/10.3390/nano10020270

Rahmani-Manglano, N. E., García-Moreno, P. J., Espejo-Carpio, F. J., Pérez-Gálvez, A. R., & Guadix-Escobar, E. M. (2020). The Role of Antioxidants and Encapsulation Processes in Omega-3 Stabilization. In M. A. Aboudzadeh (Ed.), *Emulsion-based Encapsulation of Antioxidants. Food Bioactive Ingredients.* (pp. 339–386). Springer, Cham. https://doi.org/10.1007/978-3-030-62052-3_10

Rahmani-Manglano, N. E., González-Sánchez, I., García-Moreno, P. J., Espejo-Carpio, F. J., Jacobsen, C., & Guadix, E. M. (2020). Development of fish oil-loaded microcapsules containing whey protein hydrolysate as film-forming material for fortification of low-fat mayonnaise. *Foods*, *9*(5).

Rahmani-Manglano, N. E., Tirado-Delgado, M., García-Moreno, P. J., Guadix, A., & Guadix, E. M. (2022). Influence of emulsifier type and encapsulating agent on the in vitro digestion of fish oil-loaded microcapsules produced by spray-drying. *Food Chemistry*, *392*, 133257. https://doi.org/10.1016/j.foodchem.2022.133257

Ramakrishnan, S., Ferrando, M., Aceña-Muñoz, L., Mestres, M., de Lamo-Castellví, S., & Güell, C. (2014). Influence of Emulsification Technique and Wall Composition on Physicochemical Properties and Oxidative Stability of Fish Oil Microcapsules Produced by Spray Drying. *Food and Bioprocess Technology*, *7*(7), 1959–1972. https://doi.org/10.1007/s11947-013-1187-4

Serfert, Y., Drusch, S., & Schwarz, K. (2009). Chemical stabilisation of oils rich in long-chain polyunsaturated fatty acids during homogenisation, microencapsulation and storage. *Food Chemistry*, *113*(4), 1106–1112. https://doi.org/10.1016/j.foodchem.2008.08.079

Shahidi, F. (2001). Headspace volatile aldehydes as indicators of lipid oxidation in foods. In *Headspace Analysis of Food and Flavors: Theory and Practice* (Vol. 488, pp. 113–123). Plenum Publishers. https://doi.org/10.1007/978-1-4615-1247-9_9

Siemons, I., Politiek, R. G. A., Boom, R. M., van der Sman, R. G. M., & Schutyser, M. A. I. (2020). Dextrose equivalence of maltodextrins determines particle morphology development during single sessile droplet drying. *Food Research International*, *131*(November 2019), 108988. https://doi.org/10.1016/j.foodres.2020.108988

Stijnman, A. C., Bodnar, I., & Hans Tromp, R. (2011). Electrospinning of food-grade polysaccharides. *Food Hydrocolloids*, *25*(5), 1393–1398. https://doi.org/10.1016/j.foodhyd.2011.01.005

Turchiuli, C., Jimenez Munguia, M. T., Hernandez Sanchez, M., Cortes Ferre, H., & Dumoulin, E. (2014). Use of different supports for oil encapsulation in powder by spray drying. *Powder Technology*, *255*, 103–108. https://doi.org/10.1016/j.powtec.2013.08.026

Unnikrishnan, P., Puthenveetil Kizhakkethil, B., Annamalai, J., Ninan, G., Aliyamveetil Abubacker, Z., & Chandragiri Nagarajarao, R. (2019). Tuna red meat hydrolysate as core and wall polymer for fish oil encapsulation: a comparative analysis. *Journal of Food Science and Technology*, *56*(4), 2134–2146. https://doi.org/10.1007/s13197-019-03694-w

van Ruth, S. M., & Roozen, J. P. (2000). Release of volatile oxidation products from sunflower oil and its oil-in-water emulsion in a model mouth system. *ACS Symposium Series*, *763*(7), 309–320. https://doi.org/10.1021/bk-2000-0763.ch025

Xiang, J., Liu, F., Wang, B., CHen, L., Liu, W., & Tan, S. (2021). A Literature Review on Maillard Reaction Based on Milk Products : Advantages , Disadvantages , and Avoidance Strategies. *Foods*, *10*, 1998.

Xu, L., Yu, X., Li, M., Chen, J., & Wang, X. (2018). Monitoring oxidative stability and changes in key volatile compounds in edible oils during ambient storage through HS-SPME/GC–MS. *International Journal of Food Properties*, *20*(3), S2926–S2938. https://doi.org/10.1080/10942912.2017.1382510

6. SUPPLEMENTARY MATERIAL

(A)

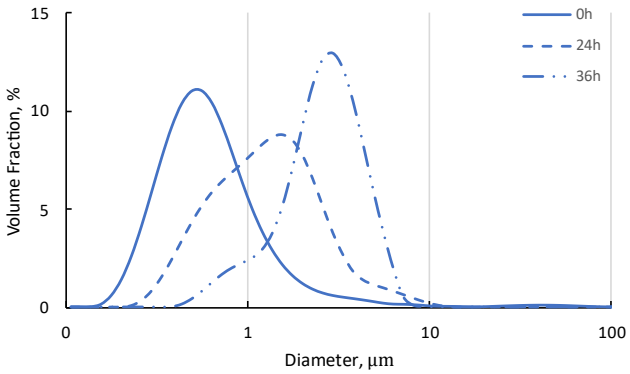

(B)

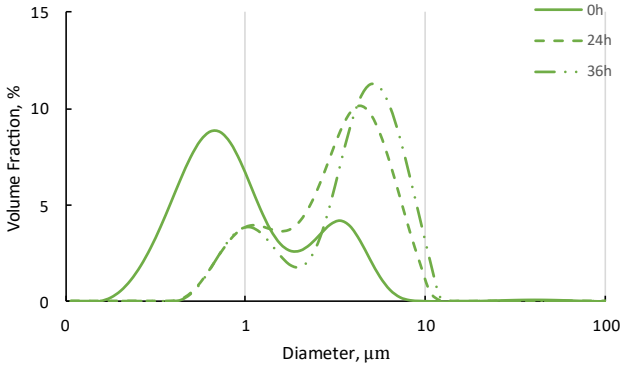

Figure S 1. Oil droplet size distribution of the fish- oil-loaded emulsions produced for monoaxial electrospraying during processing (0h, 24h, 36h): GS-mo (A) and MD-mo (B).

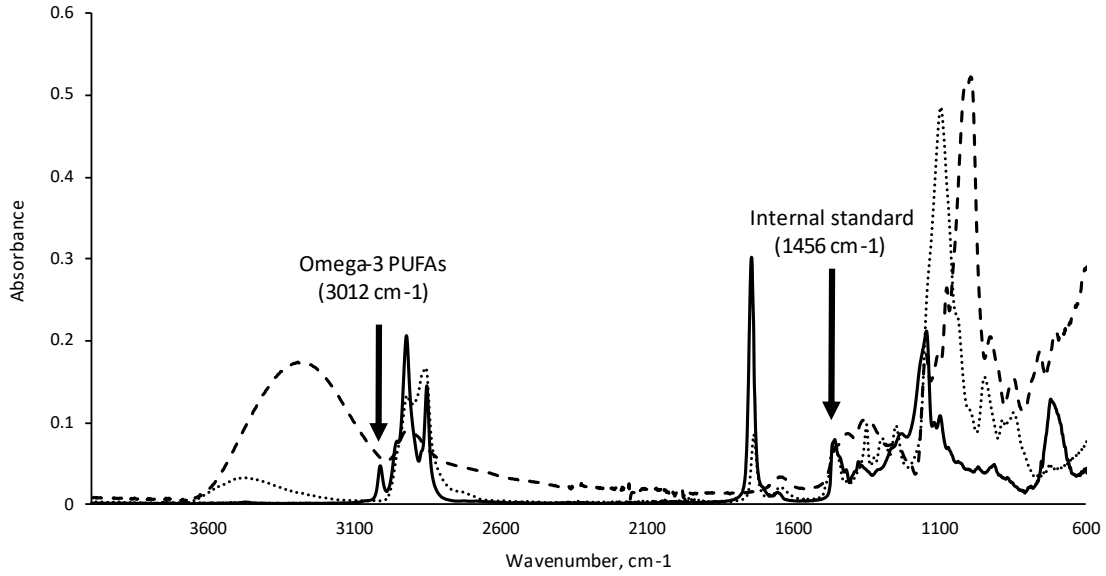

Figure S 2. ATR-FTIR spectra of the fish oil (solid line), glucose syrup (dashed line), and Tween-20 (dotted line).

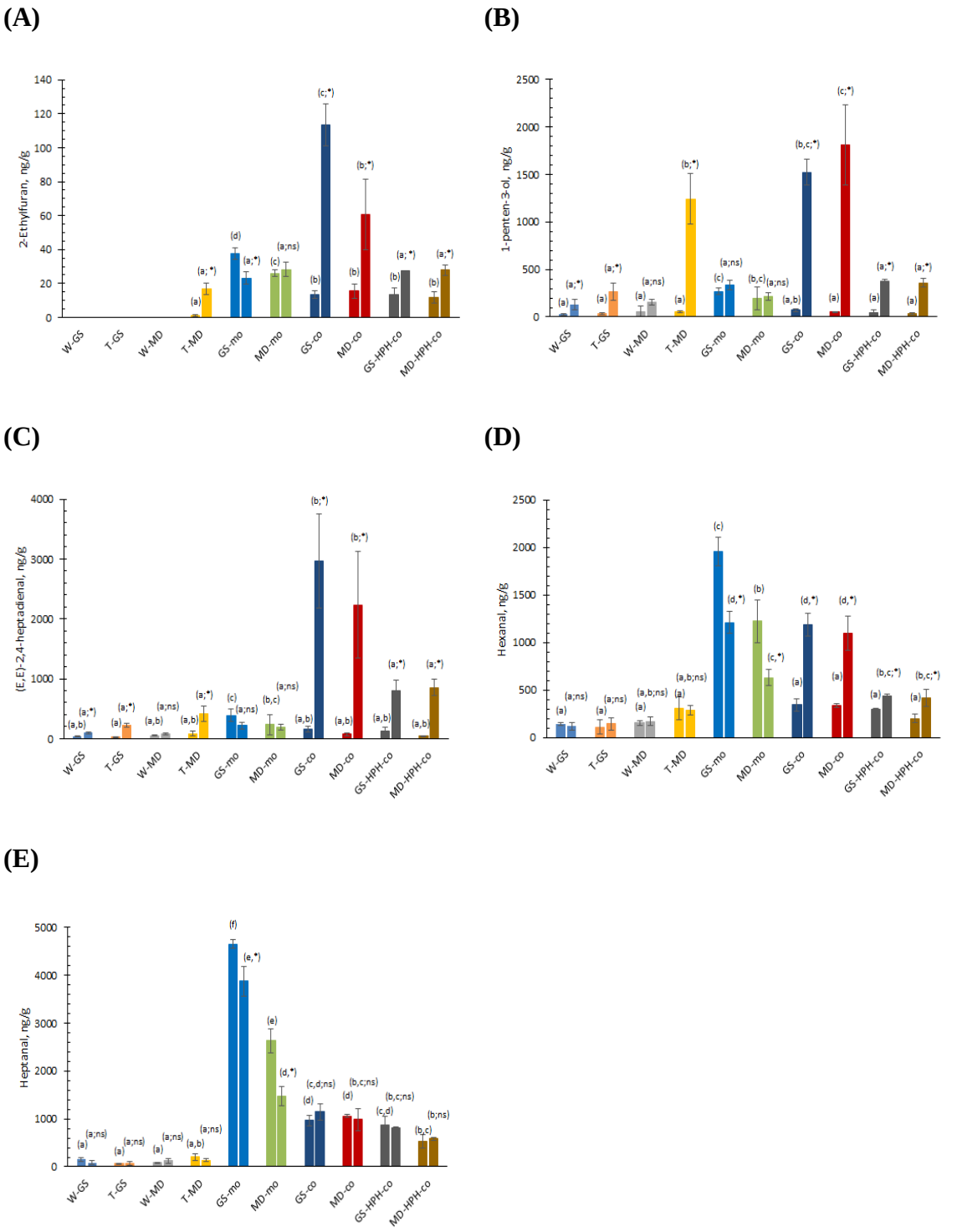

Figure S 3. Secondary volatile oxidation products (SVOPs) of the fish-oil-loaded capsules produced by spray-drying or electrospraying (monoaxial and coaxial) at week 0 and week 6 of storage: 2-ethylfuran (A); 1-penten-3-ol (B); (E,E)-2,4-heptadienal(C); hexanal (D); heptanal (E).

III. Antioxidant location affects the oxidative stability of spray-dried microcapsules loaded with fish oil *

The oxidative stability of fish oil-loaded capsules (~15 wt% oil load) produced by spray-drying and containing natural antioxidants of different polarity was investigated. For this purpose, three commercial rosemary extracts (e.g., polar; K1 or non-polar; K2, K3) and whey protein concentrate hydrolysate (WPCH), exhibiting surface-active properties, were evaluated. The capsules showed similar physicochemical properties (e.g., morphology, size and encapsulation efficiency > 91%), regardless of the formulation. However, the polarity of the antioxidant used significantly influenced the oxidative stability. The microcapsules containing hydrophobic antioxidants showed the lowest peroxide value (PV) after drying, followed by the WPCH-containing capsules, although the PV evolution over storage was similar among the samples. Nonetheless, WPCH was the most effective antioxidant reducing the formation of volatile secondary oxidation products in the capsules. This was attributed to its partition at the oil/matrix interface, resulting in an enhanced protective effect when combined with tocopherols present in the encapsulated oil.

* MANUSCRIPT SUBMITTED FOR PUBLICATION: N.E. Rahmani-Manglano, P.J. García-Moreno, A.R. Pérez-Gálvez & E.M. Guadix-Escobar. (2023). Antioxidant location affects the oxidative stability of spray-dried microcapsules loaded with fish oil.

1. INTRODUCTION

Food fortification with omega-3 polyunsaturated fatty acids (PUFAs) has gained great interest over the last decades due to the health benefits attributed to their intake, especially to EPA (eicosapentaenoic acid, C20:5n-3) and DHA (docosahexaenoic acid, C22:6n-3) (Patel et al., 2022). However, their inclusion into complex food matrices is still challenging for the food industry, mainly because of their low oxidative stability. As it has been extensively reported, lipid oxidation of omega-3 PUFAs results in the loss of their nutritional properties and also has an impact on their organoleptic properties (e.g., development of flavor/odor active compounds) (Arab-Tehrany et al., 2012; Baik et al., 2004; Encina et al., 2016; Velasco et al., 2003), both lowering the quality of the enriched food product. Therefore, the addition of omega-3 rich oils (e.g., fish oil) in the form of a delivery system has been proposed as a promising approach to enhance the oxidative stability of both, the omega-3 PUFAs and the fortified foodstuff (Sørensen et al., 2021). In this regard, the use of encapsulation technologies for the development of efficient dried omega-3 delivery systems (e.g., fish oil-loaded capsules) is of special interest.

Spray-drying is the most common encapsulation technique used for the food industry and it has been extensively used in the production of fish oil-loaded encapsulates aimed as omega-3 delivery systems (Rahmani-Manglano et al., 2020). Encapsulation by spray-drying entraps the fish oil within a glassy encapsulating matrix, generally carbohydrate-based, that acts as a physical barrier against environmental prooxidants (e.g., oxygen) aimed to prevent its degradation. However, it has been demonstrated that the onset of lipid oxidation already occurs during the encapsulation process (Baik et al., 2004; Serfert et al., 2009). The intense mechanical stress exerted during the emulsification step (i.e., production of a coarse emulsion followed by a homogenization step) leads to the inclusion and distribution of prooxidant species (e.g., oxygen, metal traces) within the system and, in most cases, this process is accompanied by a significant temperature increase (Berton-Carabin et al., 2014). Furthermore, since drying is carried out at high temperatures (inlet/outlet temperature ranging from 200 to 80 °C, respectively), lipid oxidation is also likely to occur during spray-drying if the process is not efficiently designed (e.g., low encapsulation efficiency and high residence time of the capsules in the drying chamber) (Santos et al., 2018). The initial oxidative status of the encapsulated oils (right after drying) is of outmost importance as it will further influence the oxidative stability of the encapsulated system during storage since,

once lipid radicals are present in the oil, lipid oxidation rapidly propagates (Johnson & Decker, 2015). A strategy to minimize lipid oxidation during processing, and in consequence enhance the oxidative stability of the capsules during storage, is the addition of antioxidants to the formulation (Serfert et al., 2009). Nowadays, the focus is placed on finding natural ingredients with antioxidant activity (e.g., plant extracts or protein hydrolysates) since, not only they are better considered by the consumer in terms of clean label and sustainability, but also allows to avoid the health hazards related to traditional synthetic antioxidants (e.g., butylated hydroxylanisole (BHA) or butylated hydroxytoluene (BHT), among others) (Hrebień-Filisińska, 2021). Natural plant-derived antioxidants, such as rosemary extract, are the most frequently used in the stabilization of fish oil (Anwar & Qadir, 2021; Hrebień-Filisińska, 2021). The antioxidant activity of rosemary extract is related to its content of carnosic acid (CA) and its oxidation product, carnosol (CN), which act as efficient radical scavengers (Hopia et al., 1996). Furthermore, CA has been reported to exhibit protective effect towards tocopherols (e.g., α-tocopherol or δ-tocopherol) during lipid oxidation, thus acting as a synergistic antioxidant (García-Moreno et al., 2017; Hopia et al., 1996). Additionally, protein hydrolysates have shown high potential as antioxidants, gaining more attention in the last years the use of peptides as natural antioxidants in food (Hrebień-Filisińska, 2021).

Several studies carried out in wet heterogeneous systems (i.e., oil-in-water emulsions) have shown that one of the most important factors influencing the efficacy of an antioxidant is its partition in the system, which is influenced by its polarity (e.g., lipophilic, amphiphilic or hydrophilic) (Laguerre et al., 2015; Shahidi & Zhong, 2011). Generally, it is assumed that antioxidants with a tendency to accumulate at the oil/water interface (e.g., amphiphilic antioxidants) are more efficient in wet emulsified systems since this microenvironment has been proposed to be the place where lipid oxidation is initiated (i.e., contact area between prooxidants and the oil) (Aslam & Schroën, 2023; Berton-Carabin et al., 2014; Laguerre et al., 2015; Shahidi & Zhong, 2011). Therefore, although the behaviour of antioxidants in dried heterogeneous systems is not fully understood yet (Baik et al., 2004; ten Klooster et al., 2022; Velasco et al., 2003), it is plausible to speculate that for dried emulsions, such as oil-loaded capsules, the antioxidant activity might also be strongly influenced by its location within the dehydrated system (e.g., at the encapsulated oil droplets, at the oil/matrix interface or at the glassy matrix) (Velasco et al., 2003). In this line, a recent study evaluated the influence of the polarity of gallic acid esters on the oxidative stability of spray-dried oil-

loaded capsules (ten Klooster et al., 2022). Interestingly, propyl gallate exhibiting amphiphilic properties did not significantly enhanced the oxidative stability of the encapsulated oil contrary to what could be expected based on its antioxidant activity in wet oil-in-water emulsions (ten Klooster et al., 2022). On the contrary, these authors reported that the more non-polar gallates (i.e., octyl, lauryl and hexadecyl gallate) were more efficient preventing lipid oxidation of the encapsulated oil, being the latter attributed to their partition within the oil phase of the capsules. It should be borne in mind, however, that the antioxidant activity of gallic acid and its derivatives arise from the radical scavenger activity of the polar phenolic head (Garrido et al., 2012). Unfortunately, the effect of amphiphilic compounds with antioxidant activity in both their polar and non-polar part (i.e., peptides) on the oxidative stability of dry heterogeneous systems has not been investigated to date.

Therefore, taken altogether, the aim of the study was to investigate the oxidative stability of fish oil-loaded capsules produced by spray-drying containing natural antioxidants of different polarity. For this purpose, the capsules were produced using three different commercial antioxidants: i) a water-soluble rosemary extract, ii) an oil-soluble rosemary extract, iii) an oil-soluble mixture of antioxidants including rosemary extract, tocopherols, ascorbic acid, citric acid and lecithin. Moreover, whey protein concentrate hydrolysate (WPCH, degree hydrolysis of 10%), which was previously reported to exhibit high antioxidant and emulsifying activity (Padial-Domínguez et al., 2020), was also evaluated as amphiphilic antioxidant. The results of this work will provide new insights on the effect of antioxidants location within dried emulsions and their ability to retard lipid oxidation.

2. MATERIALS AND METHODS

2.1 Materials

Omega Oil 1812 TG Gold with a peroxide value (PV) of 0.88 ± 0.02 meq O2/kg oil (measured as described in Section 2.4.1), was purchased from BASF Personal Care and Nutrition GmbH (Illertissen, Germany) and stored at -80 °C until use. The tocopherol content was determined as described in our previous work (Rahmani-Manglano et al., 2020) and was as follows: alpha-, gamma- and delta-tocopherol content of 500.8 ± 1.3, 2108.8 ± 123 5.3 and 677.4 ± 2.0 μg/g oil, respectively. Glucose syrup (GS; DE38, C*Dry 1934) was kindly donated by Cargill Germany GmbH (Krefeld, Germany). Tween 20 (T20) was purchased

from Sigma-Aldrich (Darmstadt, Germany). The three rosemary-based extracts of different polarities under the commercial name of: Herbalox® HT-P (K1, water-soluble), Herbalox® XT-O (K2, lipid-soluble) and Duralox® MAN-5 (K3, lipid-soluble) were kindly donated by Kalsec, Inc. The whey protein concentrate hydrolysate (WPCH), also used as an antioxidant, was produced by enzymatic hydrolysis with Alcalase 2.4L (Novozymes, Bagsvaerd, Denmark) as described elsewhere (Rahmani-Manglano et al., 2020). The rest of the reagents used were of analytical grade.

2.2 Production of the capsules

Fish oil-in-water emulsions containing one of the aforementioned antioxidants (K1, K2, K3 or WPCH) were subjected to spray-drying to produce the capsules (~ 15 wt% oil load), as reported in our previous work (Rahmani-Manglano et al., 2020). The antioxidant concentration in the emulsions was fixed to 200 ppm of carnosic acid and carnosol (CA+CN) for the rosemary extract-based antioxidants (K1, K2, K3) or 200 ppm of protein in case of the protein-based antioxidant, WPCH, with respect to fish oil. A control sample without antioxidants was also produced. The aqueous phase of the emulsions was produced by dissolving the encapsulating agent (GS, 28 wt%), the emulsifier (T20, 0.35 wt%) in distilled water and stirring overnight at ambient temperature. Then, a coarse emulsion was produced by dispersing the fish oil (5 wt%) in the aqueous phase during the first minute of mixing at 15,000 rpm using an Ultraturrax T-25 homogenizer (IKA, Staufen, Germany). The total processing time was 2 min. The polar antioxidants (K1 and WPCH) were added to the aqueous phase, whereas the nonpolar antioxidants (K2 and K3) where added to the oil. The coarse emulsion was further processed in a high-pressure homogenizer at a pressure range of 450/75 bar, applying 3 passes (PandaPLUS 2000; GEA Niro Soavi, Lübeck, Germany). Spray-drying was conducted in a pilot plant scale spray-drier (Mobile Minor; Niro A/S, Copenhagen, Denmark) at 190/80ºC inlet/outlet temperature, respectively, with the pressure of the pneumatic air activating the rotary atomizer set to 4 bar (22,000 rpm).

2.3 Characterization of the spray-dried capsules

2.3.1 Oil droplet size distribution (ODSD)

The oil droplet size distribution (ODSD) of the emulsions before (parent emulsions) and after drying (reconstituted emulsions) was measured by laser diffraction in a Mastersizer

2000 (Malvern Instruments, Ltd., Worcestershire, UK) as previously reported by Rahmani-Manglano et al. (2022). The emulsions were reconstituted by dissolving the microcapsules in distilled water in order to obtain the same solid content as the original emulsion. Then, the samples were diluted in recirculating water (3000 rpm) to achieve an obscuration in the range 12 - 15%. The refractive indexes of fish oil (1.481) and water (1.330) were used as particle and dispersant, respectively. Measurements were made in triplicate.

2.3.2 Morphology and size

A thin layer of powder was placed on carbon tape and carbon-coated (EMITECH K975X Turbo-Pumped Thermal Evaporator, Quorum Technologies, UK) to investigate their morphology and size by scanning electron microscopy (SEM) using a FESEM microscope (LEO 1500 GEMINI, Zeiss, Germany) (Rahmani-Manglano, Tirado-Delgado, et al., 2022). The SEM images were acquired in the range 250X – 2KX magnification with a 5-kV accelerating voltage. The ImageJ software (National Institute of Health) was used to analyze the images. Approximately, 135 randomly-selected capsules were measured to determine the particle size distributions and mean diameters.

2.3.3 Encapsulation Efficiency (EE)

The encapsulation efficiency (EE) was determined by extracting the non-encapsulated surface oil as described elsewhere (Rahmani-Manglano, Tirado-Delgado, et al., 2022). Briefly, 2.5 g of powder was weighed and mixed with 15 mL of hexane in a vortex mixer for 2 min and then centrifuged at 2720g for 20 min. Then, 5 mL of supernatant were collected in a Pyrex tube (previously weighted) and evaporated under a constant flow of nitrogen. Afterwards, the Pyrex tube was weighed again. The concentration of non-encapsulated surface oil was then adjusted to the original volume of hexane added.

2.4 Oxidative stability of the spray-dried capsules

To investigate the oxidative stability of the microcapsules, 5 g of powder was stored in brown bottles (30 mL and 26-mm inner diameter) at 25 ºC in the dark for 6 weeks. Samples were taken every week (week 0, 1, 2, 3, 4, 5, 6) and placed at −80ºC under a nitrogen atmosphere until analysis.

2.4.1 Peroxide Value (PV)

First, the fish oil was extracted from the capsules using hexane:2-propanol (1:1, v/v) solvent. For the extraction, 2 g of powder was dissolved in 10 mL of distilled water prior mixing with the extracting solvent and then, the mixture was centrifuged at 670g for 2 min. The extractions were carried out in duplicates. The peroxide value (PV) was quantified on the lipid extracts using the colorimetric ferric-thiocyanate method at 485 nm, according to Drusch et al. (Drusch et al., 2012), with some modifications. In brief, the extracted oil was diluted in purified 2-propanol prior to the addition of iron-II-chloride and ammonium thiocyanate solutions. Then, the mixture was incubated for 5 min at room temperature. Measurements were carried out in duplicates for each lipid extract. Results were expressed in meq O2 per kg of oil.

2.4.2 Determination of secondary volatile oxidation products (SVOPs)

The content of secondary volatile oxidation products (SVOPs) of the capsules was determined as described by Thomsen et al. (2016), with some modifications. Approximately, 3 g of powder and 30 mg of internal standard (4-methyl-1-pentanol and 30µg/g water) were added to a 20-mL glass vial and mixed with 7 mL of water. The vials were then placed in the SPME tray and equilibrated for 3 min at 60 °C. The extraction of the volatile compounds was performed in the headspace of the vials by a SPME fiber 50/30 µm CAR/PDMS 57,295-U (Supelco, Bellefonte, USA) during 45 min at 60 °C. The agitation speed was set to 500 rpm. Afterwards, the extracted compounds were transferred from the SPME fiber to the capillary column Zebron^{TM} ZB-1701 column (30 m × ID 0.25 mm × 0.25 µm film thickness, Phenomenex, USA) using helium gas flow (1.0 mL/min) in the split/spitless injector set at 250 °C. The injection was done in the split mode (split 20:1). The GC oven temperature program was as follows: initial temperature of 35 °C for 3 min, increment of 3.0 °C/min to 70 °C, increment of 7.0 °C/min to 200 °C and increment of 15.0 °C/min to 250 °C. This temperature was kept there for 2 min. The released volatile compounds were then identified by MS-library searches in the National Institute of Standards and Technology (NIST) database (NIST v2.0).

2.5 Statistical analysis

Data were subjected to one-way analysis of variance (ANOVA) by using Statgraphics version 5.1 (Statistical Graphics Corp., Rockville, MD, USA). A multiple sample

comparison using Tukey's test was carried out to identify significant differences between means at a level of confidence of 95% ($p < 0.05$).

3. RESULTS AND DISCUSSION

3.1 Characterization of the spray-dried capsules

3.1.1 Oil droplet size distribution (ODSD)

Before drying, the parent emulsions presented a similar oil droplet size distribution (ODSD) with the curves showing a monomodal distribution with the main peak centred at ~0.2 μm and a shoulder, less representative, centred at ~0.7 μm (Figure 22). Conversely, the reconstituted emulsions showed a bimodal ODSD with a small peak at high diameter values (~7 μm). From Figure 22, it can be clearly observed that for the reconstituted emulsions the proportion of the main peak decreased as the proportion of the shoulder increased, whilst both peaks were displaced to larger diameter values (i.e., the main peak was displaced from ~0.20 μm to ~0.30 μm). An increase in the oil droplet size of reconstituted powders is often related to flocculation/coalescence of the non-encapsulated oil fraction after redispersion, as a result of emulsion destabilization during processing (Drusch et al., 2007). Thus, our results are indicative that the T20 used as the emulsifier could not efficiently retain the integrity of the oil/water interface for all the oil droplets during spray-drying, leading to oil droplets coalescence during processing and later redispersion of the capsules (Taboada et al., 2021). These results are in agreement with previous studies in which the original fine and monomodal ODSD of a T20-stabilized parent emulsion changed to a bimodal ODSD of larger oil droplets after redispersion of the resulting spray-dried powder in water (Hernández Sánchez et al., 2016; Rahmani-Manglano, Tirado-Delgado, et al., 2022).

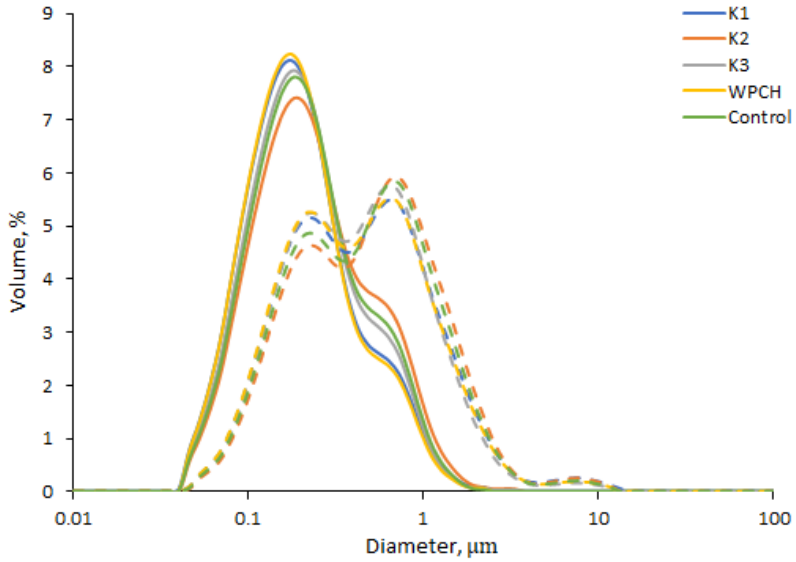

Figure 22. Oil droplet size distribution (ODSD) of the parent emulsions before drying (solid lines) and the reconstituted emulsions after drying (dashed lines).

3.1.2 Morphology and size

Figure 23A-E shows that spherical particles with mostly smooth surfaces were obtained. The mean diameter of the different type of capsules varied from 12.2 ± 7.6 µm to 13.7 ± 7.4 µm ($p > 0.05$), with more than 80% of the particles presenting a size below 20 µm (Figure 23F). As expected, no significant differences were observed regarding the morphology and size of the capsules since these properties are influenced by the composition of the emulsions (e.g., type and concentration of the encapsulating agent) and the processing conditions (e.g., inner/outer drying temperature) (Encina et al., 2016). Thus, it was confirmed that at the fixed drying conditions used to produce the capsules, neither the nature (i.e., hydrophobic/hydrophilic) nor the concentration of the antioxidant added to the formulation (i.e., 200 ppm with respect to the oil) affected the microstructure of the particles, as previously reported by other authors (Hernández Sánchez et al., 2016).

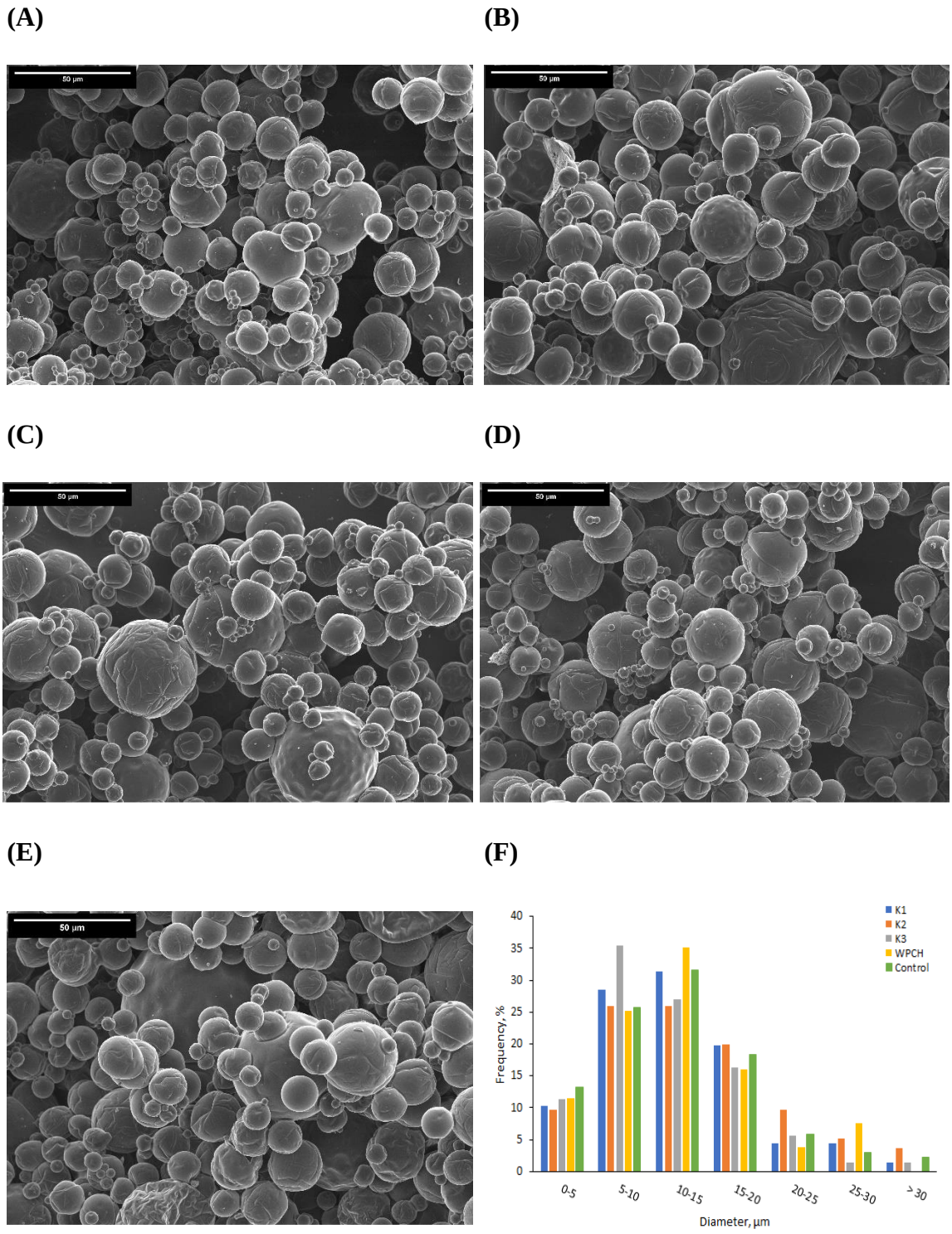

Figure 23. SEM images (A-E) and particle size distribution (F) of the spray-dried microcapsules: K1 (A); K2 (B); K3 (C); WPCH (D); Control (E). Scale bar: 50 µm.

3.1.3 Encapsulation Efficiency (EE)

High EE values were achieved in all the encapsulated systems studied (EE > 91%, Figure 24) indicating a high retention of the oil droplets within the encapsulating matrix during drying. Therefore, taking into account the results of the ODSD of the reconstituted emulsions

(Section 3.1.1), it could be speculated that the significantly larger oil droplets found in the reconstituted emulsions ($p < 0.05$) occurred as a result of oil droplets flocculation/coalescence during processing rather than flocculation/coalescence of the non-encapsulated oil fraction due to its low amount (< 8% non-encapsulated oil). Therefore, although the integrity of the T20-stabilized oil/water interface was not retained during atomization, the larger fish oil droplets were efficiently trapped within the GS-based encapsulating matrix after drying.

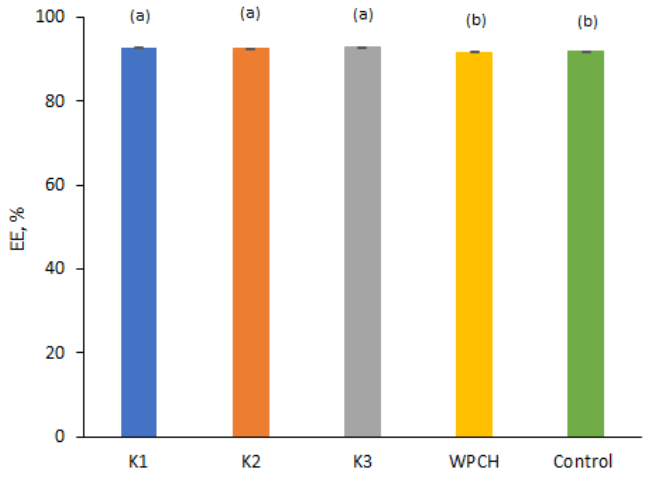

Figure 24. Encapsulation efficiency of the fish oil-loaded microcapsules. Samples followed by letter, a-b, indicates statistical differences ($p \leq 0.05$) between microcapsules.

Our results also show that the antioxidant used in the formulation had a minor effect on the EE values despite the statistical analysis results showing significant differences for WPCH and Control samples compared to the CA+CN-based antioxidants (K1, K2, K3) ($p < 0.05$, Figure 24). In this line, other authors have reported minor differences in the EE values when producing fish oil-loaded capsules by spray-drying containing antioxidants, the latter not being affected by the amount or type of antioxidant/s used in the formulation (Hogan et al., 2003; Serfert et al., 2009). The EE values achieved in the current study are slightly lower than others reported in the literature in which GS was used as the main encapsulating agent (EE > 91%) (Polavarapu et al., 2011; Rahmani-Manglano et al., 2020; Serfert et al., 2009; Tamm et al., 2015). It should be noted, however, that the aforementioned studies used either modified carbohydrates (e.g., n-octenylsuccinate-derivatised starch) or proteins/protein hydrolysates as emulsifiers (e.g., whey protein concentrate hydrolysate), all exerting film-forming properties contrary to T20.

Taken altogether, from the results on physicochemical properties of the capsules (i.e., ODSD, morphology and size, and EE), we can state that the potential differences on their

oxidative stability will arise as a result of the different antioxidant activity of the natural antioxidants added to the formulation (i.e., K1, K2, K3 or WPCH).

3.2 Oxidative stability of the spray-dried capsules

3.2.1 Peroxide Value (PV)

Figure 25 shows the content of primary oxidation products (i.e., peroxide value, PV) of the capsules during 6 weeks of storage at ambient temperature (25 ºC). After drying, a significant increase in the PV occurred in all the samples compared to the fresh fish oil (i.e., PV of the capsules in the range 2.8 ± 0.2 – 5.3 ± 0.5 meq O2/kg oil after drying). These results further confirm that the onset of lipid oxidation already occurred during processing as a result of the emulsification step and subsequent drying at high temperatures (Baik et al., 2004; Serfert et al., 2009). Nonetheless, different initial oxidation extents could be observed depending on the antioxidant used in the formulation (Figure 25). The lowest PV after drying was found in K3 sample, followed by K2 and WPCH samples, respectively. On the contrary, the K1 and the Control samples were the most degraded after processing (Figure 25, $p > 0.05$). As shown in Figure S 4 of the Supplementary Material, the rosemary-based antioxidants were consumed during processing since only ~63 – 67% of the initial concentration of CA+CN remained after drying. The lowest concentration of CA+CN found corresponded to the K3 sample, which is consistent with the lowest PV reported for this system after drying due to a higher consumption of antioxidants. However, K1 and K2 antioxidants were consumed to a similar extent during processing although their initial PV was significantly different (Figure S 4 of the Supplementary Material and Figure 25, respectively). In liquid heterogeneous systems, such as the wet spray-dried emulsions, the location of the antioxidant highly influences its protective effect against lipid oxidation. In fact, lipophilic and/or amphiphilic antioxidants have been reported to be more efficient than hydrophilic antioxidants since they tend to accumulate near to or at the oil/water interface where lipid oxidation is initiated (Shahidi & Zhong, 2011). In this line, ten Klooster et al., (2022) reported that the PV after spray-drying sunflower oil-in-water emulsions stabilized with whey protein isolate in presence of gallic acid decreased as the alkyl chain length of gallates increased (i.e., increasing hydrophobicity of the antioxidant molecule). Furthermore, in a previous study, Serfert et al. (2009) pointed out that lipid oxidation could be significantly reduced during spray-drying processing when a synergistic combination of antioxidants with different mechanisms of action was used in the formulation (e.g., lipophilic antioxidants,

synergistic compounds and metal chelator. Therefore, our results are in the same line than those previously reported since the capsules containing the lipid-soluble rosemary extract in combination with tocopherols, ascorbic acid, citric acid and lecithin (K3 sample) prevented the formation of hydroperoxides more efficiently during processing, followed by the lipid-soluble rosemary extract alone (K2 sample) and the whey protein concentrate hydrolysate (WPCH sample), the latter exhibiting surface-active properties (Padial-Domínguez et al., 2020) (Figure 25). Thus, although the water-soluble K1 antioxidant was consumed during processing (Figure S 4 of the Supplementary Material), it was less effective in preventing lipid oxidation, presumably due to its tendency towards the aqueous phase of the wet spray-dried emulsion (Shahidi & Zhong, 2011; ten Klooster et al., 2022).

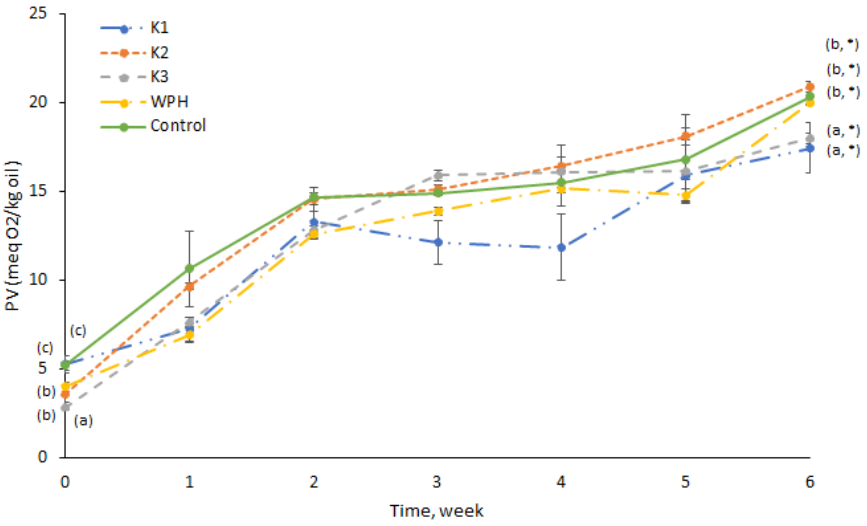

Figure 25. Peroxide value (PV) of the fish oil-loaded microcapsules stabilized with antioxidants of different polarity during 6 weeks of storage at ambient temperature (25 ºC). Samples followed by a letter, a-c, indicates statistical differences ($p \leq 0.05$) between microcapsules. Means within the same sample followed by an asterisk (*) indicates statistical differences ($p \leq 0.05$) between week 0 and week 6.

It is worth mentioning that, although initial lipid oxidation was reduced in the presence of the non-polar/amphiphilic antioxidants (i.e., K2, K3 and WPCH samples), it could not be completely avoided, as also reported by other authors (Baik et al., 2004; Hogan et al., 2003; Serfert et al., 2009; ten Klooster et al., 2022). Moreover, during storage, the presence of antioxidants in the fish oil-loaded capsules (samples K1, K2, K3 and WPCH) did not reduced the formation of lipid peroxides compared to the Control sample, since no lag phase was observed for any of the encapsulated systems produced (Figure 25). On the contrary, a rather similar sharp increase in the PV could be noticed in all the samples until the second week of storage (Figure 25). Then, from week 2 onwards, a sustained increase in the PV was observed for all the capsules to final values comparable among the samples (i.e., final PV in the range

17.5 ± 1.4 – 20.9 ± 0.3 meq O2/kg oil). Interestingly, the lowest PV after 6 weeks of storage was found for sample K1. However, low PVs may be indicative of an advanced oxidation state due to hydroperoxides decomposition to secondary oxidation products (e.g., aldehydes) rather than being indicative of a good performance of the antioxidant, as will be discussed below.

3.2.2 Secondary volatile oxidation products (SVOPs)

The content of selected secondary volatiles oxidation products (SVOPs) derived from the oxidation of omega-3 PUFAs (e.g., 2-ethylfuran, 1-penten-3-ol, 2-pentenal, 2-hexenal, (Z)-4-heptenal, (E,E)-2,4-heptadienal and nonanal) was quantified at the beginning (week 0) and at the end (week 6) of the storage time (Figure 26).

Overall, our results indicate that the water-soluble rosemary extract (sample K1) was less effective inhibiting lipid oxidation both, during processing and during storage. This was confirmed by the highest PV found after drying for K1 sample (Figure 25) and by the highest content of SVOPs developed during processing (e.g., 2-pentenal and nonanal) and subsequent storage of the capsules (e.g., 2-ethylfuran, 1-penten-3-ol, 2-pentenal, 2-hexenal, (Z)-4-heptenal and nonanal, Figure 26). This is once again attributed to the partition of K1 antioxidant within the wet (i.e., fish oil-in water emulsion) and subsequently dried (i.e., fish oil-loaded capsules) heterogeneous systems. Due to its polarity, K1 antioxidant is more likely to be dispersed in the aqueous phase of the wet spray-dried emulsion. Therefore, after water removal, K1 antioxidant is expected to be trapped within the glassy encapsulating matrix. In low moisture systems the antioxidant activity is assumed to be diffusion-limited (Barden & Decker, 2013), thus antioxidant molecules located within the encapsulating matrix – where the mobility is significantly limited – might be less effective preventing lipid oxidation. Indeed, previous studies which evaluated the effect of polar antioxidants and their non-polar analogues (e.g., α-tocopherol and Trolox or gallic acid and its ester derivatives) in dried encapsulated systems, reported that non-polar antioxidants, readily present in the oil phase, prevented lipid oxidation during storage more efficiently than their polar counterpart (Hogan et al., 2003; Velasco et al., 2009). The latter is in agreement with our observations since the oxidative stability of the fish oil-loaded capsules was significantly enhanced in the presence of the lipid-soluble rosemary extract analogue (K2 sample) compared to its polar equivalent (K1 sample) as confirmed by the significantly lower content of all the selected SVOPs found after storage (Figure 26).

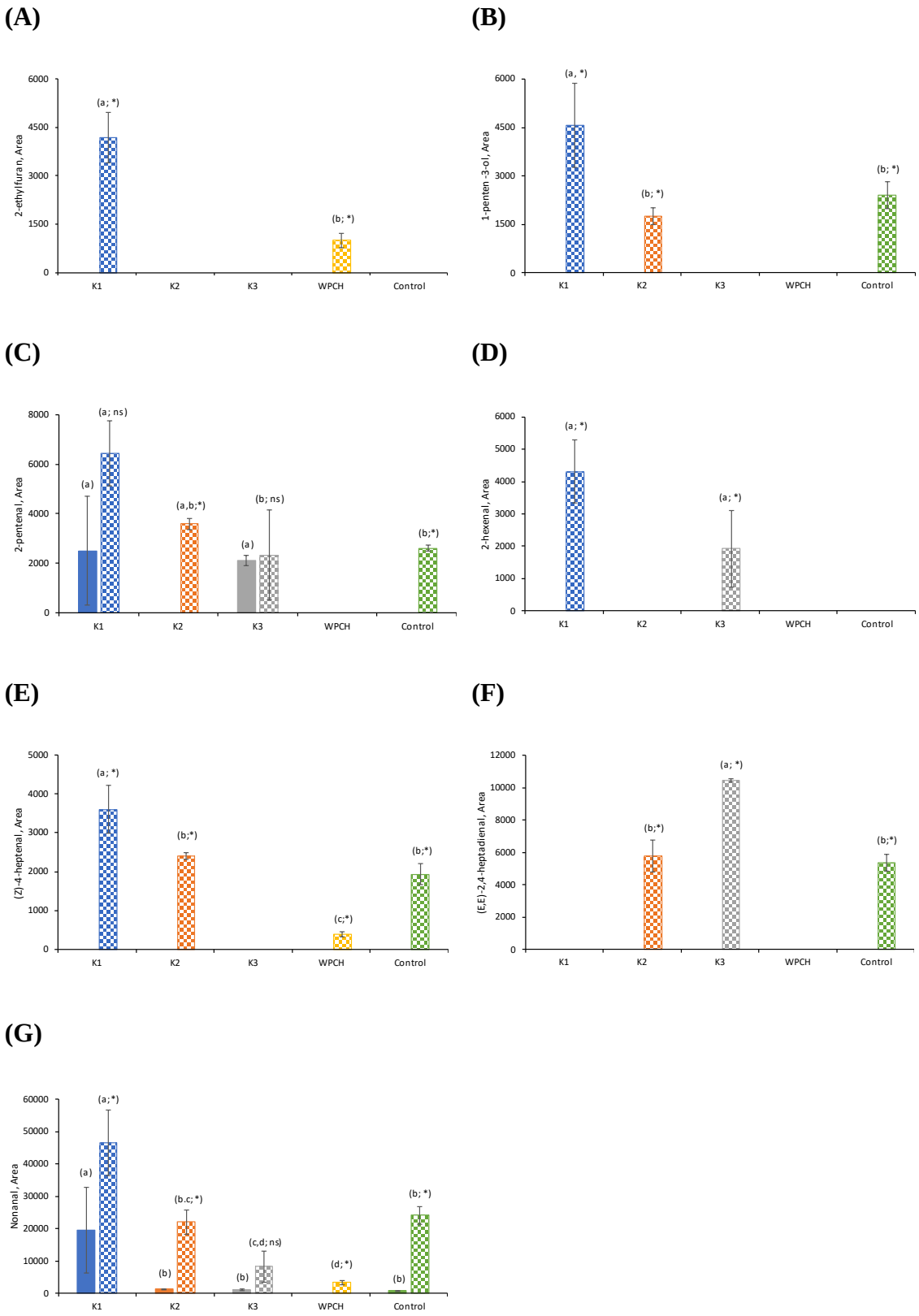

Figure 26. Secondary volatile oxidation products (SVOPs) content of the fish oil-loaded microcapsules after production (filled bars) and after 6 weeks of storage (dashed bars) at ambient temperature (25 ºC). Samples followed by a letter, a-d, indicates statistical differences ($p \leq 0.05$) between microcapsules. Means within the same sample followed by an asterisk (*) indicates statistical differences ($p \leq 0.05$) between week 0 and week 6. Means within the same sample followed by "ns" indicates no statistical differences ($p > 0.05$) between week 0 and week 6.

Interestingly, although additional stabilization with mixed antioxidants (K3 sample) prevented lipid oxidation more efficiently during processing (i.e., lowest initial PV, Figure 25), it did not significantly enhance the oxidative stability of the capsules during storage compared to single addition of the lipid-soluble rosemary extract (K2 sample) (Figure 26). This phenomenon was already observed by other authors who found that the synergistic effects derived from the combination of antioxidants which efficiently stabilized bulk or emulsified oils did not notably improve the oxidative stability of the encapsulated oil due to the different nature of the oil-loaded heterogeneous systems (i.e., wet heterogeneous system or dehydrated heterogeneous system) (Serfert et al., 2009; Velasco et al., 2000). The lower protective effect of the combined antioxidants was attributed to the lower contribution of the hydrosoluble constituents, hindered by their reduced mobility in the dehydrated system compared to the wet system (Serfert et al., 2009; Velasco et al., 2000). Therefore, our results suggest that despite the lipid-soluble nature of K3 antioxidant, the components of the antioxidants mixture partitioned within the capsules based on their polarity (e.g., ascorbic acid and citric acid are polar antioxidants whilst tocopherols are non-polar), resulting in a lower overall protective effect of the encapsulated fish oil.

As for WPCH, which exhibits both antioxidant and emulsifying properties, it was able to reduce lipid oxidation of the encapsulated fish oil as confirmed by the lower amount of the selected SVOPs (e.g., 2-pentenal, nonanal, 1-penten-3-ol) developed after storage compared to the other antioxidant-containing samples (Figure 26). These results contrast with previous studies which reported that amphiphilic antioxidants were less efficient preventing lipid oxidation in oil-loaded encapsulated systems than more non-polar antioxidants (e.g., α-tocopherol vs. ascorbyl palmitate or propyl gallate vs. octyl gallate) (Baik et al., 2004; ten Klooster et al., 2022). For instance, ten Klooster et al. (2022) argued that the preferred partitioning of propyl gallate at the oil/water interface of the spray-dried emulsion was detrimental in terms of its antioxidant activity in the encapsulated system. This was attributed either to: i) a possible glassy state of the interface after drying or to ii) preferential location of the antioxidant within the glassy encapsulating matrix upon drying, both reducing the mobility of the antioxidant towards oxidizing lipids. However, the latter was not observed in the current study. It is well known that the distribution of the antioxidant within wet heterogeneous systems strongly depends on the concentration and type of the emulsifier used in the formulation (Shahidi & Zhong, 2011; Stöckmann et al., 2000). Thus, antioxidant molecules with amphiphilic properties may not locate at the oil/water interface depending

on the nature of the emulsifier used and how much interfacial area is covered. WPCH has been demonstrated to exhibit both high interfacial adsorption and strong interactions WPCH-oil due to its enhanced surface hydrophobicity as a consequence of the higher exposure of non-polar amino acids (Rahmani-Manglano, Jones, et al., 2022; Ruiz-Álvarez et al., 2022). Therefore, co-adsorption of WPCH at the oil/water interface of the wet emulsion stabilized with low concentration of T20 (e.g., 0.35 wt% of T20) cannot be ruled out and, in consequence, its location at the oil/matrix interface of the subsequently dehydrated system. Furthermore, based on its amino acid profile, WPCH has been proved to exhibit high antioxidant activity showing combined mechanisms of action as metal chelator and radical scavenger in its polar part (i.e., by action of His and Tyr) and reducing power and radical scavenger in its non-polar part (i.e., by action of Met) (Elias et al., 2008; Padial-Domínguez et al., 2020; Rahmani-Manglano et al., 2020). Thus, contrary to propyl gallate which shows radical scavenging activity only by its polar head (i.e., phenolic group) (Garrido et al., 2012), WPCH is capable to: i) scavenge free radicals in the oil phase of the dried system and ii) to inhibit lipid oxidation through different antioxidant paths when located at the oil/matrix interface. It should be borne in mind that the commercial fish oil used in the current study already had a high concentration of non-polar antioxidants (i.e., tocopherols) contrary to the aforementioned study, which used striped sunflower oil (ten Klooster et al., 2022). Thus, the antioxidant activity of WPCH used as amphiphilic antioxidant in this work was combined with the antioxidant activity of the tocopherols already present in the fish oil. This could further explain the differences observed between the two studies together with the enhanced oxidative stability observed for the WPCH-containing samples in the current study.

4. CONCLUSION

The influence of the polarity of natural antioxidants on the oxidative stability of spray-dried fish oil-loaded capsules was investigated. All the capsules obtained had similar morphology, size and encapsulation efficiency (EE > 91%), meaning that the physicochemical properties of the encapsulated systems were not influenced by the antioxidant used in the formulation. However, the polar rosemary extract studied was less effective preventing lipid oxidation during processing and later storage of the capsules compared to the non-polar rosemary extracts and WPCH (i.e., an amphiphilic antioxidant). This was attributed to the preferred partitioning of the polar rosemary extract within the aqueous phase of the wet emulsion, far from where lipid oxidation is initiated, and subsequently within the glassy matrix of the dried

capsules, where the mobility of the antioxidant is significantly reduced. Interestingly, additional chemical stabilization in the presence of mixed antioxidants (i.e., rosemary extract, mixed tocopherols, ascorbic acid, citric acid and lecithin) with different mechanism of action did not significantly reduce lipid oxidation during storage compared to the capsules containing the lipid-soluble rosemary extract alone. The latter was discussed on the basis of the partition of the different mixed antioxidants within the dried capsules based on their polarity (e.g., polar components trapped within the glassy matrix) resulting in a reduced combinatory effect. Nonetheless, WPCH exhibiting high surface-active properties and combined antioxidant mechanisms of action in their polar (i.e., metal chelating and radical scavenging activity) and non-polar part (e.g., radical scavenging activity and reducing power), significantly enhanced the oxidative stability of the encapsulated commercial fish oil containing tocopherols.

5. REFERENCES

Anwar, F., & Qadir, R. (2021). Carnosic acid and carnosol. In *A Centum of Valuable Plant Bioactives* (pp. 261–274). Elsevier. https://doi.org/10.1016/B978-0-12-822923-1.00012-1

Arab-Tehrany, E., Jacquot, M., Gaiani, C., Imran, M., Desobry, S., & Linder, M. (2012). Beneficial effects and oxidative stability of omega-3 long-chain polyunsaturated fatty acids. *Trends in Food Science and Technology*, *25*(1), 24–33. https://doi.org/10.1016/j.tifs.2011.12.002

Aslam, A., & Schroën, K. (2023). Lipid oxidation in food emulsions: a review dedicated to the role of the interfacial area. *Current Opinion in Food Science*, *51*, 101009. https://doi.org/10.1016/j.cofs.2023.101009

Baik, M. Y., Suhendro, E. L., Nawar, W. W., McClements, D. J., Decker, E. A., & Chinachoti, P. (2004). Effects of antioxidants and humidity on the oxidative stability of microencapsulated fish oil. *JAOCS, Journal of the American Oil Chemists' Society*, *81*(4), 355–360. https://doi.org/10.1007/s11746-004-0906-7

Barden, L., & Decker, E. A. (2013). Lipid oxidation in low-moisture food: A review. In *Critical Reviews in Food Science and Nutrition* (Vol. 56, Issue 15, pp. 2467–2482). Taylor and Francis Inc. https://doi.org/10.1080/10408398.2013.848833

Berton-Carabin, C. C., Ropers, M. H., & Genot, C. (2014). Lipid Oxidation in Oil-in-Water Emulsions: Involvement of the Interfacial Layer. *Comprehensive Reviews in Food Science and Food Safety*, *13*(5), 945–977. https://doi.org/10.1111/1541-4337.12097

Drusch, S., Serfert, Y., Berger, A., Shaikh, M. Q., Rätzke, K., Zaporojtchenko, V., & Schwarz, K. (2012). New insights into the microencapsulation properties of sodium caseinate and hydrolyzed casein. *Food Hydrocolloids*, *27*(2), 332–338. https://doi.org/10.1016/j.foodhyd.2011.10.001

Drusch, S., Serfert, Y., Scampicchio, M., Schmidt-Hansberg, B., & Schwarz, K. (2007). Impact of physicochemical characteristics on the oxidative stability of fish oil microencapsulated by spray-drying. *Journal of Agricultural and Food Chemistry*, *55*(26), 11044–11051. https://doi.org/10.1021/jf072536a

Elias, R. J., Kellerby, S. S., & Decker, E. A. (2008). Antioxidant activity of proteins and peptides. *Critical Reviews in Food Science and Nutrition*, *48*(5), 430–441. https://doi.org/10.1080/10408390701425615

Encina, C., Vergara, C., Giménez, B., Oyarzún-Ampuero, F., & Robert, P. (2016). Conventional spray-drying and future trends for the microencapsulation of fish oil. *Trends in Food Science and Technology*, *56*, 46–60. https://doi.org/10.1016/j.tifs.2016.07.014

García-Moreno, P. J., Damberg, C., Chronakis, I. S., & Jacobsen, C. (2017). Oxidative stability of pullulan electrospun fibers containing fish oil: Effect of oil content and natural antioxidants addition. *European Journal of Lipid Science and Technology*, *119*(12). https://doi.org/10.1002/ejlt.201600305

Garrido, J., Garrido, E. M., & Borges, F. (2012). Studies on the food additive propyl gallate: Synthesis, structural characterization, and evaluation of the antioxidant activity. *Journal of Chemical Education*, *89*(1), 130–133. https://doi.org/10.1021/ed900025s

Hernández Sánchez, M. del R., Cuvelier, M. E., & Turchiuli, C. (2016). Effect of α-tocopherol on oxidative stability of oil during spray drying and storage of dried emulsions. *Food Research International*, *88*, 32–41. https://doi.org/10.1016/j.foodres.2016.04.035

Hogan, S. A., O'Riordan, E. D., & O'Sullivan, M. (2003). Microencapsulation and oxidative stability of spray-dried fish oil emulsions. *Journal of Microencapsulation*, *20*(5), 675–688. https://doi.org/10.1080/0265204031000151974

Hopia, A. I., Huang, S.-W., Schwarz, K., German, J. B., & Frankel, E. N. (1996). *Effect of Different Lipid Systems on Antioxidant Activity of Rosemary Constituents Carnosol and Carnosic Acid with and without r-Tocopherol*. https://pubs.acs.org/sharingguidelines

Hrebień-Filisińska, A. (2021). Application of natural antioxidants in the oxidative stabilization of fish oils: A mini-review. *Journal of Food Processing and Preservation*, *45*(4), 1–12. https://doi.org/10.1111/jfpp.15342

Johnson, D. R., & Decker, E. A. (2015). The role of oxygen in lipid oxidation reactions: A review. *Annual Review of Food Science and Technology*, *6*, 171–190. https://doi.org/10.1146/annurev-food-022814-015532

Laguerre, M., Bayrasy, C., Panya, A., Weiss, J., McClements, D. J., Lecomte, J., Decker, E. A., & Villeneuve, P. (2015). What Makes Good Antioxidants in Lipid-Based Systems? The Next Theories Beyond the Polar Paradox. *Critical Reviews in Food Science and Nutrition*, *55*(2), 183–201. https://doi.org/10.1080/10408398.2011.650335

Padial-Domínguez, M., Espejo-Carpio, F. J., García-Moreno, P. J., Jacobsen, C., & Guadix, E. M. (2020). Protein derived emulsifiers with antioxidant activity for stabilization of omega-3 emulsions. *Food Chemistry*, *329*(127148). https://doi.org/10.1016/j.foodchem.2020.127148

Patel, A., Desai, S. S., Mane, V. K., Enman, J., Rova, U., Christakopoulos, P., & Matsakas, L. (2022). Futuristic food fortification with a balanced ratio of dietary ω-3/ω-6 omega fatty acids for the prevention of lifestyle diseases. In *Trends in Food Science and Technology* (Vol. 120, pp. 140–153). Elsevier Ltd. https://doi.org/10.1016/j.tifs.2022.01.006

Polavarapu, S., Oliver, C. M., Ajlouni, S., & Augustin, M. A. (2011). Physicochemical characterisation and oxidative stability of fish oil and fish oil-extra virgin olive oil microencapsulated by sugar beet pectin. *Food Chemistry*, *127*(4), 1694–1705. https://doi.org/10.1016/j.foodchem.2011.02.044

Rahmani-Manglano, N. E., González-Sánchez, I., García-Moreno, P. J., Espejo-Carpio, F. J., Jacobsen, C., & Guadix, E. M. (2020). Development of fish oil-loaded microcapsules containing whey protein hydrolysate as film-forming material for fortification of low-fat mayonnaise. *Foods*, *9*(5). https://doi.org/10.3390/foods9050545

Rahmani-Manglano, N. E., Jones, N. C., Hoffmann, S. V., Guadix, E. M., Pérez-Gálvez, R., Guadix, A., & García-Moreno, P. J. (2022). Structure of whey protein hydrolysate used as emulsifier in wet and dried oil delivery systems: Effect of pH and drying processing. *Food Chemistry*, *390*, 133169. https://doi.org/10.1016/j.foodchem.2022.133169

Rahmani-Manglano, N. E., Tirado-Delgado, M., García-Moreno, P. J., Guadix, A., & Guadix, E. M. (2022). Influence of emulsifier type and encapsulating agent on the in vitro digestion of fish oil-loaded microcapsules produced by spray-drying. *Food Chemistry*, *392*, 133257. https://doi.org/10.1016/j.foodchem.2022.133257

Ruiz-Álvarez, J. M., del Castillo-Santaella, T., Maldonado-Valderrama, J., Guadix, A., Guadix, E. M., & García-Moreno, P. J. (2022). pH influences the interfacial properties of blue whiting (M. poutassou) and whey protein hydrolysates determining the physical stability of fish oil-in-water emulsions. *Food Hydrocolloids*, *122*(107075). https://doi.org/10.1016/j.foodhyd.2021.107075

Santos, D., Maurício, A. C., Sencadas, V., Santos, J. D., Fernandes, M. H., & Gomes, P. S. (2018). Spray Drying: An Overview. *Biomaterials - Physics and Chemistry - New Edition*. https://doi.org/10.5772/intechopen.72247

Serfert, Y., Drusch, S., & Schwarz, K. (2009). Chemical stabilisation of oils rich in long-chain polyunsaturated fatty acids during homogenisation, microencapsulation and storage. *Food Chemistry*, *113*(4), 1106–1112. https://doi.org/10.1016/j.foodchem.2008.08.079

Shahidi, F., & Zhong, Y. (2011). Revisiting the polar paradox theory: A critical overview. *Journal of Agricultural and Food Chemistry*, *59*(8), 3499–3504. https://doi.org/10.1021/jf104750m

Sørensen, A.-D. M., García-Moreno, P. J., Yesiltas, B., & Jacobsen, C. (2021). Introduction to delivery systems and stability issues. In *Omega-3 Delivery Systems* (pp. 107–117). Elsevier. https://doi.org/10.1016/b978-0-12-821391-9.00015-6

Stöckmann, H., Schwarz, K., & Huynh-Ba, T. (2000). The Influence of Various Emulsifiers on the Partitioningand Antioxidant Activity of Hydroxybenzoic Acidsand Their Derivatives in Oil-in-Water Emulsions. *AOCS Press*, *77*(5), 535–542. https://doi.org/http://dx.doi.org/10.1007/s11746-000-0085-6

Taboada, M. L., Heiden-Hecht, T., Brückner-Gühmann, M., Karbstein, H. P., Drusch, S., & Gaukel, V. (2021). Spray drying of emulsions: Influence of the emulsifier system on changes in oil droplet size during the drying step. *Journal of Food Processing and Preservation*, *45*(9), 1–11. https://doi.org/10.1111/jfpp.15753

Tamm, F., Gies, K., Diekmann, S., Serfert, Y., Strunskus, T., Brodkorb, A., & Drusch, S. (2015). Whey protein hydrolysates reduce autoxidation in microencapsulated long chain polyunsaturated fatty acids. *European Journal of Lipid Science and Technology*, *117*(12), 1960–1970. https://doi.org/10.1002/ejlt.201400574

ten Klooster, S., Villeneuve, P., Bourlieu-Lacanal, C., Durand, E., Schroën, K., & Berton-Carabin, C. (2022). Alkyl chain length modulates antioxidant activity of gallic acid esters in spray-dried emulsions. *Food Chemistry*, *387*. https://doi.org/10.1016/j.foodchem.2022.132880

Thomsen, B. R., Yesiltas, B., Sørensen, A. -. M., Hermund, D. B., Glastrup, J., & Jacobsen, C. (2016). Comparison of three methods for extraction of volatile lipid oxidation products from food matrices for GC–MS analysis. *JAOCS, Journal of the American Oil Chemists' Society*, 93(7), 929-942. doi:10.1007/s11746-016-2837-2

Velasco, J., Dobarganes, C., & Márquez-Ruiz, G. (2003). Variables affecting lipid oxidation in dried microencapsulated oils. *Grasas y Aceites*, *54*(3), 304–314.

Velasco, J., Dobarganes, M. C., & Márquez-Ruiz, G. (2000). Application of the accelerated test Rancimat to evaluate oxidative stability of dried microencapsulated oils. *Grasas y Aceites*, *51*(4), 261–267. https://doi.org/https://doi.org/10.3989/gya.2000.v51.i4.422

Velasco, J., Holgado, F., Dobarganes, C., & Márquez-Ruiz, G. (2009). Antioxidant activity of added phenolic compounds in freeze-dried microencapsulated sunflower oil. *JAOCS, Journal of the American Oil Chemists' Society*, *86*(5), 445–452. https://doi.org/10.1007/s11746-009-1365-8

6. SUPPLEMENTARY MATERIAL

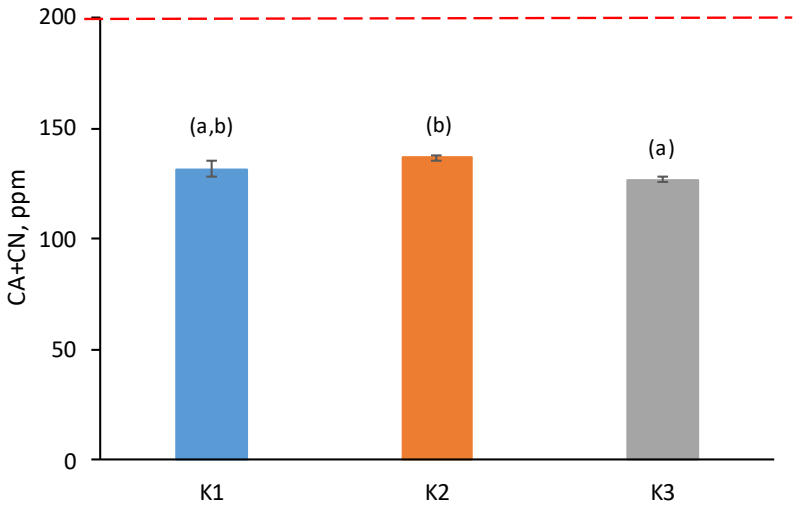

Figure S 4. Content of Carnosic acid (CA) and Carnosol (CN) present in the spray-dried capsules after processing with respect to the initial concentration added to the formulation. Samples followed by a letter, a-b, indicates statistical differences ($p \leq 0.05$) between microcapsules.

IV. Oxidative stability and oxygen permeability of fish oil-loaded capsules produced by spray-drying or electrospraying measured by Electron Spin Resonance*

The oxidative stability and the oxygen permeability of fish oil-loaded capsules were investigated by Electron Spin Resonance (ESR). The capsules were produced by spray-drying or electrospraying in the monoaxial or coaxial configuration using glucose syrup as the encapsulating agent. ESR-spin trapping results showed that electrosprayed capsules oxidized faster and during the early stages of incubation, irrespective of the emitter configuration (monoaxial or coaxial), when compared to those produced by spray-drying. Furthermore, ESR oximetry showed that oxygen inside the spray-dried capsules reached equilibrium with the surrounding atmosphere significantly slower than the monoaxially electrosprayed capsules (i.e., ~2h and ~10min, respectively). These findings have been attributed to the larger particle size of the spray-dried capsules influencing the oxygen diffusion area (i.e., lower surface-to-volume ratio) and diffusion path (i.e., thicker encapsulating wall for a fixed oil load). Together, the lower oxygen uptake reported for the spray-dried capsules correlated well with their higher oxidative stability.

* MANUSCRIPT SUBMITTED FOR PUBLICATION: N.E. Rahmani-Manglano, M.L. Andersen, E.M. Guadix, P.J. García-Moreno. (2023). Oxidative stability and oxygen permeability of fish oil-loaded capsules produced by spray-drying or electrospraying measured by Electron Spin Resonance.

1. INTRODUCTION

As a result of the health benefits related to the intake of omega-3 polyunsaturated fatty acids (omega-3 PUFAs), especially EPA and DHA, the enrichment of common food products with oils rich in these bioactives (e.g., fish oil) has gained great interest (Patel et al., 2022). However, stabilization techniques are required since these compounds are very prone to lipid oxidation, which may comprise the nutritional and organoleptic properties of the fortified food product. In this regard, the development of dry omega-3 delivery systems through encapsulation techniques has been a promising approach for the incorporation of these sensitive bioactive compounds into complex food matrices (Ghelichi et al., 2021).

By encapsulation, the oil is trapped within a (bio)polymer-based encapsulating wall which acts as a physical barrier between the bioactives and the environment, mainly aimed to prevent their degradation. However, lipid oxidation of the encapsulated oil still occurs. Prooxidant species, especially oxygen, have been demonstrated to penetrate trough the glassy encapsulating matrix, thus triggering lipid oxidation of the encapsulated oil droplets (A. B. Andersen et al., 2000; Boerekamp et al., 2019; Drusch et al., 2009; Orlien et al., 2000). Indeed, it has been reported that the oxidation rate of the non-continuous lipid phase embedded in a heterogeneous matrix (e.g., oil-loaded capsules) is affected by the physicochemical properties of the capsules (e.g., particle size), which influences the prooxidant species (e.g., oxygen) reaching the encapsulated oil droplets (Velasco et al., 2003, 2006).

Spray-drying of fish oil-in-water emulsions has been extensively used in the production of dry encapsulates using food-grade (bio)polymers (e.g., carbohydrates) as encapsulating agents (Singh et al., 2022). Moreover, the performance of spray-dried omega-3 delivery systems has been evaluated in a wide range of food products (e.g., dressings, baked products or meat products) (Ghelichi et al., 2021). However, initial lipid oxidation is susceptible to occur during emulsification (e.g., air/oxygen inclusion and distribution) and subsequent spray-drying by using inlet air at high temperature (e.g., 160-200 °C) (Serfert et al., 2009). Therefore, in the last decades, significant progress has been made in the development of non-thermal encapsulation techniques such as electrospraying to produce dry omega-3 delivery systems. By conventional electrospraying, the fish oil-loaded emulsion/dispersion is dried by means of the high-electrostatic field applied, which produces a spray of highly charged

droplets allowing solvent evaporation at room temperature (Gómez-Mascaraque & López-Rubio, 2016). Furthermore, in the coaxial configuration, fish oil-loaded capsules can be produced without first emulsifying or dispersing the oil within the (bio)polymer-based encapsulating solution since two immiscible solutions can be simultaneously electrosprayed (Rahmani-Manglano et al., 2023). Thus, by electrospraying technology, initial lipid oxidation due to processing could be significantly reduced or even theoretically avoided, depending on the emitter configuration (e.g., monoaxial or coaxial configuration). Moreover, as a result of electrohydrodynamic atomization, smaller dry particles are produced compared to spray-drying, and the particle size distribution is also narrower (García-Moreno et al., 2021). This is desirable when it comes to food fortification since smaller capsules are easier to disperse in the food matrix and the structure of the original foodstuff is expected to be less modified. Nonetheless, it should be born in mind that an increased specific surface area of the electrosprayed encapsulates might result in a lower oxidative stability of the system due to a higher contact area with prooxidants species (e.g., oxygen).

In a recent study, we investigated the oxidative stability of fish oil-loaded capsules produced by spray-drying or electrospraying in the monoaxial and the coaxial configuration (Rahmani-Manglano et al., 2023). Interestingly, our results suggested that the physicochemical properties of the encapsulated systems (e.g., particle size or thickness of the encapsulating wall) played a major role on lipid oxidation. This might be attributed to its effect on oxygen permeability, which was not investigated.

Electron spin resonance (ESR) has been proven to be a useful technique to measure oxygen concentrations in food systems (ESR-based oximetry) (Zhou et al., 2011). This technique is based on the broadening of the ESR spectra of stable radicals (i.e., paramagnetic spin probes) in the presence of other paramagnetic molecule such as oxygen. The interaction between the spin probe and oxygen produces a spin exchange between these two compounds (e.g., Heisenberg spin exchange) resulting in the line broadening of the ESR spectra, which is proportional to the concentration of oxygen (M. L. Andersen, 2021). This technique has been previously used to evaluate the oxygen-barrier properties of oil-loaded encapsulated systems produced by different technologies (e.g., freeze-drying or electrospraying) (A. B. Andersen et al., 2000; Boerekamp et al., 2019; Svagan et al., 2016). Furthermore, the ESR technique has been also extensively used to monitor the early stages of lipid oxidation (ESR-spin trapping) of bulk, emulsified or encapsulated oils (M. L. Andersen, 2021). ESR-spin trapping

relies in the formation of stable radicals (spin adducts) due to the reaction of free radicals and a diamagnetic molecular spin trap (usually nitrones or nitroso compounds), which allows the indirect measurement of the highly reactive intermediate lipid-derived radicals (e.g., alkyl radicals) (M. L. Andersen, 2021; Velasco et al., 2021).

Therefore, this study aimed at investigating the oxygen permeability fish oil-loaded capsules produced by spray-drying or electrospraying by using ESR-oximetry. Furthermore, the oxidative stability of the capsules was also studied by ESR-spin trapping during 25 days of storage at ambient temperature. To our knowledge, this is the first study comparing the oxidative stability and the oxygen permeability of fish oil-loaded capsules produced by spray-drying and electrospraying measured by ESR. The results obtained from this work advance our understanding on the relation of lipid oxidation in encapsulated systems and their physicochemical properties influencing oxygen diffusivity through the encapsulating wall.

2. MATERIALS AND METHODS

2.1 Materials

Fish oil (Omega Oil 1812 TG Gold) was purchased from BASF Personal Care and Nutrition GmbH (Illertissen, Germany) and stored at -80 °C until use. MCT oil (WITARIX® MCT 60/40) was kindly donated by IOI OLEO GmBH (Hamburg, Deutschland) and stored at -20 °C until use. Glucose syrup (GS; DE38, C*Dry 1934) was purchased from Cargill Germany GmbH (Krefeld, Germany) and Pullulan was kindly donated by Hayashibara Co., Ltd. (Okayama, Japan). Tween 20 (T20) was obtained from Sigma-Aldrich (Darmstadt, Germany) and CITREM (GRINDSTED® CITREM LR 10 EXTRA MT) was provided by Danisco (Copenhagen, Denmark). Whey protein concentrate hydrolysate (WPCH) was produced by enzymatic hydrolysis (degree of hydrolysis, DH of 10%) with Alcalase 2.4L (Novozymes, Denmark) (Rahmani-Manglano et al., 2020). The hydrolysate was then freeze-dried and stored at 4 ºC until use. ESR spin probe (16-DOXYL-stearic acid, DSA) and spin trap (α-Phenyl-N-tert-butylnitrone, PBN) were purchased from Sigma Aldrich (Søborg, Denmark). Oxygen (≥99.5%) and nitrogen (≥99.999%) gases were supplied by Air Liquide (Taastrup, Denmark). The rest of the reagents used for analysis were of analytical grade.

2.2 Preparation of the ESR spin probe and spin trap

The ESR spin trap (PBN) and spin probe (DSA) were prepared and added to the lipid phase (fish oil and MCT oil, respectively), as described by Boerekamp et al. (Boerekamp et al., 2019). In brief, to investigate the oxidative stability of the encapsulated systems, PBN was added to the fish oil as an ethanol solution (50 mg/mL) in order to have a final concentration of 30 mM of PBN in the lipid phase. For the oxygen permeability measurements, DSA was added to the MCT oil as a hexadecane solution (25 mg/mL) in order to have a final concentration of 10 μM of DSA in the lipid phase.

2.3 Production of the spray-dried capsules

The oil-in-water emulsions were prepared by dispersing the lipid phase (MCT oil or fish oil, 5 wt%) in the aqueous phase containing the encapsulating agent (GS, 28 wt%) and the emulsifier (WPCH, 6 wt%). The protein/oil ratio was fixed at 0.4. First, a coarse emulsion was produced using an Ultraturrax T-25 homogenizer (IKA, Staufen, Germany) mixing at 15,000 rpm. The total mixing time was 2 min and the fish oil was added during the first minute. Then, the pre-emulsion was homogenized in a high-pressure homogenizer (PandaPLUS 2000; GEA Niro Soavi, Lübeck, Germany) at a pressure range of 450/75 bar and applying 3 passes. Right after production, the emulsions were spray-dried in a laboratory scale spray-drier (Büchi B-190; Büchi Labortechnik, Flawill, Switzerland) at 180/90 °C inlet/outlet temperature, respectively. The drying air flow was fixed to 25 Nm3/h. The oil load of the resulting encapsulates was of ~13 wt%. The capsules were stored in airtight flasks, at −80 °C in the dark until further analysis.

2.4 Production of the electrosprayed capsules

2.4.1 Monoaxially electrosprayed capsules

To produce the oil-in-water emulsions, a mixture of CITREM (1 wt%):oil (MCT oil or fish oil, 3.7 wt%) was dispersed in the aqueous phase as described in Section 2.2. The aqueous phase consisted of WPCH (4.3 wt%), P (3.0 wt%) and the encapsulating agent (GS, 15 wt%), which were previously dissolved in distilled water and stirred overnight (500 rpm) at ambient temperature. The resulting oil-in-water emulsions also had a protein/oil ratio of 0.4. Immediately after production, the emulsions were electrosprayed in the equipment described in our previous study (Rahmani-Manglano et al., 2023) consisting of a drying chamber

equipped with a variable high-voltage power supply, a syringe pump, and a stainless-steel collector plate (SpinBox Electrospinning; Bioinicia, Valencia, Spain). The flow rate was fixed to 0.2 mL/h and the voltage applied varied from 18.5 to 20 kV. The electrospraying process was carried out at ambient temperature and ambient relative humidity (19-23 °C, 22-50 % RH) in batches of 30 min. Between batches, the remaining emulsions were gently stirred (100 rpm) to minimize physical destabilization. The powder collected from the different batches was gently mixed to ensure that analyzed samples were homogeneous and representative of the obtained material. The final oil load of the capsules was ~13 wt%. The capsules were stored in airtight flasks, at −80 °C in the dark until further analysis.

2.4.2 Coaxially electrosprayed capsules

For coaxial electrospraying, the biopolymer solution (flowing through the outer capillary) was produced by dissolving the encapsulating agent (GS, 15 wt%), P (4 wt%) and T20 (1 wt%) in distilled water and stirring overnight (500 rpm). Afterwards, the solution was passed through a high-pressure homogenizer (450/75 bar, 3 passes) prior to electrospraying. MCT oil or fish oil were infused as the core solutions (flowing through the inner capillary). The electrospraying process was carried out in the setup described in Section 2.4.1, equipped with coaxial emitter consisting of two concentric needles. Thus, two syringe pumps which worked simultaneously were used. The outer flow rate (F1) was fixed to 0.60 mL/h and the inner flow rate (F2) was adjusted to achieve a final oil load of the capsules of ~13 wt% (F2 = 0.021 mL/h). The voltage was varied from 16 to 18 kV. The process was conducted at ambient temperature and ambient relative humidity (19-23 °C, 22-50 % RH) in batches of 60 min. The powder collected from the different batches were gently mixed before sampling to ensure that analyzed samples were homogeneous and representative of the obtained material. The capsules were stored in airtight flasks, at −80 °C in the dark until further analysis.

2.5 Characterization of the capsules

2.5.1 Morphology and particle size distribution

The morphology of the capsules was investigated by scanning electron microscopy (SEM) using a FESEM microscope (LEO 1500 GEMINI, Zeiss, Germany). The samples were placed on carbon tape and carbon-coated as described in our previous work (Rahmani-Manglano et al., 2023). The SEM images were acquired in the range 500X – 15KX

magnification with a 5-kV accelerating voltage. The particle size distributions and mean diameters were determined measuring 160 randomly-selected capsules using the ImageJ software (National Institute of Health).

2.6 ESR measurements

The ESR spectra of the encapsulated systems containing the spin trap (PBN) or the spin probe (DSA) were recorded using a MiniScope MS5000 (Bruker, Rheinstetten, Germany) at ambient temperature. The modulation amplitude used in all ESR measurements was kept constant in each determination at 0.2 mT.

2.6.1 Oxidative stability

To evaluate the oxidative stability of the capsules, the ESR tubes (5 mm OD) were filled with powder to obtain a sample height of ~3.5 cm in order to ensure that the resonant cavity of the equipment was covered with sample (Velasco et al., 2021). Thus, the volume of capsules was kept constant for the analyses. Three tubes were prepared per sample and subsequently stored at 25 °C in the dark for 25 days. The PBN-ESR spectra were recorded every day to monitor the changes in the peak-to-peak height of the central line of the spectra. For comparative purposes among capsules, the peak-to-peak amplitude measured for each sample was divided by the density of each capsule type (mg sample/cm tube). Thus, normalized values for peak-to-peak amplitude were obtained. The average value of the normalized peak-to-peak height of every sample was calculated.

2.6.2 Oxygen permeability

The oxygen permeability of the capsules was determined as described by Boerekamp et al. (Boerekamp et al., 2019). In brief, 200 mg of capsules were placed in quartz ERS tubes which were closed at one end with glass wool. Afterwards, the capsules were washed with heptane (10 mL) to remove the non-encapsulated surface oil fraction. For the measurements, first nitrogen (59.50 mL/min) was passed through the sample-containing tubes for 60 min to displace oxygen. Then, oxygen (50.49 mL/h) was passed through the tubes until the nitrogen atmosphere was completely replaced. By last, nitrogen (59.50 mL/min) was passed again trough the tubes for 60 min. During the analysis, the narrowing (when nitrogen was passed through the tubes) and the broadening (when oxygen was passed through the tubes) of the ESR signal of DSA was quantified as the width of the central line of the spectra, ΔHpp (Boerekamp et al., 2019; Svagan et al., 2016).

In addition, a calibration curve (R2 = 0.98) was constructed to relate the line broadening of the DSA-ESR spectra (ΔHpp) with the concentration of oxygen (Boerekamp et al., 2019). A piece of filter paper was soaked in the MCT oil containing the DSA probe (prepared as described in Section 2.2) and placed in the ESR quartz tube. First, a nitrogen atmosphere was created by passing nitrogen through the filter-containing tube for 15 min. Then, the filter paper was exposed to different oxygen/nitrogen gas compositions and the ΔHpp was quantified to construct the calibration curve. Each point of the calibration curve was measured in triplicate.

2.7 Statistical analysis

Data were subjected to one-way analysis of variance (ANOVA) by using Statgraphics version 5.1 (Statistical Graphics Corp., Rockville, MD, USA). Tukey´s HSD multiple range test was used at 95% confidence level ($p < 0.05$) to determine significant differences between mean values.

3. RESULTS AND DISCUSSION

3.1 Characterization of the capsules

3.1.1 Morphology and particle size distribution

Depending on the technology used (e.g., spray-drying or monoaxial/coaxial electrospraying), significant differences were observed on the morphology (Figure 27) and particle size distribution (Figure 28) of the encapsulated systems. Whilst spherical particles were obtained by spray-drying (Figure 27A,B), fibrils interconnecting the capsules were observed for the electrosprayed systems, irrespective of the emitter configuration (e.g., monoaxial or coaxial; Figure 27C,D or Figure 27E,F, respectively). This is ascribed to the presence of pullulan as thickening agent in the formulation of the electrosprayed capsules (GS-mo and GS-HPH-co samples) which, due to its great spinnability in water-based solutions, leads to the formation of thin fibrils even at low concentrations (e.g., <5 wt% pullulan) (García-Moreno et al., 2018; Rahmani-Manglano et al., 2023). Nonetheless, as reported in our previous work, the electrosprayed capsules had the appearance of flowing powder once the samples were detached from the collector (Rahmani-Manglano et al., 2023).

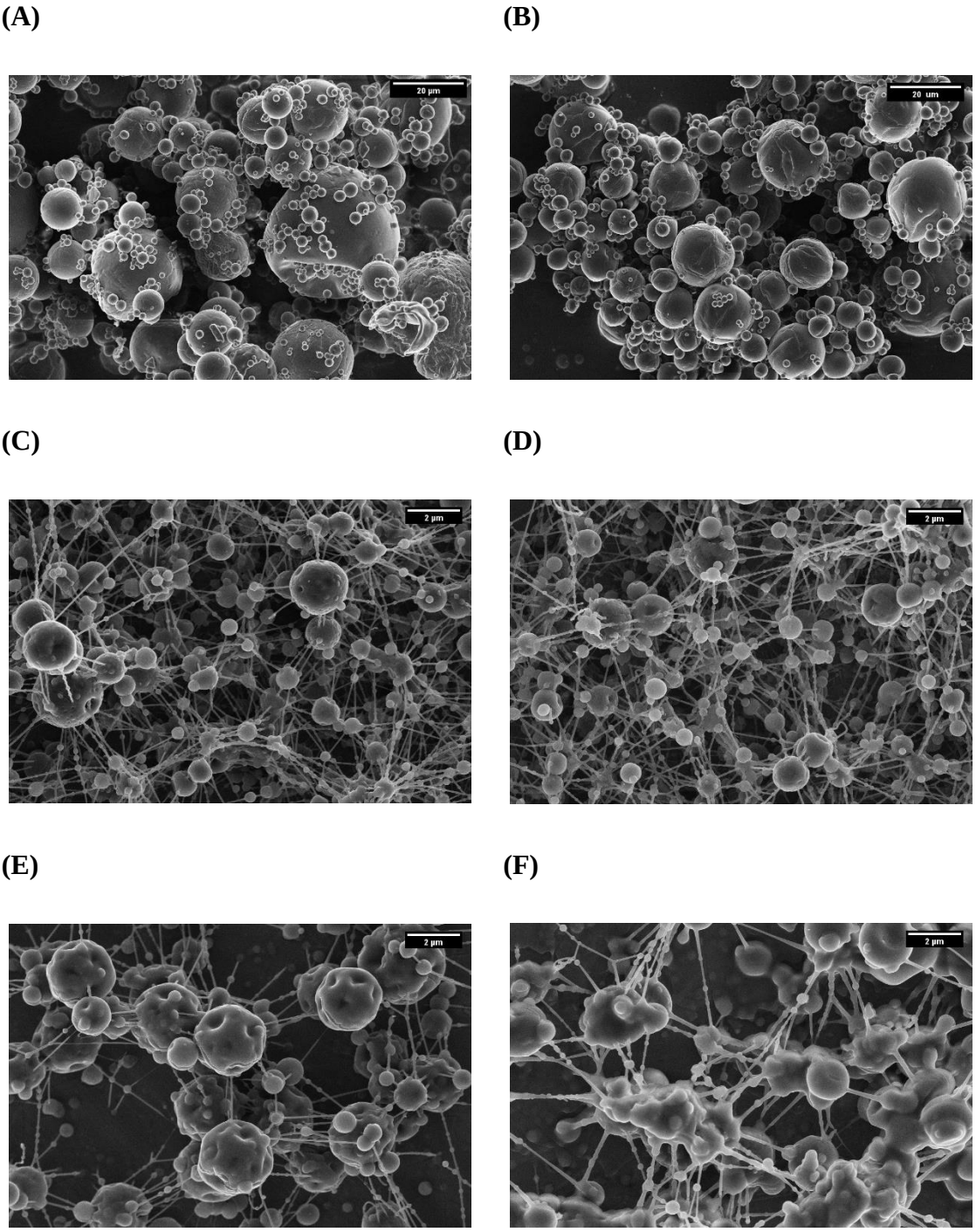

Figure 27. SEM images of the oil-loaded capsules produced by: spray-drying (fish oil, A; MCT oil, B), monoaxial electrospraying (fish oil, C; MCT oil, D) and coaxial electrospraying (fish oil, E; MCT oil, F).

Emulsion-based methods let to capsules with mostly smooth surfaces and the morphology of the particles was similar irrespective of the encapsulated oil (e.g., fish oil or MCT oil) (Figure 27A-D). Conversely, in line with our previous observations (Rahmani-Manglano et al., 2023), coaxial electrospraying resulted in dented particles when fish oil was infused as the core solution (Figure 27E). However, agglomerated capsules were observed when the

core solution consisted of MCT oil (Figure 27F). This could be explained due to the different polarities of the encapsulated oils (e.g., fish oil or MCT oil). MCT oil is more polar than fish oil (Chen et al., 2023) thus, in the absence of emulsifiers in the shell solution together with the lack of surface-active properties of the encapsulating agent (e.g., GS), a portion of the infused oil might have solubilized in the water-based encapsulating solution during processing giving rise to the agglomerated-like morphology of the resulting particles.

Figure 28 shows the particle size distribution of the fish oil-loaded systems. Spray-drying resulted in significantly larger capsules and a wider particle size distribution ($p > 0.05$; Figure 28A), compared to electrospraying (monoaxial or coaxial) (Figure 28B). In turn, monoaxially electrosprayed capsules were smaller (~90% of the capsules < 1.5μm) than coaxially electrosprayed systems (~25% of the capsules < 1.5μm) due to the difference in the operating conditions (e.g., higher infusing flow rate for coaxial electrospraying) (Rahmani-Manglano et al., 2023). The particle size of oil-loaded encapsulated systems is an important factor influencing their oxidative stability since, for a fixed oil load, a reduced particle size implies an increased specific surface area (e.g., higher area of contact with prooxidant species) and thinner encapsulating walls (e.g., reduced prooxidants diffusion path to the core of the capsules) (Linke, Hinrichs, et al., 2020).

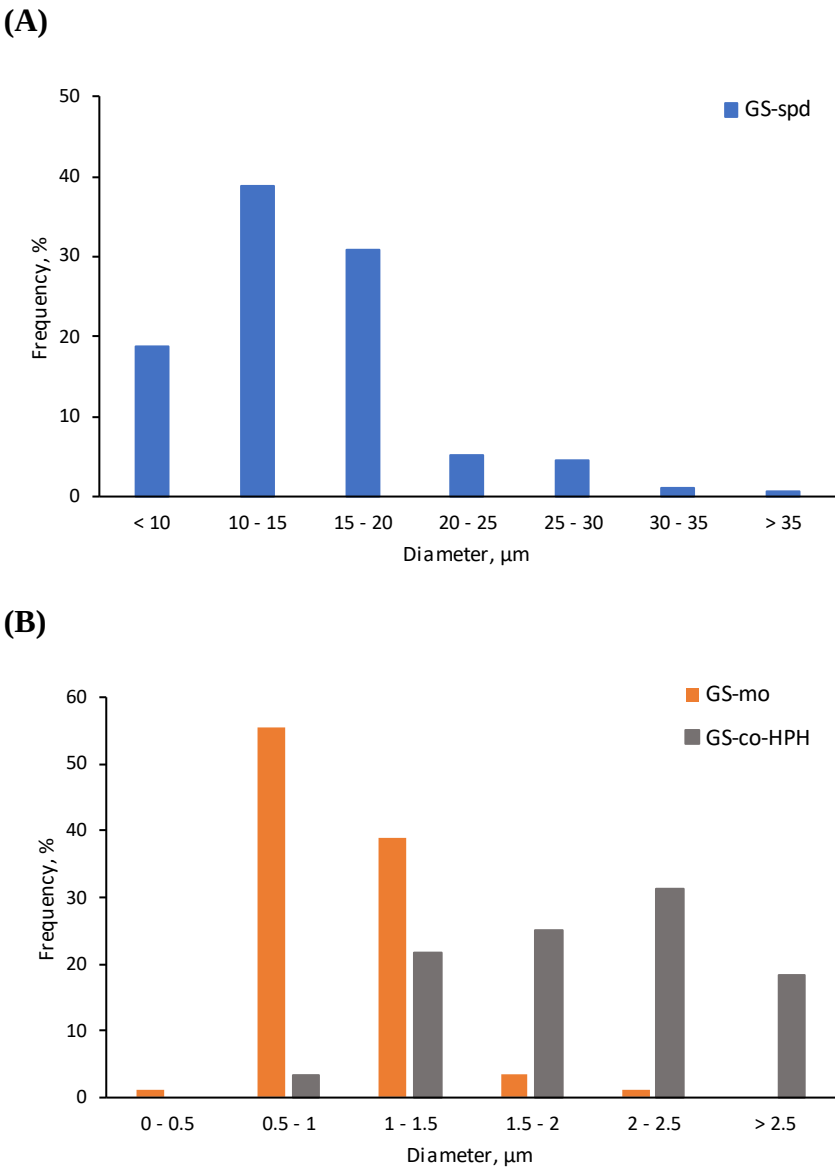

Figure 28. Particle size distribution of the fish oil-loaded capsules produced by spray-drying (A) and electrospraying (monoaxial and coaxial) (B).

3.2 Oxidative stability

The PBN-ESR spectra of the fish oil-loaded capsules showed three broad lines (Figure 29), in line with the PBN-ESR spectrum of neat fish oil (Figure S 5 of the Supplementary Material). These results are consistent with those reported by other authors for the ESR spectra of PBN-adducts formed in bulk, emulsified and encapsulated oils, where the typical coupling of nitroxyl radicals, but not the hydrogen splitting, was observed (Boerekamp et al., 2019; Velasco et al., 2005, 2021).

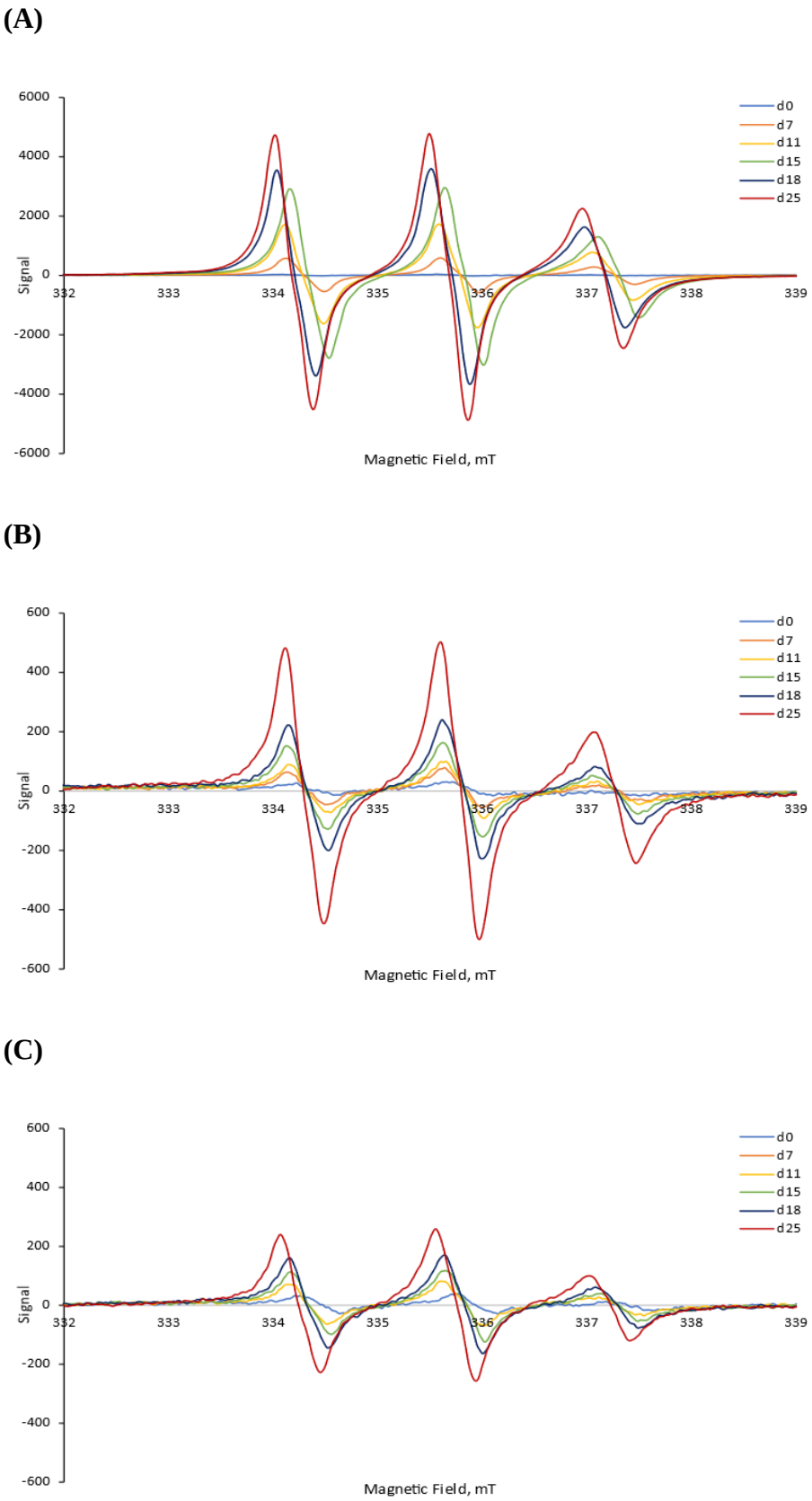

Figure 29. Evolution of ESR spectra of the fish oil-loaded capsules containing the PBN spin trap during storage at 25 °C. Capsules were produced by spray-drying (A), monoaxial electrospraying (B) and coaxial electrospraying (C).

As to the lipid-derived-radicals concentration is considered to be proportional to ESR signal intensity, the peak-to-peak amplitude of the central line of the PBN-ESR spectrum was used to monitor the lipid oxidation of the capsules (Boerekamp et al., 2019; Velasco et al., 2005). Figure 29 and Figure 30 show the evolution of the PBN-ESR spectra and the evolution of peak-to-peak amplitude of the encapsulated systems over storage, respectively. Significantly different trends were observed in both figures depending of the technology used to produce the capsules (e.g., spray-drying, monoaxial electrospraying or coaxial electrospraying).

At the beginning of the storage time, low but detectable levels of radicals were found in all the samples (Figure 29), contrary to the neat fish oil (Figure S 5 of the Supplementary Material). These results suggest that lipid oxidation already occurred during the encapsulation process, irrespective of the technology used (Velasco et al., 2021). However, it is worth mentioning that the PBN-ESR signal detected for the spray-dried capsules (GS-spd sample) after processing was smaller than that of the electrosprayed capsules (GS-mo and GS-HPH-co samples) (Figure 29 and Figure 30). During storage, the ESR signal intensity of the spray-dried capsules showed a lag-phase of 4 days, followed by a sharp increase up to day 21. Afterwards, a slower increase in the peak-to-peak amplitude was noted and the ESR signal intensity decreased by the end of the storage time (Figure 30). Nonetheless, the opposite trend was found for the electrosprayed systems (e.g., monoaxial, GS-mo and coaxial, GS-HPH-co) (Figure 30) for which a small and rather constant peak-to-peak amplitude was observed during storage.

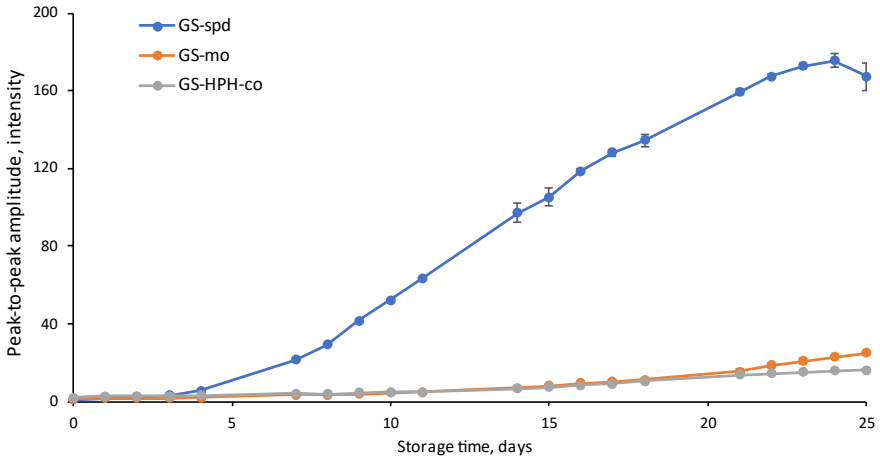

Figure 30. Peak-to-peak amplitude of the central line of the PBN-ESR spectra of the fish oil-loaded capsules containing the PBN spin trap as a function of storage time at 25 °C. Capsules were produced by spray-drying (GS-spd), monoaxial electrospraying (GS-mo) and coaxial electrospraying (GS-HPH-co)

Although it is widely accepted that high levels of radicals detected by ESR spin trapping indicate high levels of oxidation, the interpretation of our results might not be as straightforward. The detection of lipid radicals depends on several factors such as the formation rate and stability of the radical to be trapped, the rate of trapping and the stability of the spin adducts formed (Velasco et al., 2021). In addition, it has been reported that ESR spin trapping experiments should be limited to the early stages of lipid oxidation (Merkx et al., 2021; Velasco et al., 2005). Spin adducts are radicals themselves, thus they can react with other lipid-derived-radicals in conditions of advanced lipid oxidation (where their concentration is rather high) giving rise to ESR-silent compounds (e.g., diamagnetic species) (M. L. Andersen, 2021; Velasco et al., 2005). Therefore, low levels of lipid radicals might be measured in oxidized samples (M. L. Andersen, 2021). This is in agreement with previous studies that investigated the development of PBN-spin adducts at early and advanced stages of lipid oxidation in bulk oils or in oil-encapsulated systems (Falch et al., 2005; Velasco et al., 2021). In case of bulk oils (Falch et al., 2005), the lowest concentration of radicals observed corresponded to the sample that oxidized more rapidly during storage, as confirmed by the PV and TBARS measurements. Furthermore, radicals decay occurred significantly earlier compared to the more oxidatively stable oil and after that time, a low and rather constant concentration of PBN-adducts was observed until the end of the storage time (Falch et al., 2005). In a recent study, the same trend observed for bulks oils was reported for oil-loaded encapsulated systems (Velasco et al., 2021). The lowest concentration of radicals was found for the samples that were proven to oxidize more rapidly, and their concentration, after the decay of radicals occurred, did not significantly vary during the storage time. Moreover, for the less oxidatively stable encapsulated system, an initial formation of radicals followed by a decay was not noted. It was attributed to a rapid lipid oxidation during the early stages of incubation since the rate of radicals' depletion was higher than the rate of radicals' formation (Velasco et al., 2021). Taken altogether, our results suggest that the electrosprayed systems (GS-mo and GS-HPH-co samples) produced in the current study oxidized faster than those produced by spray-drying (GS-spd). Indeed, these results are in agreement with those reported in our previous study (Rahmani-Manglano et al., 2023), where a significantly higher oxidative stability was observed for the spray-dried capsules compared to the electrosprayed systems (monoaxial and coaxial), as confirmed by FT-IR measurements and the development of secondary volatile oxidation products during storage. These findings were explained due to potential differences in oxygen permeability of the encapsulated systems, which was further investigated in this study.

3.3 Oxygen permeability

Lipid autoxidation occurs as a chain reaction between lipid radicals (e.g., alkyl radicals) and oxygen (Johnson & Decker, 2015). Thus, to promote lipid oxidation of encapsulated systems, it is assumed that the environmental oxygen has to get in contact with the encapsulated oil droplets (Linke, Hinrichs, et al., 2020). Indeed, in the literature, oxygen diffusivity through the encapsulating wall has been extensively pointed out to be the key factor influencing lipid oxidation of encapsulated oils (Boerekamp et al., 2019; Drusch et al., 2009; Linke et al., 2021, 2022; Linke, Linke, et al., 2020; Linke, Weiss, et al., 2020; Velasco et al., 2006). Nonetheless, to our knowledge, there are not studies comparing the oxygen permeability of spray-dried and electrosprayed encapsulated systems neither its influence on oxidative stability.

To evaluate the oxygen-barrier properties of the encapsulating matrices, the capsules were first washed with heptane to suppress the DSA-ESR signal arising from the easily oxygen-accessible non-encapsulated oil fraction. The DSA-ESR spectra of the non-oxidizing MCT oil-loaded capsules after washing produced by spray-drying (GS-spd) and monoaxial electrospraying (GS-mo) are shown in Figure 31, where three lines can be distinguished (e.g., high field line, central line and low field line). However, a flat ESR spectrum was obtained for the capsules produced by coaxial electrospraying after washing (Figure S 6 of the Supplementary Material). The latter indicates that washing with heptane the coaxially electrosprayed capsules not only removed the non-encapsulated oil fraction, but most of the MCT oil containing the DSA probe. By optimal coaxial electrospraying, the oil is theoretically located at the core of the capsule as a single droplet surrounded by the encapsulating wall. Therefore, if the matrix is not completely solid, the encapsulated oil fraction can be easily reached, and thereby extracted, by the washing solvent that diffuses through capillary or cracks present on the surface of the capsules (Drusch & Berg, 2008). As a result, the oxygen permeability of the coaxially electrosprayed capsules (GS-HPH-co sample) could not be evaluated in the current study by ESR technology. However, our results could be regarded as an indication of the higher oxygen permeability of the coaxially electrosprayed capsules compared to those produced by the emulsion-based methods (e.g., spray-drying and electrospraying), for which the extraction of entrapped oil did not occur during washing with heptane.

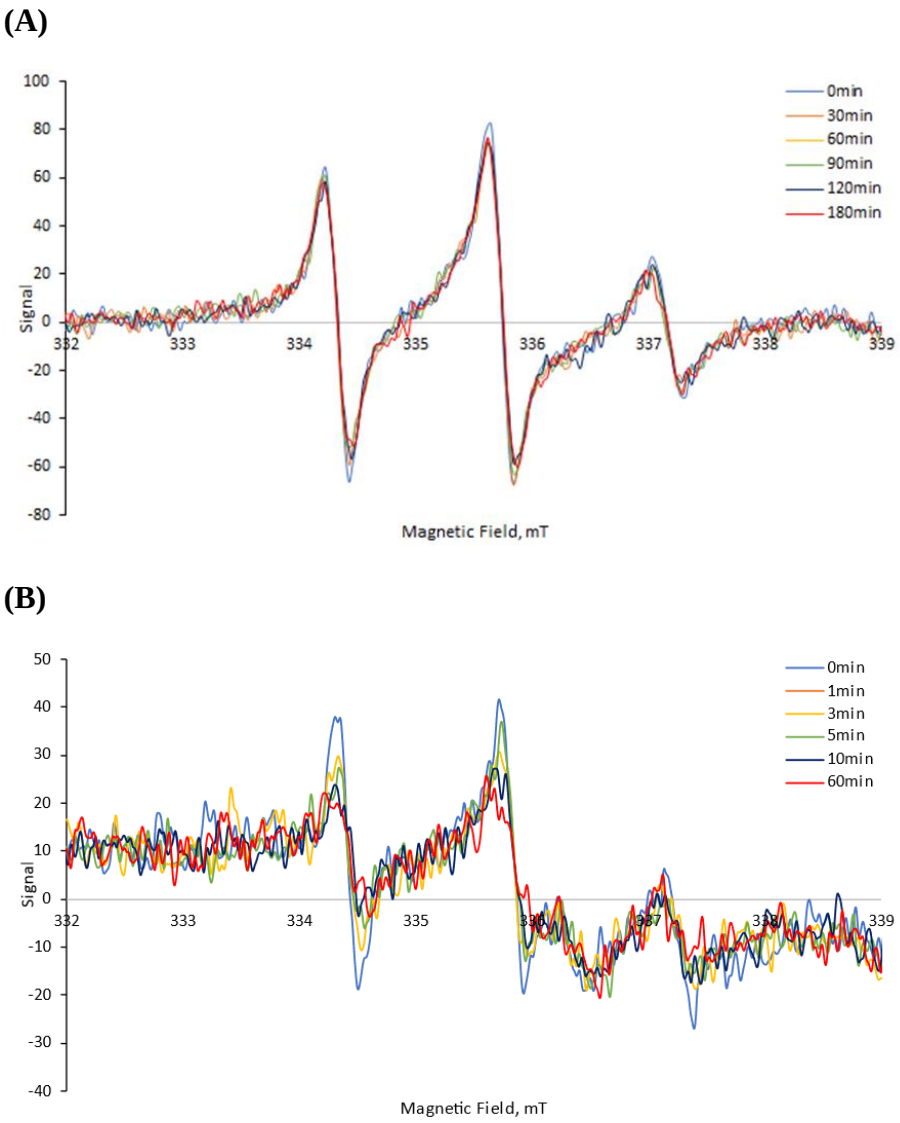

Figure 31. Evolution of the DSA-ESR spectrum of the MCT oil-loaded capsules containing the DSA probe produced by spray-drying (A) and monoaxial electrospraying (B) as the pure nitrogen atmosphere was changed to a pure oxygen atmosphere.

It should be noted that the DSA probe in pure MCT oil also showed a three-line spectrum (Figure S 7A of the Supplementary Material) which were similar to the DSA-ESR spectra of the encapsulated systems (GS-spd and GS-mo samples; Figure 31). This suggests that the DSA lipophilic probe was mainly located in the oil phase of the capsules, and therefore the broadening of the central line width (ΔHpp) of the DSA-ESR spectrum of the encapsulated systems occurred as a consequence of the interaction of the DSA probe and the oxygen dissolved in the oil (A. B. Andersen et al., 2000; Boerekamp et al., 2019; Svagan et al., 2016).

As shown in Figure 31, changing the atmosphere from pure nitrogen to pure oxygen resulted in the broadening of the central line (ΔHpp), together with the decrease of the signal intensity

with exposure time (Boerekamp et al., 2019). The changes in the DSA-ESR spectrum of the capsules produced by monoaxial electrospraying (GS-mo sample) were more extensive compared to that of the spray-dried capsules (GS-spd) (Figure 31). Figure 32 shows the narrowing and the broadening of the central line width (ΔHpp) with time upon exposure to nitrogen or oxygen atmospheres, respectively. At time zero, the atmosphere was changed from environmental air to nitrogen (i.e., the first data recorded corresponded to environmental air) and the samples were equilibrated for 1h under nitrogen exposure. After this time, the atmosphere was changed from nitrogen to oxygen until the steady-state was reached, indicating that the oxygen dissolved in the encapsulated oil was in equilibrium with the surrounding atmosphere of pure oxygen. Then, the capsules were again exposed to pure nitrogen for 1h (Figure 32). Both encapsulated systems presented a relatively high ΔHpp initial value ($p > 0.05$; Figure 32), suggesting that a high oxygen content was already present in the encapsulated oil (A. B. Andersen et al., 2000) which can be mainly attributed to air inclusion occurring during emulsification, drying and storage. However, although the initial ΔHpp values were close among the samples, their evolution with gas exposure time was significantly different depending on the technology used to produce the capsules. As expected, upon nitrogen exposure, the central line of the spectra narrowed for both systems but the liming ΔHpp values reached were different (Figure 32). According to the standard curve (Figure S 7B of the Supplementary Material), spray-dried capsules reached an asymptotic ΔHpp value of 0.24 ± 0.01 mT corresponding to a situation where the encapsulated oil is in equilibrium with an atmosphere containing ~53% nitrogen. On the contrary, our results show that the oil contained in GS-mo sample was in equilibrium with the surrounding nitrogen atmosphere (100 % nitrogen) after 1h (ΔHpp = 0.19 ± 0.01 mT). This suggests higher permeability to nitrogen of the electrosprayed capsules compared to spray-dried capsules. Accordingly, the central line width (ΔHpp) of both encapsulated systems increased with time when these were exposed to pure oxygen, but the broadening rate was again significantly different among the samples (Figure 32).

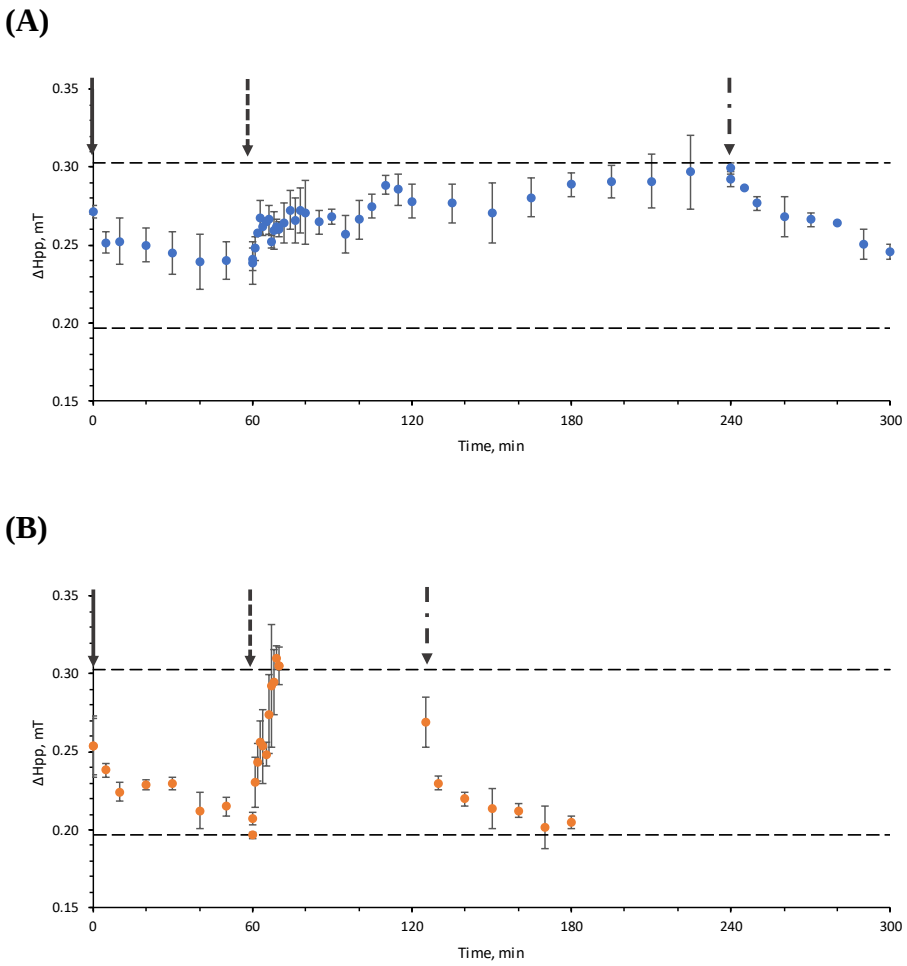

Figure 32. Broadening of the central line width (ΔHpp) of the DSA-ESR spectrum of the MCT oil-loaded capsules containing the DSA probe produced by spray-drying (GS-spd) (A) or monoaxial electrospraying (GS-mo) (B) with time. The dashed lines represent the maximum (upper line) and minimum (lower line) line width (ΔHpp) of the DSA-ESR spectrum in pure MCT oil, according to the standard curve. The solid arrow marks when the atmosphere was changed from environmental air to pure nitrogen. The dashed arrow marks when the atmosphere was changed from pure nitrogen to pure oxygen. The dotted arrow marks when the atmosphere was changed from pure oxygen to pure nitrogen.

For the spray-dried capsules, a rapid increase of the central line width (ΔHpp) was observed during the early stages of oxygen exposure (~20 min) followed by sustained increase until an asymptotic value was reached after ~2h (ΔHpp = 0.29 ± 0.01 mT). Due to the heterogeneous nature of emulsion-based encapsulating systems, in which the oil droplets are randomly distributed within the glassy encapsulating wall, a gradient in oxygen concentration inside the matrix is expected depending on the properties of the encapsulating wall and the distribution and size of the oil droplets (A. B. Andersen et al., 2000; Linke, Hinrichs, et al., 2020). Thus, the sharp increase of ΔHpp observed upon early oxygen exposure can be ascribed to the contribution of the oil droplets located near the surface of the spray-dried capsules that came fast into contact with the penetrating oxygen due to the

difference in partial pressure outside and inside the capsules. Afterwards, the rate of the central line broadening decay as the oxygen concentration increased inside the capsules until the equilibrium with the surrounding oxygen atmosphere was reached (e.g., the capsules were saturated with oxygen and the ΔHpp remained unvaried) (Kak et al., 2019; Tikekar et al., 2011). Conversely, the ΔHpp of the monoaxially electrosprayed capsules (GS-mo sample) increased exponentially and the equilibrium with the pure oxygen atmosphere was reached after 10 min (ΔHpp = 0.30 ± 0.01 mT). Oxygen diffusivity in encapsulated systems depends on the size of the capsules and the thickness and nature of the encapsulating wall. Smaller capsules result in an increased surface-to-volume ratio, implying a higher particle-air interface and therefore a higher surface area available for the diffusion process (Linke, Hinrichs, et al., 2020; Rahmani-Manglano et al., 2023). Furthermore, the oxygen diffusion path to the core of the capsules is shorter for smaller capsules when the oil load is fixed (Linke, Hinrichs, et al., 2020). This is consistent with our findings where the significantly smaller capsules produced by monoaxial electrospraying ($p \leq 0.05$; Figure 28) were significantly more permeable to oxygen than those produced by spray-drying (Figure 32).

After changing the surrounding atmosphere from pure oxygen to pure nitrogen, the ΔHpp decreased exponentially for both systems similarly as it was first observed when the atmosphere was changed from environmental air to pure nitrogen (Figure 32). Indeed, the limiting ΔHpp values reached after 1h of nitrogen exposure at the end of the test agree with those obtained at the beginning for both systems (GS-spd and GS-mo samples; Figure 32). Thus, whilst the capsules produced by monoaxial electrospraying were saturated with nitrogen at the end of the test (GS-mo; Fig. 6B), a relatively high concentration of oxygen was still present in the capsules produced by spray-drying (GS-spd; Fig. 6A). The latter suggests that not only the properties of the spray-dried capsules prevented oxygen from permeating into the oil phase, but it also prevented oxygen from permeating out. Furthermore, the ΔHpp narrowing rate of the capsules produced by monoaxial electrospraying was faster compared to those produced by spray-drying (Figure 32), further confirming the higher gas permeability of GS-mo sample. Finally, it is also noteworthy that the ΔHpp broadening rate of the spray-dried capsules was slower than the ΔHpp narrowing rate when the sample was exposed to oxygen, and subsequently to nitrogen (Figure 32A). This is once again ascribed to the heterogeneity of the encapsulated system since the random distribution of the oil droplets determine the interaction of the probe with the gases and, therefore, the ESR spectra (A. B. Andersen et al., 2000). Under non-steady state conditions,

the recorded spectrum represents the sum of the individual ESR-spectra of the system that will vary the ΔHpp, depending on the gas type (e.g., nitrogen and oxygen) and concentration (A. B. Andersen et al., 2000; Svagan et al., 2016). Furthermore, the recorded ESR spectra of heterogeneous systems are dominated by the narrow-line contributions of the DSA probe located in the oil droplets with low oxygen contents (A. B. Andersen et al., 2000; Svagan et al., 2016). Therefore, the faster ΔHpp narrowing observed for the spray-dried capsules upon nitrogen exposure can be explained by the fast contact of the oil droplets located near the surface of the capsules with the penetrating nitrogen, which significantly influence the ΔHpp of the recorded spectra (Boerekamp et al., 2019). However, for the capsules produced by monoaxial electrospraying, a fast and similar ΔHpp broadening and narrowing rate were observed (Figure 32B) as a consequence of the higher gas permeability of the matrix.

Although it is accepted that oxygen that is already present in the encapsulating matrix can contribute to lipid oxidation, the oxygen permeability through the encapsulating wall has been reported to be more important in determining the overall rate and extent of lipid oxidation (Linke et al., 2022; Linke, Linke, et al., 2020; Reineccius & Yan, 2016). Thus, encapsulating systems with low oxygen permeability are expected to be more efficient in preventing lipid oxidation of the encapsulated oil. The latter is in agreement with our findings since the spray-dried capsules were proven to be significantly less permeable to oxygen which, in turn, correlates with the higher oxidative stability reported for this system measured by ESR in this work, as well as previously reported based on the measurement of secondary volatile oxidation products (Rahmani-Manglano et al., 2023).

4. CONCLUSIONS

Oil-loaded encapsulated systems were produced by spray-drying and electrospraying in the monoaxial and coaxial configuration to compare and investigate their oxidative stability and oxygen permeability by means of ESR technology. The ESR-spin trapping results showed that spray-dried capsules oxidized slower during storage than those produced by electrospraying, irrespective of the emitter configuration. Moreover, ESR-oximetry results indicated that spray-dried capsules were more efficient in delaying gas permeability through the encapsulating matrix when compared to monoaxially electrosprayed capsules. This has been attributed to the larger particle size of the spray-dried capsules which results in a smaller surface-to-volume ratio and in thicker encapsulating walls (for the same oil load),

both affecting the diffusion process. Overall, our results confirm the key role of oxygen permeability on the oxidative stability of fish oil-loaded capsules. This fact should be borne in mind for the development of oxidatively stable electrosprayed capsules loaded with oils rich in omega-3 PUFAs.

5. REFERENCES

Andersen, A. B., Risbo, J., Andersen, M. L., & Skibsted, L. H. (2000). Oxygen permeation through an oil-encapsulating glassy food matrix studied by ESR line broadening using a nitroxyl spin probe. *Food Chemistry*, *70*(4), 499–508. www.elsevier.com/locate/foodchem

Andersen, M. L. (2021). Lipid oxidation studied by electron paramagnetic resonance (EPR). In *Omega-3 Delivery Systems*. Elsevier Inc. https://doi.org/10.1016/b978-0-12-821391-9.00004-1

Boerekamp, D. M. W., Andersen, M. L., Jacobsen, C., Chronakis, I. S., & García-Moreno, P. J. (2019). Oxygen permeability and oxidative stability of fish oil-loaded electrosprayed capsules measured by Electron Spin Resonance: Effect of dextran and glucose syrup as main encapsulating materials. *Food Chemistry*, *287*, 287–294. https://doi.org/10.1016/j.foodchem.2019.02.096

Chen, Y., Cheng, H., & Liang, L. (2023). Effect of Oil Type on Spatial Partition of Resveratrol in the Aqueous Phase, the Protein Interface and the Oil Phase of O/W Emulsions Stabilized by Whey Protein and Caseinate. *Antioxidants*, *12*(3), 589. https://doi.org/10.3390/antiox12030589

Drusch, S., & Berg, S. (2008). Extractable oil in microcapsules prepared by spray-drying: Localisation, determination and impact on oxidative stability. *Food Chemistry*, *109*(1), 17–24. https://doi.org/10.1016/j.foodchem.2007.12.016

Drusch, S., Rätzke, K., Shaikh, M. Q., Serfert, Y., Steckel, H., Scampicchio, M., Voigt, I., Schwarz, K., & Mannino, S. (2009). Differences in free volume elements of the carrier matrix affect the stability of microencapsulated lipophilic food ingredients. *Food Biophysics*, *4*(1), 42–48. https://doi.org/10.1007/s11483-008-9100-9

Falch, E., Velasco, J., Aursand, M., & Andersen, M. L. (2005). Detection of radical development by ESR spectroscopy techniques for assessment of oxidative susceptibility of fish oils. *European Food Research and Technology*, *221*(5), 667–674. https://doi.org/10.1007/s00217-005-0009-y

García-Moreno, P. J., Pelayo, A., Yu, S., Busolo, M., Lagaron, J. M., Chronakis, I. S., & Jacobsen, C. (2018). Physicochemical characterization and oxidative stability of fish oil-loaded

electrosprayed capsules: Combined use of whey protein and carbohydrates as wall materials. *Journal of Food Engineering*, *231*, 42–53. https://doi.org/10.1016/j.jfoodeng.2018.03.005

García-Moreno, P. J., Rahmani-Manglano, N. E., Chronakis, I. S., Guadix, E. M., Yesiltas, B., Sørensen, A.-D. M., & Jacobsen, C. (2021). Omega-3 nano-microencapsulates produced by electrohydrodynamic processing. In P. J. García-Moreno, C. Jacobsen, A.-D. M. Sørensen, & B. Yesiltas (Eds.), *Omega-3 Delivery Systems. Production, Physical Characterization and Oxidative Stability* (pp. 345–370). Academic Press. https://doi.org/10.1016/b978-0-12-821391-9.00017-x

Ghelichi, S., Hajfathalian, M., García-Moreno, P. J., Yesiltas, B., Moltke-Sørensen, A.-D., & Jacobsen, C. (2021). Food enrichment with omega-3 polyunsaturated fatty acids. In P. J. García-Moreno, C. Jacobsen, A.-D. M. Sørensen, & B. Yesiltas (Eds.), *Omega-3 Delivery Systems* (pp. 395–425). Academic Press. https://doi.org/10.1016/b978-0-12-821391-9.00020-x

Gómez-Mascaraque, L. G., & López-Rubio, A. (2016). Protein-based emulsion electrosprayed micro- and submicroparticles for the encapsulation and stabilization of thermosensitive hydrophobic bioactives. *Journal of Colloid and Interface Science*, *465*, 259–270. https://doi.org/10.1016/j.jcis.2015.11.061

Velasco, J., Dobarganes, C., & Márquez-Ruiz, G. (2003). Variables affecting lipid oxidation in dried microencapsulated oils. *Grasas y Aceites*, *54*(3), 304–314.

Johnson, D. R., & Decker, E. A. (2015). The role of oxygen in lipid oxidation reactions: A review. *Annual Review of Food Science and Technology*, *6*, 171–190. https://doi.org/10.1146/annurev-food-022814-015532

Kak, A., Bajaj, P. R., Bhunia, K., Nitin, N., & Sablani, S. S. (2019). A Fluorescence-based Method for Estimation of Oxygen Barrier Properties of Microspheres. *Journal of Food Science*, *84*(3), 532–539. https://doi.org/10.1111/1750-3841.14453

Linke, A., Hinrichs, J., & Kohlus, R. (2020). Impact of the powder particle size on the oxidative stability of microencapsulated oil. *Powder Technology*, *364*, 115–122. https://doi.org/10.1016/j.powtec.2020.01.077

Linke, A., Linke, T., & Kohlus, R. (2020). Contribution of the Internal and External Oxygen to the Oxidation of Microencapsulated Fish Oil. *European Journal of Lipid Science and Technology*, *1900381*, 1900381. https://doi.org/10.1002/ejlt.201900381

Linke, A., Teichmann, H., & Kohlus, R. (2022). Simulation of the oxidation of microencapsulated oil based on oxygen distribution – Impact of powder and matrix properties. *Powder Technology*, *401*. https://doi.org/10.1016/j.powtec.2022.117289

Linke, A., Weiss, J., & Kohlus, R. (2020). Oxidation rate of the non-encapsulated- and encapsulated oil and their contribution to the overall oxidation of microencapsulated fish oil particles. *Food Research International*, *127*. https://doi.org/10.1016/j.foodres.2019.108705

Linke, A., Weiss, J., & Kohlus, R. (2021). Impact of the oil load on the oxidation of microencapsulated oil powders. *Food Chemistry*, *341*(September 2020), 128153. https://doi.org/10.1016/j.foodchem.2020.128153

Merkx, D. W. H., Plankensteiner, L., Yu, Y., Wierenga, P. A., Hennebelle, M., & Van Duynhoven, J. P. M. (2021). Evaluation of PBN spin-trapped radicals as early markers of lipid oxidation in mayonnaise. *Food Chemistry*, *334*. https://doi.org/10.1016/j.foodchem.2020.127578

Orlien, V., Andersen, A. B., Sinkko, T., & Skibsted, L. H. (2000). Hydroperoxide formation in rapeseed oil encapsulated in a glassy food model as influenced by hydrophilic and lipophilic radicals. *Food Chemistry*, *68*, 191–199. https://doi.org/https://doi.org/10.1016/S0308-8146(99)00177-6

Patel, A., Desai, S. S., Mane, V. K., Enman, J., Rova, U., Christakopoulos, P., & Matsakas, L. (2022). Futuristic food fortification with a balanced ratio of dietary ω-3/ω-6 omega fatty acids for the prevention of lifestyle diseases. In *Trends in Food Science and Technology* (Vol. 120, pp. 140–153). Elsevier Ltd. https://doi.org/10.1016/j.tifs.2022.01.006

Rahmani-Manglano, N. E., González-Sánchez, I., García-Moreno, P. J., Espejo-Carpio, F. J., Jacobsen, C., & Guadix, E. M. (2020). Development of fish oil-loaded microcapsules containing whey protein hydrolysate as film-forming material for fortification of low-fat mayonnaise. *Foods*, *9*(5).

Rahmani-Manglano, N. E., Guadix, E. M., Jacobsen, C., & García-Moreno, P. J. (2023). Comparative Study on the Oxidative Stability of Encapsulated Fish Oil by Monoaxial or Coaxial Electrospraying and Spray-Drying. *Antioxidants*, *12*(2). https://doi.org/https://doi.org/10.3390/antiox12020266

Reineccius, G. A., & Yan, C. (2016). Factors controlling the deterioration of spray dried flavourings and unsaturated lipids. In *Flavour and Fragrance Journal* (Vol. 31, Issue 1, pp. 5–21). John Wiley and Sons Ltd. https://doi.org/10.1002/ffj.3270

Serfert, Y., Drusch, S., & Schwarz, K. (2009). Chemical stabilisation of oils rich in long-chain polyunsaturated fatty acids during homogenisation, microencapsulation and storage. *Food Chemistry*, *113*(4), 1106–1112. https://doi.org/10.1016/j.foodchem.2008.08.079

Singh, H., Kumar, Y., & Meghwal, M. (2022). Encapsulated oil powder: Processing, properties, and applications. In *Journal of Food Process Engineering* (Vol. 45, Issue 8). John Wiley and Sons Inc. https://doi.org/10.1111/jfpe.14047

Svagan, A. J., Bender Koch, C., Hedenqvist, M. S., Nilsson, F., Glasser, G., Baluschev, S., & Andersen, M. L. (2016). Liquid-core nanocellulose-shell capsules with tunable oxygen permeability. *Carbohydrate Polymers*, *136*, 292–299. https://doi.org/10.1016/j.carbpol.2015.09.040

Tikekar, R. V., Johnson, A., & Nitin, N. (2011). Real-time measurement of oxygen transport across an oil-water emulsion interface. *Journal of Food Engineering*, *103*(1), 14–20. https://doi.org/10.1016/j.jfoodeng.2010.08.030

Velasco, J., Andersen, M. L., & Skibsted, L. H. (2005). Electron spin resonance spin trapping for analysis of lipid oxidation in oils: Inhibiting effect of the spin trap α-phenyl-N-tert-butylnitrone on lipid oxidation. *Journal of Agricultural and Food Chemistry*, *53*(5), 1328–1336. https://doi.org/10.1021/jf049051w

Velasco, J., Andersen, M. L., & Skibsted, L. H. (2021). ESR spin trapping for in situ detection of radicals involved in the early stages of lipid oxidation of dried microencapsulated oils. *Food Chemistry*, *341*(June 2020), 128227. https://doi.org/10.1016/j.foodchem.2020.128227

Velasco, J., Marmesat, S., Dobarganes, C., & Márquez-Ruiz, G. (2006). Heterogeneous aspects of lipid oxidation in dried microencapsulated oils. *Journal of Agricultural and Food Chemistry*, *54*(5), 1722–1729. https://doi.org/10.1021/jf052313p

Zhou, Y. T., Yin, J. J., & Lo, Y. M. (2011). Application of ESR spin label oximetry in food science. In *Magnetic Resonance in Chemistry* (Vol. 49, Issue SUPPL. 1). https://doi.org/10.1002/mrc.2822

6. SUPPLEMENTARY MATERIAL

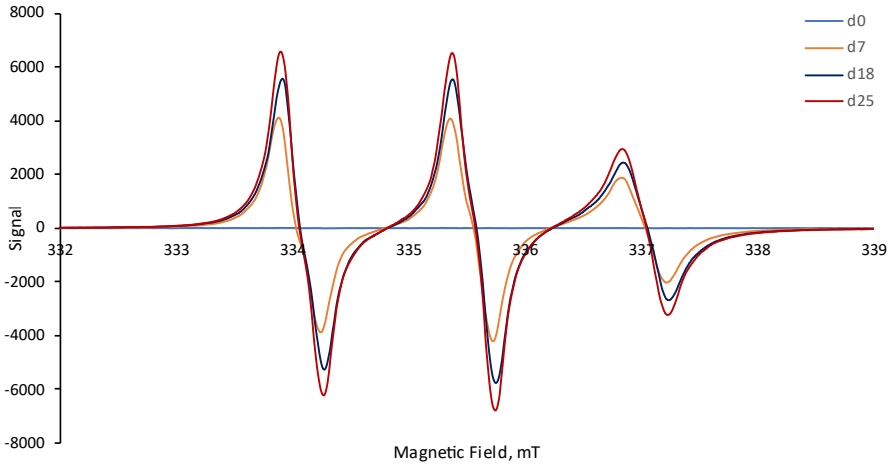

Figure S 5. Evolution of the PBN-ESR spectra of pure fish oil during 25 days of storage.

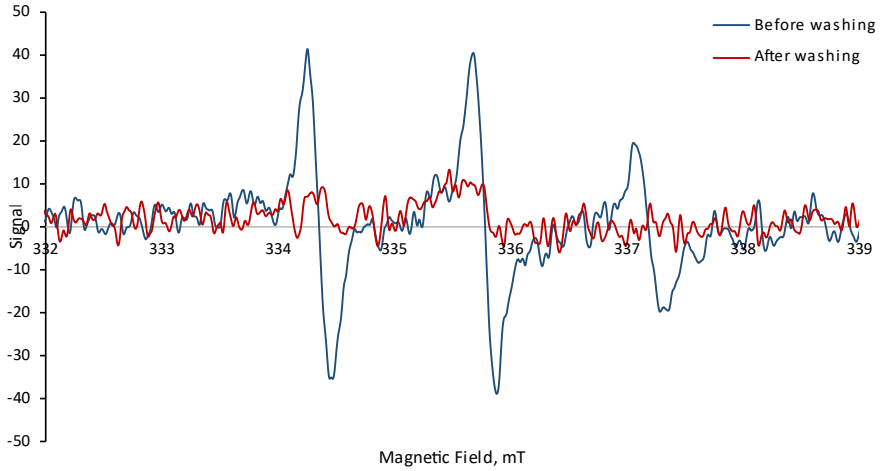

Figure S 6. DSA-ESR spectrum of the MCT oil-loaded capsules containing the DSA probe produced by coaxial electrospraying before and after washing with heptane.

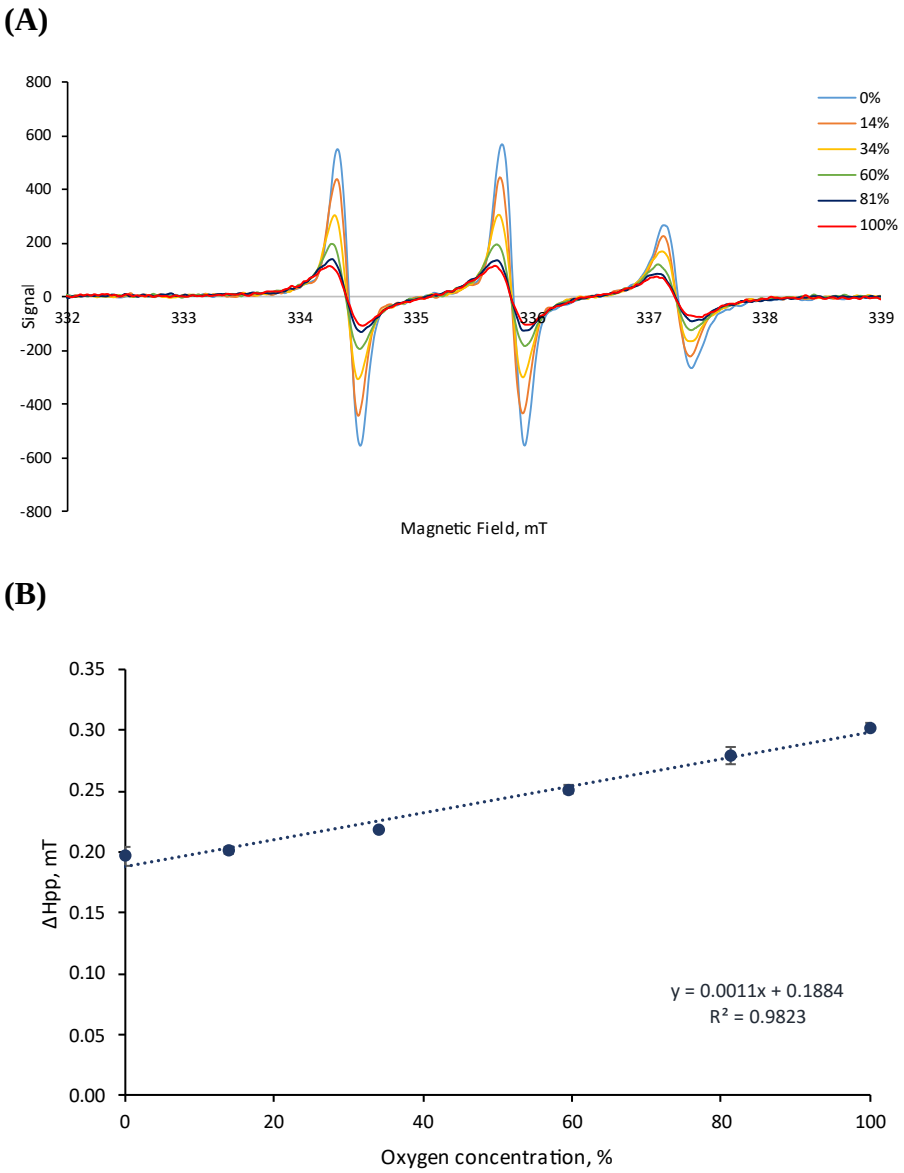

Figure S 7. (A) Broadening of the central line width (ΔHpp) of the DSA-ESR spectrum of pure MCT oil as the pure nitrogen atmosphere changes to pure oxygen atmosphere. (B) Broadening of the central line width (ΔHpp) as a function of different oxygen concentrations.

V. Structure of whey protein hydrolysate used as emulsifier in wet and dried oil delivery systems: Effect of pH and drying processing*

The secondary structure of whey protein concentrate hydrolysate (WPCH), used as an emulsifier in oil delivery systems, was investigated using Synchrotron Radiation Circular Dichroism (SRCD). The effect of pH on the conformation of peptides in solution and adsorbed at the oil/water interface, as well as the thermal stability of the systems was studied. Furthermore, oil-loaded microcapsules were produced by spray-drying or electrospraying to investigate the influence of encapsulating agents (glucose syrup, maltodextrin) and drying technique on the secondary structure of WPCH at the oil/water interface. Enzymatic hydrolysis resulted in peptides with a highly unordered structure (~60% turns and unordered regions) in solution. However, WPCH adsorption onto the oil/water interface increased the α-helical content resulting in an improved thermal stability. The encapsulating agents and spray-drying process did not modify the conformation of WPCH at the oil/water interface. Nonetheless, electrospraying affected the SRCD spectra obtained for WPCH adsorbed at the oil/water interface.

* JOURNAL PAPER: N.E. Rahmani-Manglano, N.C. Jones, S.V. Hoffmann, E.M. Guadix, R. Pérez-Gálvez, A. Guadix, P.J. García-Moreno. (2022). Structure of whey protein hydrolysate used as emulsifier in wet and dried oil delivery systems: Effect of pH and drying processing. *Food Chemistry*, 390: 133169 (IF: 9.231; category: FOOD SCIENCE & TECHNOLOGY - SCIE; position: 8/144; Q1/D1)

1. INTRODUCTION

Bioactive oils (e.g., oils rich in omega-3 polyunsaturated fatty acids) present numerous health effects and thus the food industry is highly interested in the development of fortified food products rich in these bioactive lipids (Punia et al., 2019). However, the extremely low oxidative stability, together with other inherent drawbacks of bioactive oils (e.g., low solubility), still represent a challenge to the food industry when it comes to their inclusion in complex food matrices. Hence, the design and development of efficient oil delivery systems, such as oil-in-water emulsions or oil-loaded micro/nanocapsules, is of utmost importance. To produce oil delivery systems, it is necessary to emulsify the oil in the continuous phase, which is normally water-based, and then drying is carried out when dried encapsulates are required (Rahmani-Manglano, García-Moreno, et al., 2020).

Proteins are amphiphilic molecules that have been extensively used in the food industry as emulsifiers to stabilize oil-in-water emulsions used as: i) a liquid delivery system itself (Horn et al., 2012; Nielsen & Jacobsen, 2013), or ii) employed as feed emulsion to the dryer to produce dry micro/nanocapsules (Miguel et al., 2019; Takeungwongtrakul et al., 2015). Moreover, protein hydrolysates have shown enhanced functional properties (e.g., emulsifying and antioxidant) with respect to their parent proteins (Liceaga & Hall, 2018). Enzymatic hydrolysis of proteins to a low degree of hydrolysis (DH; DH $\leq$ 10%) results in the release of surface-active peptides, which diffuse, adsorb, unfold and reorient faster at the oil/water (O/W) interface when compared to the parent protein (Peighambardoust et al., 2021). Furthermore, the conformational changes induced during hydrolysis also favor the exposure of hydrophobic groups, originally buried inside the protein structure, that also contribute to the improved emulsifying activity of protein hydrolysates (Liceaga & Hall, 2018). In addition, and depending on the proteolysis conditions (e.g., type of enzyme, temperature, pH, time), protein hydrolysates might also exhibit higher antioxidant activity than the native proteins as a result of an increased exposure of amino acid residues capable of inhibiting lipid oxidation through different mechanisms, e.g., radical scavenging and/or metal chelation (Elias et al., 2008; Peighambardoust et al., 2021). The latter is of special relevance since protein hydrolysates exhibiting both emulsifying and antioxidant activities allow the location of antioxidants at the oil/aqueous phase (in emulsions) or at the oil/shell phase (in dried encapsulates), which is the place where lipid oxidation is initiated in heterogeneous systems (García-Moreno et al., 2021; Padial-Domínguez, Espejo-Carpio,

García-Moreno, et al., 2020; Tamm et al., 2015). In this line, whey protein concentrate hydrolysates (WPCHs) have been reported to exhibit high emulsifying (Padial-Domínguez, Espejo-Carpio, Pérez-Gálvez, et al., 2020) and antioxidant activities (e.g., radical scavenging activity, metal chelating and reducing power) (Padial-Domínguez, Espejo-Carpio, García-Moreno, et al., 2020) and have been used as emulsifier/antioxidant to stabilize either oil-in-water emulsions (Padial-Domínguez, Espejo-Carpio, García-Moreno, et al., 2020) or oil-loaded microcapsules (Rahmani-Manglano, González-Sánchez, et al., 2020) showing high oxidative stability.

Some research has already studied the structure of pure proteins contained in whey (e.g., α-lactalbumin, β-lactoglobulin and bovine serum albumin; BSA) (Day et al., 2014; Zhai et al., 2010, 2011, 2012). However, to the best of our knowledge, no studies have yet been reported on the structure of peptides present in hydrolysates when adsorbed at the O/W interface. Structural organization and interaction of emulsifier peptides at the O/W interface affect the mechanical properties of the interfacial peptides film (e.g., viscoelasticity) (García-Moreno et al., 2021). The latter strongly affect the physical and oxidative stability of O/W emulsions, as well as the encapsulation efficiency (EE) and oxidative stability of dried micro/nanocapsules loaded with bioactive oils. Moreover, the effect of pH on the interfacial structure of peptides needs further investigation since above or below the isoelectric point (pI) the peptides will be negatively or positively charged, respectively. This is extremely important since it determines the adsorption of peptides onto the O/W interface as well as the viscoelasticity of the peptide interfacial layer (Ruiz-Álvarez et al., 2021). Furthermore, to the best of the authors' knowledge, the influence of the encapsulating agent (e.g., carbohydrates), and of the drying method used to produce oil-loaded micro/nanocapsules (e.g., spray-drying or electrospraying) on the structure of the peptides at the O/W interface remains to be investigated.

Synchrotron radiation circular dichroism (SRCD) is an advanced technique used to study the secondary structure of proteins and peptides in scattering and/or absorbing media such as O/W emulsions (Wallace & Janes, 2001). The high flux of synchrotron radiation light sources allows spectra collection at the vacuum ultraviolet (VUV) wavelength region (< 190 nm) with higher signal-to-noise ratios than conventional circular dichroism (CD), allowing better and more accurate determination of secondary structure (Wallace & Janes, 2001; Zhai et al., 2013). Indeed, SRCD has been recently employed to determine the secondary structure of proteins (Day et al., 2014; Zhai et al., 2010, 2011, 2012) and synthetic peptides (García-

Moreno et al., 2021) both in solutions and at the O/W interface. Nevertheless, the use of SRCD to determine the predominating structure of peptides present in protein hydrolysates and their thermal stability both in solution and at the O/W interface have not been yet studied.

Therefore, this work aimed at: i) quantitatively evaluating by SRCD the secondary structure of WPCH in solution or adsorbed at the O/W interface at different pH (pH 2 or pH 8), ii) investigating the thermal stability of WPCH in solution or adsorbed at the O/W interface at different pH (pH 2 or pH 8), and iii) studying the changes in the secondary structure of WPCH used as an emulsifier to produce oil-loaded micro/nanocapsules using different encapsulating agents (e.g., glucose syrup or maltodextrin) and obtained by different drying techniques (e.g., spray-drying or electrospraying). Thus, this research will advance our knowledge on the interfacial structure of emulsifier peptides present in whey protein hydrolysate, which will open up its use for the development of more efficient liquid and dried oil delivery systems.

2. MATERIALS AND METHODS

2.1 Materials

Whey protein concentrate (WPC: 35 wt% protein, 52 wt% lactose, 2.8 wt% fat, 2.5 wt% moisture and 7.7 wt% ash), lactose and maltodextrin (MD; DE21) were kindly donated by Abbott Laboratories (Granada, Spain). Glucose syrup (GS; DE38, C*Dry 1934) and pullulan (PUL) were provided by Cargill Germany GmbH (Krefeld, Germany) and Hayashibara Co., Ltd. (Okayama, Japan), respectively. Tricaprylin oil and sodium phosphate (monobasic anhydrous and dibasic dihydrate) were purchased from Sigma-Aldrich (St. Louis, MO). Ortho-Phosphoric acid (85%) was supplied by Merck (Darmstadt, Germany). Sodium dodecyl sulfate (SDS) was provided by Panreac Quimica S.A. (Barcelona, Spain).

2.2 Production of whey protein concentrate hydrolysate (WPCH)

WPCH was produced with Alcalase® (Novozymes, Bagsværd, Denmark) to a degree of hydrolysis of 10% (DH 10%), as described by Rahmani-Manglano, González-Sánchez, et al., (2020). In brief, WPC was diluted in distilled water to a final protein content of 40 g/L. The reaction was carried out at 50 °C and pH 8 and the DH was determined using the pH-stat method by employing an automatic titrator 718 Stat Titrino (Metrohm AG, Herisau,

Switzerland) (Rahmani-Manglano, González-Sánchez, et al., 2020). The protein hydrolysate solution was then heated to 100 °C for 5 min to deactivate the enzyme, before being freeze-dried in a Labconco freeze-drying system (Kansas City, MO, USA) and stored at 4 °C until further use. The protein content of the resulting WPCH was ca. 33% (Padial-Domínguez, Espejo-Carpio, García-Moreno, et al., 2020). A heat treatment without enzyme addition (WPC + heat) was carried out at the hydrolysis conditions mentioned (50 °C and pH 8) to evaluate the effect of only heat on the structure of WPC. The protein solution obtained was also heated to 100 °C for 5 min and then freeze-dried and stored at 4 °C.

2.3 Preparation of solutions and emulsions

Stock solutions were prepared dissolving ca. 6 wt% of WPC or WPCH in phosphate buffer 10 mM (pH 8 or pH 2), stirring overnight (500 rpm) at 4 °C. From the stock solutions, protein solutions and emulsions were produced either by addition of phosphate buffer or emulsification of tricaprylin oil. Oil-in-water (O/W) emulsions were produced by dispersing 5 wt% of tricaprylin oil in the aqueous phase containing WPC or WPCH. The protein content of the emulsions was fixed at 2 wt%. First, a coarse emulsion was produced using an Ultraturrax T-25 homogenizer (IKA, Staufen, Germany) at 15,000 rpm for 2 min. The oil was added during the first minute, and the coarse emulsion was then homogenized using a two-valve homogenizer (PandaPLUS 2000; GEANiro Soavi, Lübeck, Germany) at a pressure range of 450/75 bar, applying 3 passes. An SDS-stabilized O/W emulsion was also prepared by homogenizing 5 wt% tricaprylin oil with 95 wt% aqueous solution (2 wt% SDS in 10 mM phosphate buffer, pH 8) under the same conditions as described above. This emulsion and dilutions from it were used for SRCD baseline correction.

2.4 Production of spray-dried capsules

The emulsions fed to the spray-dryer consisted of 5 wt% tricaprylin oil-in-water emulsions stabilized with WPCH (6 wt%, which is equivalent to 2 wt% protein), containing GS or MD as encapsulating agent (28 wt%). The aqueous phase (10 mM phosphate buffer, pH 8) and the emulsions were produced as described in Section 2.3 by also dissolving the encapsulating agents in the aqueous phase. The oil load of the resulting spray-dried capsules was ca. 13 wt%. The drying process was carried out in a lab-scale spray-drier (Büchi B-190; Büchi Labortechnik, Flawill, Switzerland) at 180/90 °C as the inlet/outlet temperature, respectively. The drying air flow was fixed to 25 Nm3/h.

2.5 Production of electrosprayed capsules

For electrosprayed emulsions, the aqueous phase was produced dissolving WPCH (3.5 wt%), PUL (1.5 wt%) and GS or MD (15 wt%) in phosphate buffer 10 mM at pH 8. Again, the aqueous phase and the emulsions were produced as described in Section 2.3. The final tricaprylin oil load of the emulsion was 3 wt%. Pullulan was added as thickening agent in order to increase the stability of the Taylor cone during the electrospraying process. It should be noted that despite the differences in the formulation when compared to spray-drying, the protein/oil ratio (P/O = 0.4) and the oil load (ca. 13%) of the resulting capsules was the same irrespective of the drying method. The electrospraying process was carried out using SpinBox equipment (Bioinicia-Fluidnatek S.L.U., Valencia, Spain) consisting of a syringe pump, a drying chamber equipped with a variable high voltage power supply and a 15 x 15 cm collector plate made of stainless steel. The flow rate was fixed to 1 mL/h. The voltage applied was 17 kV. A 16G needle (Proto Advantage, Canada) was coupled to the monoaxial injector and the needle tip was 15 cm from the collector plate. The electrospraying process was carried out at room temperature (relative humidity, RH: 35 - 43%) in batches of 1 h.

2.6 SRCD measurements

SRCD measurements were carried out on the AU-CD beamline at the ASTRID2 synchrotron radiation source, (ISA, Department of Physics & Astronomy, Aarhus University in Denmark) with slight differences from our previous work (García-Moreno et al., 2021). As usual the operation of the SRCD spectrometer was confirmed daily using camphorsulfonic acid for optical rotation magnitude and wavelength (Miles et al., 2004). A 0.01 cm path length quartz Suprasil cell (Hellma GmbH & Co., Germany) was used for far-UV SRCD measurements at 25 °C. The far-UV SRCD spectra were recorded in triplicate from 270 to 170 nm in 1 nm steps, with a dwell time of 2.1 s per point.

For SRCD measurements, the solutions of WPC or WPCH were diluted in phosphate buffer at pH 8 or pH 2 (1:19, v/v) to reduce absorbance. All emulsion samples were measured untreated and after centrifugation (Eppendorf Minispin®, Eppendorf Nordic, Denmark). Centrifugation was conducted at 13,400 rpm for 15 min to separate the resulting bottom phase (aqueous phase) from the top phase (oil phase). The top phase was later re-suspended. This was carried out to separate the excess WPC or WPCH in the aqueous phase, which allowed the CD signal to be obtained from only the peptides located at the O/W interface.

The re-suspended emulsions were further diluted in phosphate buffer at pH 8 or pH 2 (1:3, v/v) to adjust the maximum absorbance measured.

Temperature scans were carried out for WPCH in solution and at the O/W interface both at pH 8 and pH 2, with SRCD measurements taken at temperatures from 5.7 °C to 84.5 °C in steps of 5°C, recorded in triplicate at each step.

2.7 SRCD data analysis and calculation of peptides secondary structure

The samples of WPC and WPCH naturally contain lactose, which itself has a CD spectrum starting below 193 nm (Figure S 26). Therefore, in order to remove this contribution from the solution spectra, a spectrum of lactose at the appropriate concentration was subtracted from each spectrum. This same treatment was applied to the aqueous portion of the emulsion samples, where it is assumed that the majority of the lactose is free in solution and therefore largely removed from the re-suspended oil-droplet portion of the emulsions. The spectra were converted to delta epsilon units using the peptide concentration obtained from absorbance at 205 nm (Anthis & Clore, 2013) and corrected for scattering where necessary (Nordén et al., 2010). There are several factors which may affect the accuracy of the concentration determined in this way, most particularly for the emulsion samples. When light is elastically scattered from particles with a size similar to or smaller than the wavelength, it may not be detected by the detector. Where scattering occurs, it is evident in the absorbance spectrum which is measured simultaneously with the CD spectrum. A long, non-zero sloping tail of the absorbance curve can be fitted using an equation based on Rayleigh scattering to simulate the effect of scattering over the full spectrum (Nordén et al., 2010), allowing for a corrected absorbance at 205 nm to be obtained. Another factor involved, is that the emulsions are being separated into aqueous and oil-droplet portions, leaving unknown quantities of oil remaining in each portion. The latter means that it is difficult to match an underlying baseline for absorbance due to the oil, which results in an incorrect absorbance calculation for the peptide. A best estimate of both the underlying scattering and absorbance from the oil was carried out through combining baselines of different oil concentrations, at or less than the dilution factor from the original emulsion concentration. Therefore, if a re-suspended emulsion was diluted by a factor of 4 for measurement, baselines of the SDS stabilized emulsion at this same dilution factor were combined with a higher dilution factor (e.g., 1/8), until absorbance matched the sample at

long wavelength. The amino acid composition of WPCH was used to determine the molar extinction coefficient and mean residual weight (Anthis & Clore, 2013) for all samples.

Another effect of light scattering from the emulsions is a change in the underlying CD baseline, due to the very different paths of light through the system compared to normal solution measurements. The SDS stabilized emulsion, produced in the same way as for the WPCH, enables the light scattering effects to be reasonably-well reproduced and therefore allowing a baseline correction of the peptide stabilized emulsions. Before analysis, all spectra were zeroed at long wavelength (270-280 nm), where no CD signal from the sample occurs.

The proportions of each secondary structure components were determined using a web-based calculation server DICHROWEB that incorporates various methods and a wide range of protein spectral databases (Whitmore & Wallace, 2007). The calculation method used in this study was CDSSTR with the reference set SMP180 (Abdul-Gader et al., 2011; Sreerama & Woody, 2000). These data were supported through additional fitting using SELCON3 analysis and the SMP180 reference set. Further details can be found in Section S3 of the Supplementary Information. Due to the nature of the emulsions, in particular due to the scattering which occurs from the droplets, the accuracy of peptide concentration determination is lower than for those in solution. In view of this, although the CDSSTR and SELCON3 routines report both regular and distorted α-helix and β-sheet structures, we report only the total helix and sheet structure to avoid over interpretation of the details of the structure content calculations. However, despite these higher uncertainties for the emulsions, which may affect the absolute values obtained through the secondary structure fitting, relative changes in the structure determination are still credible and the changes in CD spectral shapes from solution to emulsion samples reflecting significant folding changes are clearly observed.

2.8 Statistical analysis

The secondary structure fitting data were subjected to analysis of variance (ANOVA) by using Statgraphics version 5.1 (Statistical Graphics Corp., Rockville, MD, USA). Tukey´s multiple range test was used to determine significant differences between mean values. Differences between mean values were considered significant at a level of confidence of 95% ($p < 0.05$).

3. RESULTS AND DISCUSSION

3.1 Secondary structure of WPCH in solution and at the O/W interface

The far-UV SRCD spectra and the secondary structure composition (% α-helix, β-strands, turns and unordered) of WPC and WPCH in solution and at the tricaprylin oil-water interface (pH 2 or pH 8) are shown in Figure 33 and Figure 34 (with full data sets shown in Figure S 8).

Irrespective of the pH, the SRCD spectra of WPC in solution (Figure 33A,B) showed a minimum at ca. 210 nm, a zero crossing at ca. 200 nm and a maximum at 190 nm, which is characteristic of proteins with a β-sheet-rich structure (Zhai et al., 2011). Although a high content of α-helical structure in solution has been found for other proteins contained in whey (e.g., α-lactalbumin and BSA) (Day et al., 2014; Zhai et al., 2012), β-lactoglobulin (β-LG) has been reported to exhibit a β-sheet-dominant conformation (Zhai et al., 2010, 2011; Zhang & Keiderling, 2006). The latter could explain our results since β-LG constitutes ca. 60% of whey proteins (Khan et al., 2019) and its high content may mask the contribution of other proteins present in lower quantity in terms of the secondary structure (e.g., ~15% of α-lactalbumin and ~8% BSA). The calculated ordered secondary structure composition of WPC is in agreement with previous studies of β-LG secondary structure in solution (16 and 33% of α-helix and β-sheet, respectively) (Zhai et al., 2011), with disordered structures (turns and unordered regions) of WPC in solution accounting for ~54% (Figure 34A).

On the contrary, the far-UV SRCD spectra of WPCH showed a maximum at ca.185 nm and only a minimum at 200 nm (Figure 33C,D), indicating a predominantly unordered structure in aqueous solution (Hoffmann et al., 2016), both at pH 2 and pH 8 (around 60% is made up of turns and unordered regions) (Figure 34A). The ordered structure is predominantly β-sheet, with less than 10% α-helix structure (Figure 34A). These changes in the conformation of WPCH in solution with respect to the WPC are a consequence of protein hydrolysis, since similar heat treatment using the hydrolysis conditions, but without enzyme (WPC + heat), did not significantly modify the secondary structure of WPC (Figure S 9 and Figure S 10). Hence, it can be concluded that enzymatic hydrolysis resulted in peptides with lower α-helix structure and higher unordered regions in solution than the parent protein, regardless of the pH (Figure 34A).

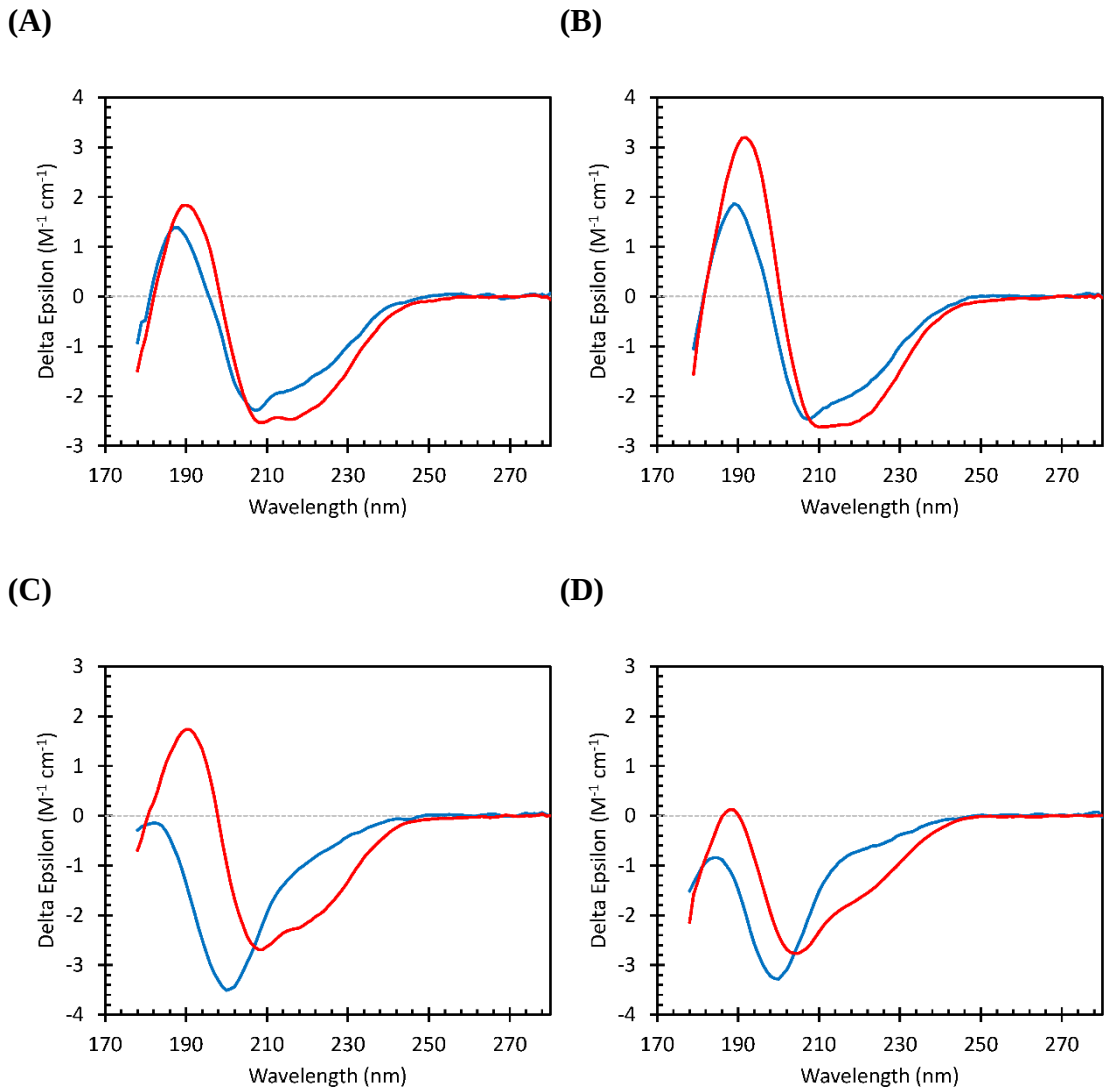

Figure 33. Far-UV SRCD spectra in solution (blue line) or at the tricaprylin oil-water interface (red line) of (A) WPC at pH 8, (B) WPC at pH 2, (C) WPCH at pH 8, and (D) WPCH at pH 2. Light scattering of oil droplets in the emulsions was corrected using sodium dodecyl sulfate (SDS)-stabilized emulsions. WPC: whey protein concentrate; WPCH: whey protein concentrate hydrolysate. The data presented here are averaged over several replicates for each sample. Fig S 7 includes the spectra of all replicates, plotted with the averaged data. Secondary structure analysis was carried out on the averaged curves.

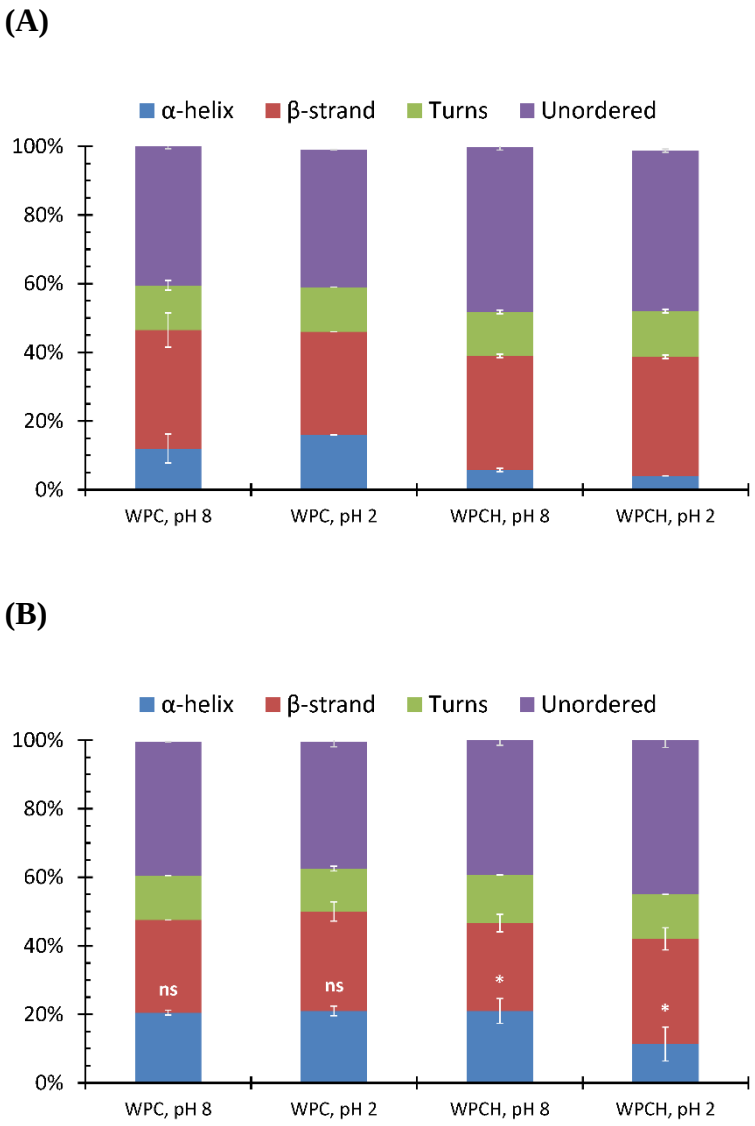

*Figure 34. Secondary structure composition (% α-helix, β-strand, turns and unordered) of whey protein concentrate (WPC) or whey protein concentrate hydrolysate (WPCH) in (A) solution, and (B) adsorbed at the tricaprylin oil-water interface at pH 8 or pH 2. The results derived from deconvolution of the respective SRCD spectra. For each emulsifier at fixed pH, ns: denotes not significant differences ($p > 0.05$) in % α-helix between solution and at the tricaprylin oil-water interface, whereas *: denotes significant differences ($p < 0.05$).*

In order to study the conformational changes induced by the adsorption of the native protein (WPC) or peptides (WPCH) at the O/W interface, the excess of un-adsorbed protein/peptides in the continuous phase was removed by centrifuging the parent emulsions (Section 2.6). The far-UV SRCD spectrum of an emulsion is comprised of signals from both protein/peptides present in the aqueous phase and at the O/W interface. Thus, to study solely the protein/peptides conformation at the O/W interface, there should be a minimum of un-adsorbed protein in the system (Zhai et al., 2010, 2012). As shown in Figure S 12, the emulsions had a very high content of un-adsorbed protein/peptides in the aqueous phase,

since the CD spectra of the untreated emulsions were practically the same that the ones obtained for the solutions. Indeed, the spectra shown for the aqueous phase separated from the emulsions were almost identical to those of untreated emulsions and solutions (Figure S 12), which highlights the importance of the centrifugation step for studying protein/peptide conformation at the interface. Figure 33 shows that the adsorption of WPC and WPCH at the O/W interface induced changes in their secondary structure when compared to the structure in solution. The CD spectra of WPC and WPCH adsorbed at the O/W interface are characteristic of a more α-helix-rich secondary structure showing two double minima at 209 nm and 222 nm and a maximum at ca. 190 nm (Hoffmann et al., 2016). In the case of WPC, the α-helical content increased by around 10% going from the solution to the tricaprylin O/W interface, which was accompanied by a slight decrease in both the β-sheet content and disordered structures. These structural changes are due to the reorientation of hydrophobic residues of proteins in WPC towards the oil phase in the emulsion, thus enhancing the interaction protein-oil (Zhai et al., 2011). However, although these results are consistent with previous studies on the secondary structure of β-LG upon adsorption at the O/W interface (Zhai et al., 2010, 2011), the increase of α-helical structure, compared to that in solution, was not statistically significant ($p > 0.05$) in the case of WPC (Figure 34B). On the contrary, a significant ($p < 0.05$) increase in α-helical structure was found for WPCH at the O/W interface when compared to solution (Figure 34B). Although protein hydrolysis of WPC gave rise to peptides with a highly unordered structure in aqueous solution (~60%) and high β-sheet content, adsorption of peptides present in WCPH at the O/W interface resulted in a slight lipid-induced β-to-α conformational transition. The non-native α-helical content increased by more than 10% going from aqueous solution to the O/W interface, with a concomitant β-sheet reduction. Furthermore, and similarly to WPC, the emulsion pH (pH 2 or pH 8) had a minor effect on the secondary structure of protein/peptides upon adsorption at the O/W interface. However, it should be noted that the pH 2 emulsions had a lower physical stability than those at pH 8, noticeable at time of measurement as inhomogeneity of the sample, resulting in a more significant variation in resulting spectra of peptide at the O/W interface (Figure S 8). These results contrast with previous studies on the role of electrostatic interactions on whey proteins (β-LG)-lipids associations (Zhang & Keiderling, 2006). The authors reported that these associations were strongly affected by the protein net charge since at pH values under the protein isoelectric point (pI = 5.5) the lipid-induced non-native α-helical structure could be further increased at the expense of both β-sheet and unordered structures, contrary to what occurred at pH values above the pI. However, our

results suggest that hydrophobic interactions played a major role (over electrostatic interactions) on conformational changes of protein/peptides when adsorbed at the O/W interface. It has been previously reported that structural changes of protein/peptides upon adsorption to the interface in emulsions are largely driven by the hydrophobic effect due to reorientation and solvation of the hydrophobic region of proteins/peptides towards the oil phase (Bañuelos & Muga, 1996).

Furthermore, our results show that hydrophobic interactions were enhanced in the case of WPCH over WPC, since the content of α-helical structure significantly increased at the O/W interface compared to that in solution (Figure 34B). This is explained on the basis that protein hydrolysis resulted in smaller and more flexible peptides, thus favouring the exposure and interaction of the hydrophobic residues with the oil phase (O. Regan & Mulvihill, 2010; Rahali et al., 2000).

3.2 Thermal stability of WPCH in solution and at the O/W interface

The thermal stability of WPCH in aqueous solution and adsorbed at the tricaprylin O/W interface (pH 2 and pH 8) was investigated by recording the far-UV SRCD spectra of the samples at different temperatures (from ca. 6 °C to 85 °C) (Figure 35 and Figure 36). These measurements were carried out on two replicates of each solution sample. After heating, the samples were cooled back to 25 °C. In addition, at the spectra minima wavelengths (WLs), the CD signal evolution with temperature was extracted and fit to a sigmoidal curve from which the melting (transition) temperature (Tm) of the system was determined (Section 6.5 in the Supplementary Information).

In solution, the CD spectra of WPCH remained relatively unaltered up to ca. 38 °C regardless of the pH (Figure 35). However, from 43 °C onward, the intensity of the spectra decreased gradually with the shape changing slightly, and was then completely lost at temperatures above 66 °C (flat spectra). These changes in the CD spectra of the peptides in solution are representative of a heat-induced denaturation of the secondary structure and the stability of the sample in the cell, yet this was partially reversible since some of the structure was recovered after re-cooling to 25 °C. The Tm of WPCH in solution was not affected by the pH, with similar values at pH 2 or pH 8 of ~52 ±1 °C (determined from the sigmoidal fits, Section 6.5 of the Supplementary Information, with the CD signal data recorded at 200 nm for all sample replicates).

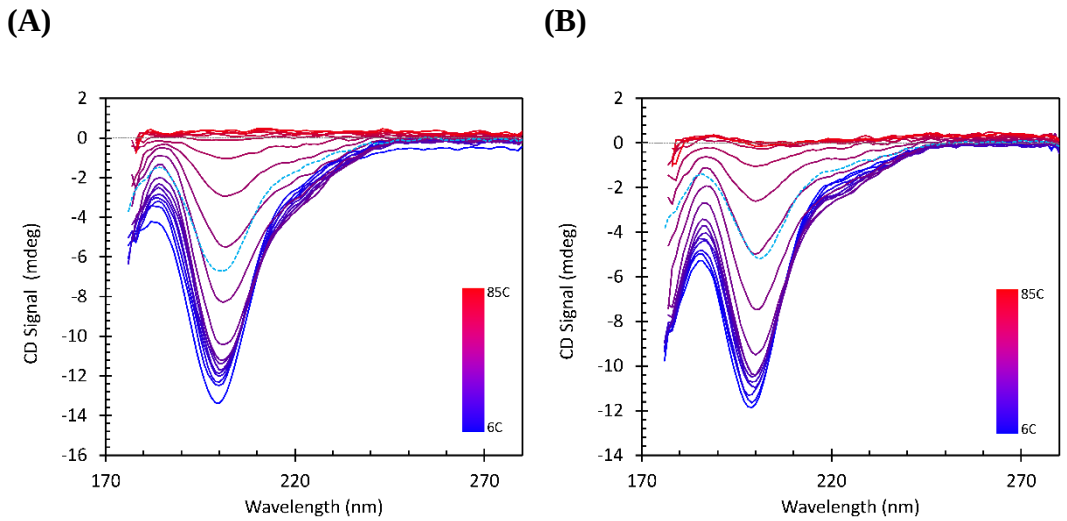

Figure 35. Effect of temperature on the conformation of whey protein hydrolysate WPCH in solution at pH 8 (A) and at pH 2 (B). The data have been treated using 10 mM sodium phosphate buffer baselines and zeroed at long wavelengths (270-280 nm). The spectra also contain a small contribution from lactose at wavelengths below 193 nm. The light blue dotted curves are the spectra measured after the system was re-cooled to 25 °C.

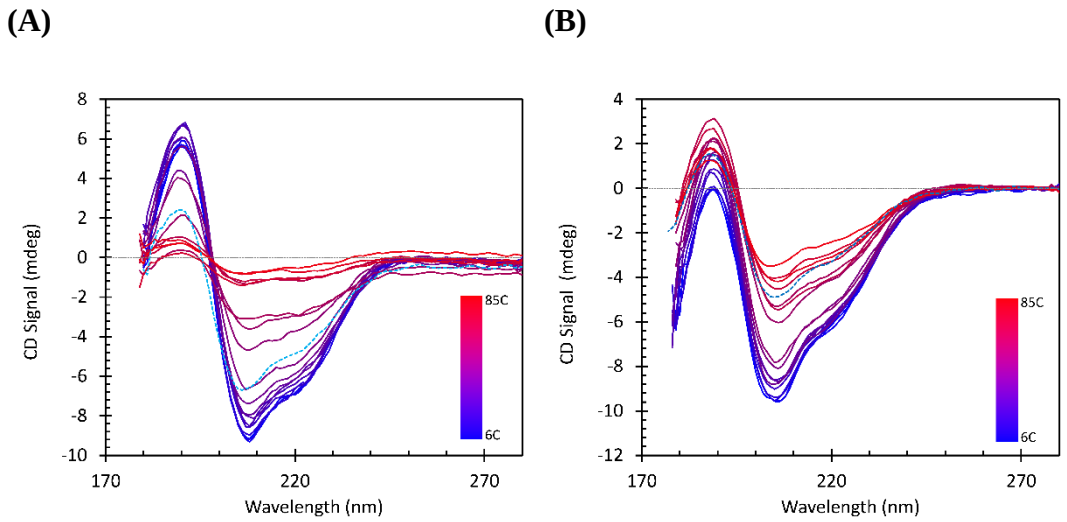

Figure 36. Effect of temperature on the conformation of whey protein hydrolysate (WPCH) at the tricaprylin oil/water interface at pH 8 (A) and pH 2 (B). The data have been treated using an SDS stabilized emulsion measured at each temperature and zeroed at long wavelengths (270-280 nm). See S6.5 in the SI for more details.

There is a higher degree of uncertainty interpreting the temperature measurements on the emulsion samples (Figure 36). Due to the scattering nature of the system and the change in scattering occurring as the temperature is increased, matching an underlying baseline for each temperature step is difficult. Figure S 17 shows the scans of an SDS stabilized emulsion taken with the same scanning parameters as for the samples. It clearly shows the changing nature of the scattering from the emulsion and therefore the underlying CD baseline of the system which will occur in these samples. However, there is no guarantee that an SDS

stabilized emulsion will change in the same way as one containing the WPCH peptide. Therefore, in order to determine how much the baseline may affect the outcome, temperature scans were also treated using a single SDS emulsion baseline taken at room temperature for all temperatures. A full description and all data produced in this way are presented in Section 6.5 of the Supplementary Information. Another factor which may affect these emulsion temperature scans is the stability (due to the age) of an emulsion sample. Measurements of WPCH emulsions at both pH 8 and pH 2 were repeated on separately prepared samples, though prepared at the same time, and more significant differences in behavior were seen compared to the solution samples.

The data presented in Figure 36 have been treated with baselines measured on an SDS emulsion taken at the same temperature as the sample. Despite these additional difficulties, the behavior of WPCH at the O/W interface system with increasing temperature is apparently different to that in solution. Although the CD signal for the solution samples at higher temperature becomes zero from temperatures around 70 °C (Figure 35 and Figs in Section 6.5.1 of the Supplementary Information), the emulsion systems appear to show a higher level of stability, with a significant CD signal from the peptide remaining even at the highest temperature (Figure 36), particularly at pH 2. These results suggest that the α-helical structure of WPCH at the O/W interface was retained to a higher extent at pH 2, so the peptides adsorbed at the interface are less prone to unfolding and aggregation upon heating. Furthermore, the range of temperatures over which the CD signal changed along the sigmoidal (data recorded at 209 nm and 222 nm) was broader at pH 2 than at pH 8 (Figure S 18-Figure S 25). These results contrast with the calculated secondary structure of the peptides in WPCH adsorbed at the O/W interface (Figure 34B) since slightly higher α-helical content was found for WPCH adsorbed at the O/W interface at pH 8 than at pH 2, which does not explain the observed slightly lower thermal stability of WPCH at the O/W at pH 8 when compared to pH 2.

The errors associated with the repeated measurements of the samples (Section 6.5.3 of the Supplementary Information) make it difficult to be certain of a change in stability of the peptides at the O/W interface based on the thermal stability alone. For samples at pH 8 there is no apparent difference in the transition temperature, and for pH 2, the difference in transition temperature between the solutions and O/W interface is marginally outside one standard deviation of the error. However, combined with the CD spectra, which indicate that a signal from the peptide could still be observed at the highest temperatures for those in the

O/W interface samples, this suggests an improvement of stability of the peptide at the O/W interface. These results are consistent with other studies on the thermal stability of whey proteins at the O/W interface (e.g., α-lactalbumin, β-LG, BSA), which reported that protein adsorption at the O/W interface resulted in an enhanced resistance to thermal denaturation compared to proteins in solution (Day et al., 2014; Zhai et al., 2010, 2011, 2012; Zhang & Keiderling, 2006). The latter might be attributed to an enhanced hydrophobic accessible surface area while these peptides are in contact with oil at the oil/water interface.

Although WPCH adsorption to the O/W interface only slightly improved the thermal stability of peptides at pH 8 in the present study, it has been reported that at these conditions their emulsifying properties are optimal (Padial-Domínguez, Espejo-Carpio, Pérez-Gálvez, et al., 2020). These authors studied the influence of pH on the emulsifying activity index (EAI) and the emulsifying stability index (ESI) of WPCH and found that these were maximized at pH 8. Furthermore, a recent study on the interfacial properties of WPCH reported that WPCH at pH 8 showed higher interfacial adsorption and led to an interface with higher dilatational modulus than at pH 2. These enhanced interfacial properties of WPCH at pH 8 favored the formation of smaller oil droplets in emulsions and a more resistant interfacial peptide layer leading to higher physical stability of emulsions stabilized with WPCH at pH 8 compared to pH 2 (Ruiz-Álvarez et al., 2021). Indeed, it is worth mentioning that differences in the physical appearance of emulsions was observed before measuring SRCD, with the emulsion stabilized with WPCH at pH 2 exhibiting creaming which was not observed for the emulsion stabilized at pH 8. Thus, the creaming in emulsion at pH 2 could affect the interaction of peptides at the interface influencing their thermal stability, although further research is required to confirm this.

WPCH has been used as emulsifier to produce fish oil-in-water emulsions (Padial-Domínguez, Espejo-Carpio, García-Moreno, et al., 2020) and fish oil-loaded microcapsules (Rahmani-Manglano, González-Sánchez, et al., 2020), both at pH 8, showing high physical and oxidative stability. Hence, in the following section we aim to study the influence of the encapsulating agent and the drying method on the secondary structure of WPCH at the O/W interface at pH 8.

3.3 Effect of the encapsulating agent and the drying method on the secondary structure of WPCH at the O/W interface

Before studying the influence of the drying method, e.g., spray-drying or electrospraying, on the secondary structure of WPCH used as emulsifier to produce tricaprylin-loaded micro/nanocapsules, the influence of the encapsulating agents used for that purpose (e.g., GS, MD, PUL) on the secondary structure of WPCH in solution and at the O/W interface (pH 8) was investigated (Figure 37). The spectra have been treated using the appropriate concentration of encapsulating agent included in the baseline scans as GS, MD and PUL have significant CD signals at low wavelengths starting below 200 nm, in order to remove any contribution from them in the final spectra (Section 6.6 of the Supplementary Information).

In aqueous solution, the delta epsilon plots of all the different samples overlapped, showing the same shape with the positive and negative peaks at ca. 185 nm and 200 nm, respectively (Figure 37A). The similarities of the plots indicate that the addition of the encapsulating agents (e.g., GS, MD and/or PUL) did not modify the secondary structure of the peptides present in WPCH in solution. This indicates that there is not a significant interaction between these carbohydrates and WPCH. For samples of WPCH adsorbed at the O/W interface (pH 8), these were treated in the same way as the other emulsions samples, centrifuging the emulsion to remove the majority of the aqueous portion and re-suspending the oil portion in the buffer. However, while any minimal remaining contribution from lactose in previous samples could be ignored due to the very low starting concentration and CD signal (Section 6.6 of the Supplementary Information), these samples contain significant amounts of encapsulating agents with large CD signals. These may not be completely removed in the process of separating the oil portion from the emulsion, leaving an unknown quantity of encapsulating agents in the measured O/W interface samples. As it is not known how much remains, the spectra have not been treated to remove them thus the resulting spectra may have contributions from these encapsulating agents below 200 nm. Despite this, the addition of the encapsulating agents does not appear to significantly change the CD signal intensities of the spectra and, as has occurred with WPCH in solution, the shape and peaks of the spectra remained similar among the samples (Figure 37B). Hence, the results found for the peptides' CD spectra in emulsion in the presence of encapsulating agents (Figure 37B) are consistent with those of the peptides' CD spectra in solution (Figure 37A) such that the same conclusion

was drawn: the addition of encapsulating agents did not affect the secondary structure of WPCH at pH 8 in solution or at the O/W interface in any significant way.

(A)

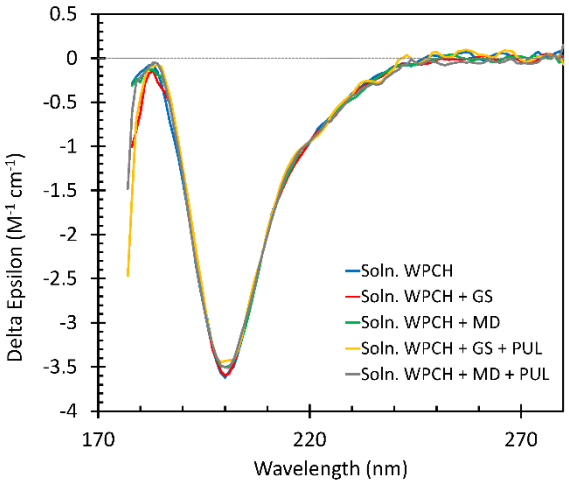

(B)

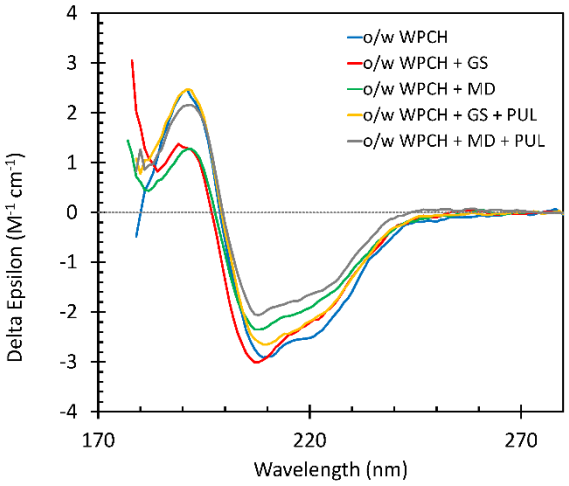

Figure 37. Effect of the encapsulating agent on the conformation of whey protein hydrolysate (WPCH) in (A) solution, and (B) at the tricaprylin oil/water interface. GS: glucose syrup. MD: maltodextrin. PUL: pullulan.

Figure 38 shows the far-UV SRCD spectra of the parent emulsions dried to produce the micro/nanocapsules and the reconstituted emulsions, i.e., those produced after re-dissolving the obtained micro/nanocapsules in buffer at pH 8. It should be noted that both parent and reconstituted emulsions were centrifuged as described in Section 2.6 in order to remove the excess of WPCH in the aqueous phase.

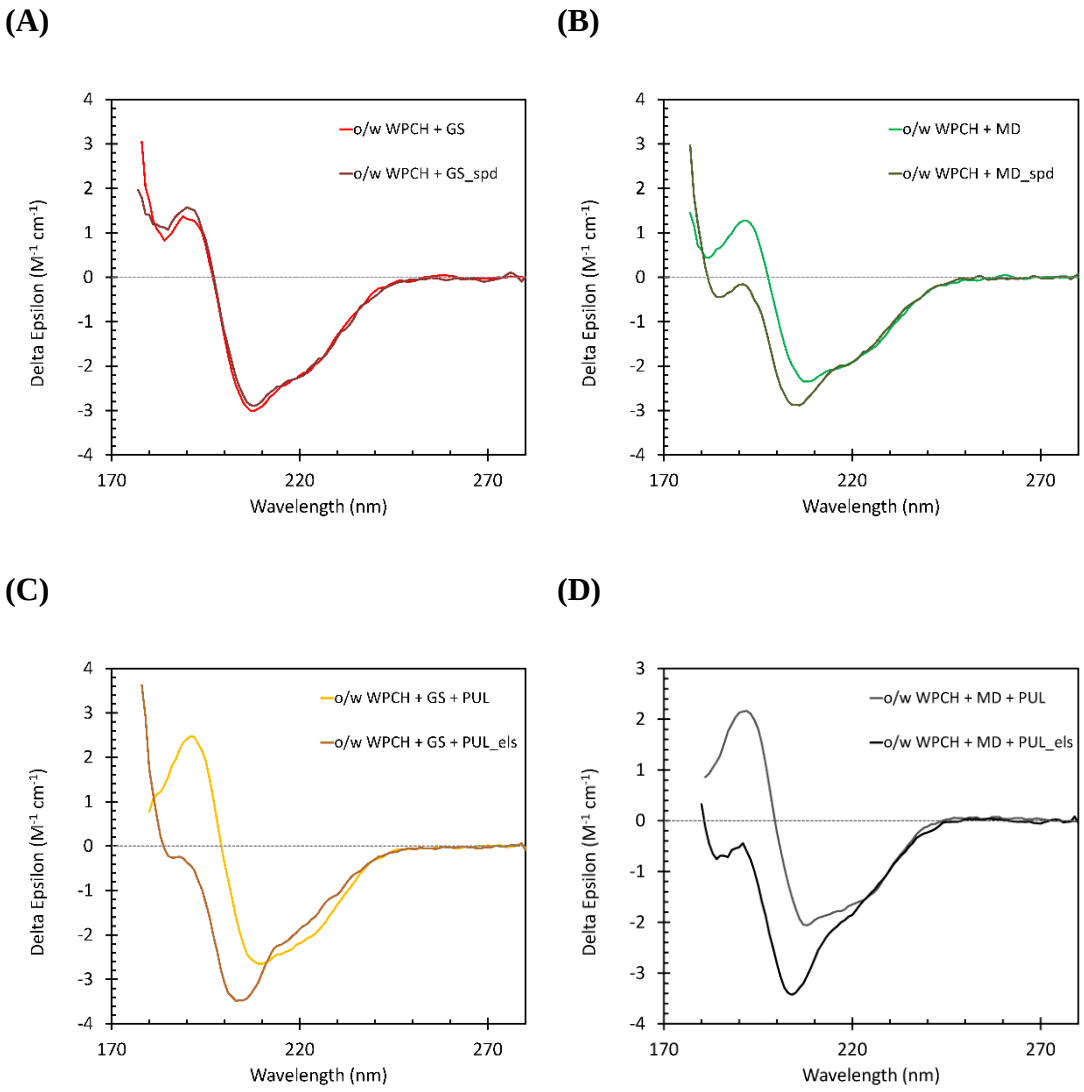

Figure 38. Effect of the drying method on the conformation of whey protein hydrolysate (WPCH) at the tricaprylin oil/water interface at pH 8: (A) and (B) capsules obtained by spray-drying (spd), (C) and (D) capsules obtained by electrospraying (els). GS: glucose syrup. MD: maltodextrin. PUL: pullulan.

After spray-drying for both encapsulating agents, GS or MD, it was found that the structure of WPCH adsorbed at the O/W interface remained practically unaltered since the shape of the CD spectra of both the parent and reconstituted emulsions were the same (Figure 38A,B). After drying, it could be observed that the positive and negative peaks were found at practically the same WLs (190, 209, and 222 nm, respectively). Spray-drying might denature proteins due to thermal stress, shear stress, air-liquid interfacial stress and/or dehydration stress (Kusonwiriyawong et al., 2009). Nonetheless, our results show that these stresses were not sufficient to significantly change the conformational structure of the peptides present in WPCH and adsorbed at the O/W interface during spray-drying. In this line, Anandharamakrishnan et al. (2007) reported that moderate outlet gas temperatures (60 - 80

°C) could prevent excessive denaturation of whey protein isolate (WPI) during spray-drying, which was studied by differential scanning calorimetry (DSC). Likewise, Haque et al. (2015) spray-dried WPI at 180/80 °C (inlet/outlet air temperature, respectively) without significant protein loss due to denaturation and/or aggregation, although the secondary structure composition was different from that of unprocessed WPI (slight decrease in α-helix and β-sheet content). Furthermore, Kusonwiriyawong et al. (2009) studied the secondary structure of untreated BSA and BSA (5 or 10 %w/w) after spray-drying in the presence of chitosan (1 %w/v) at 100/63 °C (inlet/outlet air temperature) and found that the respective CD spectra, represented as molar ellipticity, overlapped. The latter is line with our results, where no conformational changes of WPCH at the O/W interface were observed between the parent and reconstituted emulsions when spray-drying the parent emulsions (180/90 °C inlet/outlet air temperature). Despite the use of high drying temperatures (100 - 200 °C), spray-drying (in the co-current operational mode) has been reported as a suitable method to produce microcapsules loaded with heat-sensitive bioactive compounds (Rahmani-Manglano, García-Moreno, et al., 2020). Atomization of the infeed emulsion/dispersion results in fine droplets which assures that the internal mass transfer rate is high enough to evaporate most of the solvent at the inlet air wet bulb temperature (T_{wb}) (constant- rate drying period). Subsequently, in the falling-rate drying period, the external mass transfer (from the surface of the droplet to the air) is also high allowing a reduced contact time, therefore very short residence time of the microcapsules in the drying chamber (5 - 30s). Furthermore, in the co-current operational mode, the temperature of the dried product is 15 - 20 °C lower than that of the outlet air temperature, thus limiting thermal degradation (Anandharamakrishnan et al., 2007; Kusonwiriyawong et al., 2009).

On the other hand, the CD spectra of WPCH adsorbed at the O/W interface prior to and after electrospraying were different for both of the main encapsulating agents assayed, GS or MD (Figure 38C,D), suggesting that the secondary structure of WPCH at the O/W interface changed during processing by electrospraying. The shape of the CD spectra after electrospraying for both emulsions containing GS and MD are representative of proteins/peptides with a high content of irregular structure showing a sharp minimum at ca. 200 nm (Figure 38C,D) (Hoffmann et al., 2016). Electrospraying is based on applying a high-voltage electrostatic field to charge the surface of a solution that is ejected from the tip of the injector in the form of fine droplets due to Coulombic repulsion forces (Jacobsen et al., 2018). The process is carried out at room temperature, thus thermal degradation is

avoided. Therefore, this technique has gained attention as an alternative to conventional spray-drying for the production of micro/nanocapsules loaded with thermo-sensitive compounds (e.g., vitamins, probiotics, antioxidants, and omega-3 oils) (Jacobsen et al., 2018). However, the dispersion/emulsion to be dried is subjected to electrostatic stresses, which could also cause some degradation of the components during processing. In this regard, Xiang et al. (2008) studied the effect of pulsed electric fields (PEFs) on the structural modification of WPI, by tryptophan emission fluorescence spectroscopy. This technique gives information on the hydrophobicity or hydrophilicity of the environment to which tryptophan residues (Trp), originally buried in the hydrophobic core of globular proteins, are exposed. At an excitation WL of ca. 295 nm, Trp buried inside the globular protein core emits at WLs with a maximum at ca. 335 nm. However, when Trp are exposed to a hydrophilic environment (e.g., aqueous solvent due to protein denaturation) a red shift to higher WLs occurs, with a maximum at ca. 355 nm (Zhai et al., 2013). This technique has been widely used to study conformational changes of proteins contained in whey (e.g., α-lactalbumin, β-LG or BSA) either in solution or adsorbed at the O/W interface (Casterlain & Genot, 1994; Zhai et al., 2011, 2012). In the study by Xiang et al. (2008), the authors reported that increasing the electric field intensity (from 20 kV/cm to 30 kV/cm) and the number of pulses (from 10 to 20 pulses) resulted in an increased fluorescence intensity of WPI, related to protein conformational changes which was further confirmed by DSC. The results showed that WPI subjected to an electric field of 20 kV/cm and 30 pulses denatured ~44% of the protein. Correspondingly, Perez & Pilosof (2004) found that β-LG was denatured by PEF (an electric field intensity of 12.5 kV/cm denatured 40% of protein after 10 pulses). The authors explained protein denaturation on the basis that, under an electric field, β-LG underwent conformational changes that would have exposed hydrophobic residues and the sulfhydryl group (SH), promoting hydrophobic and SH/S-S interactions, and therefore leading to protein aggregation. In the same line as the aforementioned studies, our results point to the electrostatic field applied between the injector and the collector of the electrospraying setup while the parent emulsions are sprayed/dried causing the secondary structural changes of the peptides present in WPCH and adsorbed at the O/W interface. Moreover, it is worth mentioning that electrosprayed capsules (80% of the capsules were below 1 μm) had a considerably lower size when compared to spray-dried capsules (90% of the capsules were below 20 μm) (results not shown). The reduced size of the electrosprayed capsules, when compared to spray-dried capsules, could also affect the observed changes in interfacial structure. In any case, further research is required to investigate how the

electrospraying processing conditions (e.g., voltage, flow-rate, and distance from injector to collector) and particle size influence protein/peptide conformation when adsorbed at the O/W interface.

4. CONCLUSIONS

Protein hydrolysis of WPC to a low DH (10%) resulted in peptides (WPCH) with a lower α-helical structure in solution than the parent protein, and with a more unordered structure (< 10% α-helix structure and ca. 60% turns and unordered regions). However, WPC and WPCH adsorption to the O/W interface led to an increase in the α-helical content (> 10% increase in the case of WPCH), accompanied by a concomitant slight reduction of β-sheet and unordered regions. This lipid-induced conformational transition was more pronounced in the case of WPCH. Moreover, our results showed that pH (pH 2 and pH 8) had little effect on the WPC or WPCH conformation in solution and at the O/W interface. Although protein/peptides-lipid interactions are governed by electrostatic and hydrophobic interactions, our results show that the latter was the major driving force since pH, and thus the protein/peptides net charge, did not modify WPC nor WPCH secondary structure either in solution or at the O/W interface. In addition, it was found that WPCH adsorbed at the O/W interface slightly enhanced its thermal stability, particularly at pH 2. The presence of the encapsulating agents (e.g., glucose syrup or maltodextrin) did not affect the secondary structure of WPCH both in solution and at the O/W interface. Finally, it was found that the stresses exerted by spray-drying (e.g., thermal stress, shear and interfacial stress) were not sufficient to denature the peptides present in WPCH when adsorbed at the O/W interface. However, although electrospraying was carried out at room temperature, electrostatic stresses derived of applying high voltage to the emulsion caused structural changes in the peptides present in WPCH when adsorbed at the O/W interface.

5. REFERENCES

Abdul-Gader, A., Miles, A. J., & Wallace, B. A. (2011). A reference dataset for the analyses of membrane protein secondary structures and transmembrane residuesusing circular dichroism spectroscopy. *Bioinformatics*, *27*(12), 1630–1636. https://doi.org/10.1093/bioinformatics/btr234

Anandharamakrishnan, C., Rielly, C. D., & Stapley, A. G. F. (2007). Effects of process variables on

the denaturation of whey proteins during spray drying. *Drying Technology*, *25*(5), 799–807. https://doi.org/10.1080/07373930701370175

Anthis, N. J., & Clore, G. M. (2013). Sequence-specific determination of protein and peptide concentrations by absorbance at 205 nm. *Protein Science*, *22*(6), 851–858. https://doi.org/10.1002/pro.2253

Bañuelos, S., & Muga, A. (1996). Structural requirements for the association of native and partially folded conformations of α-lactalbumin with model membranes. *Biochemistry*, *35*(13), 3892–3898. https://doi.org/10.1021/bi951468v

Casterlain, C., & Genot, C. (1994). Conformational changes of bovine serum albumin upon its adsorption in dodecane-in-water emulsions as revealed by front-face steady-state fluorescence. *BBA - General Subjects*, *1199*(1), 59–64. https://doi.org/10.1016/0304-4165(94)90096-5

Day, L., Zhai, J., Xu, M., Jones, N. C., Hoffmann, S. V., & Wooster, T. J. (2014). Conformational changes of globular proteins adsorbed at oil-in-water emulsion interfaces examined by synchrotron radiation circular dichroism. *Food Hydrocolloids*, *34*, 78–87. https://doi.org/10.1016/j.foodhyd.2012.12.015

Elias, R. J., Kellerby, S. S., & Decker, E. A. (2008). Antioxidant activity of proteins and peptides. *Critical Reviews in Food Science and Nutrition*, *48*(5), 430–441. https://doi.org/10.1080/10408390701425615

García-Moreno, P. J., Yang, J., Gregersen, S., Jones, N. C., Berton-Carabin, C. C., Sagis, L. M. C., Hoffmann, S. V., Marcatili, P., Overgaard, M. T., Hansen, E. B., & Jacobsen, C. (2021). The structure, viscoelasticity and charge of potato peptides adsorbed at the oil-water interface determine the physicochemical stability of fish oil-in-water emulsions. *Food Hydrocolloids*, *115*(July 2020). https://doi.org/10.1016/j.foodhyd.2021.106605

Haque, M. A., Chen, J., Aldred, P., & Adhikari, B. (2015). Denaturation and Physical Characteristics of Spray-Dried Whey Protein Isolate Powders Produced in the Presence and Absence of Lactose, Trehalose, and Polysorbate-80. *Drying Technology*, *33*(10), 1243–1254. https://doi.org/10.1080/07373937.2015.1023311

Hoffmann, S. V., Fano, M., & van de Weert, M. (2016). Circular Dichroism Spectroscopy for Structural Characterization of Proteins. In *Analytical Techniques in the Pharmaceutical Sciences* (pp. 223–251). https://doi.org/10.1007/978-1-4939-4029-5_6

Horn, A. F., Green-Petersen, D., Nielsen, N. S., Andersen, U., Hyldig, G., Søgaard Jensen, L. H., Horsewell, A., & Jacobsen, C. (2012). Addition of fish oil to cream cheese affects lipid oxidation, sensory stability and microstructure. *Agriculture (Switzerland)*, *2*(4), 359–375. https://doi.org/10.3390/agriculture2040359

Jacobsen, C., García-Moreno, P. J., Mendes, A. C., Mateiu, R. V., & Chronakis, I. S. (2018). Use of Electrohydrodynamic Processing for Encapsulation of Sensitive Bioactive Compounds and Applications in Food. *Annual Review of Food Science and Technology*, *9*(1), 525–549. https://doi.org/10.1146/annurev-food-030117-012348

Khan, I. T., Nadeem, M., Imran, M., Ullah, R., Ajmal, M., & Jaspal, M. H. (2019). Antioxidant properties of Milk and dairy products: A comprehensive review of the current knowledge. *Lipids in Health and Disease*, *18*(1), 1–14. https://doi.org/10.1186/s12944-019-0969-8

Kusonwiriyawong, C., Pichayakorn, W., Lipipun, V., & Ritthidej, G. C. (2009). Retained integrity of protein encapsulated in spray-dried chitosan microparticles. *Journal of Microencapsulation*, *26*(2), 111–121. https://doi.org/10.1080/02652040802190937

Lam, R. S. H., & Nickerson, M. T. (2013). Food proteins: A review on their emulsifying properties using a structure-function approach. *Food Chemistry*, *141*(2), 975–984. https://doi.org/10.1016/j.foodchem.2013.04.038

Liceaga, A. M., & Hall, F. (2018). Nutritional, functional and bioactive protein hydrolysates. In *Encyclopedia of Food Chemistry*. Elsevier. https://doi.org/10.1016/B978-0-08-100596-5.21776-9

Miguel, G. A., Jacobsen, C., Prieto, C., Kempen, P. J., Lagaron, J. M., Chronakis, I. S., & García-Moreno, P. J. (2019). Oxidative stability and physical properties of mayonnaise fortified with zein electrosprayed capsules loaded with fish oil. *Journal of Food Engineering*, *263*, 348–358. https://doi.org/10.1016/j.jfoodeng.2019.07.019

Miles, A. J., Wien, F., & Wallace, B. A. (2004). Redetermination of the extinction coefficient of camphor-10-sulfonic acid, a calibration standard for circular dichroism spectroscopy. *Analytical Biochemistry*, *335*(2), 338–339. https://doi.org/10.1016/j.ab.2004.08.035

Nielsen, N. S., & Jacobsen, C. (2013). Retardation Of Lipid Oxidation In Fish Oil-Enriched Fish Pâté- Combination Effects. *Journal of Food Biochemistry*, *37*(1), 88–97. https://doi.org/10.1111/j.1745-4514.2011.00605.x

Nordén, B., Rodger, A., & Dafforn, T. (2010). *Linear Dichroism and Circular Dichroism: A textbook on polarized-light spectroscopy*. Royal Society of Chemistry.

O'Regan, J., & Mulvihill, D. M. (2010). Sodium caseinate-maltodextrin conjugate hydrolysates: Preparation, characterisation and some functional properties. Food Chemistry, 123(1), 21–31. https://doi.org/10.1016/j.foodchem.2010.03.115

Padial-Domínguez, M., Espejo-Carpio, F. J., García-Moreno, P. J., Jacobsen, C., & Guadix, E. M. (2020). Protein derived emulsifiers with antioxidant activity for stabilization of omega-3 emulsions. *Food Chemistry*, *329*(November 2019), 127148.

https://doi.org/10.1016/j.foodchem.2020.127148

Padial-Domínguez, M., Espejo-Carpio, F. J., Pérez-Gálvez, R., Guadix, A., & Guadix, E. M. (2020). Optimization of the emulsifying properties of food protein hydrolysates for the production of fish oil-in-water emulsions. *Foods*, *9*(5). https://doi.org/10.3390/foods9050636

Peighambardoust, S. H., Karami, Z., Pateiro, M., & Lorenzo, J. M. (2021). A review on health-promoting, biological, and functional aspects of bioactive peptides in food applications. *Biomolecules*, *11*(5), 1–21. https://doi.org/10.3390/biom11050631

Perez, O. E., & Pilosof, A. M. R. (2004). Pulsed electric fields effects on the molecular structure and gelation of β-lactoglobulin concentrate and egg white. *Food Research International*, *37*(1), 102–110. https://doi.org/10.1016/j.foodres.2003.09.008

Punia, S., Sandhu, K. S., Siroha, A. K., & Dhull, S. B. (2019). Omega 3-metabolism, absorption, bioavailability and health benefits–A review. *PharmaNutrition*, *10*, 100162. https://doi.org/10.1016/j.phanu.2019.100162

Rahali, V., Chobert, J. M., Haertlé, T., & Guéguen, J. (2000). Emulsification of chemical and enzymatic hydrolysates of β-lactoglobulin: Characterization of the peptides adsorbed at the interface. *Nahrung - Food*, *44*(2), 89–95. https://doi.org/10.1002/(sici)1521-3803(20000301)44:2<89::aid-food89>3.0.co;2-u

Rahmani-Manglano, N. E., García-Moreno, P. J., Espejo-Carpio, F. J., Pérez-Gálvez, A. R., & Guadix-Escobar, E. M. (2020). The Role of Antioxidants and Encapsulation Processes in Omega-3 Stabilization. In A. M.A. (Ed.), *Emulsion-based Encapsulation of Antioxidants. Food Bioactive Ingredients.* (pp. 339–386). Springer, Cham. https://doi.org/10.1007/978-3-030-62052-3_10

Rahmani-Manglano, N. E., González-Sánchez, I., García-Moreno, P. J., Espejo-Carpio, F. J., Jacobsen, C., & Guadix, E. M. (2020). Development of fish oil-loaded microcapsules containing whey protein hydrolysate as film-forming material for fortification of low-fat mayonnaise. *Foods*, *9*(5). https://doi.org/10.3390/foods9050545

Ruiz-Álvarez, J. M., Castillo-Santaella, T. del, Maldonado-Valderrama, J., Guadix, A., Guadix, E. M., & García-Moreno, P. J. (2021). pH influences the interfacial properties of blue whiting (M . poutassou) and whey protein hydrolysates determining the physical stability of fish oil-in-water emulsions. *Food Hydrocolloids*.

Sreerama, N., & Woody, R. W. (2000). Estimation of protein secondary structure from circular dichroism spectra: Comparison of CONTIN, SELCON, and CDSSTR methods with an expanded reference set. *Analytical Biochemistry*, *287*(2), 252–260. https://doi.org/10.1006/abio.2000.4880

Takeungwongtrakul, S., Benjakul, S., & H-Kittikun, A. (2015). Characteristics and oxidative stability of bread fortified with encapsulated shrimp oil. *Italian Journal of Food Science*, *27*(4), 476–486. https://doi.org/10.14674/1120-1770/ijfs.v380

Tamm, F., Gies, K., Diekmann, S., Serfert, Y., Strunskus, T., Brodkorb, A., & Drusch, S. (2015). Whey protein hydrolysates reduce autoxidation in microencapsulated long chain polyunsaturated fatty acids. *European Journal of Lipid Science and Technology*, *117*(12), 1960–1970. https://doi.org/10.1002/ejlt.201400574

Wallace, B. A., & Janes, R. W. (2001). Synchrotron radiation circular dichroism spectroscopy of proteins: Secondary structure, fold recognition and structural genomics. *Current Opinion in Chemical Biology*, *5*(5), 567–571. https://doi.org/10.1016/S1367-5931(00)00243-X

Whitmore, L., & Wallace, B. A. (2007). Protein secondary structure analyses from circular dichroism spectroscopy: Methods and reference databases. *Biopolymers*, *89*(5), 392–400. https://doi.org/10.1002/bip.20853

Xiang, B. Y., Ngadi, M. O., Simpson, M. V, & Ochoa-Martínez, L. A. (2008, July). *Effect of pulsed electric field on structural modification and thermal properties of whey protein isolate*. Conference paper for presentation at the CSBE/SCGAB 2008 Annual Conference, North Vancouver, British Columbia

Zhai, J., Day, L., Aguilar, M. I., & Wooster, T. J. (2013). Protein folding at emulsion oil/water interfaces. *Current Opinion in Colloid and Interface Science*, *18*(4), 257–271. https://doi.org/10.1016/j.cocis.2013.03.002

Zhai, J., Hoffmann, S. V., Day, L., Lee, T. H., Augustin, M. A., Aguilar, M. I., & Wooster, T. J. (2012). Conformational changes of α-lactalbumin adsorbed at oil-water interfaces: Interplay between protein structure and emulsion stability. *Langmuir*, *28*(5), 2357–2367. https://doi.org/10.1021/la203281c

Zhai, J., Miles, A. J., Pattenden, L. K., Lee, T. H., Augustin, M. A., Wallace, B. A., Aguilar, M. I., & Wooster, T. J. (2010). Changes in β-lactoglobulin conformation at the oil/water interface of emulsions studied by synchrotron radiation circular dichroism spectroscopy. *Biomacromolecules*, *11*(8), 2136–2142. https://doi.org/10.1021/bm100510j

Zhai, J., Wooster, T. J., Hoffmann, S. V., Lee, T. H., Augustin, M. A., & Aguilar, M. I. (2011). Structural rearrangement of β-lactoglobulin at different oil-water interfaces and its effect on emulsion stability. *Langmuir*, *27*(15), 9227–9236. https://doi.org/10.1021/la201483y

Zhang, X., & Keiderling, T. A. (2006). Lipid-induced conformational transitions of β-lactoglobulin. *Biochemistry*, *45*(27), 8444–8452. https://doi.org/10.1021/bi0602967

6. SUPPLEMENTARY MATERIAL

6.1 All data for WPC and WPCH in solution and at the O/W interface

Solution spectra have been treated to remove the contribution of lactose through subtraction of a lactose spectrum at the appropriate concentration (See 6.6). As the samples for the O/W interface are produced through centrifugation and removal of the majority of the aqueous portion of the emulsion, it is assumed that the lactose is largely removed and therefore no adjustment for lactose is made to the O/W interface spectra. It is possible that a very minor contribution from lactose remains, but it is not possible to determine how much this may be.

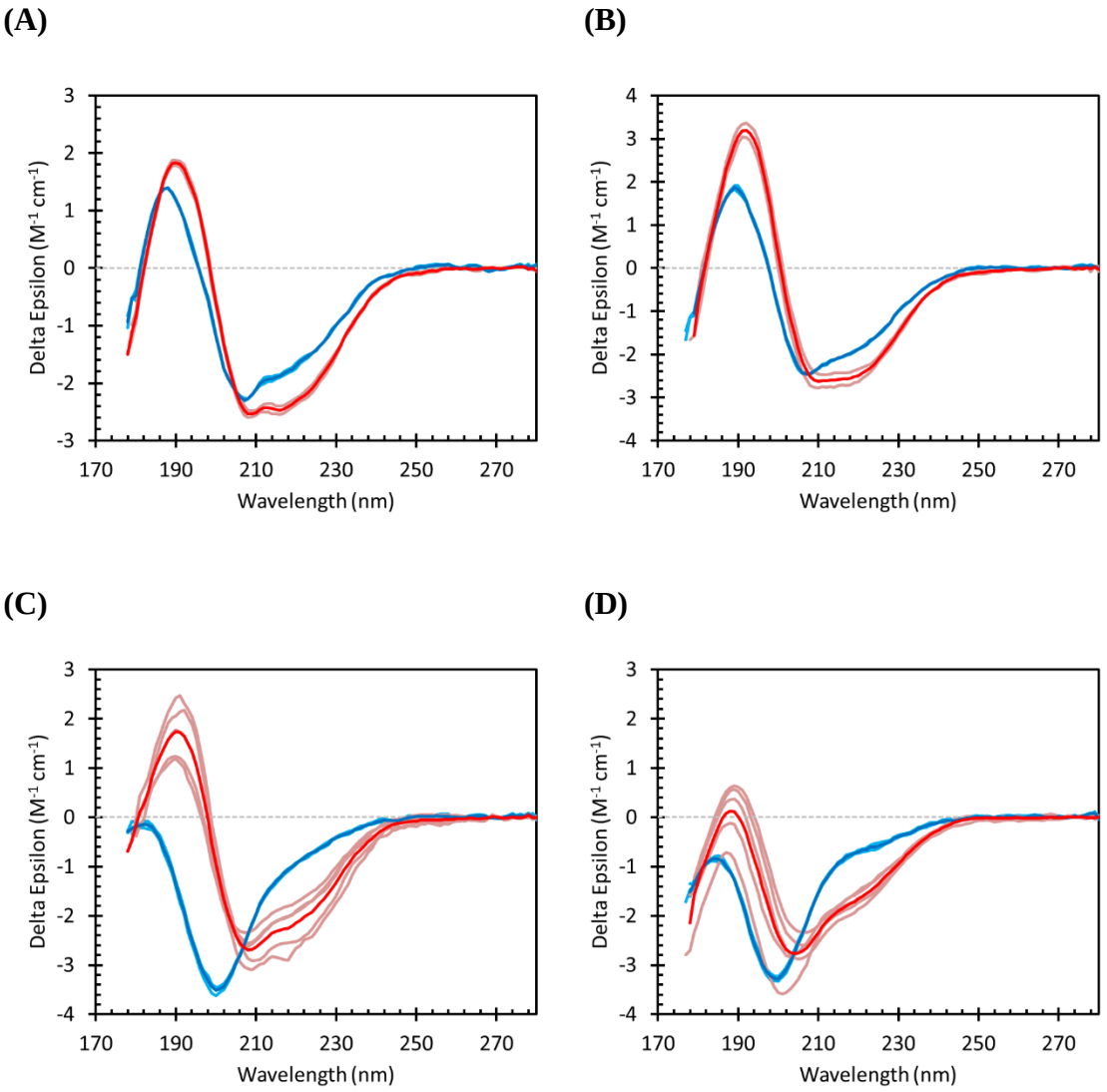

Figure S 8. Spectra of all replicates and averages (solutions, light blue with average in dark blue, at the O/W interface in brown with average in red), for (A) WPC pH 8, (B) WPC pH 2, (C) WPCH pH 8 and (D) WPCH pH 2.

6.2 Comparison of WPC with heat-treated WPC

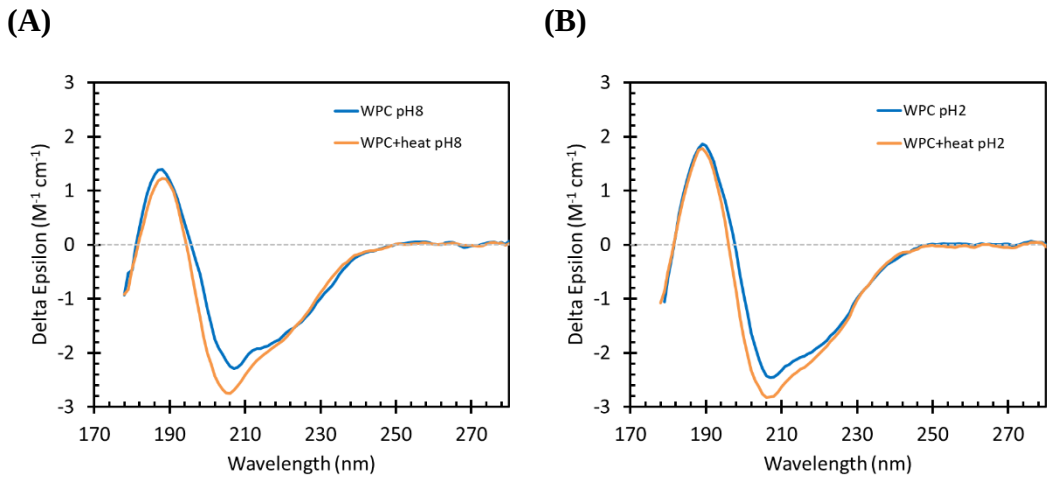

Figure S 9. Far-UV SRCD spectra in solution of WPC or WPC with heat treatment at (A) pH 8 or (B) pH 2.

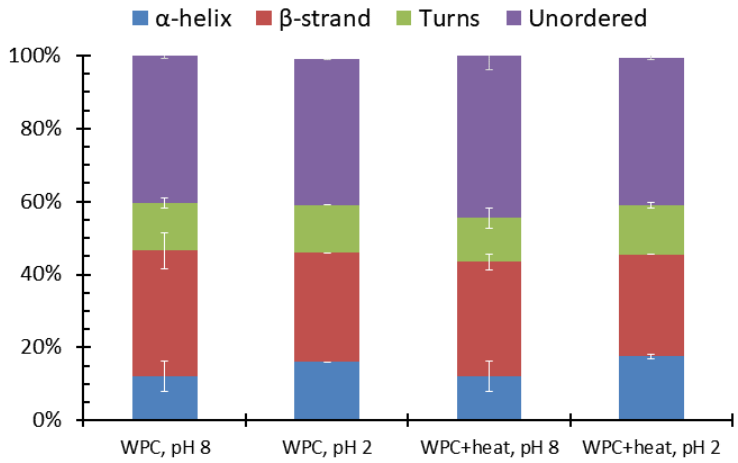

Figure S 10. Secondary structure composition (% α-helix, β-strand, turns and unordered) of whey protein concentrate (WPC) or WPC with heat treatment in solution at pH 8 or 2. The results are derived from deconvolution of the respective SRCD spectra.

6.3 Secondary structure fitting using SELCON3

To complement the CDSSTR secondary structure analysis performed using the webserver DichroWeb, the analysis was repeated using the SELCON3 (Sreerama1993, Sreerama2000) routine. Although this routine is available in the CDPro software package, to allow the use of the SMP180 (Abdul-Gader2011) CD spectra reference set for the analysis, we modified the MATLAB based SELMAT3 routine provided by Prof. B.A. Wallace (Lees2006) into a Python script, SelconsPy. This script has the same functionality as the original SELCON3 routine, i.e., the SELCON1 solutions are those that have a sum of the secondary structure

fractions of 100% within 5%, each fraction is above -2.5% and SELCON2 valid solutions have a root mean square difference between the query protein CD spectrum and the reconstructed spectrum of less than 0.25 Δε. Finally, the valid SELCON3 solutions arise from a selection based on the calculated α-helical content (Johnson1999). SelconsPy is available on request from the authors. The CD spectra comprising the SMP180 reference dataset is available as download via the Protein Circular Dichroism Data Bank (PCDDB) (Whitmore2017) as the 57 spectra in the MP180 and 71 spectra in the SP175 reference set list on PCDDB. The secondary structure assignments for the SMP180 CD reference data set used for SELCON3 leads to the same secondary structure fractions as the CDSSTR in DichroWeb: α-helix regular, α-helix distorted, β-strand regular, β-strand distorted, turns and unordered such that the distorted parts correspond to four residues per α-helix and two residues in a β-strand. The remaining residues counts as regular.

The result of this SELCON3 analysis yields a similar result to that obtained using CDSSTR, supporting the outcome from CDSSTR analysis that the α-helical content increases by ~10% when the peptides are adsorbed at the O/W interface when compared to solution. Figure S 11 shows the result of fitting to WPC and WPCH at either pH 8 or pH 2, in solution and at the O/W interface (i.e., for all spectra presented in Figure S 8). This analysis allows the determination of errors (deviations) for each of the structure fractions, based on the various solutions found for fitting to a specific spectrum. The error bars included in these plots therefore represent the combined standard deviations from the fitting of each structure across all measured spectra and not just a standard deviation of the fraction across the sample set. Where there is zero error (for example for WPC at pH 2), this indicates that there was either only a single SELCON3 solution to the fitting, or that there are only SELCON2 results.

(A) **(B)**

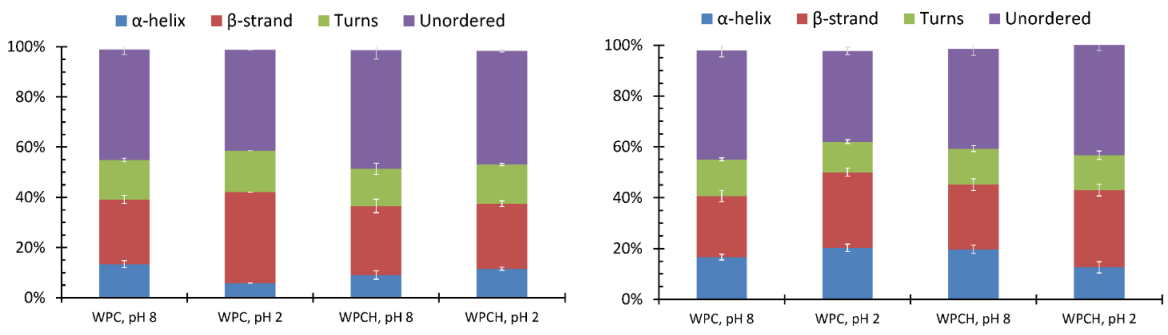

Figure S 11. Results of the secondary structure fitting using SELCON3 to the CD spectra presented in figure 28 of the manuscript. (A) are in solution, (B) at the O/W interface.

References:

Lees2006: J.G. Lees, A.J. Miles, F. Wien and B. A. Wallace, BIOINFORMATICS, 22, 2006, 1955–1962. doi:10.1093/bioinformatics/btl327

Abdul-Gader2011: A. Abdul-Gader, A.J. Miles and B. A. Wallace, BIOINFORMATICS, 12, 2011, 1630–1636. doi:10.1093/bioinformatics/btr234

Sreerama1993: N. Sreerama and R.W. Woody. (1993). Anal. Biochem. 209, 32–44.

Sreerama2000: N, Sreerama and R.W. Woody (2000). Anal. Biochem., 287, 252–260.

Whitmore2017: L. Whitmore, A.J. Miles, L. Mavridis, R.W. Janes and B.A. Wallace, PCDDB: new developments at the Protein Circular Dichroism Data Bank. Nucleic Acids Research (2017) 45 (D1): D303-D307.

Johnson1999: Johnson, W. C., Jr. (1999) Analyzing protein circular dichroism spectra for accurate secondary structures. Proteins: Struct. Funct. Genet. 35, 307–312.

6.4 Comparison of solution, aqueous phase of emulsions, and diluted emulsion samples

Measurements were carried out on samples which were diluted to be 5% of the original concentration of the stock samples. Concentrations used for delta epsilon spectrum calculations were based on measured absorbance at 205 nm.

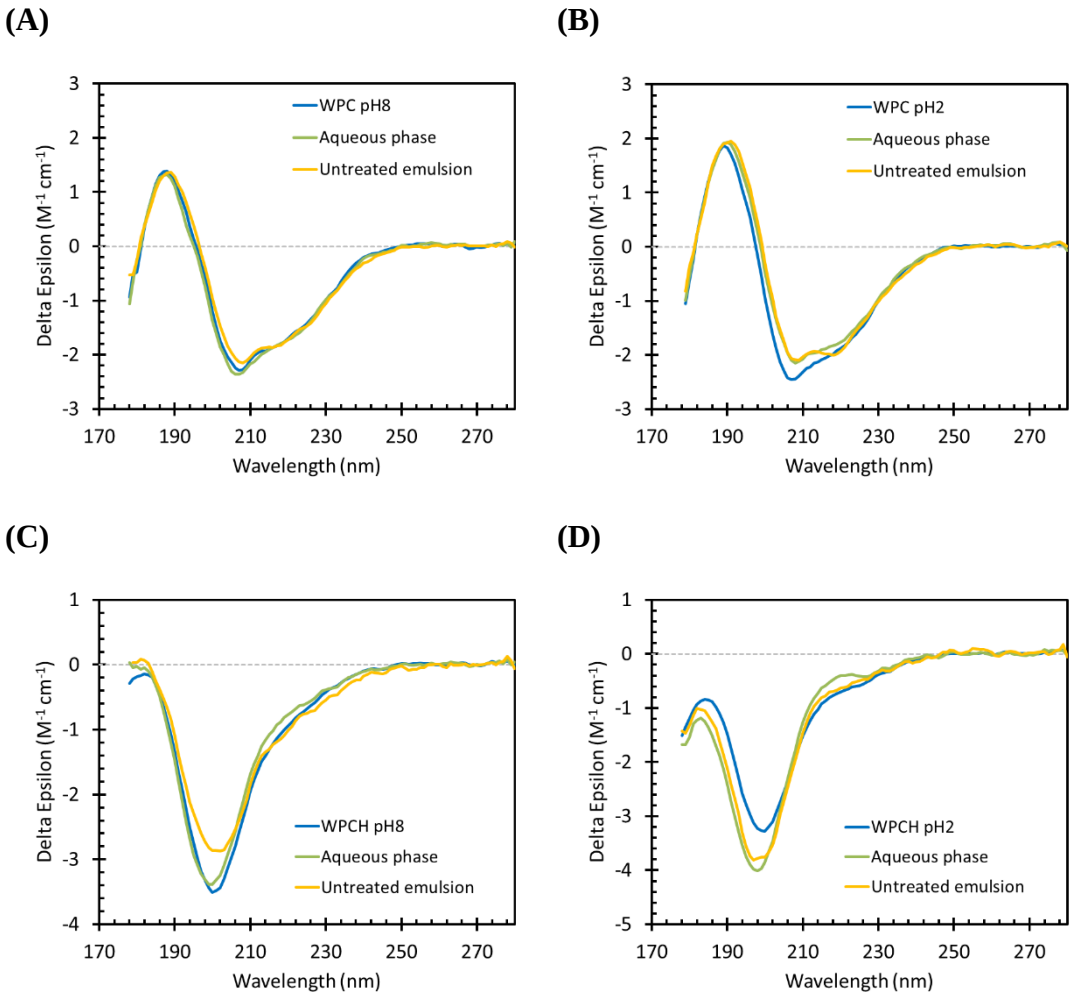

Figure S 12. Far-UV SRCD spectra in solution (blue), untreated emulsion (yellow) or aqueous phase (green) of (A) WPC at pH 8, (B) WPC at pH 2, (C) WPCH at pH 8, and (D) WPCH at pH 2.

6.5 The effect of temperature on WPCH in solution and at the O/W interface

In this section all of the data measured for temperature scans (including all replicates) of WPCH in solution or at the O/W interface are presented.

6.5.1 WPCH in solution

These data were worked up using scans of 10 mM sodium phosphate buffer at the appropriate pH for the baseline. No correction for lactose has been made to these data as it is not known how this may vary for the system through the course of the temperature scans, therefore the low wavelength region contains a small contribution from lactose (see 6.6). The underlying baseline of the system may change as the temperature increases, reflected in the non-alignment of the sample scans with the buffer baseline, noticeable at longer wavelengths. Data are presented with and without zeroing at long wavelength (270-280 nm) to be able to see what effect this may have on the determination of the transition temperature.

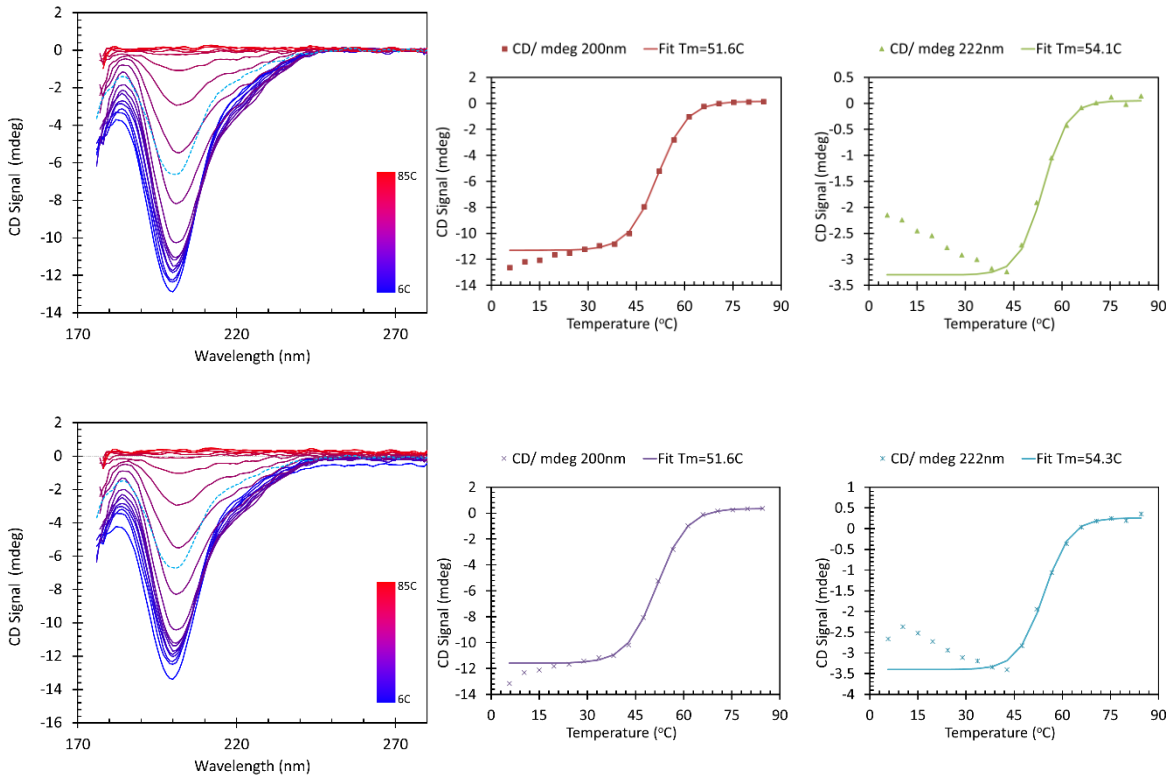

Figure S 13. WPCH in solution at pH 8, replicate 1, evolution of the CD signal with changing temperature at 200 nm (middle) and 222 nm (right). Zeroed data (top): Mid-point of the sigmoidal fits are 51.6 °C and 54.1°C respectively. Non-zeroed data (bottom): Mid-point of the sigmoidal fits are 51.6 °C and 54.3 °C respectively.

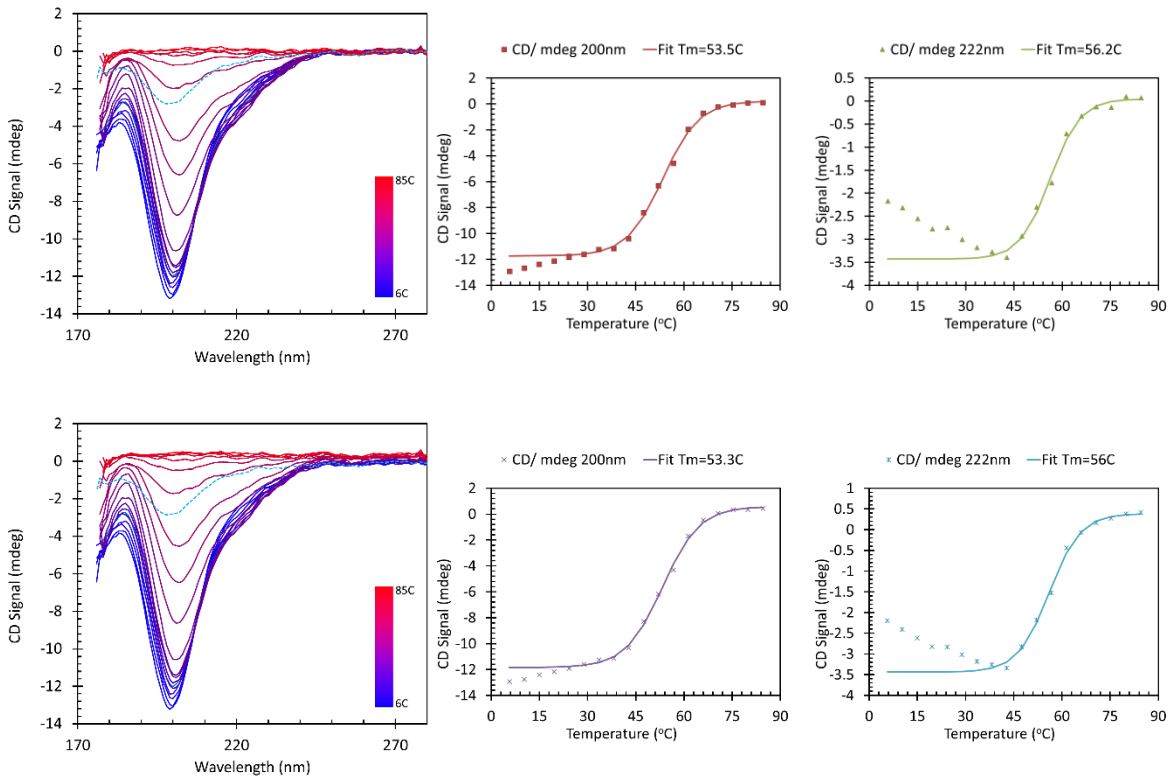

Figure S 14. WPCH in solution at pH 8, replicate 2, evolution of the CD signal with changing temperature at 200 nm (middle) and 222 nm (right). Zeroed data (top): Mid-point of the sigmoidal fits are 53.5 °C and 56.2 °C respectively. Non-zeroed data (bottom): Mid-point of the sigmoidal fits are 53.3 °C and 56 °C respectively.

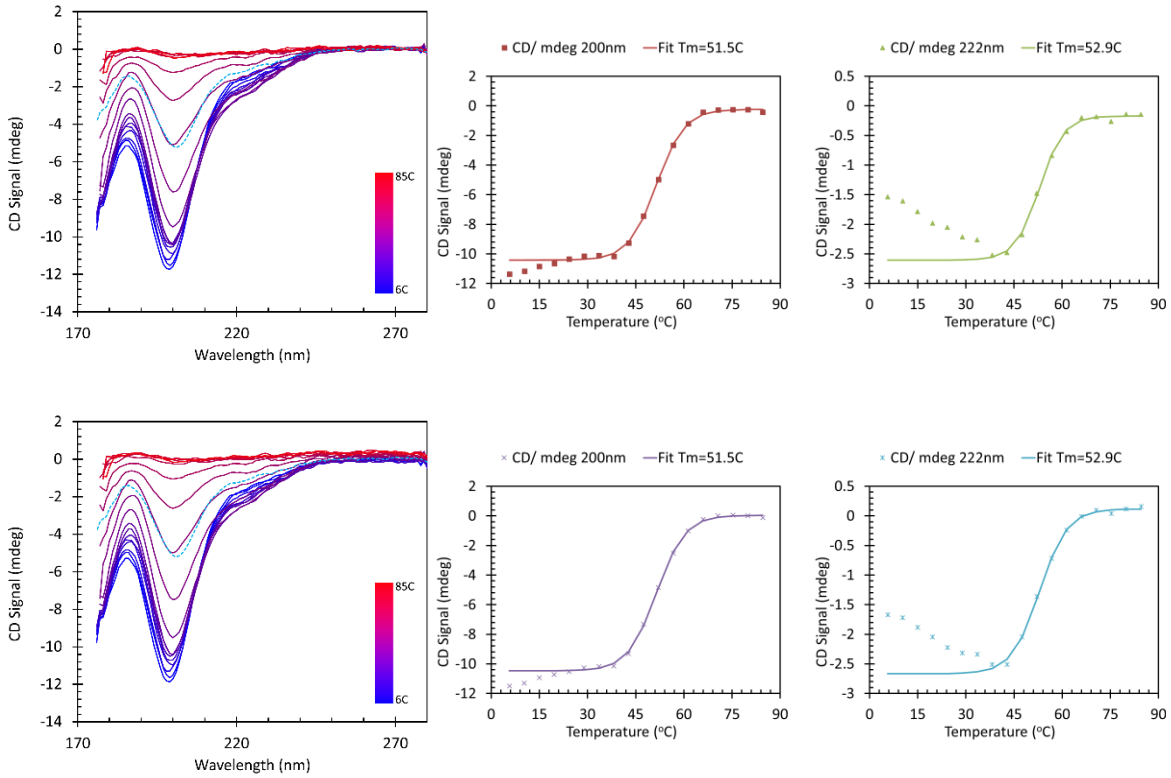

Figure S 15. WPCH in solution at pH 2, replicate 1, evolution of the CD signal with changing temperature at 200 nm (middle) and 222 nm (right). Zeroed data (top): Mid-point of the sigmoidal fits are 51.5 °C and 52.9 °C respectively. Non-zeroed data (bottom): Mid-point of the sigmoidal fits are 51.5 °C and 52.9 °C respectively.

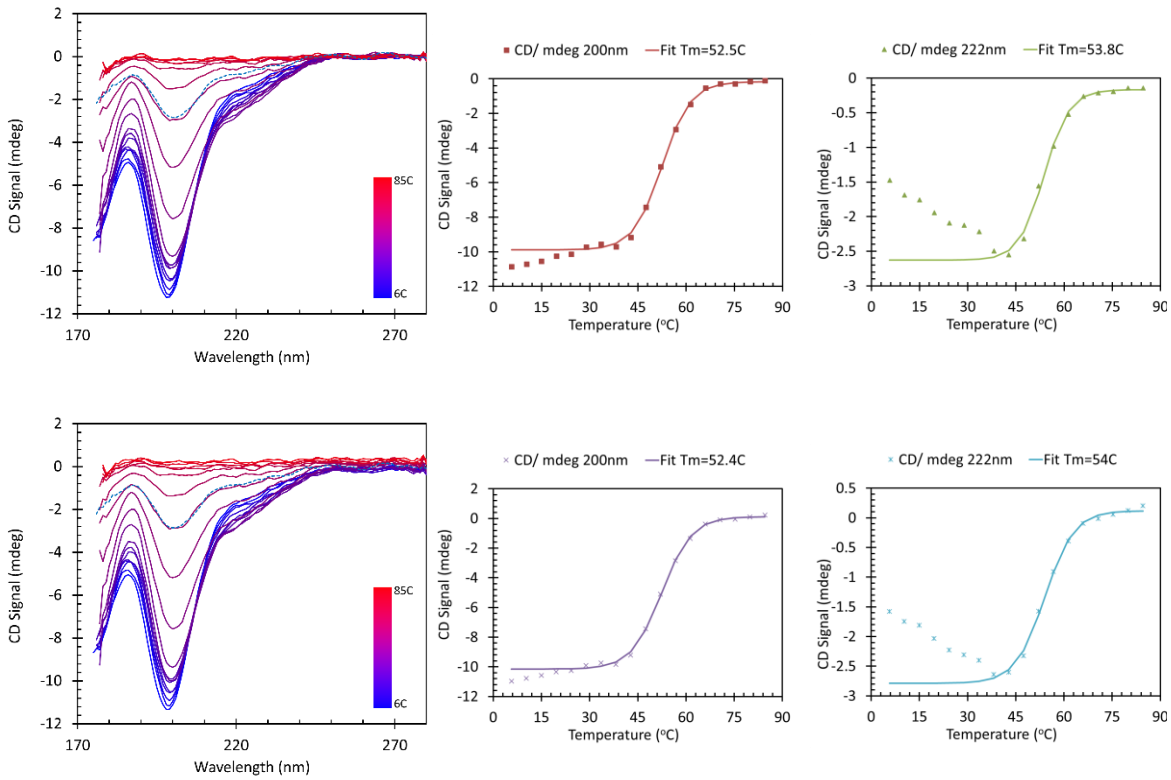

Figure S 16. WPCH in solution at pH 2, replicate 2, evolution of the CD signal with changing temperature at 200 nm (middle) and 222 nm (right). Zeroed data (top): Mid-point of the sigmoidal fits are 52.5 °C and 53.8 °C respectively. Non-zeroed data (bottom): Mid-point of the sigmoidal fits are 52.4 °C and 54 °C respectively.

6.5.2 WPCH at the O/W interface

There are many difficulties arising in measurement and treatment of CD spectra of emulsion samples (scattering, matching of baselines etc.). As the temperature of the emulsion increases the nature of the scattering is changed and therefore so is the underlying baseline of the system.

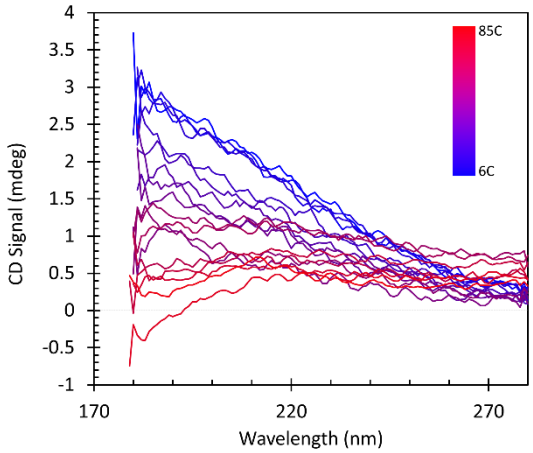

Figure S 17. Baselines recorded for a temperature scan of an SDS stabilised emulsion using the same parameters as those for WPCH sample measurement.

Figure S 17 shows the changing CD baseline of the SDS stabilized emulsion with increasing temperature. However, there is no guarantee that the scattering of peptide systems will be the same as for the SDS stabilized emulsion and therefore can result in baselines not matching. In order to see how the resulting transition temperature may be affected through possible inaccuracies in baseline matching, where possible data for emulsions have been analyzed in two ways, one using the baseline measured at each temperature of the SDS stabilized emulsion temperature scan and the other using a single emulsion baseline taken at room temperature. This second method would represent a clear error in baseline matching across the full data set for a temperature scan (matching only the first few temperatures where the scattering effect is similar) and therefore gives an indication of how significant an effect this would have on the resulting transition temperatures that are determined over the full temperature range.

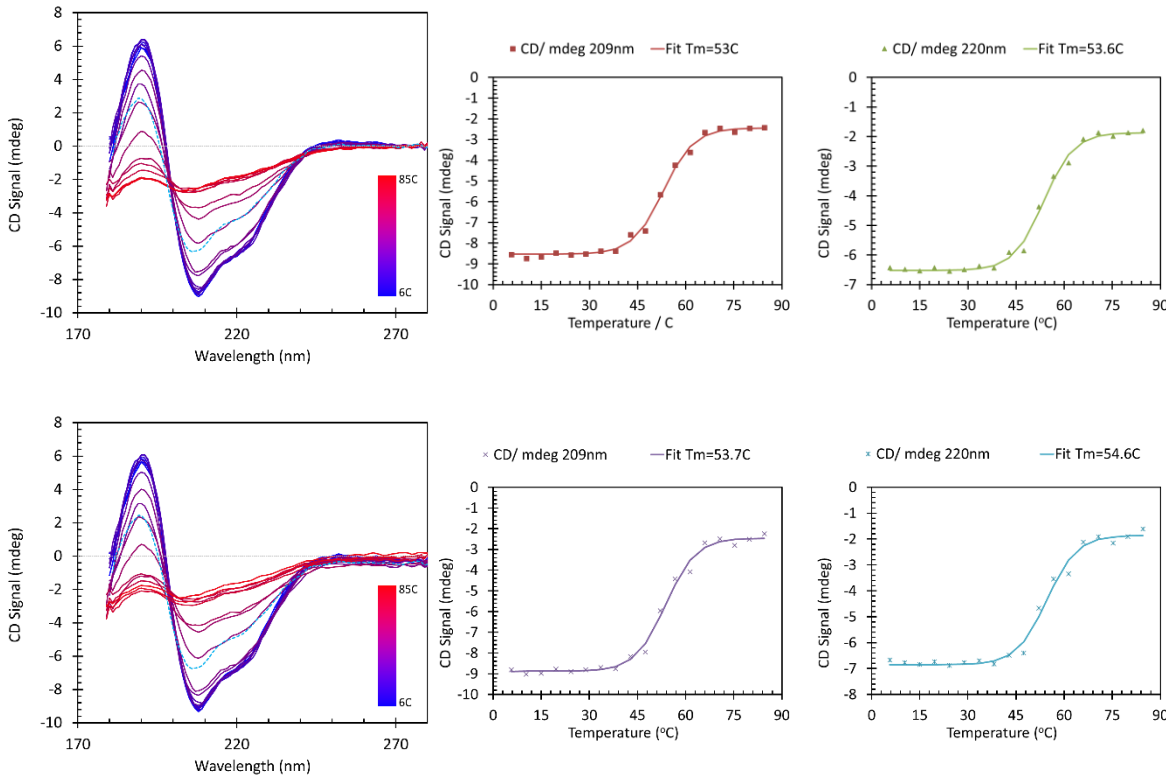

Figure S 18. WPCH at the O/W interface at pH 8, replicate 1, treated using the same baseline for all temperature steps. Evolution of the CD signal with changing temperature at 209 nm (middle) and 220 nm (right). Zeroed data (top): Mid-point of the sigmoidal fits are 53 °C and 53.6 °C respectively. Non-zeroed data (bottom): Mid-point of the sigmoidal fits are 53.7 °C and 54.6 °C respectively.

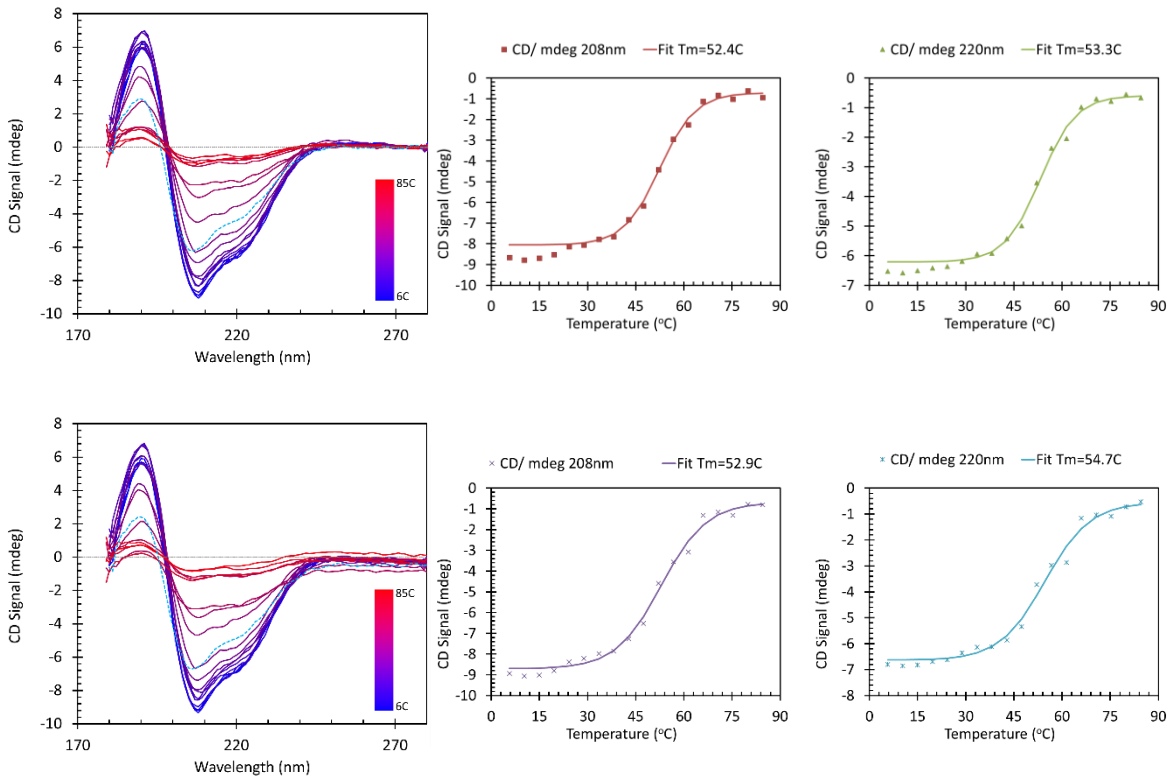

Figure S 19. WPCH at the O/W interface at pH 8, replicate 1 treated using the SDS stabilised emulsion baseline measured at the same temperature steps. Evolution of the CD signal with changing temperature at 208 nm (middle) and 220 nm (right). Zeroed data (top): Mid-point of the sigmoidal fits are 52.4 °C and 53.3 °C respectively. Non-zeroed data (bottom): Mid-point of the sigmoidal fits are 52.9 °C and 54.7 °C respectively.

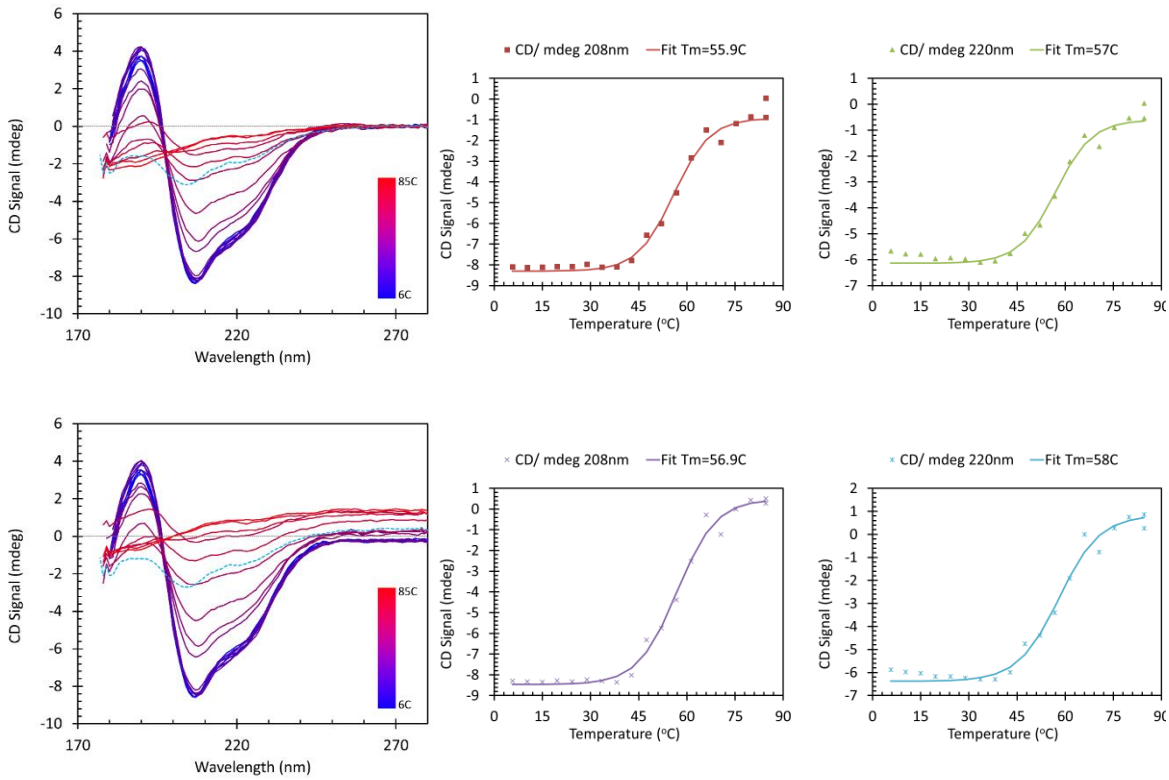

Figure S 20. WPCH at the O/W interface at pH 8, replicate 2 treated using the same baseline for all temperature steps. Evolution of the CD signal with changing temperature at 208 nm (middle) and 220 nm (right). Zeroed data (top): Mid-point of the sigmoidal fits are 55.9 °C and 57.0 °C respectively. Non-zeroed data (bottom): Mid-point of the sigmoidal fits are 56.9 °C and 58.0 °C respectively.

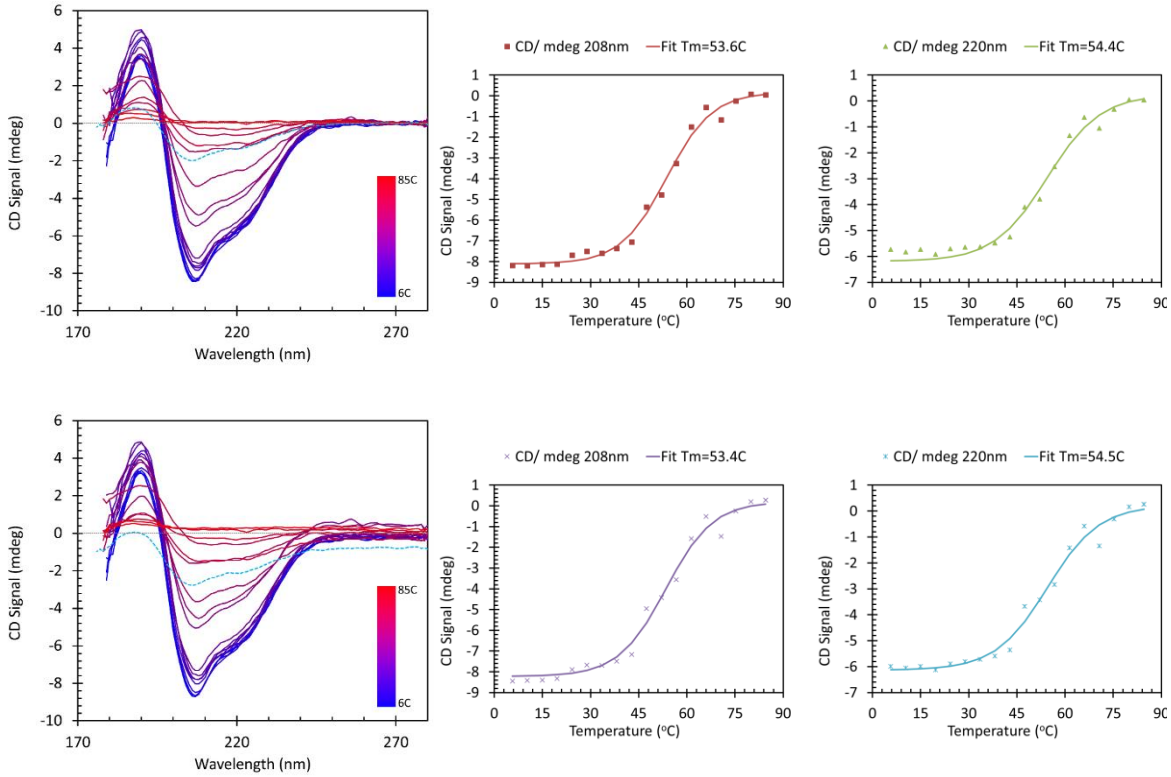

Figure S 21. WPCH at the O/W interface at pH 8, replicate 2 treated using the SDS stabilised emulsion baseline measured at the same temperature steps. Evolution of the CD signal with changing temperature at 208 nm (middle) and 220 nm (right). Zeroed data (top): Mid-point of the sigmoidal fits are 53.6 °C and 54.4 °C respectively. Non-zeroed data (bottom): Mid-point of the sigmoidal fits are 53.4 °C and 54.5 °C respectively.

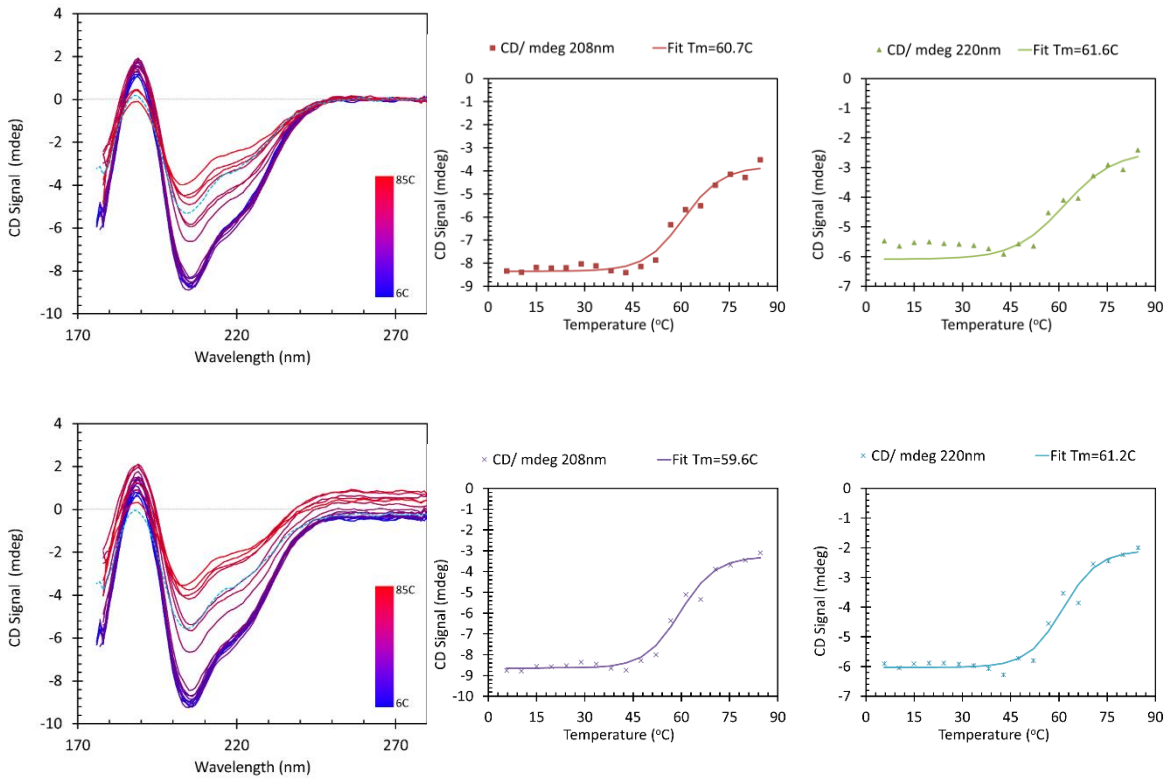

Figure S 22. WPCH at the O/W interface at pH 2, replicate 1 treated using the same baseline for all temperature steps. Evolution of the CD signal with changing temperature at 208 nm (middle) and 220 nm (right). Zeroed data (top): Mid-point of the sigmoidal fits are 60.7 °C and 61.6 °C respectively. Non-zeroed data (bottom): Mid-point of the sigmoidal fits are 59.6 °C and 61.2 °C respectively.

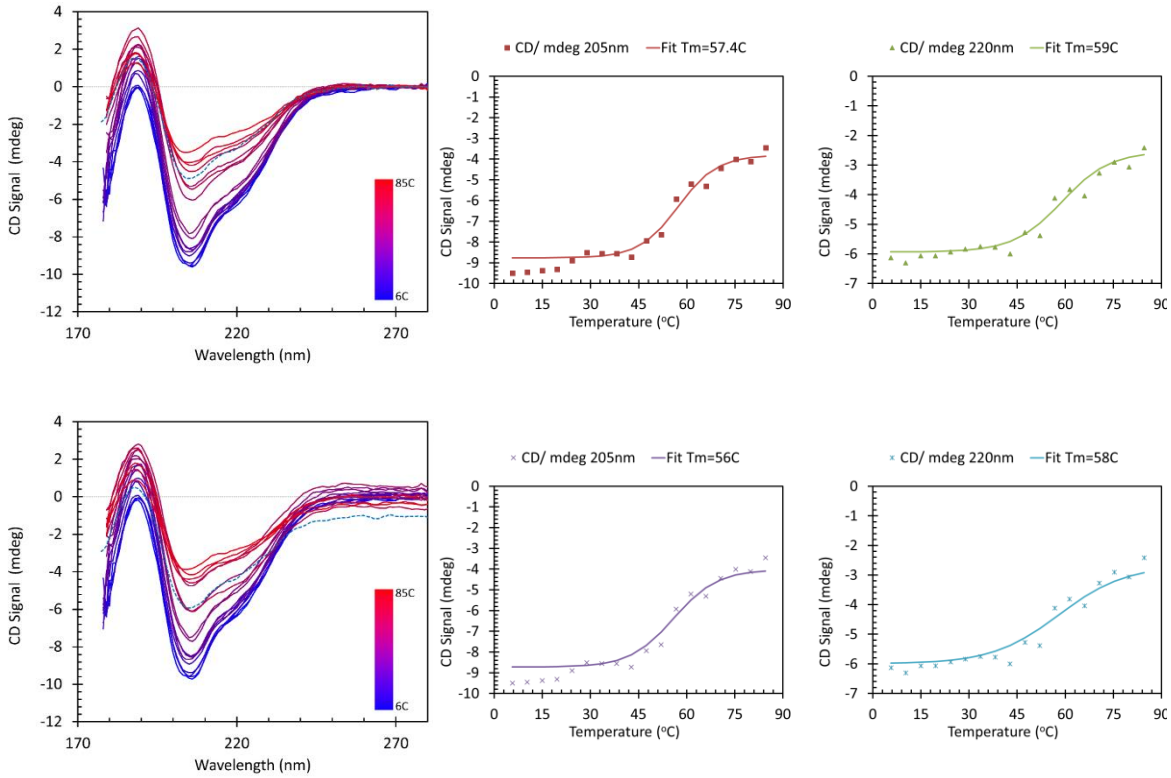

Figure S 23. WPCH at the O/W interface at pH 2, replicate 1 treated using the SDS stabilised emulsion baseline measured at the same temperature steps. Evolution of the CD signal with changing temperature at 208 nm (middle) and 220 nm (right). Zeroed data (top): Mid-point of the sigmoidal fits are 57.4 °C and 59.0 °C respectively. Non-zeroed data (bottom): Mid-point of the sigmoidal fits are 56.0 °C and 58.0 °C respectively.

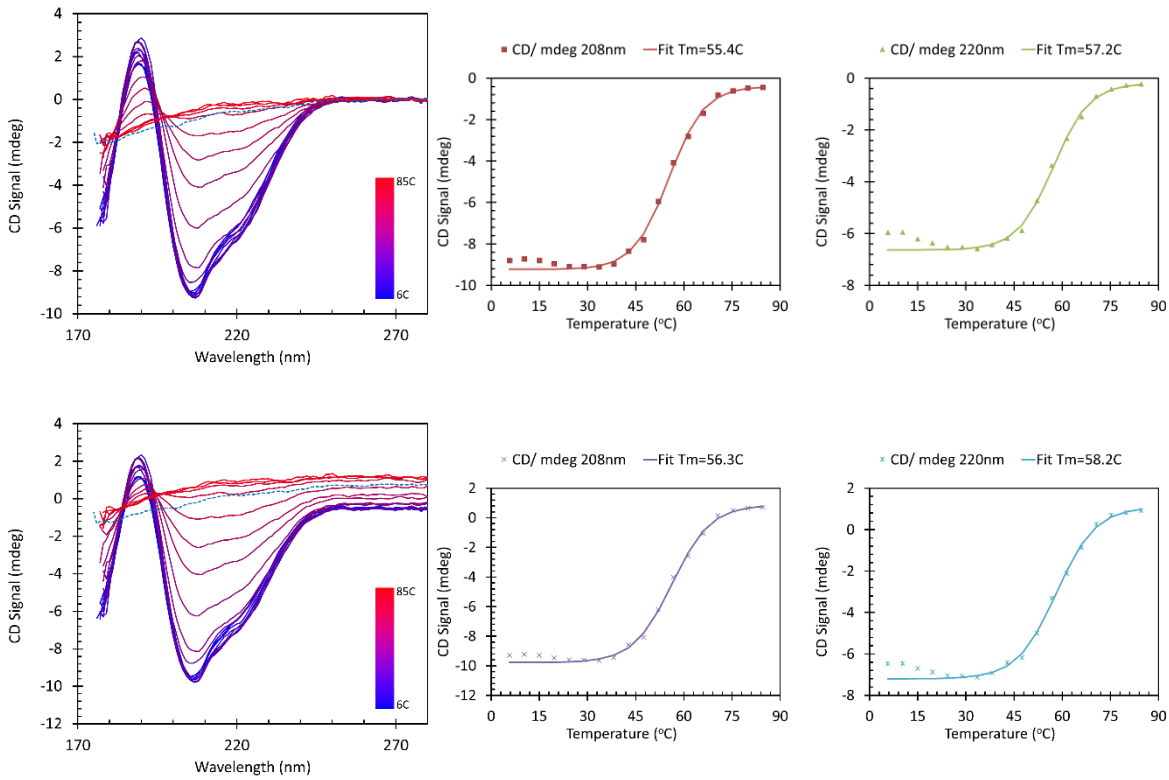

Figure S 24. WPCH at the O/W interface at pH 2, replicate 2 treated using the same baseline for all temperature steps. Evolution of the CD signal with changing temperature at 208 nm (middle) and 220 nm (right). Zeroed data (top): Mid-point of the sigmoidal fits are 55.4 °C and 57.2 °C respectively. Non-zeroed data (bottom): Mid-point of the sigmoidal fits are 56.3 °C and 58.2 °C respectively.

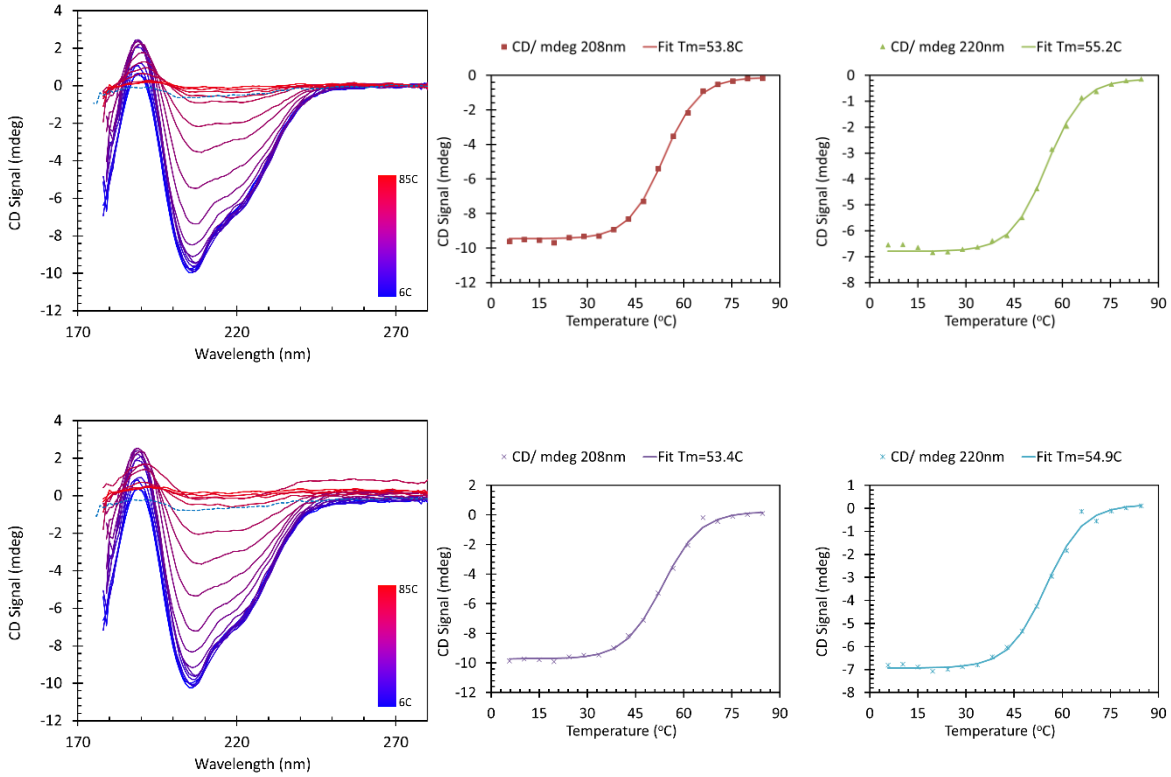

Figure S 25. WPCH at the O/W interface at pH 2, replicate 2 treated using the SDS stabilised emulsion baseline measured at the same temperature steps. Evolution of the CD signal with changing temperature at 208 nm (middle) and 220 nm (right). Zeroed data (top): Mid-point of the sigmoidal fits are 53.8 °C and 55.2 °C respectively. Non-zeroed data (bottom): Mid-point of the sigmoidal fits are 53.4 °C and 54.9 °C respectively.

6.5.3 Summary of the results for analysis of the transition temperatures

The transition temperature determined through fitting to the CD data extracted from a specific wavelength at each temperature step, is largely unaffected through the process of forcing the spectra to all be zero in the long wavelength (zeroing the data between 270-280 nm). The effect on the resulting temperature is to change it by only 0.1-0.3 °C for solution spectra and for O/W interface samples this changes in a slightly larger range of 0.1-0.9 °C.

For the O/W interface samples, the effect of using the two different methods to treat the data, either using a single SDS emulsion spectrum taken at room temperature for all temperatures (a worst-case scenario) or applying baselines (BL) measured on this emulsion taken at the same temperatures of the sample (the best estimate that may be achieved), yields differences in the transition temperature of between 0.3 and 3.3 °C. The final data obtained is summarized in the tables below, taken from datasets that have been zeroed at long wavelength.

Solutions

WPCH pH8			WPCH pH2		
Sample/WL	200 nm	220 nm	Sample/WL	200 nm	220 nm
R1	51.6	54.1	R1	51.5	52.9
R2	53.5	56.2	R2	52.5	53.8
Av.	52.6	55.2	Av.	52.0	53.4
SD	0.9	1.1	SD	0.5	0.4

O/W interface

WPCH pH8

With single emulsion BL for all			*With emulsion Tscan scans as BL*	
Sample/WL	209 nm	220 nm	209 nm	220 nm
R1	53	53.6	52.4	53.3
R2	55.9	57	53.6	54.4
Av.	54.5	55.3	53.0	53.9
SD	1.5	1.7	0.6	0.6

WPCH pH2

With single emulsion BL for all			*With emulsion Tscan scans as BL*	
Sample/WL	208 nm	220 nm	208 nm	220 nm
R1	60.7	61.6	57.4	59
R2	55.4	57.2	53.8	55.2
Av.	58.1	59.4	55.6	57.1
SD	2.7	2.2	1.8	1.9

The errors associated with the repeated measurements of the samples make it difficult to be certain of a change in stability of the peptides at the O/W interface based on the thermal stability alone. For samples at pH 8 there is no apparent difference in the transition temperature and for pH 2 the difference in transition temperature between the solutions and O/W interface is marginally outside 1 standard deviation of the error.

6.6 CD and absorbance spectra of lactose and encapsulating agents

None of the encapsulating agents, nor lactose, have any significant absorbance at 205 nm which may affect the determination of peptide concentration. However, glucose syrup and maltodextrin have significant CD signals at the low wavelengths, therefore it is possible that if their concentration in the buffer used for baseline measurement is not exactly the same, there can be an effect from either under- or overcorrecting for these additives in the final peptide sample spectra. This may be evidenced in the low wavelength part of the spectra shown in Figure 37 and Figure 38 of Chapter IV.

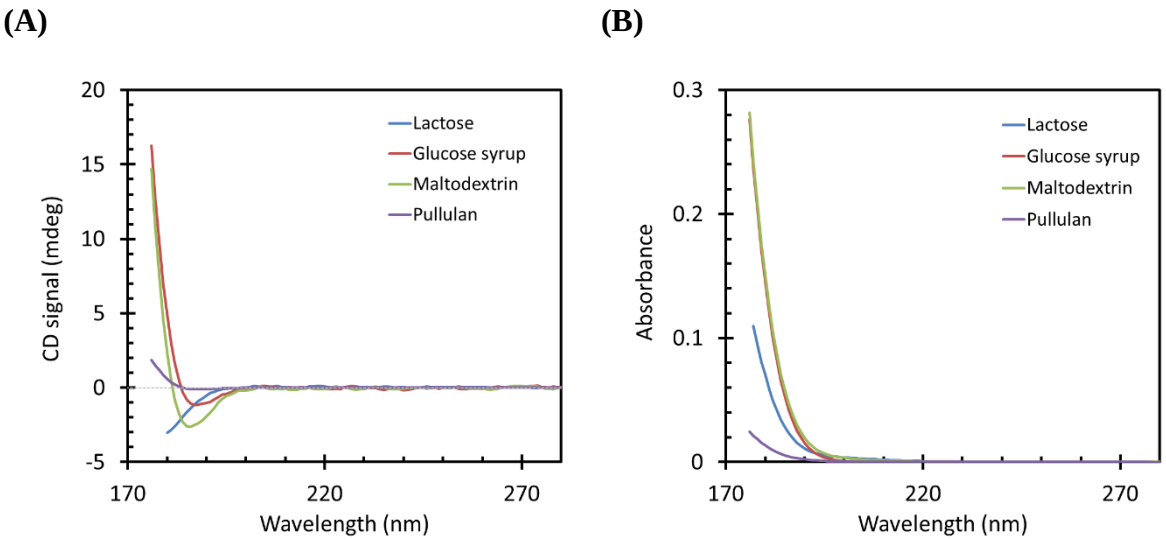

Figure S 26. Far-UV SRCD spectra (a) and absorbance (b) in solution at pH 8: for lactose (blue curves), 15% glucose syrup (brown), 15% maltodextrin (green) and pullulan (purple) scaled to the approximate concentrations used for sample measurement.

VI. Influence of emulsifier type and encapsulating agent on the in vitro digestion of fish oil-loaded microcapsules produced by spray-drying*

The influence of the emulsifier type and the encapsulating agent on the bioaccessibility of microencapsulated fish oil was investigated. Fish oil-loaded microcapsules were produced by spray-drying using carbohydrate-based encapsulating agents (glucose syrup or maltodextrin). Whey protein concentrate hydrolysate (WPCH) or Tween 20 (TW20) were used as the emulsifiers. The microcapsules were subjected to a three-phase in vitro digestion (oral, gastric, and intestinal phase) and the changes in the physicochemical properties of the samples were monitored throughout the simulated gastrointestinal tract (oil droplet size, ζ-potential, and microstructure). The lipolysis rate and extent were evaluated at the intestinal digestion phase. Contrary to the encapsulating agent, the emulsifier used in the infeed emulsion formulation significantly influenced lipid digestion. WPCH- based interfacial layer prevented oil droplets coalescence during and after processing more efficiently than TW20, which resulted in an increased specific surface area for lipases to adsorb and thus a higher bioaccessibility of the microencapsulated oil

* JOURNAL PAPER: N.E. Rahmani-Manglano, M. Tirado-Delgado, P.J. García-Moreno, A. Guadix, E.M. Guadix. (2022). Influence of emulsifier type and encapsulating agent on the in vitro digestion of fish oil-loaded microcapsules produced by spray-drying. *Food Chemistry*, 392: 133257 (IF: 9.231; category: FOOD SCIENCE & TECHNOLOGY - SCIE; position: 8/144; Q1/D1)

1. INTRODUCTION

Fish oil is an important source of long chain omega-3 polyunsaturated fatty acids (PUFAs) such as eicosapentaenoic acid (C20:5n-3, EPA), and docosahexaenoic acid (C22:6n-3, DHA) (Calder & Yaqoob, 2009). These PUFAs have been recognized to play an important role in human health by, for instance, diminishing the risk of cardiovascular disease, hypertension, or cancer (Punia et al., 2019). However, the low intake of omega-3 PUFAs through the diet makes it necessary to enrich common foods with these bioactive lipids to ensure their daily intake (Jacobsen et al., 2013). Nonetheless, EPA and DHA are highly prone to oxidation, which requires the development of delivery systems for their successful inclusion into complex food matrices (Rahmani-Manglano, García-Moreno, et al., 2020).

Microencapsulation by spray-drying is the most commonly used technique in the food industry to protect easily-degradable bioactive compounds before food enrichment (Champagne & Fustier, 2007). In the case of omega-3 PUFAs rich oils (e.g., fish oil), the process involves the emulsification of the hydrophobic phase within the wall constituents, which generally consist of an aqueous solution containing the encapsulating agent and, depending on its surface-active properties, an emulsifier. Then, the infeed emulsion is atomized in the drying chamber into a hot air stream (150-200 °C) to evaporate the solvent and produce the dried microcapsules (Rahmani-Manglano, García-Moreno, et al., 2020). Whilst the main aim of research in the field of fish oil microencapsulation has been monitoring the oxidative stability of omega-3 PUFAs during storage and subsequent inclusion into food matrices (Encina et al., 2016), recent trends in this field include the interest in understanding the digestion of these bioactive lipids throughout the gastrointestinal tract (GIT) (El-Messery et al., 2020; Shen et al., 2011; Solomando, Antequera, & Perez-Palacios, 2020a; Solomando, Antequera, & Perez-Palacios, 2020b). When microcapsules are ingested, they are exposed to fluids and enzymes present in the GIT which causes physicochemical changes. The bioaccessibility of the omega-3 PUFAs might vary depending on the components used to produce the microcapsules (Acevedo-Fani et al., 2021). Therefore, bioaccessibility can be improved by the efficient design of microcapsules using different combinations of emulsifiers and/or encapsulating agents.

Glucose syrup (GS) and maltodextrin (MD) are two commonly used encapsulating agents in spray-drying processing (Rahmani-Manglano, García-Moreno, et al., 2020).

Polysaccharides can affect lipid digestion through different mechanisms such as adhering to the surface of oil droplets impeding lipase adsorption or increasing the viscosity of the continuous phase limiting the free flow of the digestive components, among others (Chang & McClements, 2016). The emulsifier used in the formulation of the infeed emulsion also has a great impact on lipid digestion due to its influence on oil droplets aggregation, avoiding or promoting oil droplets coalescence (McClements, 2018; Solomando, Antequera, & Perez-Palacios, 2020a). Besides, highly surface-active emulsifiers may prevent bile salts and lipase adsorption onto the lipid droplets surfaces, thus limiting lipolysis (McClements, 2018).

The bioaccessibility of microencapsulated marine oils (e.g., fish oil or krill oil) within protein, carbohydrate or protein/carbohydrate-based matrices produced by spray-drying has been recently investigated as the delivery system itself (Chang & Nickerson, 2018; El-Messery et al., 2020; Sánchez et al., 2021; Zhu et al., 2021) or incorporated into different food matrices (Shen et al., 2011; Solomando, Antequera, & Perez-Palacios, 2020a; Solomando, Antequera, & Pérez-Palacios, 2020b). However, the influence of the infeed emulsion formulation and processing on both, the physicochemical changes of the microcapsules within the simulated GIT and on the extent of the microencapsulated oil digestion has not been yet studied.

Recently, whey protein concentrate hydrolysate (WPCH) has been reported to be an excellent emulsifier for the stabilization of fish oil-in-water emulsions while also exerting antioxidant activity, thus enhancing its oxidative stability (Padial-Domínguez, Espejo-Carpio, García-Moreno, et al., 2020). Furthermore, WPCH-stabilized fish oil-in-water emulsions containing carbohydrates as encapsulating agents have been successfully spray-dried to produce oxidatively stable fish oil-loaded microcapsules to be used as omega-3 delivery systems in the production of fortified low-fat mayonnaise (Rahmani-Manglano, González-Sánchez, et al., 2020). However, to the best of the authors' knowledge, the influence of WPCH, used as an emulsifier in the production of dried omega-3 PUFAs delivery systems, on lipid digestion has not been yet investigated.

Therefore, the aim of the study was to evaluate the effect of WPCH as an emulsifier on the bioaccessibility of microencapsulated fish oil produced by spray-drying when using GS or MD as encapsulating agents. The performance of WPCH was compared with a synthetic surfactant widely used by the food industry as Tween 20 (TW20). The INFOGEST standardized protocol for static in vitro digestion was employed to simulate digestion and the physicochemical changes of the dispersed microcapsules (i.e., microstructure, droplet

size, ζ-potential) throughout the different phases of the simulated GIT, as well as the lipolysis rate and extent on the intestinal phase of in vitro digestion, were evaluated.

2. MATERIALS AND METHODS

2.1 Materials

Refined fish oil (Omega Oil 1812 TG Gold) was obtained from BASF Personal Care and Nutrition GmbH (Illertissen, Germany) and stored at -80 °C until use. Glucose syrup (GS; DE38, C*Dry 1934) was kindly provided by Cargill Germany GmbH (Krefeld, Germany). Maltodextrin (MD; DE21) and whey protein (ca. 35 wt% protein content) were generously donated by Abbott (Granada, Spain). Tween 20 (TW20) was purchased from Sigma-Aldrich (Darmstadt, Germany). Alcalase was purchased from Novozymes (Denmark).

For the simulated digestion process, α-amylase (from Bacillus licheniformis 500-1500 units per mg protein, A4551), pepsin from porcine gastric mucosa (>2500 units per mg protein, P7012), bile extract (from porcine, B8631), pancreatin from porcine pancreas (8 x USP specifications, P7545), and lipase from porcine pancreas (30-90 units per mg protein using triacetin, L3126) were purchased from Sigma-Aldrich (USA). The different salts used for the simulated digestion fluids, KCl, KH2PO4, NaCl, MgCl2(H2O)6, (NH4)2CO3, HCl, and CaCl2(H2O)2 were bought either from Sigma-Aldrich (USA) or Merck (Germany). Nile red (Sigma-Aldrich S.A., USA) was used for the confocal microscopy. Enzyme activity analyses were performed according to the protocols described in (Brodkorb et al., 2019; Minekus et al., 2014).

2.2 Production of whey protein concentrate hydrolysate (WPCH)

The enzymatic hydrolysis of whey protein concentrate was carried out in an automatic titrator (718 Stat Titrino; Metrohm AG, Herisau, Switzerland) to a degree of hydrolysis of 10% (DH10) with alcalase, as described by Rahmani-Manglano, González-Sánchez, et al. (2020). The whey protein concentrate hydrolysate (WPCH) was freeze-dried and stored at 4 °C until further use.

2.3 Production of the microcapsules

Four types of microcapsules were produced depending on the encapsulating agent (i.e., GS or MD) and the emulsifier (i.e., WPCH or TW20) used in the infeed emulsion formulation. The emulsions prepared with WPCH as an emulsifier (ca. 6 wt%) had a final protein content of 2 wt%. The concentration of TW20 in the feed emulsion (0.35 wt%) was optimized to achieve a similar oil droplet size distribution compared to that of the WPCH-based emulsions. The total solids content of the emulsions was fixed to 39 wt% and depending on the emulsifier used, the concentration of the encapsulating agent varied as follows: 28 wt% when using WPCH or 34 wt% when using TW20 as emulsifiers. The aqueous phase of the emulsions was prepared by dissolving the encapsulating agent and the emulsifier in distilled water and stirring (500 rpm) overnight at room temperature. A pre-emulsion was prepared by dispersing the oil (5 wt%) in the aqueous phase for 2 min at 15,000 rpm using an Ultraturrax T-25 homogenizer (IKA, Staufen, Germany). The oil was added during the first minute. Afterwards, the coarse emulsion was homogenized in a high-pressure homogenizer (PandaPLUS 2000; GEA Niro Soavi, Lübeck, Germany) at a pressure range of 450/75 bar, applying 3 passes. The drying process was carried out in a laboratory-scale spray-drier (Büchi B-190; Büchi Labortechnik, Flawill, Switzerland) at 180/90 °C inlet/outlet temperature, respectively. The drying air flow was fixed to 25 Nm3/h. The water content of the microcapsules obtained was lower than 5% when determined using an infrared balance (AD 471A, Tokyo, Japan).

2.4 Characterization of the microcapsules

2.4.1 Morphology and size

The morphology and size of the microcapsules were investigated by means of scanning electron microscopy (SEM) using a FESEM microscope (LEO 1500 GEMINI, Zeiss, Germany). A thin layer of microcapsules was placed on carbon tape and carbon-coated using an EMITECH K975X Turbo-Pumped Thermal Evaporator (Quorum Technologies, UK). The SEM images were acquired in the range 500X – 2KX magnification with a 5-kV accelerating voltage. The images were then analyzed using the ImageJ software (National Institute of Health) and more than 150 randomly-selected microcapsules were measured to determine the particle size distributions and mean diameters.

2.4.2 Encapsulation efficiency and surface fat

The encapsulation efficiency (EE) and the surface fat content (SF) were measured as described in our previous work (Rahmani-Manglano, González-Sánchez, et al., 2020). Approximately, 2.5 g of microcapsules were immersed in 15 mL of hexane and mixed for 2 min in a vortex mixer. Then, the mixture was centrifuged at 2720g for 20 min and 5 mL of supernatant were collected in a Pyrex tube previously weighted. Then, the hexane was evaporated under a constant flow of nitrogen and the amount of extracted oil was weighed. The oil concentration was adjusted to the original volume of hexane added. The EE and the SF were calculated as follows:

$$EE, \% = \frac{A - B}{A} \cdot 100 \quad (18)$$

$$SF, \% = \frac{B}{A} \cdot 100 \quad (19)$$

where A refers to the experimental total amount of oil (g) and B to the extractable oil (g). The experimental total oil load of the microcapsules was determined by extracting the fish oil using hexane:2-propanol (1:1, v/v) solvent. For the extraction, ca. 50 mg of powder was dissolved by adding 10 mL of distilled water. The experimental total oil load was determined by measuring the absorbance of the lipid extract at 250 nm in a UV-Vis double beam spectrophotometer (Thermo Spectronic Helios Alpha 9423 UVA 1002E, Thermo Fisher Scientific, USA). The amount of oil contained in the lipid phase was determined from a calibration curve (R2 = 0.99) prepared by dissolving various quantities of fish oil in hexane (0.1 – 2.0 mg/mL). Measurements were carried out in triplicate.

2.5 Static *in vitro* digestion

The simulated digestion of the samples was carried out using an adaptation of the INFOGEST in vitro digestion method described by Brodkorb et al. (2019). The latter consists in a 3-phase digestion (i.e., mouth, stomach, small intestine) coupled with the pH-Stat method to assess the degree of hydrolysis of the fish oil (Chang & McClements, 2016). Blanks were made with either water or WPCH to evaluate the impact of the non-fatty components of the digestion on the results shown by the pH-Stat method. In vitro simulated digestions were carried out in triplicates.

2.5.1 Simulated digestion fluids

Simulated salivary fluid (SSF), simulated gastric fluid (SGF), and simulated intestinal fluid (SIF) were produced as described by Brodkorb et al. (2019) with some modifications. Since the pH-Stat method was used during the intestinal phase of digestion, NaHCO3 was replaced by NaCl at the same molar ratio to avoid the formation of bubbles and changes in the pH, as previously reported by other authors (Mat et al., 2016; Yang & Ciftci, 2020).

2.5.2 Oral digestion

Briefly, 7.5 g of microcapsules were mixed with 7.5 mL of SSF pre-heated at 37 °C and the pH was set to 7 with NaOH 0.5 M. Subsequently, α-amylase (from Bacillus licheniformis) was added to reach an activity of 75 U/mL and the mixture was introduced in a shaker instrument (Heidolph Unimax 1010) at 37 °C and 250 rpm for 2 min.

2.5.3 Gastric digestion

Gastric lipolysis only represents between 10-30% of the total lipolysis (Favé et al., 2004) and, although the optimum pH for gastric rabbit lipase is pH 4 (Moreau et al., 1988), the INFOGEST protocol uses pH 3 for this stage (Brodkorb et al., 2019; Minekus et al., 2014) which could even diminish more the lipolysis extent in the gastric phase. Therefore, gastric rabbit lipase was omitted in this study. To continue with the procedure, 17.5 ml of SGF preheated at 37 °C were added to the result of the oral phase and the pH was set to 3 using HCl 1N. Pepsin was added to reach an activity of 2000 U/mL in the final mixture, which was then introduced in the shaker at 37 °C and 250 rpm for 2 h.

2.5.4 Intestinal digestion with the pH-Stat method

Porcine bile extract to achieve a 10 mM of bile salts in the final mixture was diluted in 40 mL of SIF and heated in the shaker at 37 °C and 250 rpm for at least 30 min before the intestinal phase of in vitro digestion. The mixture obtained from the gastric digestion and the mixture of SIF and bile salts was poured into a jacketed beaker maintained at 37 ºC. The pH of the mixture was adjusted to 7 with NaOH 1 N and pancreatin and pancreatic lipase were added to achieve 100 U/mL of trypsin activity and 2000 U/mL of lipase activity, respectively. The reaction was controlled at pH 7 for 2h with a titrating instrument (902 Titrando, Metrohm, Herisau, Switzerland) by adding NaOH 0.2 M.

2.5.5 Determination of the percentage of free fatty acids

The percentage of free fatty acids (%FFA) was related to the volume of NaOH (0.2 M) added during the intestinal phase of in vitro digestion using the following equation (Yan Li & McClements, 2010):

$$\%FFA = 100 \cdot (VOil - VBlank) \cdot mNaOH \cdot \frac{MLipid}{2 \cdot WLipid} \quad (20)$$

where VOil (mL) represents the volume of NaOH added to neutralize the FFAs liberated, VBlank (mL) is the volume of NaOH added to neutralize the acid groups created by the components of the blanks, mNaOH is the molarity of the sodium hydroxide solution (0.2 M), MLipid is the molecular weight of the fish oil (930 g/mol) and WLipid is the total weight of lipid introduced in the reaction vessel (0.96 g).

2.6 Physicochemical changes during digestion

To study the fate of the microcapsules as they passed through the GIT, samples were taken from the end of the oral phase of the simulated digestion (Oral phase), as well as from the start and the end of the gastric and intestinal phases of in vitro digestion (Gastric/Intestinal phase 1 and Gastric/Intestinal phase 2, respectively). The parent emulsions before spray-drying were also characterized to evaluate the impact of processing on the reconstituted emulsions.

2.6.1 Oil droplet size

The oil droplet size distribution and oil droplet size of the samples was determined using a static light scattering instrument (Mastersizer 3000, Malvern Instruments, Worcestershire, United Kingdom). Samples were diluted in recirculating water (3000 rpm) to achieve an obscuration in the range 12 - 15%. The refractive indexes of fish oil (1.481) and water (1.330) were used as particle and dispersant, respectively. Measurements were made in triplicate.

2.6.2 Zeta potential

The ζ-potential of the samples was measured using a Zetasizer Ultra (Malvern Instruments Ltd., Worcestershire, UK) at 25ºC. Samples were previously diluted in a volume proportion

of 2/1000 with distilled water at the pH of the respective GIT phase (pH 3 or pH 7), adjusted with either HCl (1 M) or NaOH (1 M). Measurements were made in triplicate.

2.7 Microstructure of the emulsion

For better understanding the microstructure of the systems studied, samples from the end of the oral phase and the end of the intestinal phase of in vitro digestion were stained with Nile Red to be observed using a confocal scanning laser microscopy instrument (Leica DMI6000 B, Germany). Staining was carried out by mixing 2 mL of the samples with 0.1 mL of a Nile Red solution (1mg/mL in ethanol). To capture the images, a 60 x oil immersion objective lens was used with x3 zoom. The images were recorded with the software Leica Microsystems, establishing the spectrums of Nile Red in 543 nm for excitation and 650 nm for emission.

2.8 Statistical analysis

Data were subjected to analysis of variance (ANOVA) by using Statgraphics version 5.1 (Statistical Graphics Corp., Rockville, MD, USA). Tukey´s multiple range test was used to determine significant differences between mean values. Differences between mean values were considered significant at a level of confidence of 95% ($p \leq 0.05$).

3. RESULTS AND DISCUSSION

3.1 Characterization of the microcapsules

3.1.1 Morphology and size

All the microcapsules showed a spherical shape with both, smooth and wrinkled surfaces (Figure 39A-D). Moreover, no particle agglomeration was observed. Overall, the encapsulating agent and the emulsifier used had little effect on the particle size since no significant differences in the mean diameter nor in the particle size distribution of the microcapsules was observed ($p > 0.05$) (Figure 40A). The microcapsules mean diameter varied from 9.37 ± 5.20 μm to 10.54 ± 5.26 μm, and approximately 90% of the particles had a size below 20 μm for all the samples (Figure 40A).

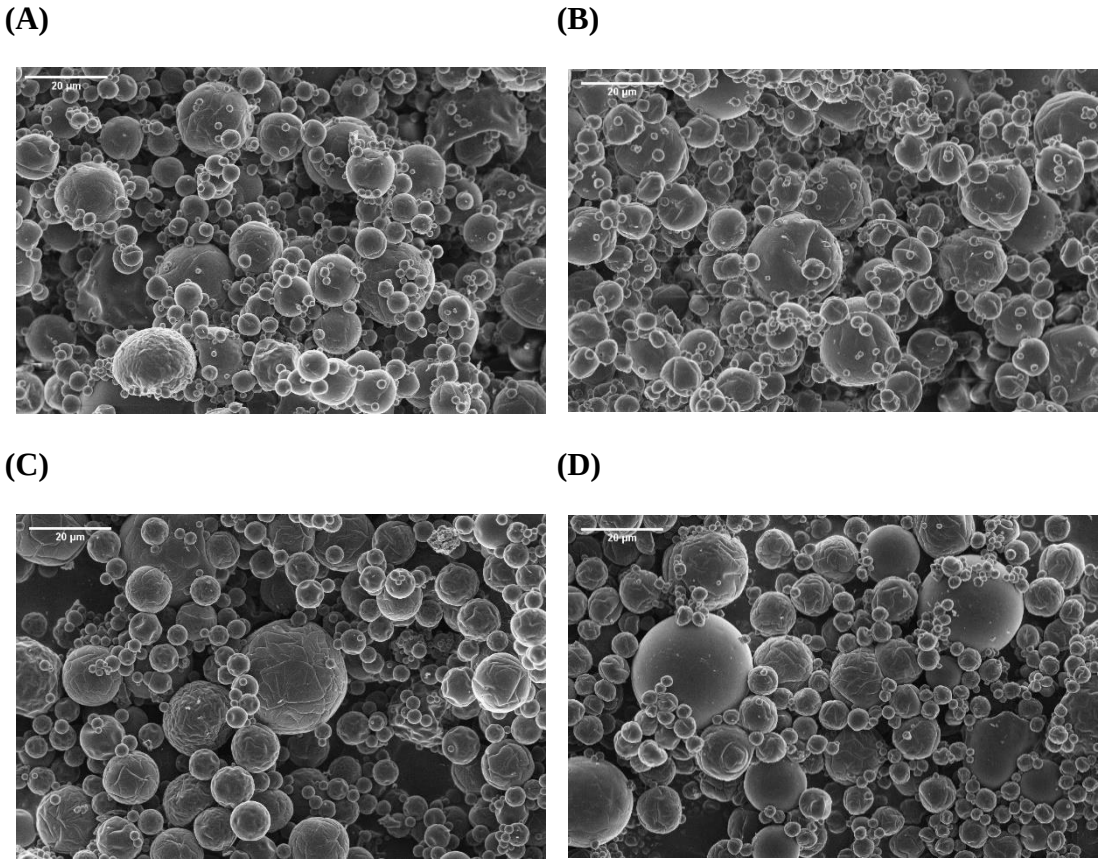

Figure 39. SEM images of the fish oil-loaded microcapsules produced by spray-drying: WPCH+GS (A), WPCH+MD (B), TW20+GS (C), TW20+MD (D). Scale bar: 20 µm.

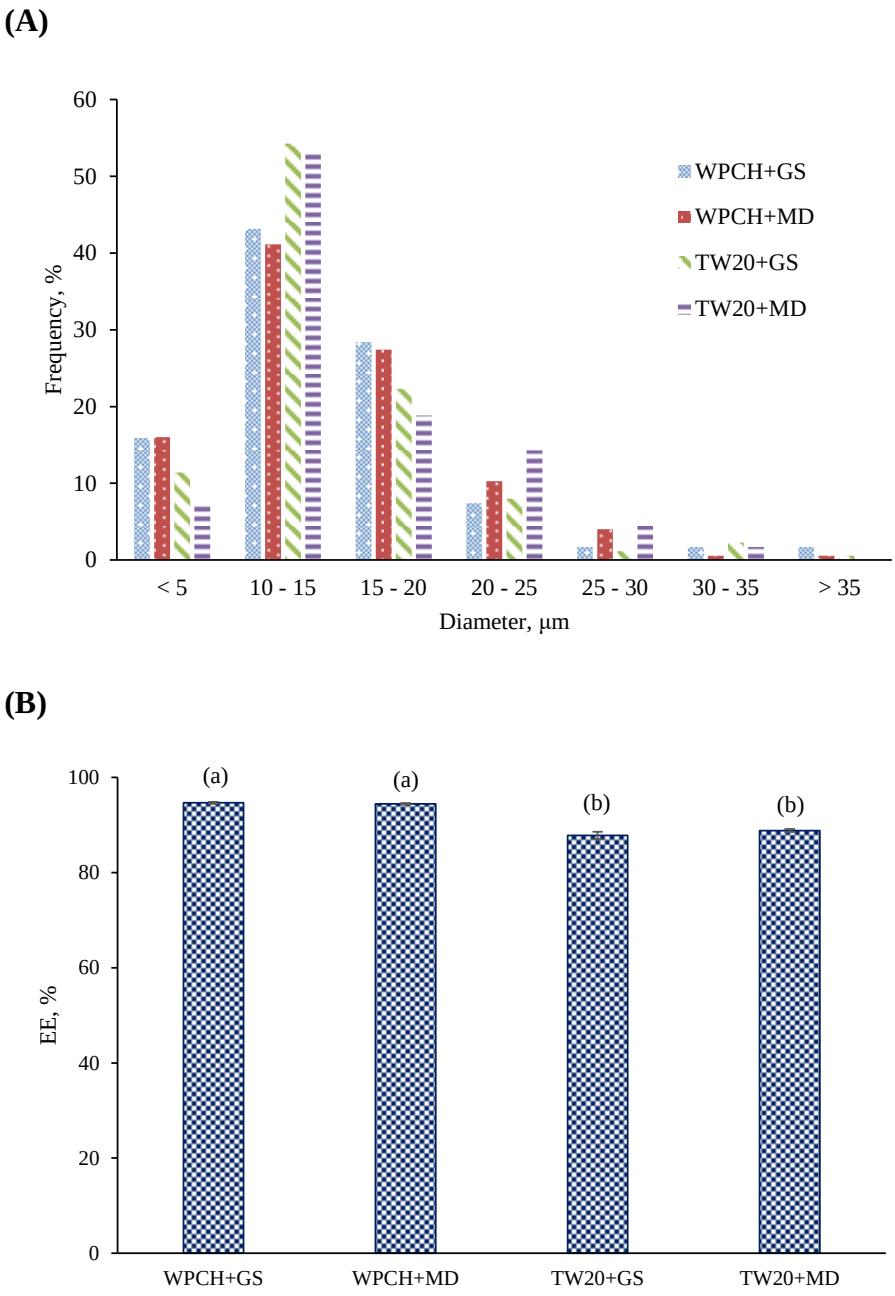

Figure 40. Particle size distribution (A) and encapsulation efficiency (EE) (B) of the spray-dried microcapsules loaded with fish oil. Samples followed by a letter, a-b, indicates statistical differences ($p \leq 0.05$) between systems.

3.1.2 Encapsulation efficiency and surface fat

High EE was achieved in the four systems studied (> 87%). However, significant differences ($p < 0.05$) were observed depending on the emulsifier used in the formulation (Figure 40B). Irrespective of the encapsulating agent, WPCH-based microcapsules showed higher EE and thus lower SF than the TW20-based microcapsules counterparts. EE is largely dependent on the wall material composition and the infeed emulsion stability (Ramakrishnan et al., 2014). High EE values are generally related to fine and monodisperse emulsions stabilized with

emulsifiers that are also able to maintain the integrity of the O/W interface during spray-drying (e.g., preventing oil droplets coalescence during atomization). Therefore, although the droplet size distribution of the parent emulsions before drying was similar for the different samples (D[4,3] = 0.451 ± 0.01 – 0.558 ± 0.007 μm) (Figure 41), our results show that WPCH stabilized the oil droplets more efficiently during processing allowing a better entrapment of the oil within the carbohydrate wall matrix. In this regard, a recent study has shown that WPI alone prevented oil droplets coalescence during spray-drying more efficiently than WPI and low molecular weight emulsifiers combinations (e.g., WPI/Citrem) due to differences in the viscoelastic behavior of the interfacial layer (Taboada et al., 2021). High viscoelasticity of the interfacial layer is related to high molecular interactions emulsifier-oil and emulsifier-emulsifier, resulting in robust interfaces capable of preventing coalescence when the oil droplets come into close contact during atomization and drying (Taboada et al., 2021). Furthermore, it has been demonstrated that protein hydrolysis to a moderate degree of hydrolysis (DH; DH ≤ 10) results in peptides with enhanced emulsifying activity (Liceaga & Hall, 2018), which could increase the interfacial stability during processing to a higher extent. The magnitude of the complex dilatational modulus of the WPCH-based interfacial layer (E = 18.5 ± 0.9 mN/m) confirms its high viscoelastic behavior, with a predominant elastic behavior (interfacial elasticity: εd = 18.4.1 ± 1.0 mN/m, when measured at a frequency of 0.1 Hz, amplitude of deformation 5% and pH 8 for a concentration of WPCH of 0.1 mg/mL), as reported in our previous work (Ruiz-Álvarez et al., 2022).

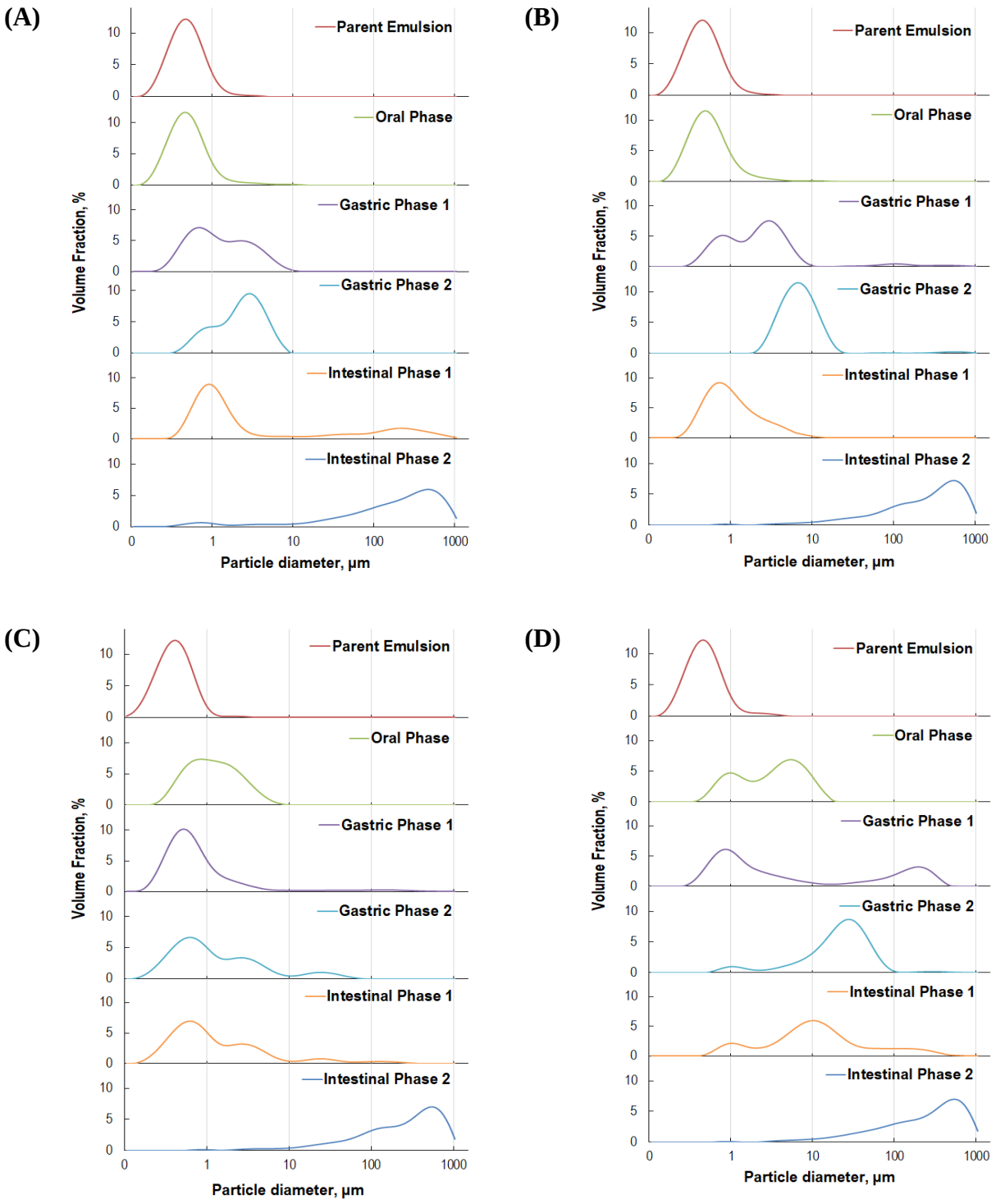

Figure 41. Droplet size distribution of emulsions before (parent emulsion) and during in vitro digestion of samples: WPCH+GS (A), WPCH+MD (B), TW20+GS (C), TW20+MD (D). Gastric phase 1 and Intestinal phase 1 represent the droplet size distribution of oil droplets before adding the respective enzymes of the phase and Gastric phase 2 and Intestinal phase 2 represent the droplet size distribution of oil droplets at the end of each phase.

3.2 *In vitro* digestion

The influence of the encapsulating agent (i.e., GS or MD) and the emulsifier (i.e., WPCH or TW20) used to produce the fish oil-loaded microcapsules on lipid bioaccessibility was investigated by measuring the rate and extent of lipolysis at the intestinal phase of the in vitro digestion. Previously, due to the water-soluble nature of the encapsulating agents used in this study, the fate of the microcapsules within the different stages of GIT was monitored by measuring the main emulsion stability indicators (e.g., droplet size distribution, charge of the interfacial layer, and microstructure).

3.2.1 Oral phase

After the oral phase of in vitro digestion, the droplet size of all the reconstituted emulsions increased with respect to the parent emulsions before drying (D[4,3] = 0.66 ± 0.01 – 4.24 ± 0.11 μm) (Figure 41). WPCH-based systems showed a monomodal droplet size distribution and a similar droplet size that the respective parent emulsions, regardless of the encapsulating agent (D[4,3] = 0.66 ± 0.01 – 0.75 ± 0.01 μm) (Figure 41A,B). However, the systems stabilized with TW20 showed both, wider and bimodal droplet size distributions and larger oil droplet size (D[4,3] = 1.54 ± 0.01 μm for sample TW20-GS and D[4,3] = 4.24 ± 0.11 μm for sample TW20-MD) (Figure 41C,D). These results are consistent with the EE values reported for the microcapsules (Figure 40B) since those containing WPCH as an emulsifier showed the lowest content of non-encapsulated oil, hence less oil was available to coalesce after the dispersion of the microcapsules in the SSF.

The latter was also confirmed by confocal microscopy images, where smaller oil droplets could be observed for the samples containing WPCH when compared to those produced with TW20 (Figure 42A). Confocal microscopy images also showed differences in the oil droplets distribution within the sample depending on the encapsulating agent used in the formulation (Figure 42A). Whilst for GS-containing systems the oil droplets were evenly distributed throughout the aqueous phase, droplets aggregation in the form of flocs were observed when MD was used as the encapsulating agent (Figure 42A). This could be attributed to MD-induced depletion flocculation as a result of the different dextrose equivalence (DE) of the carbohydrates (DE21 for MD and DE38 for GS). Due to the lack of surface-active properties of the encapsulating biopolymers (i.e., GS or MD), these remained unabsorbed within the aqueous phase of the reconstituted emulsions. At the same free (bio)polymer concentration, depletion flocculation has been reported to be more strongly induced by molecules of higher

molecular weight (Asakura & Oosawa, 1958), hence higher polymerization degree. This is the case of MD (DE21) over GS (DE38) since decreasing the DE of the carbohydrate leads to larger oligosaccharides of higher molecular weight. Furthermore, it could be observed that MD-induced depletion flocculation promoted coalescence of oil droplets to a higher extent for sample TW20+MD compared to sample TW20+GS, despite the SF content was similar for both microcapsules (12.1 ± 0.3% and 12.3 ± 0.8%, respectively). This was confirmed by the droplet size distribution of sample TW20+MD, where a population of relatively large droplets could be noted (Figure 41D). Interestingly, in the case of sample WPCH+MD, although flocs were formed, our results show that the integrity of the interfacial layer was retained avoiding droplets coalescence (Figure 42A). The droplet size distribution of the aforementioned sample (Figure 41B) also indicates that the MD-induced attractive forces were sufficiently low to be disrupted by the stirring conditions of the equipment used to do the measurements, as previously reported by other authors (Chang & McClements, 2016).

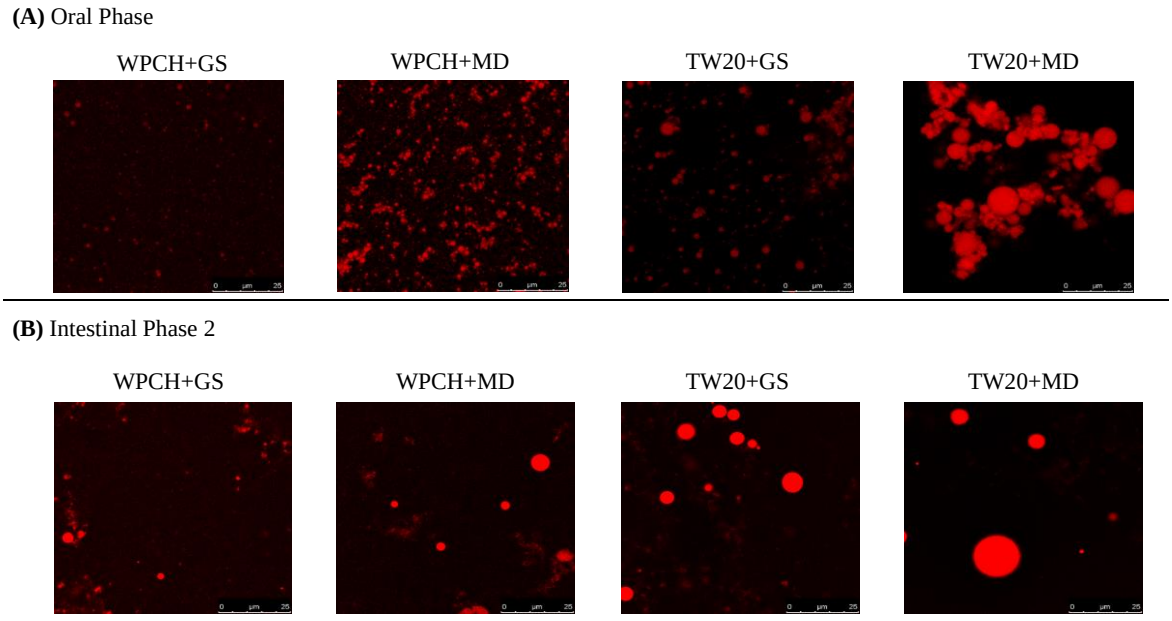

Figure 42. Confocal microscopy images of the microstructure of the emulsions at the start (oral phase) (A), and at the end (after intestinal phase) (B) of the in vitro digestion process. Scale bar 25 µm.

Figure 43 shows that the interfacial layer coating the oil droplets after the oral phase of in vitro digestion was negatively charged for all the systems despite the different nature of the emulsifiers. TW20 is a non-ionic surfactant, and although no charge should be expected, it has been reported that oil droplets coated by Tweens are negatively charged at neutral pH (Chang & McClements, 2016; Infantes-Garcia et al., 2021; Yang Li et al., 2020; Mun et al., 2007). The latter has been attributed either to the presence of impurities coming from the

surfactant and/or the oil (i.e., free fatty acids), or due to the preferential adsorption of OH- species from water. On the other hand, the negative ζ-potential values of the WPCH-stabilized systems were expected since the pH of the SSF (pH 7) is above the WPCH isoelectric point (pI = 4.06) (Ruiz-Álvarez et al., 2022). It should be noted that the magnitude of the electrical charge of the systems stabilized with WPCH did not significantly change with respect to the parent emulsions before drying ($p > 0.05$) (Figure 43). Changes in the interfacial charge of oil droplets are related to changes in the O/W interface electrostatic interactions which further affect the overall emulsion stability (Infantes-Garcia et al., 2021). Therefore, taken altogether, it can be concluded that drying and subsequent re-dispersion of the microcapsules in SSF did not modify the properties of the WPCH-based interfacial layer. This is in agreement with our current work reporting that spray-drying does not affect the secondary structure of WPCH peptides adsorbed at the O/W interface (Rahmani-Manglano et al., 2022).

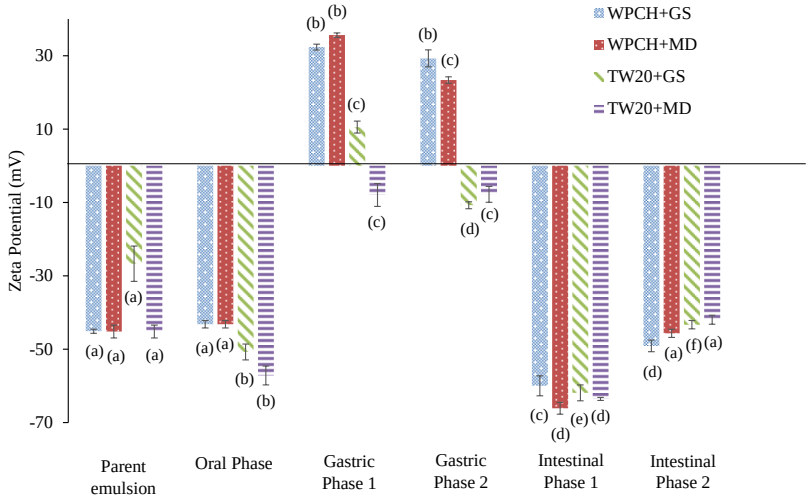

Figure 43. ζ-potential of emulsions before (parent emulsion) and during in vitro digestion of samples. Gastric phase 1 and Intestinal phase 1 represent the ζ-potential of emulsions before adding the respective enzymes of the phase and Gastric phase 2 and Intestinal phase 2 represent the ζ-potential of emulsions at the end of each phase. Samples followed by a letter, a-d, indicates statistical differences ($p \leq 0.05$) between the different stages of the GIT.

3.2.2 Gastric phase

At the initial stage of the gastric phase of in vitro digestion (Gastric phase 1) the samples were adjusted to the gastric conditions (SGF, pH 3) but the enzyme was not added. As expected, passing through the WPCH isoelectric point (pI) altered the charge of the peptides' interfacial layer and the ζ-potential switched from negative to positive values (Figure 43). The magnitude of the electrical charge was slightly reduced for both WPCH-based systems

(from -43 mV to ca. 33 mV), which could be attributed to the electrostatic screening effect of the SGF (Chang & McClements, 2016). Changes in the medium pH and ionic strength have been reported to induce droplet aggregation in protein-stabilized emulsions (Chang & McClements, 2016; Singh & Ye, 2013), thus explaining the appearance of a population of large droplets on the droplet size distributions of the WPCH-containing emulsions (Figure 41A,B). On the contrary, the ζ-potential absolute values of the TW20-based samples decreased significantly from ca. 51 – 57 mV to 8 - 10 mV (Fig. 5). The latter could be attributed to the presence of less negatively-charged ions in the continuous phase at the acidic conditions as well as to the electrostatic screening effect. Regarding the oil droplet size, this drastically increased for sample TW20+MD, as shown in the oil droplet size distribution (Figure 41D) suggesting further coalescence of the already coalesced oil droplets, which was not observed for sample TW20+GS.

After the addition of the enzyme, and at the end of the simulated gastric phase of in vitro digestion (Gastric phase 2), the oil droplets surface net charge of TW20-based systems remained unvaried although TW20+GS sample switched from positive to negative ζ-potential values. This could be attributed to the adsorption of negatively-charged pepsin molecules onto the surface of the positively-charged oil droplets at the acidic conditions of the simulated gastric phase due to the low isoelectric point of pepsin (pI = 1) (Andreeva & James, 1991). On the contrary, the electrical charge of the oil droplets coated by WPCH slightly decreased (Figure 43). These results are in line with previous studies which showed that the surface charge of protein-stabilized emulsions decreases due to protein hydrolysis of the interfacial layer by pepsin (Singh & Ye, 2013). Proteolysis of whey proteins to a DH over 10% decrease their emulsifying properties (Padial-Domínguez, Espejo-Carpio, Pérez-Gálvez, et al., 2020) since smaller peptides adsorbed at the O/W interface are unable to prevent droplet coalescence due to insufficient electrostatic and steric repulsions, as confirmed in Figure 41A,B. Conversely, the results found for the TW20-based systems contrast with previous studies on the stability of Tween-stabilized emulsions under simulated gastric conditions (Chang & McClements, 2016; Infantes-Garcia et al., 2021; Yang Li et al., 2020). These authors reported that tweens, due to their non-ionic nature, efficiently stabilized the oil droplets due to steric repulsions irrespective of the medium pH. Therefore, little changes in the droplet size and on the droplets' aggregation state were observed after simulated gastric digestion (with respect to the emulsion at the begging of the

gastric phase of each study) (Chang & McClements, 2016; Infantes-Garcia et al., 2021; Yang Li et al., 2020).

However, our results show that after the gastric phase of in vitro digestion the droplet size and droplet size distribution significantly changed (Figure 41C,D). It is worth noting that the aforementioned studies did not subject the emulsions to spray-drying which may be indicative that the TW20-based interfacial layer integrity was not retained after processing.

3.2.3 Intestinal phase

Again, at the initial stage of the intestinal phase of in vitro digestion (Intestinal phase 1), the samples were adjusted to the intestinal conditions (SIF, bile extract, pH 7) but the enzymes were not added. At pH 7 and in the presence of bile extract, the ζ-potential values for all samples were highly negative and significantly different from that of the reconstituted emulsions after the oral phase of in vitro digestion ($p < 0.05$) (Figure 43). Bile salts are amphiphilic molecules able to: i) emulsify bulk lipids entering the small intestine and ii) partially or totally displace the original emulsifier from the surface of already emulsified oil droplets (Maldonado-Valderrama et al., 2011). Bile salts adsorption upon the O/W interface is the crucial step of lipid digestion since the key role of these surface-active molecules is to promote lipolytic enzymes adsorption at the surface of oil droplets to initiate lipid hydrolysis (Bellesi & Pilosof, 2021). An increase in the negative charge of oil droplets under the simulated intestinal conditions (in the absence of enzymes) has been attributed to the presence of bile salts which could either adsorb upon the O/W interface together with the original emulsifier, partially or totally displace the original emulsifier or adsorb to the surface of the original emulsifier (Mun et al., 2007; Sarkar et al., 2016). Nonetheless, due to the nature of the emulsifiers used in this study, the decrease observed on the surface charge of the oil droplets is more likely to occur due to partial displacement of WPCH or TW20 originally adsorbed at the O/W interface (Maldonado-Valderrama et al., 2011).

The presence of bile extract in SIF also influenced the droplet size distribution of the samples in the absence of enzymes. As shown in Figure 41, the presence of bile salts appears to exert a re-emulsifying effect for the samples studied, although it was more pronounced for WPCH-containing systems. TW20 have been reported to adsorb strongly to the surface of oil droplets hindering bile salts adsorption (Salvia-Trujillo et al., 2021), which could explain the droplet size results obtained. Whilst WPCH-based systems showed a mostly monomodal droplet size distribution notably different from that at the end of the gastric phase of in vitro

digestion (Figure 41A,B), TW20-based emulsions showed trimodal oil droplet size distributions similar to that at the end of the gastric phase (Figure 41C,D). It should also be noted that the systems containing WPCH as emulsifier showed a large portion of small oil droplets at the beginning of the intestinal phase of in vitro digestion (main peak centered in ca. 0.7 – 0.9 μm) (Figure 41A,B), confirming that bile salts displaced WPCH from the O/W interface leading to re-emulsification more efficiently than TW20 samples. These results contrast with other studies which reported that the oil droplet size of all the emulsions investigated increased after setting the samples to the simulated intestinal conditions in absence of enzymes regardless of the nature of the originally adsorbed emulsifier (Chang & McClements, 2016).

Lipid digestion is an interfacial process since lipase must adsorb onto the surface of the oil droplets to catalyze lipid hydrolysis. Therefore, the droplets' size and the droplets' aggregation state are important factors that have a high impact on omega-3 PUFAs bioaccessibility, especially at the beginning of the intestinal phase of digestion (McClements, 2018). Small oil droplets evenly distributed within the continuous phase are digested faster and more efficiently. This is related to a greater access of bile salts and lipase to the oil droplets surface and to the greater specific surface area available for lipase to be adsorbed (McClements, 2018; Salvia-Trujillo et al., 2021). Right after the addition of the enzymes (Intestinal phase 2), the rate of lipid digestion was monitored (Figure 44A) and the total amount of FFA released after 2h of incubation was calculated (Figure 44B). Overall, the four types of microcapsules studied showed similar digestion profiles from which two regions could be clearly distinguished (Figure 44A). During approximately the first 5 mins of incubation, a sharp increase in the release of the FFA could be observed for all the samples (region 1) followed by a sustained release until the end of the incubation time (region 2). The first region of the curve is related to a high lipolysis rate due to a fast adsorption of lipase onto the O/W surface and a rapid release of FFA to the continuous phase. Afterwards, the lipolysis rate tends to constant values because the products generated at the O/W interface (e.g., FFA, MAG) limit lipase adsorption and reduce enzyme activity (McClements, 2018). However, different trends on lipolysis rate and extent could be observed depending on the emulsifier used in the formulation of the fish oil-loaded microcapsules. The initial rate of FFA release (Figure 44A) and the extent of lipolysis (Figure 44B) of WPCH-based systems was higher than for those using TW20 as emulsifier. These results are in line with other studies which also reported lower lipid digestion on

systems stabilized with TW20 over protein-based interfacial layers (Yang Li et al., 2020; Mun et al., 2007). This small-molecular weight emulsifier has been described to limit lipolysis because of its higher surface-activity compared to lipase which limits enzyme-substrate binding and subsequent reaction (Yang Li et al., 2020; Mun et al., 2007). However, the lower lipid digestion obtained for these samples cannot only be attributed to TW20 surface-activity. The oil droplets distribution within the continuous phase of TW20-containing samples compared to WPCH-stabilized systems at the beginning of the intestinal phase (Figure 41) may have lowered lipolysis to a higher extent due to a reduction in the specific surface area available for lipase to adsorb in TW20-based samples as a consequence of oil droplets coalescence. Furthermore, although at the end of the simulated intestinal phase of digestion the droplet size and droplet size distribution were fairly similar among the samples (D[4,3] = 289.3 ± 39.3 – 342.0 ± 11.8 μm) (Figure 41), confocal microscopy images (Figure 42B) showed larger oil droplets for the systems containing TW20, most likely due to their lower lipid digestion. Conversely, the smaller oil droplets observed for WPCH-containing systems (Figure 42B) may be attributed to the higher conversion of the TAG to FFA and MAG (Chang & McClements, 2016), thus confirming the higher lipolysis extent reported for the aforementioned samples (Figure 44B). After the intestinal phase of in vitro digestion, all the samples showed negative surface charge (Figure 43) which could be attributed to the presence of undigested protein aggregates or undigested lipid droplets (Chang & McClements, 2016).

By last, it is also worth mentioning that, although not significantly ($p > 0.05$), the encapsulating agent also seems to affect the overall lipolysis (Figure 44B). Irrespective of the emulsifier used, the systems containing GS as encapsulating agent showed a slightly higher lipolysis rate (Figure 44A) and a higher percentage of FFA released (Figure 44B) at the end of the intestinal phase of in vitro digestion when compared to MD-containing samples. This could be attributed to the lower viscosity of the continuous phase in presence of GS compared to MD as a result of the different DE of the carbohydrates (Rahmani-Manglano, González-Sánchez, et al., 2020). The higher viscosity of the aqueous phase in presence of MD may difficult the diffusion of GIT components (e.g., digestive enzymes) through the medium to the oil droplets' surface, as well as the diffusion of lipolysis products (e.g., FFA, MAG) from the oil droplets' surface to the medium (Chang & McClements, 2016).

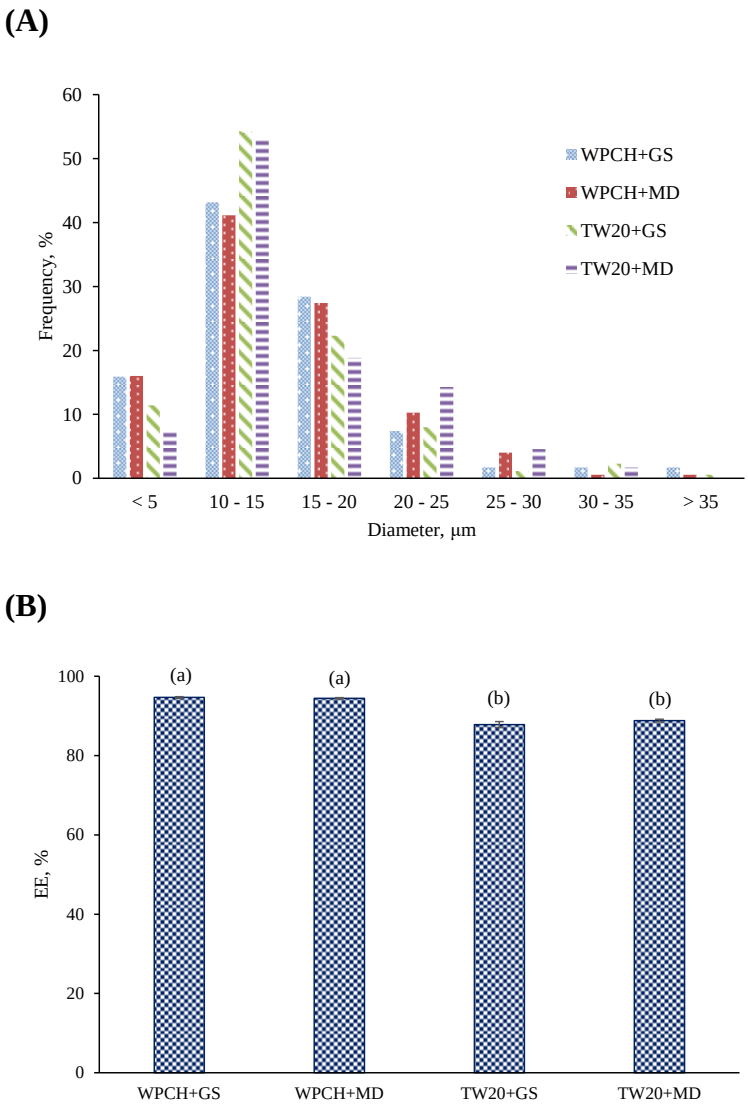

Figure 44. Volume of NaOH (0.2 M) added during the intestinal phase of the in vitro digestion (A) and percentage of Free Fatty Acids (FFAs) released during the intestinal phase of the in vitro digestion measured using the pH-stat method (B). Samples followed by a letter, a-b, indicates statistical differences ($p \leq 0.05$) between systems.

4. CONCLUSIONS

The emulsifier used in the feed emulsion formulation for spray-drying had a major impact on the bioaccessibility of microencapsulated fish oil. WPCH prevented oil droplet coalescence during processing and after re-dispersion of the microcapsules in the simulated fluids of the GIT, contrary to TW20. This resulted in a higher specific surface area of the WPCH-stabilized systems for adsorption of bile salts and lipase, hence a higher lipolysis rate and extent was obtained for the aforementioned samples. Furthermore, although not significantly, the encapsulating agent also affected lipid digestion. Irrespective of the emulsifier used, GS-containing systems showed higher percentages of FFA released after

the intestinal phase of in vitro digestion. The latter has been attributed to the different viscosities of the digest in presence of GS or MD. Overall, our results show the high bioaccessibility of fish oil-loaded microcapsules produced by spray-drying when using WPCH as emulsifier.

5. REFERENCES

Acevedo-Fani, A., Guo, Q., Nasef, N., & Singh, H. (2021). Aspects of food structure in digestion and bioavailability of LCn-3PUFA-rich lipids. In P. J. García-Moreno, C. Jacobsen, A.-D. M. Sørensen, & B. Yesiltas (Eds.), *Omega-3 Delivery Systems* (pp. 427–448). Academic Press. https://doi.org/10.1016/b978-0-12-821391-9.00003-x

Andreeva, N. S., & James, M. N. G. (1991). WHY DOES PEPSIN HAVE A NEGATIVE CHARGE AT VERY LOW pH? AN ANALYSIS OF CONSERVED CHARGED RESIDUES IN ASPARTIC PROTEINASES. In *Structure and Function of the Aspartic Proteinases. Advances in Experimental Medicine and Biology* (pp. 39–45). https://doi.org/https://doi.org/10.1007/978-1-4684-6012-4_4

Asakura, S., & Oosawa, F. (1958). Interaction between Particles Suspended in Solutions of Macromolecules. *Journal of Polymer Science*, *XXXIII*, 183–192.

Bellesi, F. A., & Pilosof, A. M. R. (2021). Potential implications of food proteins-bile salts interactions. *Food Hydrocolloids*, *118*(106766). https://doi.org/10.1016/j.foodhyd.2021.106766

Brodkorb, A., Egger, L., Alminger, M., Alvito, P., Assunção, R., Ballance, S., Bohn, T., Bourlieu-Lacanal, C., Boutrou, R., Carrière, F., Clemente, A., Corredig, M., Dupont, D., Dufour, C., Edwards, C., Golding, M., Karakaya, S., Kirkhus, B., Le Feunteun, S., … Recio, I. (2019). INFOGEST static in vitro simulation of gastrointestinal food digestion. *Nature Protocols*, *14*(4), 991–1014. https://doi.org/10.1038/s41596-018-0119-1

Calder, P. C., & Yaqoob, P. (2009). Omega-3 polyunsaturated fatty acids and human health outcomes. *BioFactors*, *35*(3), 266–272. https://doi.org/10.1002/biof.42

Champagne, C. P., & Fustier, P. (2007). Microencapsulation for the improved delivery of bioactive compounds into foods. *Current Opinion in Biotechnology*, *18*(2), 184–190. https://doi.org/10.1016/j.copbio.2007.03.001

Chang, C., & Nickerson, M. T. (2018). Stability and in vitro release behaviour of encapsulated omega fatty acid-rich oils in lentil protein isolate-based microcapsules. *International Journal of Food Sciences and Nutrition*, *69*(1), 12–23. https://doi.org/10.1080/09637486.2017.1336513

Chang, Y., & McClements, D. J. (2016). Influence of emulsifier type on the in vitro digestion of fish oil-in-water emulsions in the presence of an anionic marine polysaccharide (fucoidan): Caseinate, whey protein, lecithin, or Tween 80. *Food Hydrocolloids*, *61*, 92–101. https://doi.org/10.1016/j.foodhyd.2016.04.047

El-Messery, T. M., Altuntas, U., Altin, G., & Özçelik, B. (2020). The effect of spray-drying and freeze-drying on encapsulation efficiency, in vitro bioaccessibility and oxidative stability of krill oil nanoemulsion system. *Food Hydrocolloids*, *106*(105890). https://doi.org/10.1016/j.foodhyd.2020.105890

Encina, C., Vergara, C., Giménez, B., Oyarzún-Ampuero, F., & Robert, P. (2016). Conventional spray-drying and future trends for the microencapsulation of fish oil. *Trends in Food Science and Technology*, *56*, 46–60. https://doi.org/10.1016/j.tifs.2016.07.014

Favé, G., Coste, T. C., & Armand, M. (2004). Physicochemical properties of lipids: new strategies to manage fatty acid bioavailability. Cellular and Molecular Biology (Noisy-Le-Grand, France), 50(7), 815–831. https://doi.org/10.1170/T575

Infantes-Garcia, M. R., Verkempinck, S. H. E., Gonzalez-Fuentes, P. G., Hendrickx, M. E., & Grauwet, T. (2021). Lipolysis products formation during in vitro gastric digestion is affected by the emulsion interfacial composition. *Food Hydrocolloids*, *110*(106163). https://doi.org/10.1016/j.foodhyd.2020.106163

Jacobsen, C., Nielsen, N. S., Horn, F. F., & Sørensen, A. D. M. (2013). Food enrichment with omega-3 fatty acids. In *Food Enrichment with Omega-3 Fatty Acids*. https://doi.org/10.1533/9780857098863

Li, Yan, & Mcclements, D. J. (2010). New mathematical model for interpreting ph-stat digestion profiles: Impact of lipid droplet characteristics on in vitro digestibility. Journal of Agricultural and Food Chemistry, 58(13), 8085–8092. https://doi.org/10.1021/jf101325m

Li, Yang, Li, M., Qi, Y., Zheng, L., Wu, C., Wang, Z., & Teng, F. (2020). Preparation and digestibility of fish oil nanoemulsions stabilized by soybean protein isolate-phosphatidylcholine. *Food Hydrocolloids*, *100*(105310). https://doi.org/10.1016/j.foodhyd.2019.105310

Liceaga, A. M., & Hall, F. (2018). Nutritional, functional and bioactive protein hydrolysates. In *Encyclopedia of Food Chemistry*. Elsevier. https://doi.org/10.1016/B978-0-08-100596-5.21776-9

Maldonado-Valderrama, J., Wilde, P., MacIerzanka, A., & MacKie, A. (2011). The role of bile salts in digestion. *Advances in Colloid and Interface Science*, *165*(1), 36–46. https://doi.org/10.1016/j.cis.2010.12.002

Mat, D. J. L., Le Feunteun, S., Michon, C., & Souchon, I. (2016). In vitro digestion of foods using pH-stat and the INFOGEST protocol: Impact of matrix structure on digestion kinetics of macronutrients, proteins and lipids. *Food Research International*, *88*, 226–233. https://doi.org/10.1016/j.foodres.2015.12.002

McClements, D. J. (2018). Enhanced delivery of lipophilic bioactives using emulsions: A review of major factors affecting vitamin, nutraceutical, and lipid bioaccessibility. *Food and Function*, *9*(1), 22–41. https://doi.org/10.1039/c7fo01515a

Minekus, M., Alminger, M., Alvito, P., Ballance, S., Bohn, T., Bourlieu, C., Carrière, F., Boutrou, R., Corredig, M., Dupont, D., Dufour, C., Egger, L., Golding, M., Karakaya, S., Kirkhus, B., Le Feunteun, S., Lesmes, U., MacIerzanka, A., MacKie, A., … Brodkorb, A. (2014). A standardised static in vitro digestion method suitable for food-an international consensus. *Food and Function*, *5*(6), 1113–1124. https://doi.org/10.1039/c3fo60702j

Moreau, H., Gargouri, Y., Lecat, D., Junien, J. L., & Verger, R. (1988). Purification, characterization and kinetic properties of the rabbit gastric lipase. *Biochimica et Biophysica Acta (BBA)/Lipids and Lipid Metabolism*, 960(3), 286–293. https://doi.org/10.1016/0005-2760(88)90036-7

Mun, S., Decker, E. A., & McClements, D. J. (2007). Influence of emulsifier type on in vitro digestibility of lipid droplets by pancreatic lipase. *Food Research International*, *40*(6), 770–781. https://doi.org/10.1016/j.foodres.2007.01.007

Padial-Domínguez, M., Espejo-Carpio, F. J., García-Moreno, P. J., Jacobsen, C., & Guadix, E. M. (2020). Protein derived emulsifiers with antioxidant activity for stabilization of omega-3 emulsions. *Food Chemistry*, *329*(127148). https://doi.org/10.1016/j.foodchem.2020.127148

Padial-Domínguez, M., Espejo-Carpio, F. J., Pérez-Gálvez, R., Guadix, A., & Guadix, E. M. (2020). Optimization of the emulsifying properties of food protein hydrolysates for the production of fish oil-in-water emulsions. *Foods*, *9*(5). https://doi.org/10.3390/foods9050636

Punia, S., Sandhu, K. S., Siroha, A. K., & Dhull, S. B. (2019). Omega 3-metabolism, absorption, bioavailability and health benefits–A review. *PharmaNutrition*, 10, 100162. https://doi.org/10.1016/j.phanu.2019.100162

Rahmani-Manglano, N. E., García-Moreno, P. J., Espejo-Carpio, F. J., Pérez-Gálvez, A. R., & Guadix-Escobar, E. M. (2020). The Role of Antioxidants and Encapsulation Processes in Omega-3 Stabilization. In M. A. Aboudzadeh (Ed.), *Emulsion-based Encapsulation of Antioxidants. Food Bioactive Ingredients.* (pp. 339–386). Springer, Cham. https://doi.org/10.1007/978-3-030-62052-3_10

Rahmani-Manglano, N. E., González-Sánchez, I., García-Moreno, P. J., Espejo-Carpio, F. J., Jacobsen, C., & Guadix, E. M. (2020). Development of fish oil-loaded microcapsules

containing whey protein hydrolysate as film-forming material for fortification of low-fat mayonnaise. *Foods*, *9*(5). https://doi.org/10.3390/foods9050545

Rahmani-Manglano, N. E., Jones, N. C., Hoffmann, S. V., Guadix, E. M., Pérez-Gálvez, R., Guadix, A., & García-Moreno, P. J. (2022). Structure of whey protein hydrolysate used as emulsifier in wet and dried oil delivery systems: Effect of pH and drying processing. Food Chemistry, 390, 133169. https://doi.org/10.1016/j.foodchem.2022.133169

Ramakrishnan, S., Ferrando, M., Aceña-Muñoz, L., Mestres, M., De Lamo-Castellví, S., & Güell, C. (2014). Influence of Emulsification Technique and Wall Composition on Physicochemical Properties and Oxidative Stability of Fish Oil Microcapsules Produced by Spray Drying. *Food and Bioprocess Technology*, *7*(7), 1959–1972. https://doi.org/10.1007/s11947-013-1187-4

Ruiz-Álvarez, J. M., del Castillo-Santaella, T., Maldonado-Valderrama, J., Guadix, A., Guadix, E. M., & García-Moreno, P. J. (2022). pH influences the interfacial properties of blue whiting (M. poutassou) and whey protein hydrolysates determining the physical stability of fish oil-in-water emulsions. *Food Hydrocolloids*, *122*(107075). https://doi.org/10.1016/j.foodhyd.2021.107075

Salvia-Trujillo, L., McClements, D. J., & Martín-Belloso, O. (2021). Nanoemulsion design for the delivery of omega-3 fatty acids: formation, oxidative stability, and digestibility. In P. J. García-Moreno, C. Jacobsen, A.-D. M. Sørensen, & B. Yesiltas (Eds.), *Omega-3 Delivery Systems* (pp. 295–319). Academic Press. https://doi.org/10.1016/b978-0-12-821391-9.00016-8

Sánchez, C. A. O., Zavaleta, E. B., García, G. R. U., Solano, G. L., & Díaz, M. P. R. (2021). Krill oil microencapsulation: Antioxidant activity, astaxanthin retention, encapsulation efficiency, fatty acids profile, in vitro bioaccessibility and storage stability. *Lwt*, *147*(April). https://doi.org/10.1016/j.lwt.2021.111476

Sarkar, A., Ye, A., & Singh, H. (2016). On the role of bile salts in the digestion of emulsified lipids. *Food Hydrocolloids*, *60*, 77–84. https://doi.org/10.1016/j.foodhyd.2016.03.018

Shen, Z., Apriani, C., Weerakkody, R., Sanguansri, L., & Augustin, M. A. (2011). Food matrix effects on in vitro digestion of microencapsulated tuna oil powder. *Journal of Agricultural and Food Chemistry*, *59*(15), 8442–8449. https://doi.org/10.1021/jf201494b

Singh, H., & Ye, A. (2013). Structural and biochemical factors affecting the digestion of protein-stabilized emulsions. *Current Opinion in Colloid and Interface Science*, *18*(4), 360–370. https://doi.org/10.1016/j.cocis.2013.04.006

Solomando, J. C., Antequera, T., & Perez-Palacios, T. (2020a). Lipid digestion products in meat derivatives enriched with fish oil microcapsules. *Journal of Functional Foods*, *68*. https://doi.org/10.1016/j.jff.2020.103916

Solomando, J. C., Antequera, T., & Pérez-Palacios, T. (2020b). Study on fish oil microcapsules as

neat and added to meat model systems: Enrichment and bioaccesibility of EPA and DHA. *Lwt*, *120*(108946). https://doi.org/10.1016/j.lwt.2019.108946

Taboada, M. L., Heiden-Hecht, T., Brückner-Gühmann, M., Karbstein, H. P., Drusch, S., & Gaukel, V. (2021). Spray drying of emulsions: Influence of the emulsifier system on changes in oil droplet size during the drying step. *Journal of Food Processing and Preservation*, *45*(9), 1–11. https://doi.org/10.1111/jfpp.15753

Yang, J., & Ciftci, O. N. (2020). In vitro bioaccessibility of fish oil-loaded hollow solid lipid micro- and nanoparticles. *Food and Function*, *11*(10), 8637–8647. https://doi.org/10.1039/d0fo01591a

Zhu, Y., Peng, Y., Wen, J., & Quek, S. Y. (2021). A comparison of microfluidic-jet spray drying, two-fluid nozzle spray drying, and freeze-drying for co-encapsulating β-carotene, lutein, zeaxanthin, and fish oil. *Foods*, *10*(7). https://doi.org/10.3390/foods10071522

VII. Development of Fish Oil-Loaded Microcapsules Containing Whey Protein Hydrolysate as Film-Forming Material for Fortification of Low-Fat Mayonnaise *

The influence of the carbohydrate-based wall matrix (glucose syrup, GS, and maltodextrin, MD21) and the storage temperature (4 °C or 25 °C) on the oxidative stability of microencapsulated fish oil was studied. The microcapsules (ca. 13 wt% oil load) were produced by spray-drying emulsions stabilized with whey protein hydrolysate (WPH), achieving high encapsulation efficiencies (>97%). Both encapsulating materials showed an increase in the oxidation rate with the storage temperature. The GS-based microcapsules presented the highest oxidative stability regardless of the storage temperature with a peroxide value (PV) of 3.49 ± 0.25 meq O2/kg oil and a content of 1-penten-3-ol of 48.06 ± 9.57 ng/g oil after six weeks of storage at 4 °C. Moreover, low-fat mayonnaise enriched with GS-based microcapsules loaded with fish oil and containing WPH as a film-forming material (M-GS) presented higher oxidative stability after one month of storage when compared to low-fat mayonnaise enriched with either a 5 wt% fish oil-in-water emulsion stabilized with WPH or neat fish oil. This was attributed to a higher protective effect of the carbohydrate wall once the microcapsules were incorporated into the mayonnaise matrix.

* JOURNAL PAPER: N.E. Rahmani-Manglano, I. González-Sánchez, P.J. García-Moreno, F.J. Espejo-Carpio, C. Jacobsen, E.M. Guadix. (2020). Development of fish oil-loaded microcapsules containing whey protein hydrolysate as film-forming material for fortification of low-fat mayonnaise. *Foods*, 9(5): 545 (IF: 5.561; category: FOOD SCIENCE & TECHNOLOGY - SCIE; position: 35/144; Q1)

1. INTRODUCTION

Food fortification with omega-3 polyunsaturated fatty acids (ω-3 PUFAs) has gained increased scientific and industrial interest in the last decades (Jacobsen, 2010). This is mainly due to the health benefits attributed especially to eicosapentaenoic (EPA; C20:5 n-3) and docosahexaenoic (DHA; C22:6 n-3) fatty acids (Calder, 2014; Jacobsen, 2016). However, the high number of bis-allylic hydrogens present in these ω-3 PUFAs make them highly prone to oxidation, leading to: (i) the loss of their nutritional properties and (ii) the appearance of odor/flavor-active and/or other potentially toxic compounds (Arab-Tehrany et al., 2012). Hence, the development of efficient delivery systems which prevent ω-3 PUFAs oxidation prior (e.g., delivery system production); during (e.g., food processing) and after its incorporation into complex food matrices (e.g., food storage) is of great importance. In this regard, encapsulation technologies are of special interest for the food industry, since they allow the design of functional food systems overcoming the inherent drawbacks of ω-3 PUFAs rich oils (e.g., fish oil), such as low oxidative stability, low solubility and oily texture. Encapsulation consists of entrapping the core material (e.g., fish oil) within a homogeneous/heterogeneous matrix (e.g., encapsulating agent/s) to develop a physical barrier between the bioactive compound and the environment, thus preventing its degradation, easing its handling and/or controlling the bioactive release (Desai & Park, 2005). Among all the available encapsulation techniques (e.g., freeze-drying or coacervation), spray-dying is the most commonly used by the food industry to encapsulate bioactive ingredients (Jacobsen et al., 2018). Fish oil microencapsulation by spray-drying has been widely studied over the last decade, being the most commonly used encapsulating agents of carbohydrates, proteins and their combinations (Encina et al., 2016).

Nonetheless, additional stabilization techniques are required (e.g., addition of antioxidants to the formulation), since it has been demonstrated that the emulsification process and subsequent drying using air at high temperatures (170−200 °C) result in the initial oxidation of the oil (Morales-Medina et al., 2016; Serfert et al., 2009). Bioactive compounds such as protein hydrolysates or peptides, which exhibit both emulsifying and antioxidants properties, are a promising alternative to conventional antioxidants (e.g., tocopherols). In heterogeneous systems such as fish oil-in-water emulsions (which is the feed to the spray-drier), the location of the antioxidants determines their antioxidant activity (McClements & Decker, 2018; Shahidi & Zhong, 2011). The same is also the case for the resulting microcapsule.

Antioxidants located at the oil/water interface (in emulsions) or at the oil/encapsulating agent interface (in spray-dried microcapsules) will be preferred to inhibit lipid oxidation. This is because these interfaces are the place where oxidation is started by the contact of prooxidants (e.g., trace of metals and oxygen) and the oil.

Whey protein hydrolysates (WPH) have been reported to exhibit antioxidant activity (e.g., radical scavenging activity, metal chelating and reducing power) (Eberhardt et al., 2019; Hernández-Ledesma et al., 2005; Padial-Domínguez et al., 2020). Moreover, due their high emulsifying activity, WPH have also been used to produce fish oil microcapsules in combination with maltodextrin (DE 16.5−19.5) (Ramakrishnan et al., 2013, 2014). Nevertheless, the protective effect of WPH on the reduction of lipid oxidation in the microcapsules was not investigated in any of the latter studies. More recently, Tamm et al. (2015) produced fish oil-loaded microencapsulates using glucose syrup as the wall material in the presence of unmodified or hydrolyzed β-lactoglobulin (β-LG). The unmodified and hydrolyzed proteins were used as a film-forming material around the oil droplets. The authors found that β-LG hydrolysates enhanced the oxidative stability of microencapsulated fish oil when compared to the unmodified protein. This fact was attributed to an improved accessibility of the resulting amino acid residues with antioxidant properties after enzymatic hydrolysis. Thus, the results reported by Tamm et al. (2015) showed a promising potential for the use of spray-dried microcapsules loaded with fish oil and obtained with WPH as a delivery system of ω-3 PUFAs. However, the enrichment of food products with ω-3 microencapsulates having WPH as a film-forming material, and its effect on the physicochemical properties of the fortified product remains to be evaluated.

In this regard, the aims of the present study were to investigate: (i) the effect of the carbohydrate-based wall material (glucose syrup or maltodextrin) and (ii) the storage temperature (4 °C or 25 °C) on the oxidative stability of spray-dried microcapsules loaded with fish oil and produced using WPH as a film-forming material. In addition, the feasibility of using spray-dried microcapsules containing WPH for fortifying a low-fat mayonnaise (40 wt% of total oil) with ω-3 PUFAs was assayed. For that purpose, the physical and oxidative stabilities of low-fat mayonnaise enriched either with microcapsules loaded with fish oil, a fish oil-in-water emulsion stabilized with WPH or neat fish oil were investigated during one month of storage.

2. MATERIALS AND METHODS

2.1 Materials

Whey protein (34.6 wt% protein content) and maltodextrin (DE 21) were kindly provided by Abbott (Granada, Spain), while the glucose syrup (DE38, C*Dry 1934) was kindly donated by Cargill Germany GmbH (Krefeld, Germany). Alcalase 2.4 L was purchased from Novozymes (Bagsvaerd, Denmark). Refined fish oil (Omega Oil 1812 TG Gold) was acquired from BASF Personal Care and Nutrition GmbH (Illertissen, Germany) and stored at −80 °C until use. The fatty acid composition of the fish oil was determined by gas chromatography (GC), as described in Morales-Medina et al. (2015), and it was as follows (major fatty acids in %, w/w): 7.0% myristic acid (C14:0), 16.7% palmitic acid (C16:0), 8.8% palmitoleic acid (C16:1n-7), 4.1% stearic acid (C18:0), 8.2% oleic acid (C18:1n-9), 19.3% eicosapentaenoic acid (C20:5n-3) and 16.1% docosahexaenoic acid (C22:6n-3). Peroxide value (PV) of the fish oil was measured as described in Section 2.5.4 and was 0.36 ± 0.03 meq O2/kg oil. Tocopherol content (TC) of the fresh oil was measured as described in Section 2.5.4 and was: 427.0 ± 0.0 µg/g oil, 48.0 ± 1.4 µg/g oil, 1891.0 ± 12.7 µg/g oil and 644.3 ± 4.1 µg/g oil for alpha-, beta-, gamma- and delta-tocopherol, respectively. Refined sunflower oil (SFO), for the production of mayonnaise, was purchased from the local market. The specified fats compositions as given by the supplier were: 10.77 wt% saturated fats, 30.47 wt% monounsaturated fats and 58.76 wt% polyunsaturated fats. Peroxide value (PV) of the sunflower oil was measured as described in Section 2.7.2 and was of 3.5 ± 0.2 meq O2/kg oil. Stabilizer Grinsted FF 1149 was kindly donated by DuPont (DuPont Nutrition Biosciences Aps, Haderslev, Denmark). The rest of the ingredients used in the production of the mayonnaises were purchased in the local market. The rest of reagents used for analysis were of analytical grade.

2.2 Enzymatic Hydrolysis of Whey Protein

Enzymatic hydrolysis of whey protein (WP) was carried out in an automatic titrator 718 Stat Titrino (Metrohm AG, Herisau, Switzerland) to a degree of hydrolysis 10% (DH 10) with alcalase. For this purpose, a solution containing 36 g of protein was prepared with distilled water to a final volume of 0.9 L. The process conditions were set to 50 °C and the pH to 8, and the enzyme-substrate ratio was fixed to 0.55 (w/w). The degree of hydrolysis was

estimated with the pH-stat-method, as described by Camacho et al. (2001). The hydrolysis reaction took ca. 1.5 h, and the enzyme was deactivated at 100 °C for 5 min. The whey protein hydrolysate (WPH) solution was stored at −20 °C until further use.

2.3 Microencapsulation of Fish Oil by Spray-Drying

Previous to spray-drying, fish oil-in-water emulsions stabilized with WPH and containing one of the encapsulating agents were produced. The aqueous phase of the emulsions was prepared by dissolving the glucose syrup (GS) or maltodextrin (MD21) (28%, w/w) in the WPH solution and adding distilled water in order to have a protein content of 2 wt%. Then, the pH was adjusted to pH 8. A pre-homogenization process was carried out for 2 min at 15,000 rpm using an Ultraturrax T-25 homogenizer (IKA, Staufen, Germany), while the oil (5%, w/w) was added during the first minute. The coarse emulsions were then homogenized in a high-pressure homogenizer (PandaPLUS 2000; GEA Niro Soavi, Lübeck, Germany) at a pressure range of 450/75 bar, applying 3 passes. The temperature during the emulsification process was kept under 32 °C. Subsequently, the emulsions were dried in a pilot plant scale spray-drier (Mobile Minor; Niro A/S, Copenhagen, Denmark) at 190/80 °C inlet/outlet temperature, respectively. The pressure of the pneumatic air activating the rotary atomizer was set to 4 bar, which implies a rotational speed of the atomizer of 22,000 rpm.

2.4 Oil Droplet Size Distribution (ODSD)

The oil droplet size distribution (ODSD) of both the parent emulsions (emulsions fed to the spray-drier) at day 0 and the reconstituted emulsions (emulsions resulting of redispersing the microcapsules in water) at days 0 (week 0), 14 (week 2), 28 (week 4) and 42 (week 6) were measured by laser diffraction in a Mastersizer 2000 (Malvern Instruments, Ltd., Worcestershire, UK), as described by García-Moreno et al. (2018). The emulsions were reconstituted by dissolving the powder in distilled water in order to achieve the same solids content as the original emulsion. Measurements were made in duplicate, and the results are given in 90th percentile.

2.5 Physicochemical Characterization of Microencapsulates

2.5.1 Moisture Content (MC) and Water Activity (aw)

The moisture content of the microcapsules was determined using an infrared balance (AD-471A, Tokyo, Japan) where ca. 1 g of powder was heated at 105 °C for 90 min until a constant weight. The water activity was measured using a LabMASTER-aw (Novasina AG, Lachen, Switzerland) at 20 °C. The measurements were carried out in duplicates.

2.5.2 Encapsulation Efficiency (EE)

The encapsulation efficiency (EE) was determined by extracting the surface oil, as described by Danviriyakul et al. (2002), with some modifications. In brief, 2.5 g of powder was weighed and mixed with 15 mL of hexane in a vortex mixer for 2 min and then centrifuged at 2720× g for 20 min. Five mL of supernatant were collected on a Pyrex tube, previously weighed, and the solvent was evaporated under a constant flow of nitrogen. After total solvent evaporation, in order to calculate the surface oil, the Pyrex was weighed again, and the oil concentration was adjusted to the initial volume of hexane added. The EE was calculated as follows:

$$EE, \% = \frac{A - B}{A} \cdot 100 \tag{21}$$

where A refers to the total theoretical amount of oil (g) and B to the non-encapsulated oil (g). Measurements were carried out in triplicate.

2.5.3 Morphology and Size

The morphology and size of the microcapsules were studied by means of scanning electron microscopy (SEM) using a FEI microscope (FEI Inspect, Hillsboro, OR, USA). For this purpose, a thin layer of microcapsules was placed on a carbon tape and sputter-coated with gold, 8 s, 40 mA using a Cressington 208HR Sputter-Coater (Cressington Scientific Instruments, Watford, England). The SEM images were taken in the range 830×–870× magnification with a 10-kV accelerating voltage. Then, they were analyzed using the ImageJ software (National Institute of Health). To determine the mean diameters of the microcapsules, more than 150 randomly selected microcapsules were measured.

2.5.4 Oxidative Stability

Spray-dried microcapsules loaded with fish oil were stored at 4 °C and 25 °C during 6 weeks in brown bottles (30 mL and 26-mm inner diameter). Each bottle contained 10 g of microcapsules. Samples were taken at days 0 (week 0), 7 (week 1), 14 (week 2), 21 (week 3), 28 (week 4), 35 (week 5) and 42 (week 6) and placed at −80 °C under a nitrogen atmosphere until the determination of the peroxide value (PV), tocopherol content (TC) and content of secondary volatile oxidation products (SVOP) was carried out.

2.5.4.1 Peroxide Value (PV)

Fish oil was extracted from the microcapsules, as described by Bligh and Dyer (1959) using a reduced amount of chloroform/methanol (1:1, w/w) solvent. For the extraction, ca. 2 g of powder were weighed and then dissolved by adding 10 mL of distilled water. Peroxide value (PV) was then quantified on the lipid extracts using the colorimetric ferric-thiocyanate method at 500 nm, according to Shantha and Decker (1994). In brief, the extracted oil was diluted in chloroform/methanol (7:3, v/v) prior to the addition of iron-II-chloride and ammonium thiocyanate solutions. Then, the mixture was incubated for 5 min at room temperature. Measurements were carried out in duplicates. Results were expressed in meq O2 per kg of oil.

2.5.4.2 Tocopherol Content (TC)

Tocopherol content of the microencapsulated oil was determined by HPLC (Agilent 1100 Series) according to the American Oil Chemists' Society (AOCS) official method (AOCS, 1998). In brief, about 2 g of the chloroform extract was evaporated under nitrogen and dissolved in 1-mL n-heptane, and from this, 0.8 mL were taken into separate vials before injection of an aliquot (40 µL) on a Spherisorb S5W column (250 × 4.6 mm) (Phase Separation Ltd., Deeside, UK). Elution was performed with an isocratic mixture of n-heptane/2-propanol (100:0.4, v/v) at a flow of 1 mL/min. Detection was done using a fluorescence detector with excitation at 290 nm and emission at 330 nm, according to the AOCS (AOCS, 1998). Measurements were performed in duplicate and quantified by authentic standards. Results were expressed in µg tocopherol per g of oil.

2.5.4.3 Secondary Volatiles Oxidation Products (SVOP)—Dynamic Headspace GC-MS

Approximately, 1 g of powder and 30 mg of internal standard (4-methyl-1-pentanol and 30 µg/g water) were weighed in a purge bottle and mixed with 10 mL of distilled water. Then, the bottle content was heated for 30 min in a water bath at 45 °C while purging with nitrogen (flow rate 150 mL/min). The volatile compounds released were retained in Tenax GR tubes (Perkin Elmer 1/4″ stainless steel tubes packed with 225 ± 3 mg Tenax GR 60–80 mesh). Then, these compounds were desorbed again by means of helium and heat (200 °C) in an Automatic Thermal Desorber (ATD-400; Perkin Elmer, Norwalk, CN), cryofocused on a cold trap (−30 °C), released again (220 °C) and led to a gas chromatograph (HP 5890IIA; Hewlett Packard, Palo Alto, CA, USA and Column: DB-1701, 30 m × 0.25 mm × 1.0 µm; J&W Scientific, Folsom, CA, USA). The individual compounds were analyzed by mass-spectrometry (HP 5972 mass-selective detector; Agilent Technologies, Santa Clara, California, USA; electron ionization mode: 70 eV and mass to charge ratio scan between 30 and 250). The released volatile compounds were then identified by MS-library searches (Wiley 138K, John Wiley and Sons, Hoboken, New Jersey, USA and Hewlett-Packard, San Jose, California, USA) and quantified through calibration curves using external standards (butanal, pentanal, 1-penten-3-ol, hexanal, (E)-2-hexenal, heptanal, octanal, (E,E)-2,4-heptadienal, (Z)-4-heptenal and nonanal) dissolved in 96% ethanol. The standard solutions were diluted to concentrations of approximately 2.5, 5, 10, 50, 100 and 500 µg/mL, and 1 µL of each was directly injected on the Tenax tubes. Measurements were made in triplicates for each sample. Results were expressed as ng/g oil.

2.6 Production of Fortified Mayonnaise

Light mayonnaise (40 wt% of total oil) fortified with ω-3 PUFAs (2.5 wt% fish oil) was produced following three different approaches: (i) incorporating neat fish oil (M-NFO), (ii) incorporating a fish oil-in-water emulsion stabilized with WPH (M-EM) and (iii) incorporating spray-dried microcapsules loaded with fish oil and obtained with WPH as a film-forming material and glucose syrup as the encapsulating agent (M-GS). In all cases, 300 g of mayonnaise containing: 2.5 wt% of fish oil, 37.5 wt% of SFO, 4 wt% of egg yolk, 1 wt% of vinegar, 0.4 wt% of lemon juice and 0.3 wt% of salt were prepared as described by Miguel et al. (2019), with some modifications. In the case of M-NFO and M-EM samples, 1 wt% of sugar was also added. For the mayonnaise preparation, first, distilled water, salt,

sugar and 6 mL of sodium azide solution (0.0125 g/mL) were mixed in a blender (Taurus robot, 300 inox.) for 15 s. For the M-EM sample, also 150 g of emulsified fish oil were added in the first step. Then, the egg yolk was incorporated and mixed for 15 s. Stabilizer Grinsted FF was manually dissolved in 10 g of sunflower oil (and fish oil in the case of the M-NFO sample) and added to the blender (15 s mixing). Then, the rest of the oil was added in three steps (except ca. 10 wt%) and mixed for 30 s each. Vinegar and lemon juice were dispersed manually to the remaining oil (ca. 10 wt%) and added as the last step. Mixing in this case lasted 30 s. In the case of the M-GS sample, 58.5 g of microcapsules were added to the blender at this last step and mixed for 45 s to complete the dispersion.

2.7 Characterization of Fortified Mayonnaise

2.7.1 Physical Stability: Droplet Size Distribution and Viscosity

The droplet size distribution and viscosity of the fortified mayonnaises were evaluated after production and during 28 days of storage at 25 °C.

The droplet size distribution was measured as described in Section 2.4. For this purpose, 1 g of mayonnaise was dissolved in sodium dodecyl sulfate (SDS) buffer (10-mM NaH2PO4, pH 7) to a ratio of 1:5 (w/w). Then, the solution was sonicated for 15 min to avoid droplets agglomeration. Measurements were made in triplicate, and the results are given in surface area mean diameter (D[3,2]) and volume weighted mean diameter (D[4,3]).

The viscosity of the fortified mayonnaise samples was measured using a rotatory Kinexus Malvern rheometer (Malvern Panalytical Ltd., Worcestershire, UK) equipped with a plate-plate geometry. An increasing gradient of stress was applied from 0.1–200 Pa at 25 °C. Measurements were made in triplicate.

2.7.2 Oxidative Stability

To monitor the oxidative stability of low-fat fortified mayonnaise, 40 g of each sample were stored in polyethylene containers (60 mL) at 25 °C during 28 days. Samples were taken at days 0 (week 0), 7 (week 1), 14 (week 2), 21 (week 3) and 28 (week 4) and kept under an inert atmosphere at −80 °C until analysis.

2.7.2.1 Peroxide Value (PV)

Oil extraction from the low-fat mayonnaise for the PV determination was made as follows: ca. 0.5 g of mayonnaise were weighed and mixed with 5 mL of distilled water. Then, 20 mL

of hexane/2-propanol (1:1, v/v) solvent was added and mixed for 5 min. The resulting mixture was centrifuged at 670× g for 2 min. PV was measured using the thiocyanate assay, as described in Drusch et al. (2012), with some modifications. Extracted oil was diluted with 2-propanol prior to the addition of iron-II-chloride and ammonium thiocyanate solutions and then was incubated for 5 min at 25 °C. Oil extraction was made in duplicate for each sample. The PV measurements were made in triplicate for each oil extract. Results were expressed in meq O2 per kg of oil.

2.7.2.2 P-Anisidine Value (AV)

For the p-anisidine value determination, 2.5 g of mayonnaise were weighed to carry out the oil extraction, as described in Section 2.7.2. Oil extraction was made in duplicate for each sample. The AV measurements were made in triplicate according to the ISO 6885:2006 method (ISO 6885:2006, 2006) for each oil extract.

2.8 Statistical Analysis

For data analysis, the software Statgraphics Centurion XV (Statistical Graphics Corp., Rockville, MD, USA) was used. First, one-way ANOVA was performed to identify if there were differences between the samples. Then, a multiple sample comparison using Tukey's test allowed to identify means which were significantly different from each other. Differences between means were considered significant at $p \leq 0.05$.

3. RESULTS AND DISCUSSION

3.1 Oil Droplet Size Distribution (ODSD) of Emulsions

The parent emulsions and reconstituted emulsions presented values of the 90th percentile below 2 μm (Table 7), indicating that the WPH efficiently stabilized the oil droplets by maintaining the structural integrity of the oil/water interface prior, during and after the microencapsulation process (Tamm et al., 2015). Despite the lack of surface-active properties of the encapsulating agents used, the results show significant differences ($p < 0.05$) for the ODSD of the parent emulsions prior to drying, which are mainly attributed to minor differences in pressure adjustments in the homogenizer. In this line, Hogan et al. (2001) found that the volume average diameter (D[4,3]) of soy oil emulsions stabilized with

sodium caseinate did not differ irrespective of the dextrose equivalence (DE) of the non-surface-active carbohydrate used as a wall constituent.

Table 7. Oil droplet size distribution (ODSD) of fresh and reconstituted emulsions during storage time at 4 and 25 °C.

		d_{90}, µm	
		GS	**MD21**
Parent emulsions		$0.587 \pm 0.001^{+,*}$	$0.555 \pm 0.001^{+,*}$
Reconstituted emulsion after spray-drying			
Week 0		$0.613 \pm 0.006^{+,a,u,*}$	$0.663 \pm 0.001^{+,a,u,*}$
4 °C	Week 2	$0.624 \pm 0.006^{a,j,*}$	$0.699 \pm 0.005^{b,j,*}$
	Week 4	$0.653 \pm 0.002^{b,j,*}$	$0.730 \pm 0.001^{c,j,*}$
	Week 6	$0.654 \pm 0.004^{b,j,*}$	$0.825 \pm 0.001^{d,j,*}$
25 °C	Week 2	$0.599 \pm 0.001^{u,k,*}$	$0.703 \pm 0.011^{v,j,*}$
	Week 4	$0.669 \pm 0.005^{v,j,*}$	$0.717 \pm 0.003^{v,k,*}$
	Week 6	$0.659 \pm 0.010^{v,j,*}$	$0.882 \pm 0.002^{w,k,*}$

GS: glucose syrup and MD21: maltodextrin with DE 21. Means within the same column followed by a plus sign, +, indicates statistical differences ($p \leq 0.05$) between the parent and reconstituted (week 0) emulsions. Means within the same column followed by different letters, a–c, indicate statistical differences ($p \leq 0.05$) between sampling points for the same encapsulating agent at 4 °C. Means within the same column followed by different letters, u–w, indicate statistical differences ($p \leq 0.05$) between sampling points for the same encapsulating agent at 25 °C. Means within the same column followed by different letters, j,k, indicate statistical differences ($p \leq 0.05$) between samples stored at different temperatures for the same encapsulating agent at the same sampling point. Means within the same row followed by an asterisk, *, indicates statistical differences ($p \leq 0.05$) between encapsulating agents.

After drying, a small but significant ($p < 0.05$) increase in the ODSD occurred in both samples at week 0, suggesting coalescence of the non-encapsulated oil after reconstitution (Drusch et al., 2007). In the case of GS-based reconstituted emulsions, the ODSD during six weeks of storage was in the range 0.61–0.66 µm for both storage temperatures. On the other hand, for MD21-based emulsions, the ODSD increased progressively during the storage time from 0.66 to 0.82 µm at 4 °C and 0.66 to 0.88 µm at 25 °C. These results suggest oil leakage in the MD21 microcapsules, which increased the surface fat content and led to more oil available to coalesce after reconstitution. This finding may be related to the poorer retention properties of MD21 as a wall material when compared to GS, attributed to the lower molecular weight of the oligosaccharides present in the glucose syrup. Moreover, the results show that the storage temperature had little effect on the retention properties of the encapsulating agents used, despite the statistical analysis results showing significant differences for some sampling points for both storage temperatures assayed.

3.2 Physicochemical Characterization of Microencapsulates

3.2.1 Moisture Content, Water Activity and Encapsulation Efficiency (EE)

The moisture content (MC) was of 4.7% ± 0.4% and 4.2% ± 0.1% for the GS and MD21-based microencapsulates, respectively. These low MC values, together with the low water activity (aw) of the microencapsulates (GS, 0.184 ± 0.004 and MD21, 0.187 ± 0.001), are desired in order to confer long-term microbiological stability for the microcapsules. Moreover, as no significant differences could be observed between the samples ($p > 0.05$), it can be assumed that the MC and aw are independent of the encapsulating agent used (while maintaining constant the spray-drying processing variables).

High EE values were obtained for both types of microcapsules, although a significantly higher EE value was found for the GS-based microencapsulates when compared to the MD21-based microcapsules (98.07 ± 0.04% vs. 97.66 ± 0.06%). Interestingly, the slightly higher EE value of the GS-based microencapsulates cannot be attributed to a smaller droplet size of the parent emulsion (Table 7). Thus, differences in the EE may be consequence of a positive correlation between the EE of encapsulates and DE of the carbohydrates used as wall materials (Hogan et al., 2001; Sheu & Rosenberg, 1995; Young et al., 1993). This fact is explained on the basis that increasing the DE of the carbohydrate leads to smaller oligosaccharides, which are thought to form a more uniform and denser packaging of the core material, which favors oil encapsulation.

3.2.2 Morphology and Size

Figure 45 shows the morphology and particle size distribution of the microcapsules. Both types of microcapsules showed a spherical shape with smooth surfaces, even though a few microcapsules with wrinkled surfaces could also be observed. Furthermore, no particle agglomerations were detected, which can be attributed to the low surface fat content of the microencapsulates produced (Hogan et al., 2001). Microcapsules prepared with MD21 presented a wider particle size distribution when compared to the microcapsules produced with GS. The percentage of microcapsules with diameters below 20 µm was 92.9% and 70.5% for the GS and MD21-based microencapsulates, respectively (Figure 45), while the particle mean diameters were 12.5 ± 5.5 µm and 16.8 ± 10.2 µm, respectively. Since the rotational speed of the atomizer was kept constant, the larger particle size of the MD21-based microencapsulates was most likely due to the higher viscosity of the MD21-feed emulsion, which led to larger emulsion droplets after atomization and, hence, larger dried

microcapsules when compared to the GS-feed emulsion (Gharsallaoui et al., 2007; Hogan et al., 2001).

(A)

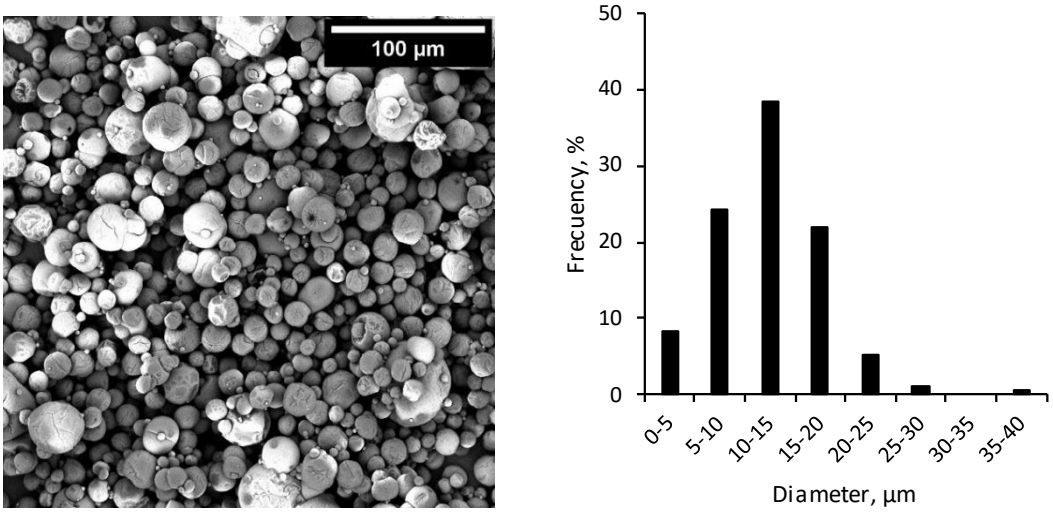

(B)

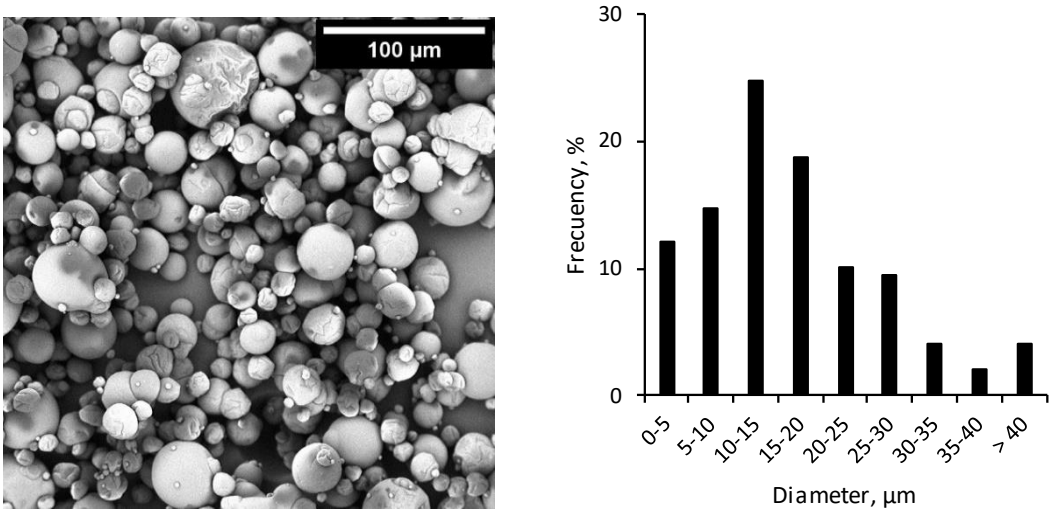

Figure 45. SEM micrographs and diameter distribution of fish oil-loaded microcapsules containing whey protein hydrolysate (WPH) as a film-forming material and glucose syrup (A) or maltodextrin DE21 (B) as the encapsulating agents.

3.2.3 Oxidative Stability of the Microencapsulates

3.2.3.1 Peroxide Value (PV) and Tocopherol Content (TC)

Oxidative stability of the microencapsulates was first evaluated by determining the formation of the primary oxidation products during storage (Figure 46). Right after

production, PV of 3.24 ± 1.38 and 3.73 ± 0.66 meq O2/kg oil were obtained for the GS and MD21-based microcapsules, respectively. No significant differences ($p > 0.05$) in the PV were observed between the two types of microcapsules at day 0, although a significant increase on the hydroperoxide content compared to the fresh oil (PV = 0.36 ± 0.03 meq O2/kg oil) could be noted. This is attributed to the encapsulation process itself, which involves mechanical stress, shear forces and heat, leading to the initial oil oxidation (Morales-Medina et al., 2016; Serfert et al., 2009). As expected, lipid oxidation was accelerated for the two types of microcapsules when increasing the storage temperature from 4 to 25 °C. For lipid autoxidation, an increase of 10 °C temperature results in a two-fold increase in the reaction rate (Jacobsen et al., 2009). However, the effect was more pronounced in the MD21-based microcapsules (PV = 9.01 ± 0.13 meq O2/kg oil after six weeks storage at 25 °C). This positive correlation between the lipid oxidation rate and storage temperature on microencapsulated fish oil has also been reported by other authors (Jeyakumari et al., 2018; Unnikrishnan et al., 2019) and could be attributed to the loss of natural antioxidants, as well as an increase in diffusivity of the prooxidant agents (e.g., oxygen, radicals and trace of metals) at higher temperatures.

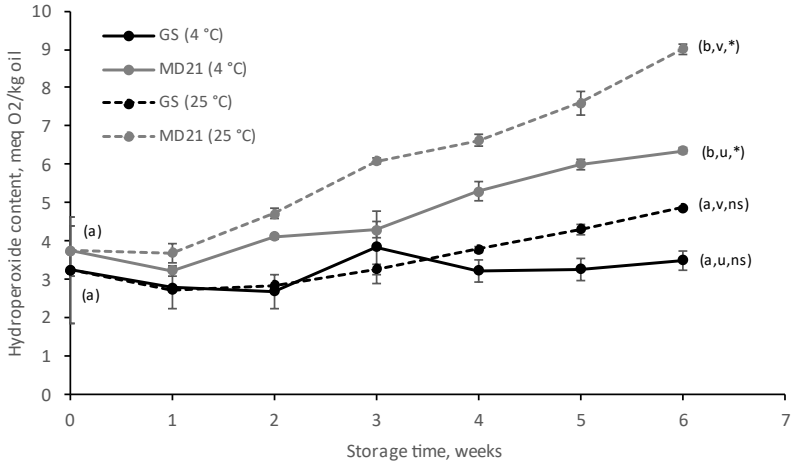

Figure 46. Peroxide value (PV) of spray-dried microcapsules loaded with fish oil during storage at: 4 °C (solid line, —•—) and 25 °C (broken line, - -•- -) encapsulated with glucose syrup (black) or maltodextrin (grey). Means within the same sampling point followed by a letter, a-b, indicates statistical differences ($p \leq 0.05$) between encapsulating agents for the same storage temperature. Means within the same sampling point followed by a letter, u-v, indicates statistical differences ($p \leq 0.05$) between storage temperatures for the same encapsulating agent. Means within the same sample followed by an asterisk (*) indicates statistical differences ($p \leq 0.05$) between week 0 and week 6. Means within the same sample followed by "ns" indicates no statistical differences ($p > 0.05$) between week 0 and week 6.

Nonetheless, although the temperature influenced lipid oxidation, higher PV values were found in MD21-based microcapsules in all cases. These results indicate that the influence of

the wall material (e.g., which determines the permeability to prooxidant species and retention properties) predominated over the storage temperature on microencapsulated fish oil oxidative stability. The lower PV of the GS-based microencapsulates has been attributed to the DE differences between carbohydrates and, thus, the molecular weight. Such differences affect the matrix free volume elements and the oxygen diffusivity through the wall. The latter increases with the increasing molecular weight of the carbohydrate (Boerekamp et al., 2019; Drusch et al., 2009). Moreover, the ODSD results showed oil leakage during the storage time for MD21-based microencapsulates (Section 3.1), which resulted in lower EE for MD21-based microcapsules and increased the content of easily oxidizable oil on the surface of these microcapsules.

Moreover, it is noteworthy that the PV results of this study were lower than others reported in literature that also produced fish oil microencapsulates within carbohydrate matrices. For instance, Drusch and Berg (2008) produced fish oil-loaded microcapsules (30 wt% or 50 wt%) by spray-drying into a matrix of nOSA-starch and GS at two drying temperature settings (160/60 °C or 210/90 °C) with PV of ca. 160–340 meq O2/kg oil after six weeks of storage at 20 °C. Likewise, Morales-Medina et al. (2016) microencapsulated fish oil using fish protein hydrolysates as emulsifiers and GS as the encapsulating material. The PV of the microencapsulates reported by the authors after six weeks of storage at 20 °C were also higher than those values obtained in the current study (ca. 120–160 meq O2/kg oil). It should be noted that both the GS used and the inlet/outlet drying temperatures were similar to the present work.

In addition to the PV, alpha-, beta-, delta- and gamma-tocopherols were quantified in the microcapsules during storage (see Figure S 27 in the Supplementary Material). A significant decrease ($p < 0.05$) was observed in the content of alpha-, delta- and gamma-tocopherols for the microcapsules when compared to the fresh oil. This indicates the formation of radicals during emulsification and drying processes and that tocopherols were consumed as a consequence of their radical scavenging activity. It is worth mentioning that the high initial content of tocopherols in the fresh fish oil is a consequence of the addition of these compounds to the oil by the producer. The tocopherol content of the microencapsulates slightly changed over the storage time, regardless of the encapsulating agent used and the storage temperature. The latter leads us to conclude that the oxidative stability of the microcapsules during storage was not influenced by their tocopherol content but was mainly

determined by the protection provided by the encapsulating agents, as well as the stabilization provided with the WPH.

3.2.3.2 Secondary Volatile Oxidation Products (SVOP)

Figure 47 shows the content of the SVOP (1-penten-3-ol, hexanal, (E)-2-hexenal, (Z)-4-heptenal and nonanal) in the microcapsules during storage. Despite the fact that hexanal and nonanal are compounds mainly derived from the oxidation of omega-6 and omega-9 fatty acids, these compounds have also been identified in oxidized fish oil. The rest of the identified SVOP (1-penten-3-ol, (E)-2-hexenal and (Z)-4-heptenal) are typical secondary oxidation products derived from omega-3 PUFAs, and all are related to undesirable odors and flavors (Frankel, 2012b). For instance, the odor of 1-penten-3-ol, hexanal and (E)-2-hexenal have been described as earthy and grassy, while (Z)-4-heptenal and nonanal have been described as creamy and tallowy, respectively (Frankel, 2012a; Fu et al., 2009). The odor threshold values for these compounds in oxidized oils range from 0.04 to 3.0 ppm (Frankel, 2012b).

As occurred with the PV, the higher storage temperature favored lipid oxidation for both types of microencapsulates, since the highest SVOP content was found in the samples stored at 25 °C compared to those stored at 4 °C. However, different trends in the SVOP curves can be observed during the storage time (Figure 47). In the case of 1-penten-3-ol (Figure 47A) and (Z)-4-heptenal (Figure 47D), the influence of the storage temperature predominated over the wall material regarding lipid oxidation, since the lower contents of these compounds were found in the encapsulates stored at 4 °C, regardless of the encapsulating agent. Nonetheless, it is noteworthy that, in both cases, the GS-based microcapsules were the less-oxidized after six weeks of storage (48.06 ± 9.57 ng of 1-penten-3-ol/g oil and 14.85 ± 2.14 ng of (Z)-4-heptenal/g oil). On the contrary, the trend of hexanal (Figure 47B), (E)-2-hexenal (Figure 47C) and nonanal (Figure 47E) curves are in line with the PV results (Section 3.2.3.1, with MD21-based microcapsules presenting higher contents of the these volatiles independently of the storage temperatures when compared to GS-based microcapsules. This indicates, for the latter SVOP, a clear influence of the wall material over the storage temperature on microencapsulated fish oil oxidative stability.

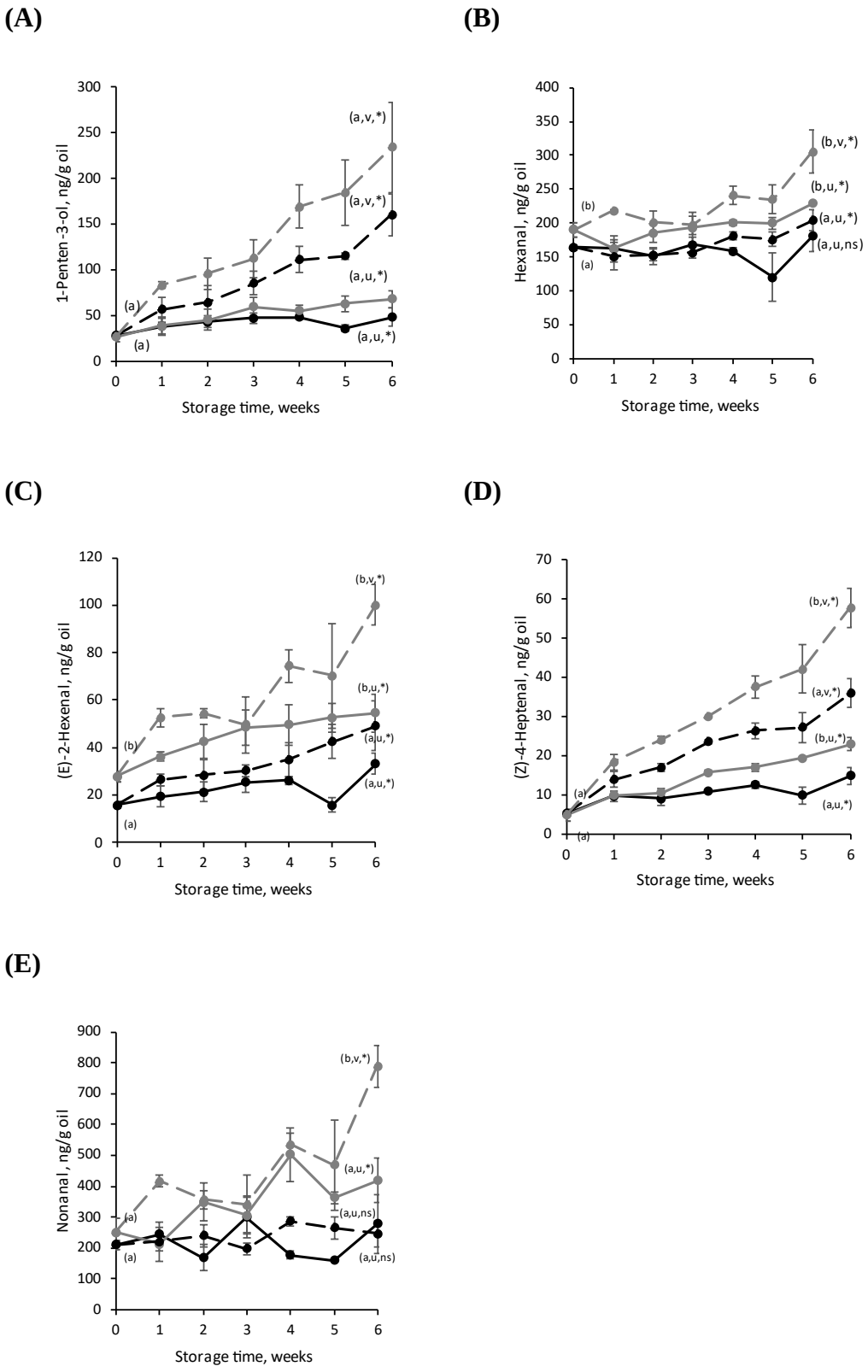

Figure 47. Secondary volatile oxidation products (1-penten-3-ol (A), hexanal (B), (E)-2-hexenal (C), (Z)-4-heptenal (D) and nonanal (E)) of spray-dried microcapsules loaded with fish oil during storage at: 4 °C (solid line, —•—) and 25 °C (broken line, - -•- -) encapsulated with glucose syrup (black) and maltodextrin (grey). Means within the same sampling point followed by a letter, a-b, indicates statistical differences ($p \leq 0.05$) between encapsulating agents for the same storage temperature. Means within the same sampling point followed by a letter, u-v, indicates statistical differences ($p \leq$

0.05) between storage temperatures for the same encapsulating agent. Means within the same sample followed by an asterisk (*) indicates statistical differences ($p \leq 0.05$) between week 0 and week 6. Means within the same sample followed by "ns" indicates no statistical differences ($p > 0.05$) between week 0 and week 6.

Most of the studies published regarding the oxidative stability of microencapsulated fish oil by spray-drying have only analyzed the course of propanal during storage, since it is an important SVOP resulting from the oxidation of both EPA and DHA DHA (Drusch et al., 2006, 2009; Drusch & Berg, 2008; Serfert et al., 2009). However, our results show that different trends can be observed when studying more than one SVOP. Likewise, García-Moreno et al. (2018) studied the course of 1-penten-3-ol, (E)-2-pentenal, heptanal and nonanal during 21 days of storage at 20 °C for electrosprayed microcapsules loaded with fish oil (20 wt%) into a matrix of pullulan blended with dextran or GS. For 1-penten-3-ol, the authors reported values ranging from 500–2000 ng/g oil, while, for nonanal, the values ranged from 2000–5000 ng/g oil. In any case, the values reported by these authors were much higher than those of the current work, which are well below the compounds odor threshold limits in oil, indicating that the microcapsules may be stable in regard to their organoleptic properties.

Taken altogether, the PV and SVOP content results show that the most oxidatively stable microcapsules were those produced with GS as a wall material. This is directly related to the lower molecular weight of GS as a result of its higher DE when compared to MD21, which led to microencapsulates: (i) with higher EE and retention of the core material and (ii) less porous and, thus, less permeable to prooxidant species (e.g., oxygen). However, the higher oxidative stability of the GS-based microencapsulates reported in the current study cannot only be attributed to the protective effect of the wall material. Tamm et al. (2015) produced microcapsules (ca. 31 wt% oil load) spray-drying emulsions stabilized with β-LG hydrolysates (2.2 wt%) and GS as wall material. The authors reported a higher oxidative stability (based on the PV) of the microencapsulates containing hydrolysates when compared to those containing unmodified protein, which clearly revealed the additional protective effect of using whey protein hydrolysates for microencapsulating fish oil. These results are in line with those of our study, where the content of both the hydroperoxides (PV) and SVOP of GS-based microcapsules containing WPH as a film-forming material remained low during six weeks of storage. The protective effect of the WPH used in this study is related to its high emulsifying and antioxidant activities (both radical scavenging, EC50 = 4.45 ± 0.00 mg/mL, and metal chelating, EC50 = 0.95 ± 0.01 mg/mL), as reported in our previous work (unpublished results). The antioxidant activity of the WPH is mainly attributed to its high

content in Tyr, Met and, to a lesser extent, His. Tyr has been related to possess radical scavenging activity due to the capacity of the phenolic group to serve as the hydrogen donor (Elias et al., 2005; Hernández-Ledesma et al., 2005), Met reduces lipid hydroperoxides to the non-reactive species by oxidation to Met sulfoxide (Elias et al., 2008; Hernández-Ledesma et al., 2005) and His possesses both radical scavenging and chelating activity (Aluko, 2015). Moreover, the small peptides produced as a result of protein hydrolysis (ca. 50% of the peptides between 0.5–3 kDa) (Padial-Domínguez et al., 2020) could have also improved the encapsulating matrix protective effect by acting as copolymers or fillers of the wall, thus limiting prooxidant diffusivity to a higher extent. This fact combined with an already low permeable wall matrix (e.g., GS) and low storage temperatures resulted in long-term oxidatively stable microcapsules.

Hence, GS-based microcapsules loaded with fish oil and containing WPH as a film-forming material were further evaluated as an omega-3 delivery system to produce fortified low-fat mayonnaise.

3.3 Physical and Oxidative Stabilities of Fortified Low-Fat Mayonnaise

The feasibility of using fish oil-loaded microcapsules produced by spray-drying (using GS as the encapsulating agent and WPH as the film-protein material) to enrich low-fat mayonnaise was evaluated. For this purpose, the physical and oxidative stabilities of low-fat mayonnaise samples fortified with: (i) neat fish oil (M-NFO), (ii) emulsified fish oil (M-EM) and (iii) microencapsulated fish oil (M-GS) were investigated.

3.3.1 Physical Stability: Droplet Size Distribution and Viscosity

Droplet size distributions of the mayonnaise samples indicate their physical stability but also the specific surface area, which influences lipid oxidation in the system. After production (day 0), the mayonnaise enriched with neat fish oil (M-NFO) showed a bimodal droplet size distribution with a main peak centered in ca. 1 µm and a second one, less representative, centered in ca. 4.7 µm (Figure 48A). Likewise, the mayonnaise sample containing microencapsulated fish oil (M-GS) showed a bimodal droplet size distribution with the peaks centered in 0.13 and 1.8 µm, respectively (Figure 48A). When comparing this curve to that of the emulsion used for the production of the microencapsulates, the droplet size of the first peak of the mayonnaise is in agreement with the peak of the monomodal curve of the

emulsion fed to the spray-drier (ca. 0.13 µm, data not shown). Therefore, the first peak of the M-GS sample represents the droplet size of the fish oil, while the second peak is a consequence of the sunflower oil droplets dispersed during the mayonnaise production. The mayonnaise fortified with emulsified fish oil (M-EM) showed a trimodal droplet size distribution with the first peak overlapping with the M-GS sample (ca. 0.13 µm) and the other two peaks centered as those of the M-NFO sample (ca. 1 and 4.7 µm, respectively) (Figure 48A). The latter suggests that the fish oil emulsion maintained its physical integrity during the mayonnaise production process, despite the shear forces produced by the blender, and did not modify the sunflower oil droplet size distribution.

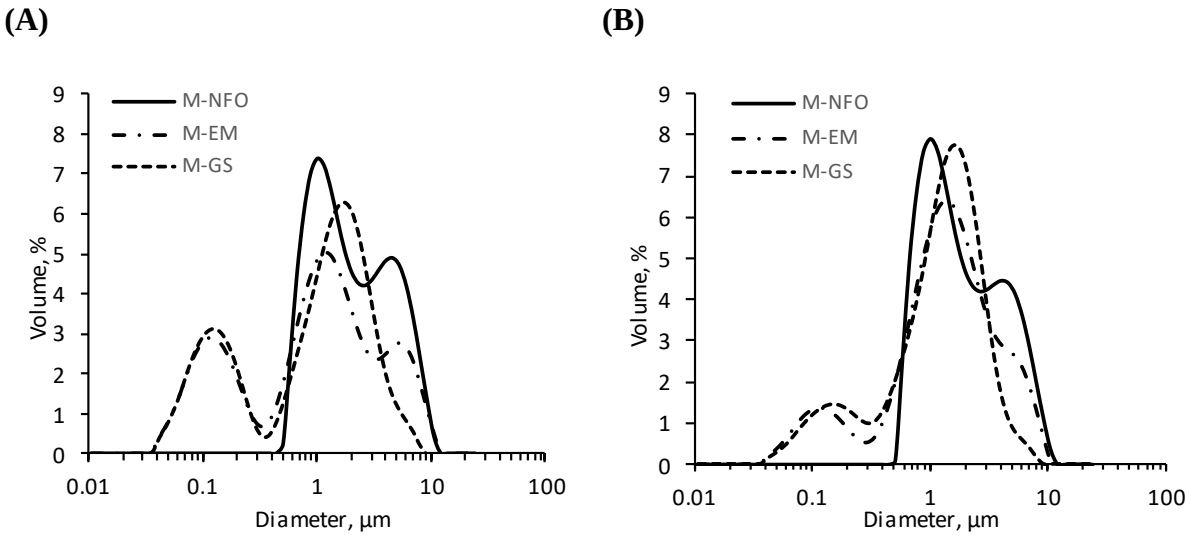

Figure 48. Droplet size distribution of low-fat mayonnaise enriched with: (i) neat fish oil (M-NFO), (ii) emulsified fish oil (M-EM) and (iii) microencapsulated fish oil (M-GS) at (A) day 0 and (B) day 28.

Table 8 shows that the mayonnaise sample containing neat fish oil (M-NFO) presented D[4,3] and D[3,2] values significantly higher ($p < 0.05$) than the rest of the samples at day 0. This is because, for the M-EM and M-GS samples, the fish oil was emulsified using a high-pressure homogenizer prior to the addition to the mayonnaise, which resulted in a lower size of the fish oil droplets when compared to the complete homogenization of the sunflower and fish oils while using the kitchen blender. It should be noted that, for the M-GS sample, the microcapsules were dispersed for 45 s into an already produced mayonnaise, which could have led to a further decrease of the size of the bulk droplets (sunflower oil droplets), explaining the lower D[4,3] values observed for this sample. Contrary to other studies, which found that the fortified mayonnaise with microencapsulated fish oil was the one with a higher D[4,3] value (Hermund et al., 2019; Miguel et al., 2019), our results may indicate that the capsules were intact and well-dispersed in the mayonnaise matrix at day 0. It should be noted

that the differences in the D[4,3] values between our results and those reported in the previous studies mentioned (Hermund et al., 2019; Miguel et al., 2019) are mainly attributed to the different equipment used for mayonnaise production.

Table 8. Droplet size and apparent viscosity ($\gamma = 10\ s^{-1}$) of fortified low-fat mayonnaise enriched with neat fish oil (M-NFO), emulsified fish oil (M-EM) or microencapsulated fish oil (M-GS).

	Droplet Size				**Apparent Viscosity**	
	Day 0		**Day 28**		**($\gamma = 10\ s^{-1}$), Pa·s**	
Sample	**D[3,2], µm**	**D[4,3], µm**	**D[3,2], µm**	**D[4,3], µm**	**Day 0**	**Day 28**
M-NFO	1.555 ± 0.020 ^{a}	2.724 ± 0.035 ^{a}	1.487 ± 0.006 ^{a,*}	2.553 ± 0.011 ^{a,*}	2.6 ± 0.3^{a}	2.0 ± 0.1 ^{a,*}
M-EM	0.310 ± 0.008 ^{b}	1.865 ± 0.052 ^{b}	0.516 ± 0.038 ^{b,*}	1.985 ± 0.045 ^{b,ns}	4.8 ± 0.1^{b}	5.1 ± 0.5 ^{b,ns}
M-GS	0.302 ± 0.001 ^{b}	1.436 ± 0.039 ^{c}	0.519 ± 0.027 ^{b,*}	1.538 ± 0.068 ^{c,ns}	9.7 ± 0.3^{c}	9.4 ± 0.2 ^{c,ns}

After 28 days of storage, fortified mayonnaise samples retained their physical integrity, since no phase separation or creaming were observed. However, changes in the droplet size distribution occurred (Figure 48B and Table 8). Contrary to the M-EM and M-GS samples, the D[4,3] and D[3,2] values of M-NFO decreased after 28 days of storage, suggesting that right after mayonnaise production, oil floccules were present, which may have disintegrated during storage (Miguel et al., 2019). For the M-EM and M-GS samples, a significant increase in the D[3,2] value suggested the coalescence or flocculation of oil droplets during storage caused by: (i) partial physical destabilization of the fish oil-in-water emulsion (in the case of the M-EM sample) or (ii) partial disintegration of the encapsulating wall, resulting in oil release (in the case of the M-GS sample) when these delivery systems were added to the food matrix.

All fortified low-fat mayonnaise samples presented pseudoplastic behaviors (see Figure S 28 in the Supplementary Material). Table 8 shows the apparent viscosity values at a shear rate of 10 s−1 for the mayonnaise samples. It was observed that the M-GS presented a significantly higher apparent viscosity, followed by the M-EM and M-NFO mayonnaises. These results are in line with those previously reported by Miguel et al. (2019), who attributed the higher viscosity of the mayonnaise sample enriched with zein-based fish oil microencapsulates to the intact microcapsules' thickening effect in the aqueous phase. Moreover, it has been stated that the larger the oil droplet size, the lower the apparent viscosity, since a reduced surface-to-volume ratio of the disperse phase leads to less friction

between the droplets (Pal, 1996). The latter correlates well with these results, since as the droplet size of the fortified mayonnaise samples increased (e.g., higher for the M-NFO), their apparent viscosity decreased (e.g., lower for the M-NFO) (Table 8). After 28 days of storage, the apparent viscosity of the M-EM and M-GS samples did not change significantly ($p > 0.05$), contrary to the M-NFO sample. This may be explained by the presence of WPH in the M-EM and M-GS mayonnaises, the latter also containing GS. This fact resulted in an improved physical stability of the M-EM and M-GS samples, which was attributed to an increased viscosity (Schröder et al., 2017).

Overall, the GS-based enrichment system led to a fortified mayonnaise with a high physical stability caused by an increased viscosity.

3.3.2 Oxidative Stability of the Fortified Mayonnaise

3.3.2.1 Peroxide Value (PV)

Figure 49 shows the evolution of the PV for the enriched low-fat mayonnaise samples during storage. It was observed that the PV at day 0 was similar among the three mayonnaise samples (4.0 ± 0.2 to 4.6 ± 0.1 meq O2/kg oil), despite the different degrees of initial oxidation of the enrichment systems: (i) NFO (PV = 1.3 ± 0.4 meq O2/kg oil; AV = 6.6 ± 0.7), (ii) fish oil-in-water emulsion stabilized with WPH (PV = 4.8 ± 1.2 meq O2/kg oil; AV = 6.2 ± 1.1) and (iii) fish oil-loaded glucose syrup microcapsules containing WPH as a film-forming material (PV = 7.0 ± 1.0 meq O2/kg oil; AV = 11.9 ± 1.5). This can be explained, because the majority of the oil present in the mayonnaise was SFO (PV = 3.5 ± 0.2 meq O2/kg oil; AV = 8.1 ± 1.1), which is more oxidatively stable than fish oil and may have masked the contribution of fish oil oxidation in the mayonnaise samples after production.

Over storage time, the PV course showed a lag phase of 1 week for the three enriched mayonnaise samples (Figure 49). However, from week 2 onwards, the PV of the three samples assayed increased progressively to final values significantly different ($p < 0.05$) from those of the beginning of the storage time. Interestingly, at day 28, the mayonnaise fortified with NFO presented a significantly higher PV (15.22 ± 1.45 meq O2/kg oil) compared to M-GS and M-EM. It should be also noted that, although the final PV of M-GS was significantly higher than the PV of M-EM, a slight decrease in the PV of M-EM was observed after day 21. This indicates that the rate of hydroperoxide decomposition was higher compared to the rate of hydroperoxide formation after day 21 for M-EM.

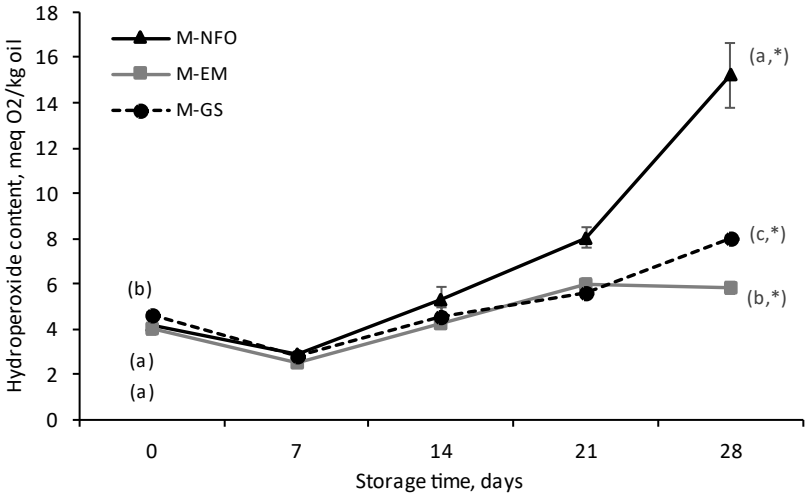

Figure 49. Peroxide value (PV) of low-fat fortified mayonnaise enriched with neat fish oil (M-NFO), emulsified fish oil (M-EM) or microencapsulated fish oil (M-GS) over storage time at 25 °C. Means within the same sampling point followed by a letter, a-c, indicates statistical differences ($p \leq 0.05$). Means within the same sample followed by an asterisk (*) indicates statistical differences ($p \leq 0.05$) between day 0 and day 28.

It is also noteworthy that our results are not aligned with those reported by Hermund et al. (2019). These authors found a lower oxidative stability for low-fat mayonnaise enriched with GS-based electrosprayed microcapsules (PV = 8–12 meq O2/kg oil) when compared to low-fat mayonnaise enriched with NFO (PV = 2 meq O2/kg oil) after 28 days storage at 25 °C. This finding was attributed to the partial disintegration of the hydrophilic biopolymer-based wall matrix of the electrosprayed microcapsules during mayonnaise production, which led to the release of already oxidized fish oil. On the other hand, Miguel et al. (2019) produced fortified mayonnaise enriched with zein-based electrosprayed microcapsules with a high oxidative stability during storage (PV = 2 meq O2/kg oil after 21 days of storage at 25 °C). In the latter work, the authors confirmed that the microencapsulates remained intact after mayonnaise production, which explained the enhanced oxidative stability of the fortified product. Taking both studies' results into account leads us to speculate that, in the current study, the physical integrity of the encapsulating wall was not severely affected either by the fortified mayonnaise production process (high-speed blending to disperse the capsules) nor the food matrix (water-based emulsion). However, the latter requires further investigation.

3.3.2.2 P-Anisidine Value (AV)

The p-anisidine value (AV) indicates the formation of secondary oxidation products, principally 2-alkenals and 2,4-alkadienals, which arise as a consequence of decomposition of the primary oxidation products (hydroperoxides) (Yang & Boyle, 2016). The initial AV

of the fortified mayonnaises ranged from 6.2 ± 1.4 to 6.9 ± 0.3, with no significant differences among the samples ($p > 0.05$) (Figure 50).

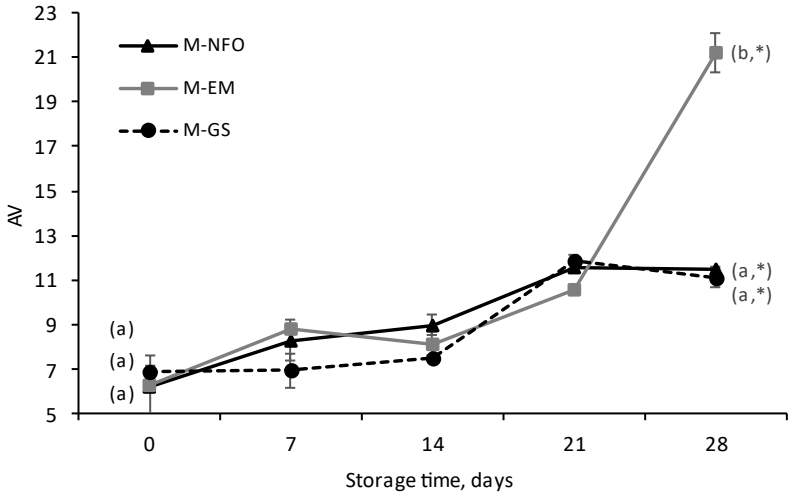

*Figure 50. P-anisidine value (AV) of low-fat fortified mayonnaise enriched with neat fish oil (M-NFO), emulsified fish oil (M-EM) or microencapsulated fish oil (M-GS) over storage time at 25 °C. Means within the same sampling point followed by a letter, a-c, indicates statistical differences ($p \leq 0.05$). Means within the same sample followed by an asterisk, *, indicates statistical differences ($p \leq 0.05$) between day 0 and day 28.*

During storage, the AV increased progressively for all the samples until day 21, from which a sharp increase in only the M-EM sample occurred. These results are in line with those previously reported for PV since, after day 21, the hydroperoxide content of the M-EM sample decreased (Figure 50), suggesting the appearance of secondary oxidation products. The poorer oxidative stability of the M-EM sample could be result of the emulsification process itself (production of a coarse emulsion and subsequent homogenization). The first step involves intense mechanical stress, which favors air inclusion, while the latter disrupts/rearranges the oil droplets, favoring a better distribution of the prooxidant species within the matrix (e.g., oxygen or metal ions) (Serfert et al., 2009). Moreover, high-pressure homogenization causes a significant increase in a specific surface area, as denoted by the lower D[4,3] values of M-EM when compared to M-NFO (Table 8), which results in a larger surface of contact between the oil and prooxidants. Likewise, Let at al. (2007) reported a lower oxidative stability (based on the content of 2-hexenal, 4-heptenal and 2,4-heptadienal during storage) for a salad dressing enriched with emulsified fish oil when compared to the addition of neat fish oil. The authors also reported that the oxidative stability of neat fish oil-fortified yogurt was higher than that of the yogurt fortified with emulsified fish oil.

After 28 days of storage, no significant differences were observed in the AV when comparing the M-NFO and M-GS samples ($p > 0.05$). However, M-GS showed a lag phase

of one week, contrary to M-NFO (Figure 50), which could suggest a protective effect of the microencapsulates against fish oil oxidation during the early stages of storage. In this line, Nielsen and Jacobsen (2013) investigated the fish oil-enrichment approach for a fish oil-fortified cod pâté and reported that the addition of microencapsulated fish oil resulted in a better oxidative stability after storage (based on 1-penten-3-oil content) than the samples fortified either with emulsified fish oil or neat fish oil.

Taken altogether, the PV and AV results indicate that the most oxidatively stable mayonnaise sample after one month of storage was M-GS, closely followed by M-NFO, while M-EM showed the lowest oxidative stability. Hence, the enhanced protection against lipid oxidation could be the result of the maintenance of the physical integrity of the encapsulating wall during mayonnaise production, which provides a physical barrier limiting the contact between fish oil droplets and prooxidants. Moreover, the higher apparent viscosity of M-GS as a result of the thickening effect of the microencapsulates may have also limited prooxidant species diffusivity, reducing lipid oxidation (Sims et al., 1979).

Our findings revealed that the use of WPH as a film-forming material, besides its metal chelating activity, which is of special interest to reduce lipid oxidation in egg yolk-based products (Hermund et al., 2019), was only beneficial for the production of microcapsules but not emulsions to be used as omega-3 delivery systems. Hence, the processing stages required to obtain the fish oil-loaded microcapsules containing WPH as a film-forming material (e.g., homogenization and spray-drying) are justified, since they result in an omega-3 delivery system that better protects the fish oil when it is incorporated into low-fat mayonnaise.

4. CONCLUSIONS

Oxidatively stable microcapsules loaded with fish oil (ca. 13 wt%) were produced via spray-drying using either GS or MD21 as wall materials and WPH as a film-forming material. GS-based microcapsules showed a higher oxidative stability when compared to MD21-based microcapsules at the two storage temperatures assayed (4 and 25 °C), which was mainly attributed to the lower oxygen diffusivity in GS-microcapsules. However, the higher oxidative stability for the GS-based microcapsules obtained, when compared to previous studies, also suggested a positive influence of the use of WPH as a film-forming material exhibiting antioxidant activity. Moreover, our results showed that the delivery system used

to enrich low-fat mayonnaise played a major role on the oxidative stability of the fortified product. Adding the fish oil in the form of a fish oil-in-water emulsion stabilized with WPH-favored lipid oxidation in the enriched product when compared to the addition of either neat or microencapsulated fish oil. This may be explained by successive emulsification processes that contributed to dispersing oxygen and prooxidant agents within the matrix, as well as to increasing the interfacial area. Fortified mayonnaise with GS-based microcapsules loaded with fish oil and containing WPH as a film-forming material showed the higher oxidative stability after storage. This was mainly explained because the physical integrity of the microencapsulates may have remained intact after mayonnaise production. Thus, our results show the potential of using WPH as a film-forming material for the production of fish oil-loaded microcapsules to be used as omega-3 delivery systems.

5. REFERENCES

Aluko, R. E. (2015). Amino acids, peptides, and proteins as antioxidants for food preservation. In *Handbook of Antioxidants for Food Preservation* (pp. 105–140). Elsevier Ltd. https://doi.org/10.1016/B978-1-78242-089-7.00005-1

AOCS Official Method CE 8-89. Determination of Tocopherols and Tocotrienols in Vegetable Oils and Fats by HPLC. (1998). *AOCS Press, Champaing*. https://doi.org/10.5650/jos1956.37.1169

Arab-Tehrany, E., Jacquot, M., Gaiani, C., Imran, M., Desobry, S., & Linder, M. (2012). Beneficial effects and oxidative stability of omega-3 long-chain polyunsaturated fatty acids. *Trends in Food Science and Technology*, *25*(1), 24–33. https://doi.org/10.1016/j.tifs.2011.12.002

Bligh, E. G., & Dyer, W. J. (1959). A rapid method of total lipid extraction and purification. *Canadian Journal of Biochemical Physiology*, *37*(8), 911–917. https://doi.org/10.1145/3163918

Boerekamp, D. M. W., Andersen, M. L., Jacobsen, C., Chronakis, I. S., & García-Moreno, P. J. (2019). Oxygen permeability and oxidative stability of fish oil-loaded electrosprayed capsules measured by Electron Spin Resonance: Effect of dextran and glucose syrup as main encapsulating materials. *Food Chemistry*, *287*, 287–294. https://doi.org/10.1016/j.foodchem.2019.02.096

Calder, P. C. (2014). Very long chain omega-3 (n-3) fatty acids and human health. *European Journal of Lipid Science and Technology*, *116*(10), 1280–1300. https://doi.org/10.1002/ejlt.201400025

Camacho, F., González-Tello, P., Páez-Dueñas, M. P., Guadix, E. M., & Guadix, A. (2001). Correlation of base consumption with the degree of hydrolysis in enzymic protein hydrolysis. *Journal of Dairy Research*, *68*(2), 251–265. https://doi.org/10.1017/S0022029901004824

Danviriyakul, S., McClements, D. J., Decker, E., Nawar, W. W., & Chinachoti, P. (2002). Physical stability of spray-dried milk fat emulsion as affected by emulsifiers and processing conditions. *Journal of Food Science*, *67*(6), 2183–2189. https://doi.org/10.1111/j.1365-2621.2002.tb09524.x

Desai, K. G. H., & Park, H. J. (2005). Recent developments in microencapsulation of food ingredients. *Drying Technology:An International Journal*, *23*(7), 1361–1394. https://doi.org/10.1081/DRT-200063478

Drusch, S., & Berg, S. (2008). Extractable oil in microcapsules prepared by spray-drying: Localisation, determination and impact on oxidative stability. *Food Chemistry*, *109*(1), 17–24. https://doi.org/10.1016/j.foodchem.2007.12.016

Drusch, S., Rätzke, K., Shaikh, M. Q., Serfert, Y., Steckel, H., Scampicchio, M., Voigt, I., Schwarz, K., & Mannino, S. (2009). Differences in free volume elements of the carrier matrix affect the stability of microencapsulated lipophilic food ingredients. *Food Biophysics*, *4*(1), 42–48. https://doi.org/10.1007/s11483-008-9100-9

Drusch, S., Serfert, Y., Berger, A., Shaikh, M. Q., Rätzke, K., Zaporojtchenko, V., & Schwarz, K. (2012). New insights into the microencapsulation properties of sodium caseinate and hydrolyzed casein. *Food Hydrocolloids*, *27*(2), 332–338. https://doi.org/10.1016/j.foodhyd.2011.10.001

Drusch, S., Serfert, Y., Scampicchio, M., Schmidt-Hansberg, B., & Schwarz, K. (2007). Impact of physicochemical characteristics on the oxidative stability of fish oil microencapsulated by spray-drying. *Journal of Agricultural and Food Chemistry*, *55*(26), 11044–11051. https://doi.org/10.1021/jf072536a

Drusch, S., Serfert, Y., Van Den Heuvel, A., & Schwarz, K. (2006). Physicochemical characterization and oxidative stability of fish oil encapsulated in an amorphous matrix containing trehalose. *Food Research International*. https://doi.org/10.1016/j.foodres.2006.03.003

Eberhardt, A., López, E. C., Ceruti, R. J., Marino, F., Mammarella, E. J., Manzo, R. M., & Sihufe, G. A. (2019). Influence of the degree of hydrolysis on the bioactive properties of whey protein hydrolysates using Alcalase®. *International Journal of Dairy Technology*, *72*(4), 573–584. https://doi.org/10.1111/1471-0307.12606

Elias, R. J., Kellerby, S. S., & Decker, E. A. (2008). Antioxidant activity of proteins and peptides. *Critical Reviews in Food Science and Nutrition*, *48*(5), 430–441. https://doi.org/10.1080/10408390701425615

Elias, R. J., McClements, D. J., & Decker, E. A. (2005). Antioxidant activity of cysteine, tryptophan, and methionine residues in continuous phase β-lactoglobulin in oil-in-water emulsions. *Journal of Agricultural and Food Chemistry*, *53*(26), 10248–10253. https://doi.org/10.1021/jf0521698

Encina, C., Vergara, C., Giménez, B., Oyarzún-Ampuero, F., & Robert, P. (2016). Conventional spray-drying and future trends for the microencapsulation of fish oil. *Trends in Food Science and Technology*, *56*, 46–60. https://doi.org/10.1016/j.tifs.2016.07.014

Frankel, E. N. (2012a). Foods. In *Lipid Oxidation* (pp. 299–354). https://doi.org/10.1533/9780857097927.299

Frankel, E. N. (2012b). Methods to determine extent of oxidation. In *Lipid Oxidation* (2nd Ed., pp. 99–127). Woodhead Publishing Limited. https://doi.org/10.1533/9780857097927.99

Fu, X., Xu, S., & Wang, Z. (2009). Kinetics of lipid oxidation and off-odor formation in silver carp mince: The effect of lipoxygenase and hemoglobin. *Food Research International*, *42*(1), 85–90. https://doi.org/10.1016/j.foodres.2008.09.004

García-Moreno, P. J., Pelayo, A., Yu, S., Busolo, M., Lagaron, J. M., Chronakis, I. S., & Jacobsen, C. (2018). Physicochemical characterization and oxidative stability of fish oil-loaded electrosprayed capsules: Combined use of whey protein and carbohydrates as wall materials. *Journal of Food Engineering*, *231*, 42–53. https://doi.org/10.1016/j.jfoodeng.2018.03.005

Gharsallaoui, A., Roudaut, G., Chambin, O., Voilley, A., & Saurel, R. (2007). Applications of spray-drying in microencapsulation of food ingredients: An overview. In *Food Research International* (Vol. 40, Issue 9, pp. 1107–1121). https://doi.org/10.1016/j.foodres.2007.07.004

Hermund, D., Jacobsen, C., Chronakis, I. S., Pelayo, A., Yu, S., Busolo, M., Lagaron, J. M., Jónsdóttir, R., Kristinsson, H. G., Akoh, C. C., & García-Moreno, P. J. (2019). Stabilization of Fish Oil-Loaded Electrosprayed Capsules with Seaweed and Commercial Natural Antioxidants: Effect on the Oxidative Stability of Capsule-Enriched Mayonnaise. *European Journal of Lipid Science and Technology*, *121*(4). https://doi.org/10.1002/ejlt.201800396

Hernández-Ledesma, B., Dávalos, A., Bartolomé, B., & Amigo, L. (2005). Preparation of antioxidant enzymatic hydrolysates from α-lactalbumin and β-lactoglobulln. Identification of active peptides by HPLC-MS/MS. *Journal of Agricultural and Food Chemistry*, *53*(3), 588–593. https://doi.org/10.1021/jf048626m

Hogan, S. A., McNamee, B. F., O'Riordan, E. D., & O'Sullivan, M. (2001). Emulsification and microencapsulation properties of sodium caseinate/carbohydrate blends. *International Dairy Journal*, *11*(3), 137–144. https://doi.org/10.1016/S0958-6946(01)00091-7

ISO 6885:2006. Animal and vegetable fats and oils — Determination of anisidine value. (2006). https://www.iso.org/standard/40052.html

Jacobsen, C. (2010). Enrichment of foods with omega-3 fatty acids: A multidisciplinary challenge. *Annals of the New York Academy of Sciences*, *1190*, 141–150. https://doi.org/10.1111/j.1749-6632.2009.05263.x

Jacobsen, C. (2016). Fish Oils: Composition and Health Effects. *Encyclopedia of Food and Health*, 686–692. https://doi.org/10.1016/B978-0-12-384947-2.00295-6

Jacobsen, C., García-Moreno, P. J., Mendes, A. C., Mateiu, R. V., & Chronakis, I. S. (2018). Use of Electrohydrodynamic Processing for Encapsulation of Sensitive Bioactive Compounds and Applications in Food. *Annual Review of Food Science and Technology*, *9*(1), 525–549. https://doi.org/10.1146/annurev-food-030117-012348

Jacobsen, C., Rustad, T., Nielsen, N. S., Falch, E., Jansson4, S., & Storrø, I. (2009). Processing of marine lipids and factors affecting their quality when used for functional foods. In J. B. Luten (Ed.), *Marine Functional Food* (pp. 89–114). https://doi.org/10.3920/978-90-8686-658-8

Jeyakumari, A., Zynudheen, A. A., Parvathy, U., & Binsi, P. K. (2018). Impact of chitosan and oregano extract on the physicochemical properties of microencapsulated fish oil stored at different temperature. *International Journal of Food Properties*, *21*(1), 942–955. https://doi.org/10.1080/10942912.2018.1466319

Let, M. B., Jacobsen, C., & Meyer, A. S. (2007). Lipid oxidation in milk, yoghurt, and salad dressing enriched with neat fish oil or pre-emulsified fish oil. *Journal of Agricultural and Food Chemistry*, *55*(19), 7802–7809. https://doi.org/10.1021/jf070830x

McClements, D. J., & Decker, E. (2018). Interfacial Antioxidants: A Review of Natural and Synthetic Emulsifiers and Coemulsifiers That Can Inhibit Lipid Oxidation. *Journal of Agricultural and Food Chemistry*, *66*(1), 20–25. https://doi.org/10.1021/acs.jafc.7b05066

Miguel, G. A., Jacobsen, C., Prieto, C., Kempen, P. J., Lagaron, J. M., Chronakis, I. S., & García-Moreno, P. J. (2019). Oxidative stability and physical properties of mayonnaise fortified with zein electrosprayed capsules loaded with fish oil. *Journal of Food Engineering*, *263*, 348–358. https://doi.org/10.1016/j.jfoodeng.2019.07.019

Morales-Medina, R., García-Moreno, P. J., Pérez-Gálvez, R., Muñío, M., Guadix, A., & Guadix, E. M. (2015). Seasonal variations in the regiodistribution of oil extracted from small-spotted catshark and bogue. *Food and Function*, *6*(8), 2646–2652. https://doi.org/10.1039/c5fo00448a

Morales-Medina, R., Tamm, F., Guadix, A. M., Guadix, E. M., & Drusch, S. (2016). Functional and antioxidant properties of hydrolysates of sardine (S. pilchardus) and horse mackerel (T. mediterraneus) for the microencapsulation of fish oil by spray-drying. *Food Chemistry*, *194*, 1208–1216. https://doi.org/10.1016/j.foodchem.2015.08.122

Nielsen, N. S., & Jacobsen, C. (2013). Retardation Of Lipid Oxidation In Fish Oil-Enriched Fish Pâté- Combination Effects. *Journal of Food Biochemistry*, *37*(1), 88–97. https://doi.org/10.1111/j.1745-4514.2011.00605.x

Pal, R. (1996). Effect of Droplet Size on the Rheology of Emulsions. *AIChE Journal*, *42*(11), 3181–3190. https://doi.org/10.1002/aic.690421119

Ramakrishnan, S., Ferrando, M., Aceña-Muñoz, L., De Lamo-Castellví, S., & Güell, C. (2013). Fish Oil Microcapsules from O/W Emulsions Produced by Premix Membrane Emulsification. *Food and Bioprocess Technology*, *6*(11), 3088–3101. https://doi.org/10.1007/s11947-012-0950-2

Ramakrishnan, S., Ferrando, M., Aceña-Muñoz, L., Mestres, M., De Lamo-Castellví, S., & Güell, C. (2014). Influence of Emulsification Technique and Wall Composition on Physicochemical Properties and Oxidative Stability of Fish Oil Microcapsules Produced by Spray Drying. *Food and Bioprocess Technology*, *7*(7), 1959–1972. https://doi.org/10.1007/s11947-013-1187-4

Schröder, A., Berton-Carabin, C., Venema, P., & Cornacchia, L. (2017). Interfacial properties of whey protein and whey protein hydrolysates and their influence on O/W emulsion stability. *Food Hydrocolloids*, *73*, 129–140. https://doi.org/10.1016/j.foodhyd.2017.06.001

Serfert, Y., Drusch, S., & Schwarz, K. (2009). Chemical stabilisation of oils rich in long-chain polyunsaturated fatty acids during homogenisation, microencapsulation and storage. *Food Chemistry*, *113*(4), 1106–1112. https://doi.org/10.1016/j.foodchem.2008.08.079

Shahidi, F., & Zhong, Y. (2011). Revisiting the polar paradox theory: A critical overview. *Journal of Agricultural and Food Chemistry*, *59*(8), 3499–3504. https://doi.org/10.1021/jf104750m

Shantha, N. C., & Decker, E. A. (1994). Rapid, sensitive, iron-based spectrophotometric methods for determination of peroxide values of food lipids. *Journal of AOAC International*, *77*(2), 421–424. https://doi.org/10.1093/jaoac/77.2.421

Sheu, T.-Y., & Rosenberg, M. (1995). Microencapsulation by Spray Drying Ethyl Caprylate in Whey Protein and Carbohydrate Wall Systems. *Journal of Food Science*, *60*(1), 98–103. https://doi.org/10.1111/j.1365-2621.1995.tb05615.x

Sims, R. J., Fioriti, J. A., & Trumbetas, J. (1979). Effect of sugars and sugar alcohols on autoxidation of safflower oil in emulsions. *Journal of the American Oil Chemists' Society*, *56*(8), 742–745. https://doi.org/10.1007/BF02663053

Tamm, F., Gies, K., Diekmann, S., Serfert, Y., Strunskus, T., Brodkorb, A., & Drusch, S. (2015). Whey protein hydrolysates reduce autoxidation in microencapsulated long chain polyunsaturated fatty acids. *European Journal of Lipid Science and Technology*, *117*(12), 1960–1970. https://doi.org/10.1002/ejlt.201400574

Unnikrishnan, P., Puthenveetil Kizhakkethil, B., Annamalai, J., Ninan, G., Aliyamveetil Abubacker, Z., & Chandragiri Nagarajarao, R. (2019). Tuna red meat hydrolysate as core and wall polymer for fish oil encapsulation: a comparative analysis. *Journal of Food Science and Technology*, *56*(4), 2134–2146. https://doi.org/10.1007/s13197-019-03694-w

Yang, X., & Boyle, R. A. (2016). Sensory Evaluation of Oils/Fats and Oil/Fat-Based Foods. In *Oxidative Stability and Shelf Life of Foods Containing Oils and Fats* (pp. 157–185). Elsevier Inc. https://doi.org/10.1016/B978-1-63067-056-6.00003-3

Young, S. L., Sarda, X., & Rosenberg, M. (1993). Microencapsulating Properties of Whey Proteins. 2. Combination of Whey Proteins with Carbohydrates. *Journal of Dairy Science*, *76*(10), 2878–2885. https://doi.org/10.3168/jds.S0022-0302(93)77626-2

6. SUPPLEMENTARY MATERIAL

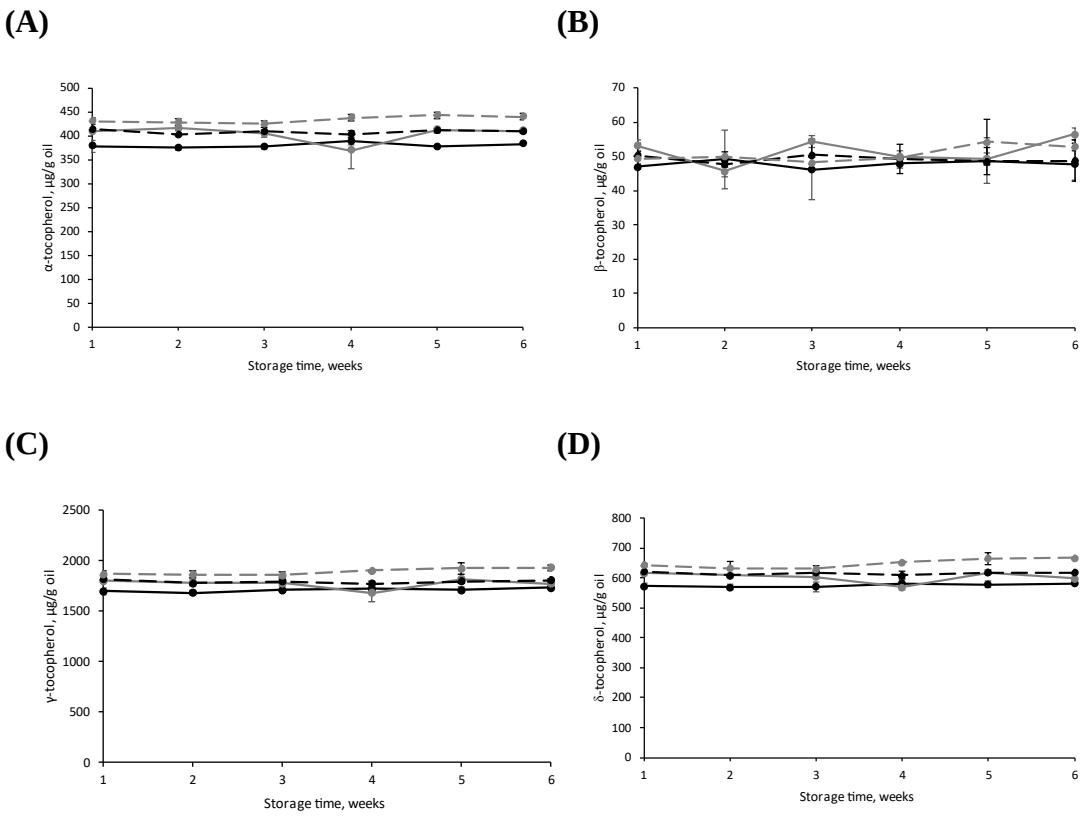

Figure S 27. Tocopherol content of spray-dried capsules loaded with fish oil during storage at: 4 °C (solid line, —•—) and 25 °C (broken line, - -•- -) encapsulated with glucose syrup (black) or maltodextrin (grey).

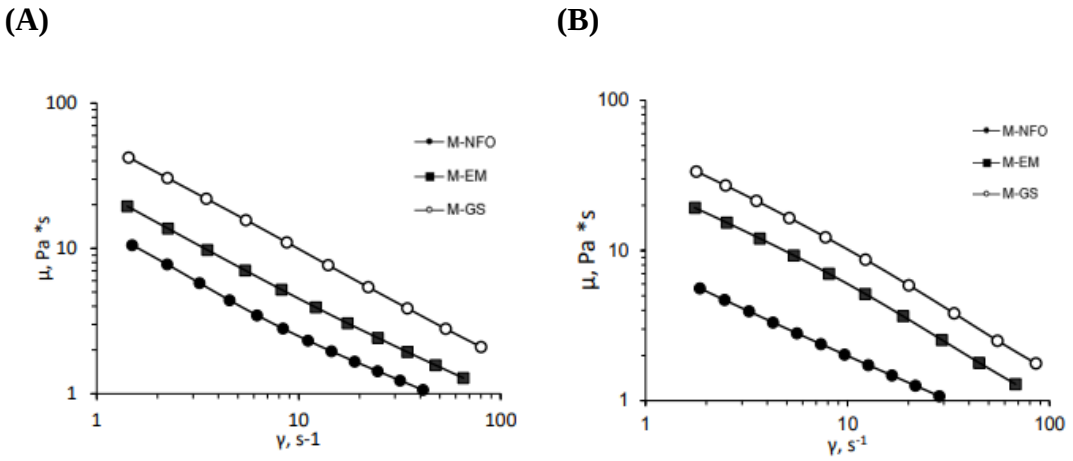

Figure S 28. Viscosity of mayonnaise enriched with: i) neat fish oil (M-NFO), ii) emulsified fish oil (M-EM) and iii) encapsulated fish oil (MGS) at (A) day 0 and (B) day 28.

VIII. Non-emulsion-based encapsulation of fish oil by coaxial Electrospraying Assisted by Pressurized Gas enhances the oxidative stability of a capsule-fortified salad dressing [*]

The influence of the encapsulation technology (spray-drying, mono- or coaxial electrospraying assisted by pressurized gas, EAPG) and the oil load (13, 26 or 39 wt%) on the oxidative stability of: i) fish oil-loaded capsules, and ii) capsule-fortified salad dressings were investigated. The highest encapsulation efficiency (EE > 83%) was achieved by the emulsion-based encapsulation methods (e.g., spray-drying and monoaxial EAPG), irrespective of the oil load. Nonetheless, monoaxially EAPG capsules were the most oxidized during storage due to their increased surface-to-volume ratio. On the contrary, non-emulsion-based coaxial EAPG resulted in low lipid oxidation after processing and subsequent storage. The oxidative stability of the capsule-fortified salad dressings correlated well with that of the encapsulates, with the dressing fortified with the coaxially EAPG capsules showing significantly lower levels of oxidation. Our results show that the fortification approach (e.g., emulsion or non-emulsion-based delivery systems) significantly influenced the oxidative stability of the enriched food matrix.

[*] MANUSCRIPT SUBMITTED FOR PUBLICATION: N.E. Rahmani-Manglano, E.M. Guadix, B. Yesiltas, C. Prieto, J.M. Lagaron, C. Jacobsen, P.J. García-Moreno. (2023). Non-emulsion-based encapsulation of fish oil by coaxial Electrospraying Assisted by Pressurized Gas enhances the oxidative stability of a capsule-fortified salad dressing.

1. INTRODUCTION

The proven health benefits related to the intake of omega-3 polyunsaturated fatty acids (PUFAs), particularly EPA (C20:5 n-3) and DHA (C22:6 n-3) (Calder, 2021), have driven the development of fortified food products rich in these bioactive compounds. However, due to their polyunsaturated nature, they are very prone to lipid oxidation. Thus, they are generally introduced into the food matrix in the form of a delivery system (Ghelichi et al., 2021; Sørensen et al., 2021). Therefore, in the last decades, the production of stable micro/nanocapsules loaded with oils rich in omega-3 PUFAs (e.g., fish oil) to be used as delivery systems has become a focus of scientific research.

Traditionally, spray-drying has been the technique of choice of the food industry to produce oil-loaded encapsulates due to its multiple advantages (e.g., high throughput) (Rahmani-Manglano, García-Moreno, et al., 2020). Nonetheless, it also presents some drawbacks that need to be considered when it comes to food fortification. Particularly, it has been demonstrated that emulsification of omega-3 rich oils followed by drying at high temperatures (e.g., 160-210 °C) results in an initial lipid oxidation if the oil is not properly stabilized and/or the process is not well designed (Serfert et al., 2009). Besides, the use of spray-dried capsules might be restrained for certain commercial food applications. By spray-drying, relatively large particles (~5-100 μm) with a polydisperse particle size distribution are produced, which may affect the reproducible performance of the encapsulates (Rahmani-Manglano et al., 2023). In the literature, fish oil-loaded capsules produced by spray-drying have been used as omega-3 delivery systems in a wide range of food products to investigate their influence on the oxidative, physical and/or sensory stability of the fortified matrix (e.g., dressings, baked, spread or meat products) (Aquilani et al., 2018; Davidov-Pardo et al., 2008; Jeyakumari et al., 2016; Nielsen & Jacobsen, 2013; Rahmani-Manglano, González-Sánchez, et al., 2020; Solomando, Antequera, & Perez-Palacios, 2020a, 2020b; Solomando, Antequera, González-Mohíno, et al., 2020). However, in the aforementioned studies, the influence of the oil load of such delivery systems on the physicochemical properties (e.g., physical and oxidative stability) of the enriched foodstuff was not investigated.

Recently, electrospraying technology has emerged as a promising alternative to spray-drying for the production of omega-3-loaded capsules aimed as delivery systems (García-Moreno et al., 2021). In conventional electrospraying, the oil-loaded solution/emulsion is subjected

to a high electric field which forms a spray of ultrathin droplets allowing solvent evaporation at room temperature (García-Moreno et al., 2021). Therefore, contrary to spray-drying, heat is not required at any point of the process, which prevents from thermal degradation and enables the use of a wider variety of (bio)polymeric wall materials (Prieto & Lagaron, 2020). In addition, by electrospraying in the coaxial configuration, two physically separated liquids can be infused simultaneously allowing to produce oil-loaded capsules without emulsifying or dispersing the oil first within the (bio)polymer-based encapsulating solution (Rahmani-Manglano et al., 2023). Thus, by electrospraying technology, initial lipid oxidation due to processing could be reduced in the monoaxial configuration, which does not use hot air to dry but requires a homogenization step, or even theoretically be avoided in the coaxial configuration, which might not require previous homogenization. Moreover, as a result of electrohydrodynamic atomization, smaller and monodispersed encapsulates are produced resulting in a more reproducible performance of the capsules, enhanced bioaccessibility and fewer modifications of the original food structure when added as delivery systems when compared to those produced by spray-drying (García-Moreno et al., 2021). Nonetheless, it should be borne in mind that the higher surface-to-volume ratio of these systems may result in lower oxidative stability of the encapsulated oil, due to the higher contact area with prooxidants species such as oxygen (Boerekamp et al., 2019), which will further affect the quality of the enriched food product.

Despite the multiple advantages of electrospraying over spray-drying, its industrial use is restrained due to the low productivity of the process (Busolo et al., 2019). In this regard, a novel high-throughput encapsulation technology based on electrospraying, and referred to as electrospraying assisted by pressurized gas (EAPG), has been recently developed (Busolo et al., 2019). This novel technology is already available at an industrial scale (Lagaron et al., 2017). The EAPG technology increases the throughput of conventional electrospraying by introducing a pneumatic injector that atomizes the oil-loaded solution/emulsion within a high electric field. Again, due to the high voltage applied, the atomized droplets are further disrupted allowing that the solvent evaporates at room temperature. The dry material is then collected as a free-flowing powder in the collection unit (Prieto et al., 2021). This technology has been previously used to produce omega-3 delivery systems (Busolo et al., 2019; García-Moreno et al., 2021; Miguel et al., 2019; Prieto & Lagaron, 2020) and their impact on the properties of selected enriched foodstuffs has been also investigated (e.g., powdered milk or low-fat mayonnaise) (Busolo et al., 2019; Hermund et al., 2019; Miguel et al., 2019).

However, the influence of the capsules' oil-load on the physicochemical properties of the enriched matrix was not studied. Moreover, to our knowledge, the potential of EAPG technology in the coaxial configuration to produce neat fish oil-loaded capsules aimed for food fortification purposes has not been reported to date.

In light of the above, the aim of the study was to investigate the influence of the encapsulation technology and the fish oil load on: i) the physicochemical properties of the dried omega-3 delivery systems, and ii) the physical and oxidative stabilities of a capsule-fortified food matrix. Salad dressing was selected as the food model system due to its high fat content, with potential for replacement with fish oil (Let et al., 2007a). First, the fish oil-loaded capsules were produced by spray-drying and EAPG technology in the monoaxial and coaxial configuration at three different fixed fish oil loads (e.g., 13, 26 or 39 wt%). The capsules' morphology and encapsulation efficiency were subsequently characterized and their oxidative stability was monitored during 6 weeks of storage at 25 °C. Selected fish oil-loaded capsules with varying oil loads and produced by different encapsulation techniques were further used for omega-3 enrichment of a salad dressing. Finally, the physical (e.g., oil droplet size, viscosity) and the oxidative (e.g., peroxide value and formation of volatile compounds) stabilities of the fortified salad dressings were studied during 28 days at ambient temperature.

2. MATERIALS AND METHODS

2.1 Materials

The fish oil (Omega Oil 1812 TG Gold) was acquired from BASF Personal Care and Nutrition GmbH (Illertissen, Germany). Cargill Germany GmbH (Krefeld, Germany) provided the glucose syrup (GS; DE38, C*Dry 1934) and the whey protein concentrate (~35 wt% protein content) was supplied by Abbott Laboratories S.A. (Granada, Spain). The whey protein concentrate hydrolysate (WPCH), used as an emulsifier, was produced by enzymatic hydrolysis as described elsewhere (Rahmani-Manglano, González-Sánchez, et al., 2020). For the production of the salad dressings, refined rapeseed oil (RSO) was provided by AAK Sweden AB (Malmö, Sweeden). The stabilizer Grinsted FF5128 was donated by DuPont (DuPont Nutrition Biosciences Aps, Haderslev, Denmark). The rest of the ingredients used

were purchased in the local market. The reagents used for the analysis were of analytical grade.

The peroxide value (PV) and the tocopherol content of the fresh oils (fish oil and rapeseed oil) were measured as described in Section 2.3.4.1. The fish oil had a PV of 0.33 ± 0.06 meq O2/kg oil and alpha-, gamma- and delta-tocopherol content of 500.8 ± 1.3, 2108.8 ± 5.3 and 677.4 ± 2.0 µg/g oil, respectively. The rapeseed oil had a PV of 0.17 ± 0.07 meq O2/kg oil and alpha- and gamma-tocopherol content of 260.5 ± 6.0 and 378.9 ± 1.1 µg/g oil, respectively.

2.2. Production of fish oil-loaded capsules

2.2.1 Emulsions preparation

The fish oil (5, 10 or 15 wt%) was dispersed in the aqueous phase containing the encapsulating agent (GS; 28, 17 or 7 wt%) and the emulsifier (WPCH; 6, 12 or 17 wt%). The protein/oil ratio (P/O ratio) was fixed to 0.4 and the solids content of the emulsions was kept constant at 39 wt%, irrespective of the oil load. First, an Ultraturrax T-25 homogenizer (IKA, Staufen, Germany) was used to produce the coarse emulsions. The fish oil was added during the first minute of mixing, and the total mixing time was 2 minutes. The coarse emulsions were then homogenized by applying three passes at 450/75 bar in a high-pressure homogenizer (PandaPLUS 2000; GEA Niro Soavi, Lübeck, Germany) (Rahmani-Manglano, González-Sánchez, et al., 2020).

2.2.2 Production by spray-drying

The fish oil-in-water emulsions (Section 2.2.1) were processed by spray-drying in a pilot plant scale spray-drier (Mobile Minor; Niro A/S, Copenhagen, Denmark) (Rahmani-Manglano, González-Sánchez, et al., 2020). The inlet and outlet air temperature were set to 190 °C and 80 °C, respectively. The rotary atomizer's activation pressure was fixed to 4 bar, which corresponds to a 22,000 rpm rotational speed. After drying, the capsules were stored in airtight flasks at −80 °C in the dark until analysis.

2.2.3 Production by EAPG in monoaxial configuration

The fish oil-in-water emulsions (Section 2.2.1) were processed by EAPG using the pilot plant equipment CapsultekTM from Bioinicia S.L. (Valencia, Spain) consisting of a nebulizer, a drying chamber and a cyclonic collector (Prieto & Lagaron, 2020). During

processing, the emulsions were kept under constant nitrogen bubbling to minimize lipid oxidation and the ambient conditions were monitored (30 °C and 25% relative humidity; RH). The emulsions flow rate was fixed to 1 mL/min and the injector worked with an assisted air pressure of 10 L/min. The electric voltage was set to 10 kV. Every 20 minutes, the capsules were collected from the cyclone and stored in airtight flasks at –20 °C in the dark until analysis.

2.2.4 Production by EAPG in coaxial configuration

For coaxial EAPG, neat fish oil (NFO) was infused as the core solution whilst through the annular gap, the water-based encapsulating agent solution consisting of a mixture GS:WPCH (~80:20, w/w) was infused. The ratio GS:WPCH was fixed in a way that the capsules with a 13 wt% of fish oil load had the same composition irrespective of the technology used for their production (e.g., spray-drying, monoaxial or coaxial EAPG). The EAPG process was carried out in the equipment described in Section 2.2.3, but this time a coaxial nebulizer was used. The core flow rate was fixed to 1 mL/min and the shell flow rate varied between 1 mL/min and 10 mL/min to achieve the desired load capacity (~13 wt%). The injector worked with an assisted air pressure of 16 L/min and the electric voltage was set to 10 kV. Every 20 minutes, the capsules were collected from the cyclone and stored in airtight flasks at –20 °C in the dark until analysis.

2.3 Physicochemical characterization of the capsules

2.3.1 Oil droplet size of the parent and the reconstituted emulsions

The oil droplet size of the parent and reconstituted emulsions was measured using a Mastersizer 3000 (Malvern Instruments, Ltd., Worcestershire, UK). For the reconstituted emulsions, the capsules were dissolved in distilled water in order to achieve the same solids content as the original emulsions. For the measurements, the samples were diluted in circulating water (3000 rpm) until an obscuration level between 12 – 15% was reached. For particle and dispersant, respectively, the refractive indexes of fish oil (1.481) and water (1.330) were used. The measurements were made in triplicate.

2.3.2 Morphology and size

A FESEM microscope (LEO 1500 GEMINI, Zeiss, Germany) was used to investigate the morphology and size of the capsules (Rahmani-Manglano et al., 2023). For this purpose, a

thin layer of powder was placed on a carbon tape and subsequently carbon-coated using an EMITECHK975X Turbo-Pumped Thermal Evaporator (Quorum Technologies, UK). The SEM images were captured at magnifications ranging from 500X to 15 KX, with a 5 kV accelerating voltage. The mean particle size and the particle size distribution were determined by measuring 160 randomly-selected capsules using the ImageJ software (National Institute of Health, USA).

2.3.3 Load capacity (LC) and encapsulation efficiency (EE)

The load capacity (LC) and the encapsulation efficiency (EE) of the capsules were determined as described in our previous work (Rahmani-Manglano et al., 2023), with some modifications. For determining the LC, 150 mg of powder was dissolved by adding 1 mL of distilled water. Then, the fish oil was extracted using a hexane/2-propanol (1:1, v/v) solvent and the total oil load was determined by measuring the absorbance of the lipid extract at 250 nm in a UV4000 spectrophotometer (Dinko Instruments, Barcelona, Spain). To measure the EE, 25 mg of powder was immersed in 10 mL of hexane and gently shaken for 30 s. Then, the mixture was filtered into a pyrex tube and the absorbance of the filtrate was measured at 250 nm. The EE was calculated as described elsewhere (Rahmani-Manglano et al., 2023). The measurements were carried out in triplicate.

2.3.4 Oxidative stability of the capsules

To investigate the oxidative stability of the capsules, these were stored for 6 weeks at ambient temperature (25 °C) in the dark to quantify the content of selected secondary volatile oxidation products (SVOPs). For the study, 4 g of capsules were stored in brown bottles. Samples were taken every week (one bottle per sampling time) and overlaid with nitrogen before storage at –40 °C until analysis.

2.3.4.1 Secondary volatile oxidation products (SVOPs) – Dynamic Headspace GC-MS

The content of selected secondary volatile oxidation products (SVOPs) was determined as described in our previous work (Rahmani-Manglano, González-Sánchez, et al., 2020). In brief, approximately 1 g of powder and 30 mg of internal standard (4-methyl-1-pentanol and 30µg/g water) were mixed with 10 mL of distilled water in a pear-shaped flask. Then, the volatile compounds were released by heating the flask content while purging with nitrogen (45 °C; flow rate 150 mL/min) for 30 min to a Tenax GR tube. The released volatile

compounds were identified by MS-library searches (Wiley 138K, John Wiley and Sons, Hoboken, New Jersey, USA and Hewlett-Packard, San Jose, California, USA) and quantified through calibration curves using external standards dissolved in 96% ethanol. The standards solution was diluted to concentrations of approximately 25, 50, 100, 200, 500, 1000 and 2000μg/mL, and 1μL of each was directly injected into the Tenax tubes. Measurements were made in triplicate.

2.4 Production and characterization of fortified salad dressing

2.4.1 Production of fortified salad dressing

The fortified salad dressings (2.5 wt% of fish oil) were produced following two different approaches: i) adding the neat fish oil (SD-NFO) or ii) adding the fish oil-loaded capsules produced either by spray-drying (SD-spd-13 or SD-spd-39), monoaxial EAPG (SD-mo-13 or SD-mo-39) or coaxial EAPG (SD-co-13). In all cases, 300 g of salad dressing was produced containing: 2.5 wt% of fish oil, 22.5 wt% of RSO, 6 wt% of vinegar, 1.2 wt% stabilizer (Grindsted FF5128) and 0.08 wt% of whey protein concentrate, following the procedure described by Let et al. (2007a) with some modifications. First, the stabilizer was dispersed in the RSO (1/3 of the total RSO) and mixed into the water phase in a Stephan Universal Mixer (Stephan, Hameln, Germany) for 2 min under vacuum. Then, the whey protein concentrate was dissolved in deionized water and added to the mixture. Fish oil (in case of SD-NFO sample), the remaining rapeseed oil, and vinegar were added slowly during mixing for 3 min and the dressing was mixed for an additional 2 min under vacuum. In case of the salad dressings fortified with the encapsulated fish oil, the capsules were dispersed into the matrix using a 4-bladed propeller stirrer for 45 s. As the last step, sodium azide solution (10 wt%) was added to all the samples to have a final concentration in the fortified salad dressings of 0.05 wt%. The solution was dispersed manually. Sodium azide was added to prevent microbial growth during storage.

2.4.2 Physical stability: oil droplet size, viscosity and color

The oil droplet size of the salad dressing samples was measured by laser diffraction as described in Section 2.3.1 at days 0 and 28. The samples were pretreated by dissolving 1 g of salad dressing in SDS buffer (10 mM NaH2PO4, 5 mM SDS) to a ratio 1:9 (w/w) and then sonicated for 15 min in a water bath at ambient temperature. The refractive index of

sunflower oil (1.4694) was used for the dispersed phase. The measurements were made in triplicate.

The viscosity of the salad dressing samples was measured at 25 °C using a Discovery Hybrid Rheometer HR-2 (Waters TA Instruments, New Castle, USA) at days 0 and 28. Plain bottom base and upper cone plate (Peltier plate Steel - 113935) were used, with a gap of 1.5 mm. An increasing gradient of stress was applied up to 200 Pa. Measurements were carried out in duplicate.

The color of the salad dressing samples was measured at days 0 and 28 of storage using a Konica Minolta CR-300 Chroma colorimeter (Minolta, Tokyo, Japan). The data were recorded by the instrument using the CIEL*a*b* color system space. Yellowness index (YI) was calculated as described by Miguel et al. (2019). All measurements were carried out in duplicate.

2.4.3 Oxidative stability

2.4.3.1 Peroxide value (PV) and tocopherol content (TC)

The peroxide value (PV) and the tocopherol content of the fortified salad dressing samples were measured as previously described elsewhere (Rahmani-Manglano, González-Sánchez, et al., 2020). Briefly, the lipids were extracted from the salad dressing samples (~9g) using a reduced amount of chloroform/methanol (1:1, w/w) solvent. Then, the peroxide value (PV) was quantified on the lipid extracts using the colorimetric ferric-thiocyanate method at 500 nm. The tocopherol content was also quantified on the lipid extract by HPLC (Agilent 1100 Series) according to the American Oil Chemists' Society (AOCS) official method (AOCS, 1998).

2.4.3.2 Secondary volatile oxidation products (SVOPs) – Dynamic Headspace GC-MS

The content of secondary volatile oxidation products (SVOPs) of the salad dressing samples was measured as described in Section 2.3.4.1. Approximately 5 g of sample and 30 mg of internal standard (4-methyl-1-pentanol, 30µg/g water) were mixed with 15 mL of distilled water and 2 mL of antifoam (Synperonic 3.2 mL/L water). The volatile compounds were released by heating the samples in a water bath at 45 °C for 30 min while purging with nitrogen (flow rate 150 mL/min) through a S-tube filled with powdered KOH (200 mg) to a Tenax GR tube. The volatiles were desorbed in the gas chromatograph as described above.

The temperature program can be found elsewhere (Let et al., 2007a). The individual volatiles were analyzed by MS, identified by both library and external standards and quantified through calibration curves. The standards solution was diluted to concentrations of approximately 0.25, 0.50, 1, 5, 10, 25, 50 and 100 μg/g, and 30 mg of each were added to a fresh salad dressing prepared with RSO. Measurements were made in triplicate.

2.5 Statistical analysis

Statgraphics software (version 5.1; Statistical Graphics Corp., Rockville, MD, USA) was used to carry out one-way analysis of variance (ANOVA). Significant differences between means were determined at 95% confidence level ($p < 0.05$) using Tukey´s HSD multiple range test.

3 RESULTS AND DISCUSSION

3.1 Physicochemical characterization of the capsules

3.1.1 Morphology and size

The morphology and the particle size distribution of the fish oil-loaded capsules are shown in Figure 51 and Figure 52, respectively. Regardless of the encapsulation technology (spray-drying or monoaxial/coaxial EAPG) and the oil load of the capsules (13, 26 or 39 wt%), a discrete distribution of spherical particles was observed for all the samples (Figure 51). However, significant differences were observed on the capsules' morphology and size, depending on the encapsulation technique used to produce the encapsulated systems. In case of the spray-dried capsules (spd- samples), the typical morphology of such powders was noted with particles showing both smooth and wrinkled surfaces (Figure 51A-C). Interestingly, less wrinkled particles were observed as the oil load of the spray-dried capsules increased, which could be related to the higher whey protein content (WPCH) of the infeed emulsions (the ratio P/O was fixed to 0.4) at the same drying conditions (Both et al., 2018). Nonetheless, the latter was not observed in case of the capsules produced by EAPG technology in the monoaxial configuration although the composition of the infeed emulsions was the same (Figure 51D-F). For these systems (EAPG-mo samples), wrinkled capsules of rather similar morphology were observed irrespective of the oil load (Figure 51D-F).

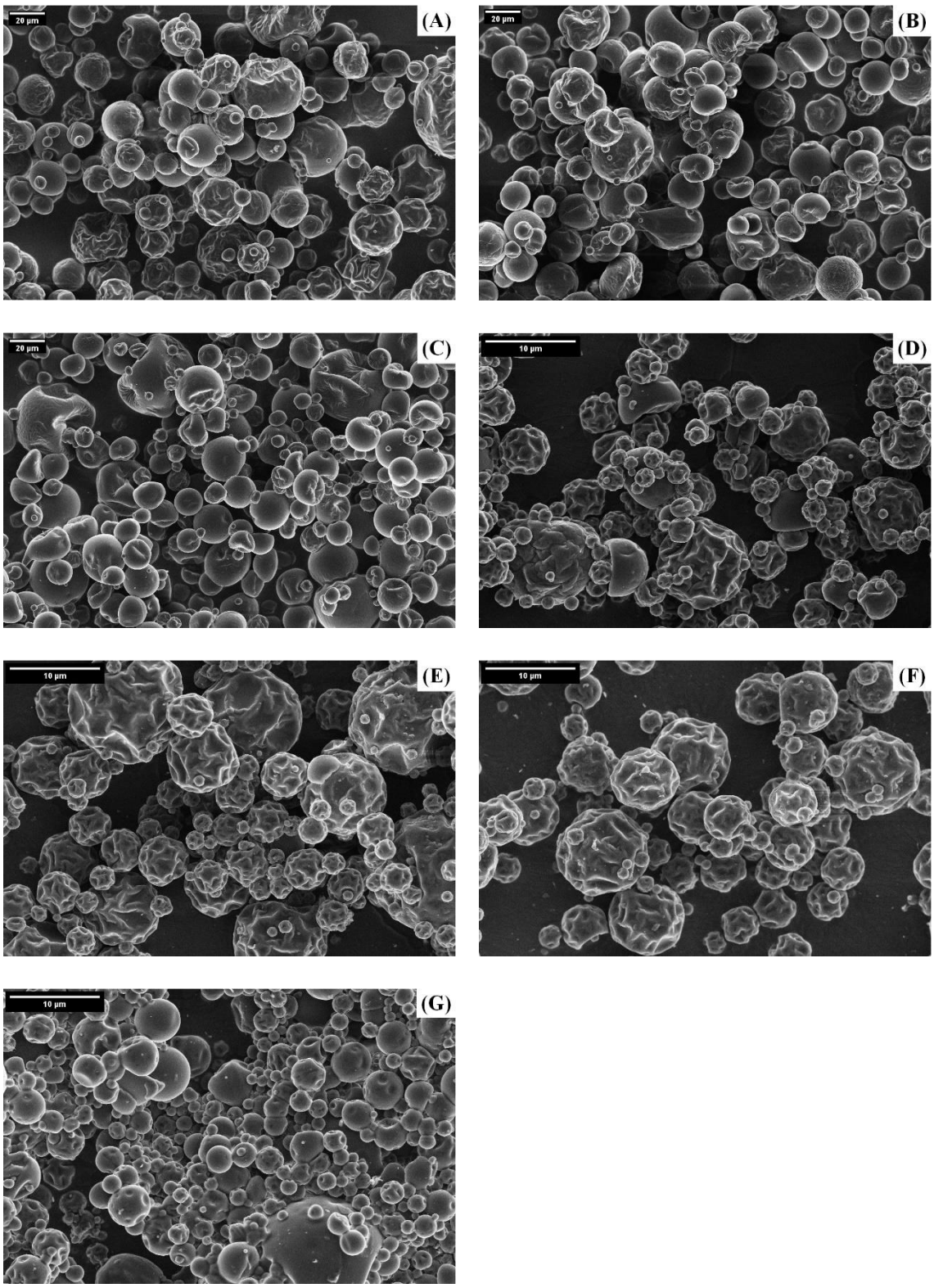

Figure 51. SEM images of the fish oil-loaded capsules (13, 26 and 39 wt% fish oil) produced by spray-drying (spd-), EAPG monoaxial (EAPG-mo-) and EAPG coaxial (EAPG-co): spd-13 (A), spd-26 (B), spd-39 (C), EAPG-mo-13 (D), EAPG-mo-26 (E), EAPG-mo-39 (F), EAPG-co-13 (G).

The morphology development of particles upon drying depends on several factors such as the composition of the dispersion/emulsion to be dried, the droplet size or the drying temperature (Both et al., 2018). At low temperature, the water evaporation rate is slower, and the structures formed during drying have more time to deform, shrink and collapse (Alamilla-Beltrán et al., 2005). Therefore, the difference between the morphology of the emulsion-based capsules produced by spray-drying or EAPG technology might be a consequence of the different solvent evaporation rate influenced by the temperature of the drying air for each process (e.g., 190 °C and ambient temperature, respectively). On the other hand, wrinkles were not observed on the surface of the coaxially electrosprayed capsules (Figure 51G) although drying also occurred at ambient temperature. This time, a water-based solution consisting of a GS:WPCH mixture was infused as the outer fluid, while NFO was infused as the core solution. Thus, during drying in the coaxial configuration, water did not have to evaporate from the core of the droplets (which consisted of neat oil) allowing a faster crust formation and, therefore, leading to more spherical particles after drying compared to those produced by monoaxial EAPG (Maria Leena et al., 2020).

As expected, the particle size and the particle size distribution of the encapsulated systems (Figure 52) were significantly influenced by the encapsulation technology. A polydisperse particle size distribution of large capsules ($17.0 \pm 8.1 – 17.3 \pm 7.6$ µm; $p > 0.05$) was obtained for the spray-dried samples (Figure 52A-C), whilst the capsules produced by EAPG technology (monoaxial or coaxial) showed a narrow particle size distribution of significantly smaller capsules ($3.2 \pm 2.1 – 4.9 \pm 2.4$ µm; $p \leq 0.05$) (Figure 52D-G). Mechanical atomization followed by electrohydrodynamic atomization, contrary to mechanical atomization alone (as is the case of EAPG technology contrary to spray-drying) leads to the formation of smaller droplets and, therefore, smaller capsules are produced after drying. Nonetheless, it was also noted that, contrary to the spray-dried capsules, a slight but significant ($p \leq 0.05$) increase of the size of the capsules occurred for the EAPG-mo systems as the oil load of the samples increased (e.g., 71% of the capsules < 10µm for EAPG-mo-13 sample over 60% of the capsules < 10µm for EAPG-mo-39 sample). This phenomenon was already observed by Prieto et al. (2020) when increasing the algae oil load of whey protein- or maltodextrin-based capsules produced by monoaxial EAPG.

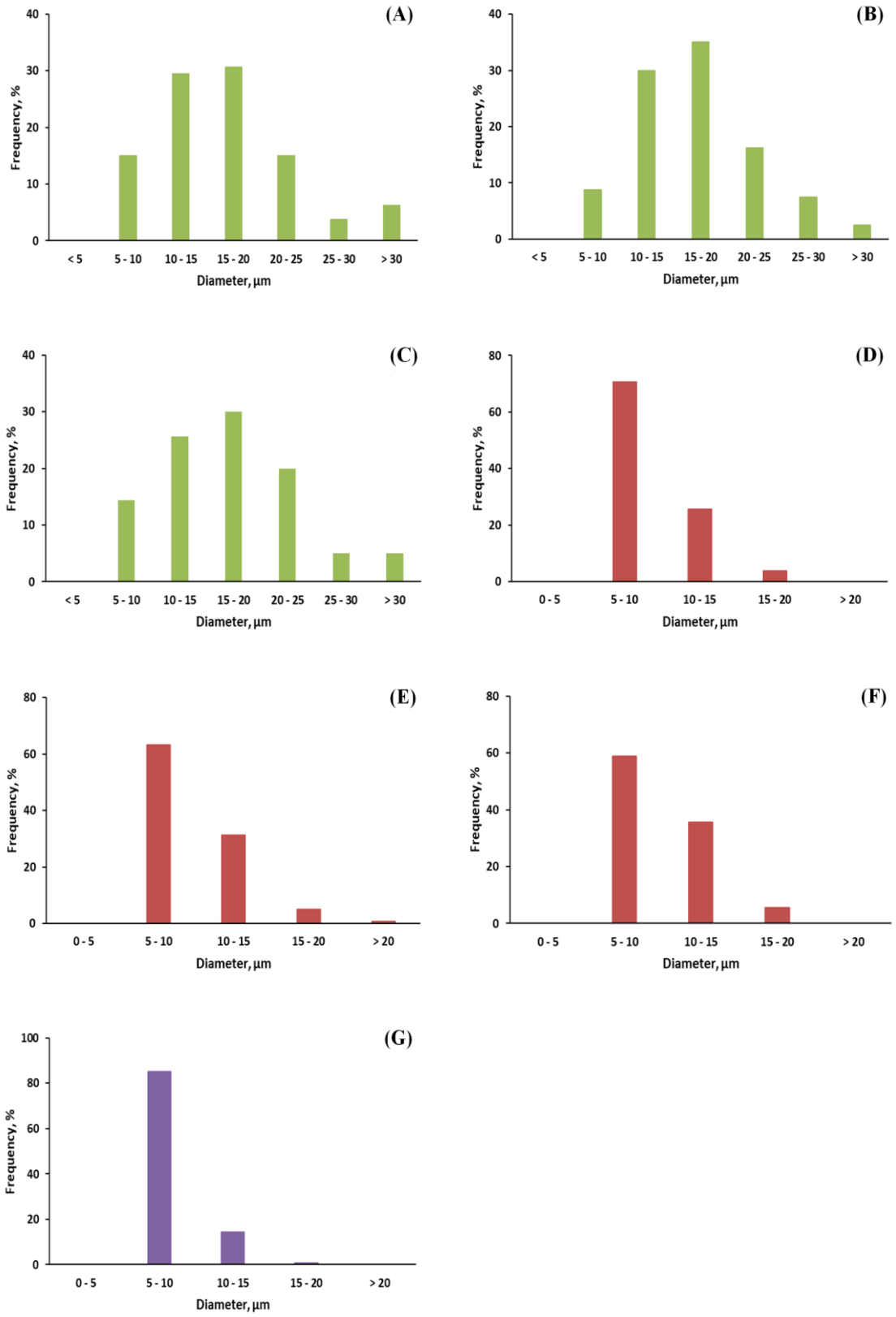

Figure 52. Particle size distribution of the fish oil-loaded capsules (13, 26 and 39 wt% fish oil) produced by spray-drying (spd-), EAPG monoaxial (EAPG-mo-) and EAPG coaxial (EAPG-co): spd-13 (A), spd-26 (B), spd-39 (C), EAPG-mo-13 (D), EAPG-mo-26 (E), EAPG-mo-39 (F), EAPG-co-13 (G).

3.1.2 Load capacity (LC) and encapsulation efficiency (EE)

Encapsulation of fish oil was successfully achieved at the assayed conditions as confirmed by the load capacity (LC) values of the different systems produced (Figure 53A). Slight deviations from the theoretical oil load (13, 26 and 39 wt%) and differences in the oil load between capsules produced by the technologies studied (e.g., spd-39 vs EAPG-mo-39) might be related to differences in the moisture content of the dry components (emulsifier and encapsulating agent) at the time of the samples' preparation.

Our results show that emulsion-based encapsulation methods (e.g., spray-drying and EAPG monoaxial) resulted in significantly higher EE values (EE > 83%), compared to coaxial EAPG (EE ~50%) (Figure 53B, $p \leq 0.05$). Drying physically stable emulsions results in high EE values (Ramakrishnan et al., 2014), which correlates with our results. As can be seen in Figure S 29A of the Supplementary Material, all the emulsions fed to the dryers showed a monomodal droplet size distribution of small oil droplets (D[4,3] = 0.4-0.5 μm) regardless of the oil load. Moreover, the reconstituted emulsions showed a droplet size distribution similar to that of the parent emulsions and these were also fairly similar among the samples (D[4,3] = 0.5-0.7 μm), except for the sample EAPG-mo-39 (D[4,3] = 1.9 μm) (Figure S 29B of the Supplementary Material). The latter is an indication that the emulsions behaved similarly upon drying irrespective of the technology used and that the integrity of the oil-water interface was retained irrespective of the atomization method (e.g., mechanical atomization or mechanical atomization followed by electrohydrodynamic atomization) (Taboada et al., 2021). Hence, the larger oil droplet size of the reconstituted emulsion for sample EAPG-mo-39 might be related to its lower EE (EE = 83%, Fig. 3B), meaning that more non-encapsulated oil was available to coalesce after the redispersion of the capsules. Indeed, at a fixed particle size, increasing the oil load might result in a reduced entrapment of the oil within the encapsulating matrix (Drosou et al., 2017), which explains our observations for small capsules as those obtained in monoaxial EAPG (e.g., thinner encapsulating wall). Nonetheless, the EE of the spray-dried capsules was not affected by their oil load ($p > 0.05$, Figure 53B) due to their large particle size (Figure 52A-C). Overall, our results are in line with other studies reported in the literature on the encapsulation of omega-3 PUFAs rich oils by EAPG in the monoaxial configuration within carbohydrates or proteins-based matrices (e.g., maltodextrin or whey protein concentrate; EE = 65-85%) (Prieto & Lagaron, 2020) and mixtures carbohydrate:protein-based matrices (e.g., glucose syrup:whey protein concentrate; EE = 78-86%) (García-Moreno et al., 2018). This could be

related to the highly-physically stable emulsions produced in the current study with considerably low droplet size (Figure S 29A of the Supplementary Material).

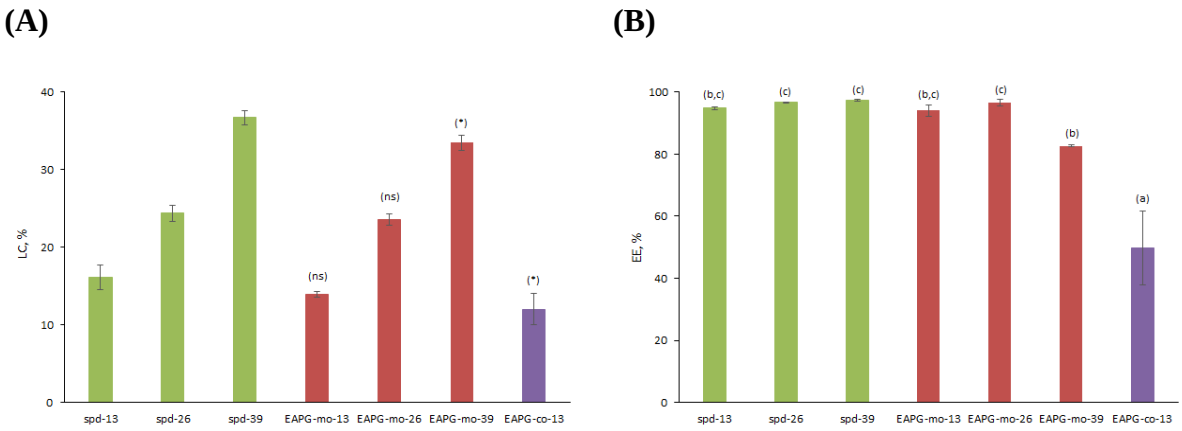

Figure 53. Load capacity (LC) (A) and encapsulation efficiency (EE) (B) of the fish oil-loaded capsules (13, 26 and 39 wt% fish oil) produced by spray-drying (spd-), EAPG monoaxial (EAPG-mo-) and EAPG coaxial (EAPG-co).

It should be noted that the lowest EE value was observed for the capsules produced by coaxial EAPG (EE ~50%) (Figure 53B). As reported in the literature, extractable oil fractions in encapsulated systems comprises both non-encapsulated surface oil and encapsulated oil that can be reached by the extracting solvent trough capillary or cracks present on the surface of the capsules and, depending on the extraction method, different fractions of the encapsulated oil can be reached (Drusch & Berg, 2008). Theoretically, optimal coaxial electrospraying leads to capsules consisting of an oil droplet located at the core of the structure surrounded by the encapsulating wall when neat fish oil is infused. Therefore, the extraction of a portion of the encapsulated oily core might be likely to occur if the dried encapsulating shell presents some capillary for solvent diffusion. In the current study, the capsules were immersed in the extracting solvent and thoroughly washed by shaking the mixture for a certain time, thus extraction of the encapsulated oil through capillary or cracks cannot be ruled out. This might explain the low EE values reported for this system (EAPG-co-13 sample), which do not correlate with its high oxidative stability, as will be further discussed below.

3.1.3 Oxidative stability

To investigate the oxidative stability of the capsules obtained, the development of secondary volatile oxidation products (SVOPs) derived from the oxidation of omega-3 PUFAs (e.g., 1-penten-3-ol) was monitored throughout 6 weeks of storage at 25 °C (Figure 54). Interestingly, our results showed that the encapsulation technology used to produce the

capsules, but not the oil load, significantly influenced ($p \leq 0.05$) their oxidative stability. The most oxidized capsules during storage were those produced by monoaxial EAPG (EAPG-mo systems), whereas the spray-dried (spd-) and the coaxially EAPG capsules (EAPG-co-13 sample) were significantly less oxidized. Furthermore, for the different oil loads evaluated, the development and the final content of the selected SVOPs found in the encapsulated systems produced either by spray-drying or monoaxial EAPG were not statistically different among the samples ($p > 0.05$; Figure 54). These results are in agreement with those previously reported by Linke et al. (2021), who found that the oil load of the capsules obtained by spray-drying (e.g., 10, 15 or 20 wt% fish oil load) did not influence the lipid oxidation rate and extent, as indicated by the hydroperoxides content and anisidine value of the samples (expressed per kg of total oil). These authors concluded that the oxygen availability and supply played a major role on the lipid oxidation of the fish oil-loaded capsules rather than the oil load (Linke et al., 2021). In fact, oxygen solubility and diffusivity through the dried encapsulating matrix has been extensively reported to be a key factor promoting lipid oxidation of encapsulated systems (Boerekamp et al., 2019; Linke et al., 2020, 2021; Rahmani-Manglano et al., 2023) and its supply will vary depending on the physicochemical properties of the capsules including EE, permeability/thickness/porosity of the encapsulating wall or the particle size. Therefore, taking into account that the formulation of the emulsion-based capsules was the same for a fixed oil load and that the EE values were not significantly different among the samples ($p > 0.05$; Figure 53B), the lower oxidative stability reported for the EAPG-mo systems compared to the spray-dried capsules could be discussed on the basis of a higher oxygen uptake during storage influenced by: i) their smaller particle size, which implies a high contact area with environmental oxygen, and ii) their thinner encapsulating walls, derived from the same oil load but lower particle size, which implies a favored contact between encapsulated oil and oxygen diffusing through the dried matrix. Based on the latter, low oxidative stability could be also expected for the capsules produced by coaxial EAPG (EAPG-co-13 sample). As previously mentioned, by coaxial electrospraying the oil is theoretically located at the core of the dried matrix, contrarily to emulsion-based encapsulation methods (e.g., EAPG monoaxial) where a random distribution of oil droplets within the encapsulating wall is achieved.

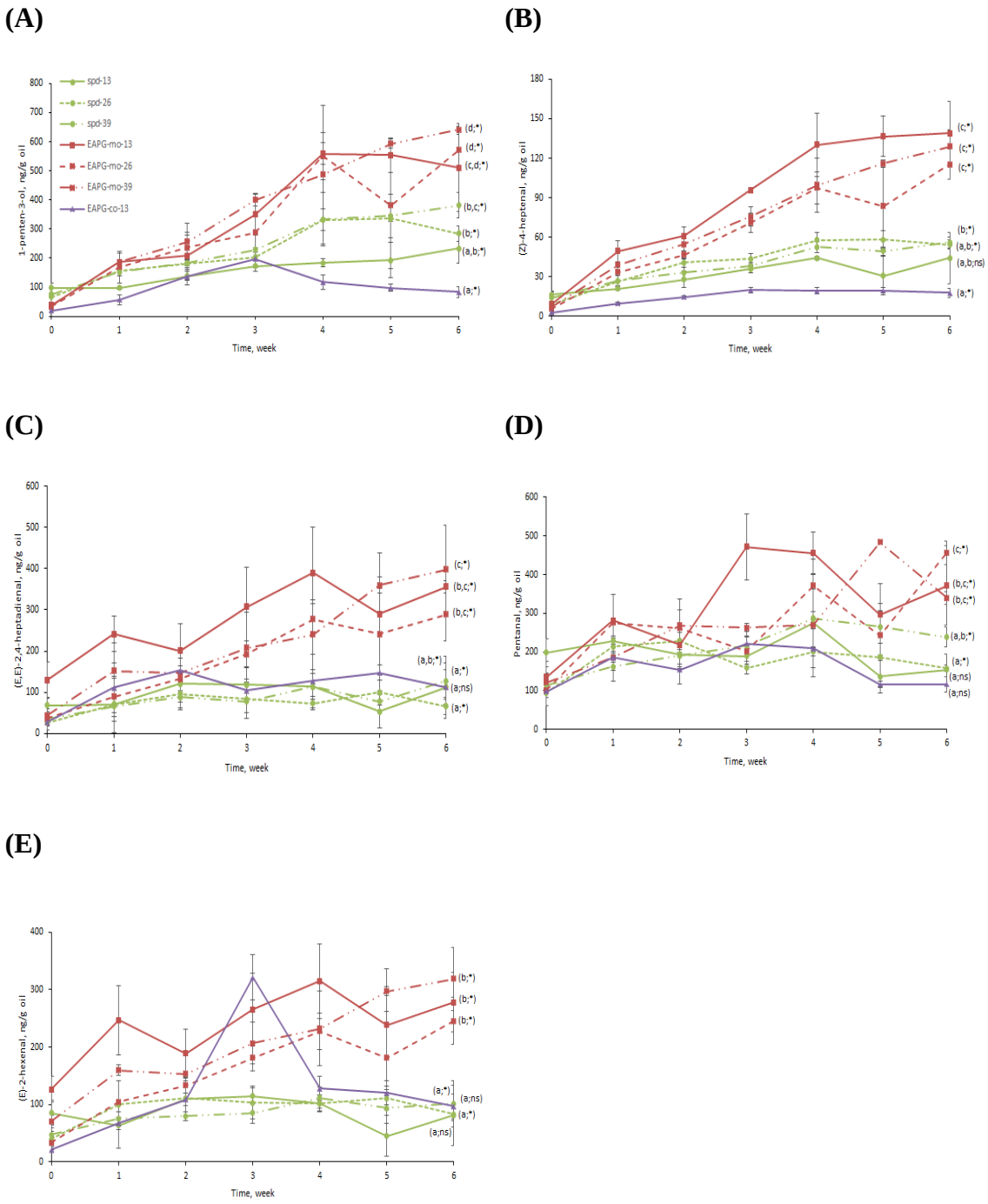

Figure 54. Secondary volatile oxidation products (SVOPs) of the fish oil-loaded capsules (13, 26 and 39 wt% fish oil) produced by spray-drying (spd-), EAPG monoaxial (EAPG-mo-) and EAPG coaxial (EAPG-co) during storage: 1-penten-3-ol (A); (Z)-4-heptenal (B); (E,E)-2,4-heptadienal (C); Pentanal (D); (E)-2-hexenal (E). Samples followed by a letter (a–e) indicate statistical differences ($p \leq 0.05$) between capsules. Means within the same sample followed by an asterisk (*) indicate statistical differences ($p \leq 0.05$) between week 0 and week 6. Means within the same sample followed by "ns" indicate no statistical differences ($p > 0.05$) between week 0 and week 6.

Our results suggest that the coaxially-encapsulated neat fish oil was more efficiently protected from environmental oxygen (i.e., the oxygen needs to penetrate throughout a thicker encapsulating wall before reaching the oily core) compared to monoaxially-encapsulated fish oil where lipid oxidation could be more easily initiated by diffusing oxygen encountering oil droplets dispersed in the encapsulating matrix closely to the capsule surface. It is also worth noting that the oxidation rate and extent of the coaxially EAPG capsules (EAPG-co-13 sample) was similar to or better than those of the spray-dried capsules (spd-systems) for all the selected SVOPs studied (Figure 54) despite their significantly different EE values ($p \leq 0.05$; Figure 53B). A low oxidative stability of encapsulated systems is often related to low EE values due to the direct contact of the unprotected non-encapsulated surface oil with environmental prooxidants (e.g., oxygen). However, it has been reported that the contribution of this non-encapsulated oil fraction to the overall lipid oxidation is minor when the fraction of the non-encapsulated surface oil is rather low compared to the fraction of the encapsulated oil (Linke et al., 2020). This is also an indication that, for the coaxially EAPG systems, a fraction of the encapsulated oil was extracted during the EE measurements, thus overestimating the non-encapsulated oil fraction (EE ~50%, Figure 53B), since a high oxidative stability was found for this system. In addition, it is particularly interesting to note that the lowest content of the selected SVOPs immediately after production was found for the coaxially EAPG capsules (EAPG-co-13 sample; Figure 54A-E). This finding further confirms that initial lipid oxidation was significantly reduced by producing the capsules in the coaxial configuration since: i) the fish oil was not emulsified (it was infused through the core as NFO), which avoids an increase in temperature and the inclusion of oxygen during homogenization, and ii) the drying process occurred at ambient temperature.

3.2 Physicochemical characterization of the fortified salad dressing

Based on the results presented, the salad dressing samples (SD-) were fortified with the selected capsules produced by the three technologies studied: spray-drying (spd-) and monoaxial EAPG (EAPG-mo) with 13 or 39 wt% fish oil loads, and coaxial EAPG (EAPG-co) with 13 wt% fish oil load. A salad dressing sample fortified with NFO (SD-NFO) was also produced as a control.

3.2.1 Physical stability: oil droplet size, viscosity and color

The physical stability of the fortified salad dressing samples was investigated by monitoring the changes in the oil droplet size, the viscosity and the color at the beginning (day 0) and at the end (day 28) of the storage time.

After production, the salad dressing samples showed different oil droplet size distributions depending on the fortification approach (e.g., emulsion or non-emulsion-based delivery systems; Figure S 30A of the Supplementary Material). The samples enriched with the capsules produced by the emulsion-based encapsulation methods (e.g., SD-spd or SD-mo samples) showed the highest proportion of small oil droplets (first peak centered at ~0.3μm), irrespective of the oil load of the capsules (Figure S 30A of the Supplementary Material). Indeed, when comparing these curves to that of the reconstituted emulsions of the emulsion-based capsules after drying (peak centered at ~0.3-0.4μm; Figure S 29B of the Supplementary Material), it can be concluded that the proportion of small oil droplets of such fortified dressings represents the droplet size of the encapsulated fish oil. Hence, the other peaks observed at larger diameter values (from 1 up to 200μm) are a consequence of the RSO droplets dispersed in the food matrix. Overall, these results are indicating that the integrity of the water-soluble encapsulating wall was retained after fortification of a food matrix with a relatively high water content (i.e., 25 wt% fat), thus the production process was efficiently optimized. Conversely, the proportion of small oil droplets was rather low (< 0.4% volume) for the samples enriched with the coaxially EAPG capsules (SD-co-13) or the NFO (SD-NFO) since in both cases the fish oil was not emulsified prior to food fortification (Figure S 30A of the Supplementary Material). In Table 9, the D[3,2] and the D[4,3] values of the enriched salad dressing samples are shown. In the fortified salad dressings, the D[3,2] value is more influenced by the size of small droplets present in the matrix whilst the D[4,3] value is more affected by the size of the bulk oil droplets (Miguel et al., 2019). As expected, higher D[3,2] values were found in the samples fortified with the non-emulsified delivery systems (e.g., SD-co-13 and SD-NFO samples) after production compared to those enriched with the emulsion-based capsules (Table 9). Furthermore, significant differences were observed in the D[4,3] values among the samples at day 0 (Table 9). High D[4,3] values of emulsion-like food products fortified with dried delivery systems (e.g., mayonnaise) have been related to a limited reduction of the oil droplet size during sample preparation in presence of the encapsulates (Hermund et al., 2019; Miguel et al., 2019). However, the opposite was found in the current study. This is explained on the basis that the dried delivery

systems were added to a previously produced salad dressing and mixed for a certain time until complete dispersion, which allowed a better reduction of the RSO oil droplets size during preparation of the food matrix. During storage, no creaming or phase separation was observed. However, changes in the oil droplet size of the samples occurred (Table 9 and Figure S 30B of the Supplementary Material). After storage, a small but significant increase in the D[3,2] and D[4,3] values was observed for the dressing samples fortified with the emulsion-based capsules, contrary to SD-co-13 and SD-NFO samples ($p \leq 0.05$, Table 9). This suggests that, for SD-co-13 and SD-NFO samples, potential oil floccules present after production disintegrated during storage (Miguel et al., 2019). Nonetheless, for the salad dressings fortified with the emulsion-based delivery systems, flocculation and/or coalescence of the oil droplets occurred, which can be in part attributed to a partial, although limited, disintegration of the encapsulating shell throughout storage (Miguel et al., 2019; Rahmani-Manglano, González-Sánchez, et al., 2020).

Table 9. Oil droplet size, apparent viscosity (γ=10 s−1) and yellowness index (YI) of the fortified salad dressing with encapsulated fish oil (SD-spd-, spray-drying; SD-mo-, EAPG monoaxial; SD-co-, EAPG coaxial) at different oil loads (13 or 39 wt%) or neat fish oil (SD-NFO).

	Oil droplet size				Apparent Viscosity		Yellowness Index	
	Day 0		Day 28		(γ = 10 s^{-1}), Pa·s		(YI)	
Sample	D[3,2], µm	D[4,3], µm	D[3,2], µm	D[4,3], µm	Day 0	Day 28	Day 0	Day 28
SD-spd-13	0.85 ± 0.02^{a}	16.31 ± 0.55^{a}	$0.94 \pm 0.02^{a;*}$	$19.45 \pm 0.90^{b;ns}$	9.80 ± 0.34^{c}	$10.01 \pm 0.36^{d;ns}$	16.00 ± 0.23^{b}	$20.14 \pm 1.44^{b,ns}$
SD-spd-39	0.86 ± 0.03^{a}	20.85 ± 0.41^{b}	$0.97 \pm 0.03^{a;*}$	$24.57 \pm 0.30^{c;*}$	6.45 ± 0.13^{b}	$6.11 \pm 0.10^{b,ns}$	$14.83 \pm 0.25^{a,b}$	$17.87 \pm 0.50^{a,b;ns}$
SD-mo-13	0.89 ± 0.04^{a}	20.35 ± 0.29^{b}	$0.99 \pm 0.02^{a;*}$	$14.69 \pm 0.04^{a;*}$	9.94 ± 0.07^{c}	$8.67 \pm 0.09^{c,*}$	16.15 ± 0.46^{b}	$24.23 \pm 0.88^{c,*}$
SD-mo-39	0.86 ± 0.01^{a}	22.04 ± 0.26^{c}	$1.10 \pm 0.03^{b;*}$	$24.85 \pm 1.09^{c;ns}$	$6.34 \pm 0.07^{a,b}$	$5.83 \pm 0.01^{b,*}$	$14.81 \pm 0.12^{a,b}$	$20.08 \pm 1.08^{b,*}$
SD-co-13	2.07 ± 0.03^{c}	24.47 ± 0.25^{d}	$1.59 \pm 0.06^{c;*}$	$23.88 \pm 0.49^{c;ns}$	8.79 ± 0.65^{c}	$8.73 \pm 0.28^{c,ns}$	19.16 ± 0.61^{c}	$20.20 \pm 0.92^{b,c;ns}$
SD-NFO	1.81 ± 0.10^{b}	25.62 ± 0.40^{e}	$1.66 \pm 0.02^{c;ns}$	$22.93 \pm 0.41^{c;*}$	5.21 ± 0.02^{a}	$4.14 \pm 0.04^{a,*}$	14.24 ± 0.03^{a}	$15.00 \pm 1.04^{a,ns}$

It should be noted that all the fortified dressings presented a pseudoplastic behavior (Figure S 31 of the Supplementary Material) and, depending on the delivery system used, different apparent viscosities were observed (Table 9). After production, the lower apparent viscosity corresponded to the sample fortified with NFO (SD-NFO sample) and it could be observed that the viscosity of the samples significantly increased as the oil load of the dried delivery systems decreased ($p \leq 0.05$; Table 9). The higher viscosity of the dressing samples fortified with the dried delivery systems is attributed to the thickening effect of the intact capsules dispersed in the food matrix (Miguel et al., 2019; Rahmani-Manglano, González-Sánchez, et al., 2020). Therefore, since more capsules with a lower oil load are required to achieve the fixed fish oil load of the food matrix, the viscosity of such samples was expected to be higher. During storage, slight, and in most cases, non-significant ($p > 0.05$) changes in the apparent

viscosity values were observed (Table 9). In the literature, changes in the apparent viscosity of emulsion-like food products during storage have been related to changes in the oil droplet size of the matrices (Miguel et al., 2019; Rahmani-Manglano, González-Sánchez, et al., 2020). Overall, a reduced specific surface area of the dispersed phase leads to less friction between the droplets, hence the larger the oil droplet size, the lower the apparent viscosity, which correlates well with our findings (Table 9).

Color measurement is a common analysis carried out in the food industry to address the quality changes of a food product as a result of processing and/or storage (León et al., 2006). As shown in Table 9, the yellowness index (YI) of the fortified dressings after production were in the same magnitude (YI = 14-19), although the value reported for the sample enriched with the coaxially EAPG capsules (SD-co-13 sample) was significantly higher ($p \leq 0.05$). After 28 days of storage, the YI of all the samples only increased slightly, which implies a high chemical stability of the food matrices (e.g., non-enzymatic browning reactions did not occur during the storage time). This was further confirmed by the pH value of the dressing samples, which was constant (pH = 4.7) during the storage time.

3.2.2 Oxidative stability

3.2.2.1 Peroxide value (PV) and tocopherol content (TC)

Figure 55A shows the evolution of the peroxide value (PV) of the fortified dressing samples during storage. After production, a low PV was found in all the samples (PV = 0.1-0.7 meq O2/kg oil) irrespective of the fortification strategy used. However, significantly different oxidation rates could be observed during storage depending on the processing of the fish oil prior to food fortification (e.g., emulsion or non-emulsion-based delivery systems). Moreover, among the dressing samples enriched with the emulsion-based capsules, also different trends could be distinguished depending on the technology used to produce such capsules (e.g., spray-drying or EAPG monoaxial). For instance, a sharp increase in the PV occurred for the samples fortified with the capsules produced by EAPG technology in the monoaxial configuration (SD-mo-13 and SD-mo-39 samples) up to the third week of storage, followed by a sharp decrease. Conversely, a sustained increase in the PV was observed for the samples fortified with the spray-dried capsules (SD-spd-13 and SD-spd-39 samples) until the end of the storage time (Figure 55A).

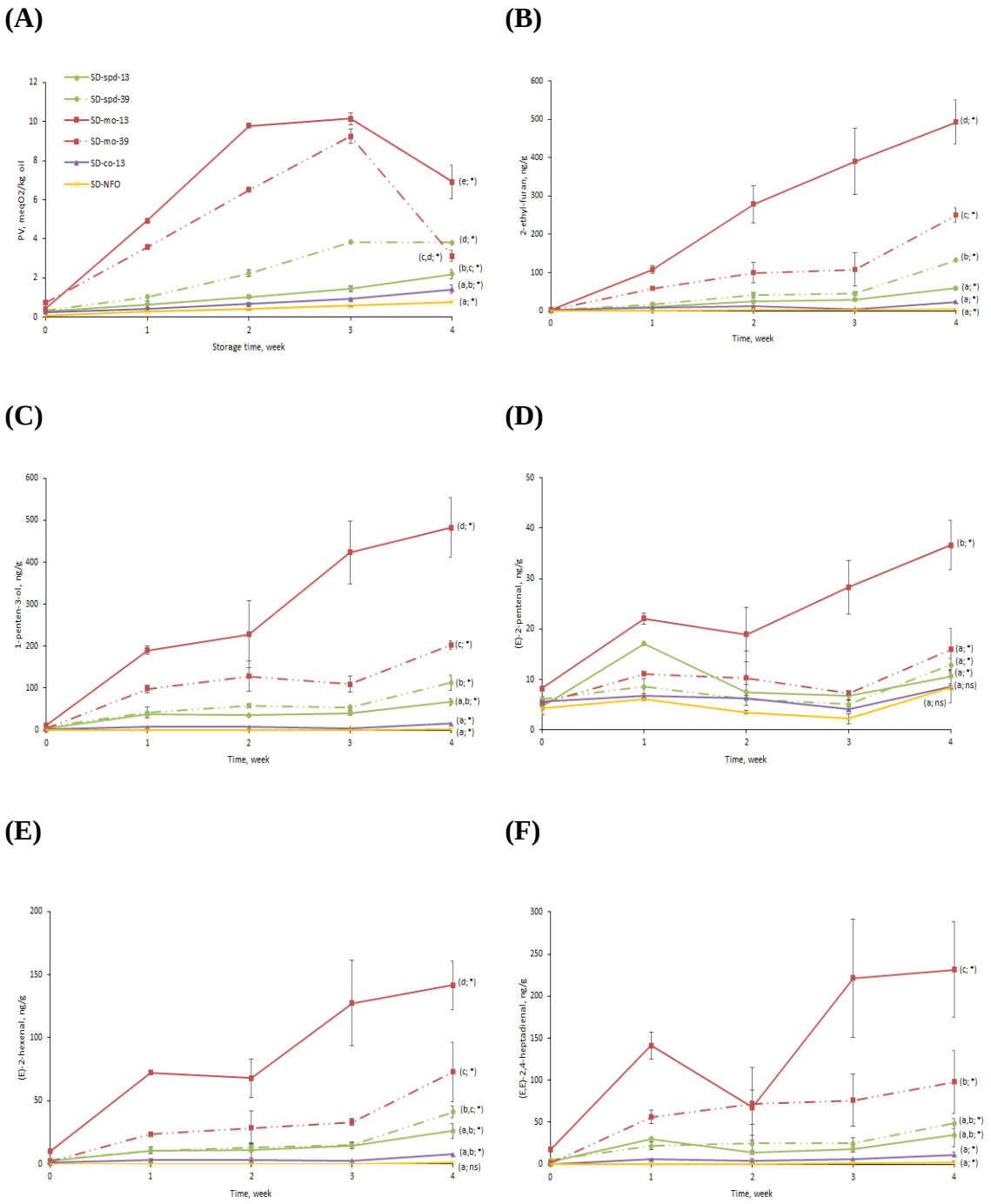

Figure 55. Peroxide value (PV) (A) and secondary volatile oxidation products (SVOPs) (B-F) of fortified salad dressing enriched with encapsulated (SD-spd-, spray-drying; SD-mo-, EAPG monoaxial; SD-co-, EAPG coaxial) at different oil loads (13 or 39 wt%) or neat fish oil (SD-NFO) during storage. Means within the same sampling point followed by a letter, a-e, indicates statistical differences ($p \leq 0.05$) between samples. Means within the same sample followed by an asterisk (*) indicates statistical differences ($p \leq 0.05$) between week 0 and week 4. Means within the same sample followed by "ns" indicate no statistical differences ($p > 0.05$) between week 0 and week 4.

These results are in line with those reported for the oxidative stability of the emulsion-based capsules, being those produced by monoaxial EAPG the less oxidatively stable throughout storage (Figure 54). The latter is also an indication that the emulsion-based capsules were not disrupted after food fortification since different oxidation trends were observed depending on the technology used to produce such encapsulates despite the formulation was the same for a fixed oil load and the EE and the droplet size of the encapsulated fish oil was not significantly different ($p > 0.05$) among the samples (e.g., spd-13 and EAPG-mo-13 or spd-39 and EAPG-mo-39; Figure 53B and Figure S 29 of the Supplementary Material).

In case of the salad dressing samples fortified with the non-emulsified delivery systems (e.g., coaxially EAPG capsules, SD-co-13 or NFO, SD-NFO) a slight increase in the PV was also noted during storage. However, although the final values were significantly higher compared to that of the beginning of the storage experiment ($p \leq 0.05$, Figure 55A), they were still very low (PV < 1.5 meq O2/kg oil). Surprisingly, the lowest PV was found for the dressing sample fortified with the "non-protected" NFO. In a previous study, Let at al. (2007a) produced a fish oil-enriched salad dressing (10 wt% fish oil) and also found that the highest oxidative stability corresponded to the sample fortified with NFO compared to the sample fortified with a fish oil-in-water emulsion. The authors argued that this finding could be attributed to the protective effect that the tocopherols present in the RSO exerted when it was mixed with the NFO before processing. Nonetheless, it seems that this is not the case in the current study. Firstly, the final PV of the salad dressing samples fortified with the non-emulsified delivery systems were comparable ($p > 0.05$) despite their different fortification approach (e.g., encapsulated fish oil by coaxial EAPG or NFO) and preparation procedures (e.g., mixing of the NFO with the RSO before processing or dispersion of the dried fish oil-loaded capsules to an already produced salad dressing). Secondly, and considering the tocopherol content of the fortified dressing samples, it can be observed that their concentration was rather constant during storage and similar among the samples, irrespective of the delivery system used (Figure S 32 of the Supplementary Material). Therefore, this led us to conclude that the oxidative stability of the dressing samples was not influenced by their tocopherol content, but it was most likely to be influenced by the fish oil oxidative status prior to food fortification (e.g., emulsified or non-emulsified), as will be further discussed below.

3.2.2.2 Secondary volatile oxidation products (SVOPs) – Dynamic Headspace GC-MS

The content of selected SVOPs of the fortified dressing samples (e.g., 2-ethyl-furan) during storage is shown in Figure 55B-F. In line with the PV of the salad dressings, the highest content of the selected SVOPs was found in the samples fortified with the emulsion-based capsules (e.g., SD-spd and SD-mo samples), being those enriched with the capsules produced by monoaxial EAPG the most oxidized at the end of the storage time (SD-mo-13 and SD-mo-39 samples; Figure 55B-F). Therefore, taking into account that the integrity of the capsules was retained after processing, the different oxidation trends of the salad dressing samples fortified with the emulsion-based delivery systems could also be attributed to the different physicochemical properties of the capsules influencing the diffusivity of prooxidant species present in the food matrix through the encapsulating wall. Nonetheless, contrary to what we observed during storage of the dried delivery systems (Figure 54), the oxidation rate and extent of the dressing samples enriched with the emulsion-based capsules were influenced by their oil load (13 or 39 wt%). Moreover, this influence was different depending on the technology used for their production (spray-drying or monoaxial EAPG) (Figure 55B-F). For instance, whilst a sharp increase in the content of all the selected SVOPs was observed for the sample SD-mo-13 from the beginning of the storage time, the oxidation rate and extent were significantly lower for the sample SD-mo-39 (Figure 55B-F). Conversely, the dressing samples fortified with the spray-dried capsules oxidized similarly throughout storage irrespective of their oil load (SD-spd-13 and SD-spd-39 samples), leading to final concentrations of the SVOPs not significantly different between the samples ($p > 0.05$; Figure 55B-F). Increasing the oil load of EAPG-mo capsules resulted in a lower proportion of small particles, approximately ~10% fewer small particles between 5-10 μm of sample EAPG-mo-39 compared to EAPG-mo-13 (Figure 52D,F), whereas the particle size distribution of the spray-dried capsules was the same irrespective of their oil load (13 or 39 wt.%, Figure 52A,C). Thus, our results suggest that although the size of the capsules had a low impact on the oxidative stability of the EAPG-mo-based delivery systems (Figure 54), it more notably influenced the differences observed on the oxidative stability of the fortified dressing samples (Figure 55B-F). In any case, it should be borne in mind that the capsules are found in different environments (e.g., stored in a bottle or dispersed in a food matrix) and therefore exposed to different prooxidant species (e.g., oxygen and/or metal ions). Prooxidants present in food promote lipid oxidation, with transition metals being one of the

most important prooxidants of food systems (Ghelichi et al., 2021). Metal ions are excellent prooxidants since they can trigger the initiation phase of lipid autoxidation and also promote the decomposition of lipid hydroperoxides giving rise to SVOPs (Jacobsen et al., 2013). Although the content of metal ions in salad dressings is suggested to be low (Jacobsen et al., 2008), it has been demonstrated that lipid oxidation mediated by transition metals is a very important factor affecting their oxidative stability (Jacobsen et al., 2008; Let et al., 2007b). In the literature, the diffusion of molecules in carbohydrate-based systems has been investigated, highlighting the importance of the molecular diameter of the diffusing molecule travelling through the cavities of the glassy matrix (Orlien et al., 2000). Furthermore, it has been reported that transition metal ions are capable to diffuse through the peptide-based interfacial layer of oil-in-water emulsions due to their small molecular size (Berton-Carabin et al., 2014). Thus, our results suggest that the higher surface-to-volume ratio of the EAPG-mo-13 capsules, compared to EAPG-mo-39 capsules, might have favored the contact and diffusion of the small-sized metal ions present in the food matrix through the encapsulating wall.

On the other hand, and also in line with the PV of the dressing samples (Figure 54), the low content of selected SVOPs observed for the samples fortified with the non-emulsified delivery systems (e.g., SD-co-13 and SD-NFO samples) was rather constant throughout storage (Figure 55B-F). These results further confirm that the oxidative stability of the fortified dressing samples was strongly influenced by the fish oil oxidative status prior to food fortification since for the non-emulsion-based delivery systems the inclusion of oxygen and the temperature increase that occurs as a result of the emulsification step, both promoting lipid oxidation during processing, was avoided (Serfert et al., 2009). Furthermore, in case of EAPG-co-13 capsules, drying was carried out at ambient temperature. In this line, it is worth noting that the emulsion-based delivery systems (e.g., spd- and EAPG-mo capsules) presented a poorer initial oxidative status than that of the coaxially EAPG capsules (EAPG-co capsules; Figure 54A-E) or the NFO (PV = 0.33 ± 0.06 meq O2/kg oil), which in turn confirms that the onset of lipid oxidation of these systems occurred during the production of the encapsulated systems (e.g., air inclusion and high temperature). This further affects the oxidative stability of the food system since, once the lipid radicals are present in the oil, lipid oxidation occurs as a chain reaction (Rahmani-Manglano, García-Moreno, et al., 2020).

4. CONCLUSIONS

Our results show that the physicochemical properties of the capsules (e.g., particle size or EE) and their oxidative stability were significantly influenced by the encapsulation technique, rather than by the oil load. Despite their high EE (EE = 83-97%), the most oxidized capsules were those produced by monoaxial EAPG, which may be attributed to their small particle size influencing the oxygen diffusivity through the encapsulating wall together with the initial degree of lipid oxidation of the encapsulated fish oil after processing due to emulsification. On the other hand, the non-emulsion-based encapsulation approach by coaxial EAPG resulted in an enhanced oxidative stability of the encapsulated fish oil during and after processing. The oxidative stability of the fortified salad dressings was in line with the oxidative stability of the dried delivery systems. The salad dressing samples fortified with the non-emulsified delivery systems (e.g., coaxially EAPG capsules or neat fish oil) showed the highest oxidative stability through storage, as confirmed by their low PV and the low content of the selected volatiles (e.g., 2-ethyl-furan). This finding can be attributed to the better oxidative status of the fish oil since it was not emulsified prior to food fortification. Taken altogether, our results showed that coaxial EAPG is a promising technique to produce neat fish oil-loaded capsules aimed as omega-3 delivery systems to produce fortified food matrices with omega-3 PUFAs.

5. REFERENCES

Alamilla-Beltrán, L., Chanona-Pérez, J. J., Jiménez-Aparicio, A. R., & Gutiérrez-Lopez, G. F. (2005). Description of morphological changes of particles along spray drying. *Journal of Food Engineering*, *67*(1–2), 179–184. https://doi.org/10.1016/j.jfoodeng.2004.05.063

AOCS Official Method CE 8-89. Determination of Tocopherols and Tocotrienols in Vegetable Oils and Fats by HPLC. (1998). *AOCS Press, Champaing*. https://doi.org/10.5650/jos1956.37.1169

Aquilani, C., Pérez-Palacios, T., Sirtori, F., Jiménez-Martín, E., Antequera, T., Franci, O., Acciaioli, A., Bozzi, R., & Pugliese, C. (2018). Enrichment of Cinta Senese burgers with omega-3 fatty acids. Effect of type of addition and storage conditions on quality characteristics. *Grasas y Aceites*, *69*(1). https://doi.org/10.3989/gya.0671171

Berton-Carabin, C. C., Ropers, M. H., & Genot, C. (2014). Lipid Oxidation in Oil-in-Water Emulsions: Involvement of the Interfacial Layer. *Comprehensive Reviews in Food Science and Food Safety*, *13*(5), 945–977. https://doi.org/10.1111/1541-4337.12097

Boerekamp, D. M. W., Andersen, M. L., Jacobsen, C., Chronakis, I. S., & García-Moreno, P. J. (2019). Oxygen permeability and oxidative stability of fish oil-loaded electrosprayed capsules measured by Electron Spin Resonance: Effect of dextran and glucose syrup as main encapsulating materials. *Food Chemistry*, *287*, 287–294. https://doi.org/10.1016/j.foodchem.2019.02.096

Both, E. M., Karlina, A. M., Boom, R. M., & Schutyser, M. A. I. (2018). Morphology development during sessile single droplet drying of mixed maltodextrin and whey protein solutions. *Food Hydrocolloids*, *75*, 202–210. https://doi.org/10.1016/j.foodhyd.2017.08.022

Busolo, M. A., Torres-Giner, S., Prieto, C., & Lagaron, J. M. (2019). Electrospraying assisted by pressurized gas as an innovative high-throughput process for the microencapsulation and stabilization of docosahexaenoic acid-enriched fish oil in zein prolamine. *Innovative Food Science and Emerging Technologies*, *51*, 12–19. https://doi.org/10.1016/j.ifset.2018.04.007

Calder, P. C. (2021). Health benefits of omega-3 fatty acids. In *Omega-3 Delivery Systems* (pp. 25–53). Elsevier. https://doi.org/10.1016/b978-0-12-821391-9.00006-5

Davidov-Pardo, G., Roccia, P., Salgado, D., León, A. E., & Pedroza-Islas, R. (2008). Utilization of Different Wall Materials to Microencapsulate Fish Oil Evaluation of its Behavior in Bread Products. *American Journal of Food Technology*, *3*(6), 384–393. https://doi.org/10.3923/ajft.2008.384.393

Drosou, C. G., Krokida, M. K., & Biliaderis, C. G. (2017). Encapsulation of bioactive compounds through electrospinning/electrospraying and spray drying: A comparative assessment of food-related applications. *Drying Technology*, *35*(2), 139–162. https://doi.org/10.1080/07373937.2016.1162797

Drusch, S., & Berg, S. (2008). Extractable oil in microcapsules prepared by spray-drying: Localisation, determination and impact on oxidative stability. *Food Chemistry*, *109*(1), 17–24. https://doi.org/10.1016/j.foodchem.2007.12.016

García-Moreno, P. J., Pelayo, A., Yu, S., Busolo, M., Lagaron, J. M., Chronakis, I. S., & Jacobsen, C. (2018). Physicochemical characterization and oxidative stability of fish oil-loaded electrosprayed capsules: Combined use of whey protein and carbohydrates as wall materials. *Journal of Food Engineering*, *231*, 42–53. https://doi.org/10.1016/j.jfoodeng.2018.03.005

García-Moreno, P. J., Rahmani-Manglano, N. E., Chronakis, I. S., Guadix, E. M., Yesiltas, B., Sørensen, A.-D. M., & Jacobsen, C. (2021). Omega-3 nano-microencapsulates produced by electrohydrodynamic processing. In P. J. García-Moreno, C. Jacobsen, A.-D. M. Sørensen, & B. Yesiltas (Eds.), *Omega-3 Delivery Systems. Production, Physical Characterization and*

Oxidative Stability (pp. 345–370). Academic Press. https://doi.org/10.1016/b978-0-12-821391-9.00017-x

Ghelichi, S., Hajfathalian, M., García-Moreno, P. J., Yesiltas, B., Moltke-Sørensen, A.-D., & Jacobsen, C. (2021). Food enrichment with omega-3 polyunsaturated fatty acids. In P. J. García-Moreno, C. Jacobsen, A.-D. M. Sørensen, & B. Yesiltas (Eds.), *Omega-3 Delivery Systems* (pp. 395–425). Academic Press. https://doi.org/10.1016/b978-0-12-821391-9.00020-x

Hermund, D., Jacobsen, C., Chronakis, I. S., Pelayo, A., Yu, S., Busolo, M., Lagaron, J. M., Jónsdóttir, R., Kristinsson, H. G., Akoh, C. C., & García-Moreno, P. J. (2019). Stabilization of Fish Oil-Loaded Electrosprayed Capsules with Seaweed and Commercial Natural Antioxidants: Effect on the Oxidative Stability of Capsule-Enriched Mayonnaise. *European Journal of Lipid Science and Technology*, *121*(4). https://doi.org/10.1002/ejlt.201800396

Jacobsen, C., Let, M. B., Nielsen, N. S., & Meyer, A. S. (2008). Antioxidant strategies for preventing oxidative flavour deterioration of foods enriched with n-3 polyunsaturated lipids: a comparative evaluation. In *Trends in Food Science and Technology* (Vol. 19, Issue 2, pp. 76–93). https://doi.org/10.1016/j.tifs.2007.08.001

Jacobsen, C., Sørensen, A. D. M., & Nielsen, N. S. (2013). Stabilization of omega-3 oils and enriched foods using antioxidants. In *Food Enrichment with Omega-3 Fatty Acids*. Woodhead Publishing Limited. https://doi.org/10.1533/9780857098863.2.130

Jeyakumari, A., Janarthanan, G., Chouksey, M. K., & Venkateshwarlu, G. (2016). Effect of fish oil encapsulates incorporation on the physico-chemical and sensory properties of cookies. *Journal of Food Science and Technology*, *53*(1), 856–863. https://doi.org/10.1007/s13197-015-1981-2

Lagaron, J. M., Castro, S., Galan, D., & Valle, J. M. (2017). *Installation and procedure of industrial encapsulation of thermolabile substances. P201631725.*

León, K., Mery, D., Pedreschi, F., & León, J. (2006). Color measurement in L*a*b* units from RGB digital images. *Food Research International*, *39*(10), 1084–1091. https://doi.org/10.1016/j.foodres.2006.03.006

Let, M. B., Jacobsen, C., & Meyer, A. S. (2007a). Lipid oxidation in milk, yoghurt, and salad dressing enriched with neat fish oil or pre-emulsified fish oil. *Journal of Agricultural and Food Chemistry*, *55*(19), 7802–7809. https://doi.org/10.1021/jf070830x

Let, M. B., Jacobsen, C., & Meyer, A. S. (2007b). Ascorbyl palmitate, γ-tocopherol, and EDTA affect lipid oxidation in fish oil enriched salad dressing differently. *Journal of Agricultural and Food Chemistry*, *55*(6), 2369–2375. https://doi.org/10.1021/jf062675c

Linke, A., Weiss, J., & Kohlus, R. (2020). Oxidation rate of the non-encapsulated- and encapsulated oil and their contribution to the overall oxidation of microencapsulated fish oil particles. *Food*

Research International, *127*(September 2019), 108705. https://doi.org/10.1016/j.foodres.2019.108705

Linke, A., Weiss, J., & Kohlus, R. (2021). Impact of the oil load on the oxidation of microencapsulated oil powders. *Food Chemistry*, *341*(September 2020), 128153. https://doi.org/10.1016/j.foodchem.2020.128153

Maria Leena, M., Gover Antoniraj, M., Moses, J. A., & Anandharamakrishnan, C. (2020). Three fluid nozzle spray drying for co-encapsulation and controlled release of curcumin and resveratrol. *Journal of Drug Delivery Science and Technology*, *57*. https://doi.org/10.1016/j.jddst.2020.101678

Miguel, G. A., Jacobsen, C., Prieto, C., Kempen, P. J., Lagaron, J. M., Chronakis, I. S., & García-Moreno, P. J. (2019). Oxidative stability and physical properties of mayonnaise fortified with zein electrosprayed capsules loaded with fish oil. *Journal of Food Engineering*, *263*, 348–358. https://doi.org/10.1016/j.jfoodeng.2019.07.019

Nielsen, N. S., & Jacobsen, C. (2013). Retardation Of Lipid Oxidation In Fish Oil-Enriched Fish Pâté- Combination Effects. *Journal of Food Biochemistry*, *37*(1), 88–97. https://doi.org/10.1111/j.1745-4514.2011.00605.x

Orlien, V., Andersen, A. B., Sinkko, T., & Skibsted, L. H. (2000). Hydroperoxide formation in rapeseed oil encapsulated in a glassy food model as influenced by hydrophilic and lipophilic radicals. *Food Chemistry*, *68*, 191–199. https://doi.org/https://doi.org/10.1016/S0308-8146(99)00177-6

Prieto, C., Evtoski, Z., Pardo-Figuerez, M., Hrakovsky, J., & Lagaron, J. M. (2021). Nanostructured Valsartan Microparticles with Enhanced Bioavailability Produced by High-Throughput Electrohydrodynamic Room-Temperature Atomization. *Molecular Pharmaceutics*, *18*(8), 2947–2958. https://doi.org/10.1021/acs.molpharmaceut.1c00098

Prieto, C., & Lagaron, J. M. (2020). Nanodroplets of docosahexaenoic acid-enriched algae oil encapsulated within microparticles of hydrocolloids by emulsion electrospraying assisted by pressurized gas. *Nanomaterials*, *10*(2). https://doi.org/10.3390/nano10020270

Rahmani-Manglano, N. E., García-Moreno, P. J., Espejo-Carpio, F. J., Pérez-Gálvez, A. R., & Guadix-Escobar, E. M. (2020). The Role of Antioxidants and Encapsulation Processes in Omega-3 Stabilization. In M. A. Aboudzadeh (Ed.), *Emulsion-based Encapsulation of Antioxidants. Food Bioactive Ingredients.* (pp. 339–386). Springer, Cham. https://doi.org/10.1007/978-3-030-62052-3_10

Rahmani-Manglano, N. E., González-Sánchez, I., García-Moreno, P. J., Espejo-Carpio, F. J., Jacobsen, C., & Guadix, E. M. (2020). Development of fish oil-loaded microcapsules

containing whey protein hydrolysate as film-forming material for fortification of low-fat mayonnaise. *Foods*, *9*(5). https://doi.org/10.3390/foods9050545

Rahmani-Manglano, N. E., Guadix, E. M., Jacobsen, C., & García-Moreno, P. J. (2023). Comparative Study on the Oxidative Stability of Encapsulated Fish Oil by Monoaxial or Coaxial Electrospraying and Spray-Drying. *Antioxidants*, *12*(2). https://doi.org/https://doi.org/10.3390/antiox12020266

Ramakrishnan, S., Ferrando, M., Aceña-Muñoz, L., Mestres, M., de Lamo-Castellví, S., & Güell, C. (2014). Influence of Emulsification Technique and Wall Composition on Physicochemical Properties and Oxidative Stability of Fish Oil Microcapsules Produced by Spray Drying. *Food and Bioprocess Technology*, *7*(7), 1959–1972. https://doi.org/10.1007/s11947-013-1187-4

Serfert, Y., Drusch, S., & Schwarz, K. (2009). Chemical stabilisation of oils rich in long-chain polyunsaturated fatty acids during homogenisation, microencapsulation and storage. *Food Chemistry*, *113*(4), 1106–1112. https://doi.org/10.1016/j.foodchem.2008.08.079

Solomando, J. C., Antequera, T., González-Mohíno, A., & Perez-Palacios, T. (2020). Fish oil/lycopene microcapsules as a source of eicosapentaenoic and docosahexaenoic acids: a case study on spreads. *Journal of the Science of Food and Agriculture*, *100*(5), 1875–1886. https://doi.org/10.1002/jsfa.10188

Solomando, J. C., Antequera, T., & Perez-Palacios, T. (2020a). Evaluating the use of fish oil microcapsules as omega-3 vehicle in cooked and dry-cured sausages as affected by their processing, storage and cooking. *Meat Science*, *162*. https://doi.org/10.1016/j.meatsci.2019.108031

Solomando, J. C., Antequera, T., & Perez-Palacios, T. (2020b). Lipid digestion and oxidative stability in ω-3-enriched meat model systems: Effect of fish oil microcapsules and processing or culinary cooking. *Food Chemistry*, *328*. https://doi.org/10.1016/j.foodchem.2020.127125

Sørensen, A.-D. M., García-Moreno, P. J., Yesiltas, B., & Jacobsen, C. (2021). Introduction to delivery systems and stability issues. In *Omega-3 Delivery Systems* (pp. 107–117). Elsevier. https://doi.org/10.1016/b978-0-12-821391-9.00015-6

Taboada, M. L., Heiden-Hecht, T., Brückner-Gühmann, M., Karbstein, H. P., Drusch, S., & Gaukel, V. (2021). Spray drying of emulsions: Influence of the emulsifier system on changes in oil droplet size during the drying step. *Journal of Food Processing and Preservation*, *45*(9), 1–11. https://doi.org/10.1111/jfpp.15753

6. SUPPLEMENTARY MATERIAL

(A)

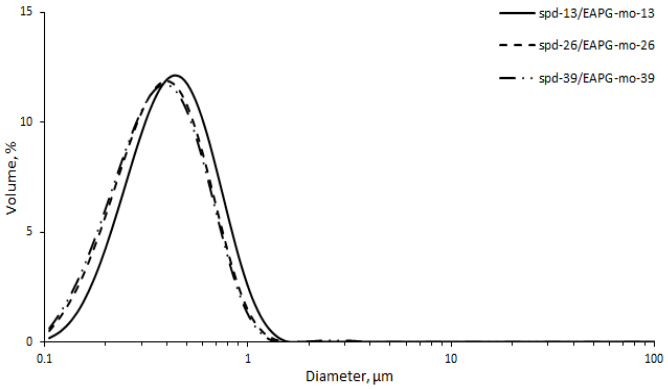

(B)

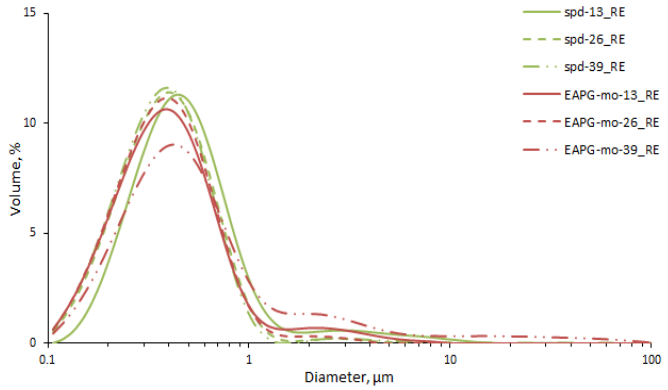

Figure S 29. Oil droplet size distribution of the parent (A) and the reconstituted emulsions (B).

(A)

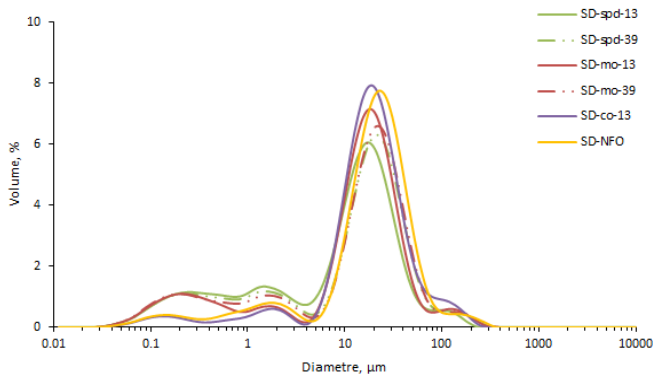

(B)

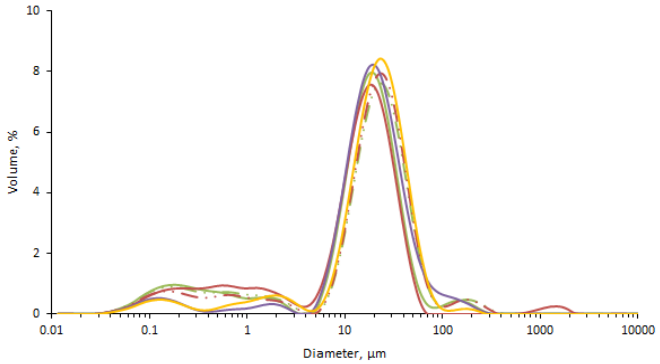

Figure S 30. Oil droplet size distribution of the fortified salad dressing samples at day 0 (A) and at day 28 (B) of the storage experiment.

(A)

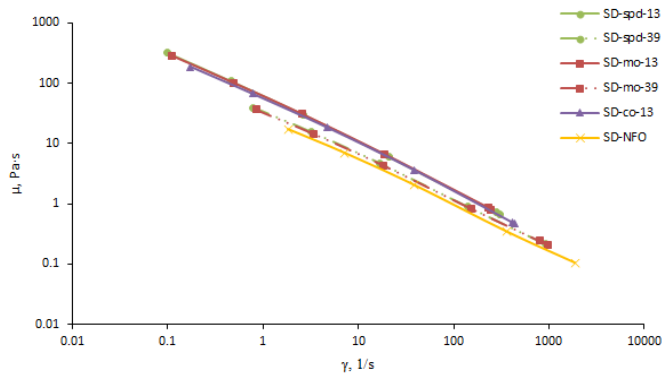

(B)

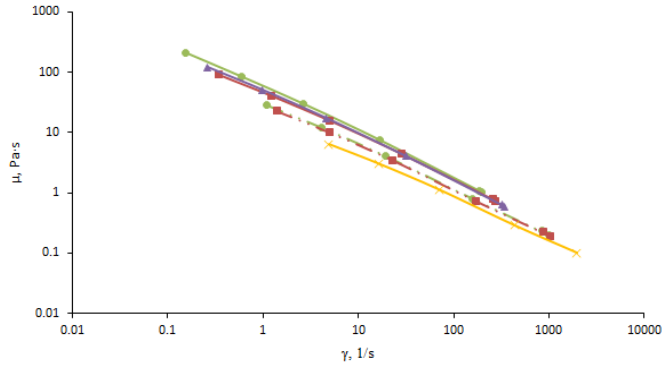

Figure S 31. Viscosity of the fortified salad dressing samples at day 0 (A) and at day 28 (B) of the storage experiment.

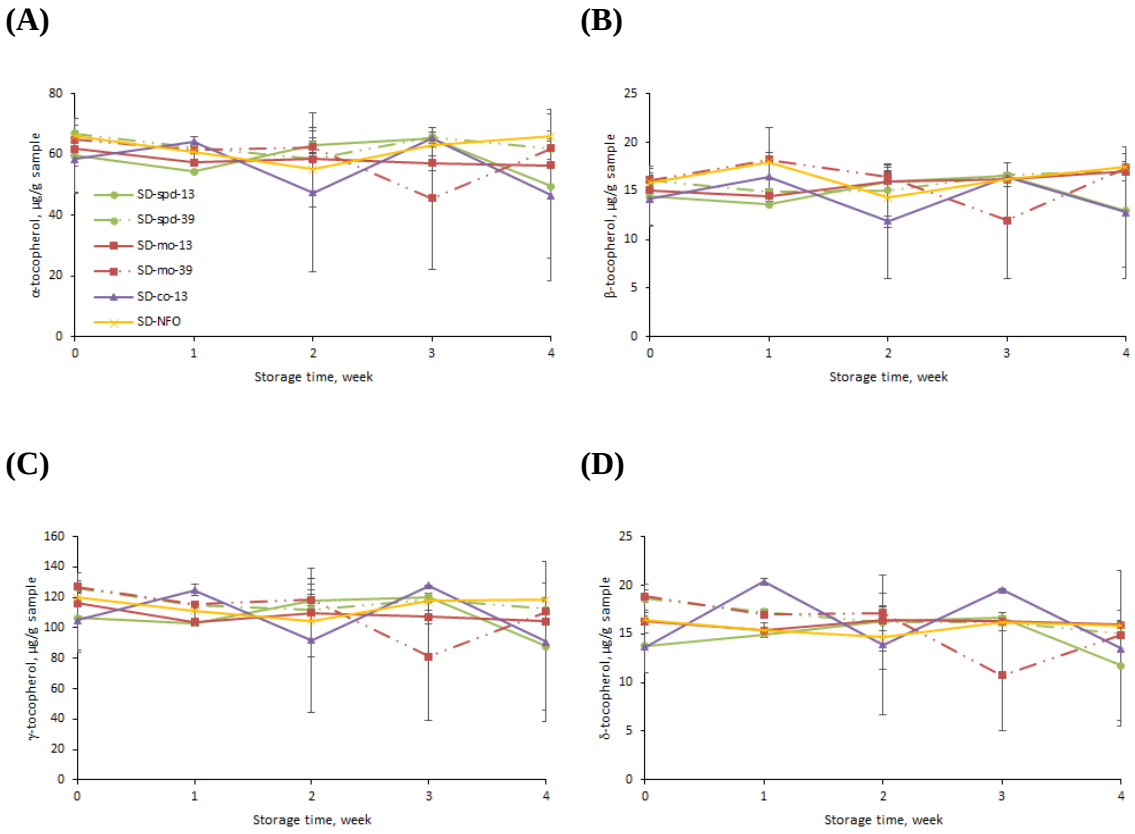

Figure S 32. Tocopherol content of fortified salad dressing enriched with encapsulated (SD-spd-, spray-drying; SD-mo-, EAPG monoaxial; SD-co-, EAPG coaxial) or neat fish oil (SD-NFO) during storage.

Appendices

APPENDIX I. Non-emulsion-based encapsulation of fish oil by coaxial electrospraying assisted by pressurized gas: combined use of whey protein concentrate hydrolysate and glucose syrup as wall materials

1. Materials and methods

The fish oil (Omega Oil 1812 TG Gold) was acquired from BASF Personal Care and Nutrition GmbH (Illertissen, Germany). Cargill Germany GmbH (Krefeld, Germany) provided the glucose syrup (GS; DE38, C*Dry 1934) and the whey protein concentrate (~35 wt% protein content) was supplied by Abbott Laboratories S.A. (Granada, Spain). The whey protein concentrate hydrolysate (WPCH), used as an emulsifier, was produced by enzymatic hydrolysis as described elsewhere (Rahmani-Manglano, González-Sánchez, et al., 2020).

The (bio)polymer-based shell solutions and the fish oil-loaded emulsion were produced as described in Chapter VIII. The samples codification and their composition are shown in Table I 1 – Table I 3.

Table I 1. Codification of the coaxially electrosprayed capsules

Code	Sample
EAPG-co-13-GS	electrosprayed solutions - coaxial; shell:core = GS:NFO
EAPG-co-13-S1	electrosprayed solutions - coaxial; shell:core = GS/WPCH(4.7):NFO
EAPG-co-13-S2	electrosprayed solutions - coaxial; shell:core = GS/WPCH(1.5):NFO
EAPG-co-13-S3	electrosprayed solutions - coaxial; shell:core = GS/WPCH(0.4):NFO
EAPG-co-13-WPCH	electrosprayed solutions - coaxial; shell:core = WPCH:NFO
EAPG-co-13-EFO	electrosprayed emulsion (oil load = 15wt%) - coaxial; shell:core = GS:EFO

Table I 2. Composition of the infeed solutions

	Composition, %					
	EAPG-co-13-GS	**EAPG-co-13-S1**	**EAPG-co-13-S2**	**EAPG-co-13-S3**	**EAPG-co-13-WPCH**	**EAPG-co-13-EFO**
GS	60	49.4	36	16.7	-	60
GS:WPCH	100:0	~82:18	60:40	~28:72	0:100	100:0
Core	NFO	NFO	NFO	NFO	NFO	EFO*
Ratio, mL:mL	1:9.9	1:9.9	1:9.0	1:8.9	1:11	1:1.1

Table I 3. Composition of the infeed emulsion

Composition, %	
EFO*	
GS	6.7
WPCH	17.3
FO	15
Water	61
GS/WPCH	0.4

The capsules were produced by coaxial EAPG as described in Chapter VIII. In brief, the core flow rate was fixed to 1 mL/min and the shell flow rate varied between 1 mL/min and

11 mL/min to achieve the desired load capacity (~13 wt%). The injector worked with an assisted air pressure of 16 L/min and the electric voltage was set to 10 kV. Every 20 minutes, the capsules were collected from the cyclone and stored in airtight flasks at –20 °C in the dark until analysis. The methodology used to characterize the coaxially electrosprayed capsules (i.e., morphology, load capacity and encapsulation efficiency) is described in Chapter VIII.

2. Results

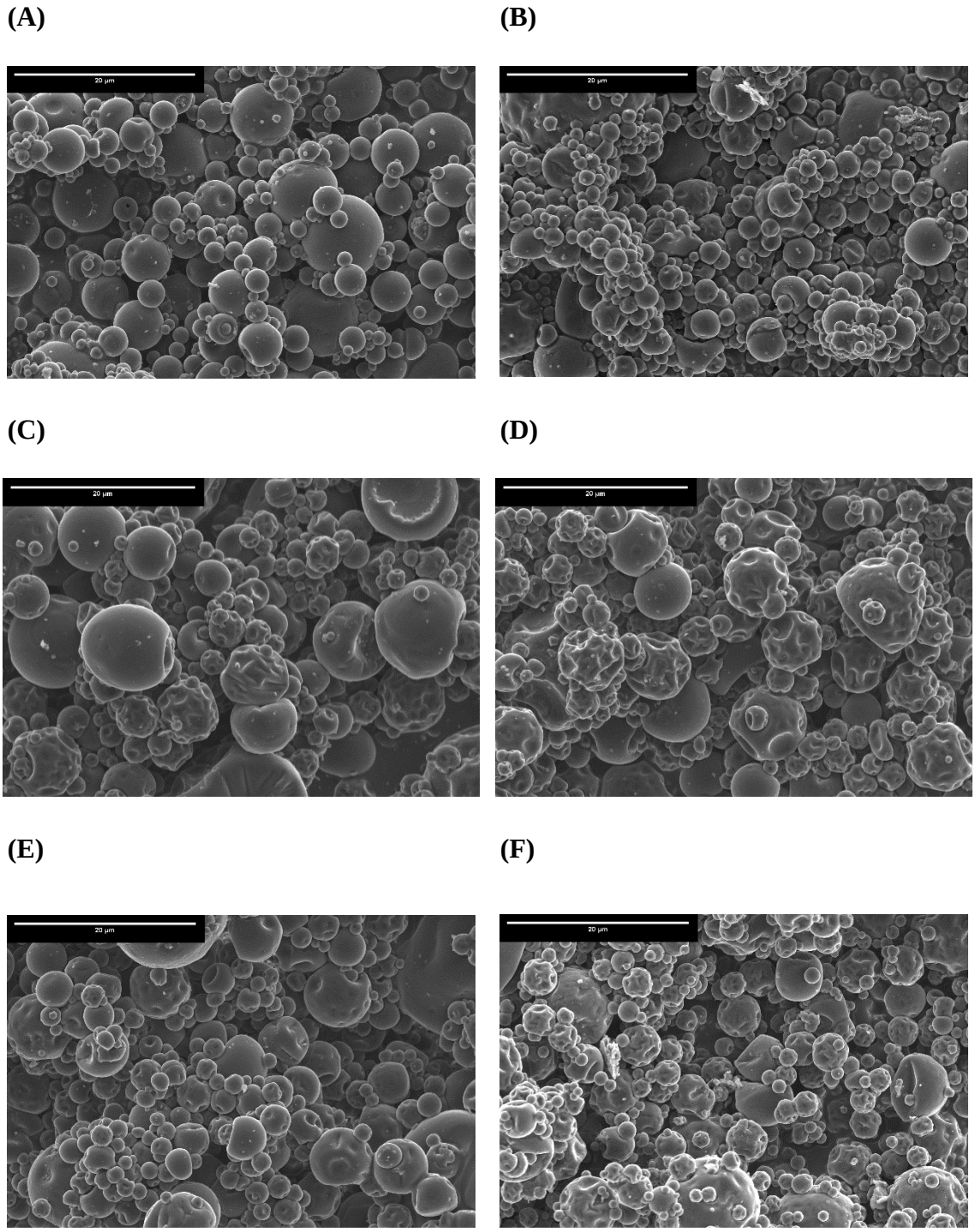

Figure I 1. SEM images of the fish oil-loaded capsules (13 wt% fish oil) produced by EAPG coaxial (EAPG-co): EAPG-co-13-GS (A), EAPG-co-13-S1 (B), EAPG-co-13-S2 (C), EAPG-co-13-S3 (D), EAPG-co-13-WPCH (E), EAPG-co-13-EFO (F). Scale bar = 20 µm.

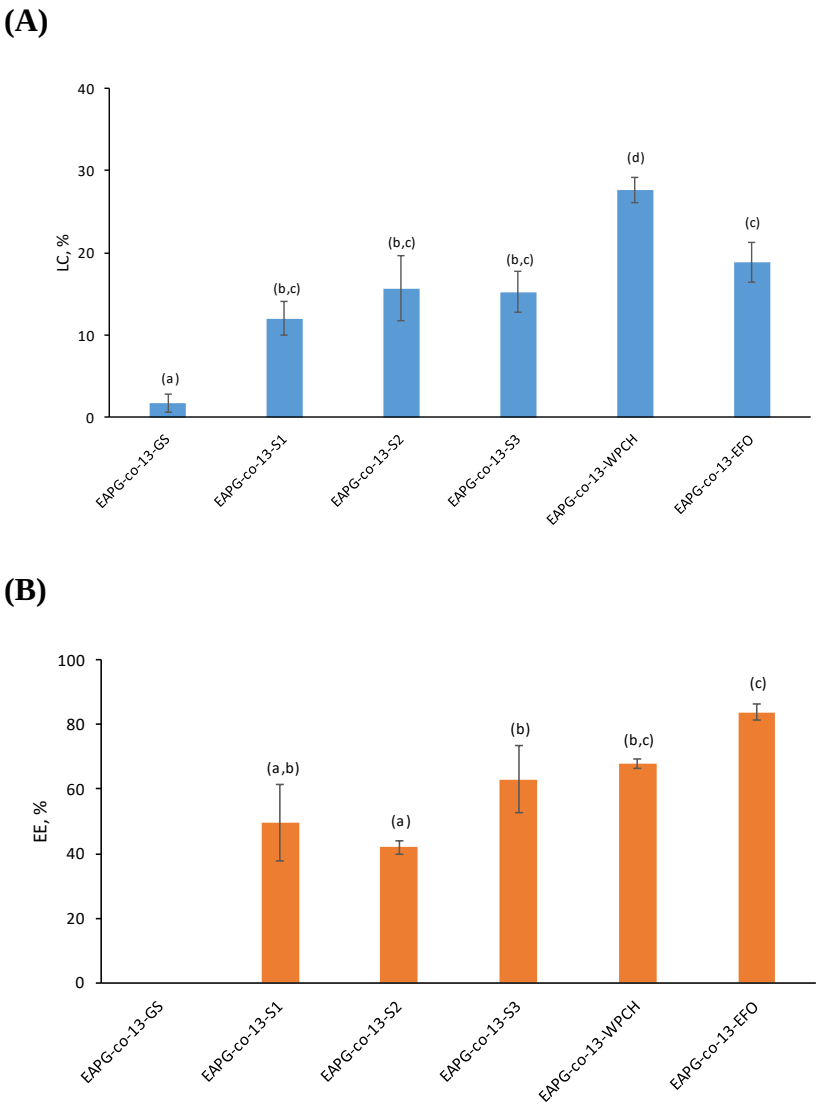

Figure I 2. Load capacity (A) and encapsulation efficiency (EE) of the fish oil-loaded capsules produced by coaxial EAPG. Samples followed by a letter, a-d, indicates statistical differences ($p \leq 0.05$) between capsules.

3. References

Rahmani-Manglano, N. E., González-Sánchez, I., García-Moreno, P. J., Espejo-Carpio, F. J., Jacobsen, C., & Guadix, E. M. (2020). Development of fish oil-loaded microcapsules containing whey protein hydrolysate as film-forming material for fortification of low-fat mayonnaise. *Foods*, 9(5). https://doi.org/10.3390/foods905054

APPENDIX II. Oxidative stability and oxygen permeability of fish oil-loaded capsules produced by electrospraying using hydrophobic proteins as the encapsulating agents

1. Materials and methods

The fish oil (Omega Oil 1812 TG Gold) was acquired from BASF Personal Care and Nutrition GmbH (Illertissen, Germany). Zein from maize, grade Z3625, was purchased from Sigma-Aldrich S.A. (Madrid, Spain). The kafirin used was extracted from sorghum as described by Cetinkaya et al. (2021). The sorghum was provided by Nu Life Market (Scott City, Kansas, United States).

The fish oil-loaded emulsions were produced to achieve and oil load of the dry capsules of ~13 wt%. For that purpose, the fish oil (2.0 wt%) was dispersed in the ethanol/water solvent (85/15, v/v) containing the kafirin or the zein protein (15 wt%) using a POLYTRON® PT1200E (Kinematic Inc., New York, USA). The fish oil was added during the first minute of mixing and the total mixing time was 2 minutes.

Electrospraying was conducted in the monoaxial configuration in the equipment described in Chapter IV. The infusing flow rate was fixed to 0.6 mL/h regardless of the protein-based emulsion and the voltage applied varied between 15 – 18 kV. Electrospraying was carried out at ambient conditions (19 – 23 °C, 22 – 50% RH) in batches of 30 min. The powder collected from the different batches was gently mixed to ensure that analyzed samples were homogeneous and representative of the obtained material. The capsules were stored in airtight flasks, at −80 °C in the dark until further analysis.

The preparation of the ESR spin probe and spin trap together with the ESR measurement conditions can be found in Chapter IV. The morphology and size of the capsules was determined as described in Chapter IV.

2. Results

(A) **(B)**

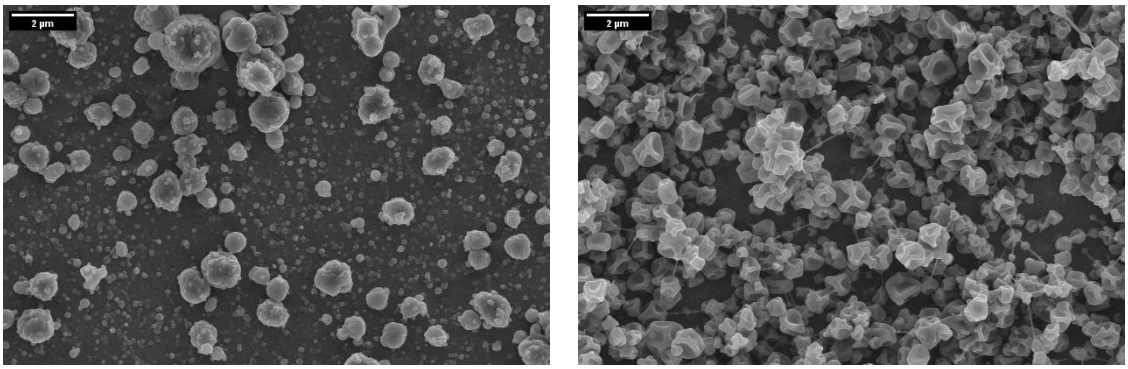

Figure II 1. SEM images of the fish oil-loaded capsules (13 wt% fish oil) produced by monoaxial electrospraying: Kafarin-mo (A), Zein-mo (B). Scale bar = 2 µm.

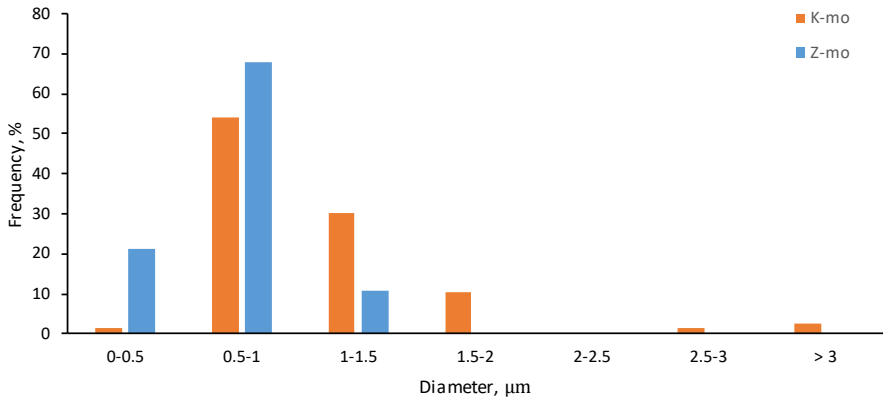

Figure II 2. Particle size distribution of the fish oil-loaded capsules produced by monoaxial electrospraying using hydrophobic proteins (i.e., kafirin, K-mo or zein, Z-mo) as the encapsulating agents.

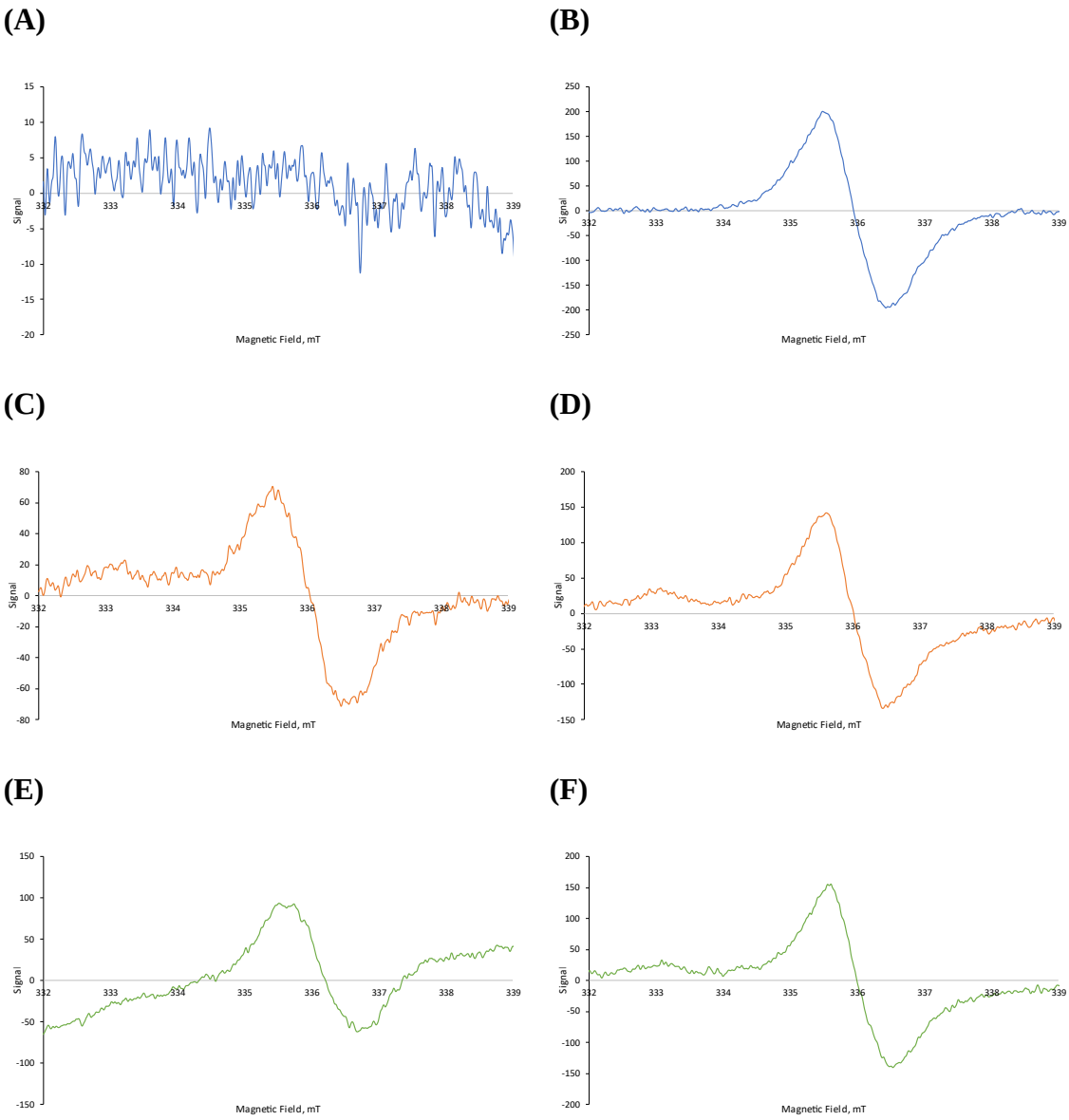

Figure II 3. ESR spectra of protein samples: K (A), Z (B), K-PBN (C), Z-PBN (D), K-mo-PBN (E), Z-mo-PBN (F).

3. References

Cetinkaya, T., Mendes, A. C., Jacobsen, C., Ceylan, Z., Chronakis, I. S., Bean, S. R., & García-Moreno, P. J. (2021). Development of kafirin-based nanocapsules by electrospraying for encapsulation of fish oil. *LWT*, 136. https://doi.org/10.1016/j.lwt.2020.11029

Final Conclusions

The following conclusions can be drawn from the research conducted:

1. The oxidative stability of the fish oil-loaded capsules produced by spray-drying at lab-scale was significantly influenced by the emulsifier used in the formulation. The combination of low molecular weight carbohydrates as the encapsulating agent (i.e., GS or MD) with WPCH as the emulsifier resulted in an improved oxidative stability of the encapsulated fish oil contrary to when T20 was used as the emulsifier, presumably due to its lack of film-forming properties and antioxidant activity.
2. The encapsulating agent used (i.e., GS or MD) played a major role on lipid oxidation when the fish oil-loaded capsules were produced by spray-drying at pilot plant scale. The highest oxidative stability was achieved when WPCH, exhibiting emulsifying and antioxidant properties, was combined with the low-molecular-weight carbohydrate, GS, as bulk material. The latter might result in less porous, and therefore less permeable, encapsulating walls and thus in an enhanced oxidative stability irrespective of the storage temperature (i.e., 4 or 25 °C).
3. The partition of the antioxidants based on their polarity (i.e., polar, non-polar or amphiphilic) within the spray-dried fish oil-loaded capsules produced at pilot plant scale influenced their protective effect against lipid oxidation during processing and subsequent storage. The use of WPCH, exhibiting high surface-activity and combined antioxidant mechanisms of action both in its polar and its non-polar part (i.e., radical scavenger and metal chelator), enhanced the oxidative stability of the encapsulated commercial fish oil already stabilized with non-polar antioxidants (i.e., tocopherols) compared to the polar and non-polar commercial rosemary-based extracts investigated.
4. The physicochemical properties (i.e., morphology, size and EE) of the fish oil-loaded capsules produced by electrospraying at lab-scale were significantly influenced by the emitter configuration (i.e., monoaxial or coaxial) and the processing conditions (i.e., infusing flow rate and voltage applied) rather than by the encapsulating agent used in the formulation (i.e., GS or MD). Emulsion-based monoaxial electrospraying enhanced the retention properties of the encapsulating wall compared to coaxial electrospraying due to the lack of surface-active properties of the encapsulating agents used in the absence of an emulsifier (i.e., GS or MD) ($EE_{monoaxial}$ = 69 –72% over $EE_{coaxial}$ = 53 – 59%).

5. Overall, scaling-up conventional electrospraying at lab-scale to pilot plant EAPG enhanced the performance of the encapsulation process (i.e., higher EE values) and the oxidative stability of the fish oil-loaded capsules (i.e., lower content of the selected SVOPs after storage). EAPG processing resulted in a discrete distribution of larger capsules (~99% of the capsules < 3μm over ~99% of the capsules < 15μm at lab-scale electrospraying and EAPG, respectively) as a result of the higher infusing flow rates (i.e., from 0.2 – 0.6 mL/h to 60 – 600 mL/h) and the combined atomization mechanisms (i.e., mechanical atomization followed by electrohydrodynamic atomization). Furthermore, monoaxial EAPG increased the EE values from 72% to 94% when the capsules were produced using GS as the encapsulating agent at a ~13 wt% fish oil load. However, the content of the selected SVOPs of the monoaxially-EAPG capsules progressively increased throughout storage, contrary to the low and rather constant content found for the coaxially-EAPG capsules (e.g., (*E*,*E*)-2,4-heptadienal or pentanal). This finding was attributed to the fish oil distribution within the capsules, being better protected from diffusing oxygen when it is located at the core of the capsules (as is the case of coaxial EAPG) contrary to when it is randomly-distributed within the encapsulating matrix (as is the case of monoaxial EAPG), especially when the particle size is reduced.
6. The physicochemical properties of the fish oil-loaded capsules, affected by the encapsulation technology, significantly influenced the oxygen diffusivity through the encapsulating wall. The capsules produced by spray-drying (~95% of the capsules < 25μm) compared to monoaxial electrospraying (~95% of the capsules < 1.5μm), both at lab-scale, were significantly less permeable to oxygen as confirmed by the ESR-oximetry results (i.e., the equilibrium with the surrounding pure oxygen atmosphere was reached after ~2h and ~10min, respectively). The latter was attributed to the lower surface-to-volume ratio and the thicker encapsulating walls of the spray-dried capsules, for a fixed oil load (i.e., ~13 wt% fish oil load), which influenced the surface area available for the oxygen diffusion process and the diffusion path to the core of the capsules. These results correlated well with the oxidative stability of the fish oil-loaded capsules measured by ESR-spin trapping, showing that the spray-dried capsules oxidized significantly slower than those produced by electrospraying, irrespective of the emitter configuration (i.e., monoaxial or coaxial).
7. The particle size of the fish oil-loaded capsules produced by the emulsion-based encapsulation methods at pilot plant scale (i.e., spray-drying or monoaxial EAPG)

significantly influenced their oxidative stability, contrary to the oil load (i.e., 13, 26 or 39 wt% fish oil load). The content of the selected SVOPs found after storage was similar among the samples produced by the same technology irrespective of the oil load (e.g., (*Z*)-4-heptenal or (*E*)-2-hexenal, $p > 0.05$), but it was significantly higher for the capsules produced by monoaxial EAPG compared to the capsules produced by spray-drying ($p \leq 0.05$). Provided that the formulation of the fish oil-loaded capsules was the same and that the EE (EE > 83%, $p > 0.05$) and the droplet size of the encapsulated fish oil was not significantly different among the samples ($D[4,3] = 0.5 – 0.7\mu m$, $p > 0.05$), this finding was attributed to the different particle size influencing the oxygen uptake during storage.

8. Protein hydrolysis of WPC (Alcalase® 2.4L, pH 8, 50 °C, DH = 10%) resulted in peptides (i.e., WPCH) with a highly unordered structure in solution (~60% of turns and unordered region). However, the content of non-native α-helical structure significantly increased (> 10%) upon adsorption at the O/W interface as a result of the enhanced hydrophobic interactions WPCH-oil. In addition, the structural conformation of WPCH adsorbed at the O/W interface was not affected by the encapsulating agent used in the formulation of the infeed emulsions before drying (i.e., GS or MD). The secondary structure of the WPCH-based interfacial layer did not change when the infeed emulsion was subjected to spray-drying, contrary to monoaxial electrospraying.
9. The composition of the encapsulating wall of the fish oil-loaded capsules produced by spray-drying influenced the bioaccessibility of the encapsulated fish oil, with the emulsifier used (i.e., WPCH or T20) playing a major role over the encapsulating agent (i.e., GS or MD). WPCH efficiently stabilized the O/W interface of the infeed fish oil-in-water emulsions during processing compared to T20 which resulted in a lower aggregation state of the fish oil droplets after re-dispersion of the WPCH-based capsules along the different phases of the simulated *in vitro* digestion (i.e., oral, gastric and intestinal phase). Furthermore, our results showed that bile salts displaced WPCH from the O/W, thus exerting a re-emulsifying effect at the beginning of the intestinal phase of lipid digestion. The later resulted in an increased interfacial specific surface are for lipases to adsorb, and therefore in a higher bioaccessibility of the encapsulated fish oil for the WPCH-containing capsules (i.e., 64 – 74% of FFA released for the WPCH-containing capsules over 42 – 51% of FFA released for the T20-containing capsules after the intestinal phase of lipid digestion).

10. The physical and the oxidative stability of low-fat mayonnaise enriched with omega-3 PUFAs was significantly influenced by the nature of the delivery system (i.e., neat fish oil, liquid fish oil-in-water emulsion or spray-dried fish oil-loaded capsules). The thickening effect of the spray-dried fish oil-loaded capsules dispersed within the food matrix resulted in an increased viscosity, and therefore, in a high physical stability. Furthermore, food enrichment with the encapsulated fish oil, contrary to the samples enriched with either the neat fish oil or emulsified fish oil, enhanced the oxidative stability of the fortified mayonnaise as confirmed by the low PV and AV of the samples after 28 days of storage at ambient temperature (PV = 8.0 ± 0.1 meq O_2/kg oil and AV = 11.1 ± 0.9). The latter suggested that the integrity of the encapsulating matrix was not significantly degraded during food processing and subsequent storage, thus preventing the direct contact of the fish oil with the prooxidant species present in the medium (i.e., oxygen and metal ions).
11. The initial oxidative status of the dry omega-3 delivery systems significantly influenced the oxidative stability of the enriched salad dressings. The salad dressing fortified with the capsules produced by coaxial EAPG showed the highest oxidative stability among the capsule-fortified samples, as confirmed by the significantly lower PV (PV < 1.5 meq O_2/kg oil, $p \leq 0.05$) and the lower content of the selected SVOPs developed after 28 days of storge (e.g., (*E*)-2-pentenal or (*E*)-2-hexenal, $p \leq 0.05$). This was attributed to the better oxidative status of the encapsulated fish oil after non-emulsion-based coaxial EAPG processing compared to the emulsion-based encapsulation methods (i.e., spray-drying and monoaxial EAPG), due to the absence of the emulsification step and subsequent drying at ambient temperature.

List of publications

JOURNAL PAPERS

1. Rahmani-Manglano, N. E., González-Sánchez, I., García-Moreno, P. J., Espejo-Carpio, F. J., Jacobsen, C., & Guadix, E. M. (2020). Development of fish oil-loaded microcapsules containing whey protein hydrolysate as film-forming material for fortification of low-fat mayonnaise. *Foods*, *9*(5). https://doi.org/10.3390/foods9050545 (IF: 5.561; category: FOOD SCIENCE & TECHNOLOGY - SCIE; position: 35/144; Q1)
2. Rahmani-Manglano, N. E., Tirado-Delgado, M., García-Moreno, P. J., Guadix, A., & Guadix, E. M. (2022). Influence of emulsifier type and encapsulating agent on the in vitro digestion of fish oil-loaded microcapsules produced by spray-drying. *Food Chemistry*, *392*, 133257. https://doi.org/10.1016/j.foodchem.2022.133257 (IF: 9.231; category: FOOD SCIENCE & TECHNOLOGY - SCIE; position: 8/144; Q1/D1)
3. Rahmani-Manglano, N. E., Jones, N. C., Hoffmann, S. V., Guadix, E. M., Pérez-Gálvez, R., Guadix, A., & García-Moreno, P. J. (2022). Structure of whey protein hydrolysate used as emulsifier in wet and dried oil delivery systems: Effect of pH and drying processing. *Food Chemistry*, *390*, 133169. https://doi.org/10.1016/j.foodchem.2022.133169 (IF: 9.231; category: FOOD SCIENCE & TECHNOLOGY - SCIE; position: 8/144; Q1/D1)
4. Rahmani-Manglano, N. E., Guadix, E. M., Jacobsen, C., & García-Moreno, P. J. (2023). Comparative Study on the Oxidative Stability of Encapsulated Fish Oil by Monoaxial or Coaxial Electrospraying and Spray-Drying. *Antioxidants*, *12*(2). https://doi.org/https://doi.org/10.3390/antiox12020266 (IF: 7.675; category: FOOD SCIENCE & TECHNOLOGY - SCIE; position: 12/144; Q1/D1)
5. Rahmani-Manglano, N. E., Guadix, E. M., Yesiltas, B., Prieto, C., Lagaron, J. M., Jacobsen, C., & García-Moreno, P. J. (2023). Non-emulsion-based encapsulation of fish oil by coaxial Electrospraying Assisted by Pressurized Gas enhances the oxidative stability of a capsule-fortified salad dressing. *Submitted for publication.*
6. Rahmani-Manglano, N. E., Andersen, M. L., Guadix, E. M., & García-Moreno, P. J. (2023). Oxidative stability and oxygen permeability of fish oil-loaded capsules produced by spray-drying or electrospraying measured by Electron Spin Resonance. *Submitted for publication.*

7. Rahmani-Manglano, N. E., García-Moreno, P. J., Pérez-Gálvez, A. R., & Guadix-Escobar, E. M. (2023). Antioxidant location affects the oxidative stability of spray-dried microcapsules loaded with fish oil. *Submitted for publication.*

BOOK CHAPTERS

1. Rahmani-Manglano, N. E., García-Moreno, P. J., Espejo-Carpio, F. J., Pérez-Gálvez, A. R., & Guadix-Escobar, E. M. (2020). The Role of Antioxidants and Encapsulation Processes in Omega-3 Stabilization. In M. A. Aboudzadeh (Ed.), *Emulsion-based Encapsulation of Antioxidants. Food Bioactive Ingredients.* (pp. 339–386). Springer, Cham. https://doi.org/10.1007/978-3-030-62052-3_10
2. García-Moreno, P. J., Rahmani-Manglano, N. E., Chronakis, I. S., Guadix, E. M., Yesiltas, B., Sørensen, A.-D. M., & Jacobsen, C. (2021). Omega-3 nano-microencapsulates produced by electrohydrodynamic processing. In P. J. García-Moreno, C. Jacobsen, A.-D. M. Sørensen, & B. Yesiltas (Eds.), *Omega-3 Delivery Systems. Production, Physical Characterization and Oxidative Stability* (pp. 345–370). Academic Press. https://doi.org/10.1016/b978-0-12-821391-9.00017-x

CONFERENCES

1. Rahmani-Manglano, N.E., Guadix, A., Jacobsen, C., Chronakis, I.S, Guadix, E.M., Garcia-Moreno, P.J. (2019, September). Development of carbohydrate-based microcapsules loaded with omega-3 fatty acids by co-axial electrospraying. Poster. 2nd Food Chemistry Conference: Shaping the Future of Food Quality, Safety, Nutrition and Health. Seville, Spain.
2. Espejo-Carpio, F.J., Padial-Domínguez, M., Rahmani-Manglano, N.E., García-Moreno, P.J., Jacobsen, C., Guadix, E.M. (2019, October). Whey Protein Hydrolysates with Emulsifying and Antioxidant Activity for the stabilisation of Omega-3 Delivery Systems. Lecture. 17th EuroFed Lipid Congress and Expo. Oils, Fats and Lipids: Driving Science and Technology to new Horizons. Seville, Spain.
3. Rahmani-Manglano, N.E.; González-Sánchez, I.; García-Moreno, P.J.; Espejo-Carpio, F.J.; Jacobsen, C.; Guadix, E.M. (2021, May). Development of spray-dried microcapsules as efficient omega-3 delivery systems for food fortification purposes.

Lecture. 2021 AOCS Annual Meeting & Expo. On-line. https://doi.org/10.21748/am21.335

4. Tirado-Delgado, M.; Rahmani-Manglano, N.E.; García-Moreno, P.J.; Guadix, A.; Guadix, E.M. (2021, May). Bioaccessibility of fish oil encapsulated by spray-drying: influence of emulsifier and encapsulating agent. Poster. 2021 AOCS Annual Meeting & Expo. On-line. https://doi.org/10.21748/am21.577
5. García-Moreno, P.J., Rahmani-Manglano, N.E., Tirado-Delgado, M., Ruiz-Álvarez, J.M., del Castillo-Santaella, T., Maldonado-Valderrama, J., Jones, N.C., Hoffmann, S. V., Jacobsen, C., Pérez-Gálvez, R., Guadix, A., Guadix, E.M. (2021, October). Interfacial Properties, Oxidative Stability and Bioaccessibility of Fish Oil-loaded Microcapsules Stabilized with Whey Protein Hydrolysate. Lecture. 18th Euro Fed Lipid Congress and Expo: Fats, Oils and Lipids: For a Healthy and Sustainable World. On-line.
6. Rahmani-Manglano, N.E., Chenxing, W., García-Moreno, P.J., Pérez-Gálvez, R., Guadix, E.M. (2021, October). Influence of Polarity of Antioxidants on the Oxidative Stability of Fish Oil-loaded Microcapsules Obtained by Spray-drying. Poster. 18th Euro Fed Lipid Congress and Expo: Fats, Oils and Lipids: For a Healthy and Sustainable World. On-line.
7. Rahmani-Manglano, N.E., Guadix, E.M., Jacobsen, C., Pérez-Gálvez, R., Guadix, A., García-Moreno, P.J. (2022, May). Impact of Drying Technology on Oxidative Stability of Encapsulated Fish Oil. Lecture. 4th International Symposium on Lipid Oxidation and Antioxidants. Vigo, Spain.
8. Padial-Domínguez, M., García-Moreno, P.J., González-Beneded, R., Almécija, M.C., Rahmani-Manglano, N.E., Guadix, E.M. (2022, May). Use of Whey Protein Hydrolysate for the Physical and Oxidative Stabilization of Fish Oil-in-Water-in-Olive Oil Double Emulsions. Poster. 4th International Symposium on Lipid Oxidation and Antioxidants. Vigo, Spain.